



Putting numbers to ideas

Using MORDRED to explore dreams and nightmares about the future of the world





Overview

The present book constitutes the first part of the 3 Pillars Project (3PP).

3PP focuses on the three pillars of social reality that constitute the world order: 'material capacities', 'rules of the game' and 'dominant ideas'. It holds that a change in all three pillars is necessary to

- achieve and preserve development possibilities of the most vulnerable human population groups on the planet;
- achieve and preserve development possibilities of the poorer half of humanity;
- preserve long-term development and survival options for human individuals and societies;
- navigate through the 21st century without major human catastrophes.

Development possibilities are defined as the opportunity to meet basic human needs and to develop one's personality, capacities, interests and virtues free from physical and structural violence.

As the first part and justification for 3PP, this book aims to

- explore future global developments and risks that emanate from the current world order and the three pillars that stabilize it;
- explore different 'sustainability transition' options and to which extent they are compatible with the current world order;
- infer the scale and direction of necessary changes in the three pillars based on the simulation results of a series of scenario exercises.

The book contains two qualitative scenario analyses and 12 quantitative simulation exercises that were implemented in MORDRED. MORDRED (Model Of Resource Distribution and Resilient Economic Development) is a computer model (an Integrated Assessment Model) of medium complexity that allows to simulate simultaneous changes in different interlinked systems at the global level. For some simulation exercises, there is supplementary material contained in excel sheets. These excel sheets are not included in the book but have been uploaded to the MORDRED GitHub (<https://github.com/Pendracus/MORDRED>).

In the following, the key content and message of every chapter of this book is shortly explained.

Chapter 1: Executive summary

Chapter 1 contains key insights derived from the simulation exercises, including the risks of business-as-usual strategies, the insufficiency of incremental political, economic and technological change, requirements for sustainability transitions, policy recommendations, open questions and some technical/methodological notes.

Chapter 2: Business as usual on the highway to hell? Limits to growth and future world orders

Chapter 2 argues that the most probable near-term future is 'business as usual', rather than a successful socio-ecological transition at the global level. It shows the unfeasibility of sustained 'green growth' but also illustrates that voluntary 'degrowth' is impossible within a capitalist,



nation-state-based world order. Four scenarios are developed: 'Hyperimperialist Exploitation', 'Interimperialist Competition', 'Global Emergency Governance' and 'Fragmented Diversity'.

Chapter 3: Limits to growth revisited: System dynamics simulations of global economic developments and the distributional implications in the 21st Century

Chapter 3 quantitatively explores the viability of 'business as usual' by simulating how multiple limits to growth might affect the development of global economic output and the per capita consumption of different classes and regions. It shows that an end to economic growth and a subsequent decline in global output and per capita consumption during the 21st century is possible, plausible and probable.

Chapter 4: Modeling systemic climate damage interactions in an input-output integrated assessment framework

Chapter 4 is a methodological chapter on the representation of climate damages in MORDRED. It shows how different climate damages might interact with each other and with changes in labor productivity. It illustrates that plausible assumed ranges regarding the damage parameters produce significant changes in projected economic development at the global level.

Chapter 5: Endogenizing demographic developments in integrated assessment models: a study of global population dynamics under climate change-induced economic degrowth

Chapter 5 is a methodological chapter on the representation of demographic dynamics in MORDRED. It serves to show how climate damages could affect mortality and fertility rates through changes in economic development. It also illustrates that projected climate-change related deaths rise strongly if indirect effects, i.e. an impairment of further economic growth, are considered.

Chapter 6: Exploring historical discontinuities in global energy scenarios: A model-based reappraisal of the shared socio-economic pathways.

Chapter 6 is a methodological chapter on comparing scenario simulations in MORDRED with and without activated feedback mechanisms. It shows that business as usual scenarios with linear, smooth changes can only be produced if critical feedback loops characterizing complex socio-ecological systems are left out from the analysis.

Chapter 7: Modeling global inequality and limits to growth: socio-economic polarization and systemic breakdown in the 21st century.

Chapter 7 simulates the 'Hyperimperialist Exploitation' scenario to test its plausibility. The main finding is that without very high and continued labor productivity improvements in the center (the Global North), a future in which rich classes and regions maintain their high levels of consumptions while poorer classes and regions perish is structurally unviable. This means that limits to growth ultimately limit the possibility of capitalist cost-shifting. It also means that a transition from 'Hyperimperialist Exploitation' to one of the other scenarios developed in Chapter 2 is likely.

Chapter 8: Toward global environmental scenarios for (and by) the 'bottom billion'?

Chapter 8 critiques commonly used global environmental scenarios because of their disregard for the well-being and reality of life of the poorest billion people on the planet from a decolonial perspective. This includes the absence of subsistence economies, the neglect for the Global South



and the marginalization of radical, just sustainability transitions, including an intentional, voluntary degrowth transition.

Chapter 9: The Rise of the Global South: Quantifying economic development and socio-ecological outcomes under alternative world orders

Chapter 9 focuses on future economic development in the Global South, and how it could affect the global distribution of power and the state of the planetary Earth system. It demonstrates the need to differentiate between the 'semiperiphery' (emerging economies) and the 'periphery' (developing countries). It makes a strong case at putting the Global South, especially the semiperiphery, into the center of the global sustainability debate, and shows that conventional development in the South will put unprecedented pressure on the planetary Earth system.

Chapter 10: Including the Bottom Billion: Integrating subsistence economies into integrated assessment modeling

Chapter 10 has a highly exploratory character. It shows how MORDRED considers the existence of economic structures outside global capitalism, and explores multiple possible interactions between rural subsistence regimes and the global economy. It explains under which conditions subsistence economies might disappear or re-emerge.

Chapter 11: Beyond Unidirectional Drivers: Endogenizing IPAT in an integrated assessment model

Chapter 11 is a methodological chapter that illustrates how demographic, economic and technological variables play out in simulations with MORDRED. It illustrates the relevance of both demographic policies (reducing birth rates) and sufficiency policies (reducing consumption per capita) alongside technological policies, and shows that only focusing on one policy is insufficient to solve socio-ecological problems.

Chapter 12: Assessing equity and mitigation outcomes in multiple degrowth pathways

Chapter 12 simulates a series of 'degrowth scenarios' to assess the environmental effects of different policies related to the idea of intentional economic degrowth. The simulations show that for degrowth policies to be effective, global, radical convergence to low levels of consumptions are required. Reductions in the consumption of richer classes and regions, a change in diet and in the way food is produced, a transition to renewable electricity and structural shift towards more labor-intensive sectors all have positive impacts on climate mitigation but fail to limit global warming to levels considered as relatively 'safe'. Thus, degrowth is necessary but not sufficient.

Chapter 13: Degrowth vs Green Growth: Multidimensional Impacts on Economy, Society and Planetary Boundaries

Chapter 13 compares degrowth and green growth strategies with regard to their effects on different planetary boundaries. Simulations show that the degrowth scenario consistently outperforms the green growth scenario. This emphasizes the need to discuss sufficiency and redistribution in global sustainability and climate policy discourses. However, even the degrowth scenarios does not succeed in navigating the Earth system back to a 'safe operating space'.

Chapter 14: Ideal vs. delayed just sustainability transitions: a comparative scenario analysis



Chapter 14 compares the environmental, economic and social effects of an early sustainability transition with a late sustainability transition at the global level. It shows that a late transition is linked to higher systemic risks. By being able to express some of these risks in numbers, it makes the case for an early transition more comprehensible.

Chapter 15: From Greener growth to sufficiency: modeling alternative global sustainability pathways

Chapter 15 compares to 'fast sustainability transition' (FST) scenarios that feature different policies in the demographic, technological, economic and social dimension. Across all simulations conducted with MORDRED, the only scenario that is able to reach international climate targets is the simulation of FST5 in which global warming is 1.9 °C by 2100. This scenario simulation features a consistent reduction in birth rates, strong sufficiency, radically egalitarian societies, a transition to renewable electricity, a transition from non-electric fossil energy to biomass-based energy, a decrease in land, water, energy and GHG intensity, as well as a 4-fold increase in product duration and product re-use, and assumes that all these policies are implemented at the global level and from the 2030s onwards.

Since the model is summarized in every chapter with a focus on those parts that are relevant for the respective simulation study, it is not necessary to read the whole model documentation before reading a chapter. Equally, the reader can jump directly to the chapter of interest with no need to start with the first chapter.



Executive summary

This executive summary contains key insights derived from the simulation exercises, including the risks of business-as-usual strategies, the insufficiency of incremental political, economic and technological change, requirements for sustainability transitions, policy recommendations, open questions and some technical/methodological notes.

Key insights

The three pillars of the current world order are characterized by:

- (I) very low (re)cycling & reuse capacities as well as production processes that depend heavily on fossil fuels as energy carriers and material feedstocks; a high inefficiency and regionally unequal effectiveness in meeting individuals' basic human needs; low capacities to engage people in meaningful, fulfilling and healthy working processes (pillar 1: material capacities);
 - (II) capitalist socio-economic production relationships, nationalist political relationships (pillar 2: rules of the game);
 - (III) objectification of nature, rejection of transcendence, illusion of equality (pillar 3: dominant ideas).
-

1. The danger of business-as-usual strategies

- (1) If the current three pillars of the world are maintained, a slowdown, halt and subsequent reversal of economic development during the 21st century due to environmental degradation cannot be ruled out. Rather, in the absence of technological breakthroughs that result in a short-term change of material capacities, a mid-term change in the rules of the game and a long-term change in dominant ideas, reversal of progress during the 21st century and a destabilized Earth system is very likely, and collapse, i.e. a sudden loss of economic complexity and population, as well as a reversal of urbanization and a rise of subsistence-based economic regimes are possible phenomena.
- (2) Even with technological breakthroughs in the energy sector it would be almost impossible to limit global warming to 1.5 °C compared to the pre-industrial period, and it would be difficult to limit global warming to 2 °C, due to the inertia of social systems and the acceleration of environmental degradation through economic growth.
- (3) Assessed drivers include climate change damages and fossil resource scarcity that interact with economic variables. However, the highest risks for the stability of the global system stem from interactions between different Earth system boundaries that are extremely complex and uncertain and cannot be assessed by the developed quantitative model. Therefore, the quantitative results of the model do not reflect the full danger caused by environmental degradation.
- (4) A reversal of economic growth at the global level can have different impacts at the regional level. If economic convergence between classes is maintained during a phase of



global economic contraction, the richer classes lose a substantial part of their consumption while the poorer classes faces substantial increases in mortality rates although their consumption losses are smaller. Extreme poverty starts to increase again while environmental degradation slows down but does not stop. If there is economic divergence between classes during a phase of global economic contraction (i.e. the richer classes in the Global North try to maintain their consumption levels at the cost of depressing consumption levels of the poorer classes in the Global South) outcomes depend on labor productivity improvements in the Global North. If the latter increases strongly and continuously, the spread of extreme poverty among poor classes leads to a populational collapse in the Global South and a regionalization of the economy in the Global North. If labor productivities in the North do not increase sufficiently, attempts of the rich to cling to high levels of consumption trigger a massive breakdown of the entire economic system because the Global North relies on the labor power of the Global South for its consumption.

- (5) A halt and reversal of economic growth under the current material capacities, rules of the games and dominant ideas implies high risks of social tensions and violent intra- and interstate conflicts that are not depicted in the model.

2. The insufficiency of incremental change

- (6) Shifting the electricity system to 100 % and shifting a substantial amount of fossil energy inputs to biomass energy input is not enough to prevent dynamics of economic contraction and collapse when economic growth and high consumption inequality are maintained.
- (7) A global one-child policy reduces environmental pressure but is insufficient to meet climate goals and in the long-term can produce labor scarcity problems if labor productivity does not rise fast and continuously.
- (8) A global convergence of consumption to 11,000 to 15,000 € per person per year slows down environmental degradation but is insufficient to meet climate goals.

3. Requirements for radical just sustainability transitions

- (9) Successful sustainability transition that manage to significantly reduce anthropogenic pressure on the Earth system start by 2030, combine population (reduction of birth rates), sufficiency (reduction of consumption of richer classes, global complete convergence of consumption to 7500 €/year) and radical technology policies (focus on meeting basic human needs, 100% renewable electricity, substitution of 60% of fossil fuels with biomass-based energy, substantial increase of product reuse and material recycling).
- (10) Transitions that occur later in the century are more probable because the impacts of environmental degradation can be expected to be more palpable, but they will occur under an already destabilized Earth system restraining long-term development options of human societies and individuals.
- (11) Required material capacities in a sustainable world order: Long duration of products, reuse of product, cycling of products, high efficiency of basic service provision.



- (12) Required rules of the game in a sustainable world order: need-based (rather than capital-based or nationality-based) allocation of economic goods; economic development/production is subject to ecological & social imperatives, rather than to the accumulation imperative; global governance bodies to coordinate the implementation (and enforcement) of technological, social and economic policies.
- (13) Required dominant ideas in a sustainable world order: cooperation, coordination, awareness for the complexity and agency of 'nature', resources as common heritage of humankind, universal human dignity, sufficiency, solidarity, sharing, overcoming othering, non-expansionist cultures.

Key policy recommendations

- (1) Recognize the contradiction between: *international state system – global economic system – planetary Earth system*.
- (2) Focus on development in the Global South:
 - (a) 'Sustainable development' in peripheral countries means capacity development aimed at delivering basic human needs through circular practices at local level informed by global socio-technological learning, not carbon lock-in or becoming a source of cheap labor and resources for the rest of the world.
 - (b) Semiperipheral countries will decisively shape political, economic and environmental outcomes in the 21st century as their population exceeds the population of current core countries multiple times.
- (3) Stop trying to grow the population of your own state.
- (4) Stop thinking that you can outsmart nature or the other states.
- (5) Stop clinging to sovereignty for sovereignty's sake.
- (6) Stop treating something that you did not create (nature, natural 'resources') as an object to be possessed and controlled.
- (7) Stop gambling with the future and present of the majority of human beings.
- (8) Start thinking about global capital regulations and a radical reform of the global financial system.
- (9) Start thinking about resilience, global disaster alleviation and coping with significant migration movements.
- (10) Start talking about converting the world's biggest private and state corporations from servants of capital into producers of goods for humanity, guided by the mission to allow every human being a life in dignity.

Open questions

The three pillars of the current world order have to change drastically to steer through the 21st century without major human tragedies and to maintain the Earth system in a state conducive to human development beyond the 21st century.

However, the processes that will change these pillars, and the new forms, shapes and colors they could acquire, are still unclear, partly due to the high complexity of the phenomenon of global social change and partly due to the scarcity of research and debate.



Hopefully, this will change soon.

Technical notes

Key methodological advances of the study constitute:

- (1) the integration of multiple feedbacks between different subsystems of the world system which leads to more holistic (and realistic) results;
- (2) the focus on regional and class inequality;
- (3) the focus on consumption (rather than on income) as central variable for living standards;
- (4) the focus on labor as central production factor that mediates limits to growth;
- (5) the representation of subsistence regimes existing at the margins of global capitalism;
- (6) the integration of multi-sectoral climate damages affecting different components of the economic process;
- (7) the systematic exploration of collapse as well as transformation scenarios.

Further information is contained in the respective simulation studies and the model documentation.

Business as usual on the highway to hell? Limits to growth and future world orders

Abstract

Combining fundamental premises from international relations, political economy and ecological economics, we show that (1) the reproduction of the current world order structurally depends on the violation of the precautionary principle in favor of 'business as usual' (BAU), understood as continued economic growth and environmental degradation; and (2) BAU rather than successful sustainability transitions constitutes the most probable short-term future, due to the difficulties of consistently implementing global 'green growth' and 'degrowth' proposals. Based on this analysis, we construct four global socio-ecological futures emerging after a period of unsustainable BAU. These scenarios feature different structural changes away from the status quo by exacerbating or transcending the capitalist, state-based world order: *Hyperimperialist Exploitation* describes an increasing polarization between the world's centers and peripheries whereas *Interimperialist Competition* includes great power rivalries similar to those leading to the first world war. In *Global Emergency Governance*, social forces achieve the establishment of a supranational organization capable of managing environmental disaster, economic development and migratory flows. Last, *Fragmented Diversity* describes a radically de-globalized world with small societies integrated in local ecosystems. The scenarios highlight the structural lock-in of the global society into a risky, potentially catastrophic development pathway but also point to the importance of societal power struggles in shaping socio-ecological futures.

Keywords

Worst-case climate change; world system; degrowth; green growth; scenario development; ecological economics

1. Introduction

Despite the rise of ‘sustainable development’ since Rio-92 and the great number of international environmental agreements, most notably the United Nations Framework Convention on Climate Change, the world has consistently failed to address a series of grave ecological and social problems (Gabric, 2023; Pawar, 2023). Renewable energies, although growing exponentially, seem to act as complement to fossil fuels, rather than as substitute, while emissions and temperatures reach all-time highs year after year (Ripple et al., 2022, 2023). Already in 1972 the ‘Limits to growth’ report illustrated the dangers of interacting source and sink problems within a capitalist growth regime (Meadows et al., 1972) but the combined forces of scientific knowledge, environmental movements, technological innovation and political ambitions have not led large-scale transformative action to prevail over ‘business-as-usual’ (BAU).

Despite this empirical dominance of ‘BAU’ during the last 50 years, in the literature concerning global environmental scenarios there is a consistent bias to explore the enablers and effects of fast sustainability transitions rather than the consequences of continued BAU for the stability of the current world order. Of the 160 scenarios classified by Hunt et al. (2012), 37 fit into the ‘Great Transition’ archetype of the Global Scenario Group (GSG) (Raskin et al., 2002) while only 27 were matched with the ‘Barbarization’ archetype, an archetype gaining momentum after the failure of ‘conventional world’ reformist strategies to tackle the environmental crisis. In a more recent review by Harmáčková et al. (2023) of the 460 scenarios assessed only 9% were classified as ‘dystopian’ (including scenarios of societal breakdown, inequality and regional competition) and 15% as ‘BAU’ whereas 49% were ‘sustainable’ scenarios. Likewise, analyzing various IPCC reports, Jehn et al. (2021) found that BAU scenarios of 3 °C degree warming, although more likely, are underrepresented compared to 1.5°C and 2°C sustainability scenarios, while dramatic temperature increases of 6 °C or more with potential catastrophic impacts were severely neglected in the literature. Last, ‘degrowth’ futures with negative economic growth and subsequent reductions in material consumption tend to be envisioned as the consequence of transformative change rather than as imposed biophysical reality (Kallis et al., 2018; Lauer, Capellán-Pérez, et al., 2025). On the other hand, frequently used ‘BAU’ scenarios - understood as futures following the historical reality of tentative incremental environmental policies often only consider the effect of socio-economic structures on environmental degradation and not the reverse effect of environmental degradation on the stability of current power structures. Ignoring that the feedback relationships between the global political economy and the living Earth lead to significant structural changes in *both* systems (Katz-Rosene & Paterson, 2018), these scenarios suggest a stability of the current politico-economic global structure which is not realistic.

In this context, a relatively small strand of the global environmental scenarios literature has focused on the consequences of BAU pathways on societies. First, the literature on societal collapse has studied the breakdown of global structures due to different stressors related to the Earth system (Brozović, 2023). Second, increasing attention is paid to the possibility of worst case climate scenarios as a consequence of BAU pathways during the coming decades (Davidson & Kemp, 2024; Kemp et al., 2022). Last, the qualitative scenario work of the GSG illustrates the growing risk of ‘barbarization’ scenarios as a consequence of BAU (Raskin et al., 2002) while Crownshaw et al. (2019) have theorized on the harsh macro-economic and political conditions in a ‘post-growth’ world facing resource constraints and wide-spread environmental damage. Also, different quantitative modeling studies have shown BAU dynamics and the subsequent end of BAU, as biophysical limits to the world system’s growth manifest themselves, causing the

world economy to decline (Capellán-Pérez et al., 2015, 2020; Meadows et al., 1972, 2004). The focus of this strand of the literature on the grave risks of BAU tendencies is justified since it serves to illustrate what is at stake in the unfolding socio-ecological crisis, and to criticize unjustified optimism (Davidson & Kemp, 2024), thereby, contributing to an integrated risk assessment necessary for decision-making within the realm of ‘deep uncertainty’ (Kemp et al., 2022).

This article complements this literature through a theory-based development exercise that produces different plausible and explorative global futures. Concretely, we aim to (i) illustrate why BAU is the most probable short-term trajectory of the world system, (ii) assess the systemic contradictions of BAU, and (iii) construct four post-BAU global futures that could potentially be further explored in quantitative models.

Our work makes several key contributions to foresight literature, particularly to the field of global environmental and economic scenario studies. First, we use ‘International Relations’ (IR) and ‘International Political Economy’ (IPE) perspectives to construct our main theoretical argumentations from which the scenarios are derived. Although the use of scenarios in the field of international political studies has been recognized (Sus & Hadeed, 2020) there is still little cross-fertilization between future studies and IR/IPE-related work. Adapting an IR-IPE theoretical framework sensitive to questions of power and to the global institutional ‘rules of the game’ allows us to link structural questions of world order with the ongoing socio-ecological crisis and to highlight the structural constraints to the implementation of different sustainability paradigms. Critical theory in IR-IPE, in particular, problematizes current world orders and emphasizes the possibility of changing world orders. Thus, our theoretical framework implies an increased awareness of the temporality of the current world order, and helps us to theorize post-BAU transformations. Second, we do not merely construct worst-case scenarios, but link BAU periods to a diversity of post-BAU pathways that include scenarios of radical de-globalization and regionalization relevant to the literature on societal collapse. Last, the four qualitative scenarios that result from our theoretical argumentation link different politico-economic world orders to environmental degradation, mitigation and adaptation as well as individual consumption, thereby taking into account multiple levels of analysis and laying the basis for a future quantification of disruptive and discontinuous pathways driven by a persistently declining global economy.

The remainder of the article is structured as follows: Section 2 establishes the theoretical background of the scenarios by arguing that the driving forces of the current politico-economic world order are fundamentally incompatible with the idea of successful and timely sustainability transitions, rendering ‘BAU’ by far the most probable scenario for the near-term¹ future (section 2.1). This section also illustrates how the system’s driving forces are themselves unsustainable, resulting in different fundamental system transformations in the medium- and long-term future² (section 2.2). The theoretical insights are used to construct four scenarios that are presented in Section 3. Section 4 compares the developed scenarios with the literature and discusses possibilities for future scenario quantification, and section 5 concludes the paper.

¹ ‘Near-term future’ in this paper refers to a period of +/- 10 years to several decades.

² ‘Medium-term future’ in this paper refers to a period of several decades to the end of the century, while ‘long-term future’ refers to time periods beyond this century.

2. Theoretical background

While technological (IPCC, 2023), legal (Aseeva, 2018; Kim & Kotzé, 2021), psychological (Mazar et al., 2021; Steg, 2023), cultural (Boström, 2021), religious (Toynbee, 1972; York, 2022) and even evolutionary (Snyder, 2020; Waring et al., 2024) factors have been found to contribute to global unsustainability, here we only illustrate how the reproduction of the global politico-economic world order depends on, and results in, continued economic growth and environmental degradation, as well as different changes in world orders as a consequence of societal reactions to emerging biophysical limits to growth.³

2.1. Business as usual as a structural result of the current politico-economic world order

Based on basic premises of International Relations and Political Economy, it can be shown that, as long as the current politico-economic world order persists, transformative changes away from hegemonic BAU, can barely take place.

2.1.1. Growth-dependency in the world system

The (global) capitalist system is characterized by the continuous accumulation of capital. Far from being a voluntary decision, capital accumulation emerges as a necessity for every capitalist enterprise participating in the system. The failure to engage in new investments, scale up production, and incorporate new technologies would lead a company to perish in the competitive struggle at the national as well as the global scale. The incorporation of more efficient technologies, which increase labor productivity, has at least two significant consequences for our analysis: on the one hand, it enables an increase in production, thus raising the amount of energy and materials processed. On the other hand, it allows for an increase in real wages while either maintaining or even increasing the level of exploitation of the working class (Marx, 1992). As a result, the system's legitimacy is reinforced without excessively harming the average profit rate.

The competition between capitalists is mirrored in the competition between states in the Westphalian international system. The state apparatus appropriates a part of the value generated within its territory and thereby is able to reproduce itself: Expenses for public goods within national borders guarantee its legitimacy while military and security expenses are the basis for preserving inner stability and gaining security and power in the absence of a supranational monopoly of violence (Waltz, 1979). The greater the national economy and productivity, the greater the state's latent power, i.e. its possibilities to transform part of its output in means of enforcing national interests on the global level (Mearsheimer, 2007). Thus, a state whose national economy stagnates risks being dominated by others and losing its position in the international hierarchy of states.

The dynamic competition between capitalists as well as between states renders relative gains more important than absolute gains: Societies not only have to grow but their growth must be faster than their competitors' growth, which creates an enormous tendency to grow productive capacities at all costs.⁴

³ This means that we leave out some important factors that would strengthen our argument by increasing the inertia of the world system's development trajectory.

⁴ This is not to say that capitalist and state do not cooperate. In fact, the reproduction of the world system relies on an adequate mix between dynamic competition and cooperation within and between firms, sectors

Thus, in the current global order, political and economic elites across the world depend on capitalist accumulation, and, in the absence of a global organization beyond state sovereignty, neglecting the ‘rules of the game’ means economic or political death.

2.1.2. Growth creates environmental degradation & resource depletion

Apart from adequate fixed capital and labor, the current global socio-economic metabolism relies on a steady flow of material and energy coming from the Earth’s (re)sources that can be transformed into economic goods. Equally, it relies on the Earth’s sinks to absorb the flow of waste generated during the production process and after the products’ consumption. Given that the Earth’s capacity to act as source and sink is limited, at a certain point in time a growing socio-economic metabolism will inevitably reach a size that in the long-term cannot be sustained by the Earth system (Fischer-Kowalski & Haberl, 1998). From this point onwards, further growth leads to a continued degradation of biophysical sources and sinks, which is reflected in a destabilization of global biogeochemical cycles and increasingly adverse global environmental change (GEC). Although the exact size of sources and sinks is currently unknown, empirical data illustrates that the continued expansion of the socio-economic metabolism has already generated a series of problems and risks related to source- and sink problems, as represented by the concept of the planetary boundaries (Rockström et al., 2009). The biophysical input requirements for an expanding capitalist world economy have led to deforestation, and land use change while the waste by-products of production and consumption have created novel chemical entities, ozone depletion, aerosol pollution, and the grave perturbation of global P-, N- and C-flows, with both resource demands and waste generation impacting freshwater resources and functional as well as genetic biodiversity integrity. As of now, the global civilization has crossed six out of nine identified planetary boundaries, thereby entering a novel space of uncertainty in which the short- and mid-term survival of human civilization, and possibly even the long-term survival of the human species is in peril (Richardson et al., 2023; Ripple et al., 2023). A global consensus, thus, exists on the need to stop further resource depletion and restore ecological integrity.

2.1.3. Proposal 1: Global Green Growth

Since the degradation of planetary health has continued during decades and has been accelerating (IPCC, 2021) the concept of ‘green’ economic growth has gained popularity among capitalist and state elites (Adamowicz, 2022). The idea is reducing the biophysical input requirements to the economic process by massive and continuous energy and material efficiency gains, as well as by reducing the economic waste generation by transitioning from a fossil fuel to a renewable energy based system. The climax of such a development would be a global circular economy, which would recycle all waste products, introducing them again as inputs into the economic process. This not only implies a decoupling of growth from environmental impacts but also a decoupling of the human economy from the restrictions to growth imposed by material scarcity.

As long as Global Green Growth works, the dynamic competition between firms and states could continue, creating ever more profit and power without threatening the integrity of the biosphere and without significant adverse GEC.

and states. For example, division of labor requires cooperation or at least coordination, and lies at the heart of (global) value chains.

2.1.4. Contradictions of Global Green Growth

Global Green Growth comes with a series of problems that render its realization highly improbable.

From a biophysical and technological viewpoint, there are thermodynamic limits to energy efficiency gains; biophysical limits to the use of solar energy stemming from the finiteness of the organic and inorganic material needed to absorb and transform this energy as well as the heat ‘pollution’ of solar-based energy technologies (Karamanov, 2022; Kümmel & Lindenberger, 2020); biophysical and practical limits to ‘dematerialization’;⁵ technical limits to material recycling (apart from exponentially rising energy requirements) and to the substitution of ecosystem services by the human economy (Ayres, 2007). Consequently, even under the most favorable conditions, global green growth could only be of temporary character and environmental degradation would continue, although to a slightly lesser extent (Haberl et al., 2020).

In practice, however, even the biophysically and technically possible levels of ‘green’ growth will probably not be reached due to the structural limitations imposed by the capitalist system.

First, given that the generation of profit is the ultimate objective of production in capitalist economies, capitalists will take investment and production decisions that best reach this objective, without consideration for environmental concerns. Although a reduction of energy and material inputs could potentially increase profits by reducing production costs, it comes with costly investments to change production processes and technologies, and the resulting cost-calculation, until now, appears to have led to energy savings less than what would be technically possible, a phenomenon described as energy-efficiency gap (Economidou et al., 2020). This is explained by two dynamics: On the one hand, a decrease in the relative costs of energy and materials due to technological improvements leads to an increase in the relative costs of labor. This creates incentives to invest in labor- rather than in further energy-saving technology. Laborsaving technology, at the same time, tends to increase the energy and material needed in the production process, given that it substitutes humans with machines. On the other hand, a reduction in the relative costs of energy and materials incentivizes capitalists to scale up production, which offsets the energy efficiency gains (rebound effect).

Second, those industries relying on the demand of resources and the clean-up of environmental pollution, such as the fossil fuel, mining, carbon capture or air purifier industry, have an interest in avoiding global green growth, and to mobilize political capital to work against it.

Third, global green growth would also require a radical greening of the military-industrial complex which is associated to significant amounts of resource use and emissions (Ahmad, 2024). Although the problem has been recognized by several great military powers and some attempts at greening the military have been initiated in several states (Jeursen & Hollants, 2024), it is highly improbable that states will substitute their military equipment with ‘greener’ products *if* this comes at the expense of losing military strength.

Thus, the development of green technology is not only subject to biophysical constraints but also to a series of politico-economic limits, which renders strong and sustained global green growth extremely unlikely.

⁵ For example, a chair needs a critical quantity of wood to sustain the weight of a human being.

2.1.5. Proposal 2: Global (Intentional) Degrowth

Given that moderately greener growth will not be sufficient to halt and reverse environmental degradation, measures to improve efficiency and recycling must be accompanied by strong reductions in the scale of economic activity to achieve a global socio-economic metabolism small enough to be integrated in the global more-than-human bioeconomy (cf. Hickel & Sullivan, 2024; Trainer, 2021). Since the downscaling of economic production is supposed to be equitable (Hickel, 2021b; Kallis et al., 2018) and to aim at meeting environmental and social goals alike, a strong convergence in the consumption between the Global North and South as well as between different social classes is necessary (Demaria et al., 2013; Hickel, 2019).⁶

To increase environmental sustainability the repair and reuse sector would grow while planned obsolescence would need to be eliminated and advertisement would be restricted to curb consumption (Fitzpatrick et al., 2022). Also, self-production and self-sufficiency would be encouraged (Fioramonti, 2024).

Last, in an economy with strongly reduced size, almost the entire production must be oriented towards the production of goods that satisfy basic human needs. Thus, the production dedicated to military ends would need to shrink drastically (Moyer, 2023; Schmelzer & Hofferberth, 2023).

Jointly, these key changes in the global economic system could be subsumed under the proposal ‘global intentional degrowth’. In what follows, we explain the contradictions of hypothetical implementation of this proposal *within* the current state-based and capitalist system. While some degrowth authors have stressed the strong links between eco-socialism and degrowth (Hickel, 2021a; Kallis, 2019), the role of the nation-state is less clear.

2.1.6. Contradictions of Global (Intentional) Degrowth

Studies are divided with regard to the technical feasibility of degrowth. For example, Moyer (2023) found that the amount of economic degrowth necessary to reach environmental goals such as greenhouse gas emission reductions is so high that it would lead to the spread of extreme poverty, i.e. that degrowth cannot simultaneously achieve its social and environmental goals. Similarly, the results of Oswald (2024) suggest a trade-off between minimum living standards and feasible climate pathways that even strong income convergence cannot completely avoid. Conversely, other studies state that basic human needs can be covered with only a fraction of today’s energy and economic production (Hickel & Sullivan, 2024; Kuhnhenn et al., 2020; Millward-Hopkins et al., 2020).

Optimistically assuming that theoretically a drastically smaller world economy would halt environmental degradation while covering basic human needs for every individual, the current politico-economic order nevertheless presents insurmountable obstacles to a realization of global degrowth.

First, global degrowth requires strong convergence between and within societies to avoid that the poorest members of world society perish in extreme poverty. Thus, in global degrowth, the consumption of capitalists would fall drastically and approach that of the rest of society. In this way, class inequality regarding consumption and privileged access to economic goods, which are fundamental incentives for capitalists to reproduce the economic system, would be eliminated.

⁶ The political project of an intentional and planned ‘degrowth’ can be contrasted with ‘unintentional degrowth’ dynamics resulting from prolonged unsustainable BAU, in which the output of the world economy declines due to escalating environmental impacts rather than because of a collective decision to reduce consumption (cf. Enríquez-Sánchez & Álvarez-Antelo, 2024).

Second, the elimination of planned obsolescence and advertisement as well as the introduction of strong resource caps and greater protagonism of self-production would reduce capitalists' opportunities for profits while decreasing workers' dependence on the output of capitalist production. With dwindling perspectives for successful accumulation, capitalists could decide to stop investing, which, without state intervention, would plunge the world economy into a grave economic crisis (Roberts, 2016; Sweezy, 2018; Tapia, 2023).

Last, opposition to global degrowth by capitalists and privileged workers (the 'labor aristocracy') who, in the short-term, would be the main losers of global degrowth, would likely translate into an opposition of states of the capitalists centers to a global degrowth project. However, even assuming values of global solidarity among capitalists and privileged workers, political elites around the world would be suspicious of global degrowth since it would require a systematic reduction of their military power, thus, putting the state in a less favorable position in the case of conflicts of interests on the global level. In the absence of a supranational enforcement, international coalitions on global degrowth would unavoidably be of temporary character because of the strong incentives for freeriding. By violating the agreement, states would not only increase their own power to defend themselves and to dominate other states but they also could increase stability and legitimization within the state by granting the citizens higher consumption levels.

2.1.7. Proposal 3: New World Order

From the argument made until here, it follows that the contradictions of global degrowth could only be solved through fundamental systemic changes toward a post-capitalist and supranational world order in which the monopoly of violence, the legislation regarding global public environmental goods and resources, the power to enforce egalitarian consumption levels and the capacity to steer the structural development of the economy over time is shifted to the global level. Avoiding the formation of a new transnational ruling class with privileged access to economic goods and high per capita consumption, and the spread of corruptive practices, could be the main difficulty for any post-capitalist and supranational world order aiming at realizing the socio-ecological objectives of equitable global degrowth. Thus, a new world order is linked to a global democratic-egalitarian system.

2.1.8. Current low probabilities of a New World Order

The cultural hegemony of ideologies like neoliberalism and meritocracy, individualism and consumerism (Laruffa, 2023; Windegger & Spash, 2023), as well as nationalism (Triandafyllidou, 2020) is being contested but is still prevalent in both the Global North and South. Together with the myth of technological progress (Burdett, 2015), these powerful ideas hide the need for a fundamental break away from BAU toward a new world order, and shape institutions and material capacities toward the maintenance of BAU. As a consequence, as of now there is a notable absence of political and economic forces aspiring the advent of a new world order aiming at transforming the current mode of societal reproduction towards more socio-economic equality and less environmental degradation. While it is not impossible that a series of social tipping points ends in a new world order of this type (cf. Lauer, De Castro, et al., 2025), such a scenario would need a series of adequate black swans that would overcome the system's inertia caused by the interaction between cultural, economic and political hegemony.

Given the low likelihood of global green growth, global degrowth and a global new world order, the most probable pathway of the world system is continued BAU with continuously increasing

source- and sink related problems and a systematic neglect for the precautionary principle (Cameron & Abouchar, 1991).

2.2. Consequences of BAU: Stagnation, collapse, transformation

Although systemic inertia renders BAU the most probable trajectory in the near-term future, BAU creates its own contradictions since capitalist accumulation ecological degradation mutually impact each other, undermining the medium- and long-term viability of BAU. When the feedback mechanisms of the Earth system on the world economy reach a critical level, world output inevitably stagnates and declines (Bovari et al., 2018; Capellán-Pérez et al., 2020; Meadows et al., 1972). A much greater uncertainty surrounds the distribution of the social costs of this kind of *involuntary* or *unintentional* global degrowth among different socio-economic groups in different parts of the world. The historical juncture posed by the end of energy and material growth, might trigger two different evolutions of the world order away from the status quo in the medium-term future: 1) an exacerbation of, rather than a break with, the current contradictions of the capitalist state system or 2) its transformation into a post-capitalist, post-state world order. These changes in world order and the accompanying changes in forms of state and social forces, as well as the resulting changes in ideas, institutions and material capabilities of different actors (Cox, 1981) determine the distribution of economic goods between different socio-economic groups as well as the means of resource allocation in this new post-BAU world order.

2.2.1. Exacerbation of the center-periphery ('North-South') contradiction

Capitalist accumulation relies on cheap labor, food, energy, and raw materials (Moore, 2015, 2017, 2018) the majority of which can be found in the world's (semi)peripheries. The exploitative relationship between centers and (semi)peripheries is reflected in the unequal exchange of labor and resources in world trade, and in cost-shifting practiced by the center whereby economic 'bads' such as pollution are shifted to marginalized territories (Emmanuel, 1972; Givens et al., 2019; Hornborg, 2001; Moran et al., 2013). To grant relatively high standards of living to the 'labor aristocracy' (Davis, 2024) in the center, thus, buying political stability, capitalists in the center have to solve the contradiction of relying both on the Global South's exploitation and its consent to this exploitation in a '*free trade*' regime. The discourse of growth and the spread of mass consumption in the South, alongside the immense military power of the US, offer one way to temporarily solve this contradiction.

In a PG regime with increasing source- and sink problems the promise of growth for the South no longer holds for the great majority of the population, while the degree of exploitation and ecologically unequal exchange continues to rise. As the South bears the brunt of involuntary global degrowth in form of environmental damages, impaired economic development and reduced consumption, hegemonic consensus falters and capitalist and political elites in center as well as periphery might increasingly recur to violent means, leading to the formation of neo-colonial regimes and a renewed importance of accumulation by dispossession already observable today (Alami et al., 2023; Monterrubio-Solís et al., 2023; Yang & He, 2021). However, by allowing the massive spread of extreme poverty and social conflicts in the South, capitalists risk the survival of the global economic system given that it relies on the continued production of cheap labor, which is only possible with minimum living standards and political stability in the (semi)peripheries.

The exacerbation of the center-periphery contradiction is based on the strengthening of the Global North's 'hyperimperialism', i.e. an alliance of the states of the center to the detriment of the rest of the world (Kautsky, 1914). However, this is not the only way to temporarily deal with the economic consequences of environmental and resource degradation. In fact, the 'hyperimperialist' strategy could break down, giving rise to 'interimperialist' competition, which will be discussed in the following section.

2.2.2. Exacerbation of the center-center/semiperiphery ('West-East') contradiction

Although the Westphalian state system is based on formal equality between states, in fact state power is highly unequally distributed, leading to a constant competition between powerful states to keep their position, and the formation of geopolitical alliances. While global economic growth gives state the possibility to gain power, the zero-sum character of relative power (Mearsheimer, 2007) becomes evident once economic growth stops and reverses, given that this sharpens rivalries between powerful states of the center and emerging powers of the semiperiphery competing for influence in the periphery to access cheap resources and labor. As powerful states prioritize 'national interest', strengthen national borders and become engaged in hostile nationalist discourses, the contradiction between national sovereignty and global environmental and resource problems aggravates. As great power rivalry is incompatible with a global economic order based on coordination and cooperation between states, strictly separated trade blocks with altered energy and material flows might emerge, constituting a first significant departure from the status quo.

Simultaneously, states of the center and semiperiphery begin to view the elimination or subjugation of rival powers as a solution to global source- and sink-related problems since this would both significantly reduce energy and material flows and associated pollution, and the need to constantly scale up power. Consequently, risks of military escalations are mounting, interacting with economic and environmental stressors to create significant threats to peace within and between societies (Buhaug et al., 2023). However, in a multipolar order based on weapons of mass destruction, rival states cannot be eliminated without great dangers to the survival of the victorious states. Thus, overt nation state competition in a world plagued by a destabilized planetary system is doomed to shovel its own grave.

2.2.3. Transformation: supranational regimes

Growing social tensions and ecological distribution conflicts caused by a break with the growth regime create risks for violent escalations but also open up a window for profound and transformative change caused by sufficient societal pressure that builds up while the legitimization for the current politico-economic order vanishes (Goldstone et al., 2022). Thus, an era in which BAU has lost its attractiveness, might give rise to social forces and institutions striving for a new world order that ends the dynamic inter-state and inter-capitalist competition. Given that the maintenance of the current order harms socio-economic groups of the world's peripheries and semiperipheries the most, these territories might be decisive for the emergence of a strong counter-hegemonic movements (Amin, 2019).

A global institution with legislative, fiscal and military competences, which does not depend on capitalist accumulation for survival, might have the capacity to regulate ecologically and socially harmful productions, control energy and material flows, limit consumption to the level of basic need satisfaction without granting privileges to certain socio-economic groups, redistribute economic output, steer global migration, and organize global disaster management.

Depending on the severity of GEC at the time of its establishment, this supranational regime might have to focus on ad-hoc reactions to rapidly changing environmental conditions or be able to adopt a longer-term perspective, including population policies, the redirection of investment flows toward the development of materially closed production technologies, or ecological restauration.

In principle, global post-capitalist orders can be hierarchical or democratic-egalitarian (Wallerstein, 2004). However, solving the ecological predicament of humankind through a supranational configuration in a post-BAU period will only be possible with low levels of inequality which are arguably more compatible with a political system based on (democratic) egalitarianism.

2.2.4. Transformation: sub-national regimes

Scientific research points to risks posed by adverse GEC, especially climate change, to the 'backbone' and 'blood' of the globalized economic system, namely:

- The global transport and trade infrastructure (especially seaports but also airports as well as the global road and rail infrastructure) (Becker et al., 2013, 2018; Christodoulou & Demirel, 2018; Forzieri et al., 2018; Izaguirre et al., 2021; Leal Filho et al., 2024; Venner & Zamurs, 2012; Voskaki et al., 2023)
- The global telecommunication infrastructure, including Internet (Clare et al., 2023; Sandhu & Raja, 2019)
- The global energy infrastructure (especially the petroleum trade system) (Dong et al., 2022; Leal Filho et al., 2024; Mikellidou et al., 2018; Rohr et al., 2013)

While single environmental risks to the global infrastructure might be managed successfully, positive feedbacks between risks, and their interactions with other local risks of political, military, social, economic, financial or health character can greatly aggravate environmental shocks, leading to domino effects and a rapid disintegration of current structures: Since the current global economy is a complex system characterized by both high connectivity and high homogeneity, it can be subject to rapid non-linear changes as impacts can cascade rapidly due to a lack of functional diversity that could buffer them (Buhaug et al., 2023; Degroot et al., 2022; Ibrahim et al., 2021; Lawrence et al., 2024).

Consequently, it cannot be ruled out that the prolongation of BAU pathways, under certain conditions, leads to a demise of the globalized economy and radical regionalization although the timing and speed of these processes remain fundamentally uncertain (S1 Supplementary Material). In such a scenario, the current global economic system would give way to significantly smaller and less complex socio-economic systems with greater protagonism of sub-national political entities. Given the material- and energy investments necessary to build up and maintain the global infrastructure, once collapsed, a return to the former degree of globalization seems highly unlikely in the medium-term and might only emerge again after centuries or millennia.

2.3. Structural constraints vs. determinism

The fact that structural constraints render BAU the most probable short- to medium-term pathway does not imply the impossibility of early deviations from BAU trajectories towards more sustainable practices. For example, the FST scenarios developed by Lauer et al. (2025) are based on the assumption that 'black swans' can trigger positive tipping points, resulting in the emergence of new historical blocs and new hegemonic structures more conducive to sustainable development. Global environmental governance cannot be reduced to international governance

fully controlled by nation states but is continuously evolving and adapting to new discourses and contextual factors. Moreover, while globally coherent and coordinated actions are difficult to implement, it is important to recognize the agency of economic and political actors at the regional and local level. As Voros (2001) rightly points out, the future is neither predetermined nor predictably, and present choices critically influence future outcomes. Especially in the context of the high level of complexity characterizing the current global system, every theoretical argument will necessarily miss some important features of the system. Thus, we caution against interpreting our analysis of structural constraints as deterministic predictions.

Another illustration of the distinction between structural constraints that condition the likelihood of certain scenarios and historical determinism lies in the development of technology, which fundamentally influences how nature is incorporated and transformed within the global economy. While our analysis does not make any deterministic statements on future evolutions of technology, we nevertheless hold that technology cannot change the basic structural constraints in the development of global futures away from BAU. In principle, technological development can both accelerate and delay environmental degradation. However, as long as technological development is subject to capital accumulation and the maximization of state power, the wide possibility-space of future 'green' technology development is greatly restrained, and only those technologies that do not threaten profit maximization and national security interests can be scaled up. Furthermore, as already mentioned, the continuous quest to replace labor with capital that characterizes capitalist development is linked to technology that replaces human by non-human energy, and that can transform more, rather than less, energy and material per worker. Of course, based on the assumption that technological fixes always emerge at the right time and that their negative side-effects are not systematically greater than the environmental problem they address, speculative green hyper-technology scenarios are possible that manage to infinitely extend the current BAU phase based on dynamic competition. Nevertheless, due to the aforementioned structural constraints and our interest in identifying risks rather than technological miracles we will not focus on such scenarios in the next section.

3. Global environmental scenarios incorporating limits to growth

3.1. Methodological remarks

Our scenario development exercise follows a five-step approach depicted in Figure 1. First, we selected the theoretical framework which combines realist, neorealist, Marxist and critical perspectives in the fields of IPE and IR. This framework allowed us in a second step to identify the three key systems and their interactions relevant for the scenario study, namely the international state system (1), the global capitalist system (2) and the planetary Earth system (3).

Analyzing the relationship between the three systems allows us to formulate structural world-order constraints to sustainability transformations in the subsequent theoretical analysis and to develop four structurally different global configurations that solve the contradictions of BAU.

The fourth step consists in formulating scenario storylines based on the four theoretical post-BAU configurations outlined in section 2.2. Given our theoretical focus on politico-economic power relations, the actors driving the storyline are different socio-economic groups with competing material interests. Since an alternative focus could result in different storylines, we

want to stress that the scenarios presented in the next section are only one possible concretization based on the theoretical argument advanced in the previous sections.

In the fifth step, the storylines can be mapped to different variables (or drivers) related to the three key systems identified in step 2 and to the socio-economic groups that appear in the scenario storylines. This mapping provides a basic 'scenario translation protocol' that serves for potential quantification exercises of the storylines in future work.

Given the importance of the IPE/IR theoretical framework in the whole scenario construction process, we refer to this method as 'theory-based' scenario development.

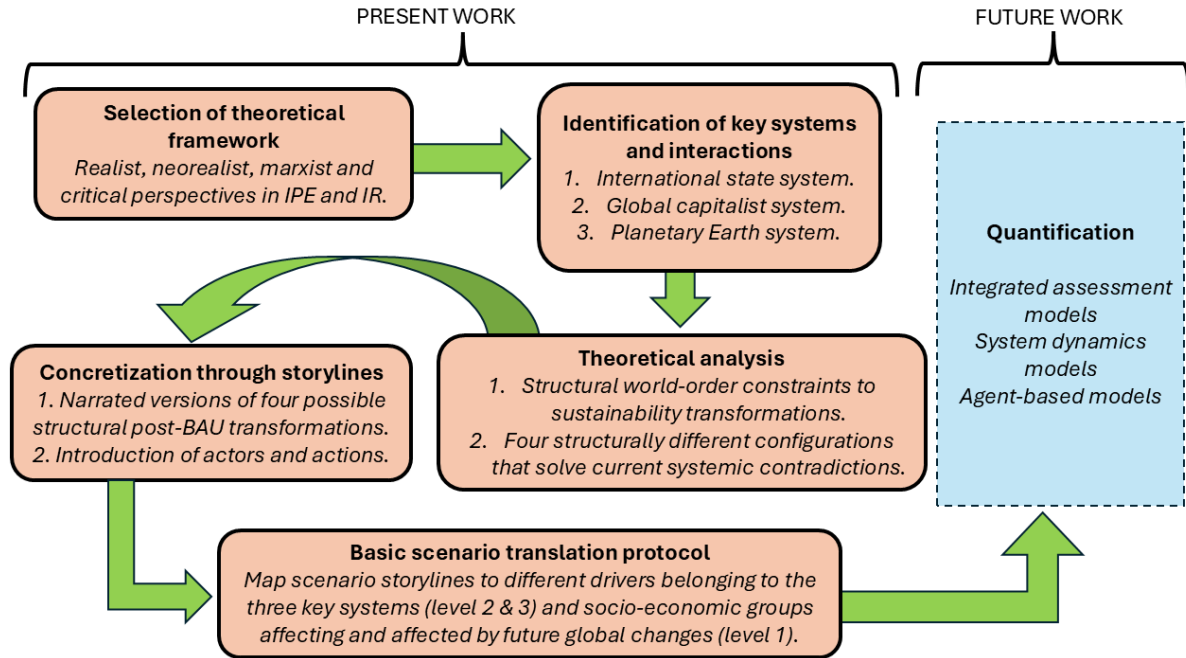


Figure 1: Methodological approach employed in this paper.

3.2. Scenario storylines

In all scenarios, the world system initially continues its trajectory of growing global economic output and environmental degradation, while maintaining intra- and international economic inequality. However, as biophysical limits to growth become increasingly evident, the system is forced to abandon its path of accumulation based on dynamic competition.

In *Hyperimperialist Exploitation* (Sc1) the capitalist elites of the center, supported by capitalist and political elites of the semiperiphery and periphery, maintain their consumption and power despite economic stagnation and degrowth, while workers of the center struggle to keep their former lifestyles, and those in the semiperiphery and periphery face declining wages and deepening poverty.

While this scenario can persist for a time, it generates mounting social tensions. As extreme poverty and despair spread, many workers in the (semi)periphery withdraw into subsistence practices, shrinking the labor force and undermining both national and global legitimacy. To sustain cheap labor without reducing their own consumption, capitalists eventually cut wages in the center as well, destabilizing it politically. The societal tensions pave the way for two alternative scenarios:

In *Interimperialist Competition* (Sc2) workers across regions remain divided.⁷ Those in the center and semiperiphery ally with their national elites, acknowledging dependence on peripheral labor and resources while competing with other states for access to them. As the periphery can no longer meet global consumption demands, rival blocs expand their influence militarily. Environmental and resource conflicts intensify, diverting growing portions of economic output to warfare and reconstruction, thereby reducing consumption for all classes worldwide.

Conversely, in *Global Emergency Governance* (Sc3) workers across regions succeed in organizing globally, fostering transnational solidarity.⁸ Capitalist elites accept or are obliged to renounce their privileged position and to support strong political transformations, in part because they are aware of the ongoing environmental catastrophe, in part because of fear of eventual violent retaliations. Finally, the social and environmental problems of the world are connected to its politico-economic system, and the need for a new economic world order becomes evident. Based on a global consensus a world emergency regime is installed. The centralized coordination and legislation, backed by global security forces, gives the new political elites an unprecedented capacity to implement stringent migratory, environmental and social policies, focusing on minimizing resource use and pollution, disaster management, the fulfillment of human needs and the development of a socio-technological regime oriented toward high reuse of materials and a better integration into the global biogeochemical cycles.

However, this arrangement may prove temporary: corruption from above and separatism from below could erode stability. Moreover, Sc3 remains viable only while global infrastructure and institutions can be sustained at acceptable costs. If maintenance costs exceed benefits, the system may transition to a scenario of *Fragmented Diversity* (Sc4). This scenario could be equally reached through a military escalation, possibly including nuclear weapons, and major inter-state wars at the end of Sc2, destroying the global infrastructure. In Sc4 there is a great diversity of different local politico-economic regimes that are only loosely connected. Societies struggling with the impacts of environmental degradation are left to their own. While some societies manage to reproduce themselves over time due to geographical advantages, technological, social, economic and cultural adaptations, others cannot stabilize their populations and disappear. Surviving societies are characterized by steady state economies with small but stable populations and economic output.

The Table in S2 Supplementary Material contains empirical trends demonstrating that BAU has been the dominant trend for the last 25 years but also shows weak signals illustrating the plausibility of the different scenario storylines. While this table does not aim to be comprehensive it nevertheless illustrates that the theoretical analysis and the resulting scenarios are compatible with important empirical trends.

While it is impossible to say how long each scenario might ‘work’, due to unresolved social and biophysical uncertainties, it is clear that the BAU future as well as the post-BAU scenarios are limited in time. Their instability make dynamic shifts between scenarios possible, with potential

⁷ Following Kautsky (1914), we use the term ‘(hyper-/inter-)imperialist’ for states capable of economically and militarily dominating agrarian or resource rich states with a lower degree of capitalist development. In the present and future context, ‘imperialist’ states, thus, potentially also include some emerging powers from the semiperiphery.

⁸ ‘Workers’ should be understood here as a very broad category comprising all individuals that do not have the chance to enter into the capitalist accumulation cycle. The fact that an individual earns a salary is neither sufficient nor strictly necessary to enter into this category.

new equilibria existing on the supranational (in the case of the emergence of a stable ‘global’, instead of national, identity) and on the infra-national level (in the case of radical de-globalization). Evidently, the four ‘pictures’ of the future, that could follow the demise of the BAU dynamic, are not predictions but rather ideal type developments resulting from past and current weak signals and dynamics observable in the politico-economic world system. Figure 2 shows the position of the four scenarios in a two-axis framework. Arrows between the scenarios illustrate the extent to which the world can move from one scenario to another as time advances.

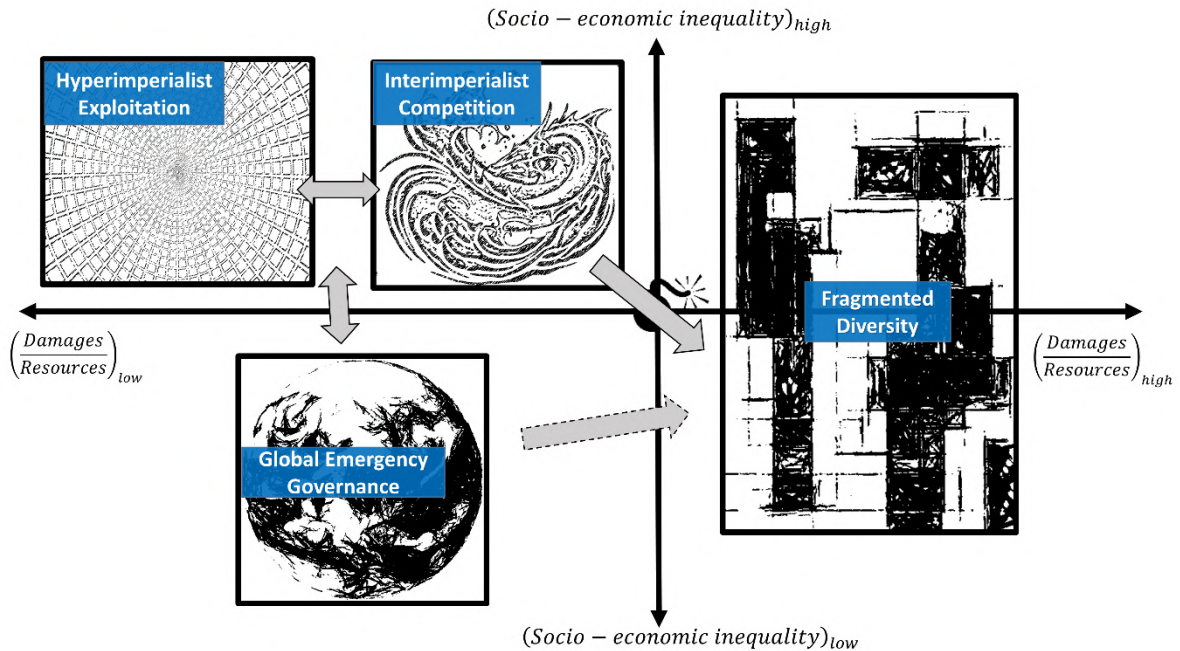


Figure 2: Position of the four scenarios with regard to two scenario characteristics: The uncertainty regarding the possibility to maintain a global infrastructure (mediated by the relationship between the severity of adverse GEC impacts on the global economy and the availability of extractable resources) (x-axis); and the degree of socio-economic inequality resulting from different allocation regimes (y-axis). Arrows indicate the possibility of shifts between scenarios.

3.3. Scenario characteristics

To avoid storylines with excessive length and to facilitate attempts to quantify the scenarios, we contrast key characteristics of the different scenarios in Table 2: Characteristics of the four scenarios at the macro (culture & governance) level. The color distribution indicates to which extent variables are present in the different scenarios. -4 which adapts the scenario representation chosen by Mora et al. (2020) and Roura-Pascual et al. (2021) to the four developed scenarios. The tables lists relevant variables on three levels (individual (Table 1); society (Table 2 & 3); Earth system (Table 4)) and illustrate to which extent the values these variables can take, appear in the respective scenarios. For example, both hard and soft conflict resolution mechanisms might appear in *Hyperimperialist Exploitation* and *Interimperialist Competition* but hard conflict resolution mechanisms have greater importance in the latter. Equally, while nature has instrumental value in all scenarios, only in *Global Emergency*

Governance and Fragmented Diversity relational and intrinsic values of nature (Pereira et al., 2020) gain some protagonism. The variables belonging to the society-level are divided into three dimensions: culture, governance and economy, following the scenario categorization developed in Lauer et al. (2024). The economic dimensions cover social as well as technological aspects of production. Last, Table 3 also describes to which extent mitigation and adaptation capacities of societies differ between the scenarios. S3 Supplementary Material justifies the values the variables take in the different scenarios.

In general, the post-BAU era is linked to reduced per capita consumption and life expectancy in all scenarios although the winners and losers are different in every scenarios, leading to varied class and geographical levels of inequality. The hegemonic ideas of every scenario legitimate the distribution of power and access to economic goods and are reproduced by the media. While Sc2 features a total control of the media by the political apparatus, in the other scenarios, especially in Sc3 the media acts as a sort of counterweight to state power due to the elimination of structural factors that currently tend to streamline the media with corporate and state interests (Herman & Chomsky, 1988).

Sc1 and Sc2 are compatible with both multipolar and bipolar world orders. Sc3, however, only works in a unipolar world order. Whereas in Sc3 the monopoly of violence necessarily is global, in Sc4 it is either local or non-existent. In Sc1, corporate and state power share the monopoly of violence which could be even extended to some transnational actors to assure capitalists' interests, something impossible in Sc2.

Sc3 is based on societal control of production and an egalitarian distribution of products designed to fulfill basic human need, whereas the maximization of both consumption and accumulation remain predominant in Sc1 and Sc2. Given that Sc4 is based on relatively isolated small societies, various different modes of production and societal organization are conceivable, which might resemble historically 'successful' relations of production such as the communitarian, tributary, slave or small simple merchant production relations (Amin, 1978). Consequently, the allocation of scarce resources in Sc4 can be determined by a range of factors beyond class and nationality, including gender or age discrimination. While Sc1 is based on state and neoliberal capitalism it is also prone to include some degree of neo-slave production. Neo-feudal and neo-slave structures would also be compatible with Sc2 variants where territories become subjugated by rival powers. Last, Sc1 to Sc3 only are feasible with high ecosystem resilience, low climate sensitivity and high adaptation speed. In contrast, Sc4 features a lower stability of the planetary system, combined with a slower but transformative adaptation away from the globalized economy.

	Scenarios	Hyperimperialist Exploitation	Interimperialist Competition	Global Emergency Governance	Fragmented Diversity
Level1: Individuals / socio-economic classes					
Life expectancy determined by					
unequal consumption					
escalating violent conflicts					
GEC damages					
Evolution of per capita consumption of the Top20% (in center, semiperiphery, periphery)					
BAU: growing					
post-BAU: high					
post-BAU: high / medium (depending on geopolitical block)					

post-BAU: low				green	yellow
Evolution of per capita consumption of the Middle50% (center/semiperiphery/periphery)					
BAU: growing		blue	yellow	green	yellow
post-BAU: medium (center); low/very low (semiperiphery/periphery)		blue			
post-BAU: medium / very low (depending on geopolitical block)			yellow		
post-BAU: low				green	yellow
Evolution of per capita consumption of the Bottom30% (in center, semiperiphery, periphery)					
BAU: growing		blue	yellow	green	yellow
post-BAU: low (center); very/extremely low (semiperiphery/ periphery)		blue			
post-BAU: low / very low / extremely low (depending on geopolitical block)			yellow		
post-BAU: low				green	
post-BAU: very low					yellow

Table 1: Characteristics of the four scenarios at the micro level. The color distribution indicates to which extent variables are present in the different scenarios. See S3 Supplementary Material for details.

	Scenarios	Hyperimperialist Exploitation	Interimperialist Competition	Global Emergency Governance	Fragmented Diversity
Level2: Society					
Culture					
Value of non-human life					
	instrumental	blue	yellow	green	yellow
	relational			green	yellow
	intrinsic			green	yellow
Hegemonic ideas legitimating social order					
	neoliberalism	blue			
	meritocracy	blue			
	nationalism		yellow		
	social Darwinism		yellow		
	universal humanism			green	
	religious('God'); naturalism/'natural order'		yellow		yellow
Media					
	depoliticized mass entertainment	blue	yellow		
	polarizing 'othering'		yellow		
	ethos of 'world union'			green	
	controlled by political elite	blue	yellow	green	yellow
	control political elite	blue		green	yellow
Governance					
Global power distribution					
	multipolar	blue	yellow		
	bipolar	blue	yellow		
	unipolar	blue		green	
	non-existent				yellow
Monopoly of violence					
	national	blue	yellow		yellow
	global	blue		green	
	corporate	blue	yellow		
	none				yellow
	local		yellow		yellow
Main political actors					
	multinational corporations	blue	yellow		
	states	blue	yellow		
	global organization(s)	blue	yellow	green	
	civil actors (workers, minorities, religious, feminists groups...)	blue	yellow	green	yellow
	communities/tribes				yellow
Conflict resolution					
	economic (money)	blue	yellow		yellow
	discursive (ideology)	blue	yellow	green	
	physical (violence)	blue	yellow	green	yellow
Trade regime					
	global	blue	yellow	green	
	regional	blue	yellow		yellow
	national	blue	yellow		
	local			green	yellow
Interregional inequality					
	low			green	yellow
	high	blue	yellow		
Class inequality					

	low						
	high						
Social policy							
	low support for workers and marginalized						
	no global fiscal and redistribution policies (no convergence)						
	global fiscal and redistribution policies (high convergence)						
Military policy							
	increasing military/security expenses						
	decreasing military/security expenses						
Migration policy							
	favor migration to cities (urbanization)						
	favor labor migration						
	migration only within geopolitical blocks						
	global migration & refugee policies						
	no migration regime, low absolute mobility						
Environmental policy							
	subordinated to economic and military policy						
	favor closed material cycles						
	favor new technologies						
	restoration & conservation of global environmental 'goods'						
Economic policy/mode of production							
	state capitalist						
	neoliberal capitalist						
	socialist						
	neo-tributary (feudal) / neo-slave						
	primitive-communal						
	small simple merchant						

Table 2: Characteristics of the four scenarios at the macro (culture & governance) level. The color distribution indicates to which extent variables are present in the different scenarios.

	Scenarios	Hyperimperialist Exploitation	Interimperialist Competition	Global Emergency Governance	Fragmented Diversity
Level2: Society					
Economy					
Social aspects					
Goal of production					
	accumulation				
	consumption				
	need satisfaction				
Allocation principle					
	class (money)				
	class (tribute)				
	ethnicity (racism)				
	geography (state)				
	egalitarian (basic human needs)				
	gender (patriarchy/matriarchy)				
	age				
Control of production					
	capitalists				
	state				
	society				
	community				
Technological aspects					
Labor productivity					
	low				
	high				
Capital productivity					
	low				
	high				
Land intensity					
	low				
	high				
Energy intensity					
	low				
	high				
Material intensity					
	low				
	high				
Energy types compatible with scenario					
	carbon				
	petroleum				



Table 3: Characteristics of the four scenarios at the macro (economy and mitigation & adaptation) level. The color distribution indicates to which extent variables are present in the different scenarios.

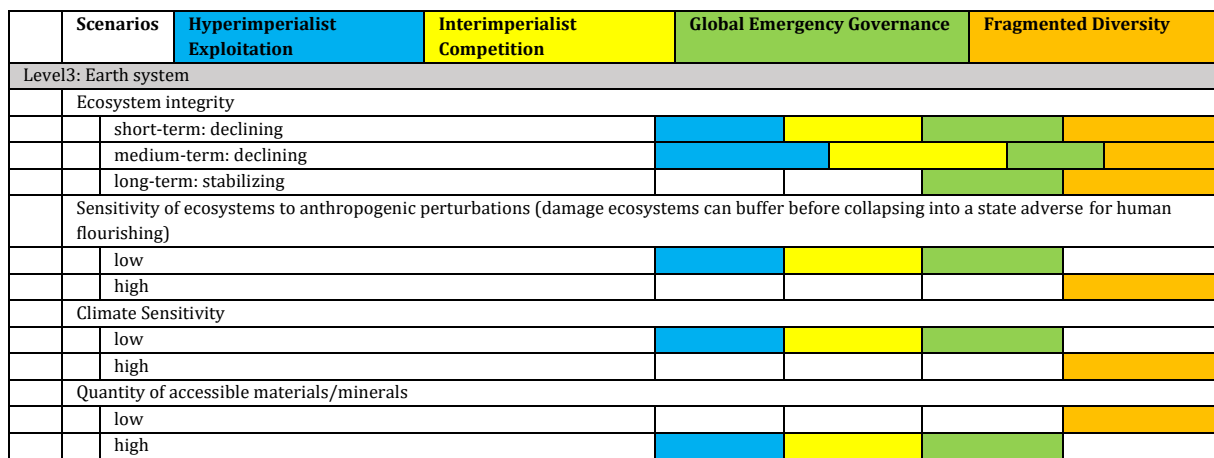


Table 4: Characteristics of the four scenarios at the Earth system level. The color distribution indicates to which extent variables are present in the different scenarios.

4. Discussion

4.1. Comparison with the global environmental scenarios literature

It is possible to compare the developed scenarios with different scenario archetypes identified in the literature (Hunt et al., 2012; Van Vuuren et al., 2012). While *Interimperialist Competition* fits the ‘regional competition’ and the ‘barbarization (fortress world)’ scenario archetype that appear frequently in scenario exercises, *Hyperimperialist Exploitation* does not easily correspond to one of the frequently used archetypes since it runs contrary to the ‘economic optimism’ and ‘reformed markets’ archetypes which reflect ‘conventional worlds’. Nevertheless, it has parallels with polarization and inequality scenarios such as ‘SSP4 - A road divided’ (Calvin et al., 2017; O’Neill et al., 2017). *Global Emergency Governance* best fits the ‘global sustainable development’ and ‘great transition’ archetype although, in contrast to many scenarios belonging to these archetypes, the transition comes very late in time and focuses more on re-actively avoiding the worst outcomes of the socio-ecological catastrophe than on proactive long-term strategies and planning. Last, *Fragmented Diversity* fits somewhat with the ‘Regional sustainable development’ archetype but also reflects some elements of the ‘Barbarization/societal collapse’ archetype. This is because, although Sc4 might in the end feature sustainable local economies capable of reproducing themselves over time, this occurs only after grave damages to the socio-ecological system during a prolonged BAU. Also, there is no guarantee that those local societies able to occupy a small niche that allows them to persist would feature governance structures commonly associated with ‘sustainable development’ such as gender equality, cultural diversity or democratic decision-making processes (Tilbury & Mulà, 2009).

The developed scenarios correspond to different analyses and discourses advanced by GEC scholars: Sc1 reflects the inherently violent and exploitative character of world capitalism repeatedly described in the literature (Alami et al., 2023; Moore, 2018), whereas elements of supranationalism and Earth governance in Sc3 can be found in proposals advanced by global environmental law scholars (Biermann, 2014; Biermann & Dingwerth, 2004; Kashwan et al., 2020; Weiss, 2009). Sc2 and Sc4 as well as a possible abrupt transition from the former to the latter resonate with different analyses of societal collapse dynamics triggered by adverse GEC (Brozović, 2023; Ehrlich & Ehrlich, 2013; Lawrence et al., 2024; Ripple et al., 2023; Scheffran, 2023).

Despite the parallels between the developed storylines and common scenario archetypes, we want to stress several important differences. First, none of the scenario archetypes links BAU dynamics to the structural features of the current world order and thus tend to underestimate the difficulty to break with BAU dynamics. Compared to our analysis, many scenario analyses do not explicitly acknowledge that a successful and timely sustainability transition very likely requires post-capitalist and post-nation-state structures. Second, while the logic and functioning of the economic system is at the center of our analysis, in other existing scenario exercises, it is seldomly problematized and only implicitly conditions scenario outcomes (Lauer et al., 2024). In this context, we also pay attention to changes in the economic mode of production. The focus on intersections between class and power also explains the strong protagonism of ‘workers’ in our scenarios, compared to other scenarios that give more agency to youth movements, civil society or businesses. Third, in contrast to the SSP scenario framework, adaptation and mitigation are not influenced by the level of economic growth but by the characteristics of the world orders in the different scenarios, which can lead to transformative or linear adaptation, and which can

foster or restrain mitigation efforts. Additionally, our scenario framework allows for dynamic transitions between different scenarios and thus the scenarios have a certain chronological relationship, which is absent in the SSP scenario architecture.

Last, compared to other climate scenarios such as the shared socio-economic pathways (SSPs), the developed scenarios are not primarily differentiated by the type of energy they use. While the energy sector in Sc3 and 4 will be without doubt much smaller and renewable than in Sc1 and Sc2 because of restrictions on extractive activities or lack of extractive technology, the latter are in principle compatible with different energy vectors and technologies used by society that could have a higher or lower share of fossils. Given that every energy type has ecological impacts and will face land and material limits, it would be only a question of time until the dynamics described in Sc1 and Sc2 would play out. This is already illustrated today by the conflict potential of materials needed for low-carbon technologies (Church & Crawford, 2018; Sovacool, 2021). While the development of nuclear fusion power would probably help to improve the stability of Sc3 this technology alone would be no guarantee for avoiding Sc1 and Sc2 as it could be captured by capitalist elites and powerful states.

4.2. Benefits of possible scenario quantifications

The value of the developed scenarios lies in their description of qualitative changes in societal systems at global level, which are difficult to fully quantify, given that they include changing political structures, institutions, values, discourses and non-linear dynamics inherent in social, geopolitical and military conflicts. Nevertheless, a quantification of key scenario elements might serve to check the plausibility of the theoretically derived scenarios by providing insights on four points missing in the conducted scenario exercise:

- **Data-derived details concerning relevant output variables:** Quantitative simulation exercises based on empirical data which is extrapolated into the future using a formalized set of equations would concretize the future evolution of a range of relevant variables in the scenarios resulting from changes in world order. Of concrete interest would be *the level and evolution* of socio-economic inequality within and between regions; per capita consumption; life expectancy; population dynamics in different regions; material and energy scarcity; and crossing of planetary boundaries (including land use change, greenhouse gas emissions and temperature change, air pollution, biodiversity loss, water consumption) as well as the implied short-, medium- and long-term consequences.
- **Impact of technological changes on scenario outcomes:** A detailed representation of technological changes in different economic sectors, especially the energy and industrial sector, would enable modelers to trace out the consequences of technological changes on GEC within different scenarios while extended input-output modeling would illustrate the material, energy, capital and labor requirements of technological changes. To render simulation results more realistic modelers would need to take into account social, administrative, legal, political, economic and practical factors influencing the speed and direction of technology development that would differ strongly in the developed scenarios. Last, quantitative simulations could test to which extent currently ‘speculative’ technologies (CCS, fusion...) would produce a greener ‘BAU’ pathway.
- **Time:** Dynamic modeling would be able to specify possible time frames for BAU and different PG scenarios, given their ability to model the rate of change of different

biophysical and societal processes. Simulations until 2200, 2300 or beyond would serve to illustrate long-term risks resulting from prolonged BAU but would also face major data uncertainties.

- **Uncertainty:** Quantitative simulations allow conducting sensitivity analyses, and thus, could demonstrate the range of assumptions regarding the rate of biophysical, technological and societal change compatible with the developed scenario storylines, with a larger range indicating a higher probability that a given scenario might occur.

Different methods have been suggested to model worst-case environmental scenarios (Davidson & Kemp, 2024) and recent attempts of scenario quantification have illustrated some risks to human life, safety and well-being posed by a prolonged BAU pathway (Kemp et al., 2022; Lenton et al., 2023). Nevertheless, given that the quantification of disruptive scenarios featuring non-linear dynamics, interacting risks and cascading shocks is highly challenging due to epistemological and data gaps, qualitative analyses and scenarios remain important.

4.3. Scenarios as tools to engage with and shape the future

Our scenario exercise aimed at detecting the risks of probable future (Pereira et al., 2021) and serves to illustrate the dire consequences of hegemonic BAU thinking prevalent in broader society and intellectual, political and economic elites alike (Thierry et al., 2023). Consequently, they should not be interpreted as fatalist predictions of the future but rather as images of the future with backward temporal influence on present decisions (Gall et al., 2022; Meadows et al., 1992).

By pointing toward threats of rising inequality, violent means of conflict resolutions and declining living standards resulting from a failure of a green growth strategy, we stress the risks caused by a narrow focus on decentralized techno-fixes. We highlight the importance of focusing on the harmful systemic interactions between current political institutions, economic modes of productions and powerful ideologies, as well as the need for profound structural change on a global level.

We also show that ‘involuntary degrowth’ regimes may not be confounded with narratives about the end of human history. Even under destabilized biogeochemical flows, there is a range of possible socio-economic scenarios that might make the most subordinated social groups in world society better or worse off. Thus, we reaffirm the hypothesis that worst-case scenarios might facilitate transformative action rather than paralyzing it (Davidson & Kemp, 2024).

Thus, our scenarios could inform current and future decision-making in at least three ways: First, publicly acknowledging the structural predicament we are facing instead of silently accepting the *status quo* and the ‘rules of the game’ would be a first step at solving it. Second, our scenarios are policy-relevant because they clearly illustrate the need for some form of strong supranational governance to overcome global capitalism and to harmonize and national economic and environmental policies, preferably before non-linear thresholds in the planetary system are crossed. Last, political risk communication should clearly highlight the dangers of an excessive and irrational faith in timely technological fixes that fails to address the structural reasons for the sustainability crisis which lie in the currently dominant economic, political and cultural systems.

5. Conclusion

The key insight of this paper for futures scholarship is the importance of taking into account questions of world order in global environmental scenario development exercises. As our IPE-IR-informed argumentation shows, a prolonged 'BAU' of economic growth followed by a collapse and/or transformation of the current world order is more probable than a timely and successful sustainability transition, due to the structural inertia of the current politico-economic world order, the biophysical, economic and political limits of global green growth, and the incompatibility of global just, voluntary and planned degrowth with the capitalist and nation-based world system. Nevertheless, the scenario exercise also illustrates that even in scenarios of an imposed decline of global economic output, social forces can positively or negatively influence the level of violence, socio-economic inequality and human suffering.

Given the theoretical focus of our work, the scenarios still lack a participatory or quantitative validation. Thus, future work could complement our study through quantifying the developed scenarios, relate the scenarios to the global polycrisis (Lawrence et al., 2024) or consider participatory extensions.

Despite these limitations, the developed scenarios reflect current experiences of 'new world disorders' more accurately than idealized sustainability transitions. By acknowledging the structural discontinuities that the world may face in the 21st century, they seek to motivate present action to prevent these risks from becoming a future reality.

References

- Adamowicz, M. (2022). Green deal, green growth and green economy as a means of support for attaining the sustainable development goals. *Sustainability*, 14(10), 5901.
- Ahmad, N. B. (2024). Military Climate Emissions. *Nevada Law Journal*, 24(3), 5.
- Alami, I., Copley, J., & Moraitis, A. (2023). The 'wicked trinity' of late capitalism: Governing in an era of stagnation, surplus humanity, and environmental breakdown. *Geoforum*, 103691.
- Amin, S. (1978). El desarrollo desigual: Ensayo sobre las formaciones sociales del capitalismo periférico. *Barcelona: Fontanella*.
- Amin, S. (2019). *The long revolution of the global south: Toward a new anti-imperialist international*. Monthly Review Press.
- Aseeva, A. (2018). (Un) sustainable development (s) in international economic law: A quest for sustainability. *Sustainability*, 10(11), 4022.
- Ayres, R. U. (2007). On the practical limits to substitution. *Ecological Economics*, 61(1), 115–128.
- Becker, A., Acciaro, M., Asariotis, R., Cabrera, E., Cretegny, L., Crist, P., Esteban, M., Mather, A., Messner, S., & Naruse, S. (2013). A note on climate change adaptation for seaports: A challenge for global ports, a challenge for global society. *Climatic Change*, 120, 683–695.
- Becker, A., Ng, A. K., McEvoy, D., & Mullett, J. (2018). Implications of climate change for shipping: Ports and supply chains. *Wiley Interdisciplinary Reviews: Climate Change*, 9(2), e508.
- Biermann, F. (2014). *Earth system governance*. MIT Press Cambridge.
- Biermann, F., & Dingwerth, K. (2004). Global environmental change and the nation state. *Global Environmental Politics*, 4(1), 1–22.
- Boström, M. (2021). Social relations and everyday consumption rituals: Barriers or prerequisites for sustainability transformation? *Frontiers in Sociology*, 6, 723464.
- Bovari, E., Giraud, G., & Mc Isaac, F. (2018). Coping with collapse: A stock-flow consistent monetary macrodynamics of global warming. *Ecological Economics*, 147, 383–398.
- Brozović, D. (2023). Societal collapse: A literature review. *Futures*, 145, 103075.
- Buhaug, H., Benjaminsen, T. A., Gilmore, E. A., & Hendrix, C. S. (2023). Climate-driven risks to peace over the 21st century. *Climate Risk Management*, 39, 100471.
- Burdett, M. S. (2015). The religion of technology: Transhumanism and the myth of progress. *Religion and Transhumanism: The Unknown Future of Human Enhancement*, 131–147.
- Calvin, K., Bond-Lamberty, B., Clarke, L., Edmonds, J., Eom, J., Hartin, C., Kim, S., Kyle, P., Link, R., & Moss, R. (2017). The SSP4: A world of deepening inequality. *Global Environmental Change*, 42, 284–296.
- Cameron, J., & Abouchar, J. (1991). The precautionary principle: A fundamental principle of law and policy for the protection of the global environment. *BC Int'l & Comp. L. Rev.*, 14, 1.
- Capellán-Pérez, I., de Blas, I., Nieto, J., de Castro, C., Miguel, L. J., Carpintero, Ó., Mediavilla, M., Lobejón, L. F., Ferreras-Alonso, N., & Rodrigo, P. (2020). MEDEAS: a new modeling framework

integrating global biophysical and socioeconomic constraints. *Energy & Environmental Science*, 13(3), 986–1017.

Capellán-Pérez, I., Mediavilla, M., de Castro, C., Carpintero, Ó., & Miguel, L. J. (2015). More growth? An unfeasible option to overcome critical energy constraints and climate change. *Sustainability Science*, 10(3), 397–411.

Christodoulou, A., & Demirel, H. (2018). Impacts of climate change on transport. *A Focus on Airports, Seaports and Inland Waterways*.

Church, C., & Crawford, A. (2018). *Green Conflict Minerals*. International Institute for Sustainable Development (IISD). <https://www.iisd.org/system/files/publications/green-conflict-minerals.pdf>

Clare, M., Yeo, I., Bricheno, L., Aksenov, Y., Brown, J., Haigh, I., Wahl, T., Hunt, J., Sams, C., & Chaytor, J. (2023). Climate change hotspots and implications for the global subsea telecommunications network. *Earth-Science Reviews*, 237, 104296.

Cox, R. W. (1981). Social Forces, States and World Orders: Beyond International Relations Theory'. *Millennium: Journal of International Studies*, 10(2), 126–155.

Crownshaw, T., Morgan, C., Adams, A., Sers, M., Britto dos Santos, N., Damiano, A., Gilbert, L., Yahya Haage, G., & Horen Greenford, D. (2019). Over the horizon: Exploring the conditions of a post-growth world. *The Anthropocene Review*, 6(1–2), 117–141.

Davidson, J. P., & Kemp, L. (2024). Climate catastrophe: The value of envisioning the worst-case scenarios of climate change. *Wiley Interdisciplinary Reviews: Climate Change*, 15(2), e871.

Davis, M. (2024). Imperialism and the labour aristocracy in Britain. *Theory & Struggle*, 125(1), 69–79.

Degroot, D., Anchukaitis, K. J., Tierney, J. E., Riede, F., Manica, A., Moesswilde, E., & Gauthier, N. (2022). The history of climate and society: A review of the influence of climate change on the human past. *Environmental Research Letters*, 17(10), 103001.

Demaria, F., Schneider, F., Sekulova, F., & Martinez-Alier, J. (2013). What is degrowth? From an activist slogan to a social movement. *Environmental Values*, 22(2), 191–215.

Dong, J., Asif, Z., Shi, Y., Zhu, Y., & Chen, Z. (2022). Climate change impacts on coastal and offshore petroleum infrastructure and the associated oil spill risk: A review. *Journal of Marine Science and Engineering*, 10(7), 849.

Economidou, M., Todeschi, V., Bertoldi, P., D'Agostino, D., Zangheri, P., & Castellazzi, L. (2020). Review of 50 years of EU energy efficiency policies for buildings. *Energy and Buildings*, 225, 110322.

Ehrlich, P. R., & Ehrlich, A. H. (2013). Can a collapse of global civilization be avoided? *Proceedings of the Royal Society B: Biological Sciences*, 280(1754), 20122845.

Emmanuel, A. (1972). *Unequal Exchange: A Study of the Imperialism of Trade*. Monthly Review Press.

Enríquez-Sánchez, J. M., & Álvarez-Antelo, D. (2024). *De la transición hacia sociedades sostenibles: Una propuesta político-jurídica* (1st ed.). Dykinson.
<https://www.torrossa.com/gs/resourceProxy?an=5748496&publisher=FZ1825>

- Fioramonti, L. (2024). Post-growth theories in a global world: A comparative analysis. *Review of International Studies*, 1–11.
- Fischer-Kowalski, M., & Haberl, H. (1998). Sustainable development: Socio-economic metabolism and colonization of nature. *International Social Science Journal*, 50(158), 573–587.
- Fitzpatrick, N., Parrique, T., & Cosme, I. (2022). Exploring degrowth policy proposals: A systematic mapping with thematic synthesis. *Journal of Cleaner Production*, 132764.
- Forzieri, G., Bianchi, A., e Silva, F. B., Herrera, M. A. M., Leblois, A., Lavalle, C., Aerts, J. C., & Feyen, L. (2018). Escalating impacts of climate extremes on critical infrastructures in Europe. *Global Environmental Change*, 48, 97–107.
- Gabric, A. J. (2023). The climate change crisis: A review of its causes and possible responses. *Atmosphere*, 14(7), 1081.
- Gall, T., Vallet, F., & Yannou, B. (2022). How to visualise futures studies concepts: Revision of the futures cone. *Futures*, 143, 103024.
- Givens, J. E., Huang, X., & Jorgenson, A. K. (2019). Ecologically unequal exchange: A theory of global environmental injustice. *Sociology Compass*, 13(5), e12693.
- Goldstone, J. A., Grinin, L., & Korotayev, A. (2022). The phenomenon and theories of revolutions. In *Handbook of revolutions in the 21st century: The new waves of revolutions, and the causes and effects of disruptive political change* (pp. 37–68). Springer.
- Haberl, H., Wiedenhofer, D., Virág, D., Kalt, G., Plank, B., Brockway, P., Fishman, T., Hausknost, D., Krausmann, F., & Leon-Gruchalski, B. (2020). A systematic review of the evidence on decoupling of GDP, resource use and GHG emissions, part II: synthesizing the insights. *Environmental Research Letters*, 15(6), 065003.
- Harmáčková, Z. V., Yoshida, Y., Sitas, N., Mannetti, L., Martin, A., Kumar, R., Berbés-Blázquez, M., Collins, R., Eisenack, K., & Guimaraes, E. (2023). The role of values in future scenarios: What types of values underpin (un) sustainable and (un) just futures? *Current Opinion in Environmental Sustainability*, 64, 101343.
- Herman, E. S., & Chomsky, N. (1988). *Manufacturing consent. The political economy of the mass media*. Pantheon Books.
- Hickel, J. (2019). Is it possible to achieve a good life for all within planetary boundaries? *Third World Quarterly*, 40(1), 18–35.
- Hickel, J. (2021a). The anti-colonial politics of degrowth. *Political Geography*, 88.
- Hickel, J. (2021b). What does degrowth mean? A few points of clarification. *Globalizations*, 18(7), 1105–1111.
- Hickel, J., & Sullivan, D. (2024). How much growth is required to achieve good lives for all? Insights from needs-based analysis. *World Development Perspectives*, 35, 100612.
- Hornborg, A. (2001). *The power of the machine: Global inequalities of economy, technology, and environment* (Vol. 1). Rowman Altamira.

Hunt, D. V., Lombardi, D. R., Atkinson, S., Barber, A. R., Barnes, M., Boyko, C. T., Brown, J., Bryson, J., Butler, D., & Caputo, S. (2012). Scenario archetypes: Converging rather than diverging themes. *Sustainability*, 4(4), 740–772.

Ibrahim, S. E., Centeno, M. A., Patterson, T. S., & Callahan, P. W. (2021). Resilience in global value chains: A systemic risk approach. *Global Perspectives*, 2(1), 27658.

IPCC. (2021). *Climate Change 2021: The Physical Science Basis. Contribution of Working Group I to the Sixth Assessment Report of the Intergovernmental Panel on Climate Change*. Cambridge University Press. Cambridge University Press, Cambridge, UK and New York, NY, USA,.

IPCC (Ed.). (2023). *Climate Change 2022 - Mitigation of Climate Change: Working Group III Contribution to the Sixth Assessment Report of the Intergovernmental Panel on Climate Change* (1st ed.). Cambridge University Press. <https://doi.org/10.1017/9781009157926>

Izaguirre, C., Losada, I. J., Camus, P., Vigh, J. L., & Stenek, V. (2021). Climate change risk to global port operations. *Nature Climate Change*, 11(1), 14–20.

Jehn, F. U., Schneider, M., Wang, J. R., Kemp, L., & Breuer, L. (2021). Betting on the best case: Higher end warming is underrepresented in research. *Environmental Research Letters*, 16(8), 084036.

Jeursen, T., & Hollants, B. (2024). Cleaner Conflicts? Energy Transition and Green Innovation in the Dutch Army. In G. Frerks, R. Geertsma, J. Klomp, & T. Middendorp (Eds.), *Climate Security and the Military* (pp. 271–288). Leiden University Press.

Kallis, G. (2019). Capitalism, socialism, degrowth: A rejoinder. *Capitalism Nature Socialism*, 30(2), 267–273.

Kallis, G., Kostakis, V., Lange, S., Muraca, B., Paulson, S., & Schmelzer, M. (2018). Research on degrowth. *Annual Review of Environment and Resources*, 43(1), 291–316.

Karamanov, D. (2022). The effect of anthropogenic heat emissions on global warming. *EGUsphere*, 2022, 1–18.

Kashwan, P., Biermann, F., Gupta, A., & Okereke, C. (2020). Planetary justice: Prioritizing the poor in earth system governance. *Earth System Governance*, 6, 100075.

Katz-Rosene, R., & Paterson, M. (2018). *Thinking ecologically about the global political economy*. Routledge.

Kautsky, K. (1914). Der Imperialismus. *Die Neue Zeit*, 32-II(21), 908–922.

Kemp, L., Xu, C., Depledge, J., Ebi, K. L., Gibbins, G., Kohler, T. A., Rockström, J., Scheffer, M., Schellnhuber, H. J., & Steffen, W. (2022). Climate Endgame: Exploring catastrophic climate change scenarios. *Proceedings of the National Academy of Sciences*, 119(34), e2108146119.

Kim, R. E., & Kotzé, L. J. (2021). Planetary boundaries at the intersection of Earth system law, science and governance: A state-of-the-art review. *Review of European, Comparative & International Environmental Law*, 30(1), 3–15.

Kuhnhenn, K., Da Costa, L. F. C., Mahnke, E., Schneider, L., & Lange, S. (2020). *A societal transformation scenario for staying below 1.5 C*. Schriften zu Wirtschaft und Soziales.

- Kümmel, R., & Lindenberger, D. (2020). Energy, Entropy, Constraints, and Creativity in Economic Growth and Crises. *Entropy*, 22(10), 1156.
- Laruffa, F. (2023). Making sense of (post) neoliberalism. *Politics & Society*, 00323292231193805.
- Lauer, A., Capellán-Pérez, I., & Wergles, N. (2025). A comparative review of de-and post-growth modeling studies. *Ecological Economics*, 227, 108383.
- Lauer, A., de Castro, C., & Carpintero, Ó. (2024). Between continuous presents and disruptive futures: Identifying the ideological backbones of Global Environmental Scenarios. *Futures*, 103460.
- Lauer, A., De Castro, C., & Carpintero, Ó. (2025). Beyond Green capitalism: Global scenarios for fast societal transitions toward sustainability. *Environmental Innovation and Societal Transitions*, 56, 100981. <https://doi.org/10.1016/j.eist.2025.100981>
- Lawrence, M., Homer-Dixon, T., Janzwood, S., Rockstöm, J., Renn, O., & Donges, J. F. (2024). Global polycrisis: The causal mechanisms of crisis entanglement. *Global Sustainability*, 7, e6.
- Leal Filho, W., Abeldaño Zuñiga, R. A., Sierra, J., Dinis, M. A. P., Corazza, L., Nagy, G. J., & Aina, Y. A. (2024). An assessment of priorities in handling climate change impacts on infrastructures. *Scientific Reports*, 14(1), 14147.
- Lenton, T. M., Xu, C., Abrams, J. F., Ghadiali, A., Loriani, S., Sakschewski, B., Zimm, C., Ebi, K. L., Dunn, R. R., & Svenning, J.-C. (2023). Quantifying the human cost of global warming. *Nature Sustainability*, 6(10), 1237–1247.
- Marx, K. (1992). *Capital: Volume I* (Vol. 1). Penguin UK.
- Mazar, A., Tomaino, G., Carmon, Z., & Wood, W. (2021). Habits to save our habitat: Using the psychology of habits to promote sustainability. *Behavioral Science & Policy*, 7(2), 75–89.
- Meadows, D. H., Meadows, D. L., & Randers, J. (1992). *Beyond the limits: Global collapse or a sustainable future*. Earthscan Publications Ltd.
- Meadows, D. H., Meadows, D., Randers, J., & Behrens, W. W. (1972). *The limits to growth. A report for the Club of Rome's Project on the Predicament of Mankind*. Universe Books.
- Meadows, D. H., Randers, J., & Meadows, D. (2004). *The limits to growth: The 30-year update*. Chelsea Green Publishing Company.
- Mearsheimer, J. (2007). Structural realism. In T. Dunne, M. Kurki, & S. Smith (Eds.), *International relations theories: Discipline and diversity* (pp. 71–88). Oxford University Press, USA.
- Mikellidou, C. V., Shakou, L. M., Boustras, G., & Dimopoulos, C. (2018). Energy critical infrastructures at risk from climate change: A state of the art review. *Safety Science*, 110, 110–120.
- Millward-Hopkins, J., Steinberger, J. K., Rao, N. D., & Oswald, Y. (2020). Providing decent living with minimum energy: A global scenario. *Global Environmental Change*, 65, 102168.
- Monterrubio-Solís, C., Barreau, A., & Ibarra, J. T. (2023). Narrating changes, recalling memory: Accumulation by dispossession in food systems of Indigenous communities at the extremes of Latin America. *Ecology and Society*, 28(1).

- Moore, J. (2015). *Capitalism in the Web of Life: Ecology and the Accumulation of Capital*. Verso Books.
- Moore, J. (2017). The Capitalocene, Part I: on the nature and origins of our ecological crisis. *The Journal of Peasant Studies*, 44(3), 594–630.
- Moore, J. (2018). The Capitalocene Part II: accumulation by appropriation and the centrality of unpaid work/energy. *The Journal of Peasant Studies*, 45(2), 237–279.
- Mora, O., Le Mouël, C., de Lattre-Gasquet, M., Donnars, C., Dumas, P., Réchauchère, O., Brunelle, T., Manceron, S., Marajo-Petitzon, E., & Moreau, C. (2020). Exploring the future of land use and food security: A new set of global scenarios. *PloS One*, 15(7), e0235597.
- Moran, D. D., Lenzen, M., Kanemoto, K., & Geschke, A. (2013). Does ecologically unequal exchange occur? *Ecological Economics*, 89, 177–186.
- Moyer, J. D. (2023). Modeling transformational policy pathways on low growth and negative growth scenarios to assess impacts on socioeconomic development and carbon emissions. *Scientific Reports*, 13(1), 15996.
- O'Neill, B. C., Kriegler, E., Ebi, K. L., Kemp-Benedict, E., Riahi, K., Rothman, D. S., van Ruijven, B. J., van Vuuren, D. P., Birkmann, J., & Kok, K. (2017). The roads ahead: Narratives for shared socioeconomic pathways describing world futures in the 21st century. *Global Environmental Change*, 42, 169–180.
- Oswald, Y. (2024). Global convergence of incomes in a climate-constrained world. *Copernicus Meetings, No. EGU24-15637*.
- Pawar, M. (2023). Poverty, policy and the poor. *The International Journal of Community and Social Development*, 5(2), 137–145.
- Pereira, L., Davies, K. K., den Belder, E., Ferrier, S., Karlsson-Vinkhuyzen, S., Kim, H., Kuiper, J. J., Okayasu, S., Palomo, M. G., & Pereira, H. M. (2020). Developing multiscale and integrative nature–people scenarios using the Nature Futures Framework. *People and Nature*, 2(4), 1172–1195.
- Pereira, L., Kuiper, J. J., Selomane, O., Aguiar, A. P. D., Asrar, G. R., Bennett, E. M., Biggs, R., Calvin, K., Hedden, S., & Hsu, A. (2021). Advancing a toolkit of diverse futures approaches for global environmental assessments. *Ecosystems and People*, 17(1), 191–204.
- Raskin, P., Banuri, T., Gallopin, G., Gutman, P., Hammond, A., Kates, R. W., & Swart, R. (2002). *Great transition: The promise and lure of the times ahead*.
- Richardson, K., Steffen, W., Lucht, W., Bendtsen, J., Cornell, S. E., Donges, J. F., Drücke, M., Fetzer, I., Bala, G., & von Bloh, W. (2023). Earth beyond six of nine planetary boundaries. *Science Advances*, 9(37), eadh2458.
- Ripple, W. J., Wolf, C., Gregg, J. W., Levin, K., Rockström, J., Newsome, T. M., Betts, M. G., Huq, S., Law, B. E., & Kemp, L. (2022). *World scientists' warning of a climate emergency 2022*.
- Ripple, W. J., Wolf, C., Gregg, J. W., Rockström, J., Newsome, T. M., Law, B. E., Marques, L., Lenton, T. M., Xu, C., & Huq, S. (2023). The 2023 state of the climate report: Entering uncharted territory. *BioScience*, 73(12), 841–850.

Roberts, M. (2016). *The long depression: Marxism and the global crisis of capitalism*. Haymarket Books.

Rockström, J., Steffen, W., Noone, K., Persson, Å., Chapin III, F. S., Lambin, E., Lenton, T. M., Scheffer, M., Folke, C., & Schellnhuber, H. J. (2009). Planetary boundaries: Exploring the safe operating space for humanity. *Ecology and Society*, 14(2).

Rohr, J. R., Johnson, P., Hickey, C. W., Helm, R. C., Fritz, A., & Brasfield, S. (2013). Implications of global climate change for natural resource damage assessment, restoration, and rehabilitation. *Environmental Toxicology and Chemistry*, 32(1), 93–101.

Roura-Pascual, N., Leung, B., Rabitsch, W., Rutting, L., Vervoort, J., Bacher, S., Dullinger, S., Erb, K.-H., Jeschke, J. M., & Katsanevakis, S. (2021). Alternative futures for global biological invasions. *Sustainability Science*, 16(5), 1637–1650.

Sandhu, H. S., & Raja, S. (2019). *No Broken Link: The Vulnerability of Telecommunication Infrastructure to Natural Hazards*. World Bank.

Scheffran, J. (2023). Limits to the Anthropocene: Geopolitical conflict or cooperative governance? *Frontiers in Political Science*, 5, 1190610.

Schmelzer, M., & Hofferberth, E. (2023). Democratic planning for degrowth. *Monthly Review*, 75(3), 142–153.

Snyder, B. F. (2020). The genetic and cultural evolution of unsustainability. *Sustainability Science*, 15(4), 1087–1099.

Sovacool, B. K. (2021). Who are the victims of low-carbon transitions? Towards a political ecology of climate change mitigation. *Energy Research & Social Science*, 73, 101916.

Steg, L. (2023). Psychology of climate change. *Annual Review of Psychology*, 74(1), 391–421.

Sus, M., & Hadeed, M. (2020). Theory-infused and policy-relevant: On the usefulness of scenario analysis for international relations. *Contemporary Security Policy*, 41(3), 432–455.
<https://doi.org/10.1080/13523260.2020.1730055>

Sweezy, P. M. (2018). *Theory of capital development*. NYU Press.

Tapia, J. A. (2023). *Six Crises of the World Economy*. Springer.

Thierry, A., Horn, L., Von Hellermann, P., & Gardner, C. J. (2023). “*No research on a dead planet*”: Preserving the socio-ecological conditions for academia. 8, 1237076.

Tilbury, D., & Mulà, I. (2009). *Review of Education for Sustainable Development Policies from a Cultural Diversity and Intercultural Dialogue: Gaps and Opportunities for Future Action*. UNESCO.

Toynbee, A. (1972). The religious background of the present environmental crisis: A viewpoint. *International Journal of Environmental Studies*, 3(1–4), 141–146.

Trainer, T. (2021). Degrowth: How much is needed? *Biophysical Economics and Sustainability*, 6(2), 5.

Triandafyllidou, A. (2020). Nationalism in the 21st century: Neo-tribal or plural? *Nations and Nationalism*, 26(4), 792–806.

- Van Vuuren, D. P., Kok, M. T., Girod, B., Lucas, P. L., & de Vries, B. (2012). Scenarios in global environmental assessments: Key characteristics and lessons for future use. *Global Environmental Change*, 22(4), 884–895.
- Venner, M., & Zamurs, J. (2012). Increased maintenance costs of extreme weather events: Preparing for climate change adaptation. *Transportation Research Record*, 2292(1), 20–28.
- Voros, J. (2001). A primer on futures studies, foresight and the use of scenarios. *Prospect: The Foresight Bulletin*, 6(1), 1–8.
- Voskaki, A., Budd, T., & Mason, K. (2023). The impact of climate hazards to airport systems: A synthesis of the implications and risk mitigation trends. *Transport Reviews*, 43(4), 652–675.
- Wallerstein, I. (2004). *World-Systems Analysis: An Introduction*. Duke University Press.
<https://doi.org/10.1515/9780822399018>
- Waltz, K. (1979). *Theory of International Politics*. Addison-Wesley Publishing Company.
- Waring, T. M., Wood, Z. T., & Szathmáry, E. (2024). Characteristic processes of human evolution caused the Anthropocene and may obstruct its global solutions. *Philosophical Transactions of the Royal Society B*, 379(1893), 20220259.
- Weiss, T. G. (2009). What happened to the idea of world government. *International Studies Quarterly*, 53(2), 253–271.
- Windegger, F., & Spash, C. L. (2023). Reconceptualising freedom in the 21st century: Neoliberalism vs. Degrowth. *New Political Economy*, 28(4), 554–573.
- Yang, B., & He, J. (2021). Global land grabbing: A critical review of case studies across the world. *Land*, 10(3), 324.
- York, M. (2022). Religion and the environmental crisis. In *Ecotheology-sustainability and religions of the world*. IntechOpen.

Supplementary Material

S1. Biophysical factors influencing de-globalization processes

Whether and how long the globalized economic system will be maintained in future scenarios depends on the relation between the costs of its maintenance and the benefits it provides to local populations, especially those with economic and political power.

Climate change damages, including sea level rise, extreme weather events and extreme temperatures will significantly increase the maintenance costs of the global infrastructure, including sea (Becker et al., 2018), air (Voskaki et al., 2023), road and train (Venner & Zamurs, 2012) transport, the electricity (Leal Filho et al., 2024) and fossil energy (Dong et al., 2022; Mikellidou et al., 2018) trade system and the global telecommunication network (Clare et al., 2023), reducing the profitability of global value chains with their reliance on inexpensive transport and just-in-time production (Curtis, 2009; Ibrahim et al., 2021). Equally, the highly connected global system favors the rapid spread of diseases (Lawrence et al., 2024), thus, increasing the societal costs of maintaining the system.

Simultaneously, the degradation of mineral ores and fossil reservoirs as well as climate change impacts and water scarcity issues (Northey et al., 2017) results in growing energy, material, capital and labor inputs necessary for the extraction process, which reduces the benefits of global trade and creates incentives to invest in local substitutes. Nevertheless, considerable scientific uncertainties remain with regard to the future evolution of input costs as resources get harder to access (Aramendia et al., 2024) as well as to the overall quantity of extractable resources (IPCC, 2021; Laherrère et al., 2022; McNulty & Jowitt, 2021; Mohr, 2015; Northey et al., 2018; Speirs et al., 2015). While an increase in energy inputs due to the degradation of mineral ores does not by itself pose a hard limit to mineral extraction, the energy inputs to the *energy* sector must be less than its energy output ($\text{EROI} >> 1$). Thus, an excessively declining global EROI poses a threat to the stability of the global energy infrastructure (Capellán-Pérez et al., 2019; Delannoy et al., 2021; Hall et al., 2014), and might add to regionalization tendencies.

Consequently, the degree of de-globalization and regionalization, depends at least on five crucial factors:

- The severity of infrastructure damages caused by global environmental change (GEC) (as well as by social dynamics such as wars)
- The input costs of the material and energy sector
- The speed at which economic flows can be redirected toward the maintenance of the global infrastructure (global adaptive capacity)
- The technological capacity to substitute goods and services of the global infrastructure by local systems (local adaptive capacity)
- Given high local adaptive capacity, the political capacity and military strength to effectively withdraw from the global economy

Figure S1 illustrates how economic complexity and size tends to decline as source- and sink-related problems increase, while the timing and extent of this decline depends on the capacities of societies to redirect and substitute resources, leaving out the political/military factor for the sake of simplicity.

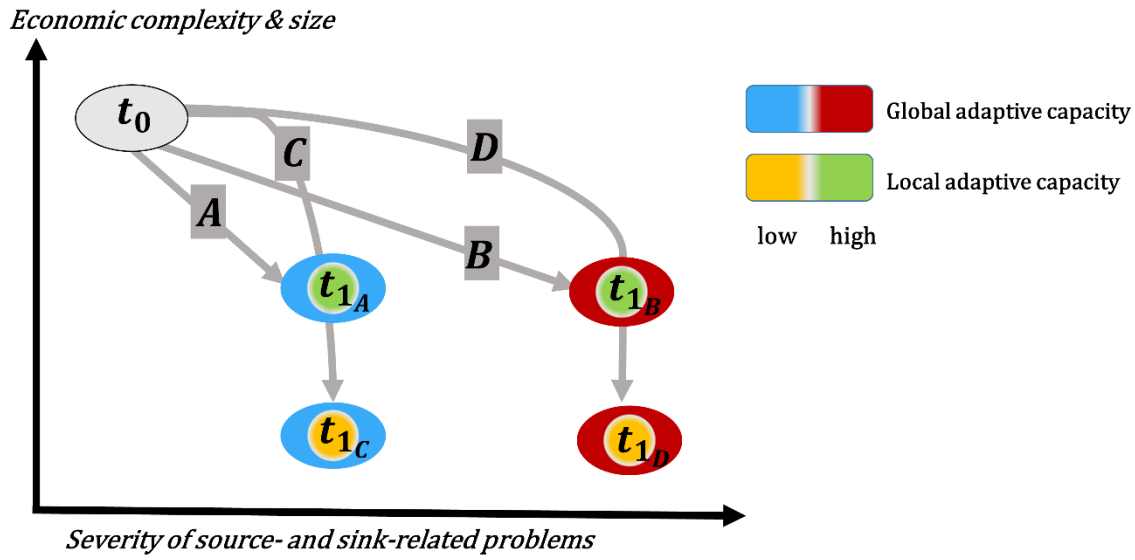


Figure S1: Four different pathways (A-D) of decreasing economic complexity and metabolism, illustrating four possible transitions towards the 'Fragmented diversity' (Sc4) scenario. In the case of low local adaptive capacity (marked orange), societies dedicate an increasing part of their production only to the maintenance of the global system and then rapidly collapse as the velocity and severity of adverse GEC surpasses their capacity to adapt. The higher the global adaptive capacity (marked red), the longer can economic complexity be maintained, although ultimately, as source- and sink-related problems escalate, economic complexity and size decline.

S2. Trends and weak signals

The following table lists empirical trends and weak signals that point to different scenarios. For certain variables, we analyze the long-term trend and indicate the percentual change for a short-term to assess whether weak signals are deviating from the long-term trend. The table does not aim to be comprehensive but only intends to illustrate that the scenarios, especially the BAU scenario period, is compatible with empirical data.

Scenario	Trend in key indicators [unit / year]	Period	Direction of change [%]	Data source
BAU	Global GDP (trillion USD)	2000 – 2024 [2023-2024]	Increasing [+4%]	World Bank (2025d)
BAU	GDP China	2000-2024 [2023-2024]	Increasing [+2.6%]	World Bank (2025d)
BAU	GDP USA	2000-2024 [2023-2024]	Increasing [+5.3%]	World Bank (2025d)
BAU	GDP India	2000-2024	[+7.4%]	World Bank (2025d)
BAU	Coal consumption (EJ)	2000-2023 [2022-2023]	increasing [+1.5%]	Ripple et al. (2024)
BAU	Oil consumption (EJ)	2000-2023 [2022-2023]	increasing [+2.5%]	Ripple et al. (2024)
BAU	Gas consumption (EJ)	2000-2023	Increasing	Ripple et al. (2024)

		[2022-2023]	[+0.04%]	
BAU	Global tree cover loss (mio. Ha)	2000-2023 [2022-2023]	Increasing [+24%]	Ripple et al. (2024)
BAU	CO2eq emissions (Gt CO2 equivalent)	2000-2023 [2022-2023]	Increasing [+2%]	Ripple et al. (2024)
BAU	Global per capita CO2eq emissions (t per person)	2000-2023 [2022-2023]	Increasing [+1%]	Ripple et al. (2024)
BAU	CH4 concentration (CH4 ppb)	2000 – 2024 [2023-2024]	Increasing [0.4%]	Ripple et al. (2024), NOAA Global Monitoring Laboratory (2025a)
BAU	N2O concentration (N2O ppb)	2000 – 2024 [2023-2024]	Increasing [+0.3%]	Ripple et al. (2024), NOAA Global Monitoring Laboratory (2025b)
BAU	Levels of 'decoupling' between economic growth and environmental impacts	2013-2019	For the 1.5°C target, considering fair shares, decoupling rates in industrial states would need to increase by a factor of 10 by 2025	Vogel & Hickel (2023)
BAU	Life expectancy LDCs	2000 – 2023 [2022 – 2023]	Increasing [+1.5%]	World Bank (2025b)
BAU	Ruminant livestock (billion individuals)	2000-2022 [2021-2022]	Increasing [+1.5%]	Ripple et al. (2024)
BAU	Per capita meat production (kg per person)	2000-2022 [2021-2022]	Increasing [+0.9%]	Ripple et al. (2024)
Sc1		2018-2020	Decreasing	
BAU, Sc2	Fossil fuel subsidies (bio. USD)	2010 – 2020 [2021-2022]	Decreasing [+106%]	Ripple et al. (2024)
BAU, Sc1	GDP sub-Saharan Africa	2000-2024 [2023-2024]	Increasing [- 5%]	World Bank (2025d)
BAU, Sc3, Sc1	Solar/wind consumption (EJ)	2000-2023 [2022-2023]	increasing [+ 15%]	Ripple et al. (2024)
BAU, Sc1, Sc2, Sc4	Global tree cover loss due to fires (mio. ha)	2000 – 2023 [2022 – 2023]	Increasing [+78%]	Ripple et al. (2024)
BAU, Sc1, Sc2, Sc4	Internally displaced persons (mio. People)	2014 – 2023 [2022 – 2023]	Increasing [-19%]	World Bank (2025a)
BAU, Sc3	Number of parties in multilateral	2000 – 2015 [2014-2015] [2014-2015]	Increasing [+0%] [+ 0.5%]	OWD (2025b)

	environmental agreements [Stockholm Convention on Persistent Organic Pollutants] [UNFCCC]			
Sc3	Jurisdictions that have declared a climate emergency (n)	2015 – 2023 [2022-2023]	Increasing [+1%]	Ripple et al. (2024)
Sc1, Sc2, (Sc3) Sc4	US heat-related mortality (rate per 100,000 person-years)	2000-2023 [2022-2023]	Increasing [+32%]	Ripple et al. (2024)
Sc1, Sc2, Sc3, Sc4	Billion-dollar floods in the US (n)	2000-2023 [2022-2023]	Increasing [+300%]	Ripple et al. (2024)
Sc1	Number of people starving	2019-2023	Increasing [+ 26%]	(FAO et al., 2024)
Sc1	Share of people living in extreme poverty (Sub-Saharan Africa)	2000 – 2024 [2019-2024]	Decreasing [+3.6%]	World Bank (2025c)
Sc1, Sc4	Non-state violent conflicts	2010-2024	Increasing: +131%	(Davies et al., 2025)
Sc2	State-based conflicts	2010-2024	Increasing: +97%	(Davies et al., 2025)
Sc2	Global military expenditures	2016-2024	Increasing: +37%	OWD (2025a), based on SIPRI (2024)

S3. Explication of scenario characteristics

This section provides more details on the variables and their values for the different scenarios as displayed in Table 1 of the main text. However, the values given to these scenarios should not be seen as absolute but rather as first approximations from the perspectives of the authors, which could be refined and improved in further work depending on the scientific questions the scenarios are intended to address. The greatest uncertainty surrounds the values of Sc4 due to its internal diversity. Additionally, it is important to keep in mind that the storylines in the main text are only particular manifestations of a set of possible storylines that could fit the underlying logic of the different scenarios. Thus, using the scenario characteristics in Table 1 of the main text would allow the construction of alternative storyline versions. For example, it would be possible to construct scenario storylines of Sc1 that are more centered on states or on corporate actors, or to construct different storylines of Sc3 featuring different kinds of energy technologies potentially compatible with this scenario. Sc4 includes the possibility of the emergence of pre-industrial and even pre-agricultural communities adopting radically different cosmovisions that could prevent the rise of social stratification. However, it is equally possible that old power

structures reemerge. Thus, to provide an in-depth characterization of Sc4 would require an extended historical analysis that is out of the scope of the present work.

Level 1: Individuals

- *Life expectancy:* In all four scenarios, life expectancy is reduced relative to a world without GEC. However, in Sc3 GEC damages have a relatively great weight in determining life expectancy compared to Sc1 and Sc2 because two other sources that reduce life expectancy (unequal consumption and escalating violent conflicts) have been greatly reduced. For Sc3 the elimination or great reduction of the latter are crucial for its stability. In Sc4 in general GEC damages are high and will heavily affect life expectancy. At the same time, consumption can be more or less unequal between different and within communities, depending on their politico-economic system and the surrounding environmental and geographical conditions although the overall level of inequality will very likely be low compared to today (see Level 2 below).
- The *per capita consumption of the top 20%* in the world's centers (high-income countries), semiperipheries (upper middle income countries) and peripheries (lower middle and low income countries) is growing in the BAU phase in all scenarios and could continue to grow in Sc1 in the post-BAU period while it stagnates in Sc2 and declines strongly in Sc3 and Sc4 as the societal structure in Sc3 and Sc4 cannot sustain such high levels of per capita consumption.
- The *per capita consumption of the middle 50%* in the world's centers, semiperipheries and peripheries grows for all scenarios in the BAU phase. In the post-BAU phase in Sc1 consumption declines to a medium level in the center and to a low (semiperiphery) or very low (periphery) level. Equally, consumption for the middle classes declines in Sc2 to a medium or very low level, depending on the geopolitical block. In Sc3 and Sc4, again, consumption declines to a low level throughout the world.
- The *per capita consumption of the bottom 30%* grows in all scenarios during the BAU period and declines in all scenarios although the decline is steepest in Sc1 and Sc2 and more moderate in Sc3.
- These trajectories for the per capita consumption of different classes and world regions reflects the dominant allocation mechanisms present in the different scenarios.

Level 2: Society

- *Nature* has instrumental value in all scenarios because societies inevitably rely on and use nature for their purposes and for their survival. However, in Sc3 and Sc4 non-human life acquires relational value, which allows those societies to achieve a higher degree of integration into the surrounding ecological systems. Equally, it is conceivable that in Sc4 some of the very diverse communities increasingly acknowledge that non-human life has intrinsic value.
- The *hegemonic ideas legitimating the social order* in Sc1 could be neoliberalism and the myth of meritocracy which allow the better-off classes to justify their position through their hard work or superior merit. Conversely, nationalism, social Darwinism and other ideologies that construct a 'natural' hierarchy or order between societies and individuals in Sc2 form the ideological basis that justify prioritizing the interest of the own political entity ('the nation', 'the alliance') and eliminating or degrading the 'other'. Sc3 is only compatible and feasible with a hegemonic idea of universal humanism that transcends class, race and territory. While the idea of universal humanism might exist in some

societies in Sc4 it arguably will not be the legitimating source of the political and social orders as societies in Sc4 in contrast to Sc3 do not need this idea for their stability. Rather, we can assume that as the societies and communities in Sc4 have a rather limited territorial reach, the own territory will become ideologically more rather than less important over time. Possibly, pre-capitalist ideologies referring to a transcendental entity or to 'natural orders' might reemerge although the rise of a fragmented, diverse post-capitalist world will constitute such a great historical discontinuity that it is difficult to pinpoint concrete hegemonic ideas in this scenario.

- The *media* in Sc1 and Sc2 is instrumentalized to serve the interests of the elites while Sc3 requires a control of the political elite through the media to maintain sufficiently low levels of corruption and to avoid sliding towards Sc1, Sc2 or Sc4 over time. Whereas in Sc3 the media would spread a discourse of 'world union', in Sc2 it would fuel geopolitical tensions and in Sc1 it would prevent political engagement and revolts from the masses through depoliticized entertainment.
- Based on the respective scenario logic, the *global power distribution* can be multipolar, bipolar or unipolar in Sc1 and multipolar or bipolar in Sc2 but only unipolar in Sc3 (although not necessarily tied to a specific country) while the concept of 'polarity' in a classical International Relations sense (Tomja, 2014) is evidently non-existent in Sc4.
- The *monopoly of violence* can be on the national level in Sc1, Sc2 and in exceptional cases (e.g. for the small countries in the current system) in Sc4. A global monopoly of violence would be very likely in Sc3 and conceivable in Sc1 whereas corporate powers will arguably have some right to exercise violence (e.g. through private 'security' firms, mercenaries) in Sc1 and Sc2. In Sc4 the monopoly of violence would likely be at the local level or even disappear in the case of very small communities without a significant division of work. Last, versions of Sc2 are possible in which the monopoly of power on the national scale breaks down in some of the geopolitical blocks due to mounting social and political tensions, giving way to local monopolies of violence.
- The *main political actors* in Sc1 are multinational corporations, states and global organizations, as well as to a small extent civil society actors which resonates with the neoliberal orientation of the scenario and the possibility of a corporate monopoly of violence. Conversely, states are the most important actors in Sc2. In Sc3, global organizations rise extremely in their importance, as well as civil society actors that act as a counterweight to the global organizations. Last, in Sc4 small-scale actors gain importance: communities as well as civil actors. Thus, the main political actors align with the variables outlined before.
- Regarding the means of *conflict resolution*, economic means are the most important in Sc1 (due to the prominence of the global economic system in this scenario), discursive means are the most important in Sc3 (due to the strong reduction of economic inequality in this scenario) and physical means are the most important in Sc2 (due to the relative weakness of the global economic system in this scenario). Given the diversity of social orders in Sc4, we have given all means equal importance.
- The *trade regime* corresponds to the economic order and the territorial reach of the socio-political order and thus, is mainly global and regional (Sc1), global and local (Sc3) and mainly national and regional (Sc2). In Sc4 the trade regime is mainly local but could have regional reach, although such a regime would be based on other technologies than those used by current societies (cf. Carrey, 2020).
- In general, *interregional inequality* and *class inequality* are high in Sc1 and Sc2 as they are exacerbations of the current world order, while they are low in Sc3 and Sc4 (in the latter,

since societies differ from each other, class inequality will vary. However, interregional inequalities like today will not be possible as the small and fragmented societies in Sc4 have no possibility to dominate societies in other world regions via colonial occupation, violent threats and/or unequal trade systems).

- The *social policy* reflects the existence of inequality in Sc1 and Sc2, with low public support for marginalized social classes and no global redistribution policies. Conversely, high convergence through global fiscal and redistribution policies is possible in Sc3 (impossible in Sc4) due to the presence (absence) of a global political system.
- The *military policy* is characterized by strongly increasing expenses in Sc1 and Sc2 to stabilize social order. In Sc3, military expenses must strongly decrease from the current level to save resources needed to fulfill basic needs of the population. Finally, given the reduced socio-economic metabolism in Sc4 absolute military expenses will be much lower than today, and depending on the concrete societal structure might cease altogether.
- The *migration regime* will favor the migration of cheap labor to cities in Sc1 while in Sc2 migration will be restrained within geopolitical blocks for ideological reasons. The migration regime could be global in the case of Sc3, and informal in Sc4.
- The *environmental policy* is always subject to the needs of other policy areas, even in Sc3,⁹ but will strongly favor the development of closed material cycles in Sc3 and Sc4.
- The *mode of production* compatible with Sc1 is neoliberal capitalism which can be paired with state capitalism and neo-tributary or neo-slave modes of production as a ‘pure’ neoliberal regime does not even exist today (cf. Alami et al., 2023). In Sc2 state capitalist and neo-tributary/neo-slave modes of production gain prominence whereas Sc3 is compatible with socialist production on the global and small simple merchant production on the local level. Sc4 is potentially compatible with a wide range of modes of production and might even give rise to new modes of production that are still unknown today.
- The *goal of production* aligns with the mode of production: in Sc1 and Sc2, the focus is on accumulation and consumption, while in Sc3 and Sc4, it shifts to need satisfaction. Additionally, the *allocation principle* and the *control of production* are determined by the mode of production
- With regard to the technological aspects, *productivities* denote ‘\$/x’, for example ‘\$/h’ would be the amount of economic output (in \$) produced with one hour of human labor (h) which would measure labor productivity. Likewise, *intensities* denote ‘x/\$’, for example ‘ha/\$’ would denote the amount of land (in ha) required for the production of one unit of economic output (in \$). Importantly, Sc3 is only feasible if land, energy and material intensities are low, given that it aims at maintaining a higher world population than the other scenarios, whereas labor and capital productivity could be low or high in this scenario. Conversely, labor and capital productivity will be high in Sc1 and Sc2, which are characterized by strong productive capacities, while the intensity variables could be low or high (in the latter case, this would translate into even stronger reductions in life expectancy and material consumption for the lower classes/the inferior geopolitical block, or into even faster environmental degradation). Last, in Sc4

⁹ Even though a stable environment is a necessary precondition for human survival, societies always have to make sure to assure their (socio-economic) reproduction before being able to act collectively in ways that we would describe as ‘environmental policy’. In ‘sustainable’ societies, the socio-economic reproduction takes forms that do not excessively affect the stability of the surrounding environmental supporting systems.

productive capacities in general will be low but intensities can vary depending on the characteristics of the bioregions and of the concrete modes of production of the respective communities.

- Regarding the *energy types compatible with the respective scenarios*, petroleum is especially important for Sc1 due to the dependence of the global transport infrastructure on petroleum. Equally, a strong development of renewable electricity in addition to other energy sources is reasonable in Sc1. In Sc2, carbon, as well as renewable electricity, could gain importance for reasons of ‘energy security’ and due to a stronger regionalization of the economic system. The energy type most compatible with Sc4 is arguably biomass whereas renewable electricity relies on the existence of a globalized system and mineral extraction, which will cease to exist in Sc4. Last, Sc3 is the only scenario displaying the necessary institutional conditions to effectively push the development of nuclear fusion although it is highly uncertain whether this technology could be developed fast enough to make up a significant amount in the energy mix in the scenario.
- Regarding *Mitigation & Adaptation* variables, Sc1 is characterized by low mitigation efforts and fast but linear adaptation, oriented towards maintaining the global structure. Sc2 features no mitigation at all as mitigation efforts can be considered a contribution to a global public good (i.e. the stability of the planetary system) which would equally benefit the competing geopolitical block. The type of adaptation in Sc2 is also fast, linear and mainly oriented towards the maintenance of the existing structure although partial substitutions of global through local structures are possible which could indicate the beginning of a transition towards Sc4. Sc3 is compatible with low or high mitigation efforts, depending on available resources and technological capacities. While the speed of adaptation must be high to prevent a collapse of the global structure, the type of adaptation in Sc3 can be linear as well as transformative, and a partial substitution of global through local structures is desirable in this scenario to increase local resilience. Finally, mitigation ceases to make sense in Sc4 as the carrying capacity of the bioregion (not of the whole world) becomes the new reference point. Adaptation speed is low, leading to a collapse of the global structure, but at the same time transformative, resulting in the substitution of global through local structures.

Level 3: Earth System

- *Ecosystem integrity* is declining equally in all scenarios in the short-term and continues to decline in the medium-term although the decline is steeper in Sc1 and Sc2 than in the other scenarios. In the long-term (centuries to millennia) ecosystem integrity stabilizes in Sc3 and Sc4 as societies manage to integrate human economies into the surrounding ecosystems. This dynamic of deterioration reflects the existence of lags in feedback processes between the human economy and the reaction of the natural environment (Meadows et al., 1992). For example, crossing certain tipping points in the climate system will likely trigger consequences unfolding over millennia (Armstrong McKay et al., 2022).
- The *sensitivity of ecosystems to anthropogenic perturbations* can also be expressed as *the damage ecosystems can buffer before collapsing into a state adverse for human flourishing*. For example, it is known that ecosystems feature critical thresholds leading to collapse (Bland et al., 2018) but it is not clear where these thresholds are. Similarly, it is not yet known at what level or rate biodiversity loss and environmental degradation might result in the failure of ecosystem services and functions that are essential for

maintaining complex human civilizations, and even for human survival. In Table1 we have also included *climate sensitivity* (covering the transient climate response but also the equilibrium climate sensitivity) given its special importance for future temperature changes (IPCC, 2021). Evidently, there are many more variables that describe the sensitivity of the Earth system to anthropogenic perturbations that have not been separately in Table1. In Sc4 these sensitivity variables have low thresholds, i.e. relatively low levels of anthropogenic perturbations suffice to produce adverse changes in the ecological supporting systems, the climate etc. which then negatively impact and destabilize human economies, eventually resulting in the collapse of the global infrastructure. In Sc1 – 3 these sensitivity variables have a higher threshold which allows them at least temporarily to maintain a global structure. In other words, the lower the Earth's sensitivity parameters (whose concrete values are still unknown) the lower the probability that Sc1-3 emerge after the BAU period, and the faster the transition to Sc4.

- Last, the *quantity of accessible materials and minerals* is low in Sc4 and high in Sc1-3 since the higher the quantity of economically extractable resources, the higher the benefits and the lower the costs of maintaining a global system (see S1 in this Supplementary Material).

References

- Alami, I., Copley, J., & Moraitis, A. (2023). The 'wicked trinity' of late capitalism: Governing in an era of stagnation, surplus humanity, and environmental breakdown. *Geoforum*, 103691.
- Aramendia, E., Brockway, P. E., Taylor, P. G., & Norman, J. B. (2024). Exploring the effects of mineral depletion on renewable energy technologies net energy returns. *Energy*, 290, 130112.
- Armstrong McKay, D. I., Staal, A., Abrams, J. F., Winkelmann, R., Sakschewski, B., Loriani, S., Fetzer, I., Cornell, S. E., Rockström, J., & Lenton, T. M. (2022). Exceeding 1.5 C global warming could trigger multiple climate tipping points. *Science*, 377(6611), eabn7950.
- Becker, A., Ng, A. K., McEvoy, D., & Mullett, J. (2018). Implications of climate change for shipping: Ports and supply chains. *Wiley Interdisciplinary Reviews: Climate Change*, 9(2), e508.
- Bland, L. M., Rowland, J. A., Regan, T. J., Keith, D. A., Murray, N. J., Lester, R. E., Linn, M., Rodríguez, J. P., & Nicholson, E. (2018). Developing a standardized definition of ecosystem collapse for risk assessment. *Frontiers in Ecology and the Environment*, 16(1), 29–36.
- Capellán-Pérez, I., De Castro, C., & González, L. J. M. (2019). Dynamic Energy Return on Energy Investment (EROI) and material requirements in scenarios of global transition to renewable energies. *Energy Strategy Reviews*, 26, 100399.
- Carrey, J. (2020). *Sans pétrole et sans charbon. Techniques et énergies dans les sociétés préindustrielles*. IS Editions.
- Clare, M., Yeo, I., Bricheno, L., Aksenov, Y., Brown, J., Haigh, I., Wahl, T., Hunt, J., Sams, C., & Chaytor, J. (2023). Climate change hotspots and implications for the global subsea telecommunications network. *Earth-Science Reviews*, 237, 104296.
- Curtis, F. (2009). Peak globalization: Climate change, oil depletion and global trade. *Ecological Economics*, 69(2), 427–434.
- Davies, S., Pettersson, T., Sollenberg, M., & Öberg, M. (2025). Organized violence 1989–2024, and the challenges of identifying civilian victims. *Journal of Peace Research*, 62(4), 1223–1240.
<https://doi.org/10.1177/00223433251345636>
- Delannoy, L., Longaretti, P.-Y., Murphy, D. J., & Prados, E. (2021). Peak oil and the low-carbon energy transition: A net-energy perspective. *Applied Energy*, 304, 117843.
- Dong, J., Asif, Z., Shi, Y., Zhu, Y., & Chen, Z. (2022). Climate change impacts on coastal and offshore petroleum infrastructure and the associated oil spill risk: A review. *Journal of Marine Science and Engineering*, 10(7), 849.
- FAO, IFAD, UNICEF, WFP, & WHO. (2024). *The State of Food Security and Nutrition in the World 2024 – Financing to end hunger, food insecurity and malnutrition in all its forms*.
<https://doi.org/10.4060/cd1254en>
- Hall, C. A. S., Lambert, J. G., & Balogh, S. B. (2014). EROI of different fuels and the implications for society. *Energy Policy*, 64, 141–152.
- Ibrahim, S. E., Centeno, M. A., Patterson, T. S., & Callahan, P. W. (2021). Resilience in global value chains: A systemic risk approach. *Global Perspectives*, 2(1), 27658.

IPCC. (2021). *Climate Change 2021: The Physical Science Basis. Contribution of Working Group I to the Sixth Assessment Report of the Intergovernmental Panel on Climate Change*. Cambridge University Press. Cambridge University Press, Cambridge, UK and New York, NY, USA,.

Laherrère, J., Hall, C. A., & Bentley, R. (2022). How much oil remains for the world to produce? Comparing assessment methods, and separating fact from fiction. *Current Research in Environmental Sustainability*, 4, 100174.

Lawrence, M., Homer-Dixon, T., Janzwood, S., Rockström, J., Renn, O., & Donges, J. F. (2024). Global polycrisis: The causal mechanisms of crisis entanglement. *Global Sustainability*, 7, e6.

Leal Filho, W., Abeldaño Zuñiga, R. A., Sierra, J., Dinis, M. A. P., Corazza, L., Nagy, G. J., & Aina, Y. A. (2024). An assessment of priorities in handling climate change impacts on infrastructures. *Scientific Reports*, 14(1), 14147.

McNulty, B. A., & Jowitt, S. M. (2021). Barriers to and uncertainties in understanding and quantifying global critical mineral and element supply. *IScience*, 24(7).

Meadows, D. H., Meadows, D. L., & Randers, J. (1992). *Beyond the limits: Global collapse or a sustainable future*. Earthscan Publications Ltd.

Mikellidou, C. V., Shakou, L. M., Boustras, G., & Dimopoulos, C. (2018). Energy critical infrastructures at risk from climate change: A state of the art review. *Safety Science*, 110, 110–120.

Mohr. (2015). *Projection of world fossil fuels by country*.

NOAA Global Monitoring Laboratory. (2025a). *Recent Global Monthly Mean CH4*. https://gml.noaa.gov/webdata/ccgg/trends/ch4_trend_gl.pdf

NOAA Global Monitoring Laboratory. (2025b). *Recent Global Monthly Mean N2O*. https://gml.noaa.gov/webdata/ccgg/trends/n2o_trend_gl.pdf

Northey, S. A., Mudd, G. M., & Werner, T. (2018). Unresolved complexity in assessments of mineral resource depletion and availability. *Natural Resources Research*, 27, 241–255.

Northey, S. A., Mudd, G. M., Werner, T. T., Jowitt, S. M., Haque, N., Yellishetty, M., & Weng, Z. (2017). The exposure of global base metal resources to water criticality, scarcity and climate change. *Global Environmental Change*, 44, 109–124.

Our World in Data. (2025a). *Military personnel and spending*. <https://ourworldindata.org/military-personnel-spending>

Our World in Data. (2025b). *Number of parties in multilateral environmental agreements*. <https://ourworldindata.org/grapher/number-of-parties-env-agreements>

Ripple, W. J., Wolf, C., Gregg, J. W., Rockström, J., Mann, M. E., Oreskes, N., Lenton, T. M., Rahmstorf, S., Newsome, T. M., Xu, C., Svenning, J.-C., Pereira, C. C., Law, B. E., & Crowther, T. W. (2024). The 2024 state of the climate report: Perilous times on planet Earth. *BioScience*, 74(12), 812–824. <https://doi.org/10.1093/biosci/biae087>

SIPRI Military Expenditure Database. (2024). [Dataset]. Stockholm International Peace Research Institute.

- Speirs, J., McGlade, C., & Slade, R. (2015). Uncertainty in the availability of natural resources: Fossil fuels, critical metals and biomass. *Energy Policy*, 87, 654–664.
- Tomja, A. (2014). Polarity and International System Consequences. *Interdisciplinary Journal of Research and Development*, 1(1), 57–61.
- Venner, M., & Zamurs, J. (2012). Increased maintenance costs of extreme weather events: Preparing for climate change adaptation. *Transportation Research Record*, 2292(1), 20–28.
- Vogel, J., & Hickel, J. (2023). Is green growth happening? An empirical analysis of achieved versus Paris-compliant CO₂-GDP decoupling in high-income countries. *The Lancet Planetary Health*, 7(9), e759–e769.
- Voskaki, A., Budd, T., & Mason, K. (2023). The impact of climate hazards to airport systems: A synthesis of the implications and risk mitigation trends. *Transport Reviews*, 43(4), 652–675.
- World Bank. (2025a). *Internally displaced persons, new displacement associated with disasters (number of cases)*. <https://data.worldbank.org/indicator/VC.IDP.NWDS>
- World Bank. (2025b). *Life expectancy at birth, total (years)—Least developed countries: UN classification*.
https://data.worldbank.org/indicator/SP.DYN.LE00.IN?locations=XL&name_desc=false
- World Bank. (2025c). *Poverty headcount ratio at \$3.00 a day (2021 PPP) (% of population)—Sub-Saharan Africa*.
https://data.worldbank.org/indicator/SI.POV.DDAY?name_desc=false&locations=ZG
- World Bank. (2025d). *World Development Indicators. GDP (current US\$)*.
<https://data.worldbank.org/indicator/NY.GDP.MKTP.CD>

Limits to growth revisited: System Dynamics Simulations of Global Economic Developments and Distributional Implications in the 21st Century

Abstract

We use a system dynamics environment-economy model to explore how multiple limits to growth might affect global economic output and consumption across different social classes until 2100. Based on a five-dimensional scenario space, we simulate global economic development in 120 scenarios that differ in labor productivity growth, per-capita consumption growth, fossil resource availability, climate change severity, and climate system sensitivity. In 92% of the simulations, output peaks and then declines persistently. Excluding scenarios without climate impacts, output in 2100 is 15–70% lower than in 2019. Scenarios with low labor productivity and consumption growth experience earlier peaks at lower levels and moderate output declines. In contrast, scenarios with high labor productivity and consumption growth show faster and longer periods of growth but eventually face economic collapse. While resource depletion and climate damages act as stressors, most simulations indicate that growth ultimately halts and reverses due to a shortage of labor hours. During the phase of unintentional economic degrowth, economic convergence and redistribution reduce consumption in high-income countries to values 3–4 times lower than initial consumption levels, while middle- and low-income countries return to consumption levels similar to those at the start of the simulations. Poverty reduction in poorer regions ends as global output peaks, while environmental destabilization caused by economic growth threatens development opportunities beyond the 21st century.

Keywords

Limits to growth; system dynamics; labor productivity; post-growth; integrated assessment modeling; global environmental scenarios

1. Introduction

The publication of *The Limits to Growth* (LTG) report (Meadows et al., 1972), sparked heated debates within academia and broader society (Higgs, 2022), and pioneered the use of computer-based integrated modeling to explore future global environmental and socio-economic dynamics (Cassen & Cointe, 2022; Vieille Blanchard, 2010). With the rise of climate change the growth-versus-environment debated has experienced a revival although the debate has shifted from concerns about resource depletion to the transgression of planetary boundaries as well as to non-biophysical factors limiting economic growth in the Anthropocene, such as social or political factors (Butler, 2024; Döring & Aigner-Walder, 2022; Jackson & Webster, 2017; Scheffran, 2023; Van Den Bergh, 2017).

Since the original publication of the World3 model, simulations were updated twice by the MIT research team (Meadows et al., 1992, 2004) and were replicated and updated by other independent researchers (Herrington, 2021; Turner, 2008, 2014). An uncertainty analysis of World3 found high sensitivity of output variables but stable trends, indicating a low probability of favorable futures for humankind (Heath et al., 2019). Likewise, a recent recalibration of the model indicates a collapse dynamic due to resource depletion that occurs with a temporal delay and after a higher peak, compared to the original simulations (Nebel et al., 2024). An extension of World3 was developed to simulate the effects of a rapid scaling of Artificial Intelligence on the limits to growth (Gulyeva et al., 2025) while a regionalized simulation of World3's 'runaway global warming' scenario shows an unequal distribution of deaths by starvation over the world (Richards et al., 2023). World3 has also inspired the development of new models such as the Integrated Global Food and Energy Security System Dynamics Model by Pasqualino et al. (2019) that was created by merging structures of World3 with a macroeconomic and an energy model, the World3-based World Energy Model by Ansell & Cayzer (2018) built to examine changes in the energy and climate system, the Earth4All model that includes social variables like a social tension and a well-being index (Stoknes et al., 2025). Further models developed to study limits to growth include WoLim (Capellán-Pérez et al., 2015) and MEDEAS (Capellán-Pérez et al., 2020). Many studies also have applied fundamental concerns of the original LTG simulations to specific sectors, such as the agriculture (Khorsandi et al., 2023) or space setor (Miraux, 2022), and have studied different potential limiting factors that have become more relevant due to recent economic and political developments such as energy efficiency (Murphy, 2022), mineral resource availability (Valero et al., 2018) and the deployment of negative emission technologies (Gambhir et al., 2023). Despite these modeling efforts and a certain reappraisal of the LTG study, international policy-making arguably is still heavily influenced by the discourse of green growth, which dismisses the possibility of collapse, assuming the feasibility of strong decoupling and continued growth in consumption and production (Gómez-Baggethun & Naredo, 2015; Smith & Ely, 2025).

This paper aims to contribute to the literature and debate on LTG by illustrating the main dynamics of a series of simulations conducted with a newly developed system dynamics model called MORDRED (Model Of Resource Distribution and Resilient Economic Development). Specifically, we seek to assess whether global collapse remains a plausible outcome within the twenty-first century (1), and to analyze how potential collapse trajectories could differentially affect living standards across social groups and regions (2). Our modeling work makes three contributions to the state of the art: First, consumption in the model is disaggregated by class and by region to address concerns raised by Global South voices that stressed the importance of economic inequality in the context of debates on (limits to) world development, which are

rendered invisible in aggregated global models (Bull & Aguilar-Støen, 2023; Grondona, 2024; Jones, 2022). Second, the model focuses on concrete changes in biophysical and technological variables, and is capable of simultaneously representing the effects of the energy transition and of unfolding climate damages on emission and temperature pathways. Third, in contrast to existing LTG related studies that sidestep the economic input factor labor or assume labor is never scarce, we treat labor, mediated by changes in population and productivity, as a key potential limiting factor to growth.

2. Methods

2.1. The MORDRED model

For our simulations, we use version 1.1.2 of the MORDRED model (*Model of Resource Distribution and Resilient Economic Development*). The model structure, mathematical equations, and data sources are described in detail by Lauer & Llases (2025). Therefore, for reasons of space, we provide only a description of the modules and variables most relevant to our scenario analysis.

MORDRED is a system dynamics model programmed in Vensim, designed to represent global-scale socio-economic dynamics and their interaction with the biophysical environment. The model consists of several modules describing the world population, economy, labor force, energy sources, land types (including natural ecosystems and economically used land), environmental stressors such as greenhouse gases, and the climate system.

The demographic module, built with UN population data (UN DESA, 2019b, 2019a, 2019c) and Exiobase3 data on household and government consumption (Stadler et al., 2018), computes the evolution of the global population, divided into three regions: the center (C) (all high-income countries), the semi-periphery (S) (all upper-middle-income countries), and the periphery (P) (all remaining countries). Population dynamics depend on age-specific birth and death rates, which are influenced by per capita consumption and public spending on education and health. These differ across world regions and among social classes within each region. At each simulation step, the population sustained by the global economy — whose labor serves as input to global production — is divided into the richest 20 % (R20), the poorest 30 % (P30), and the middle class (M50), comprising the remaining 50 %. This yields nine per-capita consumption trajectories globally.

The economic module follows an input–output structure where production is determined by final demand and factors such as technological change, climate impacts, and resource constraints. Final demand, computed globally and divided into 25 sectors, consists of private consumption, public consumption, and investment.

Private consumption is driven by the consumption demand of each social class, defined exogenously by specifying a desired growth rate for the P30 class and relative consumption multipliers linking other classes to it. The desired per capita consumption for each class and region ($Cpc_{r,cl}$) evolves according to equation (1), where $Cp_nc_{r,cl}$ denotes the desired consumption not covered by production (see equation (20)). The distribution of per capita consumption across the 25 sectors (i) is calculated with a vector denoting the sectoral share of total per capita consumption ($Cpc_ssh_{r,cl,i}$), estimated based on Exiobase3 sectoral private consumption data for different world regions, reflecting different consumption levels (2).

Multiplying sectoral per capita consumption by population yields total consumption per class and region (3). Aggregating across classes and regions gives desired global private consumption by sector (4-5).

$$Cpc_{r,cl}^d = \int_{t_0}^t (Cpc_{r,cl}^d \cdot Cpc_gr_{r,cl} - Cpc_nc_{r,cl}) dt + Cpc_{r,cl}^d(t_0) \quad (1)$$

$$Cpc_{r,cl,i}^d = Cpc_{r,cl}^d \cdot Cpc_ssh_{r,cl,i} \quad (2)$$

$$C_{r,cl,i}^d = Cpc_{r,cl,i}^d \cdot P_r \cdot share_{cl} \quad (3)$$

$$C_{r,i}^d = \sum_{cl} C_{r,cl,i}^d \quad (4)$$

$$C_i^d = \sum_r C_{r,i}^d \quad (5)$$

Desired public consumption per region (G_r^d) is defined as a share ($G2Cr_r$) of total desired private consumption per region that reflects Exiobase3 data for 2019 aggregated at the regional level (6). A constant sectoral distribution is applied for each region (7), and desired global public consumption by sector is obtained by aggregating across regions (8).

$$G_r^d = C_r^d \cdot G2Cr_r \quad (6)$$

$$G_{r,i}^d = G_r^d \cdot G_ssh_{r,i} \quad (7)$$

$$G_i^d = \sum_r G_{r,i}^d \quad (8)$$

Investment is calculated by sector at the global level and aims to maintain a specific capital stock-output ratio for each sector. It depends on sectoral capital intensity, production, and the depreciation rate of capital. Both capital intensity and depreciation have endogenous and exogenous components: the exogenous component evolves according to scenario assumptions while the endogenous component is influenced by environmental changes such as climate change impacts caused by a rise in global average temperatures (*temp*) or sea level rise (*slr*), and fossil resource depletion (*depl*). Capital intensity is calculated using equation (9), where β_i is a sector-specific damage factor influenced by temperature-related output losses in the food sector, and depletion-related fossil resource extraction difficulties in the fossil resource sectors, and $Int_i^{k,wod}$ denotes the capital intensity without damage. Sectoral depreciation is given by equation (10). Sectoral investment is then calculated using sectoral output in the previous time step, sectoral capital stock, and an adjustment parameter that regulates the investment speed to ensure that the investment is not concentrated in a single period (11). The capital stock increases with investment and decreases with depreciation (12).

The sum of investment across all sectors yields total investment. Subsequently, to calculate gross fixed capital formation as a demand component, total investment is multiplied by a vector indicating which share of the total production of investment goods belongs to each sector. Additional GFCF becomes necessary when the global temperature increase exceeds 2°C compared to pre-industrial levels.

$$Int_i^k = Int_i^{k,wod} * \beta_i^{temp,depl} \quad (9)$$

$$\delta_i = \delta_i^{wod} + \delta_i^{temp} + \delta_i^{slr} \quad (10)$$

$$Inv_i^d = \max(0; \beta^{Inv} \cdot (X_i^s(ts - 1) \cdot Int_i^k - K_i) + \delta_i \cdot K_i) \quad (11)$$

$$K_i = \int_{t_0}^t (Inv_i^s - \delta_i \cdot K_i) dt + K_i(t_0) \quad (12)$$

$$GFCF_i^d = GFCF_ssh_i \cdot \sum_i (Inv_i^d) + Extra_GFCF^{str} \quad (13)$$

The sum of the three demand components yields final demand (14). Output required to meet this demand is computed using the global input-output table of the model that evolves according to exogenous parameters reflecting assumptions about technological change, and endogenous variables such as increasing fossil resource extraction difficulties and climate change impacts in the food sector. Output by sector is derived via the Leontief inverse (15).

$$FD_i^d = C_i^d + G_i^d + GFCF_i^d \quad (14)$$

$$\bar{X}^d = (Id - A)^{-1} \cdot \bar{FD}^d \quad (15)$$

From the desired output by sector, the required inputs of land, energy, and labor are determined in the respective modules. The maximum available labor depends on the working-age population (15–64 years), participation rates, and hours worked, while labor demand depends on sectoral productivity. Land availability depends on the share of inhabitable land already in use, while land demand depends on land intensities, both of which are affected by climate change.

Because the model uses a Leontief production function, shortages in any input factor lead to proportional reductions in output. A scarcity factor (Sf), ranging from 0 to 1, is computed in each of the corresponding modules; the smallest of these is then multiplied by the demanded output to determine the actual - supplied (s) – output (16), (17). The smallest scarcity factor is also applied to final demand to calculate the actual satisfied final demand (18), as well as to the productive factors to determine the resources that have actually been used.

$$Sf = \min(Sf^{Lb}; Sf^{ff}; Sf^{Lnd}) \quad (16)$$

$$X_i^s = X_i^d \cdot Sf \quad (17)$$

$$FD_i^s = FD_i^d \cdot Sf \quad (18)$$

When total desired demand exceeds what available resources can produce, consumption across all classes is reduced proportionally to maintain consumption ratios between classes determined by convergence assumptions. Per capita consumption for each class and region is derived by dividing the consumption allocated to the corresponding group by its population, which constitutes a certain share of the total population ($clsh$) (19). The per capita consumption not covered ($Cpc_nr_{r,cl}$) is computed as the difference between the demanded and supplied per capita consumption (20).

$$Cpc_{r,cl}^s = \frac{\sum_i (C_{r,cl,i}^s)}{P_r * clsh_{cl}} \quad (19)$$

$$Cpc_nr_{r,cl} = Cpc_{r,cl}^d - Cpc_{r,cl}^s \quad (20)$$

The energy and stressor modules calculate the total amount of fossil resources extracted to produce total output, an extraction difficulty factor reflecting increasing resource depletion, and the corresponding greenhouse gas (GHG) emissions, mainly based on IEA data (IEA, 2021). The

stressor module also calculates emissions of other GHGs (CH₄, N₂O, SF₆, HFC, PFC) based on sectoral emission intensity data from the environmental extensions of Exiobase3.

The different GHG emissions are fed into the climate module, which is adapted from the Integrated Assessment Model WILIAM (Lifi et al., 2023) and has been actualized with the latest IPCC (2021) data. In this module, the increase in the global average temperature is calculated and fed back into the economy, labor and land modules.

2.2. Scenario design

For our scenario analysis, we consider five key variables that may influence the timing, pace, and scale of a decline in global economic output in response to different limits to growth: the growth in sectoral labor productivities, growth in consumption per capita across social classes, accessibility of fossil resources, the presence of climate damages, and the sensitivity of the climate system to anthropogenic perturbations. By defining a plausible range of values for each variable, a five-dimensional scenario space is constructed that covers all possible scenarios resulting from variations in the main variables' values (Fig. 1). Each main variable can take a medium state, reflecting our best guess (BG) about the model parameters, as well as a 'low' or 'high' state, corresponding to the lower and upper bounds of a plausible range. Combining different variables in various states produces unique scenarios that can be compared in terms of the model's main outputs. For example, comparing a scenario characterized by low labor productivity growth, medium consumption growth, low fossil resource accessibility, low climate damages, and medium climate sensitivity with another differing only in higher fossil resource accessibility allows us to explore how resource availability drives potential growth and unintentional degrowth patterns in global output.

In MORDRED 1.1.2, labor productivities in the 25 economic sectors are calculated by inverting sectoral labor intensities (21). Changes in labor intensities are represented by an exponentially decaying function of average per capita consumption at the global level for each sector, with the latter serving as an indicator of economic development associated with lower average labor intensities (22).

$$Lprod_i = \frac{1}{Lint_i} \quad (21)$$

$$Lint_i = \alpha_i * e^{\beta_i * Cpc_{world\ average}} \quad (22)$$

To derive the lower bound for labor productivity growth, the parameters of these functions are fitted to regional and global labor productivities and consumption levels in 2019, using EXIOBASE3 data aggregated into a high-income region and a world region. The parameters ensure that global sectoral labor productivities increase with rising average global consumption, reaching high-income country levels once global average consumption attains 97% of that of high-income countries. To calculate the BG for conceivable growth in sectoral labor productivities, the α parameter for each sector is reduced by 10%, resulting in higher productivities for a given consumption level. For the upper bound, α_i is reduced by 20%. The resulting scenario space reflects optimistic assumptions regarding future labor productivity growth since α_i is always lowered rather than increased.

As BG for consumption growth, we assume that by 2100 the per capita consumption levels in the periphery equal those of the center in 2019, that the semiperiphery is 25% above 2019 center

levels, and that consumption in the center increases by 50%. For the lower bound, consumption in the center remains constant while the semiperiphery and periphery reach 75% and 50% of the center's consumption, respectively. For the upper bound, desired consumption in the center increases by 100%, while the semiperiphery and periphery reach 150% and 125% of 2019 center levels.

We use fossil reserves and resource estimates from BGR (2020) as the quantitative basis for fossil resource availability. Limited substitutability between fuel types and low coal accessibility define the lower bound, while perfect substitutability and high coal accessibility define the upper bound. The BG assumes perfect substitutability and medium coal accessibility.

Consequently, in low-accessibility scenarios, input factors in fossil extraction sectors increase by 30% when all reserves are depleted. In BG and high-accessibility cases, input costs remain stable until all reserves are depleted but rise by 75% when all oil and gas resources and 10% of coal are extracted (BG) and by 50% when all oil and gas and 60% of coal are extracted (high). Our lower bound for fossil resources is 1.6 times higher than that in Turner's (2008) while our upper bound is 2.48 to 4.95 times higher, reflecting a certain optimism about future fossil resource availability.

For climate damages, the BG corresponds to the model's default values for all damage parameters. In the low-damages case, parameters regulating damages to capital stock and output are reduced by 25%, the parameter value causing increases in input coefficients is reduced by 8%, parameters influencing labor productivity and labor supply are reduced by 30%, and climate-induced losses of land and land productivity by 25%. In the high-damage case, the parameters impacting capital stock and output increase by 25%, the parameter impacting input coefficients increases by 10%, and the parameters influencing labor and land increase by 20% and 25%, respectively. To test extreme conditions, we also allow simulations without climate damages, though such cases are not considered plausible.

The climate sensitivity variable determines how strongly and rapidly the climate system reacts to anthropogenic greenhouse gas emissions. Higher sensitivity results in greater temperature increases under a given anthropogenic emission pathway. When sensitivity is low, feedback mechanisms are deactivated, and the equilibrium climate sensitivity (ECS) is set to 3 °C. For medium sensitivity, the ECS remains unchanged, but feedback mechanisms are activated, enhancing natural carbon and methane emissions. High climate sensitivity is obtained by activating feedbacks and increasing ECS by 10%, reflecting an increased climate sensitivity found in more recent climate modeling studies (Wyser et al., 2020).

Supplementary Material (SM) 1 contains additional boundary conditions common to all scenarios.

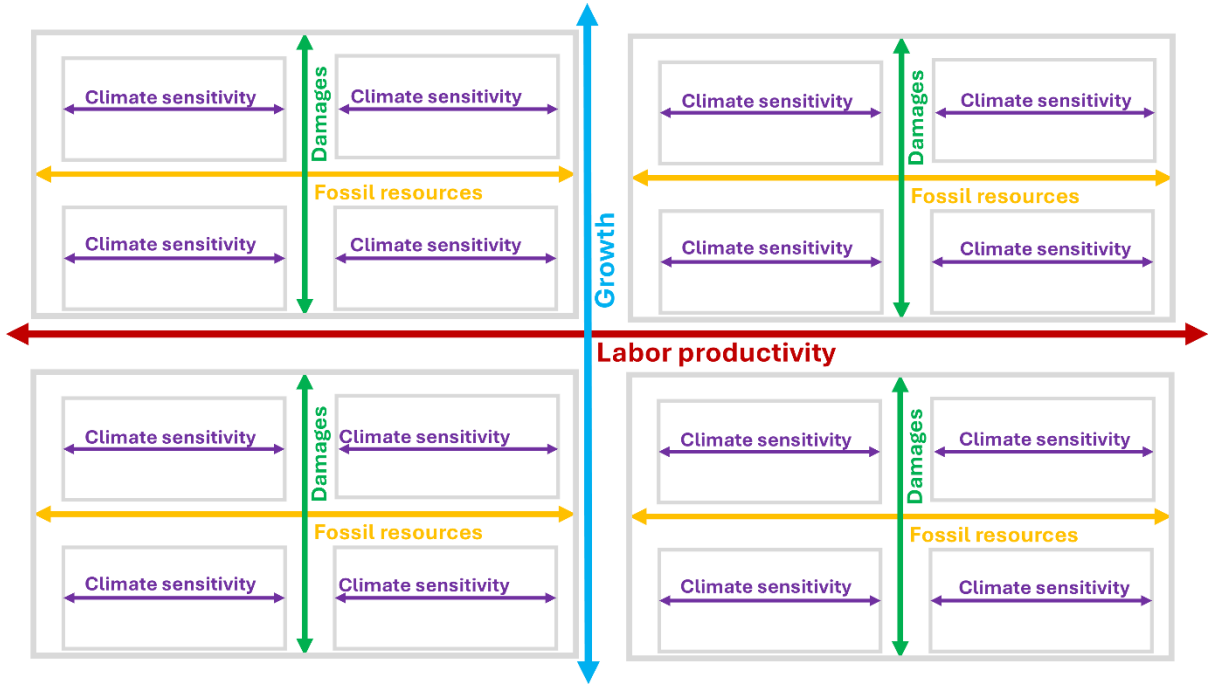


Fig. 1: Simplified representation of the scenario space constructed with the five main variables. Each variable is represented by colored bidirectional arrows indicating its value range. The left/low ends indicate 'low' states, while the right/high ends indicate 'high' states.

To simulate scenarios across the full scenario space, we divide it along labor productivity and consumption growth and simulate four scenario sets (Table 1). The first two include all scenarios with low or high labor productivity growth and medium (BG) consumption growth; the last two include scenarios with low or high consumption growth and medium (BG) labor productivity growth. We also simulate scenarios without climate damages for these four sets. As climate sensitivity does not affect dynamics in the absence of climate damages, it is not varied. Each scenario set contains 30 scenarios, resulting in 120 simulations. The simulation period is identical for all scenarios and covers 2019–2100.

Consumption growth Labor productivity	low			medium (best guess)			high		
low				12101	12201	12301			
				12111	12211	12311			
				12112	12212	12312			
				12113	12213	12313			
				12121	12221	12321			
				12122	12222	12322			
				12123	12223	12323			
				12131	12231	12331			
				12132	12232	12332			
				12133	12233	12333			
medium (best guess)	21101	21201	21301				23101	23201	23301
	21111	21211	21311				23111	23211	23311
	21112	21212	21312				23112	23212	23312

	21113	21213	21313			23113	23213	23313
	21121	21221	21321			23121	23221	23321
	21122	21222	21322			23122	23222	23322
	21123	21223	21323			23123	23223	23323
	21131	21231	21331			23131	23231	23331
	21132	21232	21332			23132	23232	23332
	21133	21233	21333			23133	23233	23333
high				32101	32201	32301		
				32111	32211	32311		
				32112	32212	32312		
				32113	32213	32313		
				32121	32221	32321		
				32122	32222	32322		
				32123	32223	32323		
				32131	32231	32331		
				32132	32232	32332		
				32133	32233	32333		

Table 1: Each five-digit number represents a scenario. The first digit denotes labor productivity growth, the second denotes consumption growth, the third fossil resource availability, the fourth climate damages, and the fifth climate sensitivity. (1) indicates a low value, (2) a medium/BG value, and (3) a high value. (0) is used only for climate damages to denote the absence of damages.

3. Results

We present the development of total economic output before proceeding to the differentiated impacts of emerging limits to growth on different social classes and world regions. Due to the input-output framework of the economic model, output is the sum of industry demand for intermediate products and final demand.

3.1. Projected development of world economic production

The most general indicator in MORDRED showing changes in world economic production is the total annual output at the global level, calculated by the economic module. The simulations show that an end of economic growth, followed by a period of persistent decline in world economic production, is a characteristic of 92% of all scenarios. Excluding the scenarios without climate damages, this figure rises to 99%, with the only exception being scenario 32311, characterized by low climate sensitivity and damages, high fossil resource availability, medium consumption growth, and high labor productivity growth. This scenario is linked to the highest output among all simulated cases, although consumption is lower than in the scenarios without climate damage impacts, indicating that a greater share of economic activity must be dedicated to countering the effects of increasing climate damage and resource scarcity. However, compared to other scenarios, the pressure on the economy is still low enough to be buffered by high labor productivity levels—at least during the simulation period, when such pressures can still be offset by productivity gains.¹ Apart from the lack of climate damages, the great majority of scenarios that grow continuously until 2100 are characterized by medium or high fossil resource availability, with the only exception being scenario 21101.

¹ Extending the simulation period between 2100, we find that this scenario collapses abruptly in 2103.

Thus, unless it is assumed that climate change impacts do not exist, or that industrial processes radically ‘dematerialize’ in unspecified ways—rendering economic production structures incomparable with current processes—an end to economic growth followed by a period of persistent economic decline can be expected to occur during the 21st century. Importantly, these findings apply only to the global level, as MORDRED does not disaggregate production into different world regions. Hence, earlier peaks and declines in some regions, as well as continued growth in others, may still be compatible with the simulation results.

Regarding changes in output compared to the start of the simulation, in 89% of the simulated scenarios output levels at the end of the period are lower than at the start, while output exceeds initial levels in only 13 scenarios, three of which peak and decline in the 2080s. All 13 scenarios are characterized by low climate sensitivity, and all but one by the absence of climate change impacts. Of all scenarios with a peak and subsequent decline, output is highest in scenarios 12101 and 32101: by 2100, global output remains 1.86 times higher than in 2019. The scenario with the lowest output in 2100 is 32211, where output is 70% lower than initially.

Fig. 2a-d shows the evolution of output for each scenario set. The scenario sets exhibit clear differences in both the timing and level of the peak in global output.

In the set with low labor productivity (and medium consumption) growth (Fig. 2a) output peaks earliest, with most scenarios peaking between 2035 and 2050. This is followed by the set with (medium labor productivity and) high consumption growth (Fig. 2d) where the first peak occurs in 2040. The first scenario in the set featuring (medium labor productivity and) low consumption growth peaks in 2043 (Fig. 2c) while the earliest peak in the set with high labor productivity (and medium consumption growth) occurs in 2049 (Fig. 2b). Under equal consumption growth rates, lower labor productivity growth leads to earlier peaks, as the point of labor scarcity caused by emerging limiting factors is reached sooner. Conversely, under equal labor productivity growth, higher consumption growth results in faster increases in emissions and temperatures, faster growth in damages, and earlier labor shortages.

While all scenarios with low labor productivity growth and some level of climate damage reach their maximum output within 15 years after the first scenario peaks, scenarios with high labor productivity growth show peaks over a 50-year span, including two late peaks in the 2080s and 2090s, followed by steep collapses in the cases of medium and low fossil resource accessibility (32211 and 32111). Both scenario sets built on low and high consumption growth see peaks and declines within approximately four decades. The output level at the peak is lowest in the low-consumption set and highest in the high-labor productivity set. Scenarios with low labor productivity and medium consumption growth tend to peak at lower levels than scenarios with medium labor productivity and high consumption growth, although those combining no climate damages with low fossil resources peak at comparable levels.

Thus, higher labor productivity growth rates increase the level at which output peaks because they allow output to grow longer, while higher consumption growth rates lead to higher peaks because output rises faster. At the same time, low labor productivity and consumption growth rates are associated with slower output reductions, creating ‘smooth’ curves, while high growth—especially high labor productivity growth—produces faster and steeper declines resembling collapse dynamics. This dynamic arises from the endogenization of labor productivity: as output grows, rising productivity allows further expansion despite emerging limits such as climate damages and resource constraints. Paradoxically, limiting factors can initially increase output growth, as they lower the ratio between final demand and output,

requiring higher output to meet desired consumption. However, once labor shortages emerge, output declines, reducing productivity further and creating a self-reinforcing downward spiral. The longer non-labor limiting factors accumulate before output peaks, the greater the subsequent economic decline.

Excluding scenarios without climate change, the 2100 output range is lowest for scenarios with high labor productivity (47.4–100.8 trillion €) and highest for scenarios with low consumption (70.1–132 trillion €). The sets with high consumption (66.7–104.7 trillion €) and low labor productivity (69.2–117.6 trillion €) fall in between. However, even in the sets with the highest final output range, the values remain significantly below the initial output of 156 trillion €.

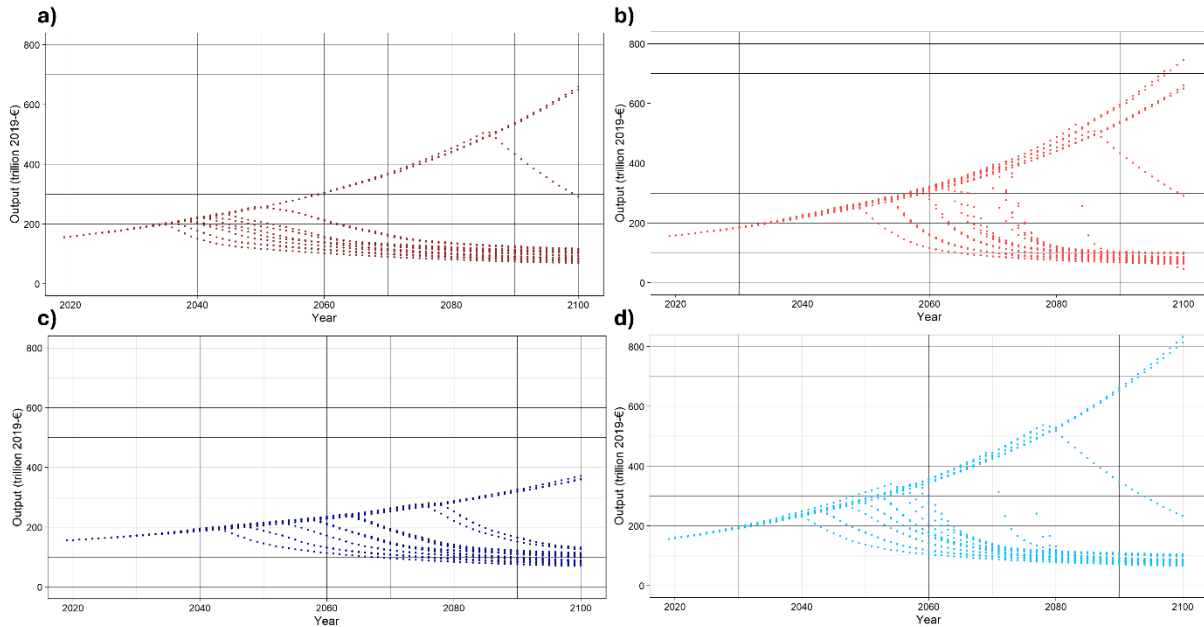


Fig. 2: Evolution of world output throughout all simulations. Scenario sets with a) low labor productivity, b) high labor productivity, c) low consumption, d) high consumption growth.

Having highlighted differences in world economic trajectories caused by varying labor productivity and consumption growth rates, we now turn to the role of resource availability, climate damages and climate sensitivity. Fig. 3a-d shows the four scenario sets with the color indicating the fossil resource availability in the scenarios. Differences in the economic trajectories between scenarios with medium or high fossil resource availability are relatively low across all scenario sets. Scenarios with low resource availability, however, tend to peak earlier. This is especially evident in the case of scenarios with no climate damages where rising extraction difficulties cause output to decline in all scenario sets except for the one with low consumption growth rates (Fig. 3c). Thus, even when climate impacts on the economy are judged insignificant, for example due to extremely high assumed adaptation capacities of society, resource constraints can still bring economic growth to a halt. In general, in scenarios with low resource accessibility the input costs of the extraction sectors increase earlier, resulting directly and indirectly (through an increase in labor intensity of the extraction sectors as well as through the necessary growth in intermediate goods and investment) in a higher labor demand, which, in combination with climate impacts, is sufficient to cause a scarcity of labor hours. Additionally, once output levels approach 500 trillion 2019-€ per year, the fossil resources have been depleted to such an extent that an additional fossil scarcity factor begins to apply in the model that slows down growth to avoid a sudden crash as accessible resources approach zero. Due to its lower consumption growth, scenario 21101 is not affected by this dynamic, reaching similar

levels of output as the scenario variants with higher resource availability. Scenarios *12201*, *12301*, *32201* and *32301* reach the same output in 2100 independently from energy resource availability and labor productivity growth rates since all scenarios have the same desired consumption growth rates that can be fulfilled due to the absence of climate damages and higher resource availability than in scenario *12101*.

The effects of climate damages and climate sensitivity are clearly visible in Fig. 3e-h and Fig. 3i-l. They both work in the same direction, and their combined effect is the main driver shaping global economic trajectories in the simulations. Across all simulations and scenario sets, scenarios with high climate damages *ceteris paribus* have the earliest peaks in world output, followed by scenarios with medium, low and no damages. The same applies to climate sensitivity: the higher the sensitivity, the earlier the peak in output occurs.

These findings reflect basic reasoning: The higher the level of damage given a certain temperature increase, the earlier climate change will start to adversely impact economic trajectories. Likewise, the higher the sensitivity of the climate system to anthropogenic perturbations, the higher the global warming response to a given emission pathway, leading to higher climate damages at every given level of emissions. Given that emission pathways are, *inter alium*, driven by output, a higher sensitivity leads to climate damages starting to impact the economy at comparatively lower levels of world output.

Unsurprisingly, scenarios with high damages and high sensitivity peak first in all scenario sets, independent from fossil resource accessibility. The reason is that the combined effect of high damages and high sensitivity lead output to peak before extraction costs start to rise in the case of low resource accessibility. Even when extraction costs begin to rise the effect on the output trajectory is negligible due to the small share of the extraction sectors in total output.

Thus, lower labor productivity growth combined with lower resource accessibility, higher consumption growth, higher damages and higher climate sensitivities accelerates a peak and decline of world economic production while higher labor productivity levels and resource accessibility combined with lower consumption, damages and sensitivity can delay this dynamic, although they might also cause a steeper and more abrupt decline resembling economic collapse.

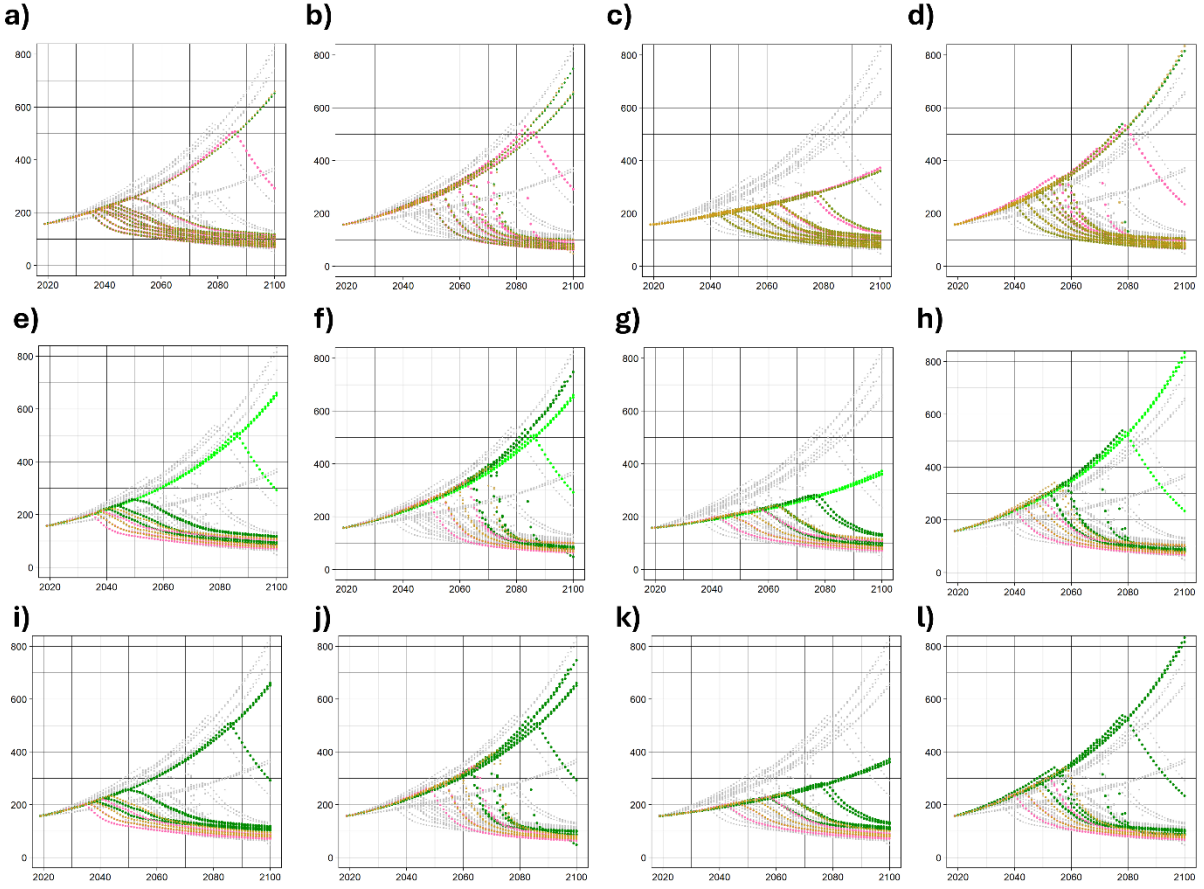


Fig. 3: Evolution of output in trillion € throughout all scenario simulations (grey dots). a)-d): Scenarios with low (pink dots), medium (yellow dots) and high (dark green dots) fossil resource accessibility. e-h): Scenarios with high (pink dots), medium (yellow dots), low (dark green dots) and no (light green dots) climate impacts (pink dots). i-l): Scenarios with high (pink dots), medium (yellow dots) and low (dark green dots) climate sensitivity. a), e), i): Colored dots represent scenarios with low labor productivity growth. b), f), j): Colored dots represent scenarios with high labor productivity growth. c), g), k): Colored dots represent scenarios with low consumption growth. d), h), l): Colored dots represent scenarios with high consumption growth.

3.2. Differentiated impacts of decline in world economic output

Given that in the current economic system the distribution of economic goods between social classes is highly unequal, different socio-economic groups might see themselves affected by a decline in world output in different ways. In our simulations, in the absence of limits to growth, a certain convergence in consumption between social classes takes place as the consumption of poorer classes grows at a higher rate than the consumption of richer classes (see SM1). In the case of emerging limits to growth, this convergence process is maintained, reflecting the optimistic assumption that in times of economic recessions and production decline redistribution aims at buffering the impacts for the poorer classes.

Fig. 4 shows the consumption per capita trajectories for three different social classes in 12 scenarios covering all scenario sets as well as low, medium and high climate impacts. Simulation results for the remaining scenarios are contained in SM2. Since consumption per capita pathways depend on the size of world output, consumption levels across all classes peak latest in scenarios with low climate impacts and reach the highest levels in scenarios with high labor productivity or high consumption growth. Unsurprisingly, the consumption pathways reproduce the same dynamics as the output trajectories, with high labor productivity and high consumption growth leading to higher consumption levels and steeper declines of per capita

consumption. Irrespective of the scenario set, at the global level, the decline in consumption following the peak is highest in the richest class and lowest in the poorest (Fig. 4a, e, i). However, while the richest 20% of the center remain above a consumption threshold of 10 € per day (Fig. 4a-d), the poorest 30% of the periphery never cross this consumption threshold, except for a period of less than 20 years in a scenario with high labor productivity growth and low climate impacts. The consumption of the middle class in the semiperiphery starts crosses the 10€-threshold during the phase of economic growth in every scenario set. However, during the period of global unintentional degrowth in output, consumption declines again and by the end of the simulation is below the threshold, except for the scenario with low climate impacts and low consumption growth (Fig. 4g). At the same time, public expenditures that might complement private consumption, such as health or education expenses per capita, are reduced as well, since they are modeled as a fixed share of household consumption at the regional level. Hence, scenarios with ongoing economic convergence throughout the whole simulation period avoid pushing the entire periphery into extreme poverty levels but at the same time strongly reduce consumption levels in the center. For example, in the 12 scenarios represented in Fig. 4, consumption levels of the richest 20% of the center in 2100 are between 72% and 85% lower than at the initial level, and between 72% and 86% lower compared to the moment where consumption levels reach their maximum. Conversely, consumption levels of the middle class of the semiperiphery at the end of the simulation are between 42% and 74% below the maximum levels reached during the simulation. Finally, the cut in consumption compared to the maximum level ranges between 24% and 71% for the poorest class of the periphery, with none of the consumption levels in 2100 being higher than 1500 € per year.

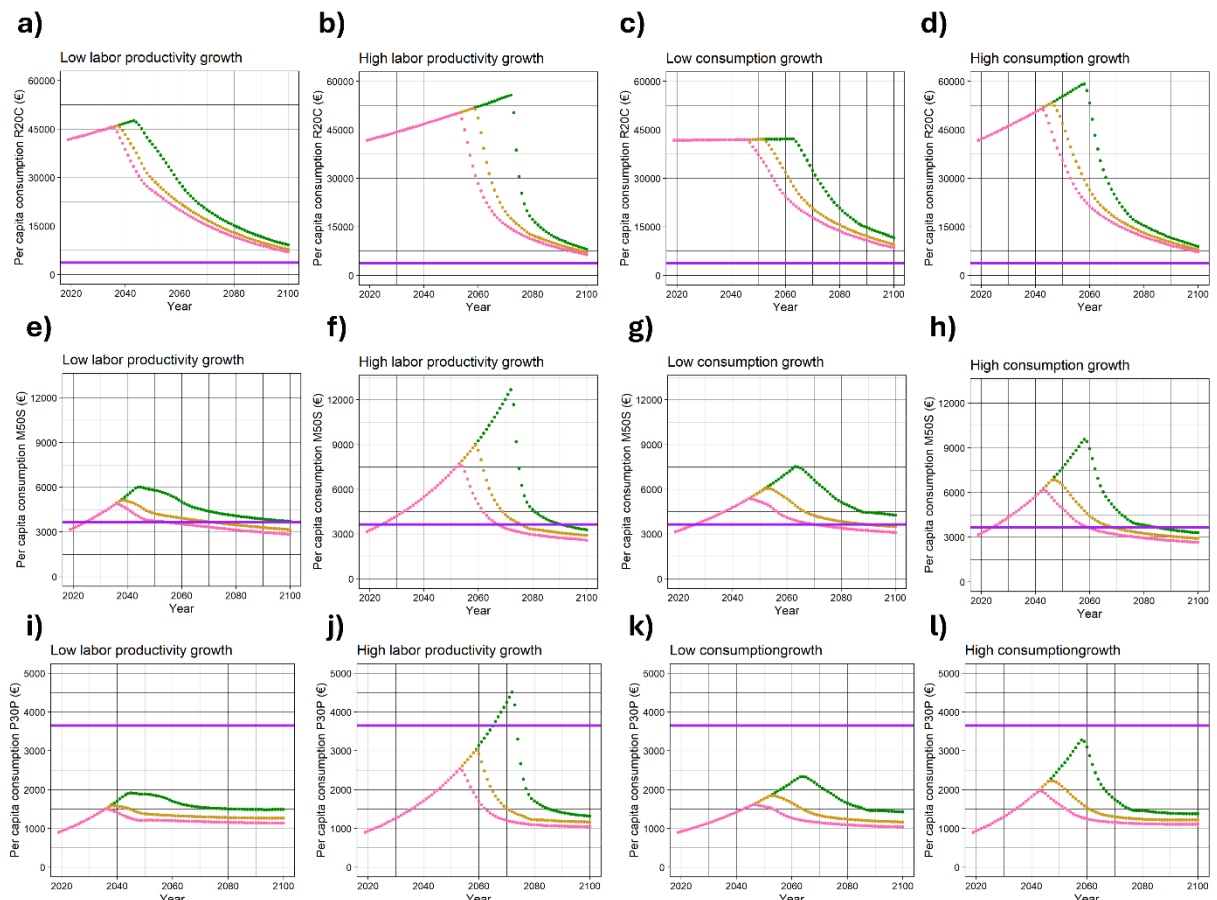


Fig. 4: Annual per capita consumption for the richest 20% of the center (a-d), the middle 50% of the semiperiphery (e-h) and the poorest 30% of the periphery (i-l) in 12 different scenarios: scenarios 12212, 12222 and 12232 in a), e) and i);

scenarios 32212, 32222 and 32232 in b), f) and j); scenarios 21212, 21222 and 21232 in c), g) and k); scenarios 23212, 23222 and 23232 in d), h) and l). Consumption pathways belonging to scenarios with low, medium and high climate impacts are colored in dark green, yellow and pink, respectively. The purple line denotes the consumption level corresponding to a per capita consumption of 10 € per day.

Fig. 5 complements Fig. 4 by displaying the consumption pathways of all social classes in MORDRED for the ‘best guess’ scenarios from every scenario set (12222, 32222, 21222, 23222), i.e. scenarios with medium resource accessibility, climate impacts and climate sensitivity. In all three regions, the richest 20% experience the highest declines in consumption in absolute terms but by the end of the century still have higher consumption levels than the poorer classes. Additionally, the three richest classes are the only classes that still consume more than 10 € per day in 2100. Comparing the consumption trajectories of the middle class in the center, semiperiphery and periphery illustrates that the consumption decline in relative terms is highest in the center since the middle class of the center has a much higher initial consumption level. However, while in the center the 10€-per-day consumption threshold is only approached by 2100 (Fig. 4b), in the semiperiphery it is already crossed between 2075 and 2085 (Fig. 4e). Finally, in the periphery, in the scenarios with low labor productivity and low consumption growth the decline in world economic output prevents the middle class from crossing the threshold in the first place (Fig. 4e). From 2075 onwards, consumption stabilizes in all scenarios between the 10€-per-day (purple line) and the 5€-per-day (orange line) threshold. The poorest classes in the three regions mirror the dynamics of the middle class but at a lower level of consumption. Around 2080, the consumption of the poorest 30% drops below the 10€-per-day threshold and by 2100, this class consumes less than the middle class of the semiperiphery in 2019 (Fig. 4c). In the semiperiphery, the consumption of the poorest class peaks at the 10€-threshold around 2060 in the high labor productivity growth scenario while the threshold is never crossed in the scenarios belonging to the other scenario sets. Between 2070 and 2100, the consumption has returned to the initial consumption values just below the 5€-threshold (Fig. 4f). Last, for the poorest class, consumption peaks at the 5€-threshold in the case of the low productivity and low consumption growth scenarios, and between the 5€- and the 10€-threshold in the case of the scenarios with high consumption and labor productivity growth. Thus, in the scenario simulations presented here, all classes of the center as well as the richest class of the semiperiphery see their consumption decline significantly below the initial level. As a result from ongoing global convergence, the consumption of the middle and poor class of the semiperiphery returns to the initial level while the consumption of all classes of the periphery stabilizes slightly above the initial level. Thus, the improvements in living standards and the reduction in the population living in poverty brought about by economic growth are short-lived. During the final three decades of the simulations, the low- and middle-income classes outside high-income countries become increasingly trapped in moderate to severe poverty. At the same time, the strong reductions in the living standards in the center constitute a radical break with historical tendencies. While situations of persistent poverty can remain compatible with societal and political stability as long as there are prospects for near-term economic growth, declines in living standards following a period of growth may undermine both social stability and the legitimacy of political systems. The results therefore point to two major potential sources of distributive conflict during the 21st century: the spread of poverty and the loss of prosperity attained during the period of economic growth. Neither higher economic growth nor moderate intra- and international redistribution can eliminate these sources of conflicts although the latter at least prevents a complete economic and demographic breakdown in the simulated scenarios.

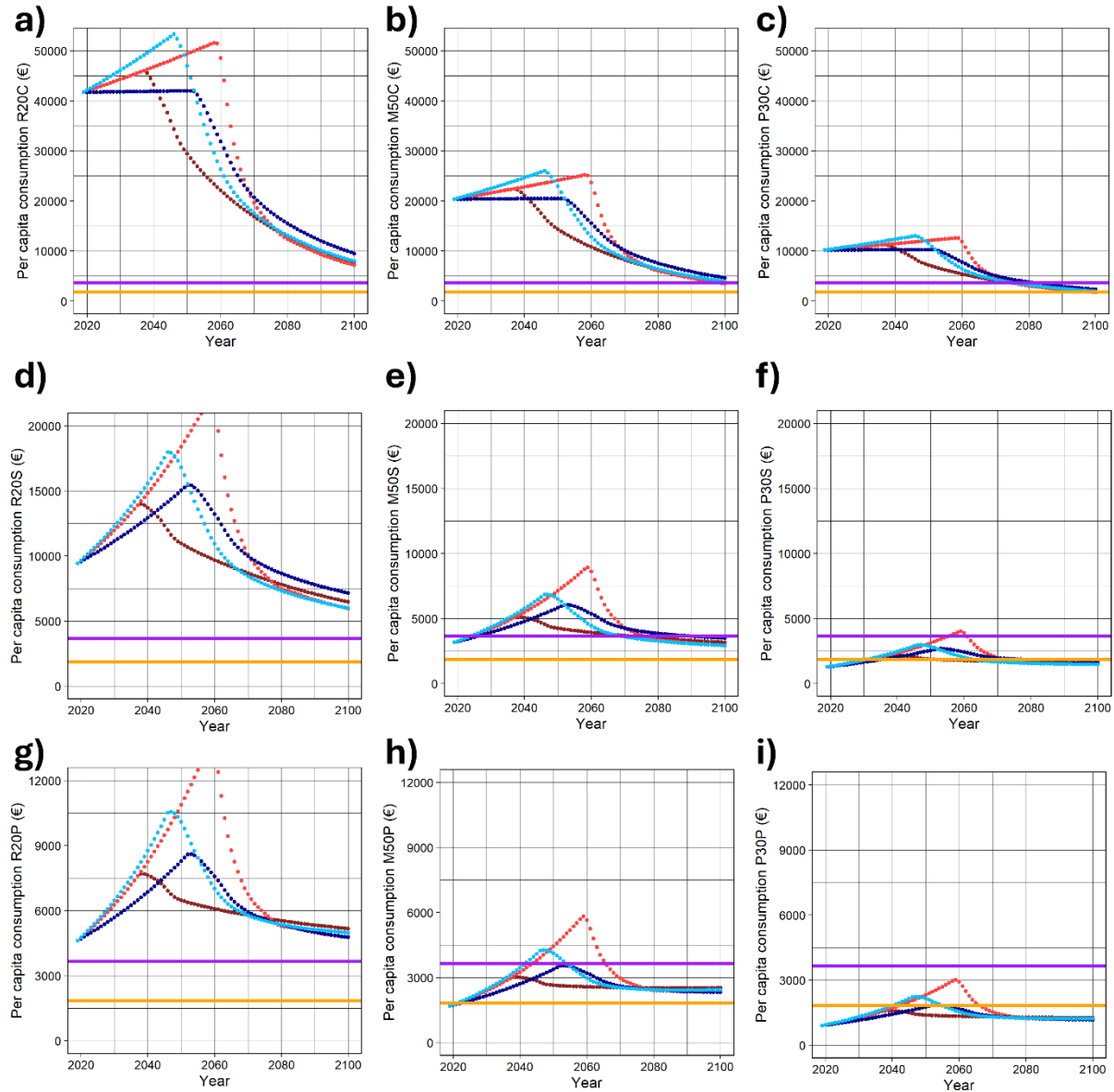


Fig. 5: Per capita consumption pathways for a) the richest 20%, b) the middle 50%, c) the poorest 30% of the center; d) the richest 20%, e) the middle 50%, f) the poorest 30% of the semiperiphery; g) the richest 20%, h) the middle 50%, i) the poorest 30% of the periphery for four scenarios belonging to the scenario sets characterized by low labor productivity (dark red), high labor productivity (light red), low consumption (dark blue) and high consumption (light blue) growth. All scenarios are characterized by medium resource accessibility, climate impacts and climate sensitivity. The purple line denotes the consumption level corresponding to a per capita consumption of 10 € per day, the orange line represents a per capita consumption of 5 € per day.

4. Discussion

Our simulations indicate that plausible assumptions regarding the evolution of key socio-economic and environmental variables result in a high likelihood of a global economic peak followed by decline during the 21st century. Nevertheless, great uncertainty remains about the future evolution of important variables such as the accessibility of resources (Capellán-Pérez et al., 2016; Höök & Tang, 2013), unexpected developments in socio-technological systems (Krupa & Jones, 2013; Lenton et al., 2022) or the scale of climate impacts (Dankers & Kundzewicz, 2020; Frisch, 2018). Additionally, the model's empirical basis and structure render it incapable of

representing societal reactions and adaptation measures in response to emerging limits to growth (cf. Abbot & Malani, 2025; Cassen & Cointe, 2022). Thus, our results should not be interpreted as predictions regarding the timing of a global economic collapse but as a risk assessment illustrating that current socio-economic developments and the environmental changes they cause entail a significant risk of historical discontinuities and persistent declines in living standards. The deep uncertainty regarding the nature, scale and velocity of global environmental change, coupled with the impossibility of excluding socio-technological developments that seem implausible in today's system, makes it impossible to state that a decline in global output is unavoidable or that it would necessarily prove harmful or catastrophic. There always exists a possibility to change model parameters in a way as to avoid a 'collapse' during the 21st century, as shown, for example, in our simulations where climate impacts are negligible. Nevertheless, using a system dynamics model representing key feedback mechanisms between the global socio-economic and environmental system, we show that an end to global economic growth and a persistent decline during the 21st century is a possibility that should not be underestimated. Assuming this possibility means acknowledging that 'business as usual' will cease to work within the next 20 to 50 years, and that even a complete 'greening' of the electricity sector is insufficient to avoid limits to growth, given that all simulated scenarios include a shift to 100% renewable electricity by 2100.

From the perspective of economic, social and environmental policy design, our results raise several questions for scholars and policymakers in the coming decades: How can investment in key sectors and critical infrastructure be maintained during a prolonged global recession? Which international social policies can alleviate the spread of poverty implied by a persistent output decline? How can low-carbon provisioning systems deliver essential services without depending on growth? Which adaptation measures can mitigate heat- and weather-related impacts on labor productivity? Which policies foster the resilience and flexibility of production structures? Our results therefore highlight the importance of building bridges between the academic fields of post-growth (Burke, 2022; Kallis et al., 2025), resilience (Cumming & Peterson, 2017; Stanley, 2020) and climate vulnerability, impacts and adaptation (IPCC, 2022) to address these questions in an integrated way.

Not confounding our scenario analysis with probability-based predictions is crucial, as our simulations omit feedback mechanisms that could further constrain growth, and thus tend to underestimate historical discontinuities. Missing biophysical dynamics include the adverse impacts of crossing non-climate Earth system boundaries (Rockström et al., 2023), the limited availability of mineral resources (Sverdrup & Ragnarsdóttir, 2014) and limits to land productivity gains caused by soil depletion (DeLong et al., 2015; Shrivastava & Kumar, 2015; Wang et al., 2024), desertification (Ahmed et al., 2024; Cherlet et al., 2018) or scarcity of chemical fertilizers (Penuelas et al., 2023). Section 2 SM1 shows the ratio between land demanded by the economy and disposable land—i.e., the Earth's habitable land without water bodies—for 12 scenarios. Under constant land intensities, land demand surpasses disposable land in all scenarios, with maximum demand between 1.1 and 4 times total disposable land. Thus, unless rapid and persistent land productivity gains are assumed for the forestry, biomass and food sectors, limited habitable land could prove a key constraint to growth, influencing the entire economy through inter-industry linkages. Integrating biosphere and land-related limits becomes even more important in scenarios with stronger bioenergy-based decarbonization (Braun et al., 2025). On the social side, the model cannot represent geopolitical conflicts, migration, eroding institutional stability, civil wars or the global financial system—all elements of a polycrisis that could accelerate declines in output (Scheffran, 2025).

Despite these limitations, our simulations enrich the literature on quantitative modeling of socio-economic and environmental dynamics. By modeling labor availability as an endogenous variable dependent on demographic, economic and biophysical developments, we show the importance of labor as a potential limiting factor of economic growth. In our scenarios, it is not the absolute scarcity of resources or abstract environmental pollution that impairs production, but the simultaneous increase in labor demand and decline in labor supply driven by environmental degradation and resource depletion. Our model thus reflects that labor productivity growth depends on exergy (Furse, 2025) and that insufficient exergy can trigger collapse dynamics driven by falling labor productivity and falling resource extraction. At the same time, such dynamics could induce societal and economic restructuring processes altering simulated trajectories. Although our model grants labor a more central role in the LTG debate, uncertainty about sectoral labor productivity developments warrants further research—e.g., via simulations with differing assumptions about productivity drivers. Another contribution lies in modeling the differentiated impacts of global output decline on sub-global consumption levels. Our simulations show increased poverty risks for poorer classes and regions—the majority of the world's population—even under optimistic assumptions of economic convergence during decline. Future work could explore whether early radical convergence reduces the spread of poverty, and whether divergence under unintended degrowth amplifies risks for systemic collapse, economic instability and extreme poverty driven by polarization triggered by emerging limits to growth.

Conclusion

In this study, we simulated 120 scenarios depicting non-linear developments in the global socio-economic and biophysical system throughout the 21st century. The results suggest that, under plausible assumptions about key variables, global economic output is likely to peak and subsequently decline within this century. Continued growth beyond 2100 occurs only under the highly improbable condition of no climate impacts combined with medium or high fossil resource availability.

These findings indicate that a 'business-as-usual' pathway is not viable: long-term global poverty eradication through economic growth alone cannot be achieved. As limits to growth emerge, the world will likely face declining consumption, rising poverty, depleted fossil resources, and a destabilized climate system constraining human development for millennia (Levermann et al., 2013; Xu et al., 2020). While the model cannot capture societal responses to these emerging limits, our simulations point to a high risk of distributive conflict within and between societies as consumption levels fall across all social classes. How such conflicts might unfold or be resolved lies beyond the scope of this scenario analysis.

References

- Abbot, D. S., & Malani, A. (2025). Revisiting the physical limits to economic growth, with a focus on the waste heat limit. *PLOS ONE*, 20(3), e0319217. <https://doi.org/10.1371/journal.pone.0319217>
- Ahmed, Z., Gui, D., Abd-Elmabod, S. K., Murtaza, G., & Ali, S. (2024). An overview of global desertification control efforts: Key challenges and overarching solutions. *Soil Use and Management*, 40(4), e13154. <https://doi.org/10.1111/sum.13154>
- Ansell, T., & Cayzer, S. (2018). Limits to growth redux: A system dynamics model for assessing energy and climate change constraints to global growth. *Energy Policy*, 120, 514–525. <https://doi.org/10.1016/j.enpol.2018.05.053>
- BGR. (2020). *BGR Energy Study 2019 – Data and Developments Concerning German and Global energy supplies*. Hannover. https://www.bgr.bund.de/EN/Themen/Energie/Downloads/energiestudie_2019_en.pdf;jsessionid=ADF18B2529B3E89FC705FDF390A57BA4.internet002?__blob=publicationFile&v=6
- Braun, J., Werner, C., Gerten, D., Stenzel, F., Schaphoff, S., & Lucht, W. (2025). Multiple planetary boundaries preclude biomass crops for carbon capture and storage outside of agricultural areas. *Communications Earth & Environment*, 6(1), 102.
- Bull, B., & Aguilar-Støen, M. (2023). Introduction to Handbook on International Development and the Environment: From limits to growth to a transformation for the Anthropocene. In B. Bull & M. Aguilar-Støen (Eds.), *Handbook on International Development and the Environment* (pp. 1–24). Edward Elgar Publishing. <https://doi.org/10.4337/9781800883789.00007>
- Burke, M. J. (2022). Post-growth policies for the future of just transitions in an era of uncertainty. *Futures*, 136, 102900.
- Butler, C. D. (2024). Bioethics, climate change, and civilization. *The Journal of Climate Change and Health*, 18, 100329. <https://doi.org/10.1016/j.joclim.2024.100329>
- Capellán-Pérez, I., Arto, I., Polanco-Martínez, J. M., González-Eguino, M., & Neumann, M. B. (2016). Likelihood of climate change pathways under uncertainty on fossil fuel resource availability. *Energy & Environmental Science*, 9(8), 2482–2496. <https://doi.org/10.1039/C6EE01008C>
- Capellán-Pérez, I., de Blas, I., Nieto, J., de Castro, C., Miguel, L. J., Carpintero, Ó., Mediavilla, M., Lobejón, L. F., Ferreras-Alonso, N., & Rodrigo, P. (2020). MEDEAS: a new modeling framework integrating global biophysical and socioeconomic constraints. *Energy & Environmental Science*, 13(3), 986–1017.
- Capellán-Pérez, I., Mediavilla, M., de Castro, C., Carpintero, Ó., & Miguel, L. J. (2015). More growth? An unfeasible option to overcome critical energy constraints and climate change. *Sustainability Science*, 10(3), 397–411.
- Cassen, C., & Cointe, B. (2022). From The Limits to Growth to Greenhouse Gas Emissions Pathways: Technological Change in Global Computer Models (1972–2007). *Contemporary European History*, 31(4), 610–626. <https://doi.org/10.1017/S096077732200042X>
- Cherlet, M., Hutchinson, C., Reynolds, J., Hill, J., Sommer, S., & von Maltitz, G. (2018). *World Atlas of Desertification*. Publication Office of the European Union. https://wad.jrc.ec.europa.eu/sites/default/files/atlas_pdf/JRC_WAD_fullVersion.pdf
- Cumming, G. S., & Peterson, G. D. (2017). Unifying research on social–ecological resilience and collapse. *Trends in Ecology & Evolution*, 32(9), 695–713.

- Dankers, R., & Kundzewicz, Z. W. (2020). Grappling with uncertainties in physical climate impact projections of water resources. *Climatic Change*, 163(3), 1379–1397.
- DeLong, C., Cruse, R., & Wiener, J. (2015). The Soil Degradation Paradox: Compromising Our Resources When We Need Them the Most. *Sustainability*, 7(1), 866–879.
<https://doi.org/10.3390/su7010866>
- Döring, T., & Aigner-Walder, B. (2022). The Limits to Growth—50 Years Ago and Today. *Intereconomics*, 57(3), 187–191. <https://doi.org/10.1007/s10272-022-1046-5>
- Frisch, M. (2018). Modeling Climate Policies: The Social Cost of Carbon and Uncertainties in Climate Predictions. In E. A. Lloyd & E. Winsberg (Eds.), *Climate Modelling* (pp. 413–448). Springer International Publishing. https://doi.org/10.1007/978-3-319-65058-6_14
- Furse, S. (2025). *Are there biophysical limits to technical change? A review of societal exergy analysis and ecological macroeconomics*.
- Gambhir, A., Mittal, S., Lamboll, R. D., Grant, N., Bernie, D., Gohar, L., Hawkes, A., Köberle, A., Rogelj, J., & Lowe, J. A. (2023). Adjusting 1.5 degree C climate change mitigation pathways in light of adverse new information. *Nature Communications*, 14(1), 5117.
<https://doi.org/10.1038/s41467-023-40673-4>
- Gómez-Baggethun, E., & Naredo, J. M. (2015). In search of lost time: The rise and fall of limits to growth in international sustainability policy. *Sustainability Science*, 10(3), 385–395.
- Grondona, A. (2024). Latin American World Model: A Third-World Voice to Face Limits to Growth. *The Journal of Imperial and Commonwealth History*, 52(6), 1003–1031.
<https://doi.org/10.1080/03086534.2024.2444997>
- Gulyayeva, N., Bhardwaj, E., & Becker, C. (2025). *Exploring the Viability of the Updated World3 Model for Examining the Impact of Computing on Planetary Boundaries* (Version 1). arXiv. <https://doi.org/10.48550/ARXIV.2510.07634>
- Heath, A. W., Stappenhelt, B., & Ros, M. (2019). Uncertainty analysis of the Limits to Growth model: Sensitivity is high, but trends are stable. *GAIA - Ecological Perspectives for Science and Society*, 28(3), 275–283. <https://doi.org/10.14512/gaia.28.3.8>
- Herrington, G. (2021). Update to limits to growth: Comparing the World3 model with empirical data. *Journal of Industrial Ecology*, 25(3), 614–626.
- Higgs, K. (2022). A Brief History of The Limits to Growth Debate. In S. J. Williams & R. Taylor (Eds.), *Sustainability and the New Economics* (pp. 123–136). Springer International Publishing. https://doi.org/10.1007/978-3-030-78795-0_8
- Höök, M., & Tang, X. (2013). Depletion of fossil fuels and anthropogenic climate change—A review. *Energy Policy*, 52, 797–809. <https://doi.org/10.1016/j.enpol.2012.10.046>
- IEA. (2021). *Key World Energy Statistics 2021*. IEA. <https://www.iea.org/reports/key-world-energy-statistics-2021>
- IPCC. (2021). *Climate Change 2021: The Physical Science Basis. Contribution of Working Group I to the Sixth Assessment Report of the Intergovernmental Panel on Climate Change*. Cambridge University Press. Cambridge University Press, Cambridge, UK and New York, NY, USA.,
- IPCC. (2022). *Climate Change 2022: Impacts, Adaptation and Vulnerability. Contribution of Working Group II to the Sixth Assessment Report of the Intergovernmental Panel on Climate Change*. Cambridge University Press. Cambridge University Press, Cambridge, UK and New York, NY, USA.,
- Jackson, T., & Webster, R. (2017). Limits to Growth revisited. In C. Deeming & P. Smyth (Eds.), *Reframing Global Social Policy* (pp. 295–322). Policy Press.
<https://doi.org/10.51952/9781447332503.ch013>
- Jones, P. (2022). *Limits to growth at 50 Years: Reframing the predicament*. Proceedings of relating systems thinking and design 2022 SYMPOSIUM (RSD11).

- Kallis, G., Hickel, J., O'Neill, D. W., Jackson, T., Victor, P. A., Raworth, K., Schor, J. B., Steinberger, J. K., & Ürge-Vorsatz, D. (2025). Post-growth: The science of wellbeing within planetary boundaries. *The Lancet Planetary Health*, 9(1), e62–e78.
- Khorsandi, M., Omidi, T., & van Oel, P. (2023). Water-related limits to growth for agriculture in Iran. *Heliyon*, 9(5).
- Krupa, J., & Jones, C. (2013). Black Swan Theory: Applications to energy market histories and technologies. *Energy Strategy Reviews*, 1(4), 286–290.
<https://doi.org/10.1016/j.esr.2013.02.004>
- Lauer, A., & Llases, L. (2025). *MORDRED: Model Of Resource Distribution and Resilient Economic Development. Model Documentation*. GitHub. <https://github.com/Pendracus/MORDRED>
- Lenton, T. M., Benson, S., Smith, T., Ewer, T., Lanell, V., Petykowski, E., Powell, T. W., Abrams, J. F., Blomsma, F., & Sharpe, S. (2022). Operationalising positive tipping points towards global sustainability. *Global Sustainability*, 5, e1.
- Levermann, A., Clark, P. U., Marzeion, B., Milne, G. A., Pollard, D., Radic, V., & Robinson, A. (2013). The multimillennial sea-level commitment of global warming. *Proceedings of the National Academy of Sciences*, 110(34), 13745–13750.
<https://doi.org/10.1073/pnas.1219414110>
- Lifi, M., de Blas, I., Capellan-Perez, I., Mediavilla, M., Miguel, L. J., Parrado-Hernando, G., Llases, L., Álvarez-Antelo, D., Calleja, M., Wergles, N., Ferreras, N., Ramos, I., Arto, I., Calheiros, T., Capela Lourenco, T., Morlin, G., D'Alessandro, S., van Allen, O., Eggler, L., ... Oakes, R. (2023). *Synthesis of the model, selected results, and scenario assessment. WP9, Task 9.2, D.9.3. LOCOMOTION*. <https://zenodo.org/records/10813034>
- Meadows, D. H., Meadows, D. L., & Randers, J. (1992). *Beyond the limits: Global collapse or a sustainable future*. Earthscan Publications Ltd.
- Meadows, D. H., Meadows, D., Randers, J., & Behrens, W. W. (1972). *The limits to growth. A report for the Club of Rome's Project on the Predicament of Mankind*. Universe Books.
- Meadows, D. H., Randers, J., & Meadows, D. (2004). *The limits to growth: The 30-year update*. Chelsea Green Publishing Company.
- Miraux, L. (2022). Environmental limits to the space sector's growth. *Science of The Total Environment*, 806, 150862. <https://doi.org/10.1016/j.scitotenv.2021.150862>
- Murphy, T. W. (2022). Limits to economic growth. *Nature Physics*, 18(8), 844–847.
<https://doi.org/10.1038/s41567-022-01652-6>
- Nebel, A., Kling, A., Willamowski, R., & Schell, T. (2024). Recalibration of limits to growth: An update of the World3 model. *Journal of Industrial Ecology*, 28(1), 87–99.
<https://doi.org/10.1111/jiec.13442>
- Pasqualino, R., Monasterolo, I., & Jones, A. (2019). An Integrated global food and energy security system dynamics model for addressing systemic risk. *Sustainability*, 11(14), 3995.
- Penuelas, J., Coello, F., & Sardans, J. (2023). A better use of fertilizers is needed for global food security and environmental sustainability. *Agriculture & Food Security*, 12(1), 5.
<https://doi.org/10.1186/s40066-023-00409-5>
- Richards, C. E., Gauch, H. L., & Allwood, J. M. (2023). International risk of food insecurity and mass mortality in a runaway global warming scenario. *Futures*, 150, 103173.
<https://doi.org/10.1016/j.futures.2023.103173>
- Rockström, J., Gupta, J., Qin, D., Lade, S. J., Abrams, J. F., Andersen, L. S., Armstrong McKay, D. I., Bai, X., Bala, G., Bunn, S. E., Ciobanu, D., DeClerck, F., Ebi, K., Gifford, L., Gordon, C., Hasan, S., Kanie, N., Lenton, T. M., Loriani, S., ... Zhang, X. (2023). Safe and just Earth system boundaries. *Nature*, 619(7968), 102–111. <https://doi.org/10.1038/s41586-023-06083-8>

- Scheffran, J. (2023). Limits to the Anthropocene: Geopolitical conflict or cooperative governance? *Frontiers in Political Science*, 5, 1190610. <https://doi.org/10.3389/fpos.2023.1190610>
- Scheffran, J. (2025). Planetary Boundaries, Polycrisis and Politics in the Anthropocene: Climate Pathways, Tipping Cascades and Transition to Sustainable Peace in Integrative Geography. In H. G. Brauch (Ed.), *Towards Rethinking Politics, Policy and Polity in the Anthropocene* (Vol. 35, pp. 339–444). Springer Nature Switzerland. https://doi.org/10.1007/978-3-031-71807-6_8
- Shrivastava, P., & Kumar, R. (2015). Soil salinity: A serious environmental issue and plant growth promoting bacteria as one of the tools for its alleviation. *Saudi Journal of Biological Sciences*, 22(2), 123–131. <https://doi.org/10.1016/j.sjbs.2014.12.001>
- Smith, A., & Ely, A. (2025). From Limits to Growth to Post-growth: The International Politics of Technology in Historical Perspective. *Science, Technology and Society*, 30(2), 230–258. <https://doi.org/10.1177/09717218251326833>
- Stadler, K., Wood, R., Bulavskaya, T., Södersten, C., Simas, M., Schmidt, S., Usubiaga, A., Acosta-Fernández, J., Kuenen, J., Bruckner, M., Giljum, S., Lutter, S., Merciai, S., Schmidt, J. H., Theurl, M. C., Plutzar, C., Kastner, T., Eisenmenger, N., Erb, K., ... Tukker, A. (2018). EXIOBASE 3: Developing a Time Series of Detailed Environmentally Extended Multi-Regional Input-Output Tables. *Journal of Industrial Ecology*, 22(3), 502–515. <https://doi.org/10.1111/jiec.12715>
- Stanley, C. (2020). Living to spend another day: Exploring resilience as a new fourth goal of ecological economics. *Ecological Economics*, 178, 106805.
- Stoknes, P. E., Collste, D., E. Cornell, S., Callegari, B., Spittler, N., Gaffney, O., & Randers, J. (2025). The Earth4All scenarios: Human wellbeing on a finite planet towards 2100. *Global Sustainability*, 8, e22. <https://doi.org/10.1017/sus.2025.10013>
- Sverdrup, H. U., & Ragnarsdóttir, K. V. (2014). Natural resources in a planetary perspective. *Geochemical Perspectives*, 3(2), 129–130.
- Turner, G. (2008). A comparison of The Limits to Growth with 30 years of reality. *Global Environmental Change*, 18(3), 397–411. <https://doi.org/10.1016/j.gloenvcha.2008.05.001>
- Turner, G. (2014). Is global collapse imminent? An updated comparison of the Limits to Growth with historical data. *MSSI Research Paper*, 4, 21.
- UN DESA. (2019a). *World Population Prospects 2019, Online Edition. Rev. 1. File FERT/7: Age-specific fertility rates by region, subregion and country, 1950-2100 (births per 1,000 women)*, WPP2019_FERT_F07_AGE_SPECIFIC_FERTILITY.xlsx. This data gives age-specific fertility rates for 7 age categories (15-19, 20-24, ..., 45-49).
- UN DESA. (2019b). *World Population Prospects 2019, Online Edition. Rev. 1. File MORT/4-1: Deaths (both sexes combined) by five-year age group, region, subregion and country, 1950-2100 (thousands)*, WPP2019_MORT_F04_1_DEATHS_BY_AGE_BOTH_SEXES.xlsx.
- UN DESA. (2019c). *World Population Prospects 2019, Online Edition. Rev. 1. File POP/7-1: Total population (both sexes combined) by five-year age group, region, subregion and country, 1950-2100 (thousands)*.
- Valero, A., Valero, A., Calvo, G., & Ortego, A. (2018). Material bottlenecks in the future development of green technologies. *Renewable and Sustainable Energy Reviews*, 93, 178–200.
- Van Den Bergh, J. C. J. M. (2017). A third option for climate policy within potential limits to growth. *Nature Climate Change*, 7(2), 107–112. <https://doi.org/10.1038/nclimate3113>

- Vieille Blanchard, E. (2010). Modelling the Future: An Overview of the 'Limits to Growth' Debate. *Centauros*, 52(2), 91–116. <https://doi.org/10.1111/j.1600-0498.2010.00173.x>
- Wang, C., Xie, Y., & Tan, Z. (2024). Soil potassium depletion in global cereal croplands and its implications. *Science of The Total Environment*, 907, 167875. <https://doi.org/10.1016/j.scitotenv.2023.167875>
- Wyser, K., Van Noije, T., Yang, S., Von Hardenberg, J., O'Donnell, D., & Döscher, R. (2020). On the increased climate sensitivity in the EC-Earth model from CMIP5 to CMIP6. *Geoscientific Model Development*, 13(8), 3465–3474. <https://doi.org/10.5194/gmd-13-3465-2020>
- Xu, C., Kohler, T. A., Lenton, T. M., Svenning, J.-C., & Scheffer, M. (2020). Future of the human climate niche. *Proceedings of the National Academy of Sciences*, 117(21), 11350–11355. <https://doi.org/10.1073/pnas.1910114117>

Supplementary Material 1

1. Boundary conditions

The following boundary conditions are common to all scenarios that have been simulated.

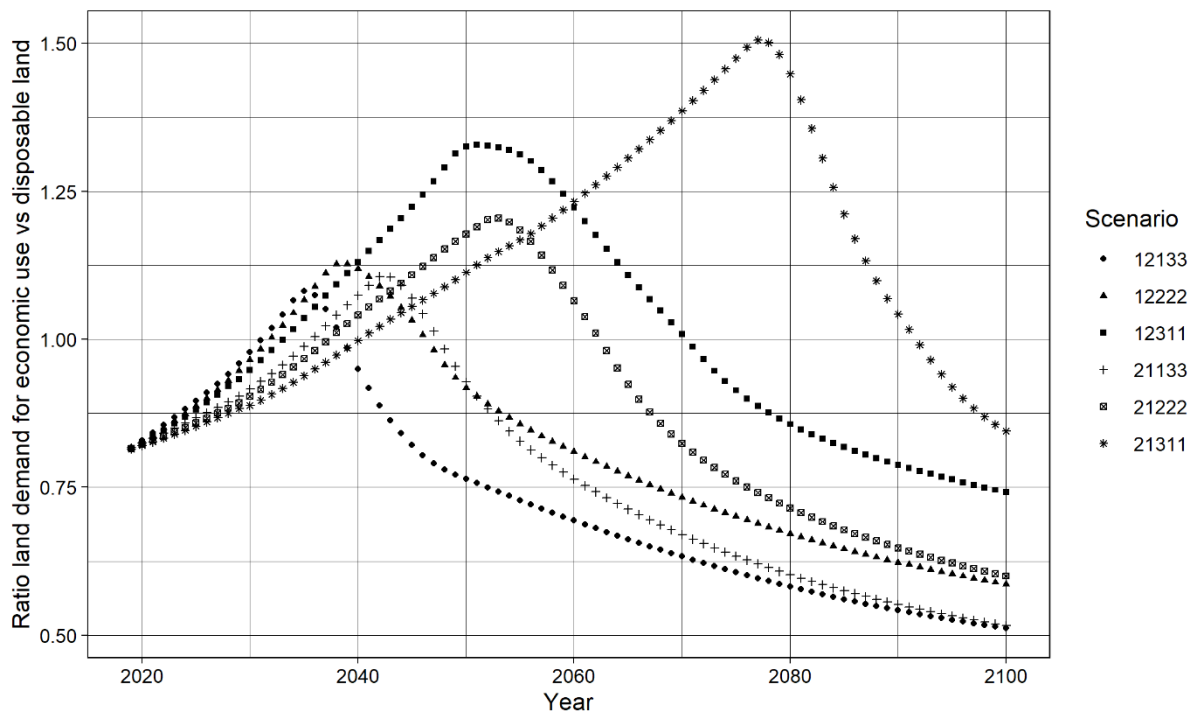
- *Demographic module*: Model default parameters adopted
- *Stressor module*: Reduction of target greenhouse gas emission intensity of 30% by 2100 for all types of greenhouse gases (CO₂, CH₄, N₂O, SF₆, HFC, PFC).
- *Land module*: Constant land intensities, default model values for remaining land parameters, land scarcity factor deactivated, which allows output to grow independent from the availability of demanded land types.
- *Labor module*: Default model values for annual working hours (2080 hours) and maximum participation rate (95%).
- *Economic module*: constant capital intensities; target consumption vector for public consumption, private consumption and GFCF: complete substitution of fossil and nuclear electricity by solar, wind and hydropower by 2100; target consumption vector corresponding to households with low consumption levels: share of food sector reduced by 20%; 10% shifted to service sector, 10% shifted to industry sector; A-Matrix: complete substitution of fossil and nuclear electricity by solar, wind and hydropower by 2100; energy efficiency improvements in industrial processes by 2100: 5% in all processes across all sectors; moderate electrification and efficiency gains in the fossil resources, bioenergy, electricity, industry, manufacturing, services, chemical, transport and renewable waste sectors; convergence in consumption

For convergence processes, the relative consumption multipliers have been specified to decrease from 46:1 to 8:1 (R20C to P30P class) in 2100 for low consumption growth scenarios, to 6:1 for medium consumption growth scenarios, and to 6.5:1 for high consumption growth scenarios.

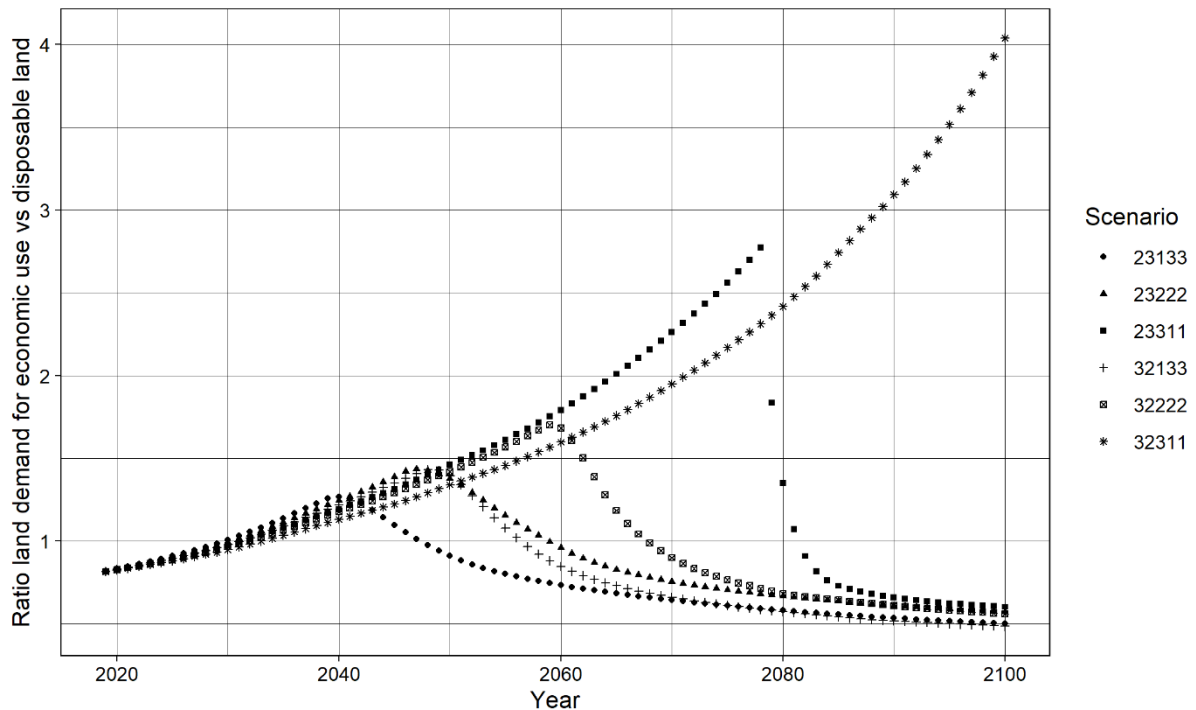
2. Land demand and disposable land

Suppl. Figure 1 and Suppl. Figure 2 show the evolution of the ratio between the amount of land required for economic production under constant land intensities (i.e. at the level of 2019) and the maximum land supply that depends on the size of habitable land, which is reduced by climate change impacts. Results are shown for 12 of the 120 simulated

scenarios.



Suppl. Figure 1: Ratio between land demanded for economic production and maximum land supply during the simulations for six scenarios with low labor productivity or low consumption growth (12133, 12222, 12311, 21133, 21222, 21311).



Suppl. Figure 2: Ratio between land demanded for economic production and maximum land supply during the simulations for six scenarios with high labor productivity or high consumption growth (23133, 23222, 23311, 32133, 32222, 32311).

Modeling Systemic Climate Damage Interactions in an Input-Output Integrated Assessment Framework

Highlights

- Framework to represent environmental damages in input-output models
- Simulation of multiple climate damage scenarios in the MORDRED-IAM
- Climate impacts are found to slow down technological progress
- Importance of adverse climate change impacts on labor
- Scenarios integrating damages exhibit lower levels of economic growth and global warming

Abstract

We present a methodological framework to incorporating generic environmental damages in economic input-output models and apply the approach to the modeling of climate change impacts in an integrated assessment model, considering potential adverse climate impacts on capital, labor, and land. We simulate multiple climate damage scenarios and compare them with a reference pathway to examine economy-climate feedbacks and interactions across damage types. Incorporating climate impacts substantially alters 21st-century economic output, emission and temperature trajectories, generally reducing world output while moderating global temperature increases in scenarios that include all parametrized damages. Assumptions regarding future labor productivity developments and the severity of adverse climate impacts significantly influence simulation outcomes, with endogenously changing labor productivities and higher impact severity being linked to an earlier peak of world output and a lower degree of climate change. Climate impacts are found to slow down improvements in the greenhouse gas intensity of economic activities, while climate-change-induced increases in land intensities can elevate emissions from land-use changes. Higher rates of capital depreciation may paradoxically stimulate economic activity while lowering consumption. Labor-related damages exert the strongest individual effect on economic development; however, the combination of output-, capital-, and labor-related damages results in a strong, non-linear effect on world economic output absent in scenarios that only feature isolated damage types. Thus, assessing climate damages in isolation can substantially underestimate their systemic effects on both economic activity and emissions.

Keywords

Climate change damages; input-output models; Integrated Assessment Models; climate change scenarios; system dynamics; global environmental change

1. Introduction

The quantitative modeling of damages on the global economy resulting from environmental degradation and the transgression of planetary boundaries supports the design of effective and efficient policies and informs the emerging legal 'loss and damage' framework under the UNFCCC [1], [2]. Integrated Assessment Models (IAMs)—such as optimal growth models, computable general equilibrium models (CGEMs), energy-system models, or macroeconometric models [3] have a decades-long history of projecting economic climate impacts and currently dominate quantitative climate change research [4]. Although these IAMs differ in structure and employ various methods to estimate adverse economic impacts, they generally rely on damage functions that vary with changes in global mean temperature [5], [6].

Complementing these established IAM types, a growing number of quantitative models have been developed to represent interactions among environmental, economic, and energy systems and the resulting economic damages. These models are built with alternative economic theories and modeling techniques such as stock-flow consistent models [7], [8], system dynamics models [9], [10], [11] or life-cycle impact assessment (LCIA) models [12]. These alternative IAMs provide valuable insights by examining climate-related financial risks, mineral and energy resources as well as non-climate damages.

The rise of new IAMs departing from neoclassical climate economics assumptions can also be explained by the methodological weaknesses underpinning damage assessments in frequently used IAMs—such as DICE, FUND or PAGE—which continue to shape policy development [13]. Criticisms include the insufficient consideration of epistemic, ethical and political dimensions of uncertainty in IAM-based modeling exercises [14]; a lack of genuine complexity within the models; the use of discount rates and overly optimistic assumptions regarding technological development [15]; the neglect of climate tipping points, the assumption that economic sectors not exposed to the weather are unaffected by climate change, and methodological inconsistencies in the estimation and representation of damages [13]. This results in damage assessments predicting only a 5.3 – 13.8% GDP loss at 7.4 – 8.6 °C of global warming relative to the pre-industrial period [5], which stands in stark contrast to scientists' dire warnings of a climate emergency [16] and the numerous already observable and projected losses and damages enumerated by the IPCC's WG II [17]. Even with updated damage parameters, the FUND model still estimates losses of only 2.82% of GDP in 2100 under a business-as-usual scenario [18].

This paper seeks to address some of the current methodological issues in modeling environmental damages to economic structures while contributing to the dynamically expanding field of non-neoclassical IAMs. It does so by modeling and exploring climate change damages in the MORDRED model, an IAM of medium complexity built on environmentally and socially extended input-output data [19]. Although the potential of combining environmentally extended input-output analysis [20] with integrated assessment modeling for studying multi-dimensional sustainability impacts, demand-side solutions and post-growth climate mitigation scenarios has been recognized [21], to the best of our knowledge, no IAM has yet been developed that draws on holistic input-output-based damage modeling.

Accordingly, this work pursues three research objectives:

- (1) the development of a new methodological framework that facilitates the systematic representation of environmental impacts in input-output models;
- (2) the application of this framework to model climate damages within an IAM; and

(3) the simulation of different ‘damage scenarios’ and the analysis of key model dynamics.

In line with these objectives, the remainder of this article is structured as follows: in the next section, we introduce the new framework for the representation of environmental impacts in input-output models and describe its application to the incorporation of climate damages in MORDRED. Subsequently, we explore the resulting model dynamics through a scenario simulation exercise. We conclude by discussing the merits and the limits of our approach, and by outlining directions for future work.

2. Methodology

2.1. Representation of damages in an input-output framework

In input-output (IO) modeling, economic processes are represented by Leontief production functions, which are characterized by the strict non-substitutability of productive factors [22]. In other words, the production of one unit of any good requires a fixed combination of inputs, and no factor can be reduced by increasing the use of another. For instance, labor cannot be substituted for capital, nor can materials be substituted by labor. Within this framework, technological change is represented as variations in the quantity of inputs required per unit of output. At any given point in time, however, the parameters of the production function remain fixed, and the condition of non-substitutability continues to hold.

In a multisectoral economy, the parameters of the Leontief production function can be expressed through a matrix and a set of intensity vectors:

- Input-output matrix (A matrix): each column indicates the quantity of inputs from each sector required to produce one unit of output in the corresponding sector.
- Labor intensity vector: each element represents the amount of labor necessary to produce one unit of sectoral output.
- Capital intensity vector: each element corresponds to the necessary stock of capital to produce one unit of sectoral output.

In an environmentally extended IO framework, biophysical input factors also enter the production function as intensity vectors. For example, a land (water, material, ...) intensity vector denotes the amount of land (water, material, ...) required to generate one unit of sectoral output. Equally, a pollution intensity vector contains information on the amount of pollution generated per unit of sectoral output.

Consequently, in an IO framework, adverse impacts from global environmental change can be represented via variations in (i) the intensities of intermediate or primary inputs (labor, capital, land, ...), and (ii) the available stock of primary inputs.

When damages alter input intensities, greater quantities of inputs are required to produce the same unit of output. For example, as mineral deposits and fossil resources become depleted, the extraction of a given quantity of material requires more inputs, which amounts to a change in the columns of the A matrix that represent the extraction sectors. Depending on the extraction method, the same process may also require more labor which would result in a change in the labor intensity vector. Likewise, additional machinery or capital stock may be needed, increasing the values of the capital intensity vector. Equally, declining soil productivity leads to a higher land demand per unit of agricultural output, i.e. a change in the land intensity vector. Thus,

increases in input intensities can be interpreted as an environmentally induced reversal of technological progress.

Alternatively, adverse environmental impacts may affect the availability of primary inputs. For labor, this can occur through two channels: a reduction in the number of workers (due to incapacity or mortality) or a reduction in working time, since total labor supply in a given period is the product of the number of workers and the hours worked. For capital, damages take the form of destruction of capital stock within a given sector, either as a discrete loss linked to a specific period of time, or as an increase in depreciation. Capital destruction in the aftermath of a flood would exemplify the former, while a reduction in the useful life of equipment due to extreme temperatures would manifest as a higher depreciation rate. For land, damages correspond to a reduction in the stock of land available for productive purposes.

Last, a part of sectoral output itself can be lost due to environmental impacts, which is modeled as an indirect increase in the factor intensity of production.

Table 1 summarizes the relevant variables in an IO model that change in respond to environmental damages.

Variable	Unit
<i>Input-output matrix A</i>	$\text{€}/\text{€}$
<i>Labor intensity vector</i>	$h/\text{€}$
<i>Capital intensity vector</i>	$\text{€}\cdot\text{year}/\text{€}$
<i>Environmental intensity vector (land, material, energy...)</i>	$(ha, kt, EJ...)\cdot\text{year}/\text{€}$
<i>Working time</i>	$h/(\text{worker}\cdot\text{year})$
<i>Labor force</i>	<i>workers</i>
<i>Capital stock</i>	€
<i>Environmental stocks (land, resources...)</i>	ha, kt, \dots

Table 1: Key variables within an input-output framework affected by environmental damages.

2.2. Realization in MORDRED

We applied the methodological framework to MORDRED (Model Of Resource Distribution and Resilient Economic Development) because the representation of the world economy in this model draws heavily on IO data and includes all relevant variables listed in Table 1.

2.2.1. Model summary

Mordred is a system dynamics model that represents broad socio-economic dynamics at a global scale and their relationship with the environment. The model consists of several coupled modules that focus on specific aspects of the world system such as demographic and economic developments as well as the consequences of the former on the demand for, and supply of, labor, land and energy, and on material extraction, pollution and the climate system.

The demographic module projects the evolution of the world population, which is divided into three regions: the center (i.e. the high-income countries), semi-periphery (upper-middle-income countries), and periphery (lower-middle- and low-income countries). Demographic changes are driven by birth and death rates, which are mainly influenced by per capita consumption levels across different regions and social classes within MORDRED. The demographic module also accounts for populations living in subsistence conditions at the margins of the global economy.

For each world region, migration between the subsistence and the world economy is modeled as a function of the difference in consumption between the poorest class and the subsistence class.

The economic module calculates the volume of goods and services produced in the economy and their distribution across regions and social classes. For the former it uses an IO framework in which the global economy is divided into 25 sectors, including the food, industry, services and mineral extraction sector, as well as different energy sectors. For the latter, in every world region, the population living outside the subsistence regime is divided into three social classes: The wealthiest 20%, the poorest 30% and the middle 50%.

For its calculations, the model relies on exogenously defined desired growth rates in per capita consumption for each class and region. Government consumption is defined as a fixed percentage of household consumption, while investment evolves endogenously as a function of the quantity of capital goods required for production. During the model simulation, actual output of goods and services may not match demand, as the former is constrained by the availability of labor, energy, labor and land.

The labor module projects the changes in the available workforce that depend on changes in the demographic module and imposes an upper limit on production capacity while the energy module calculates the total energy demanded by the system and tracks the increasing depletion of fossil resources. The land module compares land demand with supply and allocates available land between different land uses. Availability of land is primarily driven by land intensities.

The climate module is a greatly simplified and adapted version of the climate model contained in the WILIAM-IAM [23]. It calculates changes in the carbon cycle and in global average temperatures as a consequence of different greenhouse gas emission pathways.

An exhaustive description of MORDRED is available in Lauer & Llases [24]. A GitHub repository [25] provides information on different model versions and the 25 sectors of the model that were aggregated from EXIOBASE3 [19].

2.2.2. Introduction of climate damages

We applied the methodological framework to the representation of climate change damages.

In the model, climate impacts evolve as functions of global average temperature change relative to the pre-industrial (1850) period.

$$\Delta Temp = Temp(t) - Temp(1850) \quad (1)$$

We include potential climate damages in the economic, labor and land module.

In the economy module, capital stock and intensity are assumed to be affected by climate-change-induced increases in extreme weather events and sea-level rise.

Extreme weather events including droughts, floods, storms, wildfires and heatwaves are assumed to increase the depreciation rate of the capital stock in all sectors as global average temperature rises. A minimum and a maximum estimate for the annual global damage in capital stock at 4 °C degree of warming was made based on damage estimates for the US in the period 2010-2019 [26] and for Europe in the period 1981-2020 [27] as well as projected increases in the intensity and frequency of extreme weather events given in IPCC WGI's contribution to the sixth assessment report [28]. Possible higher impacts of heatwaves [29] and droughts [30] in

world regions outside the US and Europe, as well as the non-linear effects of compound extreme weather events were taken into account through adjustment factors. The resulting damage range represents losses in a hypothetical world with 4°C of global warming and the capital stock of the USA in 2015. To distinguish between impacts in different sectors, the 25 sectors in MORDRED were categorized into 'high-exposure' sectors particularly affected by extreme weather impacts (such as the food, transportation and energy sectors [31], [32]) and 'low-exposure' sectors. 70% of the overall damage at 4 °C of global warming is assumed to affect all sectors while the rest of the damage is assumed to be concentrated in high-exposure sectors.

The ratio between capital stock lost at 4 °C of warming and total capital stock constitutes the additional extreme-weather-induced capital depreciation for each sector, with $\alpha_i = 0$ for the low-exposure sectors and 1 for the high-exposure sectors (2) (3). The lower and upper bound estimates for total damages result in a low and a high depreciation estimate.

$$\delta_i^{4^\circ C, min} = 0.7 \cdot \frac{\text{Total damages}_{min}}{\sum_{i=1}^{25} K_{US_{2015}i}} + \alpha_i \cdot 0.3 \frac{\text{Total damages}_{min}}{\sum K_{US_{2015}high\ exposure}} \quad (2)$$

$$\delta_i^{4^\circ C, max} = 0.7 \cdot \frac{\text{Total damages}_{max}}{\sum_{i=1}^{25} K_{US_{2015}i}} + \alpha_i \cdot 0.3 \frac{\text{Total damages}_{max}}{\sum K_{US_{2015}high\ exposure}} \quad (3)$$

$$\delta_i^{extreme_weather} = \delta_i^{4^\circ C} \cdot \left(\frac{(\Delta Temp - 1)^2}{9} \right) \quad (4)$$

Under a high emission scenario and/or antarctic instability, 4 - 7 % of the global population could live in areas flooded annually by the end of the century [33], [34]. We assume that population is directly correlated to the size of the capital stock, and that capital assets are more concentrated in coastal areas (e.g. ports, refineries etc.). Thus, we assume that 6 - 9% of the global capital assets could be threatened by annual flooding under a temperature increase of 4 °C. Additionally, we assume that half of the capital stock can be protected by hard coastal protection while the other half is lost due to a managed retreat of the population. This leads to an overall loss of 3 - 4.5% of global capital stock as global warming approaches the 4°C mark. Since these losses do not repeat after the population has resettled and new capital stock has been constructed elsewhere, sea-level-rise-induced losses are modeled as discrete events when certain temperature thresholds are exceeded (2°C, 3°C, and 4°C), following a Gaussian function and affecting all sectors' depreciation rates equally (5).

The additional costs linked to the construction of coastal protection is represented in the model as additional GFCF in the construction sector, which is contained in sector 5 and is estimated based on Hinkel et al. [33], considering the fact that a loss of coral reef protection due to temperature changes higher than 1.5 °C to 2 °C doubles the exposure of built capital and people to flooding [35] and assuming that the coastal protection has to be renewed once during the model simulation.

The overall effect of climate impacts on depreciation in a given sector and moment of time is obtained by adding the impacts from extreme weather events and sea-level-rise (6).

$$\delta_i^{slr} = \beta 0^{2^\circ C_slr} \cdot e^{-\left(\frac{(t-10-t^{2^\circ C})^2}{\beta 1^{2^\circ C_slr}}\right)} + \beta 0^{3^\circ C_slr} \cdot e^{-\left(\frac{(t-10-t^{3^\circ C})^2}{\beta 1^{3^\circ C_slr}}\right)} + \beta 0^{4^\circ C_slr} \cdot e^{-\left(\frac{(t-10-t^{4^\circ C})^2}{\beta 1^{4^\circ C_slr}}\right)} \quad (5)$$

$$\delta_i^{climate\ change} = \delta_i^{extreme_weather} + \delta_i^{slr} \quad (6)$$

Climate-change-induced increases in input coefficients are only considered for the agricultural sector, which is contained in MORDRED sector 1. We estimate the hypothetical share of output that is destroyed due to adverse effects of insect pests [36] and heat [37] for 4 °C of warming (7) which leads to an increase in the capital intensity without damage ($Int_1^{k,wod}$) (8) and increases the intensity of intermediate goods. The latter is modeled through multiplying the column in the A matrix corresponding to sector 1 with a factor α_{loss} (9), (10), (11).

$$X_loss_1 = (\alpha_{insects}^{4^{\circ}C} + \alpha_{heat}^{4^{\circ}C}) \cdot \left(\frac{\Delta Temp - 1}{3} \right) \quad (7)$$

$$Int_1^k = \frac{Int_1^{k,wod}}{(1 - X_loss_1)} \quad (8)$$

$$\alpha_{loss}^{4^{\circ}C} = \frac{1}{1 - X_loss_1} \quad (9)$$

$$\alpha_{loss} = \beta_0 loss + \beta_1 loss \cdot \Delta Temp + \beta_2 loss \cdot \Delta Temp^2 \quad (10)$$

$$a_{i,1} = a_{i,1} \cdot \alpha_{loss} \quad (11)$$

In the labor module, the maximum supply of labor hours depends on the size of the population that belongs to the global economy and is in the working age, the participation rate (Prt_r) and the annual working hours per person (12). Although the methodological framework contains the possibility of a reduction of the working force through environmental impacts, we assume no *direct* climate-change-induced changes in mortality rates, e.g. through the spread of vector- or water-borne diseases or the increase in natural disasters, given that the actual effect of those factors on mortality are strongly mediated by the socio-economic context [38], [39]. However, we assume that annual working hours can be negatively affected by increases in deadly heat. The share of working hours lost due to heat-related damage (HD^{Max_Lb}) depends on the share of days with deadly heat at 4°C of warming, estimated based on Mora et al. [40], as well as on the assumed share of workers whose ability to work is affected due to the deadly heat conditions (13).

$$Max_Lb = Pop_{15-64\ years} \cdot Prt_r \cdot \frac{annual\ working\ hours}{worker} \cdot (1 - HD^{Max_Lb}) \quad (12)$$

$$HD^{Max_Lb} = \frac{days_{deadly\ heat}}{days_{year}} \cdot \frac{workers_{affected}}{workers} \cdot \left(\frac{(\Delta Temp - 1)^2}{9} \right) \quad (13)$$

Additionally, we assume that global warming adversely affects labor productivity. Dasgupta et al. [41] find that for 3 °C of warming global effective labor, including both productivity and hours worked, decreases by 18% ($\alpha_{Lprod_{low}}$) for low-exposure and by 25% ($\alpha_{Lprod_{high}}$) for high exposure activities. Low-exposure working conditions are defined as work outside in the shade or indoors while high-exposure working conditions are defined as works outside with no shade. The MORDRED sectors were classified as having predominantly low- or high-exposure working conditions, resulting in sectors 1, 4 and 5 (food, mining, industry) being linked to high exposure

and the rest of the sectors to low exposure. Here, for simplicity, we assume that the losses apply solely to labor productivity. Thus, the sector and temperature dependent heat-related damage to labor productivity ($HD_i^{Lb_prod}$) is calculated according to equation (14) and (15). This damage factor leads to an increase in the original sectoral labor intensity without damage ($Int_i^{Lb,wod}$) (16). In sector 1, the destroyed output further increases the labor intensity (17) while in sector 3 and 8 an extraction difficulty factor (Edf) related to the depletion of fossil resources leads to a higher labor intensity as resources become more difficult to access (18).

$$HD_{i=\text{high exposure sectors}}^{Lb_prod} = \alpha_{Lprod\text{high}} \cdot \left(\frac{(\Delta Temp - 1)^2}{4} \right) \quad (14)$$

$$HD_{i=\text{low exposure sectors}}^{Lb_prod} = \alpha_{Lprod\text{low}} \cdot \left(\frac{(\Delta Temp - 1)^2}{4} \right) \quad (15)$$

$$Int_i^{Lb} = \frac{Int_i^{Lb,wod}}{(1 - HD_i^{Lb_prod})} \quad (16)$$

$$Int_1^{Lb} = \frac{Int_1^{Lb,wod}}{(1 - X_loss_1 - HD_1^{Lb_prod})} \quad (17)$$

$$Int_{3,8}^{Lb} = \frac{Int_{3,8}^{Lb,wod}}{(1 - HD_{3,8}^{Lb_prod})} \cdot Edf \quad (18)$$

For damages in the land model, we account for land losses due to sea-level rise, river floods, temperature and humidity change, based on estimates found in the literature [33], [42], [43], [44] (19). These damages reduce the amount of habitable land that can be used for economic purposes (20). In sector 1, there is an increase in the intensity of agricultural land use (21). Lastly, it is assumed that rising temperatures and the increasing severity and frequency of extreme weather events linearly reduce the number of people that can be sustained per unit of land in the subsistence regime. This is modeled as an additional intensity factor added to the original subsistence land intensity without damages (22), (23).

$$Land_loss = \beta_{SLR,floods,temp,humidity}^{land_loss} \cdot \left(\frac{(\Delta Temp - 1)^2}{9} \right) \quad (19)$$

$$Disposable_Land = Disposable_{Land}^{wod} - Land_loss \quad (20)$$

$$Int_{agr.land}^{Land} = \frac{Int_{agr.land}^{Land,wod}}{(1 - X_loss_1)} \quad (21)$$

$$Extra_Int_{sub_land}^{Land} = \beta^{Extra_Int_Land_sub} \cdot (\Delta Temp - 1) \quad (22)$$

$$Int_{sub_land}^{Land} = Int_{sub_land}^{Land,wod} + Extra_Int_{sub_land}^{Land} \quad (23)$$

The Supplementary Material (SM) contains the numerical values for all estimated damage parameters.

2.3. Scenario design

We develop a baseline scenario projecting economic development without climate change impacts, and a set of damage scenarios demonstrating how various forms of climate damage modify the baseline trajectory.

To render the scenarios comparable the values for scenario and model parameters are the same in all scenarios, except for damage-relevant parameters. The common scenario assumptions include (1) low per capita growth rates for social classes in high-income countries and medium per capita growth rates for social classes in the rest of the world; (2) low energy intensity improvements in production processes; (3) a moderate increase in capital intensity; (4) fast declines in land intensities; (5) moderate substitution of fossil energy through renewable energy types. Rather optimistic assumptions regarding land productivity improvements and fossil energy availability, coupled with rather pessimistic assumptions regarding the energy transition and future declines in greenhouse gas intensities, provide a suitable framework to focus on the economy-climate nexus because they tend to generate medium to high-emission pathways that are less affected by potential land scarcity issues, and thus, result in higher temperature changes and higher observable impacts. This approach addresses our main research objective, i.e. to assess the influence of parameterized damage factors on economic development pathways in the model. Section 2 SM contains more information on the scenarios' boundary conditions.

The simulated damage scenarios can be categorized according to the *type* of impacts they incorporate, the *severity* of the adverse impacts, and the *evolution of sectoral labor productivity*.

First, we construct three damage categories: category 'A' includes damages related to sea-level rise and land-related damages; category 'B' includes impacts on labor productivities and supply; category 'C' includes impacts on economic production, i.e. input coefficients and capital stock. From these categories we construct 7 types of damage scenarios: A, B, C, A+B, A+C, B+C, A+B+C. We are primarily interested in the dynamics produced by the last type of damage scenarios and use scenarios with a partial representation of damages primarily to compare the strength of, and interactions between, different types of damages.

Second, we distinguish between three severity levels of impact: moderate, low and high, with moderate impacts reflecting our best guess for every damage parameter. To derive the values for a lower severity, we decrease the damage factors pertaining to category 'B' by 30%, and the damage factors pertaining to category 'A' and 'C' by 25%. For a higher severity of impacts, we increase the damage factors pertaining to category 'B' by 20%, and the damage factors pertaining to 'A' and 'C' by 25%, except for the increased depreciation rate, which is increased by 42%, reflecting our higher-end estimate related to the loss of capital stock.

Finally, the evolution of sectoral labor productivities in the damage scenarios can be purely exogenous, reflecting social learning and technological innovations happening over time, or complemented by an endogenous component. To fix an exogenous target for labor productivity improvements, we take the labor productivity (and intensity) levels of the center in 2019, given in EXIOBASE3, as reference levels because they constitute an example for empirically observed high labor productivity values. Thus, by 2100, in scenarios with purely exogenous labor productivity developments, global average productivity levels are assumed to have increased to 70% of the reference productivity levels. Conversely, in scenarios in which productivity levels are influenced by endogenous model developments, the exogenous target level is set to only 30% of the reference productivity levels. However, those scenarios also contain a labor intensity multiplier that changes labor intensities as an exponentially falling function of global average consumption. The parameters of the function are selected to reduce labor intensities by 80% when the global average consumption has reached the average consumption of the center in 2019. Thus, in a scenario with strong economic growth, the endogenous component makes labor productivities increase faster than in scenarios without this component. However, given that

climate impacts can affect both labor productivities and economic output levels, the endogenization of labor productivities also acts as a potential amplifier of economic damages.

By simulating every type of damage scenario with low, moderate and high climate impacts, and with, as well as without, endogenously evolving labor productivity levels, we build our scenario set, which contains a total of 43 scenarios (Table 2). All scenarios were simulated for the period 2019–2100 using MORDRED version 1.0.6.

<i>Scenario simulation</i>	<i>Type</i>	<i>Severity</i>	<i>Endogenous component in labor intensity changes</i>
1 (<i>Baseline</i>)	<i>none</i>	-	<i>yes</i>
2	<i>ABC</i>	<i>low</i>	<i>no</i>
3			<i>yes</i>
4		<i>moderate</i>	<i>no</i>
5			<i>yes</i>
6		<i>high</i>	<i>no</i>
7			<i>yes</i>
8		<i>low</i>	<i>no</i>
9	<i>A</i>		<i>yes</i>
10		<i>moderate</i>	<i>no</i>
11			<i>yes</i>
12		<i>high</i>	<i>no</i>
13			<i>yes</i>
14	<i>B</i>	<i>low</i>	<i>no</i>
15			<i>yes</i>
16		<i>moderate</i>	<i>no</i>
17			<i>yes</i>
18		<i>high</i>	<i>no</i>
19			<i>yes</i>
20	<i>C</i>	<i>low</i>	<i>no</i>
21			<i>yes</i>
22		<i>moderate</i>	<i>no</i>
23			<i>yes</i>
24		<i>high</i>	<i>no</i>
25			<i>yes</i>
26	<i>AB</i>	<i>low</i>	<i>no</i>
27			<i>yes</i>
28		<i>moderate</i>	<i>no</i>
29			<i>yes</i>
30		<i>high</i>	<i>no</i>
31			<i>yes</i>
32	<i>AC</i>	<i>low</i>	<i>no</i>
33			<i>yes</i>
34		<i>moderate</i>	<i>no</i>
35			<i>yes</i>
36		<i>high</i>	<i>no</i>

37			<i>yes</i>
38	<i>BC</i>	<i>low</i>	<i>no</i>
39			<i>yes</i>
40		<i>moderate</i>	<i>no</i>
41			<i>yes</i>
42		<i>high</i>	<i>no</i>
43			<i>yes</i>

Table 2: Overview of scenario simulations.

3. Results

This section contains the simulation results of selected scenarios that allow us to show key model dynamics resulting from the introduction of different types of climate impacts. We begin by analyzing damage scenarios that integrate all parameterized damages from the economic, labor, and land modules (type ABC scenarios), and subsequently examine the effects of each damage type in isolation

3.1. Economy-climate interactions

In the baseline scenario both world output and global warming rise strongly until the end of the 21st century, reaching more than 450 trillion 2019-€ and more than 3.6 °C despite the assumed changes in the energy infrastructure (Figure 1).¹ However, once damages of all types (A+B+C) are introduced, the observed dynamics change significantly.

In scenarios with endogenously evolving labor productivities, world output peaks between 2045 and 2060 and decreases afterwards, being between 2.9 and 3.6 times lower than in the baseline by 2100 (Figure 1c). In scenarios without endogenously evolving labor productivities, economic growth comes to a halt as well, albeit about 2 decades later. World output begins to decline moderately but persistently after 2075 (2080) in scenarios with high (moderate) impacts. Conversely, the difference in output between the peak in 2082 and output in 2100 in the low-impact scenario is marginal. By 2100 world output levels in scenarios without an endogenous labor productivity component are between 27% and 49% lower than in the baseline (Figure 1d).

While world output trajectories of all scenarios, including the baseline, are comparable until 2045, from 2040 onward, global temperature trajectories rise faster than in the baseline scenario in all damage scenarios (Figure 1a-b). However, in the second half of the simulation this dynamic reverses for most of the damage scenarios: after 2065, 2070 and 2080, in scenarios with endogenously evolving labor productivities and high, moderate and low impacts, temperatures in the baseline scenario rise significantly faster. As a result, by the end of the simulation, increases in global average temperature are projected to range from 2.99 °C to 3.25 °C, depending on the severity of impacts. Scenarios lacking an endogenous labor productivity component exhibit similar dynamics, albeit with a temporal delay. In the high-impact scenario, average temperature increases more rapidly than in the moderate- and low-

¹ The baseline scenario was simulated with endogenously changing labor productivity. However, the limits to growth in this baseline are sufficiently weak that a scenario with purely exogenous changes would produce comparable results. Consequently, we employ the same baseline throughout as a benchmark for comparison with the damage scenarios. The only variable exhibiting notable differences between baselines with and without endogenous labor productivity is total labor demand.

impact scenarios between 2040 and 2060. After 2060, this trend reverses, and by the final decade of the simulation, the rate of warming has slowed enough for average global temperatures to fall below those observed in the baseline scenario. The scenario with moderate impacts reaches its turning point in 2099, while the scenario with low impact displays higher degrees of warming than the baseline beyond the 21st century. In the final year of the simulation, global warming is 3.56 °C in the high-impact, 3.64 °C in the moderate-impact and 3.76 °C in the low-impact scenario. Unsurprisingly, in both types of scenarios, the lower the adverse impacts from global warming, the longer the global economy grows, resulting in higher final output levels, higher emissions and higher changes in global average temperature.

Thus, temperature and output pathways can differ significantly, depending on assumptions about the evolution of labor productivity and the severity of impacts, with endogenously changing productivities and higher impact severity being linked to an earlier peak of world output and a lower degree of climate change. At the same time, multiple economy-climate interactions can be observed across all scenarios. Taking into account the feedback effect of the climate system on the economic system produces a strong deviation from the historical trend of continuous economic expansion, and a more dynamic variation in the rate of global warming. Interestingly, in all but one scenario, the introduction of climate impacts ultimately results in a lower scale of warming.

As our scenario design features very low consumption growth rates for the social classes of the world region ‘center’, simulation results with higher growth rates in the center are displayed in Suppl. Figure 1. While output and temperature change are higher in the baseline scenario, the dynamics observed in the damage scenarios are comparable to those just discussed.

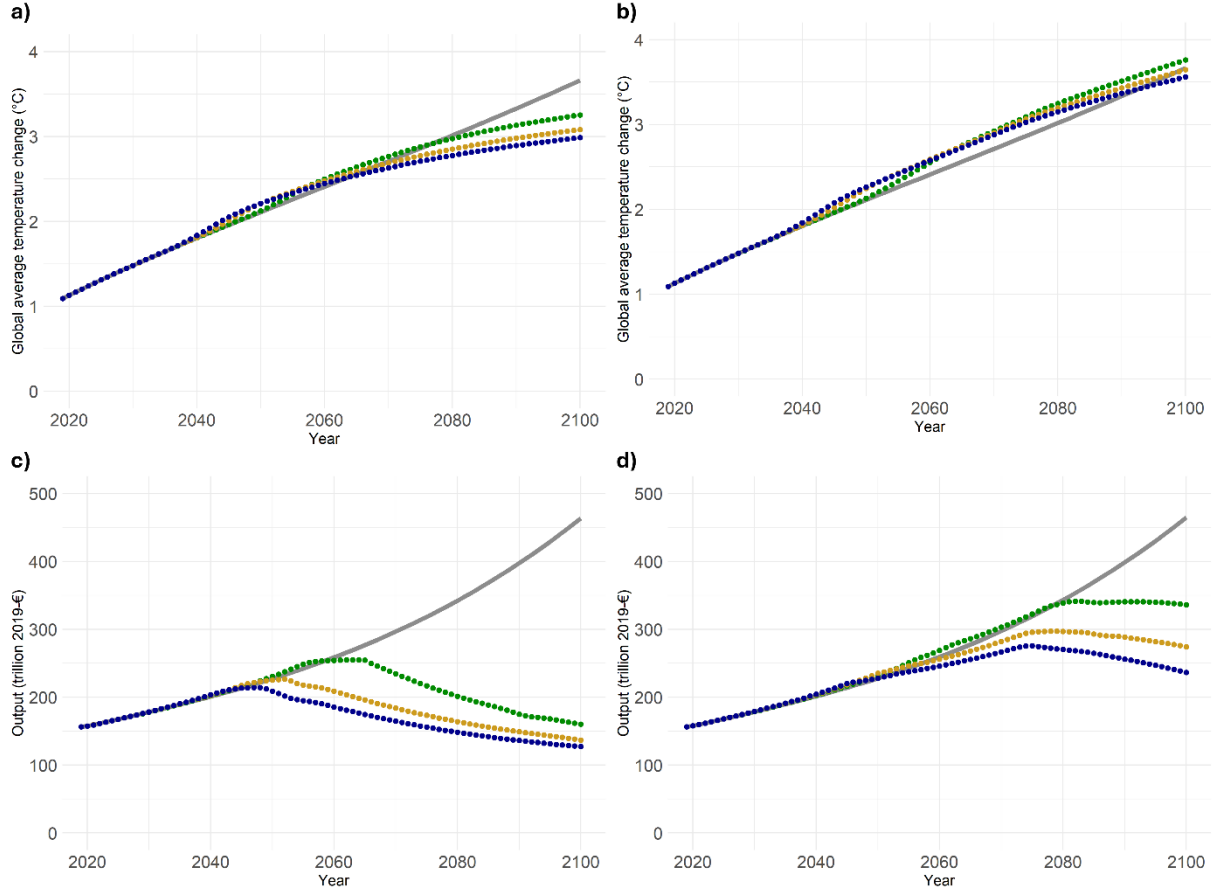


Figure 1: Change of global average temperature with respect to 1850 in the Baseline (grey), high-impact (blue), moderate-impact (yellow) and low-impact (green) scenarios with (a) and without (b) endogenously (b) evolving labor productivities. World output trajectory in the Baseline, high-impact, moderate-impact and low-impact scenarios with endogenously (c) and exogenously (d) evolving labor productivities. All damage scenarios belong to the type 'ABC'.

The differences in the rate of temperature change observed in Figure 1 can be explained by changes in total greenhouse gas (GHG) emissions and GHG intensities (Figure 2) occurring during the simulation period. The pattern of total GHG emissions in the simulated scenarios is roughly correlated with the evolution of world output. GHG emissions peak first between 2040 and 2050 in the high- and moderate-damage scenarios, independent from the type of labor productivity development (Figure 2a, d), followed by peaks between 2055 and 2075 for the low-damage scenarios. The peaks in total emissions do not correspond to the peaks in total output because they are driven by the conversion of forest into land used for the generation of food, energy, and infrastructure. Interestingly, in the baseline, emissions rise continuously but more smoothly than in the damage scenarios, indicating the absence of major land use conversions. The differences in the observed patterns are produced mainly due to a climate-change-induced increase in the intensity of agricultural land in the damage scenarios which lead to a higher land demand, and thus, higher pressure to convert non-economically used forests than in the baseline scenario. As output and land demands remain high for a longer time in scenarios with purely exogenously evolving labor productivities, those scenarios exhibit higher land pressure and higher emissions from land use changes. Nevertheless, total GHG emissions ultimately decline across all damage scenarios and are 22.2% to 69.4% lower than in the baseline scenarios at the end of the simulation. In the low-impact damage scenario without an endogenous labor productivity component, emissions by 2100 have not declined enough to lower global average

temperatures below baseline levels; however, the trend indicates that the turning point is approaching.

The GHG emissions that are not related to land use changes are driven by the scale of production and consumption as well as by the respective GHG intensities (Figure 2b, c, e, f). GHG intensities of output are comparable between scenarios with and without an endogenous labor productivity component and are the highest for scenarios with a high severity of impacts. Thus, interestingly, climate damages slow down technological progress. Nevertheless, the trend of falling GHG intensities of economic production processes are not reversed in any damage scenario.

Conversely, for private (household) and public (government) consumption the effect of climate impacts on GHG intensity is so significant that in the high-impact scenario without endogenous labor productivity component the improvement in the GHG intensity of consumption comes to a halt in 2091 and subsequently starts to increase, which amounts to another break with historical trends (Figure 2f).

Although GHG intensities are significantly lower in the baseline scenario the divergence in the scale of global production and consumption between the baseline and the damage scenarios by far offsets the difference in intensities, resulting in declining total emissions in the damage scenarios, and increasing emissions in the baseline during the second half of the simulation.

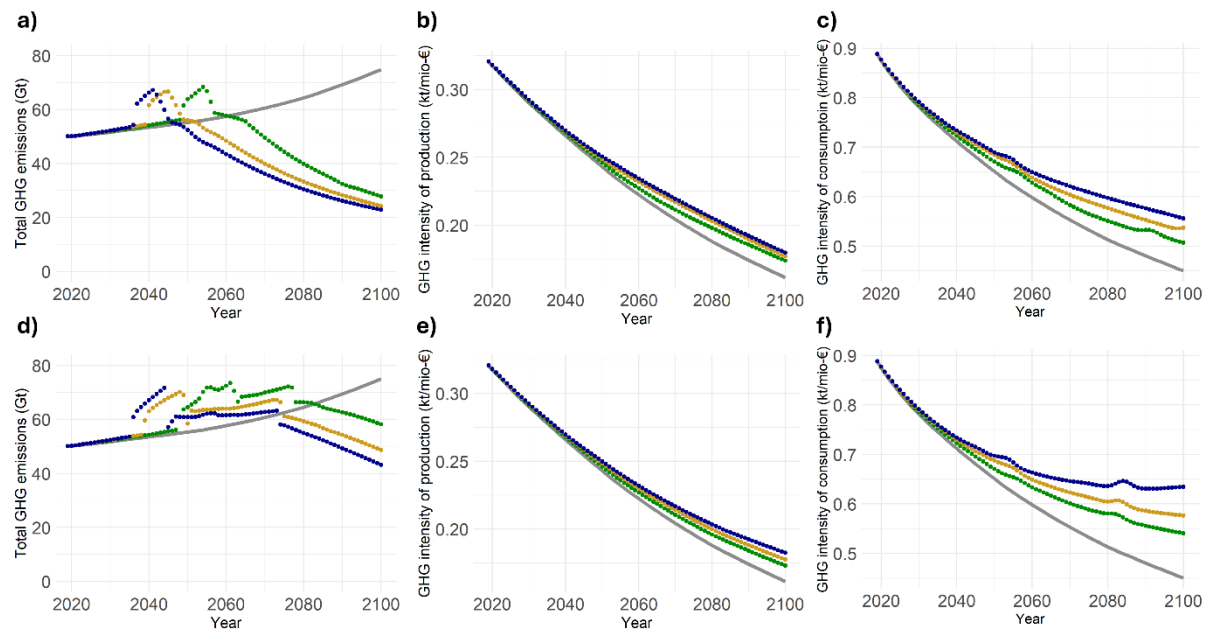


Figure 2: a) Total GHG emissions in CO₂ equivalents, b) GHG intensity of output, c) GHG intensity of consumption in the Baseline (grey), high-impact (blue), moderate-impact (yellow) and low-impact (green) scenarios with endogenously evolving labor productivities; d) total GHG emissions in CO₂ equivalents, e) GHG intensity of output, f) GHG intensity of consumption without endogenously evolving labor productivities. All damage scenarios belong to the type 'ABC'.

3.2. Interactions between different climate damage types

Comparing the evolution of world output in scenarios that only consider some types of damages (A, B, C) with scenarios incorporating various or all parametrized damages (AB, AC, BC, ABC) shows the strength of isolated and combined climate change impacts in the model (Figure 3).

Damage scenarios of type A, which capture only sea-level-rise- and land-related damages, closely track the baseline scenario irrespective of the severity of impacts. Conversely, the incorporation of labor-related damages alone (damage type B) is sufficient to halt economic growth in all scenarios and reverse it in all but the low-impact-non-endogenous-labor-productivity scenario (Figure 3e). In general, scenarios of type B produce patterns similar to scenarios of type ABC but with a temporal delay, resulting in higher output peaks. In scenarios with an endogenous labor productivity component the difference in output between scenarios of type B and of type ABC has reduced considerably, especially in the case of high and moderate impacts. Conversely, in scenarios without an endogenous labor productivity component output remains significantly higher in scenarios of type 'B', especially in the moderate and high-impact scenarios. The similarity in the patterns produced by the scenarios of type B and ABC indicate the important role of labor-related damages in shaping model outcomes. Scenarios with capital- and output-related damages (type C) differ significantly between scenarios with moderate (Figure 3a,d), weak (Figure 3b,e) and high impacts (Figure 3c,f). In scenarios with moderate impacts, the output trajectory closely resembles the baseline trajectory during the great majority of the simulation period. Interestingly, in scenarios with low impacts, the presence of damages increases the growth rate of global economic production, resulting in a significantly higher output in type-C scenarios than in the baseline scenario (526 trillion € compared to 463 trillion €). Likewise, final demand is higher in the damage scenarios. However, when disaggregating final demand into investment and consumption, we find that total consumption is slightly lower in the damage scenarios and the higher final demand is explained by higher gross fixed capital formation (GFCF) necessary due to higher capital depreciation rates from climate change impacts (Figure 4a, b). Likewise, the ratio of final demand to total output declines slightly during the simulation for the damage type-C scenarios, indicating a damage-induced increase in the production of intermediate goods. Thus, type-C scenarios illustrate the possibility of climate damages leading to an increase in economic growth but a decrease in consumption. Consequently, the assumption that an increase in production is linked to an increase in consumption might no longer hold under climate change scenarios. In type-C scenarios with high impacts the output trajectory starts to diverge from the baseline from 2060 onward. In the scenario with an endogenous labor component impacts are sufficiently strong to cause output to peak and decline (Figure 3c) while in the scenario lacking the endogenous development output increases until the end of the simulation albeit at a lower rate than in the baseline (Figure 3f). These findings point to a relatively high sensitivity of capital- and output-related damages to the assumed severity of impacts.

Combining the damages of type A and B, we find that labor-related damages strongly dominate over sea-level-rise and land-related damages since the type-AB output trajectory closely resembles the type-B trajectory, as illustrated by the blue diamonds (type B) and the red diamonds (type AB) in Figure 3. Likewise, the trajectory resulting from the combination of type-A and type-C damages clearly is influenced to a stronger degree by damage type C. Nevertheless, the trajectory in the AC scenarios differs from the trajectories of scenarios that contain only one type of damage: for moderate- and high-impact scenarios, the resulting growth rate is lower than in the type-A and the type-C scenarios; for low-impact scenarios, world output grows faster than in the type-A scenarios but slower than in the type-C scenarios. Last, BC scenarios closely resemble ABC scenarios, with the combined effect of labor-, capital- and output-related damage factors imposing an earlier decline and reversal of economic growth. This finding is not sensitive to (exogenous vs. endogenous) labor productivity assumptions. Thus, compared to capital-, output- and labor-related damages, in our scenario parametrization, sea-level-rise- and land-

related damages are relatively minor, while the interaction effect between damages in the economic and in the labor model significantly alter the simulation results.

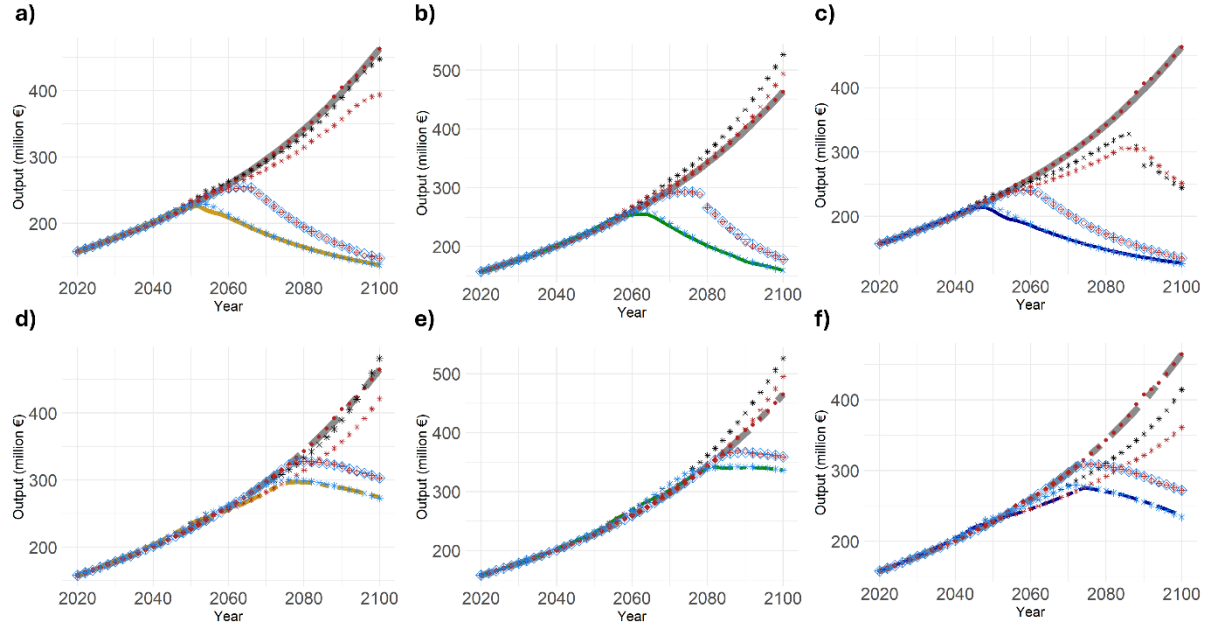


Figure 3: Evolution of world output in scenarios with (a-c) and without (d-f) endogenously evolving labor productivities and moderate (a, d), low (b, e) and high (c, f) impacts. a-f) Baseline (grey (dashed) line), scenarios with damage type A (red dots), type B (blue diamond), type C (black star), type AB (red diamond), type AC (red star), type BC (blue star), type ABC (yellow, green or blue (dashed) line).

3.2. Impacts on damages on economic production factors

Figure 4 shows different impacts of climate damages on variables related to the economic production process. As already discussed in the previous section, in type-C damage scenarios investment increases faster than in the baseline because the loss of capital stock alone does not stop economic growth but rather results in an increase in the production of capital goods to meet rising consumption demands. In type-B scenarios GFCF first exceeds investment in the ABC-type scenarios due to the higher output levels but, as output begins to decline, drops below the GFCF levels in the ABC-type scenarios because the B-type scenarios do not consider a climate-change-induced increase in capital depreciation.

Comparing ABC-type scenarios with and without an endogenous labor productivity component with the baseline we find that the annual total depreciation of capital stock increases faster in scenarios with climate impacts. In scenarios with a strong decline in output, total depreciation eventually decreases modestly, while in scenarios with a moderate decline in output total depreciation first stabilizes but then continues to increase slightly. In the scenario with purely exogenously driven labor productivities and low impacts total depreciation is still higher than in the baseline scenario in the final year of the simulation (Figure 4c). The share of the food sector's depreciation in total depreciation is significant, ranging from 6-10% (Figure 4d).

While total labor demand peaks between 2040 and 2060 in the baseline scenario and then decreases sharply—mainly due to continuous increases in labor productivity—labor demand rises strongly in all scenarios with an endogenous labor-productivity component and exceeds the baseline level by up to 15%. Even as output begins to decline, the difference in the labor

demand between the damage and the baseline scenarios increases toward the end of the simulation (Figure 4e). In damage scenarios purely driven by exogenous labor productivity improvements, because of changing sectoral productivity levels and production capacities, labor demand first decreases, then increases and eventually falls again. Conversely, due to the increasing heat-related damages impacting the labor supply, in all damage scenarios the maximum pool of labor hours is smaller than in the baseline scenario, with the difference being higher in scenarios with high impacts and higher temperature increases. In the simulations, the adverse effect of deadly heat on the ability to work, rather than the increase in mortality of the working population, proves to be the principal driver behind the reduction in available working hours (Figure 4f). The latter can also be seen in Figure 4g and Figure 4h, which show that climate damages indirectly cause both total deaths and births to increase. The strongest effects are produced in scenarios with high impacts and endogenously evolving labor productivities: by 2100, births and deaths in the high-impact-endogenous-labor-productivity scenario are 48% and 16% higher than in the baseline. Finally, Figure 4f shows how the loss of habitable land increases with increasing climate impacts. As temperature rises faster in scenarios driven only by exogenous labor productivity improvements, the resulting loss of land is higher in those scenarios.

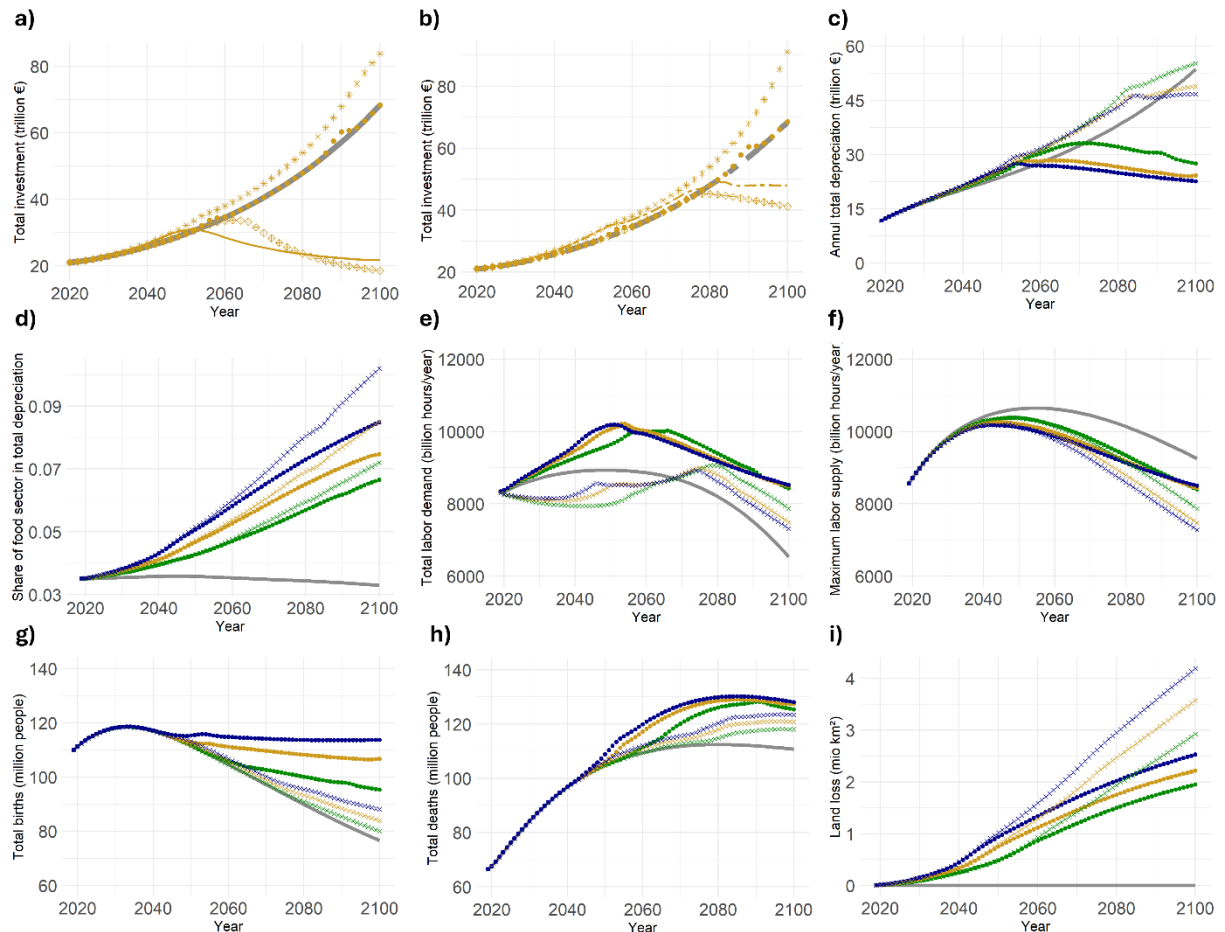


Figure 4: a-b): World GFCF in the baseline (grey (dashed) line), moderate type-A damage (dots), type-B damage (diamonds), type-C damage (stars) and type-ABC damage (yellow (dashed) line) scenarios with (a) endogenously and (b) exogenously evolving labor productivities. Evolution of c) total depreciation, d) share of the food sector's depreciation in total depreciation, e) total labor demand, f) maximum labor supply, g) total births, h) total deaths, i) damage-induced land loss in type-ABC scenarios with low (green), moderate (yellow) and high (blue) impacts as well as with (dots) and without (crosses) endogenously evolving labor productivities.

4. Discussion

We hold that our methodological framework and its implementation in MORDRED constitute a contribution to the loss and damage literature for several reasons. First, rather than modeling damages as impacts on a single parameter—losses to income—we consider the possibility of increased losses in capital stock [45] as well as losses in labor and land productivity. Second, while we distinguish between varying degrees of impact severity across economic sectors, we do not assume that non-weather-related sectors remain unaffected by climate impacts (cf.[13]).

Instead, the input-output framework captures spillover effects between more and less vulnerable sectors through the flow of intermediate goods between industries. Third, our damage modeling is sensitive to questions of equity across time and space [45]. We refrain from using discount rates, calculating the social cost of carbon, or fixing intra- or international income distributions *ex ante*. Rather, MORDRED requires scenarios to specify assumptions of future changes in consumption inequalities, thereby avoiding to incorporate questionable ethical assumptions into its default calibration [14]. In the simulated scenarios, which assume moderate convergence between social classes and regions, the forgone consumption under climate change scenarios is higher for richer classes than for poorer ones, and higher in the center than in the periphery (see Figure 2 in the SM), in line with the modeling analysis of De Bruin et al. [1] who indicate that richer households might face higher impacts. However, MORDRED also shows that the periphery and semiperiphery experience stronger increases in mortality rates in response to economic losses, underscoring the importance of coupling life expectancy to changes in per capita consumption (Figure 3 SM). Last, in contrast to optimal growth models like DICE (cf. [13]), economic trajectories in MORDRED are sensitive to climate change impacts, and the model can exhibit collapse dynamics under high damage assumptions. In this context, our simulations highlight the importance of labor productivity assumptions for scenario outcomes, demonstrating that scenarios with endogenously changing labor productivities that consider the link between exergy availability and labor productivity [46] produce development pathways that are more unstable and sensitive to environmental disruptions.

At the same time, assessments of future environmental risks and damages based on MORDRED face several limitations. With respect to parameter values, the quality of our numerical estimates for different damage factors depends on data availability, which is heavily biased toward the Global North. Furthermore, the impossibility of a comprehensive bottom-up reconstruction of climate impacts leads to the exclusion of many impact channels identified in the literature, such as direct mortality increases due to extreme heat [47] or productivity losses in the livestock industry resulting from heat stress on cattle, chicken, and poultry [48], [49]. While this incompleteness likely results in an underestimation of climate impacts, the adopted input-output framework enforces strict production limits once a single sector becomes constrained, which may be overly pessimistic. Regarding the representation of social, environmental, and economic feedback dynamics linked to climate damages, MORDRED currently omits key feedback relationships, such as the influence of climate damages on other systemic risks, including social and geopolitical conflicts [4]. We also intentionally exclude the effects of crossing climate tipping points [50] on economic production, as their quantification remains elusive – a case of *recognized ignorance*, where modelers cannot plausibly develop alternative causal representations [14]. Moreover, given our focus on production-related damage factors, the model does not account for non-economic losses arising from the intrinsic, cultural, religious, or

recreational values of nature[51], [52] which can be highly significant for perceived quality of life.

Thus, while our work enriches existing damage modeling frameworks, future research could extend it by improving parameter estimates, conducting additional sensitivity tests, and incorporating social and political variables. Investigating the possibilities and limits of climate change adaptation [53], particularly for poorer classes and regions, would also yield valuable policy insights. Furthermore, although our focus has been on climate change damages, the methodological framework can be applied to other environmental damages, thereby enhancing the comprehensiveness of environmental impact assessments based on input–output models. This would allow for simulations that explore feedbacks between climate-related and other ecological limits to growth, such as nitrogen pollution [54] and groundwater depletion [55].

While future work may address some of the model's limitations, *deep uncertainty* [56] and *total ignorance* [14] imply that neither classical risk assessment nor the prediction of societal collapse should be the goal of quantitative loss and damage modeling. As Kareiva and Carranza [51] note, the greatest existential risk from global environmental change lies in our ecological ignorance of the complex feedback dynamics within tightly coupled human–natural systems. We therefore concur with Saltelli et al. [57] on the importance of acknowledging and communicating what is not known, rather than conveying a false sense of certainty.

Conclusion

In this article, we introduced a transparent and structured framework for representing adverse impacts of global environmental change on the economy. We applied this framework to the MORDRED-IAM by introducing a set of climate damage factors and examining their effects on economic developments under different damage scenarios. Unlike neoclassical damage representations in established IAMs, the model's system-dynamics and input–output foundations produce substantial changes in key economic and technological parameters once climate damages are activated. This highlights both the threat climate change poses to economic growth and the urgency of strengthening international cooperation on climate governance. While we argue that MORDRED yields quantitative projections that are 'less wrong' than those of optimal-growth IAMs, it remains essential to acknowledge the unknowable, unpredictable positive and negative surprises waiting in the future.

References

- [1] K. C. De Bruin, C. K. Kyei, L. Henry, and A. M. Yakut, "Macroeconomic impacts of climate-induced damages in Ireland: A CGE analysis of secondary impacts," ESRI Working Paper, 2024.
- [2] D. Lemoine, C. Hausman, and J. Shrader, "A Guide to Climate Damages," National Bureau of Economic Research, Cambridge, MA, w34348, Oct. 2025. doi: 10.3386/w34348.
- [3] A. Nikas, H. Doukas, and A. Papandreu, "A detailed overview and consistent classification of climate-economy models," *Understanding risks and uncertainties in energy and climate policy*, pp. 1–54, 2019.
- [4] T. A. Undheim, "An interdisciplinary review of systemic risk factors leading up to existential risks," *Progress in Disaster Science*, vol. 22, p. 100326, Apr. 2024, doi: 10.1016/j.pdisas.2024.100326.
- [5] H. Füssel, "Modeling impacts and adaptation in global IAMs," *WIREs Climate Change*, vol. 1, no. 2, pp. 288–303, Mar. 2010, doi: 10.1002/wcc.40.
- [6] S. Hitz and J. Smith, "Estimating global impacts from climate change," *Global Environmental Change*, vol. 14, no. 3, pp. 201–218, 2004.
- [7] E. Bovari, G. Giraud, and F. Mc Isaac, "Coping with collapse: a stock-flow consistent monetary macrodynamics of global warming," *Ecological Economics*, vol. 147, pp. 383–398, 2018.
- [8] Y. Dafermos, M. Nikolaidi, and G. Galanis, "Climate change, financial stability and monetary policy," *Ecological Economics*, vol. 152, pp. 219–234, 2018.
- [9] T. Ansell and S. Cayzer, "Limits to growth redux: A system dynamics model for assessing energy and climate change constraints to global growth," *Energy policy*, vol. 120, pp. 514–525, 2018.
- [10] I. Capellán-Pérez *et al.*, "MEDEAS: a new modeling framework integrating global biophysical and socioeconomic constraints," *Energy & Environmental Science*, vol. 13, no. 3, pp. 986–1017, 2020.
- [11] J. Nieto, Ó. Carpintero, L. J. Miguel, and I. de Blas, "Macroeconomic modelling under energy constraints: Global low carbon transition scenarios," *Energy Policy*, vol. 137, p. 111090, 2020.
- [12] K. Tokimatsu and R. Yasuoka, "Multi-channel, climate and non-climate damages in an integrated assessment model," 2024.
- [13] S. Keen, T. M. Lenton, A. Godin, D. Yilmaz, M. Grasselli, and T. J. Garrett, "Economists' erroneous estimates of damages from climate change," 2021, *arXiv*. doi: 10.48550/ARXIV.2108.07847.
- [14] M. Beck and T. Krueger, "The epistemic, ethical, and political dimensions of uncertainty in integrated assessment modeling," *WIREs Climate Change*, vol. 7, no. 5, pp. 627–645, Sept. 2016, doi: 10.1002/wcc.415.
- [15] S. Asefi-Najafabady, L. Villegas-Ortiz, and J. Morgan, "The failure of Integrated Assessment Models as a response to 'climate emergency' and ecological breakdown: the Emperor has no clothes," *Globalizations*, vol. 18, no. 7, pp. 1178–1188, 2021.
- [16] W. J. Ripple *et al.*, "The 2024 state of the climate report: Perilous times on planet Earth," *BioScience*, vol. 74, no. 12, pp. 812–824, Dec. 2024, doi: 10.1093/biosci/biae087.
- [17] IPCC, "Climate Change 2022: Impacts, Adaptation and Vulnerability. Contribution of Working Group II to the Sixth Assessment Report of the Intergovernmental Panel on Climate Change." Cambridge University Press. Cambridge University Press, Cambridge, UK and New York, NY, USA, 2022.

- [18] Z.-J. Zhao *et al.*, "Global climate damage in 2 °C and 1.5 °C scenarios based on BCC_SESM model in IAM framework," *Advances in Climate Change Research*, vol. 11, no. 3, pp. 261–272, Sept. 2020, doi: 10.1016/j.accre.2020.09.008.
- [19] K. Stadler *et al.*, "EXIOBASE 3: Developing a Time Series of Detailed Environmentally Extended Multi-Regional Input-Output Tables," *J of Industrial Ecology*, vol. 22, no. 3, pp. 502–515, June 2018, doi: 10.1111/jiec.12715.
- [20] J. Kitzes, "An introduction to environmentally-extended input-output analysis," *Resources*, vol. 2, no. 4, pp. 489–503, 2013.
- [21] J. Lefèvre, "Integrated assessment models and input–output analysis: bridging fields for advancing sustainability scenarios research," *Economic Systems Research*, vol. 36, no. 4, pp. 675–698, 2024.
- [22] R. E. Miller and P. D. Blair, *Input-output analysis: foundations and extensions*. Cambridge university press, 2009.
- [23] M. Lifi *et al.*, "Synthesis of the model, selected results, and scenario assessment. WP9, Task 9.2, D.9.3." LOCOMOTION, 2023. [Online]. Available: <https://zenodo.org/records/10813034>
- [24] A. Lauer and L. Llases, "MORDRED: Model Of Resource Distribution and Resilient Economic Development. Model Documentation." GitHub, 2025. [Online]. Available: <https://github.com/Pendracus/MORDRED>
- [25] A. Lauer, "MORDRED GitHub repository." 2025. [Online]. Available: <https://github.com/Pendracus/MORDRED>
- [26] A. Smith, "U.S. Billion-dollar Weather and Climate Disasters, 1980 - present (NCEI Accession 0209268)." NOAA National Centers for Environmental Information, 2025. doi: 10.25921/STKW-7W73.
- [27] G. Forzieri *et al.*, "Escalating impacts of climate extremes on critical infrastructures in Europe," *Global environmental change*, vol. 48, pp. 97–107, 2018.
- [28] IPCC, "Climate Change 2021: The Physical Science Basis. Contribution of Working Group I to the Sixth Assessment Report of the Intergovernmental Panel on Climate Change." Cambridge University Press. Cambridge University Press, Cambridge, UK and New York, NY, USA, 2021.
- [29] I. Meza *et al.*, "Global-scale drought risk assessment for agricultural systems," *Natural Hazards and Earth System Sciences*, vol. 20, no. 2, pp. 695–712, 2020.
- [30] Y. Hu *et al.*, "Spatial characterization of global heat waves using satellite-based land surface temperature," *International Journal of Applied Earth Observation and Geoinformation*, vol. 125, p. 103604, 2023.
- [31] E. Mulholland and L. Feyen, "Increased risk of extreme heat to European roads and railways with global warming," *Climate Risk Management*, vol. 34, p. 100365, 2021.
- [32] J. Verschuur *et al.*, "Quantifying climate risks to infrastructure systems: A comparative review of developments across infrastructure sectors," *PLoS Climate*, vol. 3, no. 4, p. e0000331, 2024.
- [33] J. Hinkel *et al.*, "Coastal flood damage and adaptation costs under 21st century sea-level rise," *Proceedings of the National Academy of Sciences*, vol. 111, no. 9, pp. 3292–3297, 2014.
- [34] S. A. Kulp and B. H. Strauss, "New elevation data triple estimates of global vulnerability to sea-level rise and coastal flooding," *Nature communications*, vol. 10, no. 1, pp. 1–12, 2019.
- [35] M. W. Beck, I. J. Losada, P. Menéndez, B. G. Reguero, P. Díaz-Simal, and F. Fernández, "The global flood protection savings provided by coral reefs," *Nature communications*, vol. 9, no. 1, p. 2186, 2018.

- [36] C. A. Deutsch *et al.*, "Increase in crop losses to insect pests in a warming climate," *Science*, vol. 361, no. 6405, pp. 916–919, 2018.
- [37] C. Zhao *et al.*, "Temperature increase reduces global yields of major crops in four independent estimates," *Proceedings of the National Academy of Sciences*, vol. 114, no. 35, pp. 9326–9331, 2017.
- [38] A. Béguin, S. Hales, J. Rocklöv, C. Åström, V. R. Louis, and R. Sauerborn, "The opposing effects of climate change and socio-economic development on the global distribution of malaria," *Global Environmental Change*, vol. 21, no. 4, pp. 1209–1214, 2011.
- [39] L. H. Franklino, K. E. Jones, D. W. Redding, and I. Abubakar, "The effect of global change on mosquito-borne disease," *The Lancet Infectious Diseases*, vol. 19, no. 9, pp. e302–e312, 2019.
- [40] C. Mora *et al.*, "Global risk of deadly heat," *Nature Climate Change*, vol. 7, no. 7, pp. 501–506, 2017.
- [41] S. Dasgupta, N. van Maanen, S. N. Gosling, F. Piontek, C. Otto, and C.-F. Schleussner, "Effects of climate change on combined labour productivity and supply: an empirical, multi-model study," *The Lancet Planetary Health*, vol. 5, no. 7, pp. e455–e465, 2021.
- [42] N. W. Arnell, "Climate change and global water resources: SRES emissions and socio-economic scenarios," *Global environmental change*, vol. 14, no. 1, pp. 31–52, 2004.
- [43] J. L. Bamber, M. Oppenheimer, R. E. Kopp, W. P. Aspinall, and R. M. Cooke, "Ice sheet contributions to future sea-level rise from structured expert judgment," *Proceedings of the National Academy of Sciences*, vol. 116, no. 23, pp. 11195–11200, 2019.
- [44] X. Zhang and X. Cai, "Climate change impacts on global agricultural land availability," *Environmental Research Letters*, vol. 6, no. 1, p. 014014, 2011.
- [45] E. A. Stanton, F. Ackerman, and S. Kartha, "Inside the integrated assessment models: Four issues in climate economics," *Climate and Development*, vol. 1, no. 2, pp. 166–184, 2009.
- [46] S. Furse, "Are there biophysical limits to technical change? A review of societal exergy analysis and ecological macroeconomics," 2025.
- [47] A. Ahmadalipour and H. Moradkhani, "Escalating heat-stress mortality risk due to global warming in the Middle East and North Africa (MENA)," *Environment International*, vol. 117, pp. 215–225, 2018.
- [48] P. Thornton, G. Nelson, D. Mayberry, and M. Herrero, "Increases in extreme heat stress in domesticated livestock species during the twenty-first century," *Global Change Biology*, vol. 27, no. 22, pp. 5762–5772, 2021.
- [49] P. Thornton, G. Nelson, D. Mayberry, and M. Herrero, "Impacts of heat stress on global cattle production during the 21st century: a modelling study," *The Lancet Planetary Health*, vol. 6, no. 3, pp. e192–e201, 2022.
- [50] T. M. Lenton *et al.*, "Climate tipping points—too risky to bet against," *Nature*, vol. 575, no. 7784, pp. 592–595, 2019.
- [51] P. Kareiva and V. Carranza, "Existential risk due to ecosystem collapse: Nature strikes back," *Futures*, vol. 102, pp. 39–50, 2018.
- [52] U. Pascual *et al.*, "Valuing nature's contributions to people: the IPBES approach," *Current Opinion in Environmental Sustainability*, vol. 26–27, pp. 7–16, June 2017, doi: 10.1016/j.cosust.2016.12.006.
- [53] C. W. Callahan, "Present and future limits to climate change adaptation," *Nat Sustain*, vol. 8, no. 4, pp. 336–342, Feb. 2025, doi: 10.1038/s41893-025-01519-7.
- [54] M. Wang *et al.*, "A triple increase in global river basins with water scarcity due to future pollution," *Nature Communications*, vol. 15, no. 1, p. 880, 2024.

- [55] H. Niazi *et al.*, "Global peak water limit of future groundwater withdrawals," *Nature Sustainability*, pp. 1–10, 2024.
- [56] A. Xepapadeas, "Uncertainty and climate change: The IPCC approach vs decision theory," *Journal of Behavioral and Experimental Economics*, vol. 109, p. 102188, Apr. 2024, doi: 10.1016/j.socec.2024.102188.
- [57] A. Saltelli *et al.*, "Five ways to ensure that models serve society: a manifesto," *Nature*, vol. 582, no. 7813, pp. 482–484, June 2020, doi: 10.1038/d41586-020-01812-9.

Supplementary Material

1. Final damage parameter values

Parameter	Numerical value
Loss of capital stock due to sea-level rise (%)	at 2°C: 1% in 10 years, at 3°C: loss of 1.5 % in 10 years; at 4 °C: loss of 2% of global capital stock in 10 years
Sectoral shares of damages in capital stock for high-exposure sectors at 4°C of warming ($\delta_{high\ exposure}^{4^{\circ}C,min}$)	0.093025266458601
Sectoral shares of damages in capital stock for low-exposure sectors at 4°C of warming ($\delta_{low\ exposure}^{4^{\circ}C,min}$)	0.0160184446054674
Additional GFCF due to sea-level rise in sector 5 (mio. 2019-€) ($GFCF_5^{slr}$)	166000
Output loss factor at 4 °C of warming ($X_loss^{4^{\circ}C}$)	0.27
Parameter of the function regulating changes in input coefficients in A Matrix ($\beta_0_{output\ loss}$)	1.107237
Parameter of the function regulating changes in input coefficients in A Matrix ($\beta_1_{output\ loss}$)	0.153196
Parameter of the function regulating changes in input coefficients in A Matrix ($\beta_2_{output\ loss}$)	0.054713
Heat-related damage to labor supply (HD^{Max_Lb}) at 4 °C of warming	0.24520548
Shares of days with deadly heat per year at 4 °C of warming	0.49041096
Share of workers affected by deadly heat	0.5
Loss of labor productivity in high-exposure sectors ($\alpha_{Lprod_{high}}$) at 3°C of warming	0.25
Loss of labor productivity in low-exposure sectors ($\alpha_{Lprod_{low}}$) at 3°C of warming	0.18
Total land loss at 4°C of warming (km^2) ($\beta_{SLR,floods,temp,humidity}^{land_loss}$)	4605000
Damage factor on subsistence land intensity ($\beta^{Extra_Int_Land_sub}$)	0.002333333333333333

Suppl.Table 1: Numeric values used in the scenarios with moderate impacts.

2. Main scenario parameters

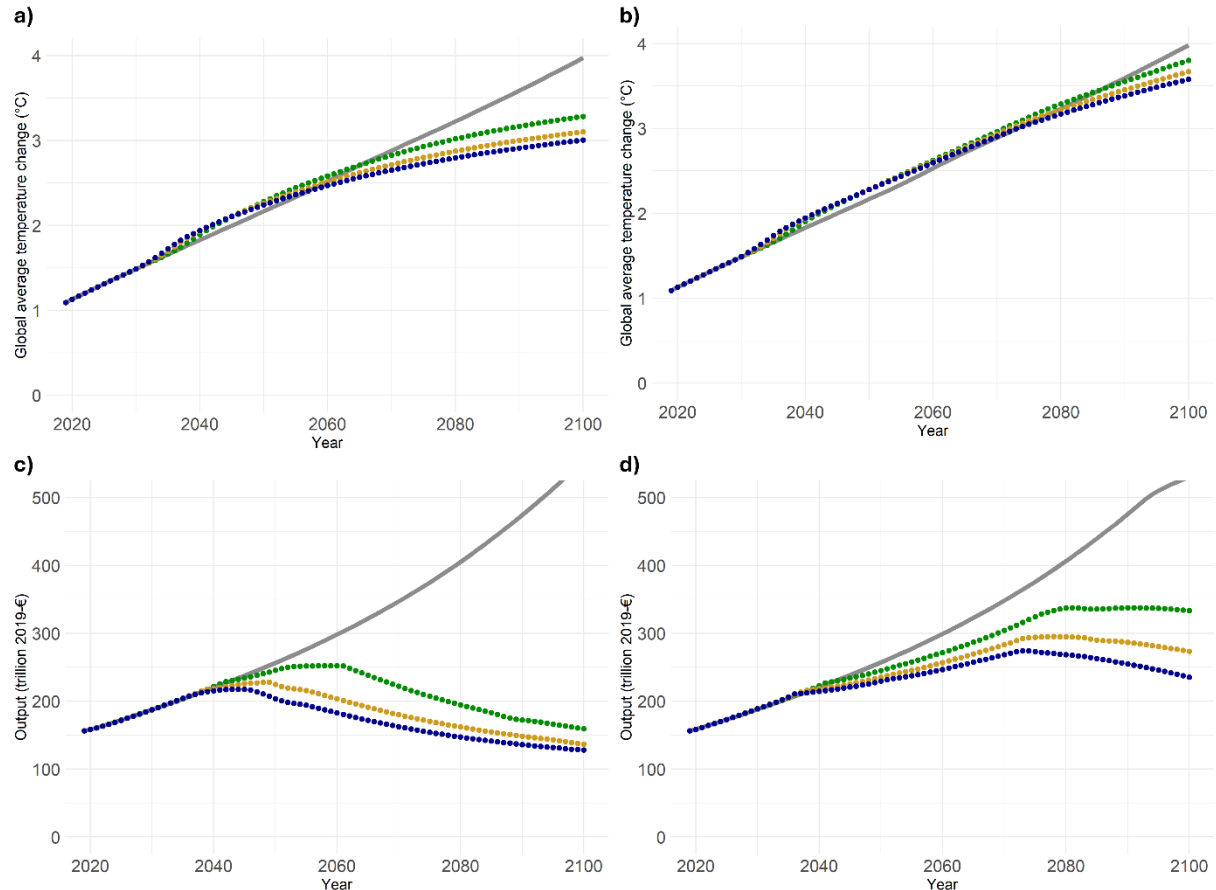
Variable	Parametrization	Comments
<i>Growth rate in per capita consumption</i>	Center richest class: 0.23% middle class: 0.58% poorest class: 0.86%	We focus on energy- and material-intensive consumption growth rather than on abstract GDP growth. As the material consumption levels of the center are already relatively high, future growth in energy- and material-intensive consumption is
	Semiperiphery richest class: 1.37% middle class: 2.24% poorest class: 2.88 %	
	Periphery richest class: 1.73 %	

	middle class: 2.43% poorest class: 3.00%	<i>assumed to be particularly low.</i>
<i>Energy efficiency</i>	10% improvement in the energy efficiency of economic processes in all sectors until the end of the simulation.	<i>The low growth in material- and energy-intensive consumption is logically linked to a slow improvement in energy efficiencies.</i>
<i>Land intensity</i>	50% reduction in land intensities until the end of the simulation for all land types (agricultural land (cropland and pastures), economically used forest, land classified as 'other land' by the FAO (demanded by the food and the biomass sector), land used for renewable energy generation (water bodies used for hydropower are not considered)).	<i>We adopt optimistic assumptions regarding land-use intensities in order to minimize constraints on economic growth stemming from land availability, thereby allowing us to focus on climate damages as potential limiting factor for economic development.</i>
<i>Capital intensity</i>	Increase in capital intensity by 20% until the end of the simulation.	
<i>Electrification</i>	Medium electrification: substitution of 25% of the non-electric energy input by electricity input in all industries and in all final demand components (public consumption, private consumption, gross fixed capital formation).	
<i>Greening of the electricity mix</i>	Reduction of fossil electricity and of nuclear power by 75% until the end of the simulation; substituted by solar PV, hydropower and wind power.	
<i>Energy availability</i>	Medium fossil resource accessibility: all oil and gas resources as well as 40% of the estimated coal resources of the BGR (2020) are assumed to be extractible. Input costs do not increase until all reserves are depleted and increase by 75% by the time all oil and gas resources as well as 10% of all coal resources have been depleted.	
<i>Substitution of fossil energy through biomass-based energy</i>	10% of fossil energy inputs are replaced by bioenergy until the end of the simulation.	
<i>Greenhouse gas (GHG) emission intensity</i>	GHG emission intensity of all economic sectors (including CH ₄ and N ₂ O emissions) reduced by 30% until the end of the simulation.	
<i>Land protection</i>	100% of the primary forest that exists at the start of the simulation is protected.	
<i>Climate sensitivity</i>	High <i>Climate feedbacks within the climate module are activated which lead to additional greenhouse gas emissions from natural systems as temperature rises. The equilibrium climate sensitivity is set to 3 °C.</i>	

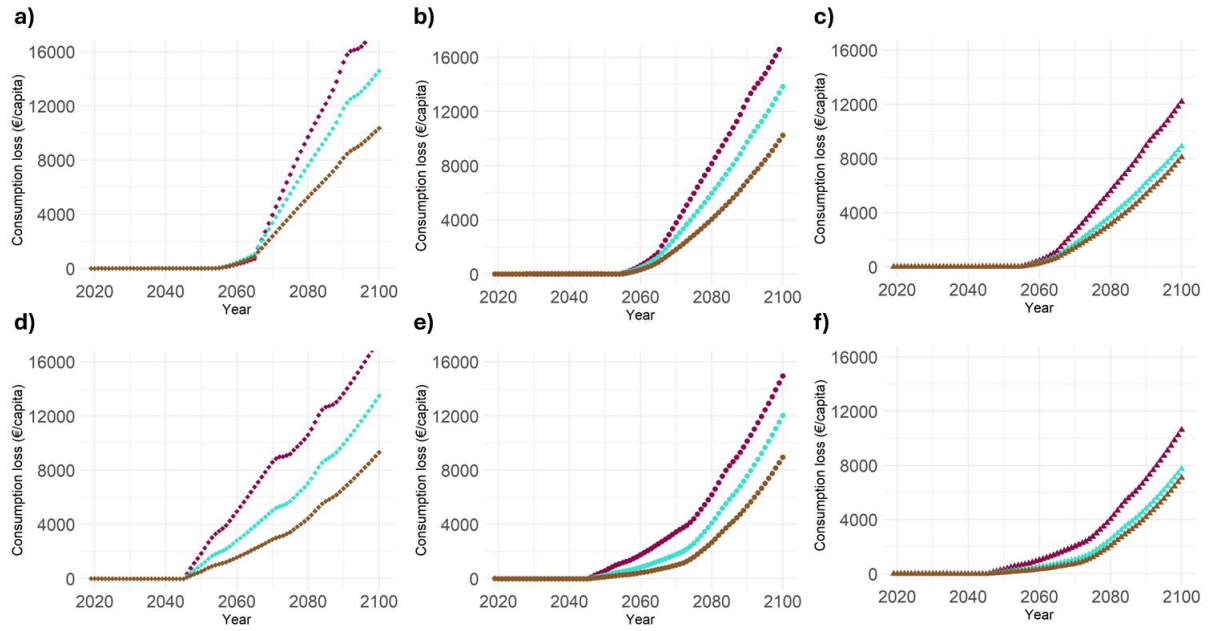
Suppl.Table 2: Parametrization of main scenario parameters common to all simulated scenarios.

Supplementary figures

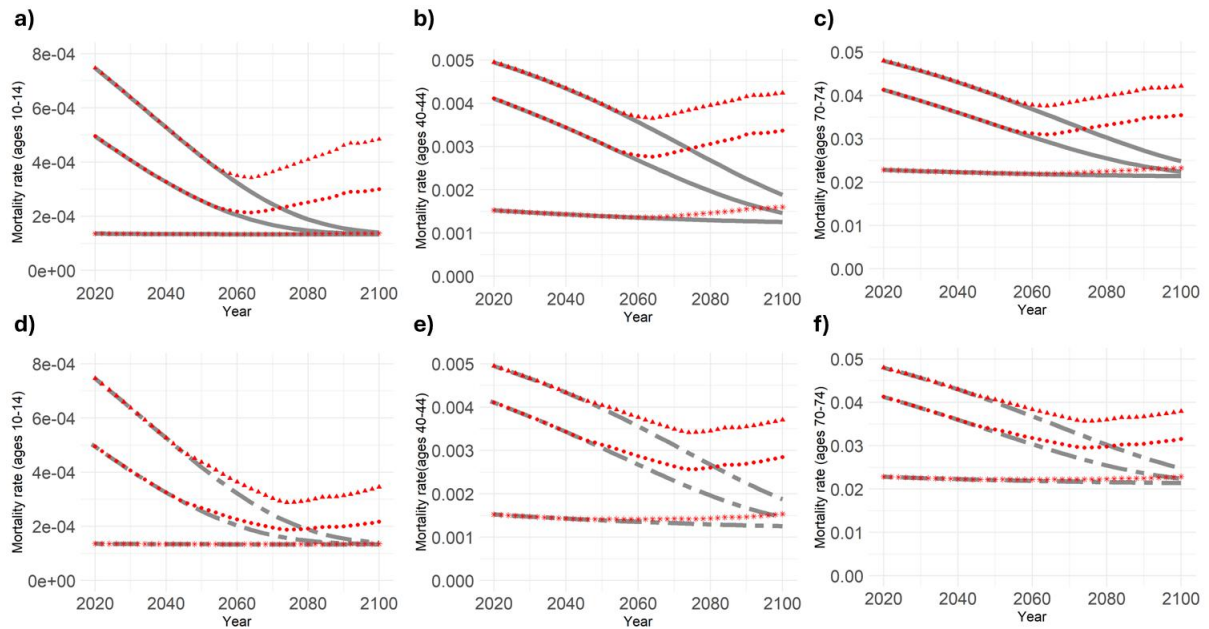
Suppl. Figure 1 displays changes in global average temperature and world output in different scenarios that are characterized by higher growth rates in the center than in the scenarios discussed in the main article. Concretely, the growth rates in per capita consumption are 0.86% for the richest 20% of the center, and 1.37% for the remaining 80% of the population.



Suppl. Figure 1: Scenario results with higher growth rates in the center. a) Change of global average temperature with respect to 1850 in the Baseline (grey), the high-damage (blue), medium-damage (yellow) and low-damage (green) scenarios with endogenously (a) and exogenously (b) evolving labor productivities. World output trajectory in the Baseline, the high-damage, medium-damage and low-damage scenarios with endogenously (c) and exogenously (d) evolving labor productivities.



Suppl. Figure 2: Annual consumption losses for the wealthiest 20% (purple), middle 50% (blue) and poorest 30% (brown) of the center (a & d), the semiperiphery (b & e), and the periphery (c & f) compared to a no-damage scenario. a-c: Scenarios with endogenously evolving labor productivity levels. d-f: Scenarios without endogenously evolving labor productivity levels.



Suppl. Figure 3: Evolution of mortality rates in the center (diamonds), semiperiphery (dots) and periphery (triangles) for different age groups in the baseline scenario (grey) and two damage scenarios (red). a-c) Mortality rates of population aged 10-14, 40-44 and 70-74 in the baseline and in the ABC-type-damage scenario with low impacts and endogenously evolving labor productivities. d-f) Mortality rates of population aged 10-14, 40-44 and 70-74 in the baseline and the ABC-type-damage scenario with high impacts and without endogenously evolving labor productivities.

Endogenizing demographic developments in integrated assessment models: a study of global population dynamics under climate change-induced economic degrowth

Abstract

We integrate a regionalized world population model into an integrated assessment model to simulate demographic dynamics until 2100 in four socio-economic scenarios that differ with regard to the presence of population policies and climate change damages to economic production. While world population peaks and declines between 2050 and 2070 in all scenarios, simulations show that both a fertility policy and climate change damages lead to a lower average age of the population and increase the number of births. In scenarios with climate change damages, the size of the world population falls faster due to a strong increase in deaths resulting from a climate change-induced and unintentional degrowth in global economic output. Although all world regions are affected, middle- and low-income countries are hit hardest, as the global convergence in mortality rates observable in the no-climate-change scenario comes to a halt and regional differences in mortality rates increase again. Simulations show that the mortality rate at the regional level in 2100 increases between 1.45- and 3.88-fold compared to scenarios without climate change, with additional deaths per year between 2070 and 2100 ranging from 0.1–1.4 million in high-income countries, 3–12 million in upper-middle-income countries, and 10–22 million in lower-middle- and low-income countries. Our simulations further indicate that a fertility policy in high-income countries, under scenarios with climate change damages, can have adverse effects on mortality rates during the phase of economic decline by lowering consumption levels across all world regions.

Keywords

System dynamics; integrated assessment modeling; world population model; climate damages; global population dynamics; socio-economic scenarios

1. Introduction

Population dynamics are central to the study of global environmental and climate change, as demographic changes both drive and are driven by changing planetary conditions (Muttarak, 2021). Yet, future demographic developments and their interactions with global economic and environmental systems remain inherently uncertain. In this context, multidimensional integrated models provide a systematic and quantitative means of addressing the demography–economy–climate nexus and conducting scenario analyses that can inform policy-making across demographic, economic, and environmental domains.

Models have been used to examine how demographic developments contribute to environmental pressure and climate change by influencing economic growth rates and greenhouse gas emission pathways (Dodson et al., 2020; Kc & Lutz, 2014). At the same time, the size and structural composition of the world's population—including educational levels and geographic distribution—determine how many people will face the socio-economic impacts of environmental degradation and shape societies' capacity for both mitigation of and adaptation to climate change (Lutz, 2017; Lutz & Striessnig, 2015).

A second strand of modeling research investigates how adverse climate change impacts may, in turn, affect demographic dynamics. This research direction resonates with scholarly calls to examine catastrophic climate scenarios (Kemp et al., 2022), and with the emerging field of the 'demography of disaster' (Karácsonyi et al., 2021). Quantitative studies have addressed a broad range of issues, including the direct impacts of climate change on mortality through various channels such as heat, malaria, dengue, diarrhoeal disease, and undernutrition under different RCP scenarios (Pottier et al., 2021); the temperature-related mortality burden under alternative climate and population scenarios (Hajat et al., 2023; Ignjačević et al., 2024; Rai et al., 2019); and changes in temperature-related mortality burdens with adaptation under different shared socio-economic pathways (SSPs) (Wan et al., 2024). Other studies have explored demographic shifts resulting from flooding (Shu et al., 2023) and the demographic implications of climate-induced migration (Hauer et al., 2024).

Nevertheless, models that simultaneously examine the effects of population on the climate system and of climate change on demographic processes remain scarce. Notable exceptions include the integrated climate–economy–demography models developed by Gerlagh et al. (2023), and by Lupi & Marsiglio (2021), the latter based on the Integrated Assessment Model (IAM) DICE. However, both are limited by their level of aggregation, which prevents them from representing demographic changes at the regional level or accounting for the demographic implications of socio-economic inequality. Moreover, although some scholars have explicitly quantified climate-induced changes in fertility rates in developing countries (Casey et al., 2019; Shayegh, 2017), changes in birth rates are often neglected in modeling exercises addressing the demography–economy–climate nexus (Grace, 2017).

In light of these gaps, the present article pursues three main objectives. First, we aim to illustrate how the interlinked evolution of world population, global economic production, and planetary environmental conditions can be endogenized by coupling a population model with an IAM. Compared to other demographic models that can be integrated into an IAM (Court & McIsaac, 2020; Rozell, 2017), the population model developed here features a higher level of complexity by incorporating disaggregation by region, age, and socio-economic class. Second, we want to analyze how demographic variables at the regional and the global level might evolve in the absence of any global environmental changes, as well as in the presence of population policies.

Last, we explore how climate change might indirectly impact demographic developments through climate-change induced losses in economic production.

The remainder of this paper is structured as follows. The next section describes the structure of the developed population model and its integration into the selected IAM. We then present the results of four simulation scenarios, highlighting unexpected findings and feedback dynamics. Finally, we discuss caveats in interpreting the simulation results, summarize the key methodological advances resulting from this modeling exercise, and outline avenues for future research.

2. Methods

2.1. A regionalized world population model

We used the system dynamics software Vensim to develop a global scale population model that serves to simulate demographic dynamics over time. For this purpose, the world population is disaggregated into three world regions—center, semiperiphery, and periphery—and into 20 age cohorts in five-year intervals, ranging from the group of zero to four-year-olds to the group of those aged at 95 or older. Thus, each age cohort, except the last, covers five years. The model distinguishes between individuals fully integrated into the global economy and those who subsist partially or entirely at the margin of it. The latter are assumed to derive their means of livelihood primarily from non-monetized sources outside the world economy. Additionally, while all people living in subsistence conditions belong to the same ‘subsistence’ class, the population that lives fully integrated in the global economy is divided into nine consumption classes. The size of the classes is derived by dividing the population at the regional level into the richest 20% (R20), the poorest 30% (P30) and the middle class which covers the remaining half of the population (M50) at every moment of the simulation.

To calculate the evolution of the population fully integrated into the global economy, the following factors are considered: the initial population stock broken down by age and region; the flow of births; the flow of deaths; the flow of population transitioning from the global economy to the subsistence regime; the flow of population moving from subsistence to the global economy; and the population shifting from one age group to another.

The population stock of the youngest age group (zero- to four-year-olds) is calculated according to equation (1), the population stock of the oldest age group (95 or older) according to (2), and the stock of the remaining age groups according to equation (3). A list of subscripts and superscripts is provided in the Appendix.

$$P_{r,c04}^{we} = \int_{t_0}^t \left(B_r^{we} - D_{r,c04}^{we} + M_{r,c04}^{sub2we} - M_{r,c04}^{we2sub} - \frac{P_{r,c04}^{we}}{5} \right) dt + P_{r,c04}^{we}(t_0) \quad (1)$$

$$P_{r,c95+}^{we} = \int_{t_0}^t \left(\frac{P_{r,c9094}^{we}}{5} - D_{r,c95+}^{we} + M_{r,c95+}^{sub2we} - M_{r,c95+}^{we2sub} \right) dt + P_{r,c95+}^{we}(t_0) \quad (2)$$

$$P_{r,am}^{we} = \int_{t_0}^t \left(\frac{P_{r,ay}^{we}}{5} - D_{r,am}^{we} + M_{r,am}^{sub2we} - M_{r,am}^{we2sub} - \frac{P_{r,am}^{we}}{5} \right) dt + P_{r,am}^{we}(t_0) \quad (3)$$

Population dynamics in the model are determined by birth and death flows.

The birth flow is calculated with the population stock and the birth rate of every age group that belongs to the reproductive age, i.e. all age groups between 15 and 44. Birth rates are

endogenously calculated based on per capita consumption ($Cpc_{r,cl}$), which differs between the 9 social classes, and public education expenses per capita ($Edpc_r$). Different functional forms are used to estimate birth rates across age groups to achieve a better statistical fit. When per capita consumption falls below the subsistence level which is constituted by the extreme poverty line of the Worldbank for 2017, a different function is applied to calculate the birth rate. This function is adopted for all age cohorts, and its parameters are adjusted so that when per capita consumption drops to half of the subsistence level, the birth rate drops to zero. If the per capita consumption of a class in the global economy is higher than the subsistence consumption, the birth rates over five years for every age group belonging to the reproductive age are calculated with equations (4) to (9), otherwise they are calculated according to equation (10). Annual birth rates are calculated by equation (11) and the number of births at the regional level is derived by summing over all age groups (12).

$$Br5y_{r,c1519}^{we} = \sum_{cl} \left(\left(yf_{c1519}^{Br5y} + (y0_{c1519}^{Br5y} - yf_{c1519}^{Br5y}) \cdot e^{-\alpha_{c1519}^{Br5y} \cdot (Cpc_{r,cl}^{we,s} + Edpc_r)} \right) \cdot clsh_{cl} \right) \quad (4)$$

$$Br5y_{r,c2024}^{we} = \sum_{cl} \left(\left(yf_{c2024}^{Br5y} + (y0_{c2024}^{Br5y} - yf_{c2024}^{Br5y}) \cdot e^{-\alpha_{c2024}^{Br5y} \cdot (Cpc_{r,cl}^{we,s} + Edpc_r)} \right) \cdot clsh_{cl} \right) \quad (5)$$

$$Br5y_{r,c2529}^{we} = \sum_{cl} \left(\left(yf_{c2529}^{Br5y} + (y0_{c2529}^{Br5y} - yf_{c2529}^{Br5y}) \cdot e^{-\alpha_{c2529}^{Br5y} \cdot (Cpc_{r,cl}^{we,s} + Edpc_r)} \right) \cdot clsh_{cl} \right) \quad (6)$$

$$Br5y_{r,c3034}^{we} = \sum_{cl} \left(\left(\beta_1_{c3034}^{Br5y} + \beta_2_{c3034}^{Br5y} \cdot \ln(Cpc_{r,cl}^{we,s} + Edpc_r) \right) \cdot clsh_{cl} \right) \quad (7)$$

$$Br5y_{r,c3539}^{we} = \sum_{cl} \left(\left(\beta_1_{c3539}^{Br5y} + \beta_2_{c3539}^{Br5y} \cdot (Cpc_{r,cl}^{we,s} + Edpc_r) \right) \cdot clsh_{cl} \right) \quad (8)$$

$$Br5y_{r,c4044}^{we} = \sum_{cl} \left(\left(yf_{c4044}^{Br5y} + (y0_{c4044}^{Br5y} - yf_{c4044}^{Br5y}) \cdot e^{-\alpha_{c4044}^{Br5y} \cdot (Cpc_{r,cl}^{we,s} + Edpc_r)} \right) \cdot clsh_{cl} \right) \quad (9)$$

$$Br5y_{r,a}^{we} = \max \left(0, \sum_{cl} \left((\beta_0_a^{Br5y} + \beta_1_a^{Br5y} \cdot Cpc_{r,cl}^{we,s}) \cdot clsh_{cl} \right) \right) \quad (10)$$

$$Br_{r,a}^{we} = \frac{Br5y_{r,a}^{we}}{5} \quad (11)$$

$$B_r^{we} = \sum_a (P_{r,a}^{we} \cdot Br_{r,a}^{we}) \quad (12)$$

Deaths are calculated from the population stock of different age groups and their respective mortality rates. These mortality rates depend on class-specific per capita consumption and public healthcare expenses per capita (Hpc_r). Death rates over five years are obtained through equation (13), annual death rates through equation (15) and total deaths per year through equation (16). When the per capita consumption of a class belonging to the global economy falls below the subsistence level, a different equation is used (14), which sets the annual mortality rate to 1 once per capita consumption has dropped to half of the subsistence consumption level, reflecting rapidly increasing mortality rates once extreme poverty can no longer be buffered by subsistence-based coping mechanisms.

$$Dr5y_{r,a}^{we} = \sum_{cl} \left(\left(yf_a^{Dr5y} + (y0_a^{Dr5y} - yf_a^{Dr5y}) \cdot e^{-\alpha_a^{Dr5y} \cdot (Cpc_{r,cl}^{we,s} + Hpc_r)} \right) \cdot clsh_{cl} \right) \quad (13)$$

$$Dr5y_{r,a}^{we} = \min \left(5, \sum_{cl} \left((\beta 0_a^{Dr5y} + \beta 1_a^{Dr5y} \cdot Cpc_{r,cl}^{we,s}) \cdot clsh_{cl} \right) \right) \quad (14)$$

$$Dr_{r,a}^{we} = \frac{Dr5y_{r,a}^{we}}{5} \quad (15)$$

$$D_{r,a}^{we} = P_{r,a}^{we} \cdot Dr_{r,a}^{we} \quad (16)$$

To calculate the population flow from the global economy to the subsistence economy, first the share of the population that wishes to migrate is calculated for each region and social class. The share is then used to determine the flow (19). The share is calculated based on per capita consumption and always ranges between 0 and 0.1 (17). The migration flow can be constrained by the amount of land available for subsistence agriculture which depends on the land productivity in the subsistence economy (18).

$$Mr_{r,cl}^{we2sub} = \max \left(0; \min \left(0.1, \beta 0 - \beta 1 \cdot Cpc_{r,cl}^{we,s} (ts - 1) \right) \right) \quad (17)$$

$$MaxP^{sub} = Lnd^s \cdot Int_{sub_lnd}^{Lnd} \quad (18)$$

$$\begin{aligned} M_{r,a}^{we2sub} &= \max \left(0; \min \left(1; \frac{MaxP^{sub} - P^{sub}}{\sum (Mr_{r,cl}^{we2sub} \cdot P_{r,a}^{we} \cdot clsh_{cl}))} \right) \right) \\ &\cdot \sum_{cl} (Mr_{r,cl}^{we2sub} \cdot P_{r,a}^{we} \cdot clsh_{cl}) \end{aligned} \quad (19)$$

Likewise, the flow from the subsistence economy to the global economy is calculated using the share of people wanting to migrate and the stock of population in the subsistence regime. The share is determined based on the per capita consumption in the lower classes of different regions within the global economy and the fixed per capita consumption in the subsistence sector. It is assumed that the willingness to migrate increases with the difference between the consumption of the poorest classes in the global economy and the consumption in the subsistence regime. If there is insufficient land to sustain the subsistence population (18), forced integration into the global economy occurs. This process serves as an adjustment mechanism when subsistence conditions cannot support the existing population.

$$Mr_r^{sub2we} = \max \left(0, \min \left(0.1; \beta 1 \cdot (Cpc_{r,low}^{we,s} - Cpc^{sub}) \right) \right) \quad (20)$$

$$M_{r,a}^{sub2we} = \max \left(Mr_r^{sub2we} \cdot P_{r,a}^{sub}; \left(\frac{\max(0; P^{sub} - MaxP^{sub})}{P^{sub}} \right) \cdot P_{r,a}^{sub} \right) \quad (21)$$

The same equations (1) to (21), which are used for the population integrated into the global economy, are also applied to the subsistence class, with only two differences. First, instead of using the sum of per capita consumption and public education or health expenses to calculate birth and death rates, only the constant per capita subsistence consumption is used because it is assumed that the subsistence class is not covered by the benefits of public expenditures. Second, in the equations used to calculate population changes, migration terms have reversed signs. This is because migration flows from the global economy to subsistence represent an inflow for the subsistence population but an outflow for the global economy's population stock. Conversely, migration from subsistence to the global economy constitutes an outflow for the subsistence population and an inflow for the global economy.

The non-demographic variables in the population module such as per capita consumption, land intensity or public spending constitute exogenous input variables. At the same time, if required for a particular scenario analysis, endogenous demographic developments can be altered by introducing exogenous variables that can replace or modify endogenous variables such as birth or death rates.

The data for the initial population stock comes from UN population data for 2020 (UN DESA, 2019c) which disaggregates population into countries and into 21 age groups. We aggregated the two oldest age groups, and aggregated countries into three world regions according to average income levels. The world region ‘center’ includes the high-income countries; the ‘semiperiphery’ includes the upper-middle income countries and the ‘periphery’ covers the lower- and low-middle income countries. The size of the subsistence population was set to 800 million in 2019 of which 85% were matched to the periphery and 15% to the semiperiphery. To determine the parameters of equations (4) - (9) and (13), a total of 25 regression models were constructed based on the disaggregated Exiobase3 final demand data on household consumption and public expenditure for health and education (Stadler et al., 2018) and age-specific mortality and fertility rates from the UN (2019b, 2019a), covering the period between 1995 and 2020. To convert household final demand into consumption per capita, the disaggregated Exiobase3 data was divided by the population size of the respective countries or world regions by using UN population data (2019c). Unlike Court & McIsaac (2020) we do not use gross world output or GDP as independent variable since we hold that only consumption goods, especially education and health services, can have an effect on mortality and fertility rates by changing living standards, while non-consumption goods might be necessary to sustain production processes but do not have a direct effect on demographic variables. While consumption per capita is the most important determinant of fertility and mortality rates we find that the statistical fit can be increased by factoring in per capita public expenses for health in the case of mortality rates, and for education in the case of birth rates. The parameters for equations (4) - (7), (9) and (13) were calculated with nonlinear least squares asymptotic regression models via the R NLS/SSasymp commands from the stats package while the parameters for equations (7) and (8) were estimated by using a logarithmic, and a linear regression model, respectively. Further information on the estimation of model parameters is provided in Lauer & Llases (2025).

2.2. Integration into MORDRED

By coupling the population model with a global economic socially and environmentally extended input-output model based on EXIOBASE3 data, we integrate the model into the IAM ‘MORDRED’ (Model of Resource Distribution and Resilient Economic Development), which is described in detail in Lauer & Llases (2025). This coupling results in the endogenization of a series of demographic, economic and environmental variables.

First, economic developments influence demographic developments through changes in the per capita consumption of the different social classes that lower or increase age-specific mortality and fertility rates in the three world regions. These class-specific changes in consumption are determined by exogenously determined desired growth rates for every class, and by the availability of economic input factors necessary to produce the desired economic output. When the amount of available input factors is insufficient to satisfy total demand an allocation rule is applied that can be set to prioritize the consumption demands of certain classes or to proportionally reduce the consumption of all classes. The main input factors in the economic model are labor, fossil resources, land and intermediate goods. To provide greater flexibility for

model users, the feedback between input factors and economic production can be deactivated—with the exception of intermediate goods—so that the economy can continue to grow even when one or several input factors become scarce.

Second, demographic developments influence economic developments through the input factor 'labor'. The share of the world population that lives outside of the subsistence sector and falls within the working age, which is set to 15 to 64 years, constitutes the global labor force sustaining the world economy. The maximum number of working hours that can be demanded by economic processes depends on the size of the working force, the participation rate and the number of annual hours worked. The size of economic output that can be produced with these working hours depends on specific labor productivities that differ among the 25 sectors of the economic module of MORDRED. The migration from the subsistence sector to the global economy leads to an increase of the working force. Thus, the input factor labor evolves endogenously in the model and is affected by changes in demographic structures in the three world regions.

Last, economic activities in MORDRED produce greenhouse gas emissions that cause the global average temperature to increase. The adverse impacts of climate change are reflected through a series of non-linear damage functions that influence the capital depreciation, output, input requirements of intermediate goods, land intensities of the subsistence and the global economy, labor productivities and hours worked. Thus, integrating the population model into MORDRED allows us to assess demographic effects of climate change through climate change impacts on economic production processes. Rather than calculating direct increases in mortality rates due to heat (Chapman et al., 2022; Gasparrini et al., 2017; Guibert et al., 2024), other extreme weather events (Ebi, 2014), or the spread of vector-borne diseases (Messina et al., 2019), the IAM simulates possible climate change-induced deteriorations in production efficiencies and declines in economic output that in turn affect both fertility and mortality rates.

Figure 1 illustrates the main links resulting from the integration of the population model into MORDRED.

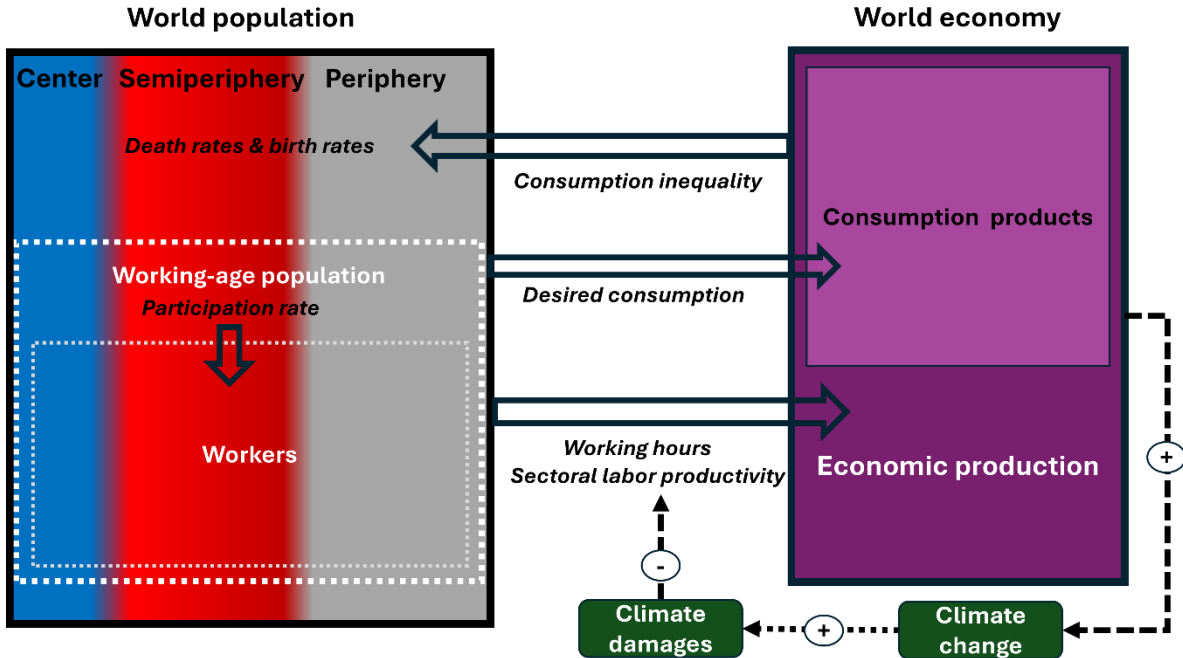


Figure 1: Main links between the demographic and the economic part of MORDRED. (+) signs indicate the increase of a variable leads to an increase in the variable it influences. (-) indicates that the increase of a variable leads to a decrease in the variable it influences.

2.2. Scenario design

We design four simple scenarios to illustrate different demographic dynamics produced by the model. They are called *Baseline* (BL), *Baseline-High fertility* (BL-HF), *Damages* (DM), and *Damages-High fertility* (DM-HF). The scenarios cover the period 2019 to 2100. To reduce the level of complexity in the model simulation, we deactivate the land scarcity feedback in the model for all scenarios, only focusing on feedbacks between the climate, economy, labor and population modules.

The *Baseline* scenario simulates demographic developments in the absence of exogeneous population policies and adverse climate change impacts. Economic development is characterized by high energy efficiency gains and reductions in greenhouse gas intensities but also by strong continuous growth of the world economy, with low- and middle-income regions (periphery and semiperiphery) growing faster than high-income regions (center). This results in a medium-emission pathway with moderate global economic convergence.

The BL-HF scenario differs from the BL only in terms of an exogenous population policy which is specified to increase fertility rates of the high-income countries by 20% for a given consumption level. The policy is applied across all age groups in the reproductive age.

Economic growth, energy and greenhouse gas intensities in the *Damages* scenario are parametrized the same way as in the *Baseline* but climate damages in MORDRED are activated that affect the labor and the economy modules.

In the DM-HF scenario the same fertility policy is added as in the BL-HF scenario.

The parametrization of the scenarios is given in Section 1 of the Supplementary Material (SM). For the simulations, we use MORDRED version 1.0.4, which, unlike version 1.0 features endogenously evolving sectorial labor productivities.

3. Results

This section presents the main demographic dynamics emerging from the different scenario simulations and links them to underlying developments in the economic and biophysical system.

3.1. Demographic developments without climate impacts

3.1.1. No population policies

In the Baseline scenario, world population stabilizes between 2050 and 2070 after an initial phase of growth, peaking in 2055 at 8.7 billion people. Thereafter, population declines markedly, reaching 7.79 billion by 2100 — similar to the level at the start of the simulation (Figure 2a). These developments closely resemble the SSP5 projections and show parallels with SSP1 (Kc & Lutz, 2017). Conversely, SSP population projections based on a continuously growing per capita gross world product by Court & McIsaac (2020) do not peak, resulting in a much larger population by century's end.

The early and relatively low population peak results from rapidly increasing affluence across regions and social classes and moderate convergence between them, accelerating fertility decline. This resonates with both SSP1 and SSP5 – scenarios characterized by strong economic growth, low fertility and mortality as well as high education levels (Cuaresma & Lutz, 2015). By 2100, global annual output reaches €1,200 trillion, and world average consumption per capita exceeds €45,000 per year.

Rising consumption among the poorest 30% in the semiperiphery and periphery drives a continuous transition from subsistence to monetized economic activity. As the consumption gap widens, more people seek to enter the global economy, leading to the near disappearance of the subsistence sector by 2100 (Figure 2b). This dynamic reflects the model's assumption of high migratory capacity and a strong absorptive ability of formal economies to integrate new labor. The Baseline scenario thus reflects a storyline imagining a smooth and successful globalization, with the spread and stabilization of industrialized and monetized production throughout the world.

At the regional level (Figure 2c), population in the center declines continuously, falling by 35% between 2020 and 2100. In the semiperiphery, population rises modestly from 2.9 billion in 2019 to 3 billion in 2031, then declines gradually to 2.44 billion in 2100. In the periphery, population grows strongly from 3.6 billion to 4.9 billion in 2070, before falling to 4.56 billion by 2100. Consequently, the periphery's population becomes increasingly dominant: in 2020 it was 12% smaller than the combined population of other regions, but by 2100 it is 40% larger.

The moderate convergence assumed in the Baseline not only drives these demographic patterns but also shifts regional consumption scales. Despite persistent per capita gaps, the periphery's total consumption rises from one fifth of the center's at the start to 1.7 times the center's and 30% more than the semiperiphery's by 2100. Nevertheless, per capita consumption levels in the periphery are still lower than in the other world regions at the end of the simulation.

Birth and death dynamics underlie these trends (Figure 2d and e). Annual births in the periphery peak in 2035—about 35 years before total population peaks. Between 2035 and 2100, births decline steadily in all regions, with a weak convergence tendency. By 2100, annual births have fallen by **37%**, **43%**, and **23%** in the center, semiperiphery, and periphery, respectively. Deaths rise strongly in the periphery due to population growth and aging (Figure 2h), while in the center they rise slightly because of an older age structure. Although deaths increase in absolute terms, the mortality index (relative to initial rates) declines continuously across regions (Figure 2f), falling by over 70% in the semiperiphery and 75% in the periphery, indicating convergence in absolute mortality by 2100.

Consequently, global population grows older: average age rises from <33 years at the start to >43 years by 2100 (Figure 2g). Demographic convergence also takes place (Figure 2h): the center's average age rises modestly (41 → 44), the semiperiphery's from 35.5 to 44, and the periphery's from <28 to 43 years.

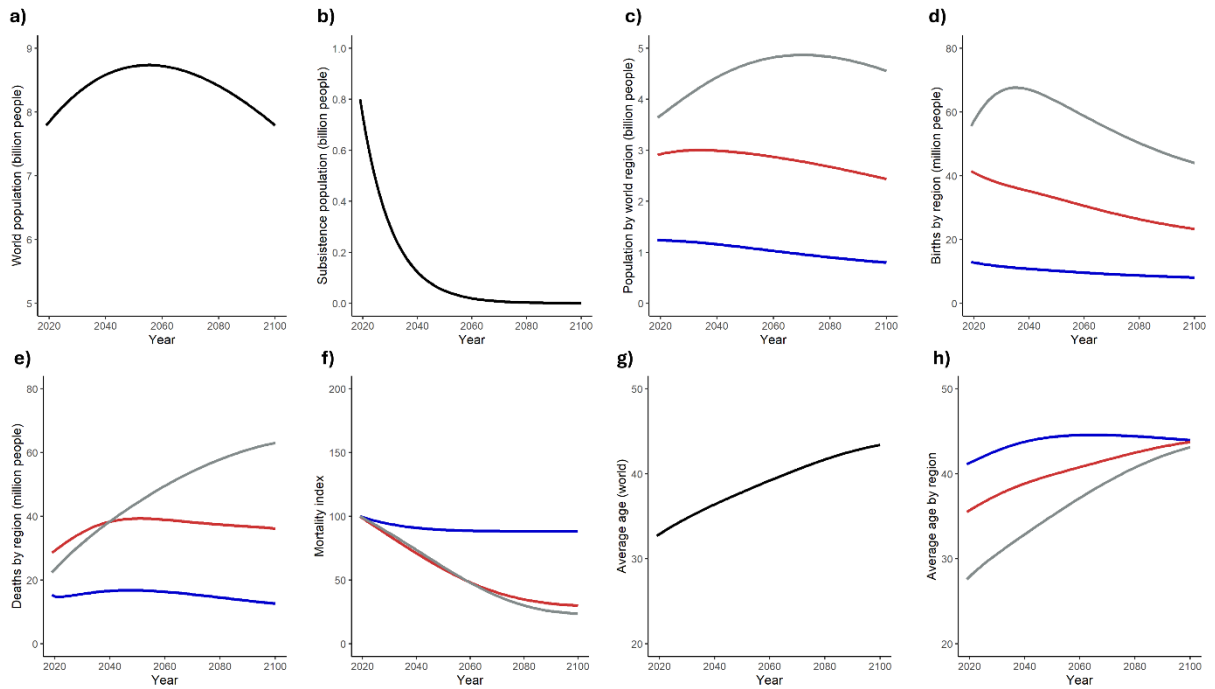


Figure 2: Main demographic dynamics of the Baseline scenario. a) World population; b) population living in subsistence; c) population in the center (blue), semiperiphery (red) and periphery (grey); d) annual births by region; e) annual deaths by region; f) mortality index (initial mortality rate in every region = 100; shows relative changes for every region); g) average age of the world population; h) average age by region.

3.1.2. Exogeneous population policies

Given the continuous decline and aging of the population in the center, it is reasonable to explore the effects of a fertility policy aimed at increasing birth rates. At the same time, it is worth emphasizing that in our scenario simulation, the semiperiphery exhibits comparable demographic dynamics from 2040 onwards. In the model, affluence and economic development raise labor productivity, allowing economies to grow despite aging. Thus, pro-natalist policies in high-income countries (BL-HF scenario) would be motivated less by internal stability concerns than by geopolitical factors, particularly in response to the population growth of other regions (Figure 2c).

As a result, world population in the BL-HF scenario grows slightly faster, peaking at 8.8 billion in 2058 (Figure 3a). In the center, the policy significantly slows population decline, yielding 280 million more people in 2100—over one third of the center’s baseline population (Figure 3b). This difference stems from birth and death dynamics: in the baseline, births decline continuously, whereas in BL-HF they stabilize after 2040 and rise slightly in the last three decades of the simulation (Figure 3c). Deaths follow a similar trajectory in both scenarios until 2070, after which they decrease more slowly under BL-HF. (Figure 3c). As a result of the policy, average age in the center peaks at 42.5 years in 2045, then declines below 41 years by 2090.

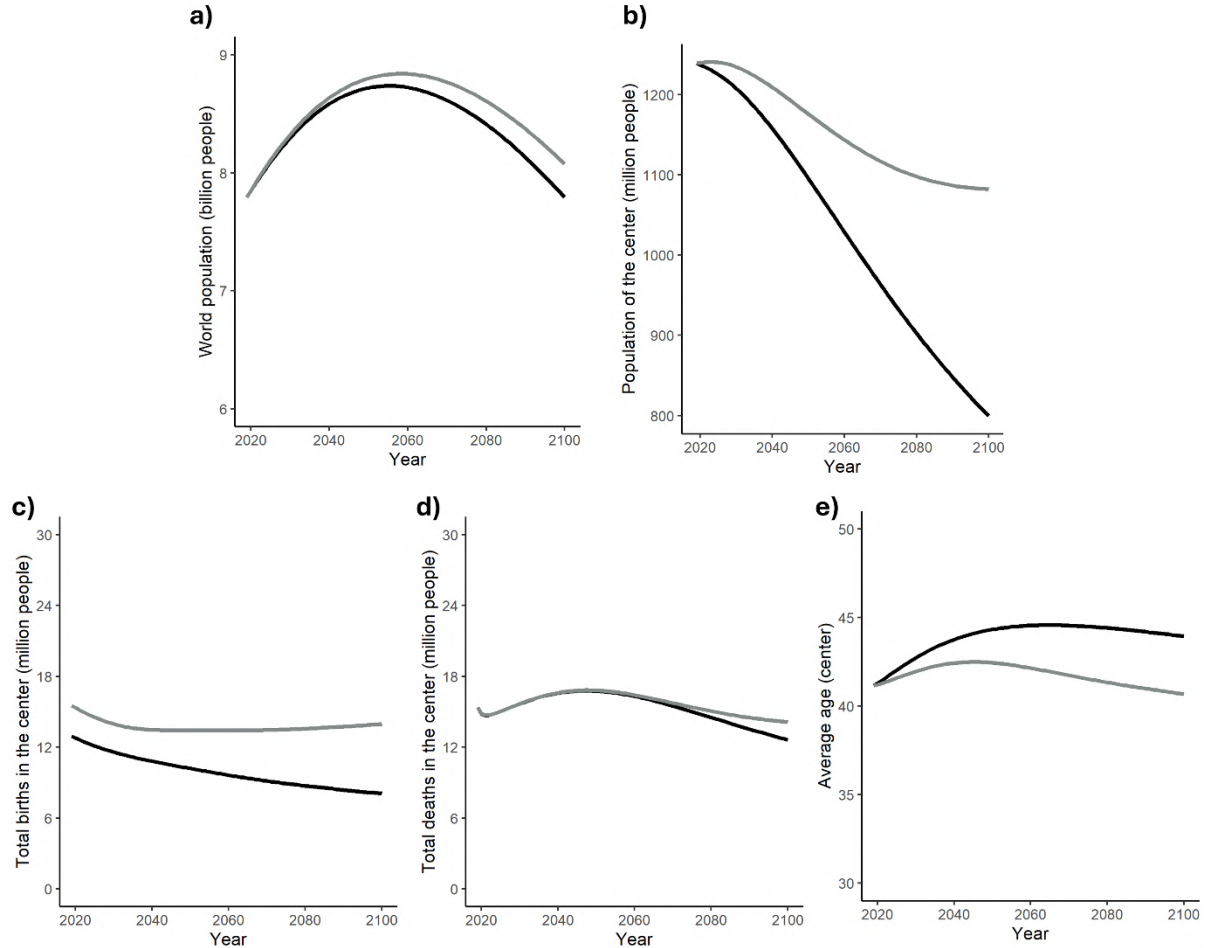


Figure 3: Demographic changes due to a fertility policy applied in high-income countries in the BL (black) and the BL-HF scenario. a) World population; b) population of the center; c) total births, d) total deaths and e) average age in the center.

3.2. Effects of climate change on demographic developments

The BL and BL-HF scenarios depict demographic change in the absence of environmental shocks. The following sections demonstrate how these trajectories alter when climate damages to the global production system are introduced.

3.2.1. No population policies

In the Damages (DM) scenario, economic losses from rising temperatures accumulate until global output halts in 2066 due to labor shortages. Economic production collapses between 2066–2075, driven by falling labor productivity, lower production, and shrinking consumption,

before stabilizing at a lower output level. These shocks transform demographic trends (Figure 4a to r). The economic collapse causes a sharper population decline than in the BL scenario (red vs. black line in Figure 4a). While subsistence-economy dynamics remain broadly similar (Figure 4b), climate change reduces land productivity and available arable land. Because land feedbacks on production are deactivated in this simulation, subsistence expansion is unconstrained by global economic land demand. Consequently, land-related damages are not reflected in demographic outcomes—rendering the simulation blind to potential forced migration from subsistence to formal sectors. If such climate-driven livelihood losses were considered, migration to the world economy would likely intensify as long as economic opportunities remained higher. Under stronger economic collapse or weaker convergence, migration could reverse, as impoverished groups re-integrate into subsistence regimes outside monetized structures.

Climate change in the DM scenario not only reduces total population faster but also yields a younger global population (Figure 4c). Average age peaks just above 40 years in 2068, then declines to 38.5 by 2100. Regional divergence grows in the final decades: in the center, population decline accelerates, while in the semiperiphery the economic collapse causes a temporary sharp fall that later stabilizes (Figure 4d and e). In the periphery, this process occurs earlier, and by 2100 its population slightly exceeds that in the BL scenario (Figure 4f).

Climate-induced economic disruption decreases births in the center (Figure 4g) but increases them sharply in the other regions (Figure 4h and i). In the periphery, births show a second peak between **2070–2080**, following the first in 2030–2040. This pattern arises from cohort-specific fertility behavior: younger cohorts (15–29 years) exhibit higher fertility under lower consumption, while older groups (30–39 years) have higher fertility with rising consumption. As economic decline reduces consumption, fertility rises in younger cohorts and falls in older ones. In the center, older groups dominate, producing a net fertility decline. In the semiperiphery and periphery, stronger fertility increases among younger cohorts offset the decline among older ones, yielding higher total births (Figures 2 & 3 in the SM).

Deaths rise sharply in all regions, especially the periphery (Figure 4j-l). In the center, deaths in DM exceed BL by 1–1.4 million annually (2070–2080) and 0.1–1 million (2080–2100). In the semiperiphery, excess deaths reach 9–12 million (2070–2080) and 3–9 million (2080–2100); in the periphery, 19–22 million and 10–19 million, respectively.

While deaths and births drive population size, mortality rates can be taken as an indicator of the quality of life of the population (Figure 4m-o). The DM scenario is characterized by an increase in the mortality rate index from 2067 onwards that affects all age cohorts and all regions. In the center, mortality rises 28% above initial levels by 2100; in the semiperiphery, it returns to initial levels after an earlier 55% decline; in the periphery, it drops to 42 by 2067 but rebounds to 93 by 2100. Thus, relative deterioration is strongest in the semiperiphery, but in absolute terms the periphery experiences the greatest mortality increase. Climate damages thus halt and reverse the mortality convergence observed in the Baseline scenario (Section 2 SM).

Population aging also reverses (Figure 4p-r). All regions become younger, though the shift is modest in the center and pronounced elsewhere: in the semiperiphery and the periphery the climate change induced demographic changes are so strong that they result in a peak and subsequent decline of the average age in the DM scenario. In 2100, the average age in the semiperiphery is 39, compared to 44 in the BL. In the periphery, average age declines from 39 in

2067 to 37 in 2100, compared to an increase to 43 in BL. Hence, the reversal of global aging stems mainly from demographic rejuvenation in poorer regions.

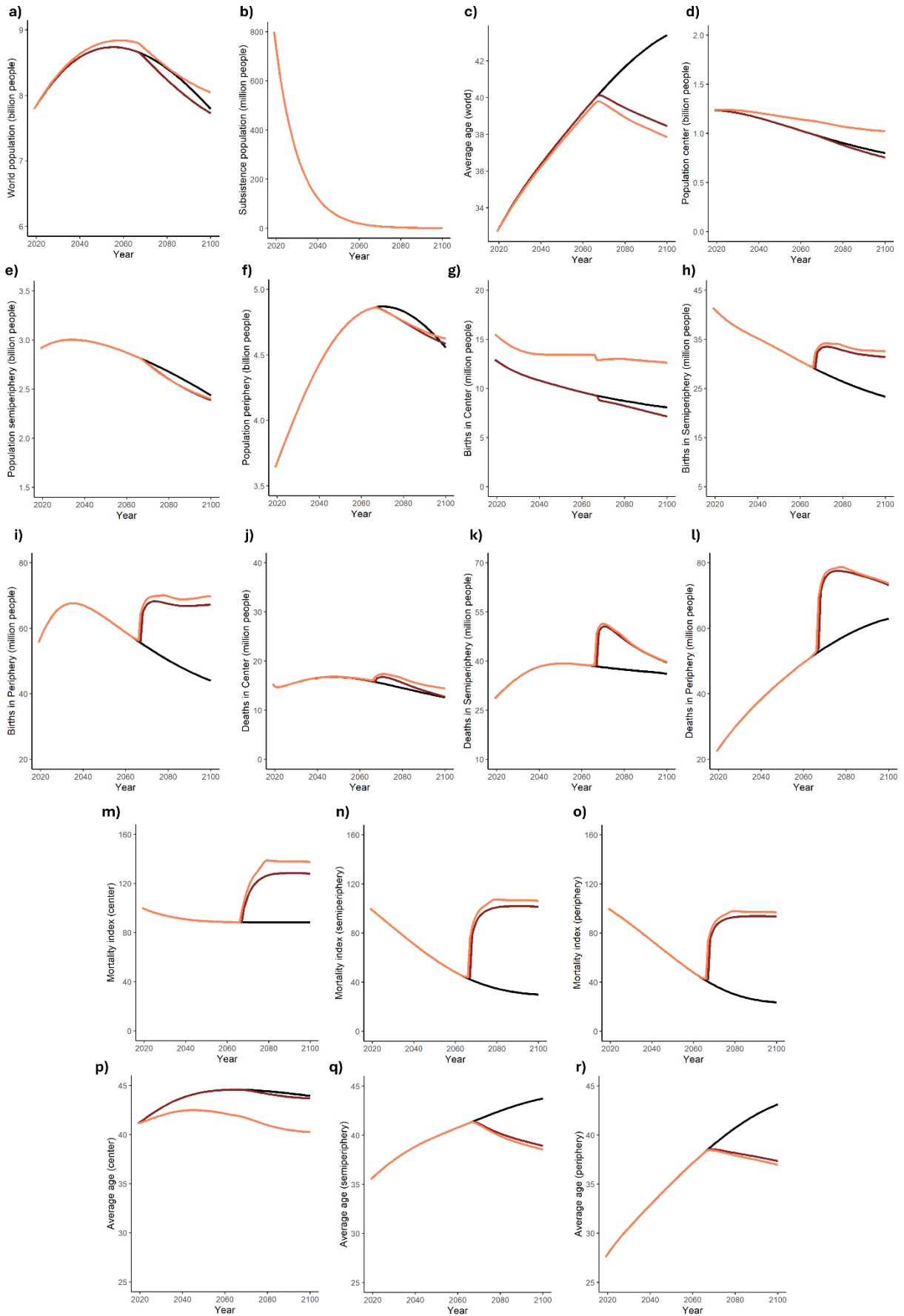


Figure 4: Evolution of key demographic variables in the DM (red) and DM-HF (orange) scenario, compared to the BL (black) scenario. a) World population; b) population living in subsistence; c) average age of the world population;

population in the center (d), semiperiphery (e) and periphery (f); annual births in the center (g), semiperiphery (h) and periphery (i); annual deaths in the center (j), semiperiphery (k) and periphery (l); mortality index in the center (m), semiperiphery (n) and periphery (o); average age in the center (p), semiperiphery (q) and periphery (r).

3.2.2. Population policies

Introducing climate damages in a scenario with a population policy applied to the high-income countries produces notable differences in demographic developments relative to the BL and the DM scenario (orange line Figure 4). World population peaks higher but declines faster, and the global average age falls further, reaching 37.9 years by 2100. However, while the change in average age in the center is the effect of the population policy, in the other regions it stems from adverse climate change impacts.

In the center, the policy raises births relative to DM, but climate impacts dampen its effectiveness—births remain below BL–HF levels. Moreover, the combination of higher fertility in the center and climate-related economic stress has unintended consequences for the demographic development in the semiperiphery and periphery: following the global output collapse, both births and deaths in the semiperiphery and periphery increase more than in DM (Figure 4h-l). As births and deaths have opposite effects on population size, these changes are harder to observe if only the total population is considered (Figure 4e and f). However, as illustrated by the mortality rate index, in the presence of a fertility policy in high-income countries, climate change effects lead to a stronger rise of mortality in all regions, with the relative change being especially pronounced in the center. These unexpected dynamics arise from additional consumption demands in the center. The larger population drives faster pre-collapse economic growth, an earlier downturn, and lower per capita consumption. The resulting pressure from sustaining a bigger wealthier population leads to higher mortality across all regions. Hence, under climate stress, a pro-natalist policy in the center not only proves unnecessary for maintaining, provided that labor productivity grows, but also worsens welfare and mortality outcomes during economic contraction.

4. Discussion

It is important to emphasize that the demographic dynamics presented in the previous section depend strongly on the underlying economic and climate scenario assumptions, particularly the exclusion of land-related feedbacks on demographic and economic developments. Adjusting parameters that influence labor productivity or emission intensities can substantially alter the trajectory of economic output and the interactions between the demographic and economic modules in the damage scenarios. Because most scenario parameters are subject to significant uncertainty, the demographic developments described must not be seen as prediction but rather as plausible dynamics under a given socio-economic and biophysical pathway. Nevertheless, the scenarios serve to illustrate the importance of considering interactions between the world population and the global economy in IAMs, given that demographic dynamics constrain, and simultaneously are constrained by, economic developments. Thus, while we acknowledge the deep uncertainty linked to global environmental changes and their interactions with the global socio-economic system (McLeman, 2025), we hold that endogenizing both demographic and economic developments in IAM related studies produces simulations that are ‘less wrong’ than those that exclude any feedback between population, economic production and climate change from the outset.

A previous study linking climate, economic, and demographic dynamics based on the relationship between gross world output per capita and age-specific fertility and mortality rates (Court & McIsaac, 2020), found that a climate-induced economic collapse could trigger higher population growth, yielding a larger and younger population. In contrast, our simulations—built on feedbacks between regionally and socio-economically disaggregated per capita consumption levels and age-dependent fertility and mortality rates—show an accelerated population decline accompanied by a younger average population, as mortality rises faster than birth rates. In MORDRED, climate damages increase the investment required to sustain production, reducing the share of consumption in final demand and total output as global temperature rises. Because it is consumption, not overall production, that determines life expectancy and fertility, models relying on output or income per capita may underestimate the demographic impacts of climate-driven economic contraction. To improve the accuracy of population–economy–climate projections, our findings suggest using consumption rather than income or production as the key driver of demographic change, while also disaggregating population dynamics by region and age.

Compared with the WHO estimate of 250,000 additional annual deaths between 2030 and 2050 (World Health Organization, 2014), the additional deaths projected in our simulations are one to two orders of magnitude higher. This discrepancy arises because the WHO study considers an earlier period, focuses on selected health outcomes, incorporates adaptation, and assumes continued economic growth rather than contraction. Thus, our findings suggest that the threat of climate change to the capacity of the economy to grow or at least to maintain stable productive processes is a currently overlooked and underestimated threat to future mortality rates. Also, although climate change impacts on fertility remain contested (Ahmed et al., 2024) the indirect effects observed in the MORDRED simulations reveal differentiated impacts across age and socio-economic groups, resulting in clear demographic deviations from a no-climate-change scenario. As noted earlier, our approach does not include direct mortality increases from climate effects such as heatwaves or floods. However, given the relatively small number of people affected compared with the large-scale demographic effects of climate-driven economic restructuring, this underestimation of mortality is likely minor.

The regionalized world population model presented here complements existing demographic models designed for IAM integration (Court & McIsaac, 2020; Rozell, 2017). The main advantage of our exploratory scenario approach lies in its integrated character, which allows simultaneous consideration of multiple drivers shaping demographic futures under severe global environmental change. For example, studies have stressed the importance of considering changes in the age structure when projecting climate change effects on demographic developments because elderly people are more vulnerable to climate change impacts such as extreme weather events (Cole et al., 2023; Lee et al., 2018). MORDRED accounts for regional changes in the age distribution, enabling an assessment of evolving vulnerabilities across world regions. Moreover, studies show that climate impacts on health, fertility, and mortality are mediated by socio-economic conditions (Liu-Helmersson et al., 2019; Messina et al., 2019). For instance, the population at risk from malaria is projected to decline by 2050 when economic growth effects are considered (Béguin et al., 2011) and evidence from India indicates falling mortality rates despite more frequent extreme weather events (Ray et al., 2021). MORDRED reflects these insights by treating socio-economic development as the primary determinant of fertility and mortality, and by framing environmental degradation as acting through changes in economic structure. By distinguishing consumption across socio-economic classes and regions,

the model captures differing vulnerability profiles, with low-consumption households disproportionately affected by indirect climate impacts.

Despite these methodological advances, many critical aspects of the population–economy–climate nexus remain beyond MORDRED’s current scope. We highlight three key directions for future work.

First, the model could be extended to represent migration flows between regions, enabling analysis of migration from the periphery to the center as an alternative to fertility policies, and of complex climate-induced migration dynamics. Such movements may result not only from deteriorating economic and environmental conditions but also from adaptation and mitigation measures, social perceptions, and narratives (Daoust & Selby, 2024) as well as non-economic climate damages currently not represented in MORDRED. For example, extreme weather events do not only affect productive processes but also reduce the quality of life due to their negative effects on mental health – including anxiety, depression and PTSD – (Batra & Erbas, 2025; Brown et al., 2025; Zhang et al., 2022) and by restricting the mobility of the affected population, particularly elderly people, adolescents, women and low-income groups (Tang et al., 2023; Wang et al., 2025; Yao et al., 2024).

Second, although the model allows for reversals in migration between the formal and subsistence economies, our simulations show no net migration back to the subsistence regime. This is because economic production stabilizes after the climate-induced growth reversal, and proportional consumption reductions across all classes prevent the poorest households from falling below subsistence levels. However, both migration propensity and the distribution of climate-induced economic losses are uncertain and could vary across scenarios. Future work should therefore explore alternative allocation mechanisms, higher migration propensities, and worst-case scenarios involving greater temperature increases and economic losses, to assess whether some pathways could plausibly trigger large-scale population movements from the global economy back to subsistence—a potential signal of radical economic reorganization.

Last, further insights could be gained by taking into account gender- and age-specific effects of climate change impacts (Alonso-Epelde et al., 2024; Prina et al., 2024) as well as to account for geographic differences (Falchetta et al., 2024; IPCC, 2022) and for direct climate change impacts on mortality and fertility rates (Lüthi et al., 2023; McElroy et al., 2022; Pottier et al., 2021).

5. Conclusion

This study integrated a population model into the IAM MORDRED and used scenario analysis to demonstrate the value of endogenizing demographic and economic dynamics in integrated assessment modeling. Our results show that both fertility policies and climate change impacts substantially influence demographic trajectories, and that population policies in one region can interact with global climate damages to produce unintended effects elsewhere due to the interconnected nature of the world economy. In our simulations, both fertility policies and climate impacts lead to a younger global population; however, fertility policies increase total population size, while climate change accelerates population decline. A climate-induced contraction of global economic production, driven by shortages of labor hours, raises both the number of births and deaths globally. The simulations indicate that mortality increases linked to economic collapse are significant: by 2100, mortality rates in the climate damage scenario are 1.45 times higher in the center and up to 3.88 times higher in the periphery compared to the no-climate-change case, corresponding to annual additional deaths of 0.1–1 million in the center

and 10–19 million in the periphery between 2080 and 2100. Future work could extend the demographic model to include interregional migration flows to better capture climate-induced migration, and further differentiate climate impacts by age, gender, and region. Finally, the methodological approach developed for MORDRED could be applied to other IAMs to enhance their ability to represent the coupled evolution of population, economy, and climate under global change.

Appendix

Subscripts and superscripts used in the model equations. The subscripts denote vectors, subvectors or vector elements. The superscripts complete the names of the variables or link parameters to the variables to be calculated.

Subscripts

Abbreviation	Type	Definition
a	Vector	Age cohort
am	Generic element created for the transition of population from one cohort to another	Middle age (generic cohort)
ay	Generic element created for the transition of population from one cohort to another. It is the cohort prior to the middle-aged cohort	Young age (generic cohort)
c04	Element (inside vector age cohort)	Cohort 0 to 4 years
c1519	Element (inside vector age cohort)	Cohort 15 to 19 years
c2024	Element (inside vector age cohort)	Cohort 20 to 24 years
c2529	Element (inside vector age cohort)	Cohort 25 to 29 years
c3034	Element (inside vector age cohort)	Cohort 30 to 34 years
c3539	Element (inside vector age cohort)	Cohort 35 to 39 years
c9094	Element (inside vector age cohort)	Cohort 90 to 94 years
c95+	Element (inside vector age cohort)	Cohort 95 years or more
cl	Vector	Class
Lnd	Vector	Land
low	Element (inside vector age class)	Poorest class
r	Vector	Region
sub_lnd	Element (inside vector land)	Land used by the population living in the subsistence sector

Superscripts

Abbreviation	Definition
Br5y	Birth rate per five years
Dr5y	Death rate per five years
s	Supply
sub	Subsistence

sub2we	Subsistence to world economy
we	World economy

References

- Ahmed, K. J., Tan, Y., & Rudd, D. (2024). Exploring the relationship between changes in fertility and disasters: A review of the literature. *Journal of Population Research*, 41(1), 1. <https://doi.org/10.1007/s12546-023-09324-9>
- Alonso-Epelde, E., García-Muros, X., & González-Eguino, M. (2024). Climate action from a gender perspective: A systematic review of the impact of climate policies on inequality. *Energy Research & Social Science*, 112, 103511. <https://doi.org/10.1016/j.jerss.2024.103511>
- Batra, M., & Erbas, B. (2025). Extreme Weather, Vulnerable Populations, and Mental Health: The Timely Role of AI Interventions. *International Journal of Environmental Research and Public Health*, 22(4), 602. <https://doi.org/10.3390/ijerph22040602>
- Béguin, A., Hales, S., Rocklöv, J., Åström, C., Louis, V. R., & Sauerborn, R. (2011). The opposing effects of climate change and socio-economic development on the global distribution of malaria. *Global Environmental Change*, 21(4), 1209–1214.
- Brown, H. E., Balakrishnan, A. K., Stamps, K. M., Obara, L. M., Witte, S. S., & Winter, S. C. (2025). Experiences of extreme weather and mental health in climate-vulnerable communities: Results from a large-scale survey of women living in informal settlements in Nairobi, Kenya. *BMC Psychology*, 13(1), 1–11.
- Casey, G., Shayegh, S., Moreno-Cruz, J., Bunzl, M., Galor, O., & Caldeira, K. (2019). The impact of climate change on fertility. *Environmental Research Letters*, 14(5), 054007.
- Chapman, S., Birch, C. E., Marsham, J. H., Part, C., Hajat, S., Chersich, M. F., Ebi, K. L., Luchters, S., Nakstad, B., & Kovats, S. (2022). Past and projected climate change impacts on heat-related child mortality in Africa. *Environmental Research Letters*, 17(7), 074028.
- Cole, R., Hajat, S., Murage, P., Heaviside, C., Macintyre, H., Davies, M., & Wilkinson, P. (2023). The contribution of demographic changes to future heat-related health burdens under climate change scenarios. *Environment International*, 173, 107836.
- Court, V., & McIsaac, F. (2020). A Representation of the World Population Dynamics for Integrated Assessment Models. *Environmental Modeling & Assessment*, 25, 611–632.
- Cuaresma, J. C., & Lutz, W. (2015). The demography of human development and climate change vulnerability: A projection exercise. *Vienna Yearbook of Population Research*, 241–261.
- Daoust, G., & Selby, J. (2024). Climate change and migration: A review and new framework for analysis. *WIREs Climate Change*, 15(4), e886. <https://doi.org/10.1002/wcc.886>
- Dodson, J. C., Dérrer, P., Cafaro, P., & Götmark, F. (2020). Population growth and climate change: Addressing the overlooked threat multiplier. *Science of The Total Environment*, 748, 141346. <https://doi.org/10.1016/j.scitotenv.2020.141346>
- Ebi, K. L. (2014). Health in the new scenarios for climate change research. *International Journal of Environmental Research and Public Health*, 11(1), 30–46.
- Falchetta, G., De Cian, E., Sue Wing, I., & Carr, D. (2024). Global projections of heat exposure of older adults. *Nature Communications*, 15(1), 3678. <https://doi.org/10.1038/s41467-024-47197-5>
- Gasparrini, A., Guo, Y., Sera, F., Vicedo-Cabrera, A. M., Huber, V., Tong, S., Coelho, M. de S. Z. S., Saldiva, P. H. N., Lavigne, E., & Correa, P. M. (2017). Projections of temperature-related excess mortality under climate change scenarios. *The Lancet Planetary Health*, 1(9), e360–e367.

- Gerlagh, R., Lupi, V., & Galeotti, M. (2023). Fertility and climate change. *The Scandinavian Journal of Economics*, 125(1), 208–252. <https://doi.org/10.1111/sjoe.12520>
- Grace, K. (2017). Considering climate in studies of fertility and reproductive health in poor countries. *Nature Climate Change*, 7(7), 479–485. <https://doi.org/10.1038/nclimate3318>
- Guibert, Q., Pincemin, G., & Planchet, F. (2024). Impacts of Climate Change on Mortality: An extrapolation of temperature effects based on time series data in France. *arXiv Preprint arXiv:2406.02054*.
- Hajat, S., Proestos, Y., Araya-Lopez, J.-L., Economou, T., & Lelieveld, J. (2023). Current and future trends in heat-related mortality in the MENA region: A health impact assessment with bias-adjusted statistically downscaled CMIP6 (SSP-based) data and Bayesian inference. *The Lancet Planetary Health*, 7(4), e282–e290.
- Hauer, M. E., Jacobs, S. A., & Kulp, S. A. (2024). Climate migration amplifies demographic change and population aging. *Proceedings of the National Academy of Sciences*, 121(3), e2206192119. <https://doi.org/10.1073/pnas.2206192119>
- Ignjačević, P., Botzen, W., Estrada, F., Daanen, H., & Lupi, V. (2024). Climate-induced mortality projections in Europe: Estimation and valuation of heat-related deaths. *International Journal of Disaster Risk Reduction*, 111, 104692.
- IPCC. (2022). *Climate Change 2022: Impacts, Adaptation and Vulnerability. Contribution of Working Group II to the Sixth Assessment Report of the Intergovernmental Panel on Climate Change*. Cambridge University Press. Cambridge University Press, Cambridge, UK and New York, NY, USA.
- Karácsonyi, D., Taylor, A., & Bird, D. (2021). *The demography of disasters: Impacts for population and place*. Springer Nature.
- Kc, S., & Lutz, W. (2014). Demographic scenarios by age, sex and education corresponding to the SSP narratives. *Population and Environment*, 35(3), 243–260.
- Kc, S., & Lutz, W. (2017). The human core of the shared socioeconomic pathways: Population scenarios by age, sex and level of education for all countries to 2100. *Global Environmental Change*, 42, 181–192. <https://doi.org/10.1016/j.gloenvcha.2014.06.004>
- Kemp, L., Xu, C., Depledge, J., Ebi, K. L., Gibbins, G., Kohler, T. A., Rockström, J., Scheffer, M., Schellnhuber, H. J., & Steffen, W. (2022). Climate Endgame: Exploring catastrophic climate change scenarios. *Proceedings of the National Academy of Sciences*, 119(34), e2108146119.
- Lauer, A., & Llases, L. (2025). *MORDRED: Model Of Resource Distribution and Resilient Economic Development. Model Documentation*. GitHub. <https://github.com/Pendracus/MORDRED>
- Lee, J. Y., Kim, E., Lee, W.-S., Chae, Y., & Kim, H. (2018). Projection of Future Mortality Due to Temperature and Population Changes under Representative Concentration Pathways and Shared Socioeconomic Pathways. *International Journal of Environmental Research and Public Health*, 15(4), 822. <https://doi.org/10.3390/ijerph15040822>
- Liu-Helmersson, J., Brännström, Å., Sewe, M. O., Semenza, J. C., & Rocklöv, J. (2019). Estimating past, present, and future trends in the global distribution and abundance of the arbovirus vector Aedes aegypti under climate change scenarios. *Frontiers in Public Health*, 7, 148.
- Lupi, V., & Marsiglio, S. (2021). Population growth and climate change: A dynamic integrated climate-economy-demography model. *Ecological Economics*, 184, 107011.
- Lüthi, S., Fairless, C., Fischer, E. M., Scovronick, N., Ben Armstrong, Coelho, M. D. S. Z. S., Guo, Y. L., Guo, Y., Honda, Y., Huber, V., Kyselý, J., Lavigne, E., Royé, D., Ryti, N., Silva, S., Urban, A., Gasparrini, A., Bresch, D. N., & Vicedo-Cabrera, A. M. (2023). Rapid increase in the risk of

- heat-related mortality. *Nature Communications*, 14(1), 4894.
<https://doi.org/10.1038/s41467-023-40599-x>
- Lutz, W. (2017). How population growth relates to climate change. *Proceedings of the National Academy of Sciences*, 114(46), 12103–12105.
<https://doi.org/10.1073/pnas.1717178114>
- Lutz, W., & Striessnig, E. (2015). Demographic aspects of climate change mitigation and adaptation. *Population Studies*, 69(sup1), S69–S76.
<https://doi.org/10.1080/00324728.2014.969929>
- McElroy, S., Ilango, S., Dimitrova, A., Gershunov, A., & Benmarhnia, T. (2022). Extreme heat, preterm birth, and stillbirth: A global analysis across 14 lower-middle income countries. *Environment International*, 158, 106902. <https://doi.org/10.1016/j.envint.2021.106902>
- McLeman, R. (2025). Coming to Terms with Deep Uncertainty in the Study of Climate-Related Displacement. *Cosmopolitan Civil Societies: An Interdisciplinary Journal*, 17(1), 14–34.
<https://doi.org/10.5130/ccs.v17.i1.9383>
- Messina, J. P., Brady, O. J., Golding, N., Kraemer, M. U., Wint, G. W., Ray, S. E., Pigott, D. M., Shearer, F. M., Johnson, K., & Earl, L. (2019). The current and future global distribution and population at risk of dengue. *Nature Microbiology*, 4(9), 1508–1515.
- Muttarak, R. (2021). Demographic perspectives in research on global environmental change. *Population Studies*, 75(sup1), 77–104.
- Pottier, A., Fleurbaey, M., Méjean, A., & Zuber, S. (2021). Climate change and population: An assessment of mortality due to health impacts. *Ecological Economics*, 183, 106967.
- Prina, M., Khan, N., Akhter Khan, S., Caicedo, J. C., Peycheva, A., Seo, V., Xue, S., & Sadana, R. (2024). Climate change and healthy ageing: An assessment of the impact of climate hazards on older people. *Journal of Global Health*, 14, 04101.
<https://doi.org/10.7189/jogh.14.04101>
- Rai, M., Breitner, S., Wolf, K., Peters, A., Schneider, A., & Chen, K. (2019). Impact of climate and population change on temperature-related mortality burden in Bavaria, Germany. *Environmental Research Letters*, 14(12), 124080. <https://doi.org/10.1088/1748-9326/ab5ca6>
- Ray, K., Giri, R. K., Ray, S. S., Dimri, A. P., & Rajeevan, M. (2021). An assessment of long-term changes in mortalities due to extreme weather events in India: A study of 50 years' data, 1970–2019. *Weather and Climate Extremes*, 32, 100315.
<https://doi.org/10.1016/j.wace.2021.100315>
- Rozell, D. (2017). Using population projections in climate change analysis. *Climatic Change*, 142(3–4), 521–529. <https://doi.org/10.1007/s10584-017-1968-2>
- Shayegh, S. (2017). Outward migration may alter population dynamics and income inequality. *Nature Climate Change*, 7(11), 828–832. <https://doi.org/10.1038/nclimate3420>
- Shu, E. G., Porter, J. R., Hauer, M. E., Sandoval Olascoaga, S., Gourevitch, J., Wilson, B., Pope, M., Melecio-Vazquez, D., & Kearns, E. (2023). Integrating climate change induced flood risk into future population projections. *Nature Communications*, 14(1), 7870.
<https://doi.org/10.1038/s41467-023-43493-8>
- Stadler, K., Wood, R., Bulavskaya, T., Södersten, C., Simas, M., Schmidt, S., Usabiaga, A., Acosta-Fernández, J., Kuenen, J., Bruckner, M., Giljum, S., Lutter, S., Merciai, S., Schmidt, J. H., Theurl, M. C., Plutzar, C., Kastner, T., Eisenmenger, N., Erb, K., ... Tukker, A. (2018). EXIOBASE 3: Developing a Time Series of Detailed Environmentally Extended Multi-Regional Input-Output Tables. *Journal of Industrial Ecology*, 22(3), 502–515.
<https://doi.org/10.1111/jiec.12715>

- Tang, J., Zhao, P., Gong, Z., Zhao, H., Huang, F., Li, J., Chen, Z., Yu, L., & Chen, J. (2023). Resilience patterns of human mobility in response to extreme urban floods. *National Science Review*, 10(8), nwad097. <https://doi.org/10.1093/nsr/nwad097>
- UN DESA. (2019a). *World Population Prospects 2019, Online Edition. Rev. 1. File FERT/7: Age-specific fertility rates by region, subregion and country, 1950-2100 (births per 1,000 women)*, WPP2019_FERT_F07_AGE_SPECIFIC_FERTILITY.xlsx. This data gives age-specific fertility rates for 7 age categories (15-19, 20-24, ..., 45-49).
- UN DESA. (2019b). *World Population Prospects 2019, Online Edition. Rev. 1. File MORT/4-1: Deaths (both sexes combined) by five-year age group, region, subregion and country, 1950-2100 (thousands)*, WPP2019_MORT_F04_1_DEATHS_BY_AGE_BOTH_SEXES.xlsx.
- UN DESA. (2019c). *World Population Prospects 2019, Online Edition. Rev. 1. File POP/7-1: Total population (both sexes combined) by five-year age group, region, subregion and country, 1950-2100 (thousands)*.
- Wan, K., Hajat, S., Doherty, R. M., & Feng, Z. (2024). Integrating Shared Socioeconomic Pathway-informed adaptation into temperature-related mortality projections under climate change. *Environmental Research*, 251, 118731. <https://doi.org/10.1016/j.envres.2024.118731>
- Wang, Y., Gao, S., & Manini, T. M. (2025). Age-Related Deficits in Mobility Resilience With an Extreme Weather and Climate Event. *JAMA Network Open*, 8(7), e2518525. <https://doi.org/10.1001/jamanetworkopen.2025.18525>
- World Health Organization. (2014). *Quantitative risk assessment of the effects of climate change on selected causes of death, 2030s and 2050s*. World Health Organization.
- Yao, Q., Shan, X., Li, M., & Wang, J. (2024). The Impact of Floods on the Mobility of Automobile Commuters in Shanghai Under Climate Change. *International Journal of Disaster Risk Science*, 15(6), 986–1000. <https://doi.org/10.1007/s13753-024-00604-3>
- Zhang, R., Zhang, Y., & Dai, Z. (2022). Impact of Natural Disasters on Mental Health: A Cross-Sectional Study Based on the 2014 China Family Panel Survey. *International Journal of Environmental Research and Public Health*, 19(5), 2511. <https://doi.org/10.3390/ijerph19052511>

Supplementary Information

1. Scenario parametrization

All simulations were realized with MORDRED 1.0.4. Differences to the original version are listed here: <https://github.com/Pendracus/MORDRED/blob/main/Versions.md>.

1.1. Baseline

Suppl.Table 1 contains the main scenario parameters and their values for the *Baseline* scenario.

Parameter	Baseline scenario value
Parameters regulating migration between subsistence and world economy (β_0, β_1)	Model default (see section 2.1 main text).
Birth rate multiplier	1
Energy intensities of production processes and final demand components (private consumption, public consumption, investment)	70% reduction in initial intensities by 2100.
Electricity mix	100% of fossil electricity replaced by renewable electricity (hydro, solar and wind power) by 2100.
Greenhouse gas emissions intensities	30% reduction in initial intensities by 2100.
Labor productivity increase	A fast increase of labor productivity in response to an increase in world average per capita consumption is assumed. Parameters are set to enable the world to reach the (higher) sectoral labor productivities of the center already at a per capita consumption 12% below the center.
Convergence in consumption	Moderate convergence through higher growth rates of the per capita consumption levels in middle- and low-income regions. Target consumption growth rate of the periphery = 3.5%. Target consumption growth rate of the semiperiphery = 3%. Target consumption growth rate of the semiperiphery = 2%. Allocation rule set to give all social classes the same consumption priority in the case of scarcity to avoid divergence.
Land related parameters	Land scarcity feedback deactivated; adaptation of model default parameters.
Climate damages (damages of capital stock due to sea level rise and extreme weather	Deactivated.

events, additional gross fixed capital formation due to sea level rise, output loss and increase of input coefficients in the agricultural sector, labor productivity losses due to heat, loss of labor supply due to heat, loss of land, increase in land intensity for the subsistence sector)	
Climate sensitivity	Default values of the model are adapted.
Resource availability	High resource availability; fossil resources are assumed to become more costly to extract once fossil reserves have been depleted.

Suppl.Table 1: Parametrization of the Baseline scenario.

1.2. Baseline - high fertility

The only difference to the parametrization of the *Baseline* scenario is the value of the birth rate multiplier which is set to 1.2.

1.3. Damages

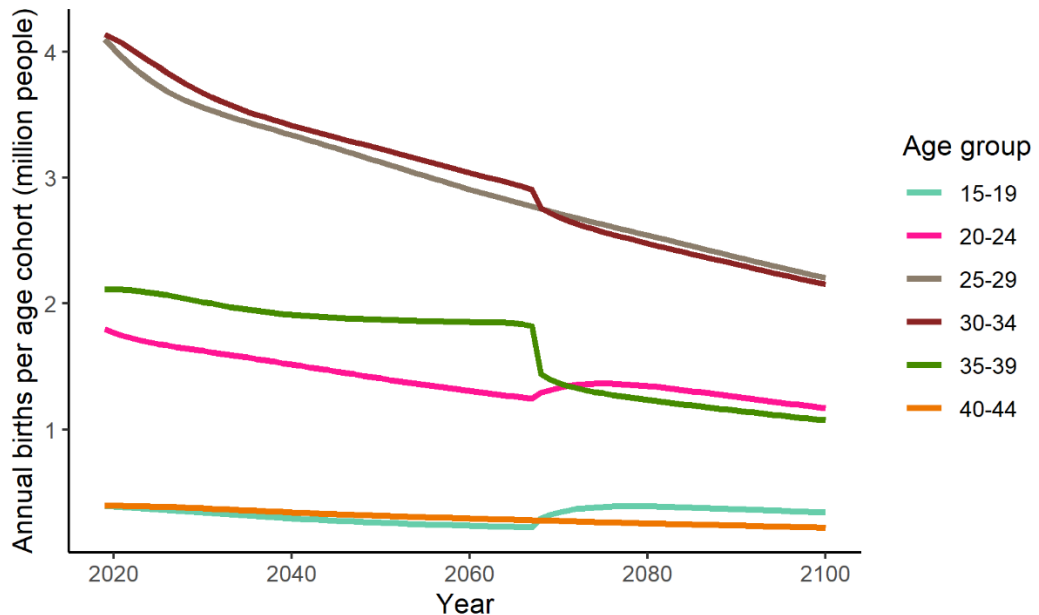
The only difference to the parametrization of the *Baseline* scenario is the activation of climate change damages. All damage parameters are taken from the default calibration of MORDRED.

1.4. Damages – high fertility

The only difference to the parametrization of the *Damages* scenario is the value of the birth rate multiplier which is set to 1.2.

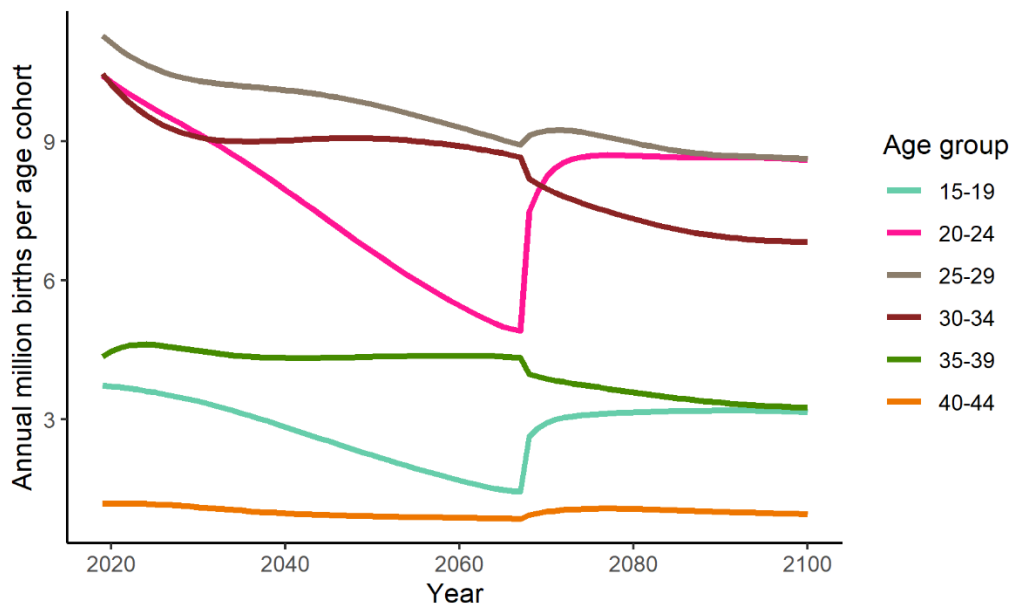
2. Supplementary Figures

All Figures display results from the *Damages* (DM) scenario. Suppl. Figure 1 shows annual births in the center by age group. As can be seen, the increase in birth rates for the younger population groups only translates into slightly increasing annual births for the two youngest age groups.

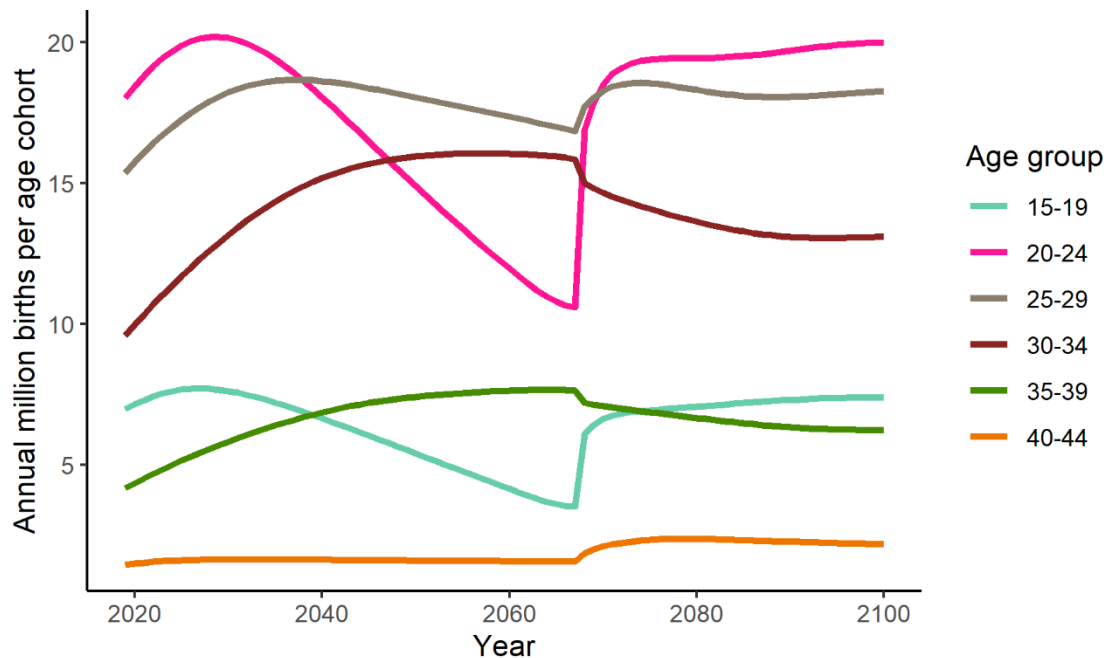


Suppl. Figure 1: Annual births per age cohort in the center (million people).

Suppl. Figure 2 and Suppl. Figure 3 show annual births in the semiperiphery and periphery by age group. Here, birth rates in the younger age groups increase sufficiently to cause a net increase in births when all age groups are aggregated.

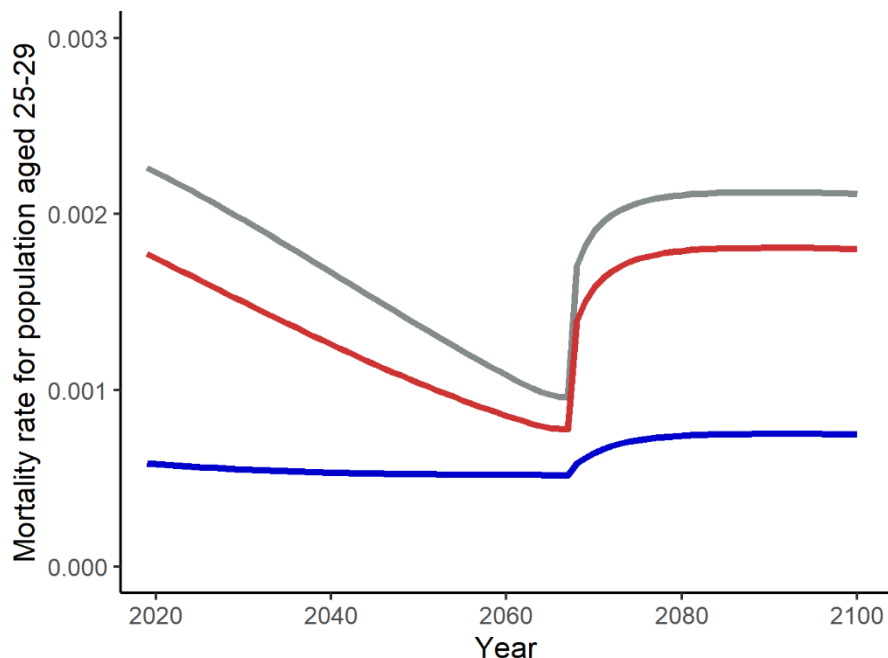


Suppl. Figure 2: Annual births per age cohort in the semiperiphery (million people).



Suppl. Figure 3: Annual births per age cohort in the periphery (million people).

Suppl. Figure 4 shows changes in mortality rate for one age group, representative of all age groups. Due to the climate change induced decline in economic production, the convergence of mortality rates between world regions is halted and reversed.



Suppl. Figure 4: Mortality rate for the population aged 25-29 in the center (blue line), semiperiphery (red line) and periphery (grey line).

Exploring historical discontinuities in global energy scenarios: A model-based reappraisal of the Shared Socio-economic Pathways

Abstract

Global environmental scenarios, such as the Shared Socioeconomic Pathways (SSPs), are central to decision-making under deep uncertainty but have been criticized for their lack of alternative economic futures. This study addresses these limitations by introducing selected SSPs into the Integrated Assessment Model *MORDRED*, which endogenizes economic, demographic, and biophysical variables through system-dynamic feedback relationships. By re-quantifying SSP2, SSP3, and SSP5 under two boundary conditions — without (SSP') and with (SSP'') biophysical feedbacks — it was examined how the incorporation of biophysical feedbacks into economic system analyses affects the plausibility and viability of the SSP storylines. While the SSP' implementations reproduce dynamics projected by previous SSP quantification exercises, introducing biophysical constraints in SSP'' variations generates nonlinear dynamics and historical discontinuities in socio-economic and environmental trajectories which are absent from, and incompatible with, the original SSPs. Projected developments include stagnation or collapse in final demand, demographic contractions, and major shifts in energy system evolution before the end of the 21st century. A positive feedback loop between environmental degradation, reduced productive capacity and declining energy efficiency emerges as a key driver of systemic instability. These findings challenge the implicit assumption of perpetual economic growth underpinning many global environmental scenarios and reveal that futures featuring economic stagnation and collapse are not only possible but plausible under less optimistic boundary conditions. Thus, current SSP-based assessments underestimate both the risks of climate–economy interactions and the scope of required institutional transformations to ensure societal resilience under biophysical constraints.

Keywords

Shared socio-economic pathways; climate scenarios; global environmental scenarios; integrated assessment modeling; limits to growth

1. Introduction

Global environmental scenarios, notably energy and climate scenarios, have come to occupy a key position in supporting decision making under deep uncertainty (DMDU), as facilitated by the IPCC (Lempert et al., 2024). Among these, a particular set of scenarios has gained prominence: the Shared Socioeconomic Pathways (SSPs) (O'Neill et al., 2017). The SSPs form part of a sophisticated scenario architecture (Kriegler et al., 2014) and have been used by the IPCC in its Sixth Assessment Report. The five storylines (SSP1–SSP5), which trace alternative socio-economic development pathways over the 21st century, have been widely applied in quantitative simulation studies (Lauer et al., 2024).

Within the SSP scenario architecture, socio-economic developments are treated separately from climate policies, climate impacts, and adaptation processes. This separation allows for isolated and counterfactual projections of economic (Dellink et al., 2017) and demographic (Kc & Lutz, 2014) developments. While this methodological choice simplifies modeling, it also neglects critical feedbacks between social, economic, and climatic systems. Consequently, the SSP storylines appear overly linear and fail to capture risks emerging from real-world interdependencies. As Szetey et al. (2023) highlight, modeling constraints narrow the SSP focus excessively, exemplified by the absence of intentional degrowth futures or other non-growth economic outcomes. Further criticisms include a lack of institutional realism and excessive optimism regarding the large-scale and timely implementation of decarbonization technologies (Lane & Montgomery, 2014).

According to Keys et al. (2024), the SSPs thus exhibit key features of *Anthropocene science*: limited “worlding capacity,” value-laden assumptions about what is possible, and a tendency to exclude alternative futures. In the context of DMDU, this last feature is especially problematic, as excessively linear futures obscure the need for policies that can respond to the complex and non-linear consequences of accelerating global environmental change.

However, despite calls for more diversity in global socio-economic climate and energy scenarios (El Skaf, 2025; Hickel et al., 2021; Otero et al., 2022; Rothman et al., 2023) and significant advances realized in the realm of modeling post-growth futures —whether through intentional societal transitions or unintentional economic contractions (Edwards et al., 2025; Lauer et al., 2025) —little is currently known about the implications of integrating biophysical feedback effects into economic system analyses, particularly regarding the plausibility and viability of the original SSP storylines.

This article addresses that gap by conducting a comparative scenario analysis using *MORDRED 1.0.2* (Model of Resource Distribution and Resilient Economic Development), a system-dynamic, non-equilibrium Integrated Assessment Model in which key economic, demographic and biophysical variables evolve endogenously and are driven by complex feedback relationships. By simulating different variations of SSP2, SSP3 and SSP5, we test how scenario outcomes change once the assumption of continuous

economic growth is removed. Our approach can thus be described as an IAM-based quantitative study that anticipates potential future risks and aims to increase societal preparedness for discontinuous socio-economic changes during the 21st century (cf. Pereira et al., 2021). Additionally, we intend to explore how numerical projections of the SSPs vary when they are quantified with a model incorporating a fundamentally different structural logic.

Consequently, the remainder of the article is structured as follows: The remainder of the article is organized as follows: first, we provide an overview of the model and the adopted parameterization approach; next, we describe and compare the key simulation results from the SSP variations; and finally, we contextualize the simulation outcomes and discuss their policy relevance.

2. Methods

2.1. The MORDRED model

MORDRED (Model Of Resource Distribution and Resilient Economic Development) is a global IAM designed to represent socio-economic inequality at global and regional levels and to incorporate key feedback relationships between its submodules. Built on a system dynamics framework, MORDRED endogenizes variables that are often treated as exogenous in other IAMs—such as economic growth, mortality and fertility rates, labor force evolution, and climate impacts. This structure provides the flexibility required to simulate a broad range of global environmental and economic scenarios. The model's principal components and feedback relationships are summarized in Fig. 1.

MORDRED is calibrated with data from the databases Exiobase3 (Stadler et al., 2018) and GCIP (Lahoti et al., 2016), as well as from climate, emissions and population data provided by the IPCC WGI (2021) and the UN (2019). It can be considered an ecological macroeconomic model (Hardt & O'Neill, 2017) due to the monetary input–output (IO) structure of its economic module and the linkages between the monetary economic structure and the biophysical components of the model, i.e., the energy, land, and climate system.

The economic module of MORDRED consists of a global input-output production matrix disaggregated into 25 sectors covering agriculture, biomass, industry, mining, services, transport, and various energy sectors. Sectors produce intermediate goods as well as consumption and investment goods demanded by the different final demand components (governments, households and Gross Fixed Capital Formation (GFCF)). Production in each sector depends on intermediate goods and the primary production factors: capital, labor, land, and energy. The latter two are subdivided into specific types—such as agricultural and forest land, and fossil fuels, bioenergy, or electricity from various sources.

The demographic module represents 20 age groups (each spanning five years), three world regions—center (high-income countries), semiperiphery (upper-middle-income

countries), and periphery (lower-middle- and low-income countries)—and four social classes (subsistence, Top20, Middle50, and Bottom30). The subsistence class includes individuals living largely outside the global capitalist economy; its size is set to zero in the center at the model's initial time step. Within each region, the population participating in the formal economy is divided into deciles, with the richest two deciles forming the Top20 class, the poorest three the Bottom30 class, and the remaining five the Middle50 class. In the SSP simulations, parameters governing the integration of the subsistence class into the formal economy lead to rapid assimilation; consequently, this class is omitted from the analysis, as global population quickly converges to that of the formal economy. Population segments generate consumption demand that drives economic development, while mortality and fertility rates for each age cohort evolve with per-capita consumption. The population aged 15–64 constitutes the potential labor force of the global economy.

The land, energy and climate modules form the bridge between economic production and environmental impacts. They enable the calculation of emissions from land-use change and fossil fuel combustion. The climate module uses information from the land and energy module as well as various sectoral emission intensities belonging to the economic module to convert different greenhouse gas emissions (CO₂, CH₄, N₂O, HFC, PFC, SF₆) into changes in global average temperatures with respect to the 1850 reference level.

The key feedback mechanisms embedded in MORDRED include:

- restrictions on economic production due to limited labor supply (demography → economy);
- constraints on population growth due to limited economic output (economy → demography);
- depletion of fossil resources driven by economic activity (economy → energy);
- reduced economic production from rising energy extraction requirements (energy → economy);
- expansion of land use from economic growth (economy → land);
- limits on production from land scarcity and conversion constraints (land → economy);
- increased emissions from economic output (economy → climate); and
- economic impacts resulting from temperature change (climate → economy; climate → labor → economy; climate → land → economy).

A detailed description of the model's development, full structure, and governing equations is provided in Lauer & Llases (2025).

For our simulations, we developed a new version of the model (MORDRED 1.0.2), characterized by the endogenization of sectoral energy intensity developments, i.e.

sectoral energy intensity evolves as a function of sectoral output per capita, which depends on demographic, economic and biophysical changes during the scenario simulation (see Supplementary Material (SM) 1 and Table 1).

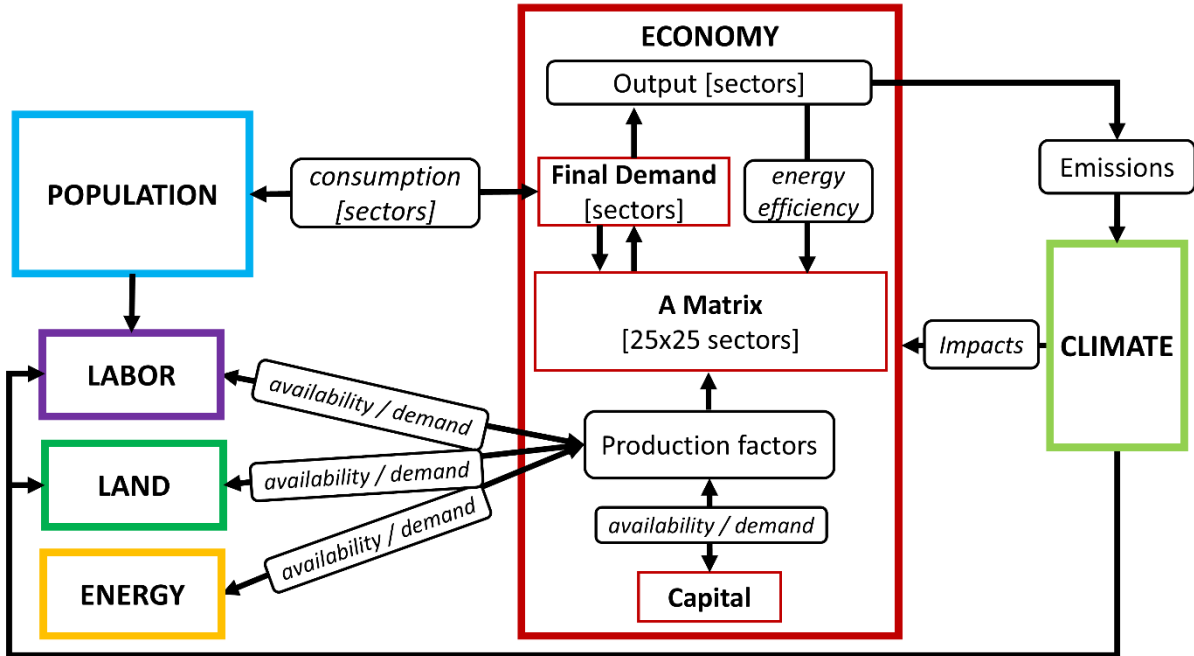


Fig. 1: Structural overview of MORDRED 1.0.2.

2.2. Scenario assumptions and parametrization

We conducted a comparative scenario analysis of three SSPs: SSP2, SSP3 and SSP5. SSP2 features a continuation of historical trends, SSP3 an increase in regional competition and security concerns, and SSP5 a strong growth in fossil-based industrialization and consumption around the world (O'Neill et al., 2017). Apart from SSP1, the selected SSPs are used most frequently in the literature (Lauer et al., 2024) and are sufficiently distinct for a comparative analysis.

For every selected SSP scenario, we ran two simulations: In the first simulation (SSP'), the feedback loops from the environment on the economy were deactivated and very optimistic assumptions were made regarding the future evolution of input factors into economic production processes. In the second simulation (SSP''), biophysical restraints were activated and less optimistic assumptions regarding the availability of input factors were adopted to explore the effects of biophysical feedback loops on the viability of the original SSP storylines.

In parameterizing SSP2, SSP3, and SSP5, we sought to balance comparability with previous SSP quantifications and the preservation of MORDRED's structural and dynamic features. To this end, we drew upon the extended SSP storylines from O'Neill et al. (2017) and the corresponding quantitative and qualitative information provided in the main scenario quantifications (Calvin et al., 2017; Fricko et al., 2017; Fujimori et al., 2017; Kriegler et al., 2017; Riahi et al., 2017).

Unlike IMAGE, MESSAGE-GLOBIOM, AIM/CGE, GCAM, and REMIND-MAgPIE, which underlie the main SSP quantifications (Riahi et al., 2017), MORDRED excludes carbon capture and storage (CCS) and bioenergy with carbon capture and storage (BECCS) technologies, given concerns about their scalability and socio-ecological implications (Braun et al., 2025; Creutzig et al., 2021; Heck et al., 2018; Sekera & Lichtenberger, 2020). Biomass-based energy technologies are represented as a single aggregated sector. Similarly, agricultural production from various crops and livestock types is consolidated into one sector; therefore, MORDRED does not explicitly model crop yields or diet-related caloric intake. The relationship between diets, caloric intake, and life expectancy is captured indirectly through the consumption-based endogenization of mortality and fertility rates, since higher consumption implies dietary and nutritional changes (Ezzati et al., 2005; Gerbens-Leenes et al., 2010; Knez et al., 2017). MORDRED also departs from conventional IAMs by not relying on carbon or energy prices to shift the energy mix during simulations. Instead, technological progress and extraction constraints are reflected through changes in the input coefficients of the model's A matrix (cf. section 1 SM1).

We test the feasibility of the SSP storylines under two conditions: (1) without biophysical constraints and feedback mechanisms (SSP2', SSP3', SSP5'), and (2) with activated biophysical constraints and feedback mechanisms (SSP2'', SSP3'', SSP5'').

Table 1 summarizes the implementation of all SSP variations simulated in MORDRED. SM1 provides further details on the parametrization process, while SM 2 lists the numerical values used in all SSP configurations. Additionally, SSP variations with only a partial activation of biophysical feedback were conducted which are described and depicted in section 3 of SM1.

Variable	Basis for parametrization	Implementation	SSP2'	SSP2''	SSP3'	SSP3''	SSP5'	SSP5''					
Population	-	endogenous in MORDRED											
GDP per capita	O'Neill et al. (2017)	desired per capita household consumption in 2100 (DC) and desired growth rate (dg) per year	MEDIUM		LOW		HIGH						
	Calvin et al. (2017)		$DC: 21,344 \text{ €}$ (dg : varies between different world regions and consumption classes [1.75% - 2.13%])		$DC: 7,749 \text{ €}$ (dg : same for all regions and classes: 0.74%)		$DC: 53,508 \text{ €}$ (dg : varies between different world regions and classes [2.75 % - 3.41%])						
<i>Energy demand</i>													
Traditional fuel use	Riahi et al. (2017)	no traditional fuel use	-										
Lifestyles / material intensity	Riahi et al. (2017)	Input coefficients column in A matrix for the service sector are multiplied with a material intensity change factor $\alpha_{material}$.	materially intensive			very materially intensive							
	own choice		$\alpha_{material} = 0.95$			$\alpha_{material} = 1.1$							
Environmental awareness	Riahi et al. (2017)	changes in households', governments' and investments' sectoral consumption shares	MEDIUM		LOW								
	own choice		shift 90% of fossil electricity demand and 40% of nuclear electricity demand to renewable electricity; substitute 10% of non-electricity demand with renewable electricity		no changes compared to initial moment of the simulation								

			demand for households, governments and investment			
Energy intensity of industry	Riahi et al. (2017)	Input coefficients from energy sectors for the column of the industry sector (s=5) are multiplied by a factor α_{ei} that changes with sector output per capita.	MEDIUM	HIGH	MEDIUM	
	own choice		$\alpha_{ei_5SSP} = \beta_5 * x_{5pc(t)}^\gamma + \varepsilon_5$ $x_{5pc(t)}$ grows faster in SSP5 than in SSP2, and slowest in SSP3. Thus, $\alpha_{ei_5SSP5} < \alpha_{ei_5SSP2} < \alpha_{ei_5SSP3}$.			
Energy intensity of buildings	Riahi et al. (2017)	Input coefficients from energy sectors for the column of the sector containing real estate (s=7) are multiplied by a factor α_{ei} that changes with sector output per capita.	MEDIUM	HIGH	MEDIUM	
	own choice		$\alpha_{ei_7SSP} = \beta_7 * x_{7pc(t)}^\gamma + \varepsilon_7$ $x_{7pc(t)}$ grows faster in SSP5 than in SSP2, and slowest in SSP3. Thus, $\alpha_{ei_7SSP5} < \alpha_{ei_7SSP2} < \alpha_{ei_7SSP3}$.			
Energy intensity of transportation	Riahi et al. (2017)	Input coefficients from energy sectors for the column of the transport sector (s=21) are multiplied by a factor α_{ei} that changes with sector output per capita.	MEDIUM	HIGH	MEDIUM	
	own choice		$\alpha_{ei_{21SSP}} = \beta_{21} * x_{21pc(t)}^\gamma + \varepsilon_{21}$ $x_{21pc(t)}$ grows faster in SSP5 than in SSP2, and slowest in SSP3. Thus, $\alpha_{ei_{21SSP5}} < \alpha_{ei_{21SSP2}} < \alpha_{ei_{21SSP3}}$.			
<i>Energy types</i>						
Importance of fossil fuels compared to	Kriegler et al. (2017), Fricko et al. (2017)	shifts in the input coefficients in A matrix between the fossil	MEDIUM	HIGH	HIGH	

renewable energies and nuclear energy	own choice	electricity, nuclear electricity, hydro, solar PV and wind electricity sectors; electrification of key sectors	shift 70% of fossil electricity demand and 10% of nuclear electricity demand to renewable electricity; key economic sectors: electrification of 20% of non-electric input through renewable electricity	shift 40% of fossil electricity demand for production to renewable electricity; shift 50% of nuclear electricity demand to fossil electricity; key economic sectors: electrification of 10% of non-electric input through renewable electricity	
Technological progress in energy technologies	Kriegler et al. (2017), O'Neill et al. (2017)	Input coefficients from main energy sectors (es=3,10,12,13,14,15,17) for the columns of energy sectors are multiplied by a factor α_{ei} that changes with sector output per capita.	MEDIUM	LOW	HIGH
<i>Fossil energy supply</i>					
Fossil fuel availability	Riahi et al. (2017)	quantity of fossil fuel resources	MEDIUM	MEDIUM	HIGH
	Fricko et al. (2017)		169000 EJ	83900 EJ (lower value for oil and gas resources and upper value for	589700 EJ (highest estimates of all fossil fuel types in the literature) 353900 EJ (lower value for oil, gas and coal resources)

				coal reserves)				
<i>Agriculture & land use change</i>								
Land use change regulation	Riahi et al. (2017)	limit on primary forest conversion	MEDIUM		LOW		MEDIUM	
	own choice		protect 50% of primary forest area in 2019		no protection		protect 50% of primary forest area in 2019	
Land productivity growth	Riahi et al. (2017)	annual growth in land productivity	MEDIUM		LOW		HIGH	
	Fricko et al. (2017); own choice for SSP5' based on Fricko et al. (2017)		annual average increase of 3% for all land types	annual average increase of 0.53% for all land types	annual average increase of 2% for all land types	annual average increase of 0.35% for all land types	annual average increase of 4% for all land types	annual average increase of 0.795% for all land types
Environmental impact of food consumption	Riahi et al. (2017)	cropland and pasture demand of the food and agricultural sector	MEDIUM		HIGH			
	own choice		75% of original land intensity		90% of original land intensity			
Inequality between societies	O'Neill et al. (2017)	inequality in per capita consumption between classes	HIGH				MEDIUM	
	own choice		maintenance of the consumption p.c. ratios between classes				Reduction of consumption ratios between classes: the growth rate of the M50 class is kept constant, the consumption of the B30 class is multiplied by 1,05 and of the T20 class by 0.925.	

Inequality within societies	O'Neill et al. (2017)	inequality in per capita consumption between regions	MEDIUM	HIGH	MEDIUM
	own choice		20% reduction in the average consumption ratios between the center and the semiperiphery ($c_c : c_{s_{2100}} = 0.8 * c_c : c_{s_{2019}}$) and 25% reduction between the center and the periphery	maintenance of the consumption p.c. ratios between regions	20% reduction in the consumption ratios between the regions ($c_{center} : c_{i_{2100}} = 0.8 * c_{center} : c_{i_{2019}}$ with $i \in semiperiphery, periphery$)
Labor productivity growth	O'Neill et al. (2017)	annual growth of labor productivity	MEDIUM	LOW	HIGH
	own choice		increase of 3% p.a.	increase of 1.5% p.a	increase of 4% p.a.
Capital intensity growth	O'Neill et al. (2017)	annual growth of capital intensity	MEDIUM	LOW	HIGH
	Kriegler et al. (2017); own choice for SSP3 based		increase of 16.1% until 2100 with respect to initial value	increase of 10.0% until 2100 with respect to initial value	increase of 22.6% until 2100 with respect to initial value
Non-combustion related GHG intensity reduction	Riahi et al. (2017)	non-combustion related (e.g. CH4, N2O, SF6) target GHG intensity	MEDIUM	LOW	LOW
	own choice		reduction of 20% until 2100 with respect to initial intensities	reduction of 10% until 2100 with respect to initial intensities	reduction of 5% until 2100 with respect to initial intensities
Other MORDRED	MORDRED	-	MORDRED baseline value		

scenario variables									
Climate impacts	MORDRED	damage factors	deactivated	activated	deactivated	activated	deactivated	activated	
Land, energy and labor scarcity factors	MORDRED	scarcity factors	deactivated	activated	deactivated	activated	deactivated	activated	

Table 1: Overview of SSP parametrization in MORDRED.

3. Results

3.1. SSP implementation without biophysical feedbacks

Scenario simulations of the SSP storylines without biophysical feedbacks generally confirm previous SSP quantifications produced with different IAMs (Fricko et al., 2017; Fujimori et al., 2017; Kriegler et al., 2017; Riahi et al., 2017). Historical discontinuities are absent, and the quantitative patterns align with the qualitative descriptions of the respective scenarios. This applies to demographic, macroeconomic, energy, and food system developments. As a result, climate conditions change rapidly over the simulation period (2019–2102).

3.1.1. Demographic and macroeconomic developments

In SSP2', world population grows moderately until 2057, reaching 8.8 billion, then stabilizes before declining to 8 billion by 2100. The population of the *center* (high-income countries) shrinks continuously to 790 million, while the *semiperiphery* (upper-middle-income countries) grows to 3 billion in 2034 before gradually declining to 2.5 billion. The *periphery* (lower-middle- and low-income countries) peaks later, at 4.96 billion in 2074, and slightly declines to 4.8 billion by 2100. Thus, while global population in 2100 is comparable to current levels, the relative demographic weight of the Global South increases considerably.

The population decline results mainly from falling fertility rates that outpace mortality reductions, driven largely by rising per-capita consumption and, to a lesser extent, higher government spending on education. Global average consumption per capita more than triples, reaching €21,669 per year by 2100, supported by steady growth in final demand, which nearly quadruples to 308.5 trillion (2019-€).

In SSP3', slower economic growth delays the population peak to 2064 at 8.9 billion, followed by a gradual decline to 8.6 billion by 2100. The center and semiperiphery show patterns similar to SSP2', while the periphery, in line with the SSP3 storyline, continues to grow until 2093, peaking at 5.2 billion. Global final demand reaches €115.7 trillion—only 37.5% of the SSP2' level. The lower productive development coupled with the higher population leads to a lower average consumption per capita level of 7,882€ per year in 2100 which is still considerably higher than the initial average consumption level. However, given the high level of inequality in this scenario, the average consumption in the periphery is only 3,705 € per year in 2100.

In the SSP5' simulation, world population peaks earlier, in 2056, at 8.7 billion and declines faster than in SSP2', reaching 7.8 billion by 2100. This is accompanied by very high growth in global final demand (819 trillion €/year in 2100, more than ten times the initial level) and average per-capita consumption (55,196 €/year, almost nine times the initial level).

Fig. 2 resumes the main demographic and macroeconomic developments for the three scenario implementations in MORDRED at the global level.

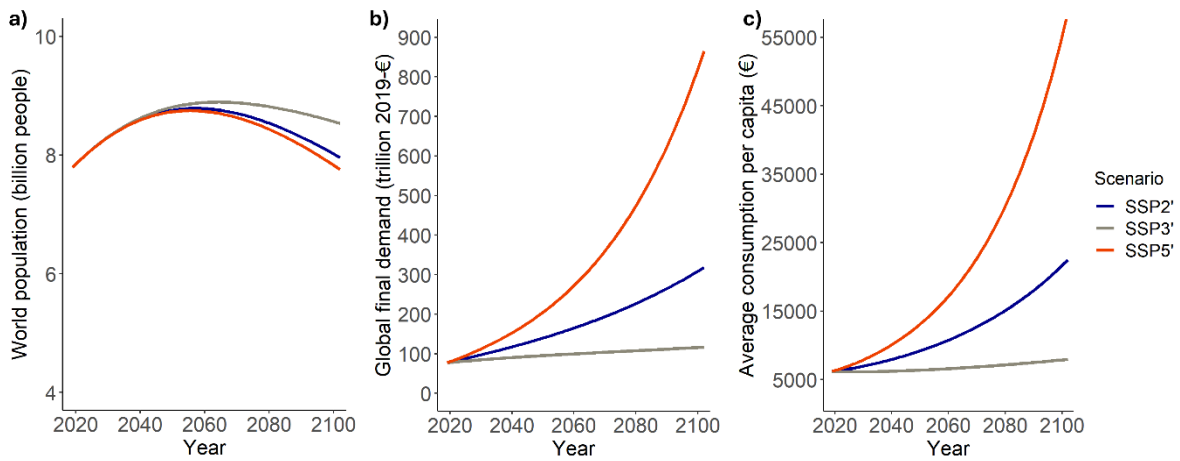


Fig. 2: a) World population, b) Global final demand, c) Consumption per capita on the global level for the scenarios SSP2' (blue), SSP3' (grey) and SSP5' (red).

3.1.2. Sectoral evolution of the economy

In SSP2', final energy use grows across all types throughout the simulation. Fossil fuel energy increases from 291 EJ in 2019 to 539 EJ in 2100. Electricity use rises sharply, accelerating toward the end of the period to 330 EJ. Electricity production quadruples, biomass energy more than doubles to 108 EJ, and renewable electricity—hydro, wind, and solar PV—reaches 82, 94, and 93 EJ, respectively, meaning each technology alone could meet current global electricity demand.

In line with the macroeconomic and demographic developments, final energy demand grows more slowly in SSP3', and although wind and solar PV expand exponentially, they reach only 21 EJ and 20 EJ by 2100. Conversely, in the SSP5' simulation, final energy demand surges: non-electric fossil energy reaches 1,424 EJ, biomass 281 EJ, and electricity 713 EJ—almost nine times the 2019 level—while the renewable share of electricity remains lower than in SSP2'.

Rising affluence in all scenarios reduces the food sector's share of total output, as higher incomes shift consumption toward other goods and services. The decline is steepest in SSP5'. In SSP3', however, the food sector share initially rises to 6.7% by 2027 due to the larger proportion of poorer populations, before declining later. Despite its reduced share, total food sector output grows exponentially in SSP5', reaching €69 trillion by 2100, compared to €13 trillion in SSP3'.

Fig. 3 summarizes energy and sectoral developments across SSP2', SSP3', and SSP5'.

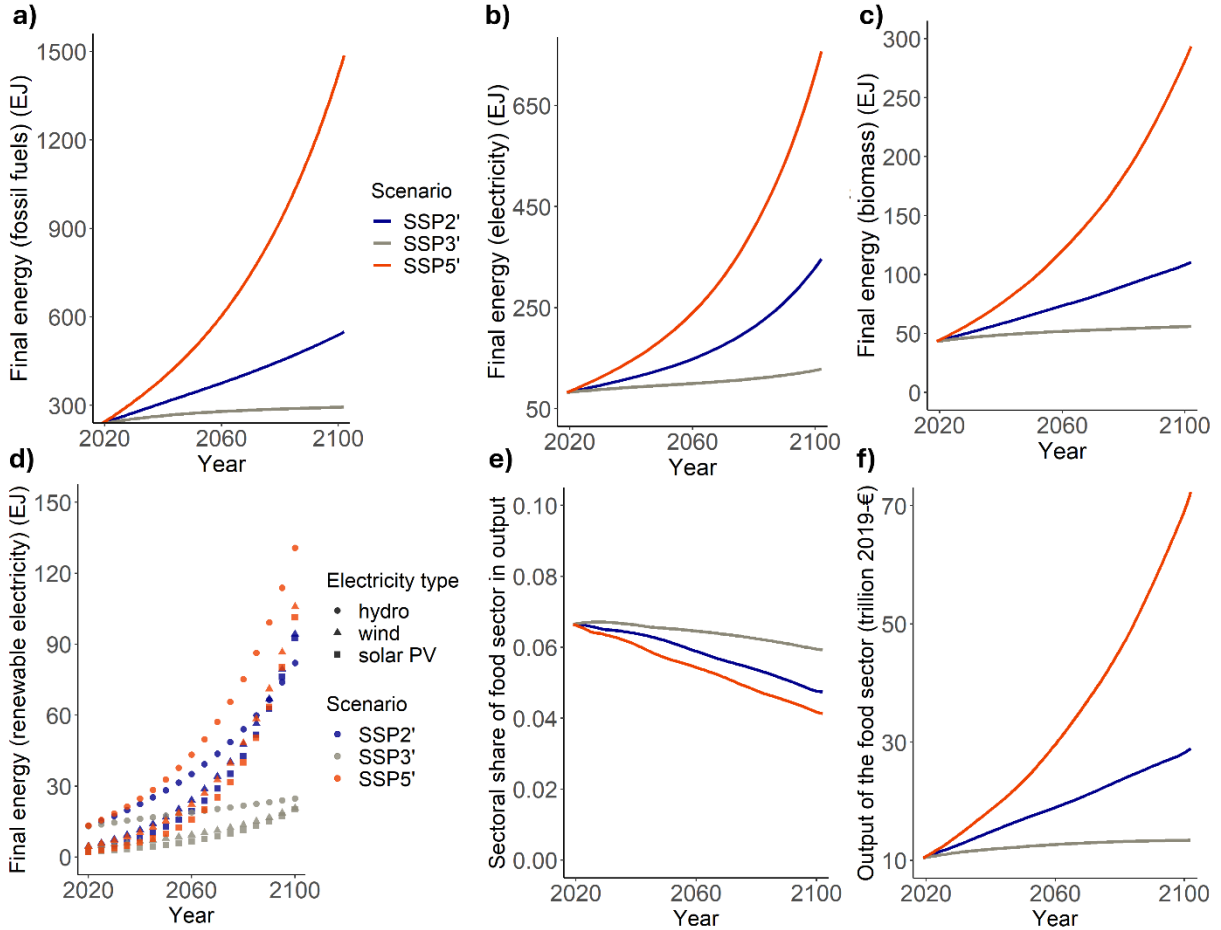


Fig. 3: Annual quantity of a) fossil fuels; b) electricity; c) biomass used by the global economy for SSP2' (blue), SSP3' (grey) and SSP5' (red). d) Evolution of renewable electricity systems (hydro, wind and solar PV based electricity) in the three scenarios; e) share of the food sector in total output on a global scale; f) annual total output of the food sector.

3.1.3. Emissions and global climate change

In line with the macroeconomic developments and the evolution of the global energy system, SSP5 emits the highest quantity of greenhouse gases and reaches the highest global temperatures, while SSP3 displays the lowest emissions and temperature increases, with SSP2 being situated in the middle.

In SSP5, GHG emissions resulting from strong economic growth and reliance on fossil fuels continue unabated and reach 325 Gt in 2100, corresponding to a temperature change of 5.98 °C compared to 1850.. In SSP2, annual emissions increase to 100 Gt by 2100, resulting in a 3.71 °C warmer world. SSP3 shows a slower rise, from 50 Gt to 59 Gt, leading to 3.02 °C of warming (Fig. 4).

Other SSP quantifications project comparable temperature outcomes for SSP2 (3.76 °C by 2100), significantly higher global warming under the SSP3 baseline (4 °C in 2100) and significantly lower levels of climate change under SSP5 baseline (5 °C in 2100)

(Riahi et al., 2017). These differences stem mainly from the parametrization of the energy system and the assumptions made for the endogenization of energy intensities.

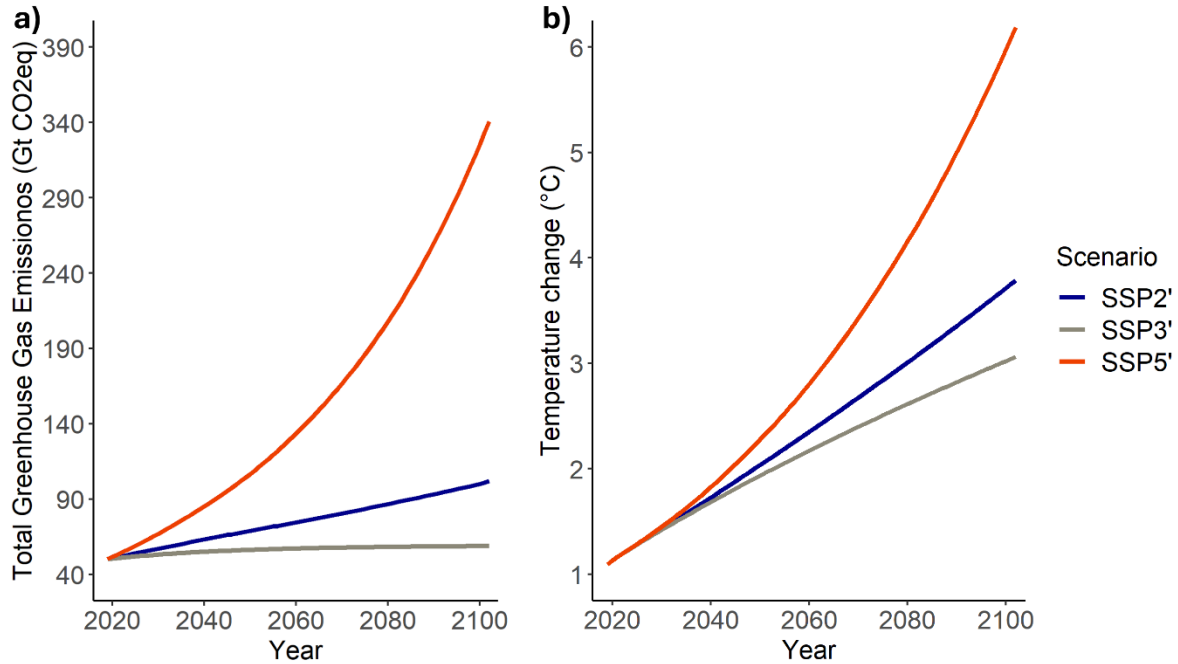


Fig. 4: a) Total greenhouse gas emissions and b) global average temperature change for the three SSP' simulations (blue: SSP2', grey: SSP3', red: SSP5').

3.2. SSP implementation with biophysical feedbacks

Including biophysical feedbacks leads to major deviations from previous SSP quantifications, revealing radically altered global trajectories characterized by strong historical discontinuities absent from the original storylines.

3.2.1. Demographic and macroeconomic developments

Introducing biophysical constraints produces significant demographic changes in the final quarter of the century. In SSP2'', population follows SSP2' until 2065, then declines more slowly before dropping sharply from 2092, falling from 8.4 to 6.6 billion by 2100. This illustrates that moderate climate impacts – through their adverse effects on the per capita consumption of different socio-economic groups and world regions – could lead to a relative increase in the population due to a relative increase in overall birth rates while severe climate impacts are linked to a population decline due to escalating mortality rates. Regionally, the decline is concentrated in the *periphery* (from 5 to 3.3 billion), while the center and semiperiphery maintain slightly higher populations than in SSP2', due to higher birth rates.

Tighter biophysical limits in SSP2'' constrain final demand throughout the simulation, causing a lower growth in economic production. Global final demand peaks in 2077 at €129 trillion—ten years after divergence from SSP2' and 15 years before the population

collapse. By 2090, it is 46% below its peak, and by 2100, 38% below the initial 2019 level (Fig. 5b). Average global consumption per capita rises with final demand, reaching a peak at about 7,750 €, and subsequently declines strongly to a minimum of less than 3,200 € in 2096. Since the rate of decline in the world population eventually exceeds the rate of decline in final demand average per capita consumption increases slightly during the last 5 years of the simulation (Fig. 5c).

SSP3'' exhibits similar dynamics but with earlier discontinuities. Population matches SSP3' until 2086, then falls by 35% within 15 years. As in SSP2'', the deep-rooted consumption inequality of the world economic system has the effect that different world regions are affected unequally by biophysical constraints to growth. As a result, in the simulation the periphery loses 65% of its population size while changes in birth and death rates in the center and the semiperiphery are not drastic enough to cause a demographic collapse. In the periphery, mortality rates spike due to the massive spread of extreme poverty among the poorer classes that see their consumption levels decline as the global economy starts to contract due to mounting climate change impacts and rising fossil resource extraction costs.

The SSP3 storyline assumes a less favorable global economic panorama, which is reflected in low growth rates in both SSP3 simulations. Thus, once biophysical limits to growth are introduced, global final demand peaks at 111 trillion € in 2076 in SSP3'', i.e. slightly earlier and at a lower level than in SSP2''. Interestingly, until its peak, final demand in SSP3'' grows faster than in SSP3'. However, disaggregating final demand into its components, we find that this difference is driven by a strong increase in investment which becomes necessary to prevent climate impacts from halting economic growth, and to ensure the accessibility of fossil resources. Conversely, consumption in the different world regions and classes already peaks more than a decade before the observed peak in world demand. This points to the possibility of global futures that feature a stagnation in living standards or even rising poverty levels despite growing final demand and production.

Although global final demand in SSP3'' peaks at a lower level than in SSP2'', by the end of the century the difference has reduced significantly (Fig. 5b), and – due to the earlier and higher population decline – average consumption reaches its minimum at an earlier and a higher level than in SSP2'' (Fig. 5c). Thus, paradoxically, average consumption by the end of the scenario is higher in SSP3'' than in SSP2'' despite the global panorama is undoubtedly less favorable. Although representing GDP (or consumption) per capita is common in modeling exercises concerned with future socio-economic developments—and implicitly serves as a proxy for well-being—substantial criticism has been raised regarding the use of GDP per capita as an indicator of population well-being at the national level (Aitken, 2019; T. Dong et al., 2024; Harvie et al., 2009; Kubiszewski et al., 2013). This critique applies even more strongly at the global level, where an even higher degree of aggregation obscures territorial, class, and gender inequalities. We therefore conclude that world average consumption (and even more so world GDP) per capita

does not constitute an adequate indicator of well-being or living standards, particularly during periods of economic crisis and unintentional economic degrowth.

The demographic trajectory of SSP5'' differs markedly: population follows SSP2'' but remains stable at the century's end, at 0.4 billion higher than in SSP5'. Global final demand continues to grow but at lower rates, reaching 152 € trillion—only 19% of SSP5' level. Growth in average consumption per capita levels slows down during the last decade of the simulation, peaks at 8,665 € per year in 2099 and then starts to decline. Again, this points to the possibility of a relative growth in investment goods and a relative decline in consumption goods in futures with significant climate change impacts, affirming that treating GDP as a central variable in research around future world economic and environmental developments is problematic due to its lack of differentiation between the benefits and cost of economic growth, the latter including necessary productive activity to alleviate the impacts of ecological degradation (Van den Bergh, 2009). Importantly, the lack of population and final demand decline in this scenario during the 21st century does not mean that this scenario is more feasible or stable than the other simulations in the mid- to long-term. Rather, the peak in average consumption per capita at the end of the century suggests that SSP5'' may be approaching a turning point beyond the temporal scope of this analysis.

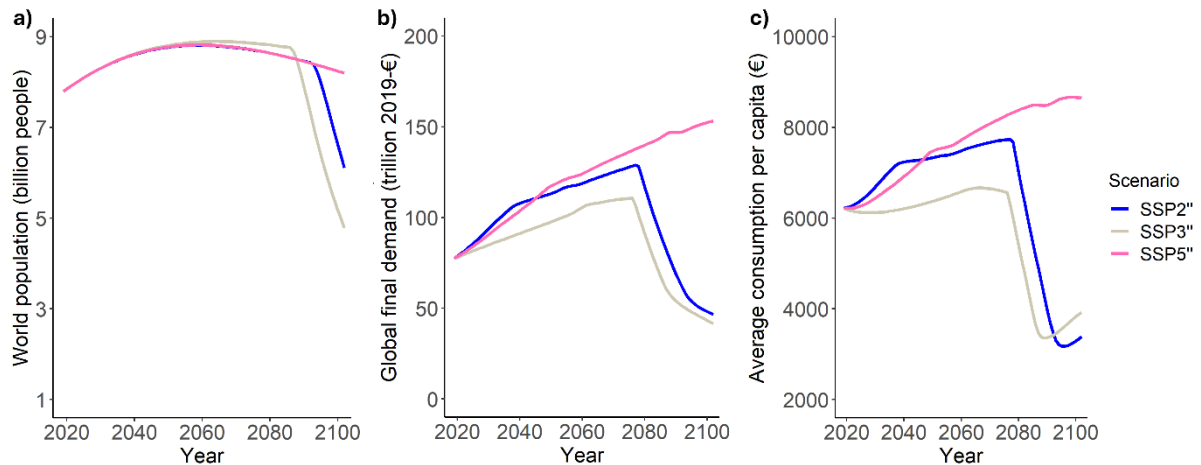


Fig. 5: a) World population, b) Global final demand, c) Consumption per capita on the global level for the scenarios SSP2'' (blue), SSP3'' (beige) and SSP5' (pink').

3.2.2. Sectoral evolution of the economy

Reflecting the demographic and macroeconomic discontinuities, sectoral dynamics diverge sharply from the SSP' simulations. In SSP2'' and SSP3'', final energy production from fossil fuels and electricity peaks at the end of the 2070s. The higher carbon intensity of the economy in SSP3'' results in fossil fuel pathways comparable to SSP2'', while electricity growth is significantly higher in SSP2'' and remains comparable to SSP5'' until the global economic downturn begins in SSP2''. Biomass production for bioenergy also peaks at the end of the 2070s, reaching 60 EJ in both scenarios (Fig. 6a-c). Conversely, in SSP5'', final energy use continues to grow throughout the century across

all energy types, albeit at a much slower rate than in SSP5'. By 2100, global production reaches 420 EJ of fossil fuels, 177 EJ of electricity, and 75 EJ of biomass—equivalent to 29%, 25%, and 27% of the respective SSP5' values. Thus, in relative terms, SSP5'' relies even more heavily on fossil fuels than SSP5'.

The renewable electricity sectors also exhibit discontinuous changes. In SSP2'', hydroelectricity declines to less than 25 EJ annually after peaking at 37 EJ in the late 2070s. The decline in global final demand, however, only temporarily slows the exponential growth of wind and solar PV (Fig. 6d). SSP3'' reproduces the same pattern but at generally lower levels of renewable electricity, particularly for wind and solar energy. Finally, the expansion of renewables in SSP5'' is slower than in SSP2'' throughout the simulation for both solar PV and wind-based electricity, while hydroelectricity in SSP5'' surpasses that in SSP2'' only when final demand starts to decline in the latter scenario.

The evolution of the global food sector's output mirrors the trajectory of final demand in all simulations (Fig. 6f). Following a moderate but steady decline in its share of total output, this share increases again during the last three decades of the simulation in SSP2'' and SSP3'' due to shifting household consumption patterns: as overall budgets fall sharply, households allocate a larger proportion of spending to food. However, ultimately, the dramatic surge in mortality rates of the poorest households at the global level lead to a strong reduction in the weight of the consumption of the poorest classes, and, consequently, the share of the food sector in total output decreases again (Fig. 6e). In contrast, in SSP5'', the food sector's output share declines moderately, stabilizes at 6% from 2080 onward, and begins to rise slightly after 2088—signaling a turning point in the global economy and foreshadowing major structural transformations in the 22nd century.

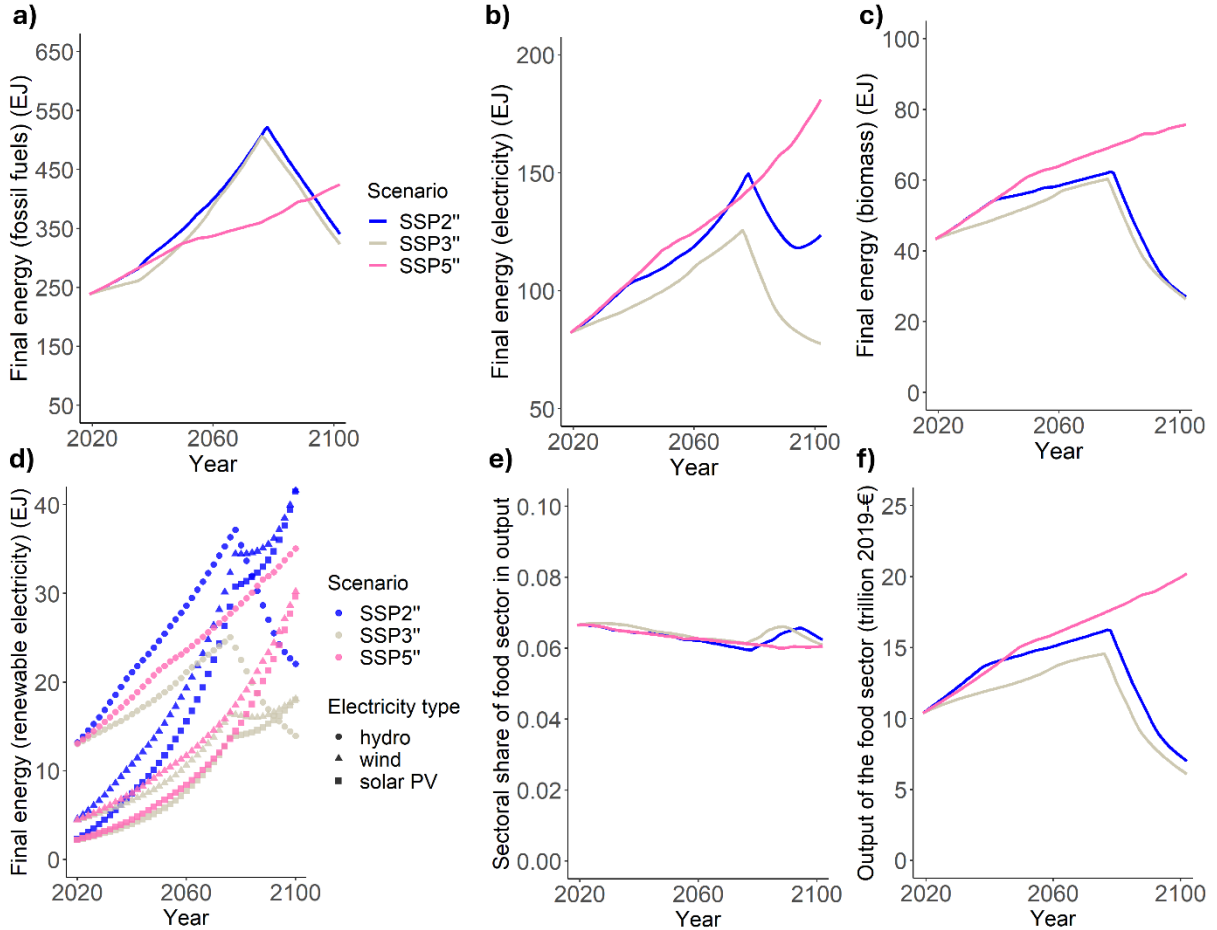


Fig. 6: Annual quantity of a) fossil fuels, b) electricity, c) biomass used by the global economy for SSP2'' (blue), SSP3'' (beige) and SSP5'' (pink). d) evolution of renewable electricity systems (hydro, wind and solar PV based electricity) in the three scenarios, e) share of the food sector in total output on a global scale, f) annual total output of the food sector in the three SSP'' scenarios.

3.2.3. Emissions and global climate change

Compared to the SSP' simulations, the SSP'' variations result in significantly lower global GHG emissions throughout the simulation period. In SSP2'' and SSP3'', global GHG emissions peak in 2077 and 2076 at 88 and 94 Gt/year, respectively, whereas in SSP5'', emissions continue to rise until the end of the century, reaching 95 Gt. The local emission peaks observed in SSP2'', SSP3'', and SSP5'' (Fig. 7b) stem from rapid land-use conversions from forests to agricultural land, driven by the lower land productivity assumptions in the SSP'' implementations. Consequently, global primary forests are completely deforested in SSP3'' by 2076, causing a temporary emission spike, while in SSP2'' and SSP5'', a primary forest protection policy preserves 50% of the initial primary forest until the end of the simulation.

Due to the highly non-linear emission dynamics in the SSP'' simulations, the increase in global average temperature is less monotonic than in the SSP' scenarios. In SSP2'' and SSP3'', the rise in global temperatures slows toward the end of the simulation, reaching 3.37 °C and 3.41 °C in 2100, respectively, whereas in SSP5'', global temperatures increase by 3.69 °C relative to the pre-industrial reference period. Nevertheless,

compared to the SSP' simulations, the differences between SSPs are much smaller. Biophysical constraints thus transform the SSP5 scenario into a fossil-fuel-dependent, low-growth trajectory. The moderate economic convergence tendencies of this scenario—combined with higher resource accessibility compared to SSP2 and SSP3, and lower global warming than in SSP5'—prevent an abrupt economic breakdown during the 21st century, although signs of systemic instability increase, indicating a growing sensitivity of the global system to even small additional deteriorations in the biophysical conditions underpinning socio-economic reproduction.

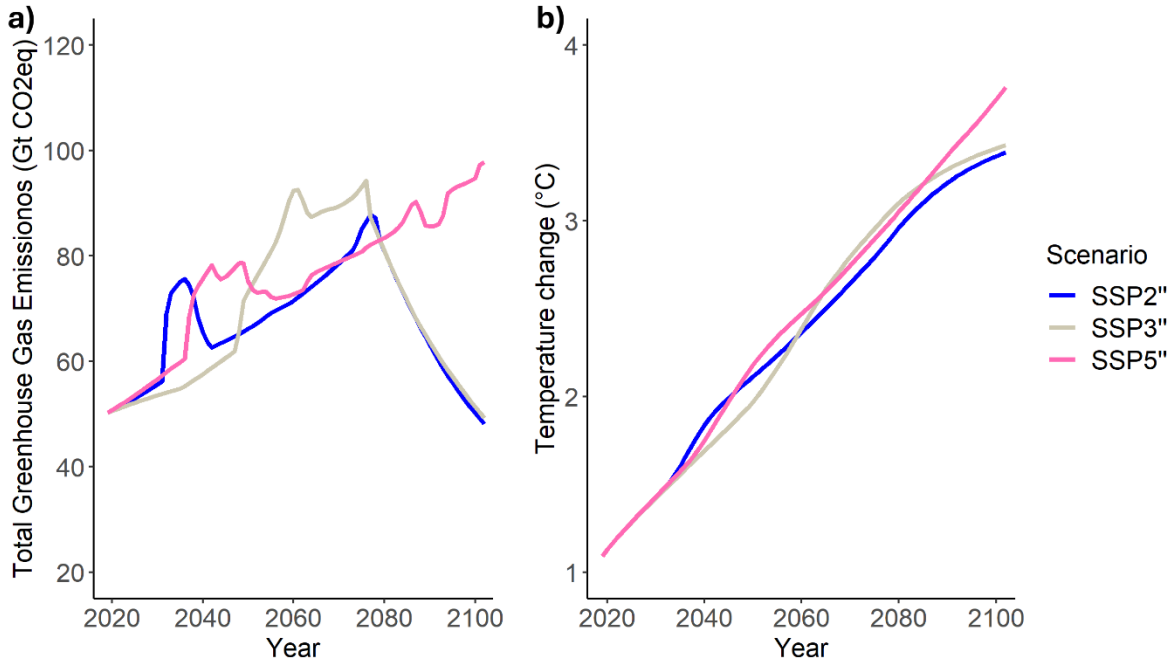


Fig. 7: a) Total greenhouse gas emissions and b) global average temperature change for SSP2'' (blue), SSP3'' (beige) and SSP5'' (pink).

4. Discussion

4.1. Energy intensity and economic development

The assumption that increasing productive capacity or rising affluence is associated with higher energy efficiency in economic activities—due to factors such as technological know-how or greater investment in research and development—is tied to the idea of relative or even absolute decoupling between economic growth and environmental impacts (B. Dong et al., 2016; Elhaj et al., 2025).

However, while the simulations run with MORDRED 1.0.2 do indeed exhibit a modest relative ‘decoupling’ as long as the global economy grows, this trend reverses when economic production begins to decline. The resulting dynamics appear across key industries, affecting fossil and biomass energy intensity as well as the intensity of fossil and renewable electricity (Figure 1 in SM1).

Thus, the same assumption that supports a relative decline in environmental pressure during growth also implies an accelerated collapse when the ‘business-as-usual’

pathway begins to break down. During growth phases, energy efficiency gains enable further expansion; during contraction, declining productive capacity causes deterioration in sectoral energy efficiencies. A vicious cycle emerges: declining energy efficiency increases demand for energy, which heightens environmental pressure; that, in turn, accelerates degradation, adversely impacts the global economy, reduces production, and further degrades energy efficiency. Although this vicious circle is facilitated by biophysical constraints, it evolves into a self-reinforcing dynamic that cannot be reduced simply to the biophysical factors—and it could, in principle, be interrupted by technological policy or structural changes not modeled here.

Nevertheless, given that most global environmental scenario quantifications do not incorporate historical discontinuities in economic growth (Lauer et al., 2024), we contend that the risks arising from a failure of ‘decoupling’ have been insufficiently emphasized in the literature. Our quantifications of SSP2” and SSP3” demonstrate that decoupling may hold long enough to lock the global economy into a decade-long ‘business-as-usual’ path—but once biophysical feedbacks intensify, the very dynamic of decoupling becomes an accelerator of economic and environmental collapse. Thus, ‘decoupling’ only denotes one side of a positive feedback loop which is overlooked in periods of economic growth but emerges as an additional pressure factor in periods of economic collapse.

Further research is required to refine projections of future energy-intensity trends across sectors and socio-economic scenarios—especially those that allow for historical discontinuities and structural shifts in the global energy–economy system (Edelenbosch et al., 2017; Stern, 2017; Tavoni et al., 2015). This task is complicated by methodological challenges in measuring energy intensity itself: it is defined as the ratio of biophysical energy inputs to monetary output, making it an inherently abstract unit whose concrete material content changes over time (cf. Fiorito, 2013).

4.2. Boundary conditions of SSP quantifications

The results of our SSP implementations reaffirm the importance of model structure and boundary conditions in shaping scenario outcomes (Sognnaes et al., 2021). In MORDRED, reproducing results akin to previous SSP quantifications (SSP2’, SSP3’, SSP5’) requires high labor productivity growth assumptions; land productivity growth assumptions significantly higher than the assumptions on future improvements in crop yield made in previous SSP quantifications (Fricko et al., 2017); optimistic assumptions about fossil fuel availability, extraction costs and substitutability between fossil fuels; and, ultimately, the absence of strong climate impacts on labor productivity (Table 1).

In contrast, the boundary conditions for the SSP” simulations assume land productivity improvements more in line with past scenario work, high labor productivity growth, greater skepticism regarding coal/lignite extraction under a favorable EROI, limited substitutability across fossil fuel types, and incorporation of climate impacts on capital, agricultural output, working hours, and labor productivity.

Importantly, the outcomes observed in SSP2'', SSP3'', and SSP5'' will likely be observed only in models with a high degree of endogenization of variables such as world population and economic growth, coupled with feedbacks linking the economy and biophysical environment, and with sectoral disaggregation (via an input–output structure). The latter implies more conservative assumptions about substitutability among energy and sectoral inputs. Consequently, we argue that as IAMs become more holistic and integrate environmental feedbacks more fully, they will tend to project global-level historical discontinuities during the 21st century.

That said, model projections should not be mistaken for precise numerical predictions. The complexity inherent in representing the global system and its long-term trajectories is so great that we can only explore plausible dynamics and pattern shifts, not exact quantitative outcomes. Like all modeling studies, the quantitative outcomes of our scenario exercise must be interpreted in light of the boundary conditions underpinning the simulations. For example, we strongly caution against interpreting SSP5 as the 'best' scenario as it does not show discontinuities as strong as SSP2 and SSP3 when feedback mechanisms are included. Given the high uncertainty regarding climate impacts, the higher level of global warming and fossil fuel dependence in SSP5 could prove disastrous in simulations adopting more pessimistic climate damage parameters. At the same time, in our simulations rising extraction costs of fossil resources play a key role driving the dynamics observed (section 3 SM1) but there are high uncertainties surrounding future developments of this variable. Equally, the model does not explore disaster and emergency policies that presumably would be developed once the economic crisis becomes evident (Nohrstedt & Parker, 2024). These policies might prevent an escalation of mortality rates and a demographic and economic breakdown in the periphery although a recovery and return to economic growth comparable to the beginning of the 21st century seems less plausible. Thus, in general, the conducted analysis principally serves to illustrate that the socio-economic future depicted by previous quantified assumptions of the SSPs is too narrow and that strong historical discontinuities cannot be ruled out *ex ante*. Previous quantifications of the SSPs could generate an unjustified impression of stability, continuity and certainty that dissolves once a more holistic, biophysically grounded and less techno-optimist approach is taken.

4.3. Policy implications

We demonstrate that scenarios that break with the historical linearity and continuity assumed in all SSP storylines, do not only enter into the realm of possible futures but appear highly plausible (Gall et al., 2022). Additionally, we argue that, considering the degree of techno-optimism of the assumptions necessary to 'produce' futures of continued linearity, scenarios featuring significant collapse dynamics of environmental and economic systems appear more probable than scenarios that picture the future as extended present. This finding has a high policy relevance given that policies based on naïve expectations about the viability of 'business-as-usual' are radically different from policies that fully take into account the risks of current environmental and economic

developments (Crownshaw et al., 2019; Jäger et al., 2024; Lawrence et al., 2024; Wesseler & Zhao, 2019).

Currently, global environmental scenarios tend to both underestimate the degree of ecosystem deterioration and climate change caused by continued economic growth, as well as the severity of adverse impacts on economic structures caused by the loss of Earth system support functions. Reorienting policies towards a precautionary approach, thus, implies even higher rates of necessary structural and institutional changes than is currently supposed to prevent drastic climate change. Rather than a ‘decoupling’ of growth from environmental deterioration, these changes would include a ‘decoupling’ of basic human need satisfaction from growth (Brand-Correa & Steinberger, 2017; Buchs et al., 2024; Millward-Hopkins et al., 2020).

Conclusion

In this article we have conducted a comparative scenario analysis of three shared socio-economic pathways (SSP2, SSP3 and SSP5), using a system dynamics based IAM incorporating key feedback mechanisms between global economic, demographic and environmental systems. While a simulation of SSPs without biophysical factors constraining economic growth produces dynamics comparable to previous scenario quantifications using other IAMs, we find that integrating biophysical feedbacks into the quantification of SSPs profoundly alters long-term socio-economic and environmental trajectories, resulting in a global panorama hardly compatible with the global future traced in the original SSP storylines. Rather than a perpetual increase affluence alongside growing environmental impacts, feedback-induced discontinuous developments—manifesting as contractions in production and final demand, population decline, and the spread of poverty—become defining features of 21st-century dynamics in some of the quantified SSP variations. Thus, outcomes from SSP quantifications are shown to be highly sensitive to scenario assumptions and the structure of the IAM used to run the simulations. Importantly, these results do not imply deterministic collapse but rather expose the fragility of the growth-dependent structures embedded in conventional IAM and in the SSP architecture itself. Our findings suggest that the perceived continuity and stability of previous SSP quantifications derive largely from methodological constraints and techno-optimistic assumptions rather than empirical plausibility. As soon as realistic biophysical limits are introduced, the linearity of the original SSPs dissolves, giving way to nonlinear, self-reinforcing dynamics that current policy frameworks remain ill-equipped to address. Consequently, the central policy implication is the urgent need to move beyond the paradigm of “decoupling” growth from environmental degradation and to explore institutional pathways that ensure human well-being independently of economic expansion. Strengthening global resilience under deep uncertainty thus requires reframing scenario design toward precautionary and post-growth perspectives capable of capturing systemic risks. The SSP architecture, while foundational for global environmental assessment, should evolve to integrate non-equilibrium dynamics, feedback-induced discontinuities, and alternative socio-economic imaginaries if it is to remain relevant for policy-making in the Anthropocene.

References

- Aitken, A. (2019). Measuring Welfare Beyond GDP. *National Institute Economic Review*, 249, R3–R16. <https://doi.org/10.1177/002795011924900110>
- Brand-Correa, L. I., & Steinberger, J. K. (2017). A framework for decoupling human need satisfaction from energy use. *Ecological Economics*, 141, 43–52.
- Braun, J., Werner, C., Gerten, D., Stenzel, F., Schaphoff, S., & Lucht, W. (2025). Multiple planetary boundaries preclude biomass crops for carbon capture and storage outside of agricultural areas. *Communications Earth & Environment*, 6(1), 102.
- Buchs, M., Koch, M., & Lee, J. (2024). Sustainable welfare: Decoupling welfare from growth and prioritising needs satisfaction for all. In L. Eastwood & K. Heron (Eds.), *De Gruyter Handbook of Degrowth. De Gruyter Handbooks in Business, Economics and Finance* (pp. 89–106). De Gruyter.
- Calvin, K., Bond-Lamberty, B., Clarke, L., Edmonds, J., Eom, J., Hartin, C., Kim, S., Kyle, P., Link, R., & Moss, R. (2017). The SSP4: A world of deepening inequality. *Global Environmental Change*, 42, 284–296.
- Creutzig, F., Erb, K., Haberl, H., Hof, C., Hunsberger, C., & Roe, S. (2021). Considering sustainability thresholds for BECCS in IPCC and biodiversity assessments. *Global Change Biology. Bioenergy*, 13(4), 510–515.
- Crownshaw, T., Morgan, C., Adams, A., Sers, M., Britto dos Santos, N., Damiano, A., Gilbert, L., Yahya Haage, G., & Horen Greenford, D. (2019). Over the horizon: Exploring the conditions of a post-growth world. *The Anthropocene Review*, 6(1–2), 117–141.
- Dellink, R., Chateau, J., Lanzi, E., & Magné, B. (2017). Long-term economic growth projections in the Shared Socioeconomic Pathways. *Global Environmental Change*, 42, 200–214.
- Dong, B., Zhang, M., Mu, H., & Su, X. (2016). Study on decoupling analysis between energy consumption and economic growth in Liaoning Province. *Energy Policy*, 97, 414–420. <https://doi.org/10.1016/j.enpol.2016.07.054>
- Dong, T., Ye, X., & Mao, Z. (2024). The effect of consumption inequality on subjective well-being: Evidence from China. *PLOS ONE*, 19(11), e0310193. <https://doi.org/10.1371/journal.pone.0310193>
- Edelenbosch, O. Y., Kermeli, K., Crijns-Graus, W., Worrell, E., Bibas, R., Fais, B., Fujimori, S., Kyle, P., Sano, F., & Van Vuuren, D. P. (2017). Comparing projections of industrial energy demand and greenhouse gas emissions in long-term energy models. *Energy*, 122, 701–710. <https://doi.org/10.1016/j.energy.2017.01.017>
- Edwards, A., Brockway, P., Bickerstaff, K., & Nijssse, F. J. (2025). Towards modelling post-growth climate futures: A review of current modelling practices and next steps. *Environmental Research Letters*.
- El Skaf, R. (2025). Post-growth and the lack of diversity in the scenario framework. *Journal of Economic Methodology*, 1–20.
- Elhaj, M., Sarabdeen, M., Almugren, H. Z., Kijas, A. C. M., & Halid, N. (2025). The Economics of Innovation, Renewable Energy, and Energy Efficiency for Sustainability: A Circular Economy Approach to Decoupling Growth from

- Environmental Degradation. *Energies*, 18(17), 4643.
<https://doi.org/10.3390/en18174643>
- Ezzati, M., Vander Hoorn, S., Lawes, C. M. M., Leach, R., James, W. P. T., Lopez, A. D., Rodgers, A., & Murray, C. J. L. (2005). Rethinking the “Diseases of Affluence” Paradigm: Global Patterns of Nutritional Risks in Relation to Economic Development. *PLoS Medicine*, 2(5), e133.
<https://doi.org/10.1371/journal.pmed.0020133>
- Fiorito, G. (2013). Can we use the energy intensity indicator to study “decoupling” in modern economies? *Journal of Cleaner Production*, 47, 465–473.
- Fricko, O., Havlik, P., Rogelj, J., Klimont, Z., Gusti, M., Johnson, N., Kolp, P., Strubegger, M., Valin, H., & Amann, M. (2017). The marker quantification of the Shared Socioeconomic Pathway 2: A middle-of-the-road scenario for the 21st century. *Global Environmental Change*, 42, 251–267.
- Fujimori, S., Hasegawa, T., Masui, T., Takahashi, K., Herran, D. S., Dai, H., Hijioka, Y., & Kainuma, M. (2017). SSP3: AIM implementation of shared socioeconomic pathways. *Global Environmental Change*, 42, 268–283.
- Gall, T., Vallet, F., & Yannou, B. (2022). How to visualise futures studies concepts: Revision of the futures cone. *Futures*, 143, 103024.
- Gerbens-Leenes, P. W., Nonhebel, S., & Krol, M. S. (2010). Food consumption patterns and economic growth. Increasing affluence and the use of natural resources. *Appetite*, 55(3), 597–608. <https://doi.org/10.1016/j.appet.2010.09.013>
- Hardt, L., & O'Neill, D. W. (2017). Ecological macroeconomic models: Assessing current developments. *Ecological Economics*, 134, 198–211.
- Harvie, D., Slater, G., Philp, B., & Wheatley, D. (2009). Economic Well-being and British Regions: The Problem with GDP Per Capita. *Review of Social Economy*, 67(4), 483–505. <https://doi.org/10.1080/00346760802245383>
- Heck, V., Gerten, D., Lucht, W., & Popp, A. (2018). Biomass-based negative emissions difficult to reconcile with planetary boundaries. *Nature Climate Change*, 8(2), 151–155.
- Hickel, J., Brockway, P., Kallis, G., Keyßer, L., Lenzen, M., Slameršák, A., Steinberger, J., & Ürge-Vorsatz, D. (2021). Urgent need for post-growth climate mitigation scenarios. *Nature Energy*, 6(8), 766–768.
- IPCC. (2021). *Climate Change 2021: The Physical Science Basis. Contribution of Working Group I to the Sixth Assessment Report of the Intergovernmental Panel on Climate Change*. Cambridge University Press. Cambridge University Press, Cambridge, UK and New York, NY, USA.,
- Jäger, W. S., de Ruiter, M. C., Tiggeloven, T., & Ward, P. J. (2024). What can we learn from global disaster records about multi-hazards and their risk dynamics? *Natural Hazards and Earth System Sciences Discussions*, 2024, 1–31.
- Kc, S., & Lutz, W. (2014). Demographic scenarios by age, sex and education corresponding to the SSP narratives. *Population and Environment*, 35(3), 243–260.
- Keys, P. W., Badia, L., & Warrier, R. (2024). The Future in Anthropocene Science. *Earth's Future*, 12(1), e2023EF003820.

- Knez, M., Nikolic, M., Zekovic, M., Stangoulis, J. C., Gurinovic, M., & Glibetic, M. (2017). The influence of food consumption and socio-economic factors on the relationship between zinc and iron intake and status in a healthy population. *Public Health Nutrition*, 20(14), 2486–2498. <https://doi.org/10.1017/S1368980017001240>
- Kriegler, E., Bauer, N., Popp, A., Humpenöder, F., Leimbach, M., Strefler, J., Baumstark, L., Bodirsky, B. L., Hilaire, J., & Klein, D. (2017). Fossil-fueled development (SSP5): An energy and resource intensive scenario for the 21st century. *Global Environmental Change*, 42, 297–315.
- Kriegler, E., Edmonds, J., Hallegatte, S., Ebi, K. L., Kram, T., Riahi, K., Winkler, H., & Van Vuuren, D. P. (2014). A new scenario framework for climate change research: The concept of shared climate policy assumptions. *Climatic Change*, 122(3), 401–414.
- Kubiszewski, I., Costanza, R., Franco, C., Lawn, P., Talberth, J., Jackson, T., & Aylmer, C. (2013). Beyond GDP: Measuring and achieving global genuine progress. *Ecological Economics*, 93, 57–68. <https://doi.org/10.1016/j.ecolecon.2013.04.019>
- Lahoti, R., Jayadev, A., & Reddy, S. (2016). The global consumption and income project (GCIP): An overview. *Journal of Globalization and Development*, 7(1), 61–108.
- Lane, L., & Montgomery, W. D. (2014). An institutional critique of new climate scenarios. *Climatic Change*, 122, 447–458.
- Lauer, A., Capellán-Pérez, I., & Wergles, N. (2025). A comparative review of de-and post-growth modeling studies. *Ecological Economics*, 227, 108383.
- Lauer, A., de Castro, C., & Carpintero, Ó. (2024). Between continuous presents and disruptive futures: Identifying the ideological backbones of Global Environmental Scenarios. *Futures*, 103460.
- Lauer, A., & Llases, L. (2025). *MORDRED: Model Of Resource Distribution and Resilient Economic Development. Model Documentation*. GitHub. <https://github.com/Pendracus/MORDRED>
- Lawrence, M., Homer-Dixon, T., Janzwood, S., Rockstöm, J., Renn, O., & Donges, J. F. (2024). Global polycrisis: The causal mechanisms of crisis entanglement. *Global Sustainability*, 7, e6.
- Lempert, R. J., Lawrence, J., Kopp, R. E., Haasnoot, M., Reisinger, A., Grubb, M., & Pasqualino, R. (2024). The use of decision making under deep uncertainty in the IPCC. *Frontiers in Climate*, 6, 1380054.
- Millward-Hopkins, J., Steinberger, J. K., Rao, N. D., & Oswald, Y. (2020). Providing decent living with minimum energy: A global scenario. *Global Environmental Change*, 65, 102168.
- Nohrstedt, D., & Parker, C. F. (2024). Revisiting the role of disasters in climate policy-making. *Climate Policy*, 24(3), 428–439. <https://doi.org/10.1080/14693062.2024.2301781>
- O'Neill, B. C., Kriegler, E., Ebi, K. L., Kemp-Benedict, E., Riahi, K., Rothman, D. S., van Ruijven, B. J., van Vuuren, D. P., Birkmann, J., & Kok, K. (2017). The roads ahead: Narratives for shared socioeconomic pathways describing world futures in the 21st century. *Global Environmental Change*, 42, 169–180.
- Otero, I., Rigal, S., Pereira, L., Kim, H., & Grêt-Regamey, A. (2022). *A degrowth scenario for biodiversity? Some methodological avenues and a call for collaboration*.

- Pereira, L., Kuiper, J. J., Selomane, O., Aguiar, A. P. D., Asrar, G. R., Bennett, E. M., Biggs, R., Calvin, K., Hedden, S., & Hsu, A. (2021). Advancing a toolkit of diverse futures approaches for global environmental assessments. *Ecosystems and People*, 17(1), 191–204.
- Riahi, K., Van Vuuren, D. P., Kriegler, E., Edmonds, J., O’Neill, B. C., Fujimori, S., Bauer, N., Calvin, K., Dellink, R., & Fricko, O. (2017). The shared socioeconomic pathways and their energy, land use, and greenhouse gas emissions implications: An overview. *Global Environmental Change*, 42, 153–168.
- Rothman, D. S., Raskin, P., Kok, K., Robinson, J., Jäger, J., Hughes, B., & Sutton, P. C. (2023). Global Discontinuity: Time for a Paradigm Shift in Global Scenario Analysis. *Sustainability*, 15(17), 12950.
- Sekera, J., & Lichtenberger, A. (2020). Assessing carbon capture: Public policy, science, and societal need: A review of the literature on industrial carbon removal. *Biophysical Economics and Sustainability*, 5, 1–28.
- Sognnaes, I., Gambhir, A., van de Ven, D.-J., Nikas, A., Anger-Kraavi, A., Bui, H., Campagnolo, L., Delpiazzo, E., Doukas, H., & Giarola, S. (2021). A multi-model analysis of long-term emissions and warming implications of current mitigation efforts. *Nature Climate Change*, 11(12), 1055–1062.
- Stadler, K., Wood, R., Bulavskaya, T., Södersten, C., Simas, M., Schmidt, S., Usabiaga, A., Acosta-Fernández, J., Kuenen, J., Bruckner, M., Giljum, S., Lutter, S., Merciai, S., Schmidt, J. H., Theurl, M. C., Plutzar, C., Kastner, T., Eisenmenger, N., Erb, K., ... Tukker, A. (2018). EXIOBASE 3: Developing a Time Series of Detailed Environmentally Extended Multi-Regional Input-Output Tables. *Journal of Industrial Ecology*, 22(3), 502–515. <https://doi.org/10.1111/jiec.12715>
- Stern, D. I. (2017). How accurate are energy intensity projections? *Climatic Change*, 143, 537–545.
- Szetey, K., Moallemi, E., Chakori, S., & Bryan, B. A. (2023). *Improving the relevance of the Shared Socioeconomic Pathways for sustainability science*.
- Tavoni, M., Kriegler, E., Riahi, K., Van Vuuren, D. P., Aboumahboub, T., Bowen, A., Calvin, K., Campiglio, E., Kober, T., & Jewell, J. (2015). Post-2020 climate agreements in the major economies assessed in the light of global models. *Nature Climate Change*, 5(2), 119–126.
- UN DESA. (2019). *World Population Prospects 2019, Online Edition. Rev. 1. File POP/7-1: Total population (both sexes combined) by five-year age group, region, subregion and country, 1950-2100 (thousands)*.
- Van den Bergh, J. C. (2009). The GDP paradox. *Journal of Economic Psychology*, 30(2), 117–135.
- Wesseler, J., & Zhao, J. (2019). Real Options and Environmental Policies: The Good, the Bad, and the Ugly. *Annual Review of Resource Economics*, 11(1), 43–58. <https://doi.org/10.1146/annurev-resource-100518-094140>

Supplementary Material

1. Additional information on scenario implementation

1.1. Land, labor and capital intensities

Land, labor and capital intensities are modeled as exogenous target values that are approached by 2100, starting from the initial values. The target values are calculated with the respective growth rates for changes in either productivity or intensity, considering that intensity = 1/productivity. Target land intensities for 2100 are multiplied by a factor <1 to reflect the environmental impact of dietary changes. All values are given in Table 1 of the main text.

1.2. Changes in the A matrix and the consumption vectors

During the simulation, the initial values of the A matrix approach targets values defined for the year 2100 in the target A matrix while the initial consumption vectors of households, governments and investment approach target consumption vectors in 2100.

These target values are obtained through various conversions of the original A matrix and the initial consumption vectors.

First, the monetary inputs belonging to the energy sectors (row numbers 3, 10, 12, 13, 14, 15, 16, 17, 18, 19, 20) of the A matrix, and the shares of the energy sectors in the consumption vectors, are converted into biophysical inputs using conversion factors that relate the monetary with the biophysical output of every energy sector.

Second, inputs from less efficient or scalable renewable energy technologies (sectors 16, 19, 20) are shifted to other renewable energy sectors (sectors 14, 15, 17).

Third, a certain percentage of the inputs (in the case of the consumption vectors, expenditure shares) from the fossil and nuclear electricity sector (number 12 and 13), which depends on the respective scenario, is shifted to renewable energies (sectors 14, 15, 17), and a certain percentage of the inputs of the non-electricity energy sectors (number 3 and 10) is shifted to renewable electricity (sectors 15 and 17) after the application of a correction factor that reflects assumed energy efficiency gains through electrification processes.

Last, in the case of the A matrix, all the inputs to the service sector (number 7) are multiplied by a material intensity factor to reflect improvements or deteriorations in the material intensity of the service economy, while in the case of the consumption vector of the richest households, half of the consumption expenditure share for the food sector is shifted to the service sector, given that the consumption vector remains constant above a

threshold per capita consumption of 24,673 € per year which without correction could lead to an overestimation of food expenditures in scenarios with high economic growth during the 21st century.

1.3. Endogenization of energy intensities

While energy intensities can be modeled exogenously through the target A matrix, for the SSP implementations we changed the model structure of MORDRED to reflect endogenous changes in the energy intensity of the economy.

The main assumption behind the endogenization of energy intensities is that as productive capacities (measured as sectoral output per capita) increase, technological know-how increases as well, which leads to an improvement in energy intensities. Evidently, the opposite is true for a decline in productive capacities.

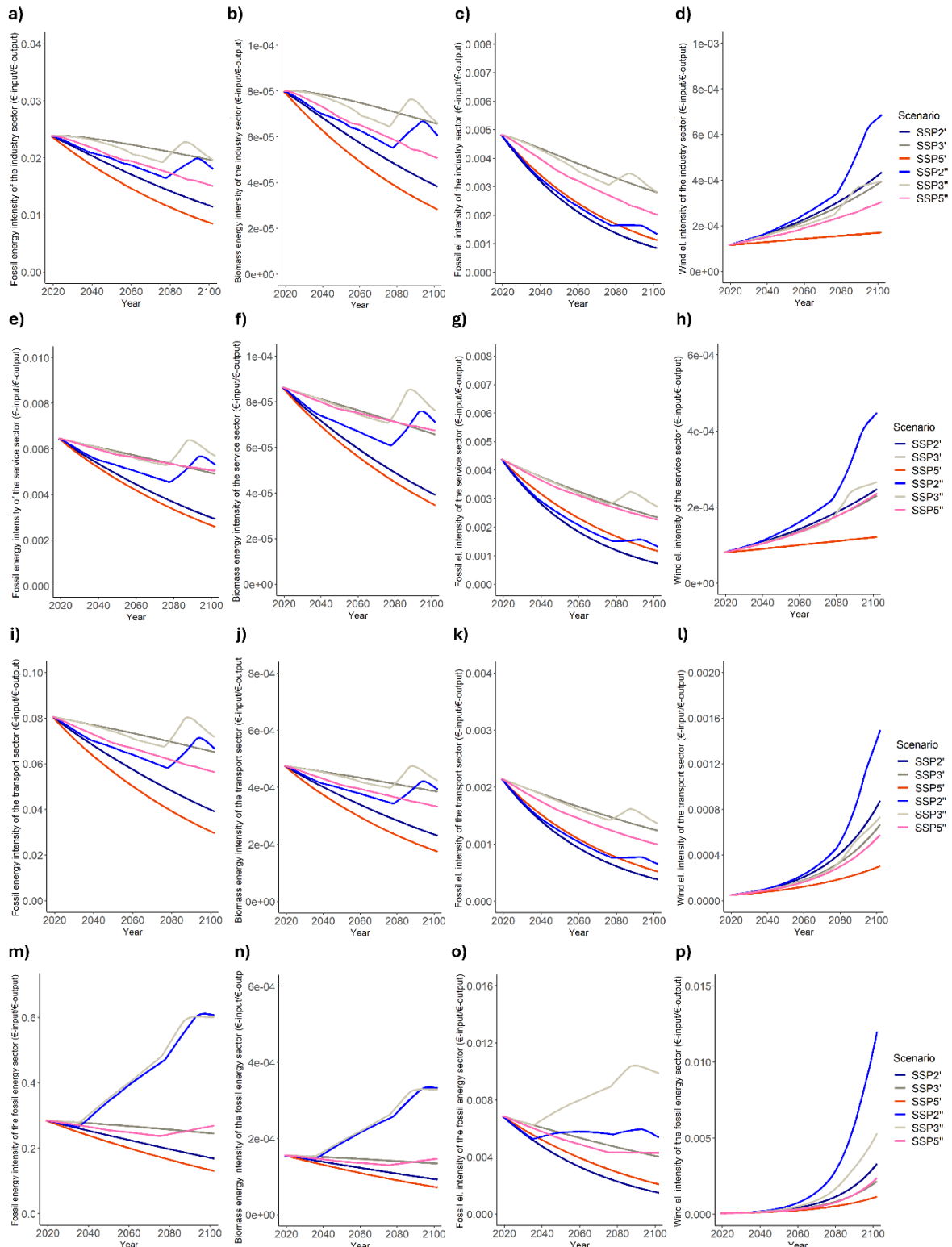
Consequently, we model the development of energy intensities with an energy intensity multiplier (*EIM*) for all the sectors (*s*) relevant to the SSP storyline implementations, i.e. the industry sector (sector 5), the services sector (sector 7), the transport sector (sector 21) and the main energy sectors (3, 10, 12, 13, 14, 15, 17). The multiplier can be expressed as:

$$EIM_s(\text{output per capita}_s) = \beta_{1s} * \text{output per capita}_s^{\beta_2} + \beta_{3s}$$

The parameters are calibrated such that the function equals 1 at the initial time step of the simulation. If the sectoral output per capita becomes greater (smaller) than the value corresponding to the initial moment EIM becomes <1 (>1).

In the adapted version of MORDRED, the dynamically changing EIM is multiplied with the rows of the A matrix corresponding to the energy sectors (3, 10, 12, 13, 14, 15, 16, 17, 18, 19, 20) in the case of all sectors for which energy intensities are endogenized (3, 5, 7, 10, 12, 13, 14, 15, 17).

2. Development of energy intensities in SSP variations

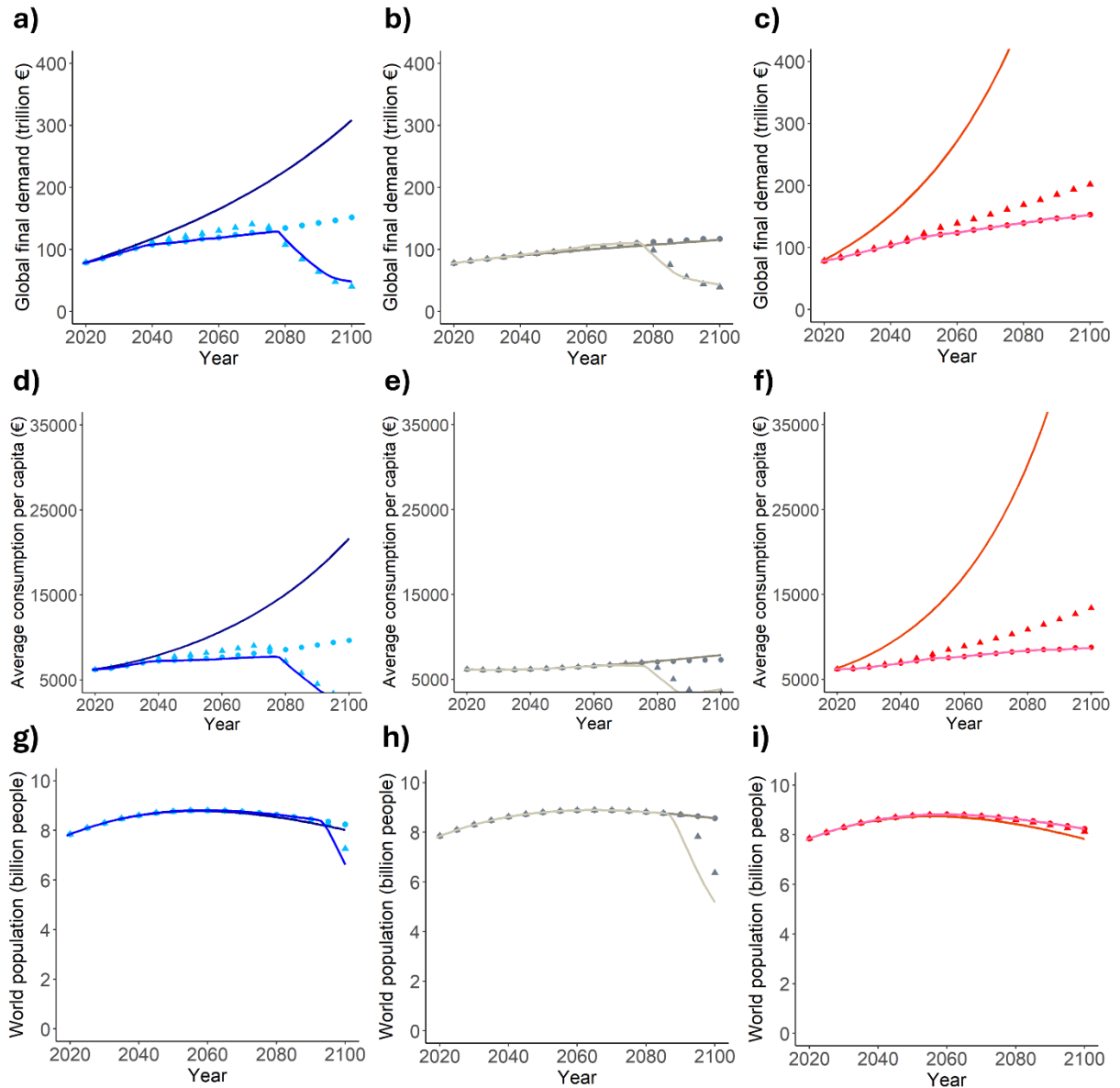


Suppl. Figure 1: Changes in energy intensities for different energy types and in different sectors across the SSP simulations (SSP2': dark blue; SSP2'': lighter blue; SSP3': grey; SSP3'': beige; SSP5': red; SSP5'': pink). a) fossil energy intensity, b) biomass energy intensity, c) fossil electricity intensity, d) wind electricity intensity of the industry sector; e) fossil energy intensity, f) biomass energy intensity, g) fossil electricity intensity, h) wind electricity intensity of the service sector; i) fossil energy intensity, j) biomass energy intensity, k) fossil electricity intensity, l) wind electricity intensity of the transport sector; m) fossil energy intensity of the fossil energy sector, n) biomass energy intensity of the fossil energy sector, o) fossil electricity intensity of the fossil energy sector, p) wind electricity intensity of the fossil energy sector.

transport sector; m) fossil energy intensity, n) biomass energy intensity, o) fossil electricity intensity, p) wind electricity intensity of the fossil energy sector.

3. Scenario variations

To test whether historical discontinuities also appear under a partial introduction of biophysical limits, additional SSP variations were simulated in which either climate impacts or rising fossil fuel extraction costs were considered independently. The inclusion of climate damage factors alone is sufficient to considerably slow the growth of global final demand and average consumption. However, no ‘tipping’ point is reached; hence, there is no radical discontinuity in demographic developments in SSP2 and SSP3. By contrast, the introduction of steeply rising fossil extraction costs generates a feedback effect strong enough to reach a global socio-economic ‘tipping point,’ although the demographic collapse in SSP2 and SSP3 occurs later than in the SSP variations with full integration of biophysical feedback. For SSP5, no significant difference in demographic development is observed between the scenarios with complete and partial inclusion of feedback mechanisms. The scenario outcomes for the key variables are displayed in Suppl. Figure 2.



Suppl. Figure 2: Evolution of global final demand (a-c), world average consumption (d-f) and world population (g-h) in all SSP variations. Lines depict the SSP' and SSP'' variations discussed in the main text (SSP2': dark blue, SSP2'': lighter blue, SSP3': grey, SSP3'': beige, SSP5': red, SSP5'': pink). Circles depict the results for SSP variations in which the climate damages represented in MORDRED are activated while rising fossil extraction costs are deactivated. Triangles depict the results for SSP variations in which there are no climate damages but increasing fossil fuel extraction costs.

Modeling Global Inequality and Limits to Growth: Socio-Economic Polarization and Systemic Breakdown in the 21st Century

Abstract

Although both rising inequality and biophysical limits to economic growth originate within the global capitalist system and increasingly strain its stability, the interactions between these dynamics remain insufficiently understood. To address this gap, this study presents a simulation-based analysis of (i) potential distributional implications of biophysical limits to growth for different socio-economic groups and world regions, (ii) the environmental consequences of economic divergence and societal polarization under such limits, and (iii) the resulting risks for global economic stability throughout the 21st century. Using the Integrated Assessment Model MORDRED, a *Hyperimperialist Exploitation* scenario is quantified in which growing biophysical constraints trigger a persistent global economic decline disproportionately affecting poorer regions and classes, while the wealthiest maintain high consumption levels. The simulations indicate that this trajectory produces escalating inequality, catastrophic socio-economic impacts in the Global South, and fails to achieve effective climate mitigation. The findings suggest that maintaining high inequality in resource and energy use—supported by continued socio-ecological cost-shifting from richer to poorer regions—is structurally unsustainable over the medium to long term due to the global economy's dependence on cheap labor and materials from the South. As economic growth ceases to function as a mechanism of social stabilization, the system's underlying fragility becomes exposed, indicating that efforts to preserve material privileges in the Global North may ultimately precipitate a comprehensive systemic breakdown.

Keywords

Limits to growth; Integrated Assessment Modeling; climate scenarios; global environmental scenarios; inequality; North-South interdependence

1. Introduction

Since the end of World War II, the stability of the current politico-economic world order depends on economic growth (Schmelzer, 2017) given that the prospective of economic development and the associated increases in living standards and geopolitical power legitimizes the existence of persistent inequalities in power and economic wealth within and between societies (Nilsen, 2016, 2025). However, the ‘great acceleration’ (Steffen et al., 2015) resulting from the persistent growth of world economic output has also exponentially increased the pressure of the global civilization on the Earth’s resources and ecological supporting systems (IPCC, 2021, 2022; Richardson et al., 2023). Today, the world faces accelerating and complex global environmental changes in several dimensions that have put into question the sustainability of the global capitalist economic system and even of industrial civilization itself (Chandler et al., 2018; Keys et al., 2024; Moore, 2017; Rockström et al., 2009). Although economic growth until the end of the 21st century is still a standard assumption in the majority of global environmental scenarios an increasing number of scenarios has recognized that growth rates could decline in the future, either through intentional political action or because of a failure to solve the sustainability crisis (Lauer et al., 2024).

Scenarios based on the former are often labeled as ‘Degrowth’ or ‘Post-growth’ scenarios, tend to concentrate on reducing output and consumption of the Global North and imply strong convergence between world regions as well as within countries (Lauer et al., 2025). Regarding the latter possibility, the problem of dynamically interrelated biophysical limits to exponential economic growth and the dynamics of overshoot and collapse caused by delayed feedback loops were already illustrated in the Limits to Growth Report to the Club of Rome (Meadows et al., 1972). Subsequent research has not only updated and confirmed the principal results of the modeling study (Herrington, 2021; Meadows et al., 2004; Turner, 2014) but also has added greater detail and complexity to the study of biophysical constraints on economic development by focusing on specific questions such as the land, material and EROI constraints on the renewable energy transition(Capellán-Pérez et al., 2017, 2019, 2020), the relationship between energy availability and economic development (Ayres et al., 2003; Espinoza et al., 2022; García-Olivares & Ballabrera, 2012; Kümmel & Lindenberger, 2020; Nieto et al., 2020) or the ways in which climate damages can impact the economy (Bovari et al., 2018; Tsigaris & Wood, 2019) and demographic developments (Court & McIsaac, 2020).

Distributional aspects and inequalities are a central area of study for researchers concerned with intentional degrowth or post-growth transitions (Hickel, 2020; Kallis, 2019; Koch, 2015) and, given the inherent inequality produced by a capitalist system (Bouchaud & Mézard, 2000; Piketty, 2017) researchers have pointed toward framework conditions and possible policy measures to prevent a rise in social inequality in a non-growing economy (Hartley et al., 2020; Jackson & Victor, 2018, 2016). Conversely, the modeling literature concerned with biophysical limits to economic growth and the risks of an imposed degrowth of world economic output has not yet exhaustively addressed the possible distributional impacts of a stagnating or declining world economic output due to escalating environmental degradation and resource constraints. For example, in the original study by Meadows et al. (1972) and in subsequent studies building on a comparable system dynamics logic (Capellán-Pérez et al., 2020) world average GDP declines but this number is not further disaggregated into different world regions or social classes. However, as repeatedly illustrated by recent historical examples such as the 2008 financial crisis, the Covid-19 pandemic or the war in Ukraine, in a global capitalist system the loss of world output due to economic, political and/or environmental shocks is not distributed

equally between different social classes and world regions (Abay et al., 2023; Behnassi & El Haiba, 2022; van Bavel & Scheffer, 2021). Rather, poorer classes and regions risks losing access to basic food and health products (e.g. Bayati et al., 2022) while the increase in wealth of the richest percentiles continues (Christensen et al., 2023).

To address this gap in the literature, in this article we conduct a quantitative scenario study to explore the conceivable distributional impacts of a prolonged stagnation and contraction of the world economy, and to analyze the social, economic and environmental impacts of rising inequality in a post-growth or post-'business as usual' era. Concretely, we seek to answer the following questions:

- How could key socio-economic and environmental variables on the global scale evolve during the 21st century without fundamental changes in the dominant political institutions and socio-economic structures shaping the production of and access to economic goods?
- How could limits to growth in the global capitalist economy affect economic inequality between classes and societies and the consumption levels of the poorest socio-economic groups of the world system?
- What might happen to the stability of world economic (re)production in global futures featuring strong 'polarization and divergence', i.e. scenarios in which rich classes and countries ('Global North') maintain their consumption levels at the cost of poorer classes and countries ('Global South')?

To this end, we use a newly developed Integrated Assessment Model (IAM) which is parametrized to fit a scenario characterized by increasing inequality once biophysical limits to world economic growth begin to manifest. We analyze the feasibility of such a scenario and discuss possible avenues for future research before concluding by highlighting the main policy implications of our findings.

2. Methods

2.1. Simulation model

To carry out the simulations, we use version 1.0.1. of MORDRED (Model of Resource Distribution and Resilient Economic Development), an Integrated Assessment Model (IAM) designed to analyze global socio-economic inequality and biophysical constraints on economic growth. Built with the software Vensim, it integrates several dynamically linked parts: Population, Economy, Labor, Energy, Land and Climate (Fig. 1). MORDRED endogenizes critical variables that are often treated as exogenous (e.g., economic growth, mortality/fertility rates, climate impacts) and provides a disaggregated view on the consumption of different socio-economic groups which allows users to simulate diverse climate and energy scenarios under varying inequality conditions. MORDRED can be categorized as ecological macroeconomic model (Hardt & O'Neill, 2017) of medium complexity that combines system dynamics with monetary input-output (IO) modeling. The main data sources for the calibration of the model are the environmentally and socially extended IO tables from Exiobase3 for the year 2019 (Stadler et al., 2018), UN (2019) population data for 2020, consumption inequality data for 2014 from the GCIP database (Lahoti et al., 2016) and climate and emission related variables from the IPCC WGI (2021). A detailed description of the model, including its structure and equations, model data and raw data sources

is provided in Lauer & Llases (2025b). Thus, in the following we only shortly explain the main characteristics of the model components that are relevant for our scenario study.

- Demography

The population or demography module is divided into 20 age groups (0-4 years, 5-9 years, 10-14 years, etc., with the last group being people aged 95+), 3 world regions (center, semiperiphery, periphery) and 4 classes (Top20 (T20), Middle50 (M50), Bottom30 (B30) and Subsistence).¹ The world region ‘center’ comprises high-income countries according to the World Bank’s country classification for 2019 (World Bank, 2025), the semiperiphery comprises upper-middle income countries and the periphery consists of countries with lower-middle and low income. In every region, the population constituting the global economy is divided into consumption deciles. Consequently, the richest two deciles constitute the Top20 class, the poorest three deciles constitute the Bottom30 class and the remaining deciles constitute the middle class. The different classes demand consumption goods and supply the labor force required to maintain and increase production. The mortality and fertility rates of the different classes depend on their per capita consumption as well as on government expenses of the respective world regions on health (in the case of mortality rates) and education (in the case of fertility rates).

- Labor

The subsegment of the population in the working age (15-64 years) constitutes the potential working force for the global economy. The total labor supply depends on the participation rate and the number of hours worked. Global temperature increases negatively affect labor supply and labor productivities (e.g. Dasgupta et al., 2021; Mora et al., 2017).

- Land

MORDRED contains information on the changing amounts of primary forest, secondary forest, economically used forest, cropland, pastures and ‘other’ land demanded by the agriculture and forestry sector, land used for infrastructure and land used for renewable energy generation. Conversion of forest land causes land-use change-related CO₂ emissions. Climate change impacts can affect the availability as well as the productivity of land.

- Energy

The energy module converts monetary into biophysical demand for energy and deducts the consumed fossil energy from the stock of fossil energy reserves and resources. The model very optimistically assumes complete substitutability between coal, oil and gas. While the fossil fuels used for energy generation cause greenhouse gas emissions, the fossil fuels used as material feedstock are assumed to cause zero CO₂ emissions during the simulation period. As the most easily accessible resources get extracted first, input requirements to the fossil fuel sectors increase with the amount of already extracted resources. The energy module also depicts changes in different types of final energy and in the electricity mix.

¹ In our scenario specification, the subsistence class rapidly gets integrated into the formal economy such that there is no longer a difference between the subsistence class and the Bottom30. Thus, we refrain from discussing subsistence related dynamics and evolutions in the present paper and only focus on the global capitalist economy.

- Economy

The economy has an input-output structure comprising 25 sectors that allow model users to differentiate between food, energy, industry and service related activities (Supplementary Table 1). World economic output is determined by final demand (including government and household consumption and investment) and the production of necessary intermediate products. Sectorial final demand of households depends on their per capita consumption while sectorial final demand of governments increases as a historical share of household consumption. Investments are made to adapt the capital stock to the size required to fulfill consumption demands. Using information about the energy, land and labor intensities of the sectorial economic activities and the desired sectorial outputs, the model calculates the required labor, energy and land input requirements (the latter two are further disaggregated into fossil fuels, bioenergy and different types of electricity, and into different land types). In the case of insufficient input requirements, it uses an allocation mechanism to prioritize the different demand components. The A matrix and the capital stock of different sectors (especially the food and energy sectors) can be affected by climate impacts as well as by rising energy extraction costs.

- Climate

The climate module converts different greenhouse gas emissions (CO₂, CH₄, N₂O, HFC, PFC, SF₆) into changes in global average temperatures with respect to pre-industrial (1850) levels.

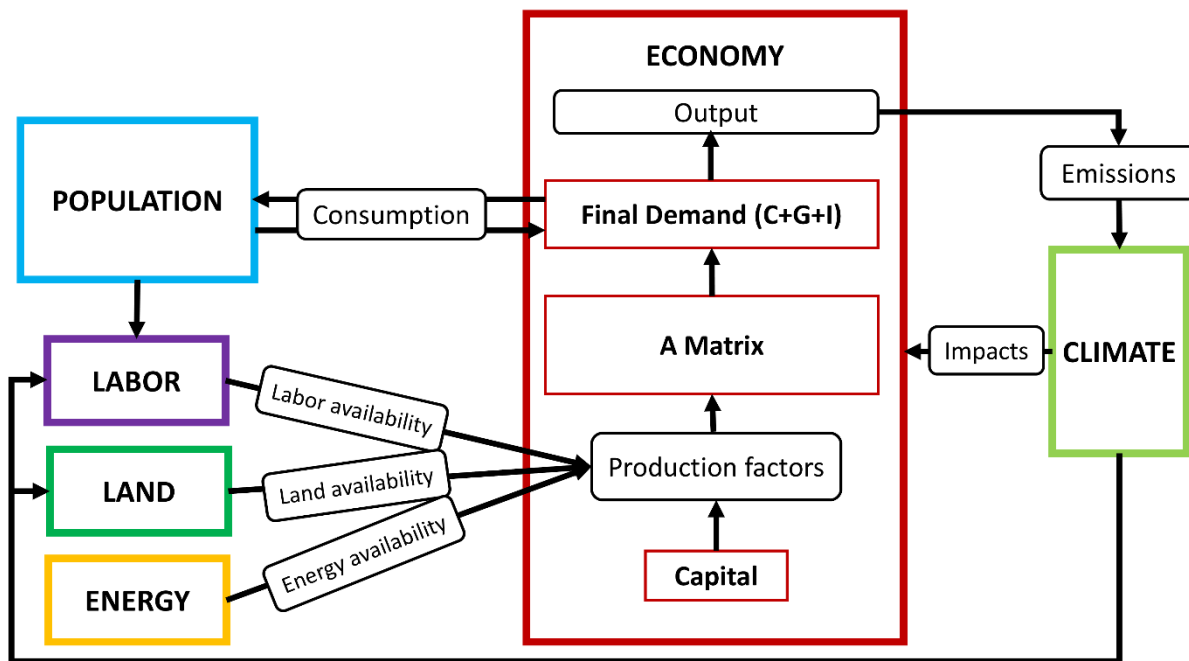


Fig. 1: Simplified representation of MORDRED, showing only the most important feedback relationships.

2.2. Scenario analysis

For the scenario analysis we selected a ‘divergence’ scenario developed in Lauer & Llases (2025a) called ‘Hyperimperialist Exploitation’ because this scenario focuses on distributional

impacts in a context of stagnating or shrinking world economic output and because the scenario storyline is coupled to a series of scenario characteristics that facilitate the scenario parametrization process.

'Hyperimperialist Exploitation' describes a scenario in which, after a period of prolonged business-as-usual economic growth, the global geopolitical, cultural and socio-economic conditions allow the upper classes of the capitalist centers (or 'Global North') to maintain their consumption despite the world economy's stagnation and subsequent degrowth. Consequently, the consumption of the remaining population declines, especially for the inhabitants of the periphery and semiperiphery. The complete storyline can be found in S1 of Supplementary Material 1 (SM1).

'Hyperimperialist Exploitation', thus, represents a scenario in which the neoliberal promise of economic growth in the Global South, which legitimizes the exploitation of cheap labor, can no longer be delivered. Consequently, in the scenario the richer classes of the world find themselves in the contradictory situation that they need to increasingly suppress the consumption of the Global South to maintain their own high consumption levels but at the same time their consumption still relies on the Global South's labor force.

To explore the storyline in MORDRED we have parametrized its key variables. The 'neoliberal promise' for the Global South is represented through desired consumption growth rates for the different classes and world regions: The growth rates of the semiperiphery and periphery are higher than in the center, and, in the absence of material restrictions, in 2100 the lower, middle and upper classes of the periphery consume like the lower, middle and upper classes of the center in 2019. The semiperiphery reaches these levels of consumption even before 2100, and in 2100 the consumption of the lower, middle and upper classes in the semiperiphery are two times as high as the consumption of the respective classes in the center in 2019. The center itself also continues to grow, consuming 4 times as much in 2100 as in 2019. Thus, in the absence of biophysical restrictions, the scenario is designed to result in a considerably richer world with slightly reduced but still significant inequalities between the Global North and South and with consistently high inequality within societies.

The input-output structure of the model, coupled with the capitalist basis of the scenario, implies that, once there are certain shocks or limitations of the required input factors that increase the costs of extraction, the total demand for goods no longer can be fulfilled, and economic output declines. The allocation rules of the model favor the consumption demands of the richest classes, reflecting the main allocation principle in a capitalist system: In the case of scarcity, the consumption demand of the richest classes are satisfied first, and of the poorest classes last. This tends to produce declines in the effective consumption of the poorest classes. Economic development in the scenario quantification reflects the historical tendency of capitalism to increase productive capacities and efficiency, resulting in significant labor and land productivity increases that are assumed to occur until the end of the 21st century. Capital productivity is optimistically assumed to increase, which can be considered an indirect material and energy efficiency improvement as less capital stock needs to be maintained and produced per unit of economic output. Regarding the energy technologies used in the scenario, we follow the original assumption of the storyline which gives a high importance to fossil fuels but also an increasing importance to renewable electricity. Changes in energy efficiency and in the electricity mix are parametrized as changes in the energy sectors of the A matrix which, during the simulation, approaches a target A matrix specifying the assumed changes in 2100.

Apart from this ‘baseline’ parametrization four scenario variations were constructed and simulated to test the robustness of the dynamics produced in the baseline (S5 SM1).

Table 1 provides an overview of the implementation of the scenario storyline in the model while S3 SM1 explains in more detail the parametrization of the A matrix as well as on the changing labor, land and capital intensities. SM2 contains the excel sheet used for the simulation of the baseline scenario and the scenario variations with all the relevant parameters.

Scenario variable	Implementation in MORDRED	
Life expectancy (unequal consumption, violent conflicts, environmental damages)	Endogenous development of life expectancy as a function of consumption per capita. Consumption per capita, in turn, is affected by biophysical impacts on production.	
Evolution of per capita consumption in the center <i>without</i> biophysical restrictions	Desired growth rate that results in a per capita consumption four times as high as in 2019.	$g_{Center_{T20}} = 1.7\%$ $g_{Center_{M50}} = 1.7\%$ $g_{Center_{B30}} = 1.7\%$
Evolution of per capita consumption in the semiperiphery <i>without</i> biophysical restrictions	Desired growth rate that results in a per capita consumption two times as high as in the center in 2019.	$g_{Semiperiphery_{T20}} = 2.8\%$ $g_{Semiperiphery_{M50}} = 3.2\%$ $g_{Semiperiphery_{B30}} = 3.5\%$
Evolution of per capita consumption in the periphery <i>without</i> biophysical restrictions	Desired growth rate that results in a per capita consumption as high as in the center in 2019.	$g_{Semiperiphery_{T20}} = 2.8\%$ $g_{Semiperiphery_{M50}} = 3.1\%$ $g_{Semiperiphery_{B30}} = 3.0\%$
Per capita consumption <i>with</i> biophysical restrictions to global economic output	Hierarchization of the final demand components	$I > G_{c,s,p} > C_{c_{T20}}, C_{c_{M50}} > C_{c_{B30}} >$ $C_{sT20}, C_{sM50}, C_{pT20}, C_{pM50} > C_{sB30}, C_{pB30}$
Interregional and intraregional inequality	High inequality levels	Initial inequality ratios: $T20_{center}:B30_{periphery} = 46$ $T20_{center}:B30_{center} = 4$ $T20_{semiperiphery}:B30_{semiperiphery} = 7$ $T20_{periphery}:B30_{periphery} = 5$
Social policy	No transfers from governments to households to reduce inequality; no transfers from governments to governments.	$transfer_{gov \rightarrow hh} = 0$ $transfer_{gov_{center} \rightarrow gov_{semip.}} = 0$ $transfer_{gov_{center} \rightarrow gov_{perip.}} = 0$
Military policy	Military expenses are included in the government demand for public security which is aggregated into the service sector.	Expenses for the military are assumed to grow at the same rate as the government demand for services grows.
Environmental policy	Moderate environmental policies subject to the imperative of economic growth through changes in the target A matrix for 2100 and changes in the consumption vectors of households, governments and investment.	Reduction of fossil electricity by 90% and of nuclear electricity by 40%; replacement through renewables; electrification of 20% of energy inputs in key sectors and final demand; no additional recycling policies; no land conservation policies.
Mode of production	The model operates at a higher level of abstraction than models representing a specific mode of production. The representation of production is purely technical (Leontief production function), and distribution does not appear as wage payments and profit appropriation. Instead, consumption levels for different social groups are exogenously imposed according to different scenarios.	
Goal of production	Output is directed to fulfill investment (accumulation) and consumption demands of governments and household, guaranteeing the reproduction and stability of the current socio-economic system	
Allocation principle	Class as indicator of personal wealth and income is the main allocation principle of scarce goods.	

Labor productivity	Change of target sectoral labor intensities in 2100	Decrease of global sectoral labor intensities to the levels of the center (Global North) in 2019.
Capital productivity	Change of target sectoral capital intensities in 2100	Capital productivity increases by 20%.
Land intensity	Change of target land intensities in 2100	Annual increase of global land productivity by 2.25% for all land types.
Energy intensity	Energy intensity declines through improvements in economic processes and through electrification, both of which is reflected in the energy sectors of the A matrix	Reduction of input coefficients from energy sectors by 5%; 20% shift from non-electricity energy sectors to renewable electricity sectors for key economic sectors.
Energy types	Energy sectors representing different energy types: sector 3 (coal, oil, gas); 10 (biomass energy); sectors 12-20 (fossil, nuclear, hydro, wind, biomass, solar PV, solar thermal, tide and geothermal electricity).	High importance of fossil fuels, especially petroleum; increasing importance of renewable electricity.
Climate Mitigation	No particular climate mitigation goals.	
Ecosystem integrity	Ecosystem integrity declines due to land use changes (conversion of forests into agricultural land and settlements).	Low priorities for land that is not used by the economy: Land demands of the global economy are fulfilled first at the detriment of land conservation.
Sensitivity of ecosystems to anthropogenic perturbations	Low sensitivity reflected through the absence of feedback mechanisms of declining biodiversity and ecosystem integrity on economic productive capacities.	
Climate Sensitivity	Best guess for climate sensitivity in climate module.	<i>Climate Sensitivity = 3°C</i>
	Climate system feedbacks.	No feedbacks assumed in the base run (cf. S5 SM1).
Quantity of accessible materials	No restrictions on the quantity of minerals that can be extracted; assumption of perfect substitutability between different types of fossil fuels resulting in relatively high amounts of accessible resources; Exponential cost modeling of input requirements to the energy sectors with respect to total fossil resources estimated by the BGR (2020); Input requirements assumed to increase by approximately 1.5 by the time coal, oil and gas reserves are depleted, and nearly triple by the time oil and gas resources are depleted.	

Table 1: Overview of scenario parametrization in MORDRED.

3. Results

The simulation results, which cover the time period 2019 to 2105, shed light on possible changes in the evolution of key socio-economic and environmental variables on the global scale (section 3.1) and changes in intraregional and interregional inequalities (section 3.2) linked to a ‘Hyperimperialist exploitation’ scenario, as well as on the stability and ‘feasibility’ of this scenario over time (section 3.3).

3.1. Socio-economic and environmental developments on the global scale

In accordance with the scenario storyline, all socio-economic variables and most environmental variables at the global level initially follow business-as-usual trends before exhibiting historically discontinuous dynamics beginning in the second half of the 21st century.

World output (the sum of final demand and intermediate production) increases continuously from €156 trillion in 2019 to a peak of €371 trillion in 2071. From 2075 onwards, global output

declines approximately linearly to €311 trillion in 2094. As illustrated in Fig. 2, from that year onwards the decline becomes exponential, and by the end of the simulation, global output is more than five times lower than in 2019. This pattern mirrors the evolution of the world population (Fig. 2b). Starting from around 7.8 billion in 2019, the population grows moderately to 8.75 billion between 2053 and 2057 before gradually declining to its initial size by 2094. However, when global economic output collapses abruptly, population size follows suit: between 2094 and 2105, the world population decreases by 6.5 billion people. As a result of these changes, global average consumption more than doubles during the first six decades of the simulation, reaching €12,590 per year in 2071. It then declines to €9,000 in 2100, before rising again as population declines faster than output. The evolution of the global energy system under this scenario is also non-linear and discontinuous but more differentiated than that of the socio-economic variables. While total output grows by 238% during the first half of the simulation, total final energy use rises more slowly but over a longer period—from 373 EJ in 2019 to a peak of 722 EJ in 2093. Between 2094 and 2105, total final energy follows world output and population in their exponential decline. By the end of the simulation, global final energy use is 80% lower than in 2019. Taken together, these economic, demographic, and technological developments indicate a large-scale systemic breakdown of the global economy by the end of the 21st century.

The increase in energy consumption levels despite stagnating and later declining world output in the final decades of the 21st century can be explained by rising input requirements for producing economic output, driven by higher fossil fuel extraction costs and the growing impacts of climate change (cf. Fig. 4d). These factors increasingly outweigh the continuing efficiency gains within the economy.

The rising energy consumption levels compared to the stagnant and subsequently declining world economic output during the last four decades of the 21st century can be explained by increasing input requirements to produce economic output, caused by an increase in the extraction costs of fossil fuels, as well as climate change impacts (cf. Fig. 4d). These factors increasingly outweigh the continuing energy efficiency gains in the economy.

Disaggregating final energy types (Fig. 2c), reveals that the simulation reflects the storyline's emphasis on the continued dominance of fossil fuels and the rising importance of electricity. While non-electric fossil energy growth slows in the 2050s and peaks in 2082, electricity demand continues to rise despite economic stagnation and contraction, though at a slower pace than in the early 21st century. In line with the scenario parameters, the electricity mix undergoes rapid and consistent "greening" (Fig. 2d). During the high-growth phase, the expansion of renewables leads only to a slow decline in fossil electricity production—from 52 EJ in 2019 to 48 EJ in 2052. However, as biophysical limits increasingly constrain accumulation while renewable expansion continues, the decline of fossil electricity accelerates, reaching a historically low value of 0.9 EJ by 2105. Nuclear electricity almost doubles, peaking at 15.4 EJ between 2058 and 2062, before declining steadily to 7.5 EJ by 2096, a level lower than at the simulation's start.

Renewable energy sources experience persistent growth despite economic stagnation: hydroelectricity expands exponentially until the global slowdown of the 2060s, after which it stabilizes at around 55 EJ between 2075 and 2095, while wind- and solar-PV-based electricity grow continuously from about 5 EJ and 2 EJ in 2019 to 70 EJ and 68 EJ in 2094, respectively. Yet, the sharp contraction in energy demand following the systemic economic collapse at the end of the century also leads to an abrupt decline in renewable generation.

Despite the expansion of renewables and the decline in global economic production, global average temperature continues to rise, reaching 3.94°C by 2100 (Fig. 1f). This outcome underscores the incompatibility of the quantified scenario storyline with effective climate mitigation strategies. The persistent temperature increase stems from global greenhouse gas (GHG) emissions (Fig. 1e), which, although decreasing after 2074, remain between 80 and 100 Gt CO₂-equivalent per year—more than 1.5 times current levels. The simulations therefore demonstrate that a sustained decline in global economic output does not necessarily result in a strong reduction of emissions or a slowdown in warming. Rather, the externalities generated during the business-as-usual growth phase—such as depletion of easily accessible resources and worsening climate impacts—manifest during the economic decline phase, due to time-lagged feedbacks between economic and environmental systems (cf. Meadows et al., 1992).

Consequently, by the end of the 21st century, the world finds itself in an extremely vulnerable position, trapped between a collapsing global economy and climate conditions unprecedented in human history.

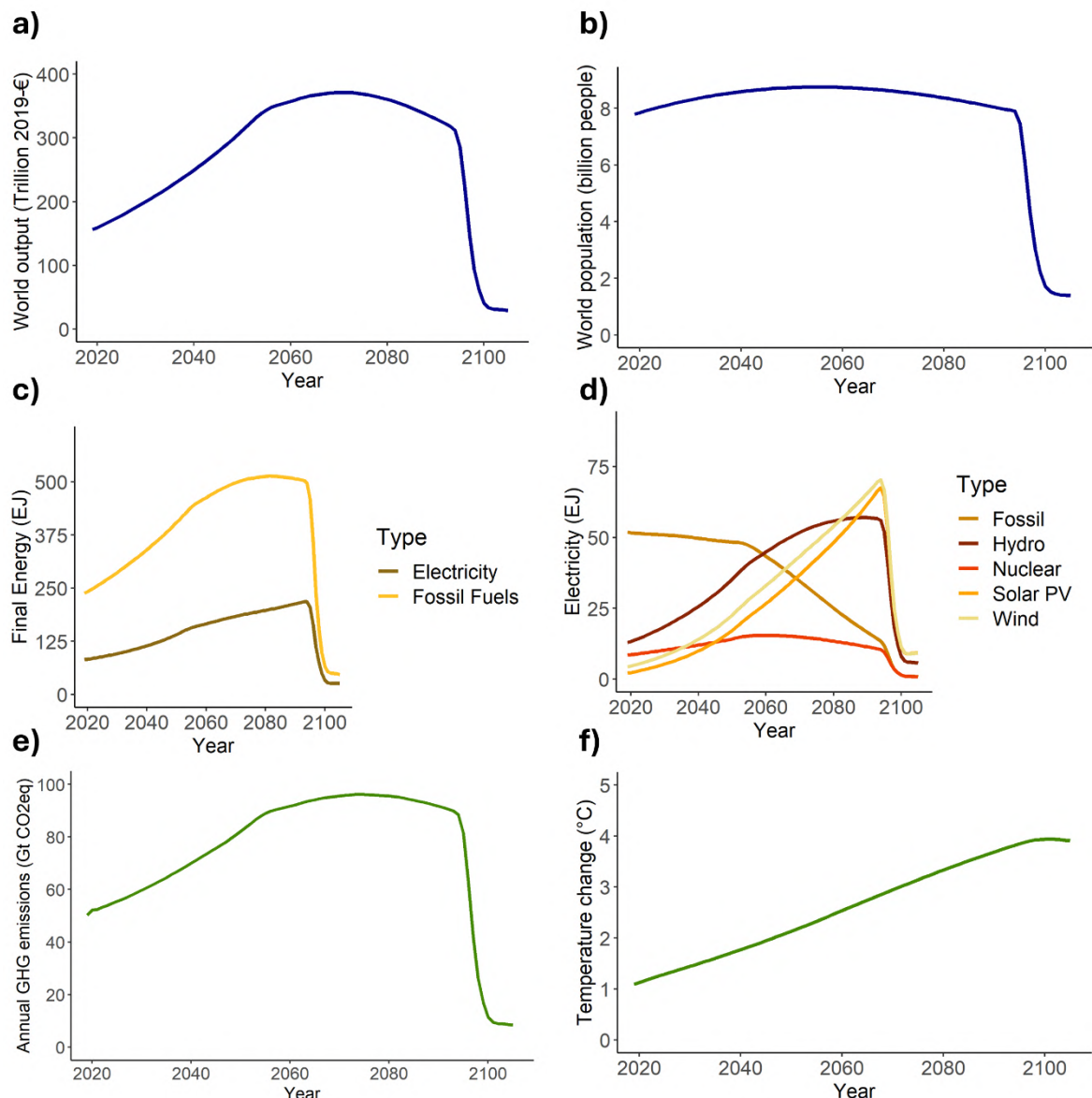


Fig. 2: Evolution of world output (a) and world population (b), fossil fuels and electricity (c), electricity mix (d), GHG emissions (e) and global average temperature with respect to 1850 (f).

3.2. Limits to growth and inequality

Although biophysical constraints on economic development emerge globally and lead to declining world output in the final quarter of the 21st century, the simulation illustrates that the distributional consequences of persistent global contraction are highly unequal and mediated by nationality and class.

As shown in Fig. 3a, consumption per capita among the upper, middle, and lower classes of the world region labeled ‘center’ (high-income countries) begins to slow in the 2050s, reaching maximum levels of €83,000, €40,500, and €20,200 per year, respectively, in 2074. Over the following two decades, these consumption levels remain roughly constant despite the global downturn and declining world average consumption. Only during the final decade of the simulation do all classes in the center experience a sharp collapse, falling to €20,000, €9,800, and €3,300 per year, respectively.

For the ‘semiperiphery’ (upper-middle-income countries), the simulation produces more differentiated trends between classes (Fig. 3b). Consumption per capita of the high and middle classes grows strongly during the first five decades, peaking in the mid-2070s at €28,000 and €11,300 per year. While consumption in the center remains stable until the systemic breakdown, the upper and middle classes of the semiperiphery experience a gradual decline from 2075 onward. The contraction is even more pronounced for the poorest class, whose consumption peaks at only €5,100 in 2074 and drops to €3,290 within a decade.

The ‘periphery,’ encompassing lower-middle- and low-income countries, mirrors these developments (Fig. 3c). Consumption across all classes peaks in the mid-2070s and declines thereafter. Given already low initial consumption levels, these decreases imply critical reductions in living standards and life expectancy. While the richest 20% in the periphery maintain a consumption level comparable to the poorest class in the center for roughly half a century, the poorest 30% reach a maximum of only €3,000 per year, and by 2092 their consumption has fallen back to the extremely low initial values of the simulation.

Hence, the ‘neoliberal promise’ of globalization holds only during the first four decades of the scenario, after which the historical gains in convergence are gradually reversed. For the lower and middle classes of the periphery and the poorest in the semiperiphery, this reversal results in severe poverty. As these groups together represent more than half of the global population, the results indicate a massive rise in poverty during the final quarter of the 21st century, driven by economic contraction and divergence. In the lowest class of the periphery, poverty-induced increases in mortality become so extreme that they trigger a demographic collapse in that region (Fig. 4a-c).

The global downturn affects the semiperiphery and periphery most severely because, starting from low consumption levels, they never reach affluence before the ‘turning point’ of the 2070s. Consequently, even small declines in consumption have strong adverse effects on health, life expectancy, and quality of life. The only exception is the top 20% of the semiperiphery, who catch up with the poorest 30% of the center by 2030 and maintain higher consumption until the 2090s. This outcome suggests the possibility of future trajectories marked by persistent inequality within the semiperiphery and a relative erosion of the lower classes in the center compared to semiperipheral elites.

Beyond per-capita measures, inequality can also be assessed through cumulative consumption over the century (Fig. 3.d-f). The three classes of the center jointly consume €2,975 trillion between 2019 and 2105, while the semiperiphery and periphery consume €2,094 trillion and €1,750 trillion, respectively. Thus, the center appropriates 44% of all goods produced during the simulation despite representing only a small and shrinking share of the global population—13% in 2040 and 10.7% by 2080. In the final year, the richest 20% of the center alone account for 17% of cumulative global consumption, while the poorest 30% of the periphery account for only 3%.

When cumulative consumption is measured per capita (Fig. 3.g-i), the contrast is even sharper: an individual born in 2019 in the richest 20% of the center consumes €5.65 million worth of goods over an 80-year lifetime; a member of the middle class in the semiperiphery consumes €0.66 million; and a person from the poorest 30% of the periphery consumes only €150,000. Overall, the simulation is characterized by moderate convergence during the growth phase, followed by accelerating divergence during the phase of unintentional global degrowth (Fig. S1a-b, SM1).

Overall, high inter- and intraregional inequality levels are compatible with a shrinking global capitalist economy, but their social effects are more severe than under continued growth. The result is widespread absolute poverty, escalating mortality rates, and increasing instability of the global system—a dynamic further explored in the following section.

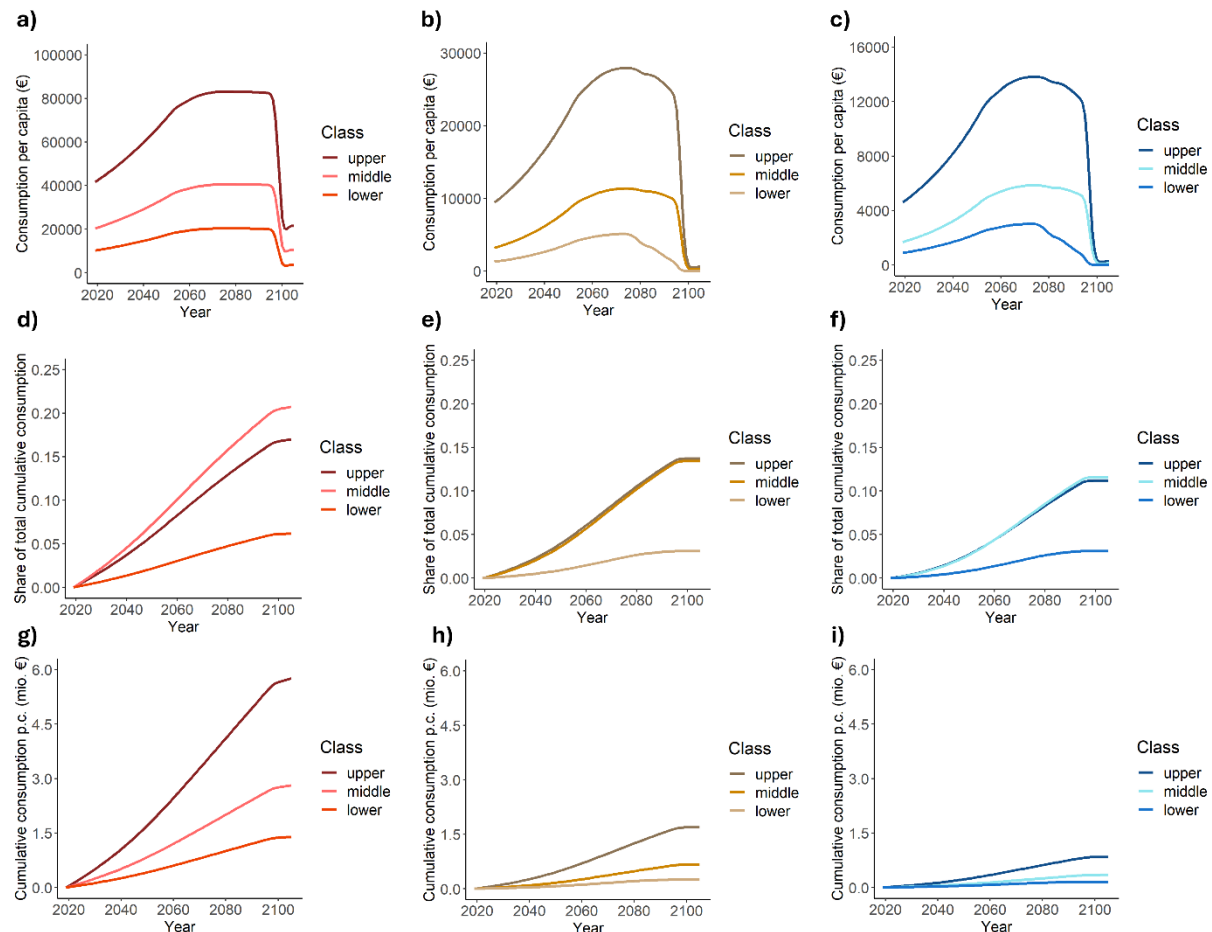


Fig. 3: Evolution of consumption per capita (€/year) for the three classes in the center (a), semiperiphery (b) and periphery (c); evolution of cumulative consumption as share of total cumulative consumption (billion €) for the three classes in the center, (d), semiperiphery (e) and periphery (f); evolution of cumulative consumption per capita (million €) for the three classes in the center (g), semiperiphery (h) and periphery (i).

3.3. Between business-as-usual and breakdown: Hyperimperialist exploitation

The scenario quantification demonstrates that the ‘hyperimperialist exploitation’ narrative is not a timeless configuration but a transient phase, sustainable only for a limited period.

In the baseline simulation, dynamics corresponding to this phase emerge after roughly four decades of business-as-usual (BAU) development and persist for about three decades, until 2093. Thereafter, a ‘breakdown’ phase begins, driven primarily by the catastrophic decline of population in non-center regions—from 4.7 to 0.6 billion in the periphery and from 2.5 to 0.3 billion in the semiperiphery between 2090 and 2100.

The BAU phase is characterized by rapid population growth in the periphery, stabilization in the semiperiphery, and decline in the center (Fig. 4a), accompanied by falling mortality rates—most pronounced in the semiperiphery and least in the center (Fig. 4c). Total deaths increase in the center due to population aging and in the other regions due to population growth (Fig. 4b). The labor-demand-to-supply ratio initially declines because labor-force growth outpaces the increase in labor demand, which is reduced by rising sectoral productivity. However, as climate impacts intensify and fossil fuel extraction costs rise, the decline in labor intensity slows, reversing the trend in the labor demand-supply ratio. Climate impacts and extraction difficulties also increase the input requirements of the food and energy sectors, reversing previous efficiency gains. Notably, these trends emerge between 2040 and 2060, several decades before global output peaks, suggesting their potential role as early-warning indicators of systemic crisis (Fig. 4d).

The subsequent ‘hyperimperialist exploitation’ phase is marked by stagnation, slow decline and a deterioration of additional key parameters contributing to the stabilization of the world economic system. Mortality rates rise across all regions, and efficiency gains fail to offset the growing input needs of the food and energy sectors. By suppressing consumption in the poorer classes of the semiperiphery and periphery, the upper and middle classes of the center maintain their living standards for several decades after the onset of global decline. However, this strategy undermines the very stability of the system that enables their affluence.

On one hand, the aspiration to reach center-level affluence historically has served as a stabilizing factor, motivating semiperipheral and peripheral countries to produce for the global market under unequal conditions. Consequently, once world output begins to stagnate and populations in the semiperiphery and periphery experience a stagnation or even a decline in their living standards, social and political pressure could lead to an end of the ‘hyperimperialist exploitation’ phase well before the 2090s. On the other hand, rising polarization within the center—between a stagnating lower class and an elite benefiting from external exploitation—could destabilize domestic politics. Importantly, the center depends structurally on the labor force of the semiperipheral and peripheral countries because its consumption levels are higher than the level it could reach by solely relying on its own labor force. Thus, once the labor force in the non-center world regions collapses due to escalating poverty-caused mortality rates, this phase of the scenario must necessarily come to an end.

This last phenomenon is shown in the model during the last years of the simulation, which constitute a ‘breakdown’ phase. Population in the non-center regions declines drastically as the

consumption of lower classes falls below subsistence levels. The resulting loss of labor—previously sustaining the consumption of wealthier regions—causes a dramatic worsening of the labor demand-supply ratio (Fig. 4d). Consequently, consumption in the remaining classes collapses rapidly (Fig. 3.a-c). The structural dependency of the Global North on the Global South for cheap labor leads to a sharp decline in living standards across the former, although the magnitude of the loss depends on regional labor productivity, the capacity for rapid re-regionalization, and other factors beyond the model's scope (cf. scenario variation 4 in SM1). During the 'breakdown' phase of the simulation, the remaining population inhabits a nearly 4 degree warmer world characterized by widespread poverty and high inequality caused by dissolving and dysfunctional global economic structures that still rely on fossil fuels.

As the model cannot capture the destabilizing effects of rising social tensions and distribution conflicts in the world system, it likely overestimates the period of the 'hyperimperialist exploitation' phase. Nevertheless, it highlights the inherent instability and unsustainability of 'polarization-and-divergence' trajectories in a contracting world economy.

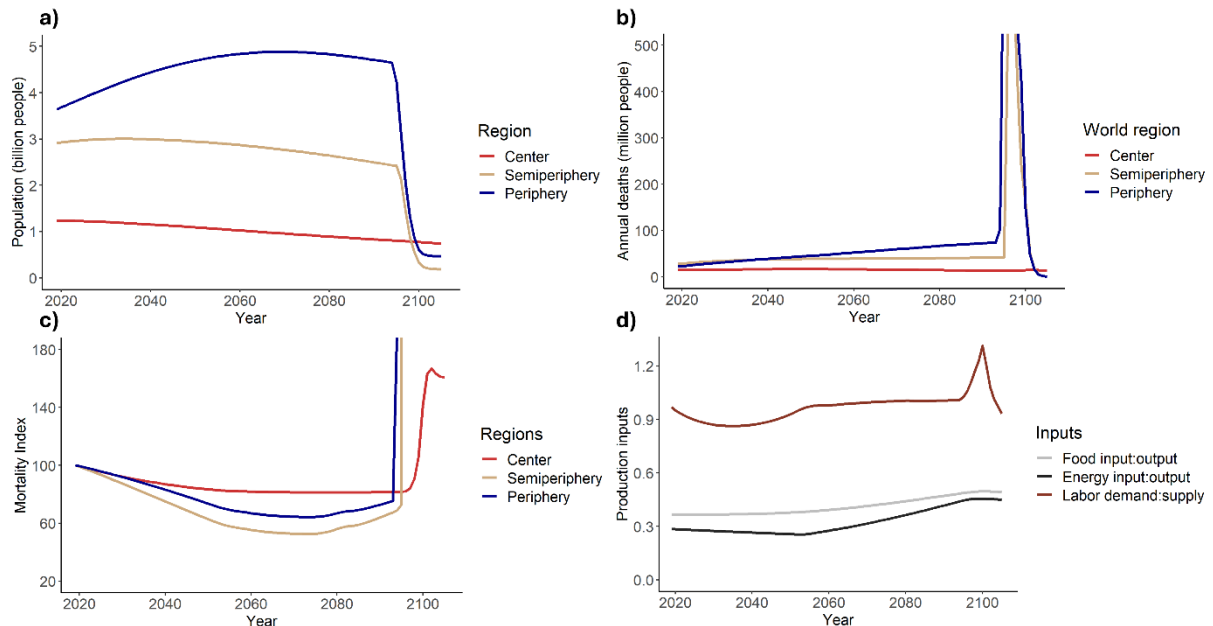


Fig. 4: Evolution of world population (a), annual deaths (b) and mortality rates (c) by region; evolution of the labor demand-supply ratio and the input-output ratios of the food sector and the fossil energy sector (d). The mortality index is calculated with the mortality rates of the age group comprising the 40- to 44-year-olds. An index value of 100 reflects the initial level of mortality in each world region.

4. Discussion

4.1. Caveats, limitations and future work

The scenario simulation presented in this article must not be regarded as a deterministic prediction of future developments but as an explorative exercise of possible dynamics of polarization under a shrinking capitalist economy and as an analysis of the long-term stability and feasibility of such dynamics. Due to some fundamental characteristics of the current global economic system, such as the unequal distribution of costs and benefits of economic development, the tendency for an increase in inequality, and the logic of the price mechanism

that excludes the poorest classes from access to consumption goods in the case of scarcity, we hold that it is probable to observe some of the tendencies explored in our scenario exercise in the future, and, as we illustrate, the potential risks and impacts for the great majority of the world population could be qualified as catastrophic.

As shown in Section 5 of SM1, alternative simulations of the same storyline—varying in the level of climate change mitigation, climate sensitivity, labor productivity, and the degree of divergence—produce dynamics similar to those presented in the previous section, although the timing and magnitude of the global system’s breakdown differ. Thus, as long as the underlying logic of the polarization and divergence scenario—namely, a strong tendency to shift the burden of unintentional economic degrowth onto poorer classes and the absence of policies to alleviate extreme poverty—is maintained, changes in key scenario variables do not fundamentally alter the overall results.

However, it is important to bear in mind that the simulated scenarios represent a certain exaggeration of the social and ecological cost-shifting from the Global North to the Global South. It is unlikely that the consumption levels of poorer classes could be suppressed to the point of endangering survival without triggering resistance dynamics that would either lead to poverty alleviation policies or to a more radical transformation of the global economic system. In fact, once its greatest legitimization – economic growth that eventually also reaches the poorest classes and regions – disappears, it can be expected that social tensions will erode the stability of the global capitalist system. This creates a huge uncertainty space whose potential content can not be discussed here.

Apart from the highly complex social and political dynamics that could unfold in a stagnating and shrinking world economy, there is also uncertainty regarding the evolution of a series of technological and biophysical variables. Assuming that our scenario parametrization of future higher labor and land productivities across sectors, and higher fossil energy extraction costs are within a plausible range, not only is the appearance of a ‘hyperimperialist exploitation’ phase a robust outcome of the scenario simulation, but also its unsustainability. Although the amount of time the ‘hyperimperialist’ phase might vary, ultimately, it causes a complete breakdown of the global system.

Consequently, the simulation results point at probable and serious risks for the poorer half of humanity as well as for the stability of the world economy, resulting from the interaction between the current distribution rules of the world economy, degrading environmental conditions and a fossil-fuel dependent energy system.

Future research could address some limitations of the present simulation study such as the exclusion of other limiting factors such as water, soil productivity or biodiversity integrity in the environmental realm. These would likely change the relatively optimistic assumptions we made in the scenario parametrization regarding land availability, land productivity and the possible rate of land use change and shed light on the role land plays in constraining economic development. Equally, future research could focus on a possible inclusion of financial or geopolitical dynamics in the simulation or reduce the uncertainties surrounding the profitability of mineral and fuel extraction. Last, another important feedback relationship that was neglected in the present study is the relationship between inequality and energy efficiency (Millward-Hopkins et al., 2020), which in our case could further reduce the duration of the ‘hyperimperialist exploitation’ phase in the simulation. However, we hold that quantitative efforts to increase the accuracy of scenario simulations featuring polarization tendencies would

need to be complemented by theoretical work applying our simulation results to questions of peace and conflict studies, sustainability transitions, North-South relationships and the study of alternative ways for societies to organize their reproduction.

4.2. Policy implications

The climate change impacts and adaptation literature has repeatedly shown that climate impacts pose a greater threat to Global South countries due to their greater vulnerability to adverse (global) environmental changes reflected in higher extreme poverty rates, weaker infrastructure, lower financial resources and higher dependence on climate-sensitive sectors (Hallegatte et al., 2016; IPCC, 2022; Thomas & Twyman, 2005). This has led to the construction of polarization scenarios such as 'Fortress World', 'Security First' or 'Slaveship Earth' (Hunt et al., 2012), which are characterized by a global upper class residing on metaphorical islands of wealth surrounded by a metaphorical ocean of misery. These scenarios are reflected in popular narratives and perceptions of the climate crisis as a distant phenomenon, which implicitly suggest that environmental degradation might deteriorate the development options and living standards of the Global South but that the population of the Global North, and especially the richest segments of those populations, although also experiencing some adverse impacts, will be able to continue their lives without major historical discontinuities (cf. Loy & Spence, 2020; Spence et al., 2012; Van Lange & Huckelba, 2021).

Our findings suggest that polarization or divergence scenarios in which the burden of adverse environmental change is systematically placed on socio-economically vulnerable populations in semiperipheral and peripheral countries are only viable during a limited period of time and in the long run undermine the conditions of their own reproduction. Because the cheap labor force of the Global South sustains the reproduction of the world economic system, which allows the upper and middle classes of the Global North – as well as the political and economic elites of the Global South – to maintain and increase their high levels of consumption, the fate of the working classes in the Global South and North cannot be separated. Our scenario study clearly shows that it is impossible for the population of high-income countries to sustain their living standards without the labor force of the Global South except in the case of extremely high labor productivity improvements. Although a fortress scenario with high inequality is still conceivable if the 'elite' with high material consumption is reduced to the wealthiest 1% or 0.1% of the world, it is highly doubtful that such a scenario would find the necessary legitimacy among the world population to be stable in the long-term.

The interesting consequence of the unequal exchange of labor and of materials (Dorninger et al., 2021; Hickel et al., 2024; Hornborg & Martinez-Alier, 2016) between center, semiperiphery and periphery in the context of biophysical limits to growth, thus, is an impossibility for rich countries to leave more vulnerable countries on their own given that a prolonged, massive cost-shifting (D'Alisa & Demaria, 2024; Martínez-Alier, 2012) of this kind drastically increases the risks of an irreversible breakdown of the world economy.

Consequently, the most relevant policy implication arising from our scenario analysis is the inadequacy of nationalist survival-of-the-fittest approaches to the global sustainability crisis. The structural interdependency characterizing the relationships between center, semiperiphery and periphery in global capitalism requires strong global cooperation to address climate change and a series of other grave environmental issues. Importantly, this cooperation is necessary not

only for mitigation efforts but also for climate change adaptation and emergency help in the face of more frequent environmental disasters.

Ultimately, it is an imperative of the wealthier and more powerful classes and countries of the world to cut down their own consumption because in the absence of a series of technological miracles of Promethean character (Georgescu-Roegen, 1986) occurring in the coming decades it seems to be the only way to prolong the life of a global economic system that disproportionately benefits these classes. Thus, we hold that a strong reduction in consumption inequalities within and between societies is to be a priority policy goal not only in potential 'degrowth' or 'ecosocialist' sustainability transitions advocated by some scholars and activists but even in an international landscape that continues to favor the development of global capitalism.

5. Conclusion

In this paper, we aimed to use the IAM MORDRED to explore possible distributional impacts of a persistent contraction of the world economy due to biophysical limits to growth. Thus, we have tested the plausibility of a 'Hyperimperialist Exploitation' scenario in which richer classes in the world's centers maintain their consumption at the cost of the rest of the world. Our findings show that such a scenario produces escalating inequality and catastrophic socio-economic consequences in the Global South and is unable to deliver any substantial climate mitigation. At the same time, we find that a scenario of high inequality in the consumption of economic goods, energy and resources between socio-economic classes, coupled with an implicit ecological cost-shifting from richer to poorer classes on a global scale, is not viable in the mid- and long-term due to the world economy's structural reliance on cheap labor and resources (Moore, 2017, 2018). Thus, maintaining or increasing inequality in a period of increasing adverse environmental impacts and resource constraints drastically undermines the stability of the capitalist global economy. This also implies that political strategies exclusively aiming at maximizing material privileges of the upper- and middle-class segments in the Global North in the long-term will cause the collapse of the very system sustaining these classes. Consequently, strong global cooperation and convergence policies would not only be adequate reactions to the global socio-ecological crisis from an ethical and justice perspective but ultimately would also be in the material interests of those disproportionately benefiting from the current world system.

References

- Abay, K. A., Breisinger, C., Glauber, J., Kurdi, S., Laborde, D., & Siddig, K. (2023). The Russia-Ukraine war: Implications for global and regional food security and potential policy responses. *Global Food Security*, 36, 100675.
- Ayres, R. U., Ayres, L. W., & Warr, B. (2003). Exergy, power and work in the US economy, 1900–1998. *Energy*, 28(3), 219–273.
- Bayati, M., Noroozi, R., Ghanbari-Jahromi, M., & Jalali, F. S. (2022). Inequality in the distribution of Covid-19 vaccine: A systematic review. *International Journal for Equity in Health*, 21(1), 122.
- Behnassi, M., & El Haiba, M. (2022). Implications of the Russia–Ukraine war for global food security. *Nature Human Behaviour*, 6(6), 754–755.
- BGR. (2020). *BGR Energy Study 2019 – Data and Developments Concerning German and Global energy supplies*. Hannover.
https://www.bgr.bund.de/EN/Themen/Energie/Downloads/energiestudie_2019_en.pdf
;jsessionid=ADF18B2529B3E89FC705FDF390A57BA4.internet002?__blob=publicationFile&v=6
- Bouchaud, J.-P., & Mézard, M. (2000). Wealth condensation in a simple model of economy. *Physica A: Statistical Mechanics and Its Applications*, 282(3–4), 536–545.
- Bovari, E., Giraud, G., & Mc Isaac, F. (2018). Coping with collapse: A stock-flow consistent monetary macrodynamics of global warming. *Ecological Economics*, 147, 383–398.
- Capellán-Pérez, I., de Blas, I., Nieto, J., de Castro, C., Miguel, L. J., Carpintero, Ó., Mediavilla, M., Lobejón, L. F., Ferreras-Alonso, N., & Rodrigo, P. (2020). MEDEAS: a new modeling framework integrating global biophysical and socioeconomic constraints. *Energy & Environmental Science*, 13(3), 986–1017.
- Capellán-Pérez, I., De Castro, C., & Arto, I. (2017). Assessing vulnerabilities and limits in the transition to renewable energies: Land requirements under 100% solar energy scenarios. *Renewable and Sustainable Energy Reviews*, 77, 760–782.
- Capellán-Pérez, I., De Castro, C., & González, L. J. M. (2019). Dynamic Energy Return on Energy Investment (EROI) and material requirements in scenarios of global transition to renewable energies. *Energy Strategy Reviews*, 26, 100399.
- Chandler, D., Cudworth, E., & Hobden, S. (2018). Anthropocene, capitalocene and liberal cosmopolitan IR: A response to Burke et al.'s 'planet politics.' *Millennium*, 46(2), 190–208.
- Christensen, M.-B., Hallum, C., Maitland, A., & Parrinello, Q. (2023). *Survival of the richest. How we must tax the super-rich now to fight inequality*. Oxfam International.
<https://oxfamlibrary.openrepository.com/bitstream/handle/10546/621477/bp-survival-of-the-richest-160123-en.pdf>
- Court, V., & McIsaac, F. (2020). A Representation of the World Population Dynamics for Integrated Assessment Models. *Environmental Modeling & Assessment*, 25, 611–632.
- D'Alisa, G., & Demaria, F. (2024). Accumulation by contamination: Worldwide cost-shifting strategies of capital in waste management. *World Development*, 184, 106725.
- Dasgupta, S., van Maanen, N., Gosling, S. N., Piontek, F., Otto, C., & Schleussner, C.-F. (2021). Effects of climate change on combined labour productivity and supply: An empirical, multi-model study. *The Lancet Planetary Health*, 5(7), e455–e465.
- Dorninger, C., Hornborg, A., Abson, D. J., Von Wehrden, H., Schaffartzik, A., Giljum, S., Engler, J.-O., Feller, R. L., Hubacek, K., & Wieland, H. (2021). Global patterns of ecologically unequal

- exchange: Implications for sustainability in the 21st century. *Ecological Economics*, 179, 106824. <https://doi.org/10.1016/j.ecolecon.2020.106824>
- Espinoza, V. S., Fontalvo, J., Martí-Herrero, J., Miguel, L. J., & Mediavilla, M. (2022). Analysis of energy future pathways for Ecuador facing the prospects of oil availability using a system dynamics model. Is degrowth inevitable? *Energy*, 259, 124963.
- García-Olivares, A., & Ballabriga, J. (2012). *The Peak of Energy and Minerals and the Economic Future*. 1–30.
- Georgescu-Roegen, N. (1986). The entropy law and the economic process in retrospect. *Eastern Economic Journal*, 12(1), 3–25.
- Hallegatte, S., Bangalore, M., Bonzanigo, L., Fay, M., Kane, T., Narloch, U., Rozenberg, J., Treguer, D., & Vogt-Schilb, A. (2016). *Shock waves: Managing the impacts of climate change on poverty*. World Bank Publications.
- Hardt, L., & O'Neill, D. W. (2017). Ecological macroeconomic models: Assessing current developments. *Ecological Economics*, 134, 198–211.
- Hartley, T., Van Den Bergh, J., & Kallis, G. (2020). Policies for equality under low or no growth: A model inspired by Piketty. *Review of Political Economy*, 32(2), 243–258.
- Herrington, G. (2021). Update to limits to growth: Comparing the World3 model with empirical data. *Journal of Industrial Ecology*, 25(3), 614–626.
- Hickel, J. (2020). Quantifying national responsibility for climate breakdown: An equality-based attribution approach for carbon dioxide emissions in excess of the planetary boundary. *The Lancet Planetary Health*, 4(9), e399–e404.
- Hickel, J., Hanbury Lemos, M., & Barbour, F. (2024). Unequal exchange of labour in the world economy. *Nature Communications*, 15(1), 6298. <https://doi.org/10.1038/s41467-024-49687-y>
- Hornborg, A., & Martinez-Alier, J. (2016). Ecologically unequal exchange and ecological debt. *Journal of Political Ecology*, 23(1), 328–333.
- Hunt, D. V., Lombardi, D. R., Atkinson, S., Barber, A. R., Barnes, M., Boyko, C. T., Brown, J., Bryson, J., Butler, D., & Caputo, S. (2012). Scenario archetypes: Converging rather than diverging themes. *Sustainability*, 4(4), 740–772.
- IPCC. (2021). *Climate Change 2021: The Physical Science Basis. Contribution of Working Group I to the Sixth Assessment Report of the Intergovernmental Panel on Climate Change*. Cambridge University Press. Cambridge University Press, Cambridge, UK and New York, NY, USA.
- IPCC. (2022). *Climate Change 2022: Impacts, Adaptation and Vulnerability. Contribution of Working Group II to the Sixth Assessment Report of the Intergovernmental Panel on Climate Change*. Cambridge University Press. Cambridge University Press, Cambridge, UK and New York, NY, USA.
- Jackson, T., & Victor, P. (2018). Confronting inequality in a post-growth world. *Basic Income, Factor Substitution and the Future of Work*, 11.
- Jackson, T., & Victor, P. A. (2016). Does slow growth lead to rising inequality? Some theoretical reflections and numerical simulations. *Ecological Economics*, 121, 206–219.
- Kallis, G. (2019). Capitalism, socialism, degrowth: A rejoinder. *Capitalism Nature Socialism*, 30(2), 267–273.
- Keys, P. W., Badia, L., & Warrier, R. (2024). The Future in Anthropocene Science. *Earth's Future*, 12(1), e2023EF003820.
- Koch, M. (2015). Climate change, capitalism and degrowth trajectories to a global steady-state economy. *International Critical Thought*, 5(4), 439–452.
- Kümmel, R., & Lindenberger, D. (2020). Energy, entropy, constraints, and creativity in economic growth and crises. *Entropy*, 22(10), 1156.

- Lahoti, R., Jayadev, A., & Reddy, S. (2016). The global consumption and income project (GCIP): An overview. *Journal of Globalization and Development*, 7(1), 61–108.
- Lauer, A., Capellán-Pérez, I., & Wergles, N. (2025). A comparative review of de-and post-growth modeling studies. *Ecological Economics*, 227, 108383.
- Lauer, A., de Castro, C., & Carpintero, Ó. (2024). Between continuous presents and disruptive futures: Identifying the ideological backbones of Global Environmental Scenarios. *Futures*, 103460.
- Lauer, A., & Llases, L. (2025a). Business as usual on the highway to hell? Limits to growth and future world orders. *Under Review*.
- Lauer, A., & Llases, L. (2025b). *MORDRED: Model Of Resource Distribution and Resilient Economic Development. Model Documentation*. GitHub. <https://github.com/Pendracus/MORDRED>
- Loy, L. S., & Spence, A. (2020). Reducing, and bridging, the psychological distance of climate change. *Journal of Environmental Psychology*, 67, 101388.
- Martínez-Alier, J. (2012). Social metabolism, environmental cost-shifting and valuation languages. *Towards an Integrated Paradigm in Heterodox Economics: Alternative Approaches to the Current Eco-Social Crises*, 94–110.
- Meadows, D. H., Meadows, D. L., & Randers, J. (1992). *Beyond the limits: Global collapse or a sustainable future*. Earthscan Publications Ltd.
- Meadows, D. H., Meadows, D., Randers, J., & Behrens, W. W. (1972). *The limits to growth. A report for the Club of Rome's Project on the Predicament of Mankind*. Universe Books.
- Meadows, D. H., Randers, J., & Meadows, D. (2004). *The limits to growth: The 30-year update*. Chelsea Green Publishing Company.
- Millward-Hopkins, J., Steinberger, J. K., Rao, N. D., & Oswald, Y. (2020). Providing decent living with minimum energy: A global scenario. *Global Environmental Change*, 65, 102168.
- Moore, J. (2017). The Capitalocene, Part I: on the nature and origins of our ecological crisis. *The Journal of Peasant Studies*, 44(3), 594–630.
- Moore, J. (2018). The Capitalocene Part II: accumulation by appropriation and the centrality of unpaid work/energy. *The Journal of Peasant Studies*, 45(2), 237–279.
- Mora, C., Dousset, B., Caldwell, I. R., Powell, F. E., Geronimo, R. C., Bielecki, C. R., Counsell, C. W., Dietrich, B. S., Johnston, E. T., & Louis, L. V. (2017). Global risk of deadly heat. *Nature Climate Change*, 7(7), 501–506.
- Nieto, J., Carpintero, Ó., Miguel, L. J., & de Blas, I. (2020). Macroeconomic modelling under energy constraints: Global low carbon transition scenarios. *Energy Policy*, 137, 111090.
- Nilsen, A. G. (2016). Power, resistance and development in the global South: Notes towards a critical research agenda. *International Journal of Politics, Culture, and Society*, 29, 269–287.
- Nilsen, A. G. (2025). *Emerging Powers and the Political Economy of the Southern Interregnum*. 1–24.
- Piketty, T. (2017). *Capital in the twenty-first century* (A. Goldhammer, Trans.). Harvard University Press.
- Richardson, K., Steffen, W., Lucht, W., Bendtsen, J., Cornell, S. E., Donges, J. F., Drücke, M., Fetzer, I., Bala, G., & von Bloh, W. (2023). Earth beyond six of nine planetary boundaries. *Science Advances*, 9(37), eadh2458.
- Rockström, J., Steffen, W., Noone, K., Persson, Å., Chapin III, F. S., Lambin, E., Lenton, T. M., Scheffer, M., Folke, C., & Schellnhuber, H. J. (2009). Planetary boundaries: Exploring the safe operating space for humanity. *Ecology and Society*, 14(2).

- Schmelzer, M. (2017). The growth paradigm: History, hegemony, and the contested making of economic growthmanship. In *Routledge Handbook of the History of Sustainability* (pp. 164–186). Routledge.
- Spence, A., Poortinga, W., & Pidgeon, N. (2012). The psychological distance of climate change. *Risk Analysis: An International Journal*, 32(6), 957–972.
- Stadler, K., Wood, R., Bulavskaya, T., Södersten, C., Simas, M., Schmidt, S., Usobiaga, A., Acosta-Fernández, J., Kuenen, J., Bruckner, M., Giljum, S., Lutter, S., Merciai, S., Schmidt, J. H., Theurl, M. C., Plutzar, C., Kastner, T., Eisenmenger, N., Erb, K., ... Tukker, A. (2018). EXIOBASE 3: Developing a Time Series of Detailed Environmentally Extended Multi-Regional Input-Output Tables. *Journal of Industrial Ecology*, 22(3), 502–515.
<https://doi.org/10.1111/jiec.12715>
- Steffen, W., Broadgate, W., Deutsch, L., Gaffney, O., & Ludwig, C. (2015). The trajectory of the Anthropocene: The great acceleration. *The Anthropocene Review*, 2(1), 81–98.
- Thomas, D. S. G., & Twyman, C. (2005). Equity and justice in climate change adaptation amongst natural-resource-dependent societies. *Global Environmental Change*, 15(2), 115–124.
<https://doi.org/10.1016/j.gloenvcha.2004.10.001>
- Tsigaris, P., & Wood, J. (2019). The potential impacts of climate change on capital in the 21st century. *Ecological Economics*, 162, 74–86.
- Turner, G. (2014). Is global collapse imminent? An updated comparison of the Limits to Growth with historical data. *MSSI Research Paper*, 4, 21.
- UN DESA. (2019). *World Population Prospects 2019, Online Edition. Rev. 1. File POP/7-1: Total population (both sexes combined) by five-year age group, region, subregion and country, 1950-2100 (thousands)*.
- van Bavel, B., & Scheffer, M. (2021). Historical effects of shocks on inequality: The great leveler revisited. *Humanities and Social Sciences Communications*, 8(1).
- Van Lange, P. A., & Huckelba, A. L. (2021). Psychological distance: How to make climate change less abstract and closer to the self. *Current Opinion in Psychology*, 42, 49–53.
- World Bank. (2025). *World Bank Analytical Classifications (presented in World Development Indicators)*. <https://datacatalogfiles.worldbank.org/ddh-published/0037712/DR0090754/OGHIST.xlsx>

Supplementary Material

S1.'Hyperimperialist Exploitation' scenario

Complete storyline:

"[...] [T]he world system continues its trajectory, leading to ever increasing global economic output and environmental degradation, but maintaining intra- and international economic inequality. However, as biophysical limits to growth become ever more evident, the system is forced to depart from its trajectory of global accumulation based on dynamic competition. In Hyperimperialist Exploitation [...] the capitalist elites of the center, with the collaboration of capitalist and political elites of the semiperiphery and periphery, maintain their consumption and power despite the world economy's stagnation and subsequent degrowth, while workers of the center struggle to keep their former lifestyles, and workers of the semiperiphery and periphery increasingly fight for survival as they see their wages stagnate and decline." (Lauer & Llases, 2025)

S2. Sectorial disaggregation in MORDRED

Sector number	Sector description
1	Agriculture, food, beverages
2	Non-energy use of biomass
3	Fossil fuels used for energy
4	Mining
5	Industry not elsewhere classified
6	Recycling industry
7	Services not elsewhere classified
8	Non-energy use of fossil fuels
9	Chemical industry
10	Biomass used for energy
11	Manufacturing
12	Fossil fuel-based electricity
13	Nuclear electricity
14	Hydroelectricity
15	Wind based electricity
16	Biomass and waste based electricity
17	Solar PV electricity
18	Solar thermal electricity
19	Tide, wave and ocean based electricity
20	Geothermal electricity
21	Transport
22	Education
23	Health
24	Waste industry
25	'Waste ,recycling' (biogasification & composting) industry

Table S1: Overview of sectoral disaggregation in MORDRED. See Model documentation of MORDRED.

S3. Scenario parametrization

S3.1. Evolution of the A matrix

The target A matrix that is reached by the initial A matrix in 2100 was derived through the following steps.

1. Monetary to energy (E) inputs

Starting from the A matrix for the world in 2019, which is disaggregated into 25 sectors, we converted the numbers contained in the rows of the A matrix representing energy sectors (3,10,12,13,14,15,16,17,18,19,20) (see S2 this Supplementary Material) from economic input per unit of economic output into energy input per unit of economic output. To this end, the original values in the rows corresponding to the energy sectors were multiplied by the energy intensity of the respective sectors.

$$\begin{aligned} a_{3,1\dots 25_E} &= [a_{3,1} * i_3] \ [a_{3,2} * i_3] \ \dots \ [a_{3,25} * i_3] \\ a_{10,1\dots 25_E} &= [a_{10,1} * i_{10}] \ [a_{10,2} * i_{10}] \ \dots \ [a_{10,25} * i_{10}] \\ a_{12,1\dots 25_E} &= [a_{12,1} * i_{12}] \ [a_{12,2} * i_{12}] \ \dots \ [a_{12,25} * i_{12}] \\ a_{13,1\dots 25_E} &= [a_{13,1} * i_{13}] \ [a_{13,2} * i_{13}] \ \dots \ [a_{13,25} * i_{13}] \\ &\vdots \\ a_{20,1\dots 25_E} &= [a_{20,1} * i_{20}] \ [a_{20,2} * i_{20}] \ \dots \ [a_{20,25} * i_{20}] \end{aligned}$$

2. Introduction of the process (P) efficiency coefficient.

To reflect energy efficiency improvements through the improvements of economic processes throughout the economy, all the biophysical inputs in the A matrix are multiplied by the factor $\alpha_{processes}$ which in the scenario parametrization takes the value 0.95, i.e. reflects a 5% increase in all economic processes requiring energy.

$$\begin{aligned} a_{3,1\dots 25_{E,P}} &= [a_{3,1_E} * \alpha_{processes}] \ [a_{3,2_E} * \alpha_{processes}] \ \dots \ [a_{3,25_E} * \alpha_{processes}] \\ a_{10,1\dots 25_{E,P}} &= [a_{10,1_E} * \alpha_{processes}] \ [a_{10,2_E} * \alpha_{processes}] \ \dots \ [a_{10,25_E} * \alpha_{processes}] \\ a_{12,1\dots 25_{E,P}} &= [a_{12,1_E} * \alpha_{processes}] \ [a_{12,2_E} * \alpha_{processes}] \ \dots \ [a_{12,25_E} * \alpha_{processes}] \\ a_{13,1\dots 25_{E,P}} &= [a_{13,1_E} * \alpha_{processes}] \ [a_{13,2_E} * \alpha_{processes}] \ \dots \ [a_{13,25_E} * \alpha_{processes}] \\ &\vdots \\ a_{20,1\dots 25_{E,P}} &= [a_{20,1_E} * \alpha_{processes}] \ [a_{20,2_E} * \alpha_{processes}] \ \dots \ [a_{20,25_E} * \alpha_{processes}] \end{aligned}$$

3. Replacement (R) of inefficient renewable energy technologies

In the target A matrix the electricity coming from biomass, solar thermal, tide and geothermal is assumed to be substituted by hydroelectricity, solar PV and wind based electricity, given the inferior performance of the former compared to the latter (e.g. De Castro, 2023; De Castro et al.,

2011). Thus, the values in the respective rows are set to zero. The inputs from wave/tidal energy are added to hydroelectricity; the inputs from geothermal electricity are added to wind electricity; the values from solar thermal and bioelectricity are added to electricity from solar PV.

$$\begin{aligned}
a_{14,1\dots25_{E,P,R}} &= [a_{14,1_{E,P}} + a_{19,1_{E,P}}] \quad [a_{14,2_{E,P}} + a_{19,2_{E,P}}] \quad \dots \quad [a_{14,25_{E,P}} + a_{19,25_{E,P}}] \\
a_{15,1\dots25_{E,P,R}} &= [a_{15,1_{E,P}} + a_{20,1_{E,P}}] \quad [a_{15,2_{E,P}} + a_{20,2_{E,P}}] \quad \dots \quad [a_{15,25_{E,P}} + a_{20,25_{E,P}}] \\
a_{16,1\dots25_{E,P,R}} &= [0] \quad [0] \quad \dots \quad [0] \\
a_{17,1\dots25_{E,P,R}} &= [a_{17,1_{E,P}} + a_{16,1_{E,P}} + a_{18,1_{E,P}}] \quad [a_{17,2_{E,P}} + a_{16,2_{E,P}} + a_{18,2_{E,P}}] \quad \dots \quad [a_{17,25_{E,P}} + a_{16,25_{E,P}} + a_{18,25_{E,P}}] \\
a_{18,1\dots25_{E,P,R}} &= [0] \quad [0] \quad \dots \quad [0] \\
a_{19,1\dots25_{E,P,R}} &= [0] \quad [0] \quad \dots \quad [0] \\
a_{20,1\dots25_{E,P,R}} &= [0] \quad [0] \quad \dots \quad [0]
\end{aligned}$$

4. Greening (G): Replacement of fossil and nuclear through renewable energy

The demand for fossil electricity in the target A matrix is assumed to decline by the factor α_{ff} (=0.9 in the scenario parametrization) while the demand for nuclear electricity is assumed to decline by the factor α_{nuc} (=0.4). At the same time, the demand for hydro, wind and solar PV electricity is assumed to grow by the same factor, i.e. fossil and nuclear electricity are substituted to equal parts by hydro, wind and solar PV.

Thus, the new input coefficients are:

$$\begin{aligned}
a_{12,1\dots25_{E,P,R,G}} &= [a_{12,1_{E,P,R}} * (1 - \alpha_{ff})] \quad [a_{12,2_{E,P,R}} * (1 - \alpha_{ff})] \quad \dots \quad [a_{12,25_{E,P,R}} * (1 - \alpha_{ff})] \\
a_{13,1\dots25_{E,P,R,G}} &= [a_{13,1_{E,P,R}} * (1 - \alpha_{nuc})] \quad [a_{13,2_{E,P,R}} * (1 - \alpha_{nuc})] \quad \dots \quad [a_{13,25_{E,P,R}} * (1 - \alpha_{nuc})] \\
a_{14,1\dots25_{E,P,R,G}} &= \left[a_{14,1_{E,P,R}} + \frac{a_{12,1_{E,P,R}} * \alpha_{ff} + a_{13,1_{E,P,R}} * \alpha_{nuc}}{3} \right] \dots \left[a_{14,25_{E,P,R}} + \frac{a_{12,25_{E,P,R}} * \alpha_{ff} + a_{13,25_{E,P,R}} * \alpha_{nuc}}{3} \right] \\
a_{15,1\dots25_{E,P,R,G}} &= \left[a_{15,1_{E,P,R}} + \frac{a_{12,1_{E,P,R}} * \alpha_{ff} + a_{13,1_{E,P,R}} * \alpha_{nuc}}{3} \right] \dots \left[a_{15,25_{E,P,R}} + \frac{a_{12,25_{E,P,R}} * \alpha_{ff} + a_{13,25_{E,P,R}} * \alpha_{nuc}}{3} \right] \\
a_{17,1\dots25_{E,P,R,G}} &= \left[a_{17,1_{E,P,R}} + \frac{a_{12,1_{E,P,R}} * \alpha_{ff} + a_{13,1_{E,P,R}} * \alpha_{nuc}}{3} \right] \dots \left[a_{17,25_{E,P,R}} + \frac{a_{12,25_{E,P,R}} * \alpha_{ff} + a_{13,25_{E,P,R}} * \alpha_{nuc}}{3} \right]
\end{aligned}$$

5. Electrification (El)

We identified the sectors that (a) do not already have high rates of electric input compared to energy inputs from other energy types, and (b) have some technical potential to be electrified. Those sectors have the numbers 3, 5, 7, 8, 9, 10, 11, 12, 14, 15, 17, 21, 25.

α_{el} denotes the share of energy inputs that is assumed to be replaced by electric energy in 2100 and is set to 0.2. It is assumed that the electricity is covered by an increase in the electricity produced by wind and solar PV (both are assumed to cover half of the additional electricity). Furthermore, it is assumed that in the process of electrification the process efficiency is also improved by a factor ($\alpha_{el,p}$) which in the scenario quantification is optimistically set to 0.5. Thus,

the increase in electricity from wind (sector 15) and solar PV (sector 17) is smaller than the reduction of non-electric energy, i.e. fossil energy (sector 3) and bioenergy (sector 10).

For the columns of the A matrix corresponding to the sectors with electrification potential, the rows corresponding to non-electric energy input and electric input were modified accordingly:

$$a_{3,1\dots 25_{E,P,R,G,El}} = \dots [a_{3,3_{E,P,R,G}} * (1 - \alpha_{el})] [a_{3,5_{E,P,R,G}} * (1 - \alpha_{el})] \dots [a_{3,25_{E,P,R,G}} * (1 - \alpha_{el})]$$

$$a_{10,1\dots 25_{E,P,R,G,El}} = \dots [a_{10,3_{E,P,R,G}} * (1 - \alpha_{el})] [a_{10,5_{E,P,R,G}} * (1 - \alpha_{el})] \dots [a_{10,25_{E,P,R,G}} * (1 - \alpha_{el})]$$

$$a_{15,1\dots 25_{E,P,R,G,El}} = \dots [a_{15,3_{E,P,R,G}} + (a_{3,3_{E,P,R,G}} + a_{10,3_{E,P,R,G}}) * \alpha_{el} * \alpha_{el_p}] \dots [a_{15,25_{E,P,R,G}} + (a_{3,25_{E,P,R,G}} + a_{10,25_{E,P,R,G}}) * \alpha_{el} * \alpha_{el_p}]$$

$$a_{17,1\dots 25_{E,P,R,G,El}} = \dots [a_{17,3_{E,P,R,G}} + (a_{3,3_{E,P,R,G}} + a_{10,3_{E,P,R,G}}) * \alpha_{el} * \alpha_{el_p}] \dots [a_{17,25_{E,P,R,G}} + (a_{3,25_{E,P,R,G}} + a_{10,25_{E,P,R,G}}) * \alpha_{el} * \alpha_{el_p}]$$

6. Target A Matrix in monetary values

Finally, we convert the energy inputs back to monetary inputs by dividing the values by the energy intensities.

$$\begin{aligned} a_{3,1\dots 25_{final}} &= \left[a_{3,1_{E,P,R,G,El}} * \frac{1}{i_3} \right] \left[a_{3,2_{E,P,R,G,El}} * \frac{1}{i_3} \right] \dots \left[a_{3,25_{E,P,R,G,El}} * \frac{1}{i_3} \right] \\ a_{10,1\dots 25_{final}} &= \left[a_{10,1_{E,P,R,G,El}} * \frac{1}{i_{10}} \right] \left[a_{10,2_{E,P,R,G,El}} * \frac{1}{i_{10}} \right] \dots \left[a_{10,25_{E,P,R,G,El}} * \frac{1}{i_{10}} \right] \\ &\vdots \\ a_{20,1\dots 25_{final}} &= \left[a_{20,1_{E,P,R,G,El}} * \frac{1}{i_{20}} \right] \left[a_{20,2_{E,P,R,G,El}} * \frac{1}{i_{20}} \right] \dots \left[a_{20,25_{E,P,R,G,El}} * \frac{1}{i_{20}} \right] \end{aligned}$$

S3.2. Evolution of final demand

The consumption shares that vary according to consumption per capita, the sectoral shares in government demand and the sectoral shares in Gross Fixed Capital Formation (GFCF) follow the changes made in the A matrix regarding the replacement (R) of inefficient electricity technologies, the greening (G) of the electricity mix and the electrification of energy demand (El). Since final demand is not engaged in production activity, the process efficiency factor was not applied.

Since the consumption vector stays constant above a threshold value of 24,673 € annual per capita consumption, the share of food expenditures could be overestimated in scenarios in which a significant proportion of the households have a consumption greater than this value. Thus, we correct the consumption vector for richest households by multiplying the share in household expenditures for the food sector by 0.5 and by adding this amount to the expenditure share for services.

S3.3. Evolution of labor, capital and land intensity

Labor productivity of the world in 2100 approximates labor productivity of the center in 2019 in all sectors as in the absence of biophysical restrictions to economic growth economic development in the Global South would likely increase the labor productivity in these regions and rise average global productivities. As sectoral labor productivity levels evolve exogenously in the scenario simulation, labor productivity could be overestimated starting from the second half of the simulation, given that sectoral productivities continue to improve although economic development in the Global South reverts its historical direction and economic development in the Global North stagnates.

Capital intensity is given as capital-stock-to-output ratio and capital productivity as output-to-stock ratio. It is assumed that, ceteris paribus, in 2100 capital productivity increases by 20% which - like the labor productivity assumption - is optimistic and is a factor contributing to an overestimation of the material and energy efficiency performance of the economy.

The target capital intensity in 2100 is given as:

$$\text{Capital intensity}_{2100_s} = \frac{1}{\frac{\text{output}_s}{\text{capital stock}_s} * 1.2} = \frac{5}{6} * \frac{\text{capital stock}_s}{\text{output}_s}$$

The last optimistic assumption concerns future land productivities. While the intensity of land demand for infrastructure depends on household demands and is assumed to remain constant, the land productivity of all other land types, including the land productivity of renewable energies and of the forestry sector, is assumed to grow by 2.25% annually, a very favorable development that is significantly higher than what would be achieved if the world merely approached the higher land productivities of the Center in 2019. Furthermore, this development is assumed to continue even in the post-BAU phase. Adopting less optimistic assumptions would very likely lead to a stagnation of global output much earlier in time.

Other scenario variables not explained in this Supplementary Material either remain constant during the simulations or take standard values chosen for the basic calibration of MORDRED given that they are not significant for the research questions addressed in this paper, and, thus, are excluded from the scope of the analysis.

S4. Consumption ratios

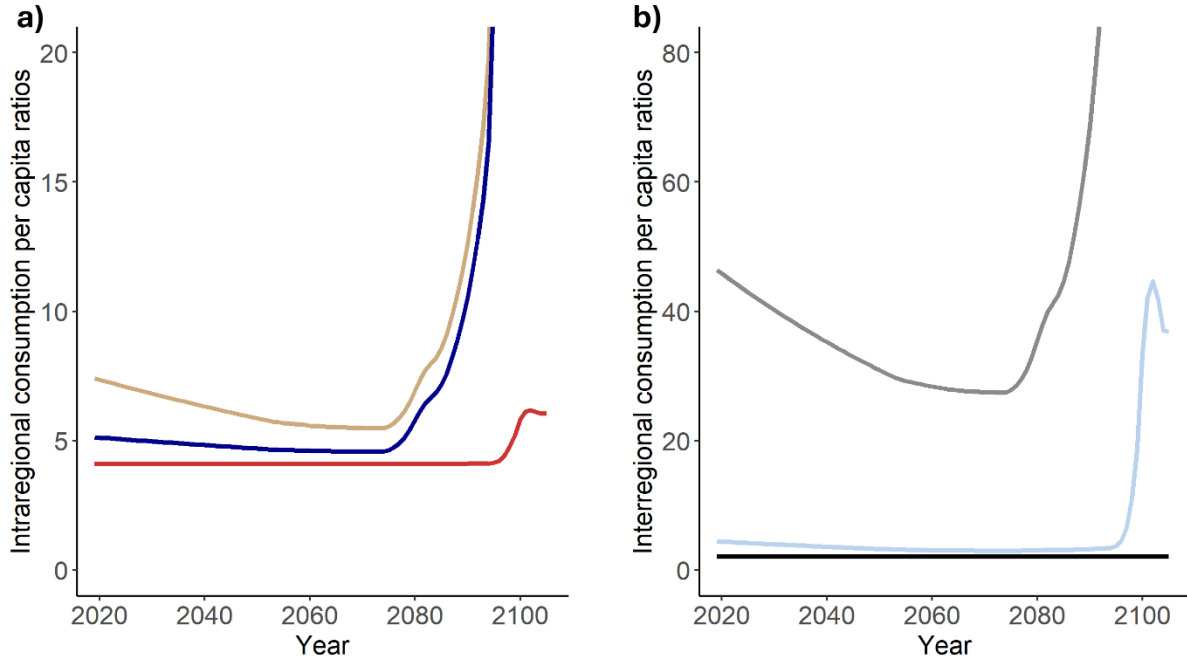


Fig. S 1: a) Evolution of intraregional consumption per capita ratios for the three world regions (consumption per capita of the richest 20% divided by the consumption per capita of the poorest 30% in a region). Red line: center, yellow line: semiperiphery, blue line: periphery. b) Evolution of interregional consumption per capita ratios. Grey line: the richest 20% of the center compared to poorest 30% of the periphery; blue line: the richest 20% of the center compared to the richest 20% of the semiperiphery; black line: the richest 20% of the semiperiphery compared to the richest 20% of the periphery).

S5. Alternative scenario runs

We have specified four alternative scenario runs — scenario variations (SV) 1 to 4 — to test the robustness of the observed dynamics in the base run presented in the main text and to gain additional insights about potential model dynamics under different scenario assumptions.

In SV1, we assume a higher level of greenhouse gas emission reductions. Therefore, the greenhouse gas intensity of non-combustion related emissions is exogenously reduced by 20% between 2019 and 2100 while in the Baseline the intensity remains constant.

In SV2, we make more pessimistic assumptions about the sensitivity of the climate system to anthropogenic pressure. Thus, we activate climate feedbacks within the climate system that lead to an increase in natural greenhouse gas emissions as global temperatures rise.

In SV3, we make more pessimistic assumptions about future exogenous growth in sectoral labor productivities, which only reach 80% of the center's 2019-productivity-levels by 2100.

In SV4, we modify the allocation priorities in the model to simulate a lower degree of divergence in consumption when scarcity issues arise.

We find that the dynamics observed in the base run presented in the main article are broadly similar to those produced in the scenario variations, although they differ in timing and magnitude. In SV2, collapse dynamics occur approximately one decade earlier than in the

baseline while in the remaining scenario variations, they appear about one decade later than in the baseline (Fig. S 2, Fig. S 3).

The higher level of climate mitigation in SV1 leads to higher maximum output levels and maximum per capita consumption levels in all social classes, a lower increase in temperatures and a stabilization of the population of the periphery at a higher level than in the other scenarios.

Conversely, the higher climate sensitivity in SV2 results in an earlier stagnation and decline of world output and consumption at a lower level, and – due to the spread of extreme poverty – an earlier decline in the population of the semiperiphery and the periphery.

The lower labor productivity in SV3 is linked to lower maximum levels of output and consumption, a lower increase in global average temperature, and a delay in the break-down of the world economy compared to the baseline simulation.

Last, the lower degree of divergence in SV4 prolongs the time period during which the scenario is stable and leads to somewhat smoother declines in world output and the consumption of the poorer classes. However, when the system finally collapses, the consumption level of the center falls to a lower level than in the other scenario simulations. In fact, the loss in consumption of the poorest class in the center is so strong that critical levels for survival are reached, and, thus, the population of the center collapses as well. Hence, less divergence delays the breakdown of the system but a longer period of overshoot and correspondingly higher levels of global warming ultimately results in higher consumption losses for the richest classes, which in SV proves catastrophic for the center.

Thus, the key dynamics discussed in the article can also be observed in alternative ‘divergence and polarization’ scenarios that differ in important scenario variables while maintaining the underlying logic of the scenario storyline, i.e. a strong cost-shifting from richer to poorer classes and an absence of policies aimed at a reduction of the most extreme forms of poverty. It is the former that creates critical risks to system instability, and the latter that triggers the demographic collapse.

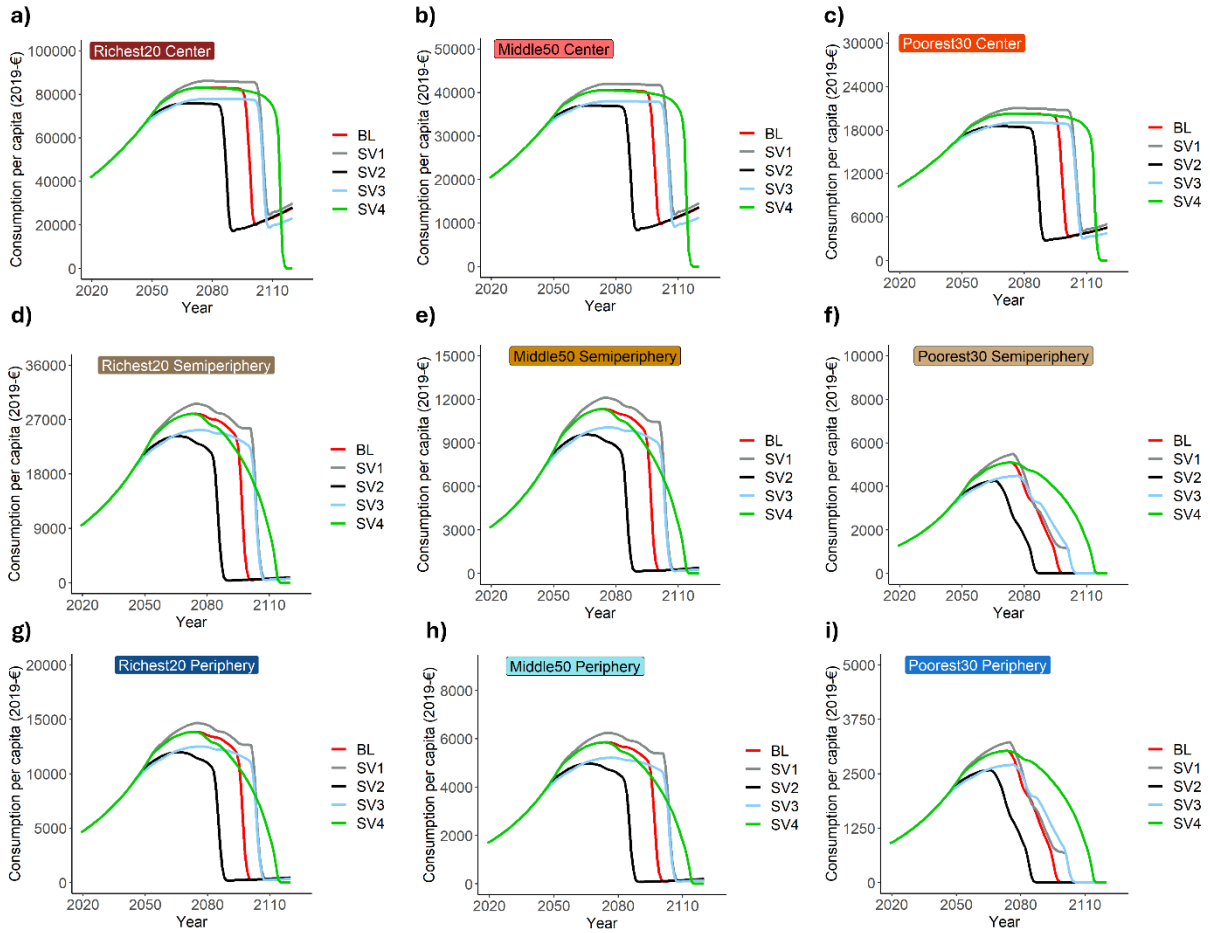


Fig. S 2: Evolution of consumption per capita of all social classes sustained by the world economy in the four scenario variations (SV) and the baseline (red line).

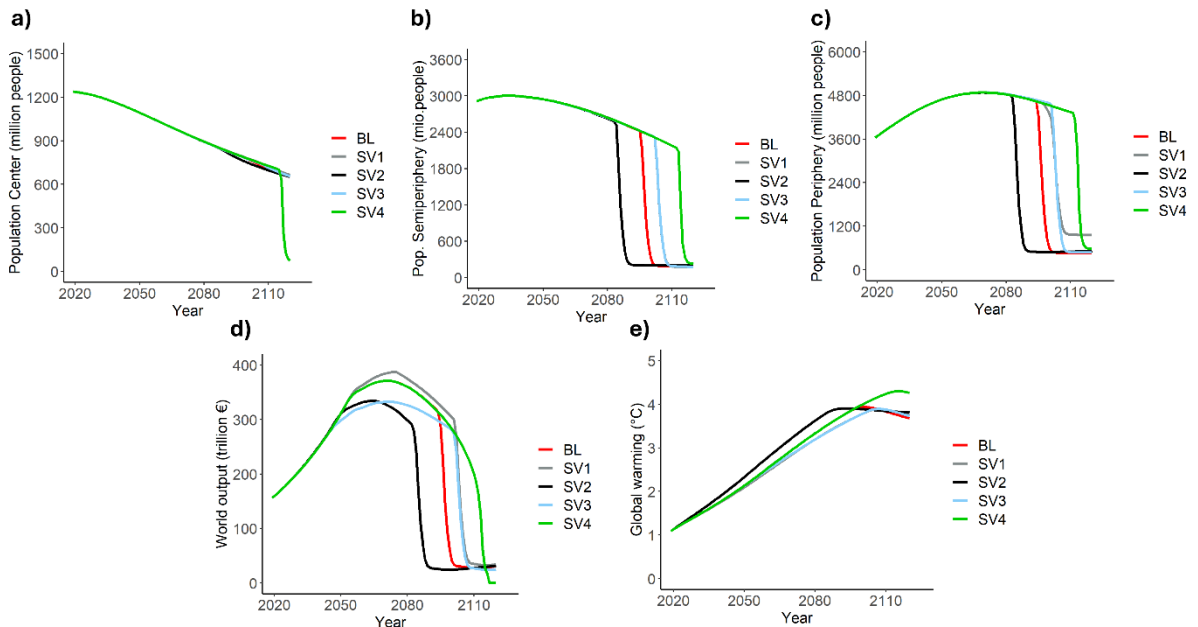


Fig. S 3: Evolution of a) the population in the center b) the population in the semiperiphery, c) the population in the periphery, d) global annual output, e) global warming with respect to 1850 in the four scenario variations and the baseline (red line).

Toward global environmental scenarios for (and by) the ‘bottom billion’?

Abstract

The current Global Environmental Scenario landscape lacks transformative socio-ecological world futures that provide pathways of liberation for the ‘bottom billion’. Drawing on decolonial thought, we develop a set of proposals for future scenario development. These proposals include participatory processes with subaltern population groups to facilitate scenario co-creation based on different ways of knowing the world; replacing fixed and ahistoric subjectivities driving global environmental and economic change with the agency of different social groups who might collectively be able to challenge the status quo of the world system; and creating visions and pathways that consistently address the colonial matrix of power by integrating decolonial environmental justice into scenario storylines. The outlined proposals pose significant challenges to conventional participatory and quantitative methods in the field of scenario research but also enable global environmental scenarios to better fulfill their potential of shaping social imaginaries towards emancipatory futures for all human beings.

Keywords

Socioecological justice; Epistemic justice; resistance; Degrowth; More-than-human; Transformation

1. Introduction

Global environmental scenarios (GES), defined as plausible stories of how the socio-ecological future of the world might unfold, are ‘boundary objects’ at the intersection between science, politics and society (Garb et al., 2008). On the one hand, they might inform sustainability related research and the exploration of different sets of environmental, social and economic policies, which might subsequently influence political decision-making processes. On the other hand, they can also shape the public opinion about the future by emphasizing certain development trends while excluding others. In any case, although scenarios constitute imaginaries of the *future*, they always act as vehicles for social change in the *present*, which are not neutral but inevitably incorporate certain value judgements and biases (Beck & Mahony, 2018; Gall et al., 2022; Metzger et al., 2010; Van Vuuren et al., 2012). Thus, the development process of scenarios as well as their content have a political character with potential distributional consequences in the real world already in the present. This is especially true for global environmental scenarios as they aim at influencing policy-making and societal imaginaries throughout the world. Furthermore, although GES explicitly focus on environmental issues such as climate change, energy transitions, biodiversity, food, water and/or land use, given that human systems develop within and interact with the living Earth/‘Gaia’ (Lovelock & Margulis, 1974) they inevitably include the development of global economic, political and cultural systems.

Given the deepening socio-ecological crises of the world system, GES related research is crucial to highlight near- and long-term future risks stemming from unsustainable economic processes at the global scale, and has the potential to act as catalyzing force for desirable socio-ecological futures by imagining and exploring decisive and bold structural and policy shifts at different levels. However, current GES are characterized by a strong continuity bias and the reproduction of dominant economic, political and cultural power structures (Lauer et al., 2024; Raskin & Swart, 2020). This points to a tendency of GES to preserve rather than to challenge the structurally unequal distribution of power across states, classes, genders and ethnicities, together with the associated ideologies that legitimate the status quo of the world system. Importantly, the reproduction of current structures of inequalities in scenarios about future worlds is implicit and characterized by the lack of change away from the status quo rather than by an explicit affirmation of the latter (Lauer et al., 2024). This finding points to the positionality of the knowledge of GES developers who might consider ‘neutral’, ‘objective’ or ‘normal’ processes, structures and realities that people in different positions of the social hierarchy experience as alienating, oppressive or unjust. Consequently, we hold that new approaches are needed to realize the potential of GES research. These approaches would draw from alternative currents still not fully acknowledged by the academic mainstream such as decolonial or degrowth thinking and would enter into a constructive and critical dialogue with the current literature on Global Change, Earth system sciences, Environmental and Ecological Economics, Integrated Assessment Modeling and sustainability policy research.

This paper aims at contributing to these new approaches by pointing out some characteristics shared by many current GES, which render subaltern population groups, especially of the Global South, invisible, and lead to an excessively narrow future space, as well as by developing a set of proposals for GES development based on decolonial thought. We conclude by discussing the methodological implications of the proposals for participatory scenario development and quantitative model simulations.

2. A narrow space of world futures

GES aim at describing ecological, economic and social developments of the whole world, which necessarily requires a certain level of abstraction. However, in practice many GES abstract from the realities of life of those at the margins of the capitalist transformation of nature and at the bottom of the global world order, which results in an excessive homogenization of the world and in biased futures of the world.

First, many GES feature a similar type of development across the world which is based on consumerism and economic growth through the expansion of market economies. For example, the Shared Socio-Economic pathways (SSPs) contrast green (sustainable) with conventional (fossil-based) development but do not envision ways of life outside a growth-based society. Thus, Western lifestyles become commonplace throughout the world. In general, the focus of GES on the ‘sustainability’ problems of the global North, i.e. ‘greening’ consumption, overlooks the socio-ecological problems in the South, such as ecological distribution conflicts that the expanding extractivist global economy already creates today (Martinez-Alier, 2004, 2021). For example, the ‘Net Zero Emissions by 2050’ (NZE) Scenario of the International Energy Agency (IEA, 2022), features some moderate behavior changes, including more recycling, a reduction in business-related long-haul trips, speed limits and fuel-efficient driving. These measures direct the attention to the lives and consumption choices of better-off classes in the Global North while socio-ecological problems of systemic character and more relevant for the rest of the world population, such as the export of (toxic and hazardous) waste to Global South countries (D’Alisa & Demaria, 2024; Mujezinovic, 2020; Stoett, 2024), deteriorations of ecological and human health due to mining activities (Le Billon & Middeldorp, 2021; Scheidel et al., 2020; Sonter et al., 2020; Temper et al., 2020), workers’ exposure to toxic substances and heat stress in the solar industry (Bakhiyi et al., 2014; Samaniego-Rascón et al., 2019) or the inability to meet basic human needs (UN, 2023) are not mentioned. Moreover, suggestions of moderate behavior change do not radically question conventional Western economic development and ways of life. For instance, car sales in the NZE scenario in 2030 are around one quarter above 2021 levels in 2030. The Agrimonde-Terra food and land use scenarios developed by Mora et al. (2020) display more diversity, including homogenized futures based on urbanization, economic growth, transnational corporations controlling the food market, ultra-processed food and generalized meat-rich diets but also collapsing economies, shorter supply chains, the spread of agroecological practices and improved access to fresh food with higher nutritional quality. However, although the Agrimonde-Terra scenarios differentiate between world regions, no special attention is paid to unequal economic relationships between those regions and how they affect the development of food systems and land use change.

Development pathways of the majority of GES, especially those coupled to quantitative simulation models, are also characterized by an anthropocentric and instrumental understanding of the living Earth that is reduced to its capacity to act as source and sink of the human economy. This implies that non-human living beings on the planet have no future besides being useful for human production and consumption. The neglect of non-human life has been recently addressed by the biodiversity scenario development exercise of the Intergovernmental Science-Policy Platform on Biodiversity and Ecosystem Services (IPBES) that has led to GES exploring various ways of ‘human-nature’ interactions, attributing relational and intrinsic value to ‘nature’ (e.g. Durán et al., 2023; Pereira et al., 2023). However, these scenarios also tend to abstract from differences between center, semiperiphery and periphery regarding ways of life, languages of valuation and interactions with the natural environment. Attempts at

combining the IPBES based Nature Futures Framework (NFF) (Lundquist et al., 2021) with the SSPs show that GES featuring alternative ‘human-nature’ interactions do not have to constitute a barrier for scenario quantification (Alexander et al., 2023; Dou et al., 2023).

Second, many GES reproduce rather than question the power structures that constitute the world system. Consequently, addressing the sustainability conundrum often involves combining economic growth with technological solutions (Lauer et al., 2024), an approach emblematic of an eco-modernist paradigm. Importantly, although economic growth and technological progress, such as the efficient use of natural resources or the transition to alternative energy systems, alleviate environmental problems GES barely envision socio-ecological futures with full convergence between countries. In this way, economic inequality is naturalized as even in ‘sustainable’ futures access to energy and economic output remains unequal between world regions. The neglect of structural factors at the economic and political level also renders GES blind to ecological and social cost-shifting processes that might be triggered by ‘green’ technological solutions (Sovacool, 2021). For example, various 1.5°C GES that try to find technological pathways to meet climate goals envision the large-scale application of bioenergy carbon capture and storage but ignore the associated risks of land rush dynamics and dispossession in the Global South (Bluwstein & Cavanagh, 2023).

Last, GES often abstract from concrete social actors driving global economic and environmental change, and from conflicts of interests between these actors. Global institutions, governments and the private sector tend to act as the main drivers of change in the scenarios whereas people are reduced to their role as consumers and producers (e.g. IEA, 2022; O’Neill et al., 2017). Even when GES include a wider range of actors such as communities, cities, local authorities, academic institutions or NGOs, marginalized social groups are typically absent.

Apart from the content, the development process of GES itself is dominated by corporate and scientific experts from the Global North. For example, the different global energy scenarios contained in the World Energy Outlook 2022 were developed by the technical staff of the IEA and included a peer review process with significant corporate involvement: 18% of the entities involved in the process were multinational corporations, mainly from the energy and mining sector (BP, Shell, Repsol, Glencore, ExxonMobil, Chevron, Iberdrola...). The remaining entities involved were public institutions like the European Investment Bank or the World Bank, research institutions, universities, lobby groups for different energy technologies and to a lesser extent NGOs, think tanks, public companies or public-private partnerships (Lauer et al., 2025). The overwhelming majority of these entities belonged to countries of the Global North, notably the US, UK, Japan and France. While the scenario development process of the SSPs did not involve corporations, the participating scientists are affiliated with a narrow range of only 34 entities, most of them universities and research institutions from Global North countries such as the US, Germany, Austria, Japan and France (cf. O’Neill et al., 2012). These are only two paradigmatic examples for a general pattern in the GES literature.

Importantly, the points just outlined do not imply that GES research is fundamentally deficient. GES are constructed to serve very different purposes, which include the exploration of very specific questions in the technological or biophysical realm (e.g. Capellán-Pérez et al., 2015, 2019; Lerede et al., 2023), and even the development of a hypothetical future space merging fictional with factual elements (e.g. Merrie et al., 2018; Pereira et al., 2023). When researchers are only interested in how social aggregates drive technical variables an abstraction from complex interdependencies, economic disparities and power inequalities on a sub-global level might appear reasonable. Also, big governments, corporations and certain international

organizations *de facto* act as the main drivers of global economic-environmental developments, and thus, it is comprehensible that GES focus on these actors. At the same time, in the current GES literature there is a striking lack of scenarios with a focus on the poorer half of the world population, especially the 1.2 billion people affected by acute multidimensional poverty (UNDP & OPHI, 2022) that could be described as ‘bottom billion’. However, these populations are of central importance when it comes to global environmental and economic futures, as they are most heavily impacted by global environmental change (IPCC, 2022), often directly rely on the environment for livelihood reasons (Martinez-Alier, 2003) and bear the brunt of ecological cost-shifting and environmentally destructive rapid industrialization of countries within the world system. For them, the capitalist promise of mass consumption has yet to be fulfilled, which through conventional capitalist development would create massive pressure on the biosphere. GES, in which necessary changes in the world system occur that allow these populations to shape their own development pathways toward materially, culturally and ecologically satisfying conditions, have yet to be developed.

3. Decolonial thought and GES

We argue that GES could become more consistent, plausible and desirable for the poorer half of humanity and the ‘bottom billion’ by engaging with decolonial critiques of Western development and decolonial approaches to environmental justice that can help to question, unlearn and undo dominant myths and practices currently obfuscating the construction of ecologically and socially just visions of global futures. Thus, in the following, we use the three core concepts of decolonial theory – the coloniality of knowledge, being and power (Maldonado-Torres, 2007; Quijano, 2000; Restrepo, 2018) – to develop a structured set of proposals that future scenario exercises could consider.

3.1. Addressing the coloniality of knowledge

Decolonial and feminist approaches to epistemological questions have in common that they reject the idea of a ‘zero point of observation’ and instead emphasize that knowledge is embodied in and produced by people with different ‘race’ and gender. Consequently, decolonial theorists criticize the claim of Western epistemology to be neutral and universally valid (Mignolo, 2013). This critique is especially pertinent for the development of GES because many conditions necessary for the successful application of the ‘classical’ reductionist scientific paradigm are not given in a nested and complex global social reality. This implies the need to question and unlearn the constructed meaning of ‘objectivity’ or ‘impartiality’ by taking positionality and embodied knowledge seriously in GES development. Decolonial approaches to environmental justice (DEJ), might support undoing epistemological violence, i.e. the imposition of one particular way of knowing, in GES construction by fostering the dialogue between different knowledge systems (Ramcilovic-Suominen, 2022; Rodríguez & Inturias, 2018). This requires not only unlearning the hierarchic dichotomy between ‘objective scientific knowledge’ from the North and non-Western, non-scientific ‘subjective experiences’ from the South (Santos, 2018) but also the active construction of ‘otherness’, given that the ‘other’ has experienced systematic oppression by colonial, patriarchal and capitalist systems: ‘other’ worldviews, conceptions of development and well-being, political practices and modes of life (Álvarez & Coolsaet, 2020; Rodriguez, 2020). Addressing the coloniality of knowledge should be understood as acknowledging limits of ‘purely’ scientific procedures in the construction of global

futures rather than as a negation of the merits of scientific theories and methodologies. A recent example of dialogues between different ways of ‘knowing’ is given by the GES exercise of the IPBES which differs from the more ‘technical’, expert-based approach of the IPCC (Borie et al., 2021).

An obvious way of ‘decolonizing’ GES is to broaden the circle of those who participate in GES development. For different purposes and scenario types, different participative methods developed by scientists and practitioners (Chambers, 1983; Ernst et al., 2018; Gonsalves et al., 2005; Pereira et al., 2021) might prove adequate. GES using direct participatory methods would undo the ‘expert paradigm’ in scenario creation to include subaltern ‘stakeholders’ of the global future such as the urban poor and homeless; the rural poor and landless; marginalized groups depending on the natural environment for their livelihoods such as small fishers, peasants and pastoralists who often intersect with indigenous communities; the ‘low-skilled’ working classes in the world’s peripheries, semiperipheries and centers;¹ refugees and migrants; and young people. Although they might not possess scientific knowledge, they all embody local and practical knowledge about their life realities which might be very different from what would be predicted according to scientific theories (Chambers, 1983). In this respect, even increasing only the diversity of ‘experts’ would constitute a step in the right direction as current GES development is dominated by scientists from few geographic territories, few disciplines, and a narrow range of theories regarding the world’s social reality.

In cases where direct participation is not the most suitable or viable method, more indirect participative methods might be employed. For example, alternative knowledge systems could be considered through focus groups or interviews with members of subaltern groups, which could subsequently inform the GES development process. Equally, reiterative rounds of feedbacks are possible in which the core themes in the storylines of already developed GES, or main results of storyline quantifications are presented to these groups, and then adapted or contextualized based on the perspectives and proposals expressed during the process.

When neither direct nor indirect participation is feasible, a thorough literature review regarding the lived experiences, priorities and knowledge of subaltern groups especially but not exclusively in the Global South prior to the scenario construction can at least reveal the current state of knowledge, and, more importantly, ignorance and data limits on the realities of life, cosmovisions and local knowledge of subaltern groups.

Actively including alternative ways of knowing the world, including local, practical and indigenous knowledge from a variety of geographic and social places can prove beneficial for different types of GES (cf. Pereira et al., 2021).

First, although the global scale is central for the governance of environmental and economic change, the impacts of environmental degradation as well as of global environmental and sustainability policies are always experienced at the local level (IPCC, 2022). Taking into account alternative knowledge systems would enable the storylines of GES to be more sensitive to the differentiated impacts of probable developments and policies favored by big corporations, states and international institutions. This would highlight different socio-ecological risks resulting from business-as-usual as well as policy scenarios that otherwise would have remained hidden. For instance, local knowledge can point to negative side-effects of low-carbon technologies and investments on the livelihood or health of different social groups (Corbera et al., 2017; Sovacool, 2021). Similarly, especially in areas where scientific data is sparsely available – which applies particularly to very poor regions and states of the outer periphery (Fatton, 2016) – local and

¹ Statistically, it is probable that these subaltern groups are constituted disproportionately by non-males and non-white people.

practical knowledge might assess to which extent people would be harmed by, and can adapt to, adverse environmental change. To offer a more realistic picture of probable global futures, GES would need to include these differentiated impacts and possible dynamics of conflict and resistance they might provoke.

On the other hand, the search for desirable global futures would also be greatly enhanced, and become more representative, if scenario developers promoted the inclusion of multiple ways of knowing the world. For instance, including 'environmental defenders' (Global Witness, 2023) and people involved in environmental distribution conflicts in Western scenario building processes such as the European bioeconomy could increase the chances of questioning, unlearning and undoing myths and paradigms in Western culture, such as technoscientific progress, economic growth, (trade) liberalization or urbanization, given that at the commodity frontiers of global capitalism the full implications of these concepts become palpable (Giuntoli et al., 2023). Based on local and practical knowledge, members of subaltern groups will be able to assess what the realization of corporate preferences for automatization or genetically modified seeds without fundamental change in the capitalist state-based world order means for their own livelihoods. For example, the inclusion of stakeholders as different as Via Campesina and Syngenta in the development of food scenarios has shown that actors' perceptions about desirable food futures varied greatly and that 'food security' futures appeared insufficient to those actors claiming 'food sovereignty' (Saghai, 2021). It is likely that the inclusion of different knowledge system will also provoke the unlearning of value systems and languages of valuation different from predominant techno-economic values (Martinez-Alier, 2013). For example, 'relational' modes of life do not reduce land to an exploitable resource but attach social and ethical meaning to it which includes reciprocal obligations that also extend to non-human beings (Álvarez & Coolsaet, 2020). Clashes between value systems also imply that there is no 'best world' for everybody but rather that one actor's desirable world might be structurally coupled with another actor's dreaded future. For example, state-based solutions might be rejected by groups that experience systematic state repression, corruption and the arbitrary exercise of power (Bocarejo & Ojeda, 2016). On the other hand, the dismantling of great corporations or global redistribution policies as proposed for example by the degrowth movement (Fitzpatrick et al., 2022), might fundamentally clash with the interests of the current power elites. Thus, the inclusion of a broad diversity of participants with different embodied knowledge would limit the possibility of the implied socio-ecological cost-shifting of certain desirable futures to go unnoticed and incite scenario developers to search for future worlds involving systemic and structural changes that appear desirable and feasible for the poorer half of humanity rather than for the world's top 1%.

3.2. Addressing the coloniality of being

The concept of the 'coloniality of being' refers to the construction of subjectivities such as the colonizer and the colonized, as well as to the experience of subaltern populations of being rendered 'less human' and inferior, all of which legitimizes oppression and injustice between humans (cf. Ndlovu-Gatsheni, 2013; Restrepo, 2018).

Thus, addressing the coloniality of being implies searching for pathways toward futures that end oppression and injustice, as well as identifying those tendencies that make unjust futures possible. In line with this, DEJ calls for systemic changes that eliminate the root causes of social and environmental harm, such as extractivism, ecologically unequal exchange and colonial violence, rather than the more equal distribution of environmental harm (cf. Álvarez & Coolsaet, 2020; Givens et al., 2019).

Current GES often concentrate on abstract entities such as ‘the world’ or on classical actors and stakeholders such as ‘businesses’, ‘decision-makers’, ‘politicians’ or ‘civil society’. The latter is understood as separate, third sphere, complementing the political and the economic sphere, rather than as a battleground for socio-cultural hegemony, and state-society-interactions are not explicitly acknowledged. This understanding of civil society in GES overlooks the potential of civil society for resistance and transformation that can take place through the development of an alternative hegemonic project pushed by oppositional movements including activists, intellectuals, the media and subaltern groups themselves (Koch, 2022).

The narrow focus on powerful actors renders invisible and nameless all other social groups that not only will bear the brunt of the negative impacts of the current and future world economy but also actively reproduce or challenge parts of global political hegemony on a daily basis. Thus, the construction of DEJ-based scenarios requires to unlearn the notion that subaltern groups are merely objects influenced by abstract forces operating above the local sphere such as governance institutions and multinational corporations or global environmental change. This can be done by directing more attention to the capacity of collective action, resistance and systemic transformation of those population groups that are not fully integrated into the capitalist world economy. Using methodological frameworks developed to study how these collectives operate between adaptation, resistance and transformation in the context of global environmental change, ‘green’ politics and the steady expansion of commodity frontiers might give insights about possible future socio-ecological-economic developments (Cui & Brombal, 2023).

A stronger focus on the potential for the transformative agency of different social collectives within the GES storylines would provoke the international and scientific institutions normally involved in GES creation to focus on the difficult question of which developments in the near future could bring about changes in subjectivities of currently oppressed agents. Importantly, subjectivities can differ greatly among subaltern groups as structural and persistent oppression can lead to apathy and resignation (Okwuadimma & Biereenu-Nnabugwu, 2021) as well as to collective resistance movements (Scheidel et al., 2020; Temper et al., 2020). In any case, granting visibility to normally neglected groups in global socio-ecological futures acknowledges not only their existence and agency but inevitably points toward the need of strong and urgent transformative action on a global scale in which those groups themselves might play a decisive role.

At the same time, the search for an active construction and inclusion of the ‘other’ in DEJ, requires the undoing of idealized, fixed and ahistoric subjectivities of subaltern groups. For example, representing indigenous people as ‘environmental conservationists’ and peasants as ‘environmental destroyers’ does not correctly depict the lived experiences and actions of any of those collectives and leads to exclusion and oppression in the context of conservation policies (Bocarejo & Ojeda, 2016). Equally, ‘local communities’ do not constitute homogeneous blocks free of power hierarchies and conflicts of interest. As a multitude of case studies in the field of political ecology have shown, the fact that subaltern groups are oppressed or marginalized by current power structures does not imply that they are unaffected by or isolated from the global and expansive character of capitalist ideologies, social relations of production and ways of integrating ever more non-human matter into the capitalist sphere of production. Subsequently, hoping to escape the ‘coloniality of being’, subaltern groups themselves might partly reproduce capitalist discourses and practices, and take reformist rather than radical standpoints (cf. David, 2013; Hilton, 2011). Last, constructing an artificial dichotomy between the ‘native (South)’ and

the ‘foreign (North)’ is also misleading given the subversive processes through which colonized population appropriated cultures and practices that were originally forced upon them (Quijano, 1999). Thus, unlearning of predetermined ontological assumptions about marginalized groups and their relationship with the world system is facilitate by the acknowledgment of the complexity of global social reality and the need to directly engage with different subaltern groups without predetermined, fixed mental frameworks.

Approaching the coloniality of being in GES would also mean to question the social construction of subjectivities such as ‘underdeveloped’, ‘developing’ or ‘developed’ in the scenario storylines. These labels create hierarchies between societies and suggest a universal, natural and objective development pathway, with ‘developed’ countries taking the lead and the non-Western world following. This implies a ‘modernization’ process through which certain ideological premises of organizing societies and economies are transferred unilaterally from the Global North to the Global South. Far from the creation of a unified and idealized westernized globe the historical reality has produced declining living standards, widespread poverty and complete dependence from foreign powers in countries of the outer periphery (Fatton, 2013, 2016), a rise of religious fundamentalism (Emerson & Hartman, 2006) and authoritarian state capitalism (Sallai & Schnyder, 2021). It is highly doubtful that the abyss between ‘ideal’ and ‘real’ development will become smaller in the future.

Besides, the terms ‘developing’ and ‘developed’ avoid the central question of GES, which is ‘Development toward *what?*’ and instead implicitly equate development with economic growth. Assuming fixed subjectivities seems to lock developing countries in a constant position of ‘backwardness’ while developed societies seem to have already reached their final destination. This discourse also ignores the triad of capitalism, imperialism and racism whose historic dynamics continue to reproduce power asymmetries and hierarchies in the world system. After all, the ‘development’ of one part of the world produced and still produces the ‘underdevelopment’ of the remaining part of the world given the reliance on capitalist development on cheap energy, materials, land and labor (Moore, 2017, 2018).

The term ‘developing’ also cannot capture the enormous heterogeneity between and within countries constituting the ‘Global South’. GES assuming homogeneous economic and technological development, political interests and reactions to socio-ecological problems greatly simplify the future and overlook conflicts between countries of the Global South as well as geopolitical North-South alliances that have their historical roots in colonialism and imperialism.

All the points just outlined imply an impossibility of constructing probable or desirable GES while abstracting from sub-global heterogeneities and conflicts of interests between actors on the regional, national and sub-national level. The global reality and its future developments are not the result of ‘one world’ but rather of many ‘worlds’ that want to unfold on planet Earth (Escobar, 2012). It is precisely the expansive character of capitalist social relations and ideologies that not only creates continuous homogenization throughout the world but also provokes constant polarization and differentiation. Destructive and inequality-increasing capitalist dynamics lead to the maintenance, production and reproduction of ‘alternative’ worlds at the margins (e.g. peasant or indigenous movements, solidarity economies) and within the center of the world economy (e.g. ecovillages, transition towns or the degrowth movement).

3.3. Addressing the coloniality of power

A decolonial approach to GES would question the legitimacy of all imagined futures that are labeled as ‘sustainable’ but implicitly reproduce the coloniality of being by maintaining those global institutions and power structures that mediate the unequal treatment of human beings. In other words, GES need to engage more explicitly with questions of power in the context of desirable futures.

The colonial matrix of power developed by Quijano consists of four interrelated domains of control: (1) the control of the economy: this includes the exploitation of labor, land appropriation and the control of natural resources; (2) the control of authority through institutions and armed forces; (3) the control of gender and sexuality; (4) the control of subjectivity and knowledge, which intersects with the coloniality of being and the coloniality of knowledge addressed in section 3.1 and 3.2.

GES could address the coloniality of power in two steps. First, visions of different futures are needed in which the colonial matrix of power has been overcome.

With regard to the economic dimension in the matrix, the research around ‘post-growth’ (Jackson, 2013, 2021) and ‘degrowth’ (Kallis et al., 2018) becomes relevant since these approaches aim at reducing the Global North’s consumption of cheap labor, land and resources from Global South countries. As a result of a profound unlearning and undoing of ‘growthism’ (Schmelzer, 2024), futures engaging with the coloniality of power in the economic realm would probably problematize the unequal exchange of labor and resources, and picture more equilibrated labor and material flows between the Global South and North. The economic control of the center over the periphery ultimately stems from an unequal distribution of capital linked to a global division of labor that traps peripheral countries in primary sector activities. Thus, in global futures where capital is redistributed on a large scale, peripheral economies would in principle be in a better position to fulfill the basic human needs of the population and to adapt to and mitigate adverse global environmental change (IPCC, 2022). Capital redistribution is related to the elimination of the global debt regime, another medium of economic control rendering heavily indebted societies completely dependent on their creditors (Kapijimpanga, 2023; Zajontz, 2022).

Reducing the scale of the global economy is necessary to halt and alleviate the persistent destabilization of biogeochemical cycles and gains importance when considering the flourishing of non-human life. Decolonial perceptions of environmental justice attempt to move beyond a human-nature dichotomy that considers humans valuable subjects and non-humans value-free (and therefore costless) objects. Expanding the concept of environmental justice to include both humans and non-humans (Menton et al., 2020) requires profound changes in production technologies but ultimately also a reduction in the global socio-economic metabolism. However, as the global metabolism shrinks, questions of distribution between social groups become even more important to avoid drastic increases in human poverty and suffering. Therefore, the integration of a strong convergence in people’s access to resources, production capacities and economic consumption in GES is crucial not only to reduce the control over the economies of the Global South but also to guarantee that basic human needs can be met in a downsized global economy (cf. Hickel, 2021).

The different types of GES could engage with these topics in their own respective ways. For example, energy scenarios could focus on strengthening renewable-based energy sufficiency and autonomous renewable-based industrial development in Global South countries rather than on

converting renewable energy from the South in a tradable commodity to be exported to industrialized countries (Okpanachi et al., 2022). Climate scenarios could integrate strong global convergence in consumption and degrowth instead of betting on speculative negative emission technologies with uncertain socio-ecological effects (Fuss et al., 2014). A small part of the literature has recently begun to move in this direction (Keyßer & Lenzen, 2021; Li et al., 2023; Nieto et al., 2020). Equally, climate scenarios could explore the relationships between inter- and intra-national capital distribution and climate finance while land scenarios could make ownership conflicts, dispossession and displacement explicit and imagine socio-ecological futures where access to land is not mediated by gender, class and race. Global food scenarios could critically examine conflicts of interest between the handful of corporations controlling the global agro-chemical and food industry and smallholder farmers that jointly provide a third of the world's food (Clapp, 2021; Lowder et al., 2021). Likewise, they could envision a global food system whose reproduction does not depend on the degradation of human and planetary health (Bodirsky et al., 2022).

The economic dimension of the colonial matrix cannot be addressed without changing the institutional/political dimension. Thus, rather than extending the current power structures into the future, GES developers could question to which extent the three main actors shaping global economic and environmental governance – states, corporations and IOs – reproduce the colonial matrix of power. For example, indigenous people manage or have tenure rights over a great amount of ecologically intact territories (Garnett et al., 2018) and claims for self-governance within these territories under informal indigenous or other customary authorities (Temper, 2019) run counter to a centralist, state-based implementation of global conservation and biodiversity governance (Schmidt & Peterson, 2009). Strong corporate presence in economic and environmental global governance entails the risk of creating regulatory frameworks which favor the profit interests of multinational corporations operating in the South over livelihood, spiritual and cultural needs affected local communities might have. Finally, the inter- and transnational economic regime, including the IMF, Worldbank, WTO, the global financial regime and investment law, constitutes the legal framework which promotes the expansion of capital from the center toward the world's peripheries and which renders an 'autonomous development' of Global South countries impossible (Schneiderman, 2022).

Decentering states, corporations and IOs in global governance, also means thinking about new and more egalitarian forms of decision-making. In this respect, GES scholars could engage with recent developments in the debate about global democracy (Scholte, 2014): While this field of political thought has been traditionally mainly concerned with liberal approaches of extending liberal (capitalist) representative democracies to the global level while ignoring economic inequalities and cultural differences, in recent years, attempts have been undertaken to approach ideas of global democracy through dialogue and mutual learning between groups from different nations, religions, ethnicities and genders (Scholte, 2020).

Last, the overwhelming majority of GES ignores the military and armed forces in spite of the significant greenhouse gas emissions of the military sector (Ahmad, 2023) and the disastrous impacts of armed conflicts not only on human but also on non-human life (Kong & Zhao, 2023). Although the monopoly of violence is the common denominator of all states in the international system, there are great military imbalances and the history of invasions of great powers into other territories they regard as within their sphere of influence illustrates that the 'free' trade regime has to be backed up by military power that can ultimately secure access to resources (cf. Le Billon, 2004). GES that do not engage with this dimension of power greatly underestimate the

future potential for armed conflicts in the Global South. Thus, from a perspective of decolonial environmental justice convergence in economic power would need to be linked to convergence in military power and a new global security regime alongside a new economic and environmental regime. This is partly reflected in degrowth policies that demand reducing military spending alongside lifestyles of sufficiency and global redistribution (Fitzpatrick et al., 2022).

Finally, the relationship between GES and control over gender roles and sexuality is less obvious in GES focused on broad ecological-economic dynamics. However, gender roles and sexuality play a key part in the reproduction of capitalist modes of production (Oksala, 2017) and in the reproduction of societies in general. Thus, these topics become relevant with regard to population policies and the debate about the size of the human population (Daily et al., 1994). It has been noted long ago that the global socio-economic metabolism and the associated environmental pressure increases with affluence as well as with population size (Holdren, 2018). Especially when attributing intrinsic value to non-human life, GES figuring reduced fertility rates and a decrease in the global population can be justified. Considering this dimension of the colonial power matrix would prompt GES researchers to search for visions of socio-ecological futures where changes in the human population are not the result of neocolonial practices of population control through gender and sexuality norms.

GES depicting different 'liberated' worlds free of the colonial matrix of power have value in themselves because scenarios can influence social imaginaries and introduce possible futures into the discourse that were unconceivable or unpronounceable before. As a second step, GES scholars could move on to develop different plausible pathways of change that might connect the present status quo and the envisioned futures. These pathways will of course differ according to the concrete content of the developed GES and could be informed by different knowledge systems and the perspectives of subaltern groups (section 3.1, 3.2). Given that addressing the coloniality of power has distributional consequences, the central question becomes under which circumstances currently powerful actors give up or lose some of their power. Importantly, these actors can be identified and analyzed: 17 global financial corporations control more than one trillion dollars in capital, are managed by only 199 interconnected directors, and are heavily invested in both giant corporate media and the top global weapon producers (Phillips, 2018). These companies also exert considerable influence over key biomes such as rainforests or boreal forests (Galaz et al., 2018). 13 corporations control 11-16% of the global marine catch and 19-40% of the most valuable stocks (Österblom et al., 2015), only 4 corporations dominate the global seed and agrochemical industry (Clapp, 2021) etc. Arguably, any feasible pathways toward 'desirable' futures for the bottom billion must particularly engage with the factual presence, intentions, fears and actions of this embodied concentrated power.

4. Discussion

4.1. Quantitative modeling and DEJ-informed GES

Our proposals for introducing decolonial perspectives into the GES literature have focused mainly on qualitative scenarios or storylines. This does not deny the importance of quantitative modeling in the field of GES research. Quantitative simulations and modeling can be useful for assessing the plausibility of GES visions and pathways in technical terms, such as finding required rates of change to achieve specific ecological or social objectives or detecting unintended side effects of certain environmental or economic policies. However, the quantitative simulation of GES based on decolonial perspectives might require significant unlearning and

undoing of common practices in the construction and logic of quantitative models. First, although Integrate Assessment Models (IAM) manage to produce detailed information on the development of a series of technological and biophysical variables, they lack the necessary disaggregation in the social realm that would be required from a DEJ viewpoint. For example, currently there is no IAM able to show the evolution of inequality under different GES along the intersecting categories of class, gender, race and geographic territories. The lack of disaggregation in the social realm is partly due to a lack of data on which IAMs rely, especially for Global South countries constituting the world's peripheries and semiperipheries. Consequently, it is practically impossible to obtain information on variables such as the evolution of ecological distribution conflicts, subsistence economy or multidimensional poverty via IAM simulations. Instead, these variables would need to be estimated from the average GDP p.c. values through regression analyses. Furthermore, due to the opacity of quantitative models, their reductionist approach to social reality and built-in biases favoring dominant structures and ideas, successful participatory processes involving different ways of knowing the world and the future become extremely challenging (Saghai, 2021).

Model development informed by DEJ-based GES probably would draw on techniques that can depict non-linear dynamics, different interacting agents and changing institutions (Köhler et al., 2018), and that include biophysical, social and economic variables which are actually significant for subaltern populations in the Global South (and North). Likely no model would be able to completely 'depict' a storyline or development pathways in quantitative terms but rather models could be developed or used to gain more insights about specific aspects of the scenario. These include changes in the ownership of land, material, labor and financial flows between regions, the evolution of the level of economic or military concentration, and climate change adaptation, mortality rates and quality of life of the 'bottom billion'.

4.2. Participation and GES

As outlined previously, GES development could greatly benefit from participatory processes including subaltern populations, rendering results both more realistic and more diverse. Incorporating a wider range of voices would help existing biases in GES which is especially important when it comes to the co-creation of 'sustainable' or 'desirable' futures. However, the inclusion of subaltern and marginalized groups in GES development poses several challenges. First, researchers might face difficulties to reach out to the rural and urban poor, migrants, peasants, indigenous people, low-skilled workers etc. as they often live in hard-to-access areas with limited or no internet and telecommunications infrastructure. Additionally, their native languages might not be English or other European languages, which further complicates communication. Second, members of those collectives might be unwilling or unable to participate in GES development processes as future global environmental and economic developments might seem too far away from every-day struggles and concerns. Unlike corporate and political stakeholders who are accustomed to expressing their opinion, potential participants might feel reluctant to be interviewed. Moreover, when asked to express perspectives on developments and social realities beyond the local realm, participants might reproduce dominant discourse promoted by corporate and state media. Third, since members of subaltern populations likely never have participated in similar exercises before, participatory GES development must avoid manipulating participants through the framing of specific problems or trends (Cooke & Kothari, 2001). Likewise, drawing on local knowledge should not become a one-sided extraction of data (Helm et al., 2023).

Despite these challenges, we believe that the participation of subaltern groups in GES development is possible. While it is true that such participation has not yet been achieved, there are other experiences with certain similarities that allow for optimism. For example, there have been successful cases at the local level in the elaboration of development plans in which indigenous communities have played a leading role. One such example is that of Life Plans (Planes de Vida), planning tools driven by and for Indigenous peoples, aimed at articulating their self-governance, vision of "good living," and autonomous development in contrast to conventional extractive models (Vieco, 2019).

In various regions of Latin America, Life Plans have served as a means for Indigenous communities to articulate visions of a less extractive and more ecologically sustainable future. One case is that of the Peruvian Amazon, where several communities have used them to strengthen collaborative management of their territories and define their development priorities (Ravikumar & Ojeda Del Arco, 2025). Similarly, in the border regions shared by Peru, Brazil, Colombia, and Ecuador, these plans have been crucial for peoples such as the Secoya (Siékopai) to defend their territorial rights and negotiate their place within broader conservation strategies (Delgado Pugley, 2024). Another case, in the Ecuadorian Amazon, is that of Kichwa organizations such as FOIN, which have worked to "indigenize" these instruments, infusing them with their own planning philosophies to model alternative futures based on their worldview (Grefa et al., 2024). These examples demonstrate the agency of these groups in constructing desired socio-ecological futures.

These successful cases can be understood within the analytical framework of Gaventa's (2006) power cube, which examines the spaces, places, and forms of power in which participation occurs. Life Plans do not emerge from closed spaces, where decisions are made exclusively by state actors or experts without any consultation. Nor are they merely invited spaces, created and defined by external authorities (governmental or non-governmental) that invite participation on their own terms. Instead, these processes fundamentally represent claimed or created spaces. They are initiatives that emerge organically from Indigenous communities and organizations based on shared concerns and identities, allowing them to autonomously articulate their visions of the future, negotiate from a position of strength with other actors, and actively shape policies and discourses affecting their territories and lives. In the case of GES development, it may be difficult to imagine that the initiative would come from the subordinate groups themselves. However, even if they are initially included by external institutions, the experience of participation could lead to the emergence of their own initiatives, which could be supported, if necessary, by other organizations belonging to those segments of the global civil society that aim at expanding alternative social spaces through counterhegemonic practices. At the same time, gradually increasing the representation of subaltern groups in policy or visioning process might provide the opportunity for these groups to engage in agenda-setting activities and strengthen counter-hegemonic projects 'from within', provided that they are not co-opted by current powers. (cf. Koch, 2022).

A methodological approach to facilitate inclusion is the use of participatory frameworks for exploring the future, such as the Three Horizons Framework (Schaal et al., 2023; Sharpe et al., 2016). This approach is particularly suited for engaging with normative futures and developing pathways towards them by valuing diverse forms of knowledge. It allows participants to identify unsustainable elements of the present system (Horizon 1), envision transformative futures grounded in their values and aspirations (Horizon 3), and explore the innovations and actions that could bridge the two (Horizon 2). By using accessible methods like storytelling, this framework can help translate subaltern groups' lived experiences and worldviews into locally meaningful

narratives of change, making their participation in GES development not only feasible but also actionable. This can empower local action and ensure that the resulting scenarios are less detached from the realities of the majority of the world's population.

Finally, it is important to highlight that GES informed by the perspectives of subaltern groups will likely be less appealing to decision-makers from the Global North and more difficult to translate into concrete policy actions. This is because, instead of 'speaking truth to power,' they would challenge 'power' itself. However, in the best case, these GES could shift the discussion about the future of humanity and the Earth from narrow academic, corporate, and political circles in the Global North to broader debates at a global level, as they would appear less detached from the reality of life for the majority of the world's population.

5. Conclusion

In this paper we have presented a series of proposals of how the field of Global Environmental Scenarios (GES) could engage with insights from decolonial theory and decolonial environmental justice to develop socio-ecological and economic global scenarios that are relevant, plausible and/or desirable for the 'bottom billion' or the poorer half of the world's population. We have shown that the design of current GES often implicitly prioritizes sustainability issues, environmental problems and realities of life of relatively privileged classes from the Global North. Likewise, GES tend to portray narrow and homogeneous development pathways and powerful actors shaping global environmental and economic development. Thus, from a decolonial perspective, GES would do well to pay more attention to different ways of knowing the world, the agency of subaltern population groups to generate profound changes in the world system and to fundamental justice concerns that address the highly unequal access to ecological and economic goods which are mediated by class, race, gender and nationality. Implementing some of our proposals will likely be challenging both with regard to successful participatory processes involving subaltern populations and with regard to the modeling of developed scenario storylines. Although we draw on decolonial thought to structure our argument the outlined proposals can be of interest to scholars from different scientific and theoretical fields who are interested in unlearning certain practices and epistemological paradigms that are often taken for granted, thereby unlocking the potential of GES to open up emancipatory options for the 'bottom billion' already today.

References

- Ahmad, N. B. (2023). Military Climate Emissions. *Nev. LJ*, 24, 845.
- Alexander, P., Henry, R., Rabin, S., Arneth, A., & Rounsevell, M. (2023). Mapping the shared socio-economic pathways onto the Nature Futures Framework at the global scale. *Sustainability Science*, 1–18.
- Álvarez, L., & Coolsaet, B. (2020). Decolonizing environmental justice studies: A Latin American perspective. *Capitalism Nature Socialism*, 31(2), 50–69.
- Bakhiyi, B., Labrèche, F., & Zayed, J. (2014). The photovoltaic industry on the path to a sustainable future—Environmental and occupational health issues. *Environment International*, 73, 224–234.
- Beck, S., & Mahony, M. (2018). The politics of anticipation: The IPCC and the negative emissions technologies experience. *Global Sustainability*, 1, 1–8.
- Bluwstein, J., & Cavanagh, C. (2023). Rescaling the land rush? Global political ecologies of land use and cover change in key scenario archetypes for achieving the 1.5° C Paris agreement target. *The Journal of Peasant Studies*, 50(1), 262–294.
- Bocarejo, D., & Ojeda, D. (2016). Violence and conservation: Beyond unintended consequences and unfortunate coincidences. *Geoforum*, 69, 176–183.
- Bodirsky, B. L., Chen, D. M.-C., Weindl, I., Sörgel, B., Beier, F., Molina Bacca, E. J., Gaupp, F., Popp, A., & Lotze-Campen, H. (2022). Integrating degrowth and efficiency perspectives enables an emission-neutral food system by 2100. *Nature Food*, 3(5), 341–348.
- Borie, M., Mahony, M., Obermeister, N., & Hulme, M. (2021). Knowing like a global expert organization: Comparative insights from the IPCC and IPBES. *Global Environmental Change*, 68, 102261.
- Capellán-Pérez, I., De Castro, C., & González, L. J. M. (2019). Dynamic Energy Return on Energy Investment (EROI) and material requirements in scenarios of global transition to renewable energies. *Energy Strategy Reviews*, 26, 100399.
- Capellán-Pérez, I., Mediavilla, M., de Castro, C., Carpintero, Ó., & Miguel, L. J. (2015). More growth? An unfeasible option to overcome critical energy constraints and climate change. *Sustainability Science*, 10(3), 397–411.
- Chambers, R. (1983). *Rural development: Putting the last first*. Longman.
- Clapp, J. (2021). The problem with growing corporate concentration and power in the global food system. *Nature Food*, 2(6), 404–408.
- Cooke, B., & Kothari, U. (2001). *Participation: The new tyranny?* Zed books.
- Corbera, E., Hunsberger, C., & Vaddhanaphuti, C. (2017). Climate change policies, land grabbing and conflict: Perspectives from Southeast Asia. *Canadian Journal of Development Studies/Revue Canadienne d'études Du Développement*, 38(3), 297–304.
- Cui, M., & Brombal, D. (2023). From resistance to transformation—The journey to develop a framework to explore the transformative potential of environmental resistance practices. *Philosophy & Social Criticism*, 49(5), 599–620.
- Daily, G. C., Ehrlich, A. H., & Ehrlich, P. R. (1994). Optimum human population size. *Population and Environment*, 469–475.
- D'Alisa, G., & Demaria, F. (2024). Accumulation by contamination: Worldwide cost-shifting strategies of capital in waste management. *World Development*, 184, 106725.
- David, E. J. R. (2013). *Internalized oppression: The psychology of marginalized groups*. Springer Publishing Company.

- Delgado Pugley, D. (2024). Planning for autonomy and conservation: 'Life Plans' and communal reserves in the Amazonian borders of Peru. *Oxford Development Studies*, 52(4), 413–428. <https://doi.org/10.1080/13600818.2024.2418370>
- Dou, Y., Zagaria, C., O'Connor, L., Thuiller, W., & Verburg, P. H. (2023). Using the Nature Futures Framework as a lens for developing plural land use scenarios for Europe for 2050. *Global Environmental Change*, 83, 102766.
- Durán, A. P., Kuiper, J. J., Aguiar, A. P. D., Cheung, W. W., Diaw, M. C., Halouani, G., Hashimoto, S., Gasalla, M. A., Peterson, G. D., & Schoolenberg, M. A. (2023). Bringing the Nature Futures Framework to life: Creating a set of illustrative narratives of nature futures. *Sustainability Science*, 1–20.
- Emerson, M. O., & Hartman, D. (2006). The rise of religious fundamentalism. *Annu. Rev. Sociol.*, 32(1), 127–144.
- Ernst, A., Biß, K. H., Shamon, H., Schumann, D., & Heinrichs, H. U. (2018). Benefits and challenges of participatory methods in qualitative energy scenario development. *Technological Forecasting and Social Change*, 127, 245–257.
- Escobar, A. (2012). Más allá del desarrollo: Postdesarrollo y transiciones hacia el pluriverso. *Revista de Antropología Social*, 12, 23–62.
- Fatton, R. (2013). *Haiti: Trapped in the outer periphery*. Lynne Rienner Publishers.
- Fatton, R. (2016). Development and the outer periphery: The logic of exclusion. *The Palgrave Handbook of Critical International Political Economy*, 119–137.
- Fitzpatrick, N., Parrique, T., & Cosme, I. (2022). Exploring degrowth policy proposals: A systematic mapping with thematic synthesis. *Journal of Cleaner Production*, 132764.
- Fuss, S., Canadell, J. G., Peters, G. P., Tavoni, M., Andrew, R. M., Ciais, P., Jackson, R. B., Jones, C. D., Kraxner, F., & Nakicenovic, N. (2014). Betting on negative emissions. *Nature Climate Change*, 4(10), 850–853.
- Galaz, V., Crona, B., Dauriach, A., Scholtens, B., & Steffen, W. (2018). Finance and the Earth system—Exploring the links between financial actors and non-linear changes in the climate system. *Global Environmental Change*, 53, 296–302.
- Gall, T., Vallet, F., & Yannou, B. (2022). How to visualise futures studies concepts: Revision of the futures cone. *Futures*, 143, 103024.
- Garb, Y., Pulver, S., & VanDeveer, S. D. (2008). Scenarios in society, society in scenarios: Toward a social scientific analysis of storyline-driven environmental modeling. *Environmental Research Letters*, 3(4), 045015.
- Garnett, S. T., Burgess, N. D., Fa, J. E., Fernández-Llamazares, Á., Molnár, Z., Robinson, C. J., Watson, J. E., Zander, K. K., Austin, B., & Brondizio, E. S. (2018). A spatial overview of the global importance of Indigenous lands for conservation. *Nature Sustainability*, 1(7), 369–374.
- Gaventa, J. (2006). Finding the Spaces for Change: A Power Analysis. *IDS Bulletin*, 37(6), 23–33. <https://doi.org/10.1111/j.1759-5436.2006.tb00320.x>
- Giuntoli, J., Oliver, T., Kallis, G., Ramcilovic-Suominen, S., & Monbiot, G. (2023). *Exploring new visions for a sustainable bioeconomy*.
- Givens, J. E., Huang, X., & Jorgenson, A. K. (2019). Ecologically unequal exchange: A theory of global environmental injustice. *Sociology Compass*, 13(5), e12693.
- Global Witness. (2023). *Standing firm—The land and environmental defenders on the frontlines of the climate crisis*.
- Gonsalves, J., Becker, T., Braun, A., Campilan, D., De Chavez, H., Fajber, E., Kapiriri, M., Rivaca-Caminade, J., & Vernooy, R. (Eds.). (2005). *Participatory research and development for sustainable agriculture and natural resource management: A sourcebook* (Vol. 1). IDRC.

- Grefa, F., Alvarado, R., Alvarado, T., & Valdivia, G. (2024). *Causaita Puruntuna* ("Let's Plan Life Together"): Planes de Vida / Life Plans and the Political Horizon of Indigenous Planning in the Ecuadorian Amazon. *Antipode*, 56(6), 2157–2179.
<https://doi.org/10.1111/anti.13062>
- Helm, P., de Götzen, A., Cernuzzi, L., Hume, A., Diwakar, S., Ruíz Correa, S., & Gatica-Perez, D. (2023). Diversity and neocolonialism in Big Data research: Avoiding extractivism while struggling with paternalism. *Big Data & Society*, 10(2), 20539517231206802.
- Hickel, J. (2021). The anti-colonial politics of degrowth. *Political Geography*, 88.
- Hilton, B. T. (2011). Frantz Fanon and colonialism: A psychology of oppression. *Journal of Scientific Psychology*, 12(1), 45–59.
- Holdren, J. (2018). A brief history of IPAT. *The Journal of Population and Sustainability*, 2(2), 66–74.
- IEA. (2022). *World Energy Outlook 2022*. <https://www.iea.org/reports/world-energy-outlook-2022>
- IPCC. (2022). *Climate Change 2022: Impacts, Adaptation and Vulnerability. Contribution of Working Group II to the Sixth Assessment Report of the Intergovernmental Panel on Climate Change*. Cambridge University Press. Cambridge University Press, Cambridge, UK and New York, NY, USA.,
- Jackson, T. (2013). Prosperity without growth. In *Globalisation, Economic Transition and the Environment* (pp. 105–128). Edward Elgar Publishing.
- Jackson, T. (2021). *Post growth: Life after capitalism*. John Wiley & Sons.
- Kallis, G., Kostakis, V., Lange, S., Muraca, B., Paulson, S., & Schmelzer, M. (2018). Research on degrowth. *Annual Review of Environment and Resources*, 43(1), 291–316.
- Kapijimpanga, O. (2023). Debt Sustainability in the Context of African Dependency and Underdevelopment. *Development*, 66(3), 251–259.
- Keyßer, L. T., & Lenzen, M. (2021). 1.5 C degrowth scenarios suggest the need for new mitigation pathways. *Nature Communications*, 12(1), 1–16.
- Koch, M. (2022). State-civil society relations in Gramsci, Poulantzas and Bourdieu: Strategic implications for the degrowth movement. *Ecological Economics*, 193, 107275.
- Köhler, J., De Haan, F., Holtz, G., Kubeczko, K., Moallemi, E. A., Papachristos, G., & Chappin, E. (2018). *Modelling sustainability transitions: An assessment of approaches and challenges*.
- Kong, L., & Zhao, Y. (2023). Remedyng the environmental impacts of war: Challenges and perspectives for full reparation. *International Review of the Red Cross*, 1–22.
- Lauer, A., Carpintero, Ó., & De Castro, C. (2025). In search of a missing South: An explorative study of biases in global climate and energy scenarios. *Globalizations*, 1–22.
<https://doi.org/10.1080/14747731.2025.2526295>
- Lauer, A., de Castro, C., & Carpintero, Ó. (2024). Between continuous presents and disruptive futures: Identifying the ideological backbones of Global Environmental Scenarios. *Futures*, 103460.
- Le Billon, P. (2004). The geopolitical economy of 'resource wars.' *Geopolitics*, 9(1), 1–28.
- Le Billon, P., & Middeldorp, N. (2021). Empowerment or Imposition? Extractive Violence, Indigenous Peoples, and the Paradox of Prior Consultation. In *Our Extractive Age* (pp. 69–93). Routledge.
- Lerede, D., Nicoli, M., Savoldi, L., & Trotta, A. (2023). Analysis of the possible contribution of different nuclear fusion technologies to the global energy transition. *Energy Strategy Reviews*, 49, 101144.

- Li, M., Keyßer, L., Kikstra, J. S., Hickel, J., Brockway, P. E., Dai, N., Malik, A., & Lenzen, M. (2023). Integrated assessment modelling of degrowth scenarios for Australia. *Economic Systems Research*, 1–31.
- Lovelock, J. E., & Margulis, L. (1974). Atmospheric homeostasis by and for the biosphere: The Gaia hypothesis. *Tellus*, 26(1–2), 2–10.
- Lowder, S. K., Sánchez, M. V., & Bertini, R. (2021). Which farms feed the world and has farmland become more concentrated? *World Development*, 142, 105455.
- Lundquist, C., Hashimoto, S., Denboba, M. A., Peterson, G., Pereira, L., & Armenteras, D. (2021). *Operationalizing the Nature Futures Framework to catalyze the development of nature-future scenarios*.
- Maldonado-Torres, N. (2007). On the coloniality of being: Contributions to the development of a concept. *Cultural Studies*, 21(2–3), 240–270.
- Martinez-Alier, J. (2003). *The Environmentalism of the poor: A study of ecological conflicts and valuation*. Edward Elgar Publishing.
- Martinez-Alier, J. (2004). Ecological distribution conflicts and indicators of sustainability. *International Journal of Political Economy*, 34(1), 13–30.
- Martinez-Alier, J. (2013). Social metabolism, ecological distribution conflicts and languages of valuation. In *Beyond Reductionism* (pp. 35–61). Routledge.
- Martinez-Alier, J. (2021). Mapping ecological distribution conflicts: The EJAtlas. *The Extractive Industries and Society*, 8(4), 100883.
- Menton, M., Larrea, C., Latorre, S., Martinez-Alier, J., Peck, M., Temper, L., & Walter, M. (2020). Environmental justice and the SDGs: From synergies to gaps and contradictions. *Sustainability Science*, 15, 1621–1636.
- Merrie, A., Keys, P., Metian, M., & Österblom, H. (2018). Radical ocean futures-scenario development using science fiction prototyping. *Futures*, 95, 22–32.
- Metzger, M. J., Rounsevell, M. D., Van den Heiligenberg, H. A., Pérez-Soba, M., & Hardiman, P. S. (2010). How personal judgment influences scenario development: An example for future rural development in Europe. *Ecology and Society*, 15(2).
- Mignolo, W. D. (2013). Introduction: Coloniality of power and de-colonial thinking. *Globalization and the Decolonial Option*, 1–21.
- Moore, J. (2017). The Capitalocene, Part I: on the nature and origins of our ecological crisis. *The Journal of Peasant Studies*, 44(3), 594–630.
- Moore, J. (2018). The Capitalocene Part II: accumulation by appropriation and the centrality of unpaid work/energy. *The Journal of Peasant Studies*, 45(2), 237–279.
- Mora, O., Le Mouél, C., de Lattre-Gasquet, M., Donnars, C., Dumas, P., Réchauchère, O., Brunelle, T., Manceron, S., Marajo-Petitzon, E., & Moreau, C. (2020). Exploring the future of land use and food security: A new set of global scenarios. *PLoS One*, 15(7), e0235597.
- Mujezinovic, D. (2020). *The Global Industrial Metabolism of E-Waste Trade: A Marxian Ecological Economics Approach*. Lancaster University (United Kingdom).
- Ndlovu-Gatsheni, S. J. (2013). Perhaps decoloniality is the answer? Critical reflections on development from a decolonial epistemic perspective. *Africanus*, 43(2), 1–11.
- Nieto, J., Carpintero, Ó., Lobejón, L. F., & Miguel, L. J. (2020). An ecological macroeconomics model: The energy transition in the EU. *Energy Policy*, 145, 111726.
- Okpanachi, E., Ambe-Uva, T., & Fassih, A. (2022). Energy regime reconfiguration and just transitions in the Global South: Lessons for West Africa from Morocco's comparative experience. *Futures*, 139, 102934.
- Oksala, J. (2017). Feminism, Capitalism, and the Social Regulation of Sexuality. *Feminism, Capitalism, and Critique: Essays in Honor of Nancy Fraser*, 67–83.

- Okwuadimma, J. C., & Biereenu-Nnabugwu, M. (2021). Frantz Fanon's Theory of Alienation, Powerlessness and Apathetic Political Behaviour in the 2019 General Elections in Nigeria. *Socialscientia: Journal of Social Sciences and Humanities*, 6(3).
- O'Neill, B. C., Kriegler, E., Ebi, K. L., Kemp-Benedict, E., Riahi, K., Rothman, D. S., van Ruijven, B. J., van Vuuren, D. P., Birkmann, J., & Kok, K. (2017). The roads ahead: Narratives for shared socioeconomic pathways describing world futures in the 21st century. *Global Environmental Change*, 42, 169–180.
- O'Neill, B., Carter, T. R., Edmonds, J., Ebi, K. L., Hallegatte, S., Kemp-Benedict, E., Kriegler, E., Mearns, L., Moss, R., Riahi, K., Van Ruijven, B., & Van Vuuren, D. (2012). *Meeting Report of the Workshop on The Nature and Use of New Socioeconomic Pathways for Climate Change Research, Boulder, CO, November 2-4, 2011*.
- Österblom, H., Jouffray, J.-B., Folke, C., Crona, B., Troell, M., Merrie, A., & Rockström, J. (2015). Transnational corporations as 'keystone actors' in marine ecosystems. *PloS One*, 10(5), e0127533.
- Pereira, L., Asrar, G. R., Bhargava, R., Fisher, L. H., Hsu, A., Jabbour, J., Nel, J., Selomane, O., Sitas, N., & Trisos, C. (2021). Grounding global environmental assessments through bottom-up futures based on local practices and perspectives. *Sustainability Science*, 16(6), 1907–1922.
- Pereira, L., Crespo, G. O., Amon, D. J., Badhe, R., Bandeira, S., Bengtsson, F., Boettcher, M., Carmine, G., Cheung, W. W., & Chibwe, B. (2023). The living infinite: Envisioning futures for transformed human-nature relationships on the high seas. *Marine Policy*, 153, 105644.
- Phillips, P. (2018). *Giants: The global power elite*. Seven Stories Press.
- Quijano, A. (1999). Colonialidad del poder, cultura y conocimiento en América Latina. *Dispositio*, 24(51), 137–148.
- Quijano, A. (2000). Coloniality of power and Eurocentrism in Latin America. *International Sociology*, 15(2), 215–232.
- Ramcilovic-Suominen, S. (2022). Envisioning just transformations in and beyond the EU bioeconomy: Inspirations from decolonial environmental justice and degrowth. *Sustainability Science*, 1–16.
- Raskin, P., & Swart, R. (2020). Excluded futures: The continuity bias in scenario assessments. *Sustainable Earth*, 3(1), 1–5.
- Ravikumar, A., & Ojeda Del Arco, A. P. (2025). Have 'life plans' delivered on their transformative aspirations for Indigenous empowerment through conservation? Evidence from four watersheds in the Peruvian Amazon. *World Development*, 190, 106972.
<https://doi.org/10.1016/j.worlddev.2025.106972>
- Restrepo, E. (2018). Coloniality of power. *International Encyclopedia of Anthropology*, 1–6.
- Rodriguez, I. (2020). Latin American decolonial environmental justice. In *Environmental Justice* (pp. 78–93). Routledge.
- Rodríguez, I., & Inturias, M. L. (2018). Conflict transformation in indigenous peoples' territories: Doing environmental justice with a 'decolonial turn.' *Development Studies Research*, 5(1), 90–105.
- Saghai, Y. (2021). Subversive future seeks like-minded model: On the mismatch between visions of food sovereignty futures and quantified scenarios of global food futures. *Ethics & International Affairs*, 35(1), 51–67.
- Sallai, D., & Schnyder, G. (2021). What is "authoritarian" about authoritarian capitalism? The dual erosion of the private-public divide in state-dominated business systems. *Business & Society*, 60(6), 1312–1348.

- Samaniego-Rascón, D., da Silva, M. C. G., Ferreira, A. D., & Cabanillas-Lopez, R. E. (2019). Solar energy industry workers under climate change: A risk assessment of the level of heat stress experienced by a worker based on measured data. *Safety Science*, 118, 33–47.
- Santos, B. de S. (2018). *Justicia entre saberes: Epistemologías del Sur contra el epistemicidio*. Ediciones Morata.
- Schaal, T., Mitchell, M., Scheele, B. C., Ryan, P., & Hanspach, J. (2023). Using the three horizons approach to explore pathways towards positive futures for agricultural landscapes with rich biodiversity. *Sustainability Science*, 18(3), 1271–1289.
<https://doi.org/10.1007/s11625-022-01275-z>
- Scheidel, A., Del Bene, D., Liu, J., Navas, G., Mingorría, S., Demaria, F., Avila, S., Roy, B., Ertör, I., & Temper, L. (2020). Environmental conflicts and defenders: A global overview. *Global Environmental Change*, 63, 102104.
- Schmelzer, M. (2024). Without growth, everything is nothing': On the origins of growthism. In L. Eastwood & K. Heron (Eds.), *De Gruyter Handbook of Degrowth* (pp. 25–40). De Gruyter.
- Schmidt, P. M., & Peterson, M. J. (2009). Biodiversity conservation and indigenous land management in the era of self-determination. *Conservation Biology*, 23(6), 1458–1466.
- Schneiderman, D. (2022). International Investment Law and Discipline for the Indebted. *European Journal of International Law*, 33(1), 65–96.
- Scholte, J. A. (2014). Reinventing global democracy. *European Journal of International Relations*, 20(1), 3–28.
- Scholte, J. A. (2020). After liberal global democracy: New methodology for new praxis. *Fudan Journal of the Humanities and Social Sciences*, 13(1), 67–92.
- Sharpe, B., Hodgson, A., Leicester, G., Lyon, A., & Fazey, I. (2016). Three horizons: A pathways practice for transformation. *Ecology and Society*, 21(2). <https://doi.org/10.5751/ES-08388-210247>
- Sonter, L. J., Dade, M. C., Watson, J. E., & Valenta, R. K. (2020). Renewable energy production will exacerbate mining threats to biodiversity. *Nature Communications*, 11(1), 1–6.
- Sovacool, B. K. (2021). Who are the victims of low-carbon transitions? Towards a political ecology of climate change mitigation. *Energy Research & Social Science*, 73, 101916.
- Stoett, P. (2024). Plastic Waste Colonialism: A Typology of Global Toxicity. In *Plastic Waste Trade: A New Colonialist Means of Pollution Transfer* (pp. 3–15). Springer.
- Temper, L. (2019). Blocking pipelines, unsettling environmental justice: From rights of nature to responsibility to territory. *Local Environment*, 24(2), 94–112.
- Temper, L., Avila, S., Del Bene, D., Gobby, J., Kosoy, N., Le Billon, P., Martinez-Alier, J., Perkins, P., Roy, B., & Scheidel, A. (2020). Movements shaping climate futures: A systematic mapping of protests against fossil fuel and low-carbon energy projects. *Environmental Research Letters*, 15(12), 123004.
- UN. (2023). *The Sustainable Development Goals Report 2023: Special edition*.
<https://unstats.un.org/sdgs/report/2023/The-Sustainable-Development-Goals-Report-2023.pdf>
- UNDP & OPHI. (2022). *Global Multidimensional Poverty Index 2022: Unpacking Deprivation Bundles to Reduce Multidimensional Poverty*.
- Van Vuuren, D. P., Kok, M. T., Girod, B., Lucas, P. L., & de Vries, B. (2012). Scenarios in global environmental assessments: Key characteristics and lessons for future use. *Global Environmental Change*, 22(4), 884–895.
- Vieco, J. J. (2019). Los planes de vida y el desarrollo propio de los pueblos indígenas de la Amazonia y Orinoquia: Opciones alternativas al desarrollo, la modernidad y la

globalización. In Milcíades Vizcaíno (Ed.), *Ciencias sociales y humanas en la Orinoquia y la Amazonia* (pp. 159–220). Ediciones Universidad Cooperativa de Colombia.

Zajontz, T. (2022). Debt, distress, dispossession: Towards a critical political economy of Africa's financial dependency. *Review of African Political Economy*, 49(171), 173–183.

The Rise of the Global South: Quantifying Economic Development and Socio-Ecological Outcomes under Alternative World Orders

Abstract

The Global South occupies a pivotal position in the global sustainability transition, simultaneously facing disproportionate climate impacts and emerging as a key economic and political actor. This study presents a quantitative scenario analysis exploring how shifts in global power distributions between the Global North and South could shape socio-economic development and environmental outcomes throughout the 21st century. Using the integrated assessment model *MORDRED*, we simulate three global scenarios to assess alternative configurations of global hierarchy and their implications for a growth, living standards, and environmental pressures: *CSP (Center>Semiperiphery>Periphery): Historical legacy*, *SCP (Semiperiphery> Center>Periphery): Diverging development*, and *SPC (Semiperiphery>Periphery> Center): Reversed fortune*. Our results show that the rise of the Global South, particularly the semiperiphery, drives global economic expansion, accelerates the reduction of poverty, and improves human development indicators. However, these socio-economic gains are accompanied by steep increases in material extraction, bioenergy demand, and greenhouse gas emissions, leading to projected global warming of 3–5 °C by 2100 despite a 90%-95% greening of electricity and the global expansion of bioenergy. Stronger economic growth in the South not only drives urbanization and the disappearance of subsistence economies but also intensifies land-use competition, endangering ecosystems and the livelihoods of vulnerable communities. We conclude that a just and sustainable global transition requires not only energy and resource convergence at low levels but also a fundamental reconceptualization of development that transcends capitalist industrial paradigms. Future global scenario studies should integrate Southern perspectives to envision post-capitalist and post-growth pathways toward ecologically sustainable and just world orders.

Keywords

Global South; international system; Integrated assessment modeling; Socio-economic scenarios; sustainable development; climate change

Introduction

The Global South occupies a pivotal position in the global quest for sustainability. On the one hand, it is and will continue to be disproportionately affected by the adverse impacts of global environmental and climate change, including economic losses and forced displacement (Almulhim et al., 2024; Shan, 2023), despite its relatively small historical contribution to the global ecological crisis and the fact that per capita emissions in most Global South countries remain lower than those in the Global North (Matthews, 2016; Our World in Data, 2024). On the other hand, economic growth in the Global South has come at a considerable environmental cost, with the region now responsible for approximately 63% of global greenhouse gas (GHG) emissions (Fuhr, 2021). At the same time, the Global South has emerged as an innovation hub for sustainable practices and technologies and has become actively engaged in climate mitigation and adaptation efforts (Anguelovski et al., 2014; Frischmann et al., 2022; Khasru & Ambrizzi, 2023). The rise of the Global South also carries profound implications for the future of the world order, as emerging powers are already reshaping global governance, including development cooperation (Das & Janakiraman, 2026; Ghimire, 2018; Klingebiel, 2023).

Scenario development in the field of international relations (IR) can be considered a valuable tool that can be used to overcome the tendency to extrapolate the structural *status quo* into the future (Sus & Hadeed, 2020). It also provides a framework to address the political uncertainties arising from global environmental and economic transformations, in which the Global South plays an increasingly active role. Nevertheless, engagement of IR and IPE (international political economy) scholars with future studies remains limited. Only a few studies (e.g. Ansari et al., 2019; Bazilian et al., 2020) have developed energy futures that incorporate geopolitical aspects (Blondeel et al., 2024). Similarly, global climate and energy scenarios tend to overlook or underestimate the agency of Global South countries and collectives (Lauer, Carpintero, et al., 2025), despite the surge of research focusing on the Global South in the fields of sustainable development and climate change (Mazzega et al., 2025). This may partly reflect the continuing dominance of the Global North within the ‘future industry’ (Muiderman et al., 2023). One effort to remedy these imbalances is represented by the ‘Fast Sustainability Scenario’ (FST) set, particularly by ‘*FST4: Greener South-led development*’, and ‘*FST5 – sufficiency economies*’, in which emerging powers assume a central role in driving social, economic, environmental and geopolitical changes (Lauer, De Castro, et al., 2025).

Likewise, scenarios that explicitly explore global governance and changing power distributions mediated by politico-economic developments in both the Global South and the Global North remain underrepresented. At present, only a limited body of work focuses on future governance-related themes and power struggles, such as the future of development cooperation (Klingebiel & Sumner, 2025), future governance in the Antarctica (Frame et al., 2022), different state futures in the Global South (Cilliers & van Rooyen, 2025) and alternative global governance scenarios that focus especially on struggles within the Global South (Cruz, 2015). These scenarios often consider the environment as a direct or indirect driver interacting with economic, social, and technological developments. However, the resulting futures are predominantly qualitative and have not been systematically examined through quantitative modeling.

To address this gap, this article presents a quantitative scenario analysis that explores the socio-economic developments associated with profound shifts in the power distribution between the Global North and the Global South, as well as the implications of these shifts for global environmental dynamics. Specifically, we address three guiding questions:

1. Which macroeconomic changes could characterize a shifting power distribution between world regions?
2. What might different macroeconomic developments imply for the living standards and ways of life of populations in different world regions?
3. How could shifts in the power distribution between the Global North and South influence future changes in anthropogenic pressures on planetary systems?

Our study constitutes a first attempt to bridge the fields of IPE, global environmental and climate change research, future studies and system dynamics modeling by representing possible global socio-economic and environmental futures with a special focus on North-South relationships through an integrated assessment model (IAM).

1. Methods

In this section, we provide an overview of the model used for the scenario analysis and describe the characteristics of the quantified scenarios.

1.1. Model

The IAM selected for our scenario analysis is *MORDRED* (Model Of Resource Distribution and Resilient Economic Development), a system dynamics model consisting of several linked sub-modules that represent different aspects of the global system. These include the world population, global economic activity, the land–energy–climate system, and the environmental impacts of economic production, such as air pollution, material extraction, and GHG emissions.

The center of MORDRED is constituted by a global input–output model that projects future economic developments across 25 sectors, based on scenario-dependent assumptions regarding future consumption growth rates. Technological development is represented as changes in the input coefficients of the model’s A matrix. The model also includes a simplified representation of a subsistence sector that operates outside the global economy. This sector is characterized by low productivity, zero material inputs from the world economy, and minimal environmental pollution. It sustains the poorest segments of the global population living at the margins of the global capitalist economy.

The demographic module of MORDRED consists of 20 age groups (0–4 years, 5–9 years, ..., 95+ years) and is used to simulate demographic developments in three world regions: the *center*, encompassing all high-income countries, the *periphery*, covering all lower-income and low-income countries, and the *semiperiphery*, including the remaining upper-middle-income countries. The model also calculates migration flows between the global economy and the subsistence sector within each region. All individuals living under subsistence conditions belong to the ‘subsistence class’, irrespective of the region. The remaining population—fully integrated into the global economy and participating in productive processes—is divided into three social classes within each region: the upper class, comprising the richest 20% of the population; the lower class, representing the poorest 30%, and the middle class with the remaining half of the population. Per capita consumption within these classes changes dynamically during simulations, influencing age-specific fertility and mortality rates.

Economic production in the world economy depends on several input factors, which vary across the 25 sectors. These include labor hours, capital, intermediate products, energy, land, and water. The model simultaneously calculates the environmental implications of economic activity

through ‘Earth intensities’ (e.g., land, water, mineral use). Impacts on the global climate system are simulated in the climate module, primarily driven by GHG emissions from fossil fuel combustion. Rising global temperatures feed back into the model through climate damage factors, which can be activated or deactivated depending on the scenario.

When required input factors are insufficient to produce the output needed to meet industrial and final demand, demand is reduced in subsequent time steps, resulting in economic contraction. However, the model can also simulate scenarios in which the scarcity of one or more input factors does not constrain economic development.

The combination of global scale and regional disaggregation of socio-demographic variables renders MORDRED particularly suitable for our study, as it allows us to track changes in both global economic–biophysical systems and sub-global development pathways. Comprehensive documentation of MORDRED, including the sectoral disaggregation, is available on GitHub (Lauer & Llases, 2025).

1.2. Scenarios

Although our scenario analysis focuses especially on development pathways in the Global South, the literature emphasizes that the Global South is not a homogeneous geopolitical, economic, social, or cultural block (Bull & Banik, 2025). There are huge disparities in economic power among Global South countries, and positions on global environmental and climate governance diverge (Mohan, 2025). However, what Global South countries have in common is a shared a common colonial heritage and/or a rather unfavorable position in the global economic order (Mazzega et al., 2025). To avoid constructing an artificial North–South dichotomy, we retain MORDRED’s division of the world into three regions—center, semiperiphery, and periphery—whose countries occupy distinct positions in the global hierarchy of economic power, reflected in differing income levels. Although the current power distribution and wealth distribution is better characterized as ‘quadrifocal’, reflected in a lower periphery, an upper periphery, the semi-periphery, and core regions (Karatasli & Kumral, 2017) for reasons of data availability and reliability we refrain from sub-dividing the periphery.

Our scenarios reflect a realist and critical traditions in IR and IPE since we focus on politico-economic power differences between regional blocs that form a hierarchical world order, despite the absence of a global monopoly of violence (cf. Beckmann & Erpul, 2024). By varying the relative positions of the center, semiperiphery, and periphery within the global politico-economic hierarchy, we derive our scenarios. In theory, six scenarios resulting from six combinations of hierarchical order are possible:

1. Center > Semiperiphery > Periphery (CSP) – *Historical legacy*

This scenario reflects the current hierarchy, characterized by considerable consumption per capita differences between the three world regions in the initial moment of the simulation that were derived based on global consumption inequality estimates (Lahoti et al., 2016). Given that this power hierarchy has persisted since the end of the Second World War, evolving from a liberal to a neoliberal international order (Ramirez, 2025) a future in which this hierarchy is maintained throughout the 21st century cannot be ruled out. Thus, in the CSP scenario, the center maintains substantial control over the world system despite its relatively small population, enjoying disproportionately high consumption levels. Cooperation between countries occurs primarily along a North-

South axis and the center is able to implicitly shape access to resources, which can create neocolonial dynamics of control and exploitation.

2. **Semiperiphery > Center > Periphery (SCP) – *Diverging development***

This configuration reflects ongoing trends of secular stagnation in high-income countries, strong growth in ‘emerging economies’ and low growth or decline in the world’s poorest regions (Carlos Bresser-Pereira, 2019; Fatton, 2013; Hurrell & Sengupta, 2012). In this global future, the divide widens between Global South countries that achieve industrialization and those that remain marginalized. International cooperation increasingly takes on a South–South character, as the semiperiphery seeks both to promote development in the periphery and to secure privileged access to its resources (Bull & Banik, 2025; Ghimire, 2018). Meanwhile, the center strives to avoid further losses of global influence.

3. **Semiperiphery > Periphery > Center (SPC) – *Reversed fortune***

In this scenario, both the semiperiphery and periphery succeed in leveraging the global economic system to their advantage, while the center fails to revive growth and gradually becomes trapped in an unfavorable position as capital flows start to shift away from the center. In this scenario, ‘development cooperation’ would acquire a South-to-North character as the current center becomes the future periphery. Although this scenario appears less likely at present, it remains plausible and yields dynamics that are rarely explored in the literature.

The remaining possible combinations (C>P>S, P>C>S, P>S>C) are deemed highly improbable and are therefore excluded from analysis.

We are interested in ‘business as usual’ scenarios lacking fundamental changes towards sustainability, given that those changes have not occurred during the last 50 years despite dire warnings and heated debates about the transgression of biophysical limits (Meadows et al., 1972). Therefore, all scenarios assume continuous economic growth along industrialization- and extraction-based development pathways. However, it is also assumed that the most powerful geopolitical actors invest in developing green technologies and implementing green structural changes. Given that the semiperiphery and periphery together represent the vast majority of the world’s population, their growing economic and political weight is expected to drive large-scale environmental policy implementation. Thus, SPC and SCP are associated with more extensive green structural transformation than CSP.

Importantly, in this scenario analysis we focus exclusively on the impacts of economic activity on planetary biophysical systems, rather than the reverse effects of altered planetary systems on the global economy—a feedback recognized as crucial for future international politico-economic developments (Katz-Rosene, 2019). This simplification reduces analytical complexity while clarifying the environmental implications of economic growth in the absence of strict biophysical limits. Accordingly, we deactivate the land scarcity feedback in the model and adopt very optimistic assumptions regarding the availability of fossil resources (BGR, 2020) in all scenarios.

Simulations project model variables to the end of the 21st century based on MORDRED version 1.1.1, which features exogenously defined consumption inequality pathways and includes an urbanization indicator. Table 1 provides an overview of the main qualitative and quantitative assumptions for the three scenarios.

Driver	CSP	SCP	SPC
International cooperation paradigm	North-South cooperation.	South-South cooperation.	South-South & South-North cooperation.
Economic development paradigm	Industrial, growth-based, extractivism, high dependency on wage labor.		
	$\Delta \frac{K}{x} = 0$ (constant sectoral capital intensities)	$\Delta_{2100-2019} \frac{K}{x} = 1.2$	$\Delta_{2100-2019} \frac{K}{x} = 1.3$
	Constant material and mineral intensities of the economy (constant input coefficients for the material extraction sector (sector 4)). $\Delta a_{4,1} = \Delta a_{4,2} = \Delta a_{4,3} = \dots = \Delta a_{4,25} = 0$ <i>annual working hours = 2080</i> <i>maximum participation rate = 0.9</i>		
Industrial development	Weak in P, strong in S, medium in C.	Strong in S, almost stagnant in C, Weak in P.	Strong in P & S, deindustrialization in C.
	$g_{C,U20} = 1.48\%$ $g_{C,M50} = 1.24\%$ $g_{C,L30} = 1.23\%$ $g_{S,U20} = 2.20\%$ $g_{S,M50} = 2.71\%$ $g_{S,L30} = 2.70\%$ $g_{S,U20} = 0.85\%$ $g_{S,M50} = 1.24\%$ $g_{S,L30} = 1.52\%$	$g_{C,U20} = 1.39\%$ $g_{C,M50} = 1.30\%$ $g_{C,L30} = 1.02\%$ $g_{S,U20} = 3.15\%$ $g_{S,M50} = 3.66\%$ $g_{S,L30} = 3.65\%$ $g_{S,U20} = 2.16\%$ $g_{S,M50} = 2.16\%$ $g_{S,L30} = 2.16\%$	$g_{C,U20} = -0.19\%$ $g_{C,M50} = 0.06\%$ $g_{C,L30} = 0.19\%$ $g_{S,U20} = 4.07\%$ $g_{S,M50} = 4.58\%$ $g_{S,L30} = 4.86\%$ $g_{S,U20} = 2.88\%$ $g_{S,M50} = 3.13\%$ $g_{S,L30} = 3.04\%$
International inequality	Moderate decrease (low convergence).	Decreasing (strong convergence).	Decreasing (medium convergence).
	$g_{C,\emptyset} = 1.29\%$ $g_{S,\emptyset} = 2.60\%$	$g_{C,\emptyset} = 1.23\%$ $g_{S,\emptyset} = 3.55\%$	$g_{C,\emptyset} = 0.05\%$ $g_{S,\emptyset} = 4.56\%$

	$g_{P,\emptyset} = 1.25\%$	$g_{P,\emptyset} = 2.16\%$	$g_{P,\emptyset} = 3.05\%$
Internal inequality	C: slightly increasing S: slightly decreasing P: decreasing.	C: increasing S: slightly decreasing P: constant.	C: decreasing S: decreasing P: slightly decreasing.
	$g_{C,U20} - g_{C,M50} = 0.24$ $g_{C,L30} - g_{C,M50} = -0.01$ $g_{S,U20} - g_{S,M50} = -0.51$ $g_{S,L30} - g_{S,M50} = -0.01$ $g_{S,U20} - g_{S,M50} = -0.39$ $g_{S,L30} - g_{S,M50} = 0.28$	$g_{C,U20} - g_{C,M50} = 0.09$ $g_{C,L30} - g_{C,M50} = -0.28$ $g_{S,U20} - g_{S,M50} = -0.51$ $g_{S,L30} - g_{S,M50} = -0.01$ $g_{S,U20} - g_{S,M50} = 0$ $g_{S,L30} - g_{S,M50} = 0$	$g_{C,U20} - g_{C,M50} = -0.25$ $g_{C,L30} - g_{C,M50} = 0.13$ $g_{S,U20} - g_{S,M50} = -0.51$ $g_{S,L30} - g_{S,M50} = 0.28$ $g_{S,U20} - g_{S,M50} = -0.25$ $g_{S,L30} - g_{S,M50} = -0.09$
Control of resource access (result of industrial development and inequality)	C>S>P	S>C>P	S>P>C
Energy transition, technological development and changes in final demand	Improvement of industrial processes: 10%. Medium greening of electricity mix: reduction of fossil electricity inputs by 90%. Low electrification: Reduction of non-electric energy inputs by 20%. Moderate greening of non-electric energy: substitution of 20% of fossil energy inputs with bioenergy (all changes refer to 2100 compared to 2019 and to both industry and final demand).	Improvement of industrial processes: 10%. Medium greening of electricity mix: reduction of fossil electricity inputs by 90%. Moderate electrification: Reduction of non-electric energy inputs by 25%. Medium greening of non-electric energy: substitution of 25% of fossil energy inputs with bioenergy.	Improvement of industrial processes: 10%. High greening of electricity mix: reduction of fossil electricity inputs by 95%. Medium electrification: Reduction of non-electric energy inputs by 30%. High greening of non-electric energy: substitution of 30% of fossil energy inputs with bioenergy.
Sectoral labor productivity development	Medium: Global sectoral labor productivities by 2100 approach labor productivity levels of the center in 2019.	High: 20% higher labor productivities than in CSP.	High: 50% higher labor productivities than in CSP.

Land productivity & land scarcity	Land scarcity feedback not activated, i.e. no limits to growth due to potential land shortages. High implicit land productivity increases.	
Control of land in rural areas	Prioritization of land demands from world economy.	Equal priority of land demands from world economy and subsistence sector.
	Land types required by global economy > land required by subsistence sector, primary forest > other ecosystems.	Land types required by global economy & subsistence sector > primary forest > other ecosystems.
Forest protection policy	Medium.	
	22200000 km ² of forests protected (50% primary forest, 50% secondary forest).	
Fossil resource availability & accessibility	High.	
	Ultimately recoverable fossil resources: 495390 EJ. Favorable extraction cost estimation.	
Climate sensitivity	Simulations with low, medium and high sensitivity of the climate system to anthropogenic perturbations.	
Adverse environmental impacts	No climate damages activated.	
Migration dynamics between subsistence and world economy	Moderate willingness to migrate from subsistence to world economy; low willingness to migrate from world economy to subsistence. Willingness to integrate into world economy increases linearly with the difference in the per capita consumption between the poorest class integrated into the world economy and the monetized consumption of the subsistence class within a world region, reaching 100% when the consumption inside the world economy is 5 times the subsistence consumption. Willingness to migrate to the subsistence economy decreases linearly with the difference in the per capita consumption between the poorest class integrated into the world economy and the consumption of the subsistence class within a world region.	

Table 1: Main qualitative and quantitative scenario assumptions.

2. Results

This section presents the key quantitative outcomes for the CSP, SCP, and SPC scenarios. Results are organized into three thematic areas: macroeconomic changes, socio-demographic developments, and environmental impacts.

2.1. Macroeconomic changes in the world system

In all scenarios, global economic output—including the production of intermediate and final goods—rises continuously throughout the simulation. As shown in Figure 1a, different power constellations in the international system are linked to distinct levels of overall economic growth. While global output triples during the 80-year simulation in CSP – Historical legacy, it increases nearly sixfold in SCP – Diverging development, and sevenfold in SPC – Reversed fortune. These results indicate that shifts away from the current power hierarchy stimulate global economic expansion and accelerate the development of productive capacities.

Interestingly, in the SPC scenario, desired consumption growth rates are so high that during the final two decades total demand can no longer be met with the available labor supply, even though both sectoral labor productivity and the global workforce grow faster than in the other scenarios. This leads to a slowdown in economic growth toward the end of the 21st century, illustrating that, even in the absence of strong biophysical limits to growth, economic development can still be constrained by labor availability.

Differences in total output growth between the scenarios are mirrored by variations in public (government) and private (household) consumption at the global level. However, at the regional level, these variables do not necessarily follow global trends (Figure 1b,c). Public consumption in the center grows by approximately 84% in both the CSP and SCP scenarios but declines by 56% in SPC. By the end of the century, government consumption in the semiperiphery exceeds that of other world regions in all scenarios. In CSP, public consumption in the semiperiphery is 1.6 times that of the center and 4.8 times that of the periphery by 2100; in SCP, the ratios are 3.6 and 4.4; and in SPC, 22 and 4.9 times higher, respectively.

In the periphery, public consumption quadruples between 2020 and 2100 in CSP and increases 11.5-fold in SPC. However, even with these high growth rates, government consumption in the periphery at the end of the century is only 9.5% higher than that of the center in CSP. This makes SPC the scenario with the greatest divergence in public consumption, particularly during the second half of the simulation. In 2060, public consumption in the center falls to 6.5 trillion €, slightly below that of the periphery (7 trillion €), while the semiperiphery rises to 23 trillion €. By 2100, the center's spending drops by another 3.1 trillion €, whereas the periphery more than doubles to 15.6 trillion €, and the semiperiphery more than triples to 76.2 trillion €, compared to their 2060 levels.

A similar pattern is observed for private consumption. In SPC, private consumption in 2100 reaches 217 trillion € in the semiperiphery, 74 trillion € in the periphery, and 11.6 trillion € in the center. Although the center's total household consumption decreases by 57% compared to the start of the simulation, it remains comparable to the semiperiphery's total in 2020 and nearly doubles that of the periphery at the beginning of the simulation, despite its smaller population size. Consumption patterns in the other scenarios show consistent growth across all regions, though faster in the semiperiphery and periphery under SCP than under CSP.

An analysis of public and private consumption at the regional level reveals that the slowdown in global output in SPC is primarily driven by reduced consumption growth in the periphery, while the semiperiphery continues to expand despite global labor shortages. Differences in workforce evolution are minor for the center and semiperiphery, both of which experience a continuous decline from 2035 onward in all scenarios. In contrast, the periphery's workforce peaks latest in CSP and earliest in SPC. By the end of the century, the working population in the periphery ranges from 3.21 billion (CSP) to 2.89 billion (SPC), with SCP falling in between (3.05 billion) (Figure 1d).

The size of the potential workforce—defined as the population integrated into the global economy and aged 15–64—serves as an indicator of a region's economic and political power, as it represents both a source of capital accumulation and of potential military recruitment. Thus, the relatively large workforce in CSP somewhat contradicts the periphery's weak global position. However, in this scenario, the periphery lacks the organizational capacity to strategically deploy its labor force, which instead functions as cheap labor stabilizing the global regime of production.

The combination of declining government and household consumption and a shrinking workforce renders the former center economically insignificant in SPC. Since it neither offers a big market nor a large and cheap working force or significant exploitable resources, this implies a strong need for the center to specialize in high-skill industries producing rare, high-value goods. Nonetheless, even in the CSP and SCP scenarios, the Global North is expected to lose relative power when considering the aggregated economic potential of the Global South.

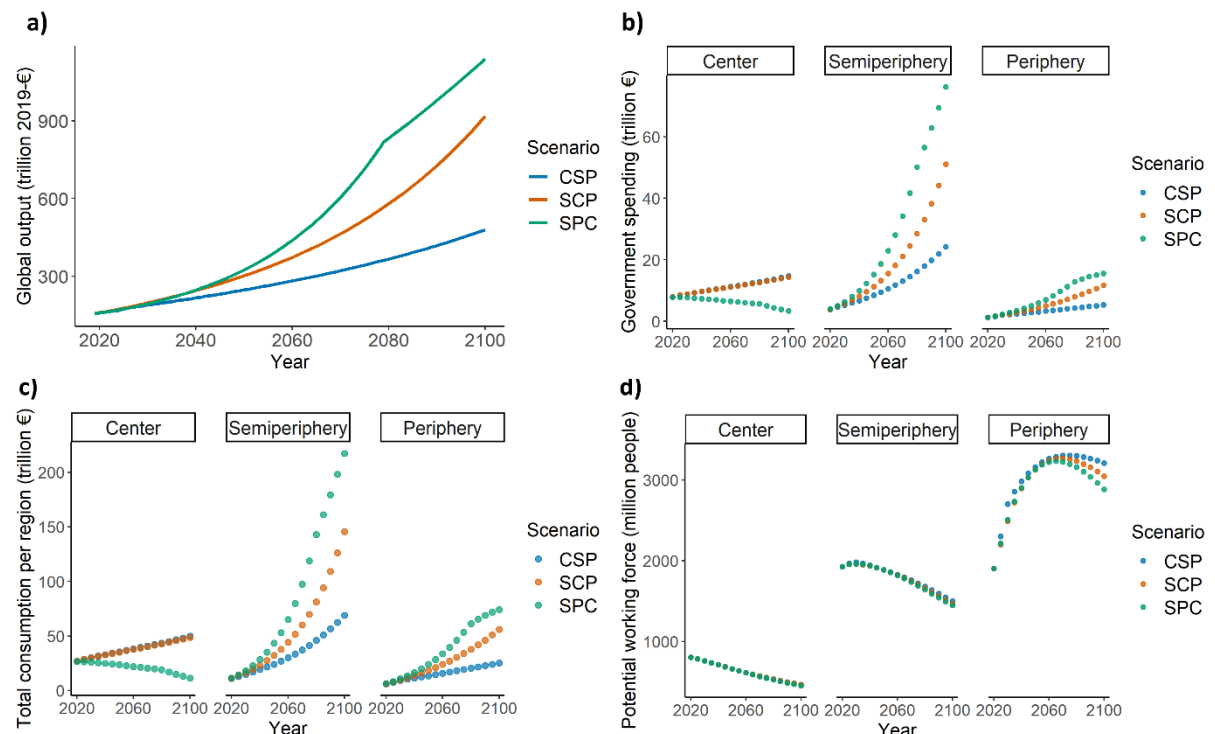


Figure 1: a) Annual world output, b) public spending, c) total household consumption and d) potential working force per world region in the CSP (blue), SCP (orange) and SPC (green) scenario.

2.2. Development indicators

Rising living standards among the poorest 30% of the semiperiphery and periphery in SCP and SPC lead to a continuous decline in the number of people dependent on the subsistence economy (Figure 2b). By 2050, over 90% of the subsistence population has transitioned into the global economy, and by 2060, the subsistence sector has virtually disappeared in all scenarios. The urbanization indicator rises from below 0.5 to 0.8, suggesting a highly urbanized Global South characterized by diminished alternative livelihoods and a nearly complete integration of workers into the global accumulation regime.

In the CSP scenario, limited protection for land used by the subsistence class leads to the integration of subsistence land into the global economy as industrial demand for land increases. Populations previously reliant on these territories are forced to join the global labor force, pointing to processes of expropriation, capitalization, and industrialization of land driven by capitalist expansion.

Economic growth also increases public expenditure on education and health, although developments differ by region and scenario. In the center, per capita public spending on these sectors more than doubles in CSP and SCP but stagnates in SPC, declining in the final two decades. In the semiperiphery, declining population combined with strong economic growth produces an increase in per capita spending across all scenarios, most notably in SPC, where it reaches far higher levels than the other regions (Figure 2a). In the periphery, per capita spending rises modestly in CSP—by 78 € between 2020 and 2060, and by 124 € between 2060 and 2100. In contrast, spending increases by 646 € in SCP and 940 € in SPC. While per capita expenditure in the semiperiphery reaches and surpasses the center's initial level between 2055 (SPC) and 2085 (CSP), the periphery does not attain the center's initial values in any scenario.

High growth rates combined with declining inequality in the semiperiphery drive exponential increases in per capita consumption among the poorest 30%. In 2060, annual per capita consumption in this class ranges from 3,800 € to 9,000 €, and by 2100, from 11,000 € to nearly 43,000 €. In contrast, consumption among the poorest 30% of the periphery ranges from 3,000 € to 7,350 € in 2100 (Figure 2c). The relatively high consumption of poorer classes in SPC contributes to the labor scarcity observed in that scenario: once lower-class consumption rises sufficiently, there are no longer large low-consuming labor groups available to sustain unequal global labor exchanges, limiting the model's ability to meet total demand.

Across all scenarios, public spending, rising consumption of the poorest classes, and declining subsistence populations lead to the global eradication of extreme poverty within the first half of the simulation. Although per capita consumption in the center declines in SPC, this does not translate into an increase in extreme poverty.

Nevertheless, regional disparities in consumption and living standards persist throughout the century, resulting in differences in life expectancy. Child mortality in the center remains low in all scenarios. In the semiperiphery, child mortality declines rapidly in the early decades, reaching the center's level by around 2065 in SPC, 2075 in SCP, and 2100 in CSP (Figure 2d). The periphery shows the highest initial child mortality, and although absolute reductions are greatest in this world region, convergence with the center's levels is achieved only in SPC. In SCP and CSP, the periphery's child mortality index remains 13% and 94% higher than that of the center by 2100.

Unlike child mortality, the adult mortality rate in the center differs between the scenarios and increases during the last decades of the SPC simulation while it continues to fall in the CSP and SCP scenarios (Figure 2e). By 2100, adult mortality in the center is still lower than in the periphery but higher than in the semiperiphery, signaling a relative decline in living standards that would be even more pronounced for the middle and lower classes if there was no reduction in internal inequality in this scenario. In the semiperiphery and periphery, adult mortality declines continuously, with faster improvements in SCP and SPC than in CSP. In CSP, the adult mortality index in the periphery is still 1.9 times that of the semiperiphery and 3.9 times that of the center in 2060; by 2100 it remains 3.2 times that of the center and twice the level observed in SPC. In the semiperiphery, adult mortality approaches the level of the center by the end of the 21st century in SCP but convergence is incomplete in CSP.

Due to demographic changes, the average age of the population dependent on the global economy increases in all regions throughout the 21st century. However, population aging occurs more slowly in the semiperiphery and periphery under CSP and SCP because of higher birth rates associated with lower consumption levels (Figure 2f).

Overall, the results indicate that changes in the global power distribution away from the status quo benefit socio-economic development in the Global South, reflected in an earlier elimination of extreme poverty, higher living standards and lower child and adult mortality.

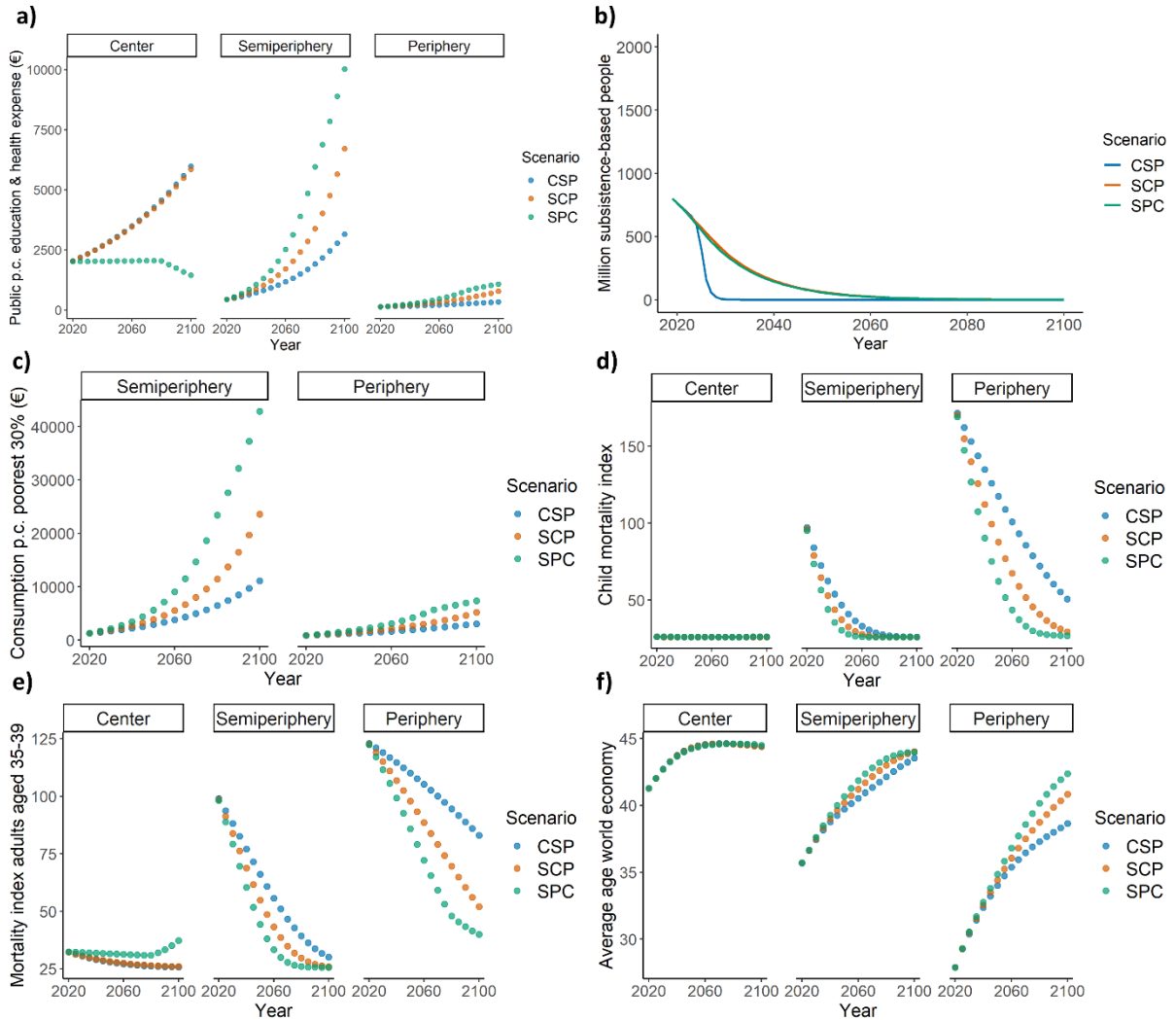


Figure 2: a) Public per capita expenses in the health and education sector in every world region, b) people depending on subsistence economies, c) consumption of the lower classes in the semiperiphery and periphery, d) child mortality index per world region (calculated with the initial child mortality rate of the semiperiphery), e) mortality index for adults per world region, based on mortality rates of adults aged 35-39, f) average age in the world economy at the regional level in the CSP (blue), SCP (orange) and SPC (green) scenario.

2.3. Environmental indicators

Environmental impacts can be classified into material extraction (Figure 3) and climate-related impacts (Figure 4).

Since all scenarios maintain an extractivist development paradigm, the production of biomass, bulk materials, and precious metals increases regardless of future power configurations (Figure 3a-c). Nevertheless, the socio-economic and political rise to power of the Global South is clearly linked to significantly higher levels of extractive activity. Global industrial roundwood production more than triples in CSP and increases fivefold in SCP. The emerging labor scarcity in SPC leads to lower increases in material extraction towards the end of the 21st century but roundwood production nevertheless increases 6-fold in the SPC scenario. Given that industrial wood extraction is linked to deforestation and biodiversity loss (Fuller et al., 2019; Goodman et al., 2024), these results suggest intensifying pressures on forest ecosystems during the 21st century.

The same pattern is observed for bulk materials such as aluminum and salt, as well as for precious metals like gold and silver. Most of the increase in extraction occurs in the second half of the simulation: between 2060 and 2100, annual aluminum and salt production rises by 83 Mt and 370 Mt in CSP, 268 Mt and 1,187 Mt in SCP, and 357 Mt and 1,551 Mt in SPC. In the same period, gold and silver production increases by 70% and 98 % in CSP, by 160% and 225% in SCP, and by 172% and 254 % in SPC, respectively.

The production levels of bulk materials reached mid-century and beyond make current extraction levels appear marginal (Figure 3b). Given the multiple types of water and air pollution linked to aluminum and salt production that can affect ecosystems as well as human health (Brough & Jouhara, 2020; Ekrami et al., 2021; Ocholla et al., 2013) the simulation outcomes point to an increased risk of ecosystem degradation and environmental distribution conflicts in the future.

Cumulatively, over the 80-years simulation more than 24% (CSP), 37% (SCP) and 48% (SPC) of the ultimately available gold resources and more than 22% (CSP), 37% (SCP) and 49% (SPC) of the ultimately available silver resources, as estimated by Henckens (2021), are extracted. For copper, between 30% and 63% of ultimately available resources are consumed. Although the simulations do not account for historical extraction or rising costs as ore grades decline, even with high technological progress, meeting mineral demand beyond the 21st century appears uncertain. This underscores the importance of recycling and material-efficiency policies, especially under scenarios where the Global South gains power and economic weight.

Another important type of material extraction comes from the fossil fuels sector given the material use of fossil resources. While coal plays a relatively minor role as industrial feedstock, the material use of natural gas and especially of oil increases strongly (Figure 3d). Thus, the non-material use of fossil resources creates a continued dependency on the fossil sector even in scenarios with a higher decarbonization rate than the scenarios simulated here.

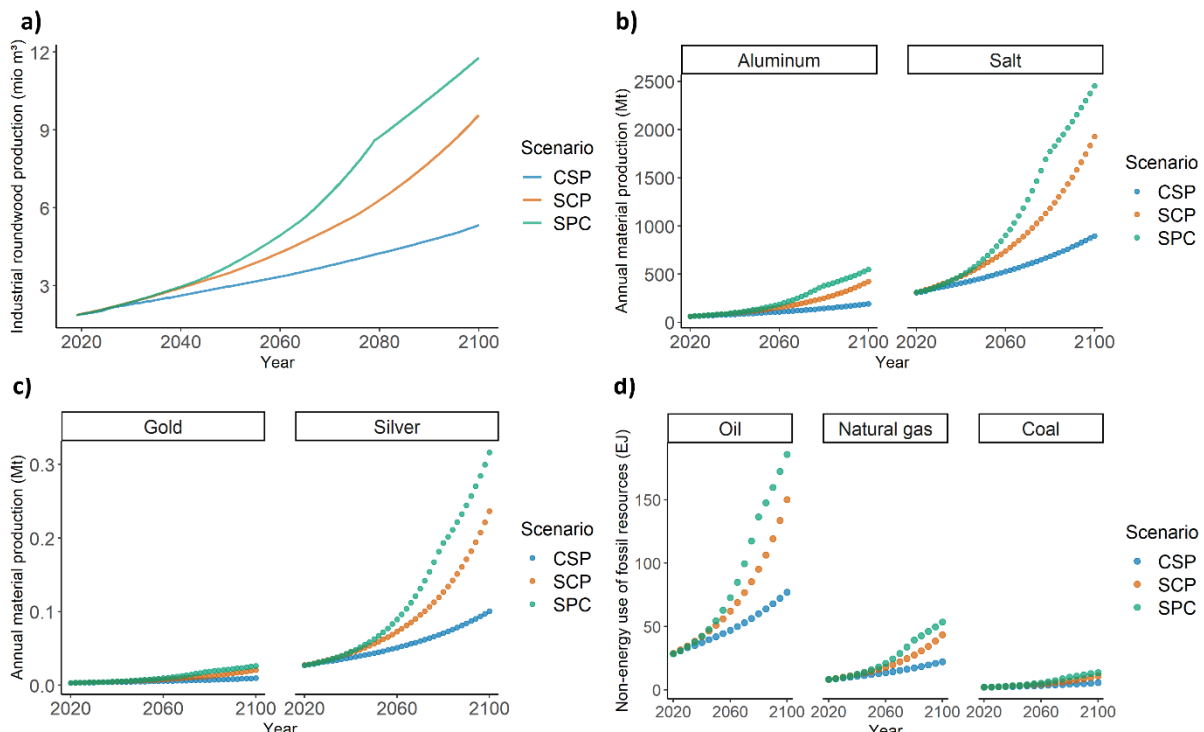


Figure 3: a) Global industrial roundwood production, b) global production of aluminum and salt, c) global production of gold and silver, d) global non-energy use of fossil resources in the CSP (blue), SCP (orange) and SPC (green) scenario.

By aggregating fossil resource extraction for energetic and material use we derive the projected changes in total fossil resource extraction during the scenarios (Figure 4a). While the extraction of oil and natural gas increases in all scenarios, coal extraction declines in the CSP scenario and stabilizes in the second half of the SPC scenario. As oil demand remains strong but reserves are more limited than for coal (BGR, 2020), future technological innovation will be crucial to prevent growth constraints from oil depletion.

Moderate environmental policies in all scenarios lead to a gradual replacement of fossil energy by electricity and biomass-based energy (Figure 4a). Although renewable energy use increases most in SPC and least in CSP, the latter produces the lowest GHG emissions overall. Assuming constant non-combustion emission intensities, annual emissions rise from 50 Gt CO₂-equivalents to 79 Gt in CSP, 142 Gt in SCP, and 163 Gt in SPC. If non-combustion-related emission intensities decrease by 40% by 2100, end-of-century emissions are 16 Gt (CSP), 15 Gt (SCP), and 36 Gt (SPC) lower—highlighting the importance of mitigating industrial emissions from CH₄, N₂O, SF₆, HFCs and PFCs.

The larger population size of the semiperiphery and the periphery is the main driver of total consumption demand in SCP and SPC. The resulting increase in the scale of economic activity results in greater demand for fossil energy resources that are not offset by the higher rate of decarbonization in those scenarios, compared to CSP. In the latter, the feedback effect between lower consumption levels and higher birth rates leads to a slower decline in the population size of the periphery and results in a somewhat higher emission pathway.

Simulated emissions correspond to an increase in global mean temperature of 3.06°C - 5.15°C by 2100 relative to the pre-industrial period, depending on assumptions regarding non-combustion GHG intensity improvements and natural climate feedbacks.

Thus, under a conventional development paradigm with moderate environmental ambition, higher living standards for the Global South are accompanied by substantially greater anthropogenic pressure on the global environment. The resulting destabilization of planetary systems (IPCC, 2021, 2022; Richardson et al., 2023) risks amplifying geopolitical tensions in the global system stemming from the Global South's rise to power in the SCP and the SPC scenario (Hurrell & Sengupta, 2012; Moore, 2024).

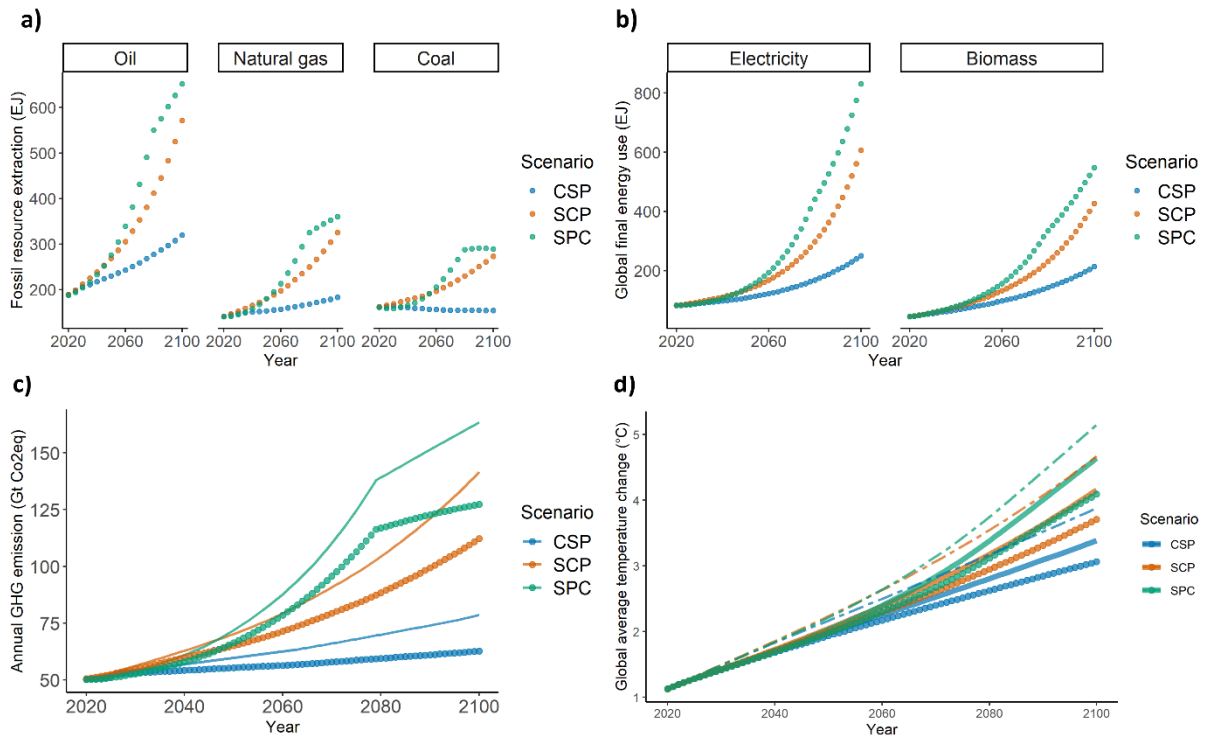


Figure 4: Changes in model variables in the CSP (blue), SCP (orange) and SPC (green) scenario. a) Global extraction of oil, natural gas and coal (given in EJ of primary energy), b) global electricity and biomass-based energy, c) world annual GHG emissions and d) global average temperature change with respect to 1850. Dots describe changes in simulations with falling GHG intensities for non-combustion-related emissions and without climate feedbacks; lines describes changes in simulations with constant GHG intensities for non-combustion-related emissions and without climate feedbacks; dashed lines describe changes in simulations with constant GHG intensities and with feedbacks within the climate systems.

3. Discussion

Our simulations explore quantitative dynamics that might accompany or signal profound changes in world orders and international power distribution due to the rise of the Global South, and, thus, constitute an attempt to complement qualitative scenario analyses in the field of IR and IPE with the additional insights that can be gained by employing modeling tools.

Nevertheless, our results must be interpreted in the context of the specific scenario assumptions made and must consider the structural features of the model used. Hence, we want to stress that the projected socio-economic and biophysical changes result from the assumption of material-intensive development, combined with the implementation of concrete green technologies that can be represented through the model's input-output structure. Our scenario analysis excludes green technologies that are not (yet) scalable or come with strong socio-ecological risks, such as carbon capture and storage (CCS), bioenergy with carbon capture and storage (BECCS), large-scale geoengineering or nuclear fusion (Braun et al., 2025; Gi et al., 2020; Günther & Ekardt, 2022; Parson & Reynolds, 2021; Sekera & Lichtenberger, 2020; Surprise, 2020). Likewise, the MORDRED model is not capable of representing new patterns of cooperation and competition that can be expected under scenarios of changing world orders. Especially, intensifying geopolitical tensions will impact future technological development, the transformation of global energy systems and climate politics. While some scholars anticipate a deceleration of mitigation efforts driven by diminished international cooperation, altered trade dynamics, diversion of financial resources, military-related emissions, and asset destruction (Block et al., 2025) others acknowledge a multitude of risks but also contend that competitive pressures may stimulate

technological innovation and increased investment in renewable energy to enhance national energy security (Blondeel et al., 2024; Moore, 2024).

Nevertheless, we hold that, overall, the growing tensions in the international system associated with a potential rise of the emerging powers among the Global South, will act as an obstacle to achieving levels of climate mitigation significantly higher than what has been simulated in the present study, especially because of the growth-enhancing effect of competition. As the scenario results show, the scale effect dominates over the effects of changes in technology and in the economy's sectoral composition, and, thus, more growth will imply a higher level of global warming.

Importantly, scenario trajectories are not only sensitive to dynamics that are presently not represented in MORDRED, such as migration, interregional trade, social conflicts and wars, but also to biophysical feedbacks that have been deactivated for the present analysis (see methods section). One consequence of this modeling decision is a relative neglect of the simulations for future land-related developments and risks. For example, if fast and continuous land productivity improvements in the Global South can no longer be maintained due to adverse effects of environmental degradation and climate change, the availability of land will become a key limiting factor to global economic development, slowing down the rise of the Global South.

In all three scenarios, rising material extraction and increasing demand for bioenergy imply strong pressures on territories in the Global South, potentially endangering the livelihoods of vulnerable socio-economic groups such as Indigenous and peasant communities (Owen, Kemp, Harris, et al., 2022; Owen, Kemp, Lechner, et al., 2022; Temper et al., 2020). The conservation and restoration of the Global South's remaining biodiversity-rich ecosystems, which perform key roles for planetary life-support systems, are clearly at odds with the strong economic expansion in all scenarios, especially in the SCP and SPC scenarios, given that large-scale agricultural land acquisitions tend to contribute to biodiversity loss and often fall within biodiversity hotspots (Davis et al., 2023). The commodification of biodiversity conservation and associated violence against marginalized population groups can thus be expected to increase in all three simulated futures (cf. Sène, 2024). Paradoxically, biodiversity conservation and mining activities increasingly overlap and are linked to land grabbing as local communities lose control over land and resources (Vuola, 2022). This is mirrored in 'renewables grabbing' (Scheidel et al., 2023) spurred by the global energy transition.

Apart from the negative effects for local communities in the Global South, the combined pressure of climate change impacts and climate change mitigation, food production and energy generation on land also generates risks for planetary environmental and international political stability (King et al., 2023) not captured in our scenario simulations. Ironically, pressure on Global South territories will be higher in scenarios with a strong economic development in the Global South than in those futures that are characterized by a continuation of Global North dominance. At the same time, a rise in the global power hierarchy will enable the South to control strategic landmasses and resource extraction situated in its own territory (cf. Mohapatra, 2017). Additionally, as emerging countries of the semiperiphery acquire 'imperial' powers in the SCP and the SPC scenario they might increasingly exert indirect territorial control over the periphery and even the center (cf. Das & Janakiraman, 2026). This could result in new dynamics of land acquisitions and investment flows with a reduced protagonism from transnational companies based in the Global North.

Given the projected demographic and economic developments in our scenario exercise, we argue that the Global South—particularly the semiperiphery—will emerge as the key political actor of the 21st century, serving not only as a major driver of climate change but also as the region most exposed to the adverse effects of local and global environmental change. Currently, the global polycrisis affects and constraints internal development in the Global South, which might render our scenarios too optimistic (Adam & Rena, 2024). However, if the Global South succeeds in expanding its economic and political influence, it will become the main protagonist in addressing, alleviating and resolving this unfolding polycrisis, with the world's long-term sustainability critically depending on its readiness to assume its new responsibilities in shaping the norms of global governance.

The land-related risks linked to our simulation scenarios not only point to the importance of including justice considerations in land-use scenarios to conserve biodiversity while preventing land-grabbing (Venier-Cambron et al., 2024) but also indicate the need to contemplate alternative development pathways for the Global South and North alike. The environmental assessment of the scenarios has shown that approximating living standards of the periphery to the levels characterizing the Global North at present under a conventional growth-based development pathway would have devastating effects on land and material extraction, and would produce emission pathways linked to very high levels of global warming, resulting in potentially catastrophic climate change effects. Additionally, the CSP and SCP scenarios reflect the possibility of growing accumulation of wealth in some parts of the global South alongside persistent poverty and structural exclusion in many other parts, reflecting a capitalist accumulation model incapable of delivering high levels of well-being to its population in a rapid, equitable and environmentally sustainable way (Nilsen, 2025). A just and sustainable transition therefore requires not only energy convergence between the Global North and South at relatively low levels (Hickel & Slamersak, 2022) but also a fundamental reconceptualization of 'development' in the Global South that transcends the paradigm of capitalist industrial growth (Gerber & Raina, 2018).

Today's emerging powers have become a key force in sustaining and globalizing capitalist accumulation logics (Hurrell & Sengupta, 2012), which appears to contradict the Global South's aspiration for systemic transformation and global justice (Bull & Banik, 2025). Nevertheless, practices, experiences, and theories from the Global South—though frequently overlooked—hold significant potential to inform social imaginaries that challenge capitalism as the dominant order (Diniz et al., 2020; Hollender, 2018; Jimenez et al., 2022; Zondi, 2016) and could act as important sources for future global environmental and economic scenario studies that are interested in radically changed global structures and world orders.

Conclusion

In this article we have conducted a quantitative scenario analysis to explore conceivable socio-economic and environmental consequences of different development pathways in the Global South and the associated changes in the global power distribution between the Global North and Global South. We found that shifts in the international power distribution towards the Global South is linked to stronger economic growth, a faster stabilization and decline of the size of the world population and global labor force, and higher public and private consumption in the South. In general, changes in world order away from the status quo foster socio-economic development

in the Global South, reflected in an earlier elimination of extreme poverty, higher living standards and mortality rates across all age groups. However, the rise of the Global South is also linked to an even faster increase in anthropogenic pressure on the Earth system, with strong growth in material extraction and land demands, as well as projected levels of global warming ranging from 3 to over 5 °C by 2100, compared to the pre-industrial reference period. Thus, although none of the development pathways of the Global South is sustainable in the long term, scenarios with strong growth in the semiperiphery and periphery further increase environmental and geopolitical risks. Consequently, it is important to explore post-capitalist and post-growth development pathways in both the Global North and South that can achieve the basic human need of the world population without destabilizing the biophysical Earth system. As the Global South unites a large and relatively young population, higher growth rates as well as higher levels of inequality and extreme poverty, emerging states from the Global South will likely become the main protagonist in the global quest for sustainability and have the potential to act as key drivers for a post-capitalist development paradigm in a radically changed global governance system and world order.

References

- Adam, H., & Rena, R. (2024). *Polycrisis and economic development in the global South*. Routledge.
- Almulhim, A. I., Alverio, G. N., Sharifi, A., Shaw, R., Huq, S., Mahmud, M. J., Ahmad, S., & Abubakar, I. R. (2024). Climate-induced migration in the Global South: An in depth analysis. *Npj Climate Action*, 3(1), 47. <https://doi.org/10.1038/s44168-024-00133-1>
- Anguelovski, I., Chu, E., & Carmin, J. (2014). Variations in approaches to urban climate adaptation: Experiences and experimentation from the global South. *Global Environmental Change*, 27, 156–167. <https://doi.org/10.1016/j.gloenvcha.2014.05.010>
- Ansari, D., Holz, F., & Al-Kuhlani, H. (2019). *Energy, climate, and policy towards 2055: An interdisciplinary energy outlook (DIW-REM Outlook)* (Issue 139). DIW Berlin: Politikberatung kompakt.
- Bazilian, M., Bradshaw, M., Gabriel, J., Goldthau, A., & Westphal, K. (2020). Four scenarios of the energy transition: Drivers, consequences, and implications for geopolitics. *WIREs Climate Change*, 11(2), e625. <https://doi.org/10.1002/wcc.625>
- Beckmann, N. A., & Erpul, O. (2024). Realism's Timeless Wisdom and its Relevance for the Global South. *All Azimuth: A Journal of Foreign Policy and Peace*, 13(1), 1–19. <https://doi.org/10.20991/allazimuth.1413433>
- BGR. (2020). *BGR Energy Study 2019 – Data and Developments Concerning German and Global energy supplies*. Hannover. https://www.bgr.bund.de/EN/Themen/Energie/Downloads/energiestudie_2019_en.pdf;jsessionid=ADF18B2529B3E89FC705FDF390A57BA4.internet002?__blob=publicationFile&v=6
- Block, K., Li, M., Gärtner, J., & Lenzen, M. (2025). Geopolitical conflict impedes climate change mitigation. *Npj Climate Action*, 4(1), 33. <https://doi.org/10.1038/s44168-025-00224-7>
- Blondeel, M., Price, J., Bradshaw, M., Pye, S., Dodds, P., Kuzemko, C., & Bridge, G. (2024). Global energy scenarios: A geopolitical reality check. *Global Environmental Change*, 84, 102781.
- Braun, J., Werner, C., Gerten, D., Stenzel, F., Schaphoff, S., & Lucht, W. (2025). Multiple planetary boundaries preclude biomass crops for carbon capture and storage outside of agricultural areas. *Communications Earth & Environment*, 6(1), 102.
- Brough, D., & Jouhara, H. (2020). The aluminium industry: A review on state-of-the-art technologies, environmental impacts and possibilities for waste heat recovery. *International Journal of Thermofluids*, 1, 100007.
- Bull, B., & Banik, D. (2025). The Rebirth of the Global South: Geopolitics, Imaginaries and Developmental Realities. *Forum for Development Studies*, 52(2), 195–214. <https://doi.org/10.1080/08039410.2025.2490696>
- Carlos Bresser-Pereira, L. (2019). Secular Stagnation, Low Growth, and Financial Instability. *International Journal of Political Economy*, 48(1), 21–40. <https://doi.org/10.1080/08911916.2018.1550949>
- Cilliers, J., & van Rooyen, M. (2025). *State Futures in the Global South*. African futures and innovation programme. <https://futures.issafrica.org/thematic/20-futures-of-the-state-in-the-global-south>
- Cruz, S. O. (2015). Alternative futures of global governance: Scenarios and perspectives from the Global South. *Foresight*.
- Das, S., & Janakiraman, K. R. (2026). Empire and International Order: Decolonial Perspective. In *Decolonising International Relations* (pp. 152–167). Routledge.
- Davis, K. F., Müller, M. F., Rulli, M. C., Tatlıhego, M., Ali, S., Baggio, J. A., Dell'Angelo, J., Jung, S., Kehoe, L., Niles, M. T., & Eckert, S. (2023). Transnational agricultural land acquisitions threaten

- biodiversity in the Global South. *Environmental Research Letters*, 18(2), 024014.
<https://doi.org/10.1088/1748-9326/acb2de>
- Diniz, S. C., Fernandes, B. S., & De Melo Monte-Mór, R. L. (2020). Social solidarity economy in a decolonial sense? Approaches from the Brazilian case. *Soziale Passagen*, 12(2), 313–329.
<https://doi.org/10.1007/s12592-020-00362-1>
- Ekrami, J., Nemati Mansour, S., Mosaferi, M., & Yamini, Y. (2021). Environmental impact assessment of salt harvesting from the salt lakes. *Journal of Environmental Health Science and Engineering*, 19(1), 365–377.
- Fatton, R. (2013). *Haiti: Trapped in the outer periphery*. Lynne Rienner Publishers.
- Frame, B., Yermakova, Y., Flamm, P., Nicklin, G., De Paula, G., Badhe, R., & Tuñez, F. (2022). Antarctica's Gateways and Gatekeepers: Polar scenarios in a polarising Anthropocene. *The Anthropocene Review*, 9(3), 392–402.
- Frischmann, C. J., Mehra, M., Alvarez, J., Jankowska, E., Jones, H., Namasivayam, A., & Yussuff, A. (2022). The Global South is the climate movement's unsung leader. *Nature Climate Change*, 12(5), 410–412. <https://doi.org/10.1038/s41558-022-01351-3>
- Fuhr, H. (2021). The rise of the Global South and the rise in carbon emissions. *Third World Quarterly*, 42(11), 2724–2746.
- Fuller, T. L., Narins, T. P., Nackoney, J., Bonebrake, T. C., Sesink Clee, P., Morgan, K., Tróchez, A., Bocuma Meñe, D., Bongwele, E., Njabo, K. Y., Anthony, N. M., Gonder, M. K., Kahn, M., Allen, W. R., & Smith, T. B. (2019). Assessing the impact of China's timber industry on Congo Basin land use change. *Area*, 51(2), 340–349. <https://doi.org/10.1111/area.12469>
- Gerber, J.-F., & Raina, R. S. (2018). Post-growth in the global south? Some reflections from India and Bhutan. *Ecological Economics*, 150, 353–358.
- Ghimire, S. (2018). Rising powers and security: A false dawn of the pro-south world order? *Global Change, Peace & Security*, 30(1), 37–55.
<https://doi.org/10.1080/14781158.2018.1431878>
- Gi, K., Sano, F., Akimoto, K., Hiwatari, R., & Tobita, K. (2020). Potential contribution of fusion power generation to low-carbon development under the Paris Agreement and associated uncertainties. *Energy Strategy Reviews*, 27, 100432.
- Goodman, R. C., Van Hensbergen, H. J., Bengtsson, K., Kaplan, A., & Persson, M. (2024). Transforming the tropical timber industry could be the key to realizing the potential of forests and forest products. *One Earth*, 7(7), 1142–1146.
<https://doi.org/10.1016/j.oneear.2024.06.016>
- Günther, P., & Ekardt, F. (2022). Human Rights and Large-Scale Carbon Dioxide Removal: Potential Limits to BECCS and DACCS Deployment. *Land*, 11(12), 2153.
- Henckens, T. (2021). Scarce mineral resources: Extraction, consumption and limits of sustainability. *Resources, Conservation and Recycling*, 169, 105511.
<https://doi.org/10.1016/j.resconrec.2021.105511>
- Hickel, J., & Slamersak, A. (2022). Existing climate mitigation scenarios perpetuate colonial inequalities. *The Lancet Planetary Health*, 6(7), e628–e631.
[https://doi.org/10.1016/S2542-5196\(22\)00092-4](https://doi.org/10.1016/S2542-5196(22)00092-4)
- Hollender, R. (2018). Anti, Alternative, and Post: A Review of Post-Growth A Review of Post-Growth Approaches to Radical Transformation in the Global South. *American Review of Political Economy*, 12(1). <https://doi.org/10.38024/arpe.147>
- Hurrell, A., & Sengupta, S. (2012). Emerging powers, North–South relations and global climate politics. *International Affairs*, 88(3), 463–484.

- IPCC. (2021). *Climate Change 2021: The Physical Science Basis. Contribution of Working Group I to the Sixth Assessment Report of the Intergovernmental Panel on Climate Change*. Cambridge University Press. Cambridge University Press, Cambridge, UK and New York, NY, USA.,
- IPCC. (2022). *Climate Change 2022: Impacts, Adaptation and Vulnerability. Contribution of Working Group II to the Sixth Assessment Report of the Intergovernmental Panel on Climate Change*. Cambridge University Press. Cambridge University Press, Cambridge, UK and New York, NY, USA.,
- Jimenez, A., Delgado, D., Merino, R., & Argumedo, A. (2022). A Decolonial Approach to Innovation? Building Paths Towards Buen Vivir. *The Journal of Development Studies*, 58(9), 1633–1650. <https://doi.org/10.1080/00220388.2022.2043281>
- Karatasli, S. S., & Kumral, S. (2017). Great convergence or the third great divergence?: Changes in the global distribution of wealth, 1500–2008. In *The world-system as unit of analysis* (pp. 36–49). Routledge.
- Katz-Rosene, R. (2019). The Treatment of Global Environmental Change in the Study of International Political Economy: An Analysis of the Field's Most Influential Survey Texts. *International Studies Review*, 21(3), 477–496.
- Khasru, S. M., & Ambrizzi, T. (2023). Climate Change & Just Energy Transition: What the North Can Learn from the South? *CEBRI-Revista: Brazilian Journal of International Affairs*, 8, 166–193.
- King, R., Benton, T., Froggatt, A., Harwatt, H., Quiggin, D., & Wellesley, L. (2023). *The emerging global crisis of land use*. Chatham house.
<https://www.chathamhouse.org/sites/default/files/2023-11/2023-11-22-emerging-global-crisis-land-use-king-et-al.pdf>
- Klingebiel, S. (2023). Geopolitics, the Global South and Development Policy. In *IDOS Policy Brief 14/2023* (Version 1.0). German Institute of Development and Sustainability.
<https://doi.org/10.23661/IPB14.2023>
- Klingebiel, S., & Sumner, A. (2025). *Four futures for a global development cooperation system in flux: Policy at the intersection of geopolitics, norm contestation and institutional shift*. IDOS Policy Brief.
- Lahoti, R., Jayadev, A., & Reddy, S. (2016). The global consumption and income project (GCIP): An overview. *Journal of Globalization and Development*, 7(1), 61–108.
- Lauer, A., Carpintero, Ó., & De Castro, C. (2025). In search of a missing South: An explorative study of biases in global climate and energy scenarios. *Globalizations*, 1–22.
<https://doi.org/10.1080/14747731.2025.2526295>
- Lauer, A., De Castro, C., & Carpintero, Ó. (2025). Beyond Green capitalism: Global scenarios for fast societal transitions toward sustainability. *Environmental Innovation and Societal Transitions*, 56, 100981. <https://doi.org/10.1016/j.eist.2025.100981>
- Lauer, A., & Llases, L. (2025). *MORDRED: Model Of Resource Distribution and Resilient Economic Development. Model Documentation*. GitHub. <https://github.com/Pendracus/MORDRED>
- Matthews, H. D. (2016). Quantifying historical carbon and climate debts among nations. *Nature Climate Change*, 6(1), 60–64. <https://doi.org/10.1038/nclimate2774>
- Mazzega, P., Rugmini, D. M., & Barros-Platiau, A. F. (2025). Where is the “Global South” located in scientific research? *Earth System Governance*, 25, 100269.
<https://doi.org/10.1016/j.esg.2025.100269>
- Meadows, D. H., Meadows, D., Randers, J., & Behrens, W. W. (1972). *The limits to growth. A report for the Club of Rome's Project on the Predicament of Mankind*. Universe Books.

- Mohan, V. (2025). In search of consensus: Examining Global South perspectives on climate security in UNSC debates. *Earth System Governance*, 23, 100231.
<https://doi.org/10.1016/j.esg.2024.100231>
- Mohapatra, N. K. (2017). Energy security paradigm, structure of geopolitics and international relations theory: From global south perspectives. *GeoJournal*, 82(4), 683–700.
<https://doi.org/10.1007/s10708-016-9709-z>
- Moore, S. (2024). Climate Action in the Age of Great Power Rivalry: What Geopolitics Means for the Climate. *Kleinman Center for Energy Policy*.
- Muiderman, K., Vervoort, J., Gupta, A., Norbert-Munns, R. P., Veeger, M., Muzammil, M., & Driessen, P. (2023). Is anticipatory governance opening up or closing down future possibilities? Findings from diverse contexts in the Global South. *Global Environmental Change*, 81, 1–19.
- Nilsen, A. G. (2025). *Emerging Powers and the Political Economy of the Southern Interregnum*. 1–24.
- Ocholla, G. O., Bunyasi, M. M., Asoka, G. W., Pacha, O., Mbugua, H. K., Mbuthi, P., Mbiti, S., Wendo, H. K., & Kamau, P. K. (2013). Environmental issues and socio-economic problems emanating from salt mining in Kenya; a case study of Magarini district. *International Journal of Humanities and Social Science*, 3(3), 213–223.
- Our World in Data. (2024). *CO₂ emissions per capita*. https://ourworldindata.org/grapher/co-emissions-per-capita?country=OWID_AFR~OWID_SAM~OWID_EUR
- Owen, J. R., Kemp, D., Harris, J., Lechner, A. M., & Lèbre, É. (2022). Fast track to failure? Energy transition minerals and the future of consultation and consent. *Energy Research & Social Science*, 89, 102665.
- Owen, J. R., Kemp, D., Lechner, A. M., Harris, J., Zhang, R., & Lèbre, É. (2022). Energy transition minerals and their intersection with land-connected peoples. *Nature Sustainability*, 1–9.
- Parson, E. A., & Reynolds, J. L. (2021). Solar geoengineering: Scenarios of future governance challenges. *Futures*, 133, 102806.
- Ramirez, C. H. (2025). The Post-War Evolution of Globalisation and International Order: From Liberal to Neoliberal International Order. *Global Society*, 1–29.
<https://doi.org/10.1080/13600826.2025.2470838>
- Richardson, K., Steffen, W., Lucht, W., Bendtsen, J., Cornell, S. E., Donges, J. F., Drücke, M., Fetzer, I., Bala, G., & von Bloh, W. (2023). Earth beyond six of nine planetary boundaries. *Science Advances*, 9(37), eadh2458.
- Scheidel, A., Sorman, A. H., Avila, S., Del Bene, D., & Ott, J. (2023). Renewables Grabbing. Land and Resource Appropriations in the Global Energy Transition. In A. Neef, C. Ngin, T. Moreira, & S. Mollett (Eds.), *Routledge handbook of global land and resource grabbing* (pp. 189–204). Routledge.
- Sekera, J., & Lichtenberger, A. (2020). Assessing carbon capture: Public policy, science, and societal need: A review of the literature on industrial carbon removal. *Biophysical Economics and Sustainability*, 5, 1–28.
- Sène, A. L. (2024). Justice in nature conservation: Limits and possibilities under global capitalism. *Climate and Development*, 16(9), 838–847.
<https://doi.org/10.1080/17565529.2023.2274901>
- Shan, Y. (2023). Discussion on How Climate Change is Disproportionately Affecting the Global South. *International Journal of Frontiers in Sociology*, 5(12).
<https://doi.org/10.25236/IJFS.2023.051202>

- Surprise, K. (2020). Stratospheric imperialism: Liberalism,(eco) modernization, and ideologies of solar geoengineering research. *Environment and Planning E: Nature and Space*, 3(1), 141–163.
- Sus, M., & Hadeed, M. (2020). Theory-infused and policy-relevant: On the usefulness of scenario analysis for international relations. *Contemporary Security Policy*, 41(3), 432–455. <https://doi.org/10.1080/13523260.2020.1730055>
- Temper, L., Avila, S., Del Bene, D., Gobby, J., Kosoy, N., Le Billon, P., Martinez-Alier, J., Perkins, P., Roy, B., & Scheidel, A. (2020). Movements shaping climate futures: A systematic mapping of protests against fossil fuel and low-carbon energy projects. *Environmental Research Letters*, 15(12), 123004.
- Venier-Cambron, C., Helm, L. T., Malek, Ž., & Verburg, P. H. (2024). Representing justice in global land-use scenarios can align biodiversity benefits with protection from land grabbing. *One Earth*, 7(5), 896–907. <https://doi.org/10.1016/j.oneear.2024.03.006>
- Vuola, M. (2022). The intersections of mining and neoliberal conservation. *World Development*, 152, 105816. <https://doi.org/10.1016/j.worlddev.2022.105816>
- Zondi, S. (2016). Ubuntu and sumak kawsay: The Inter-Parliamentary Union and the search for a global South humanist paradigm of development. *South African Journal of International Affairs*, 23(1), 107–120. <https://doi.org/10.1080/10220461.2016.1160838>

Including the Bottom Billion: Integrating Subsistence Economies into Integrated Assessment Modeling

Abstract

This study introduces *MORDRED* (Model of Regime Dynamics and Environmental Development), a system dynamics Integrated Assessment Model (IAMs) that incorporates a subsistence sector and migration flows between capitalist and non-capitalist regimes. By coupling demographic, economic, and biophysical variables, the model explores four scenarios of global development and environmental change: *Neoliberal Promises*, *Shadows of Neoliberal Development*, *Breakdown of Neoliberal Development*, and *High Adaptive Capacity of Subsistence Economies*. The results reveal dynamics of accumulation by dispossession, exploitation and contamination underpinning rural and urban economic development in the Global South. However, feedbacks between an expanding global economy characterized by high inequality, and a destabilized Earth system also can destabilize the global accumulation regime and revert the direction of rural-urban migration. Thus, while *Neoliberal Promises* replicates the narrative of smooth urbanization and growth benefitting all, other scenarios expose the instability of neoliberal development under growing biophysical constraints, culminating in potential economic collapse and partial ‘ruralization’. The findings emphasize the need to expand the scope of IAMs by representing socio-economic (re)production through subsistence and informal economies in order to arrive at more holistic assessment of impacts, vulnerabilities, adaptation and mitigation centered on poverty eradication, need-based production and resilience.

Keywords

Subsistence, Global South, smallholders, scenarios, climate change, migration.

1. Introduction

Despite the ongoing expansion of global capitalism, reflected in dynamics of ‘planetary urbanization’ (Brenner & Schmid, 2015) and continuously advancing commodity frontiers (Barbesgaard & Whitmore, 2024; Meyfroidt et al., 2024; Moore, 2000), there remain approximately 66 million pastoralists (Jenet et al., 2017), 476 million indigenous people (World Bank, 2025a) and up to 2.5 billion people belonging to smallholder farm households (Peck et al., 2013) who live at the margins of the global accumulation regime.

As these groups depend directly on the environment for survival, they are highly vulnerable to the adverse effects of environmental change and degradation (Albore et al., 2024; Gatew & Guyo, 2024; Hazarika et al., 2024; Nori et al., 2008; Widiono et al., 2024). Simultaneously, Indigenous, pastoralist, and peasant cultures and livelihoods face socio-economic threats stemming from unrestrained capitalist development linked to extended urbanization. This manifests, for example, through land grabbing in the name of rural or urban development, often backed or enforced by the state (Khan & Karak, 2018; Pratama et al., 2021; Whiting, 2022). Although accelerating the global energy transition is necessary to achieve climate goals, the large-scale deployment of renewable energy technologies risks further exacerbating these pressures through ‘renewables grabbing’ (Scheidel et al., 2023), particularly given the strong overlap between Indigenous and peasant lands and mining projects for energy transition minerals (Owen et al., 2022). The vulnerability of these socio-economic groups to adverse environmental changes is thus mediated by the political economy of global capitalism (Bernards, 2025; Ford, 2012).

In other words, although many Indigenous, pastoralist, and peasant communities live at or beyond the margins of the capitalist system they are not insulated from its dynamics. Focusing on the poorest smallholder farmers, at least three mechanisms link global capitalist development to the future of rural subsistence regimes.

First, capitalism has expanded through primitive accumulation, i.e. the expropriation of rural populations and the integration of their territories; comparable contemporary processes have been termed *accumulation by dispossession* (Harvey, 2003). Although the widespread and often interchangeable use of these concepts has been problematized (Glassman, 2006; Hall, 2013; Raju Das, 2017), both draw attention to how capitalist outward expansion secures the cheap environmental inputs (food, energy and raw materials) required for surplus value creation (Moore, 2015, 2017).

Second, primitive accumulation produces property-less workers who can be put to work for capital, resulting in *accumulation by exploitation* (Bonefeld, 2023). Cheap labor-power complements material inputs and is reproduced through rural-urban migration, where migrants swell the industrial reserve army and inadvertently contribute to the cheapening of the labor force (Li, 2020). However, in many countries, limited industrialization has given rise to a distinct form of urbanization characterized by discontinuous and contested metabolic configurations, persistent mismatches between capital and labor, an inflated informal economy and high vulnerability among urban residents (Parida & Agrawal, 2023; Schindler, 2017). The mismatch between migrants’ skills and formal employment opportunities, combined with rapid urbanization and insufficient levels industrialization, results in the de facto exclusion of these ‘marginalized of the wasteland’ from spaces of capitalist production and valorization who – in contrast to Marx’s reserve army of labor – face little chances of being incorporated into wage-labor-based production (Khan & Karak, 2018; Sanyal, 2007; Zhang et al., 2023)

Third, *accumulation by contamination* describes global ecological cost-shifting, whereby profit-maximizing activities degrade, contaminate and pollute ecosystems across the world, resulting in environmental injustice (D'Alisa & Demaria, 2024; Demaria, 2015). It can co-occur with accumulation by dispossession, for instance when waste treatment is financialized and privatized: large-scale incineration can create health-risks for residents while depriving waste pickers of recyclable materials (D'Alisa & Demaria, 2024). Climate change and toxic waste from fossil extraction constitute paradigmatic examples (Picard & Beigi, 2020).

At the same time, populations at the margins of the global economy are not merely passive victims but possess adaptive agency and may play key roles in mitigating anthropogenic environmental pressures as they often coexist with their surrounding ecosystems (Samberg et al., 2016). Smallholder farmers, pastoralists, and Indigenous communities can support carbon sequestration, fire prevention, and biodiversity conservation while sustaining their livelihoods (Ewing et al., 2023; Jenet et al., 2017; Negash & Kanninen, 2015; Nikolakis et al., 2022; Nori et al., 2008; Soto-Pinto et al., 2010). They also retain valuable local knowledge relevant for observing local climatic changes (Chanza & Musakwa, 2022; Savo et al., 2016) and developing socio-ecological systems more resilient to shocks (Altieri & Koohafkan, 2008; Caviedes et al., 2024; Estrada et al., 2022).

Despite the complex dynamics, the 'bottom billion'—those most excluded from industrial capitalist development—remain largely absent from global scenario exercises exploring potential socio-environmental futures (Lauer, Carpintero, et al., 2025; Lauer, Llases, et al., 2025). Quantitatively, Integrated Assessment Models (IAMs) generally fail to represent economies apart from the global 'market economy', leaving them blind to the mitigation potential of subsistence systems, and to how economic growth and environmental degradation jointly affect marginalized ways of life. Although IAMs quantify environmental policies such as carbon pricing, they are poorly equipped to address structural or systemic alternatives, such as food sovereignty (Saghai, 2021). To date, no IAM has modeled the different manifestations of capitalist accumulation shaping rural-urban migration and development trajectories. Instead, models rely on classical development economics' assumptions of smooth, industrialization-led urbanization and wage differentials producing an 'urban pull' on the rural population (Khan & Karak, 2018; Li, 2020). For example, in some widely used socio-economic scenarios between 80% (SSP2 and LED) and 92% (SSP1 and SSP5) of the world population is assumed to live in cities by 2100 (Bluwstein & Cavanagh, 2023). Consequently, although IAMs aim to analyze the drivers of environmental change, its impacts on vulnerable populations and possible mitigation and adaptation options (IPCC, 2023), their neglect of economies at or beyond capitalist frontiers likely results in incomplete or biased insights.

This article takes a first step toward addressing this gap by presenting and exploring an IAM that represents key relationships between the global capitalist economy and rural subsistence regimes. We pursue three research objectives. First, we demonstrate the feasibility of modeling economic structures outside the capitalist economy by integrating a simple 'subsistence economy' into an IAM. Second, we wish to explore different conceivable futures for the world's poorest under different capitalist development pathways. Last, we are interested in the associated demographic, economic and environmental consequences of these scenarios.

2. Methods

2.1. MORDRED model

Given that a detailed description of MORDRED, including data sources, calculations and relevant model equations, is provided in the model's documentation (Lauer & Llases, 2025), we only provide a brief overview of the model's structure below, focusing on the representation of the subsistence sector and its interactions with the global economy.

2.1.1. General model characteristics

MORDRED is a system-dynamics based, environmentally and socially extended global input-output model with 25 sectors, coupled with a climate, land, energy and population model. The economic model projects future changes in private and public consumption, investment, capital stock and the production of intermediate products, based on exogenously fixed target consumption growth rates. Technological developments—such as changes in energy intensities, the electricity mix, material extraction costs, or material efficiency—are captured through the A matrix, which changes endogenously as well as through exogenous scenario assumptions about future technological change.

The sector-specific demand for labor hours can be met with the labor hours provided by the population that lives fully integrated in the world economy. To survive, the population in the working age (15 – 64 years), which is assumed to sustain the rest of the population, is willing to engage in global productive processes. While the maximum supply of labor hours is determined by the size of the population in the working age and by their capacity to work –influenced by the participation rate and by heat-related climate damages – the allocation of the working force between sectors depends on the extent of sector-specific industry and final demand, which in turn depends on the purchasing power of different classes.

Within the global economy, there are 9 social classes with different consumption levels which, in the initial moment of the simulation, depend on estimates about global consumption inequality, and during the simulations change according to scenario assumptions. Three classes reside in the world region 'center' that includes all high-income countries. They are derived by diving the population into the richest 20%, the poorest 30% and the remaining 50%. The next three classes are constituted by the population of the 'semiperiphery' which consists of all upper-middle-income countries, according to the world bank's (2025b) country classification. The last three classes are part of the 'periphery' that contains all lower-middle- and low-income countries. They are derived in the same way as the classes of the center. Age-specific birth and death rates within the global economy are influenced by the different per capita consumption levels per class and region. While all 20 age groups represented in the model (0-4 years, 5-9 years, ... 95+ years) have age-specific mortality rates, only the 15- to 44-year-olds have age-specific birth rates.

The demand of global economic production for different land types (mainly forests, cropland and pastures, infrastructure, land for energy generation), and land availability are determined in the land module. The demand and supply of different types of energy is calculated in the energy module, while environmental impacts from economic activities are depicted in the 'environmental stressors' and the 'climate' modules.

The simultaneous representation of various dimensions of the global socio-economic and environmental system, and their integration into one comprehensive model, renders MORDRED an IAM of medium complexity. Nevertheless, the modeling logic of MORDRED differs from that of

most existing IAMs (for exceptions see Capellán-Pérez et al. (2020); Mediavilla et al. (2025)) due to the following characteristics: First, the model can represent scarcity of several production factors necessary for economic activities (labor, land, energy, intermediate products), and the consequences of rising scarcity for economic development pathways, including a decline or reversal of economic growth. Second, the model integrates various feedback dynamics between different parts of the model, such as the influence of consumption levels on demographic parameters, and the influence of demographic changes on labor availability. Third, the model represents several channels through which adverse climate change impacts driven by rising global average temperatures can deteriorate the conditions of economic production.

2.1.2. Representation of the subsistence sector

The subsistence economy is represented through a separation of three modules – the demographic, the land and the economic modules - into two spheres, i.e. the global or formal mode of (re)production and the subsistence mode of (re)production.

In the demographic module, in every world region, the population is divided into two segments. The larger segment is assumed to be fully integrated into the world economy, i.e., they sustain the global economy through their labor and are in turn sustained by the output of global production processes. The smaller segment is assumed to live and work in a subsistence economy at the margins of the world economy, with only occasional points of interaction.

In 2020, more than 700 million people lived in extreme poverty in 2020 (UN DESA, 2023) while the estimated number of smallholder farms with a size of 2-5 ha ranges between 380 million (Samberg et al., 2016) and 510 million (Lowder et al., 2025), sustaining between 1.5 and 2.5 billion people (Peck et al., 2013). Focusing on the high intersection between the poorest subsistence farming households and the population living in extreme poverty (Lowder et al., 2025), we set the number of people belonging to the subsistence economy to 800 million in the initial moment of the simulation, divided between the semiperiphery (15%) and the periphery (85%).

The population participating in the subsistence economy features high but constant fertility and mortality rates that correspond to a constant per capita consumption of which only the equivalent of 729 (2019-)€/year, i.e. the consumption under extreme poverty, is monetized in the global economy. Thus, fertility and mortality in subsistence are not influenced by changing per capita consumption in the global economy.

Migration movements between the subsistence and the formal economy in every world region depend on the difference in consumption per capita levels (Cpc) between the poorest class ($P30$) in the respective world region, and the subsistence class. The higher the difference in consumption, the higher the share of the population willing to leave the subsistence regime (sub) and integrate into the world economic regime (we). Equation (1) represents the region-(r) and age-(a) specific migration rate, i.e. the share of the subsistence population that wants to migrate, while equation (2) calculates the absolute region- and age-specific migration flow from the subsistence to the world economy, based on the population living in subsistence at a given moment of the simulation (P^{sub}), and the maximum population size that can be sustained through the cultivation of subsistence land ($MaxP^{sub}$). If the land that is used by the subsistence regime is reduced, the maximum population size decreases. Thus, under certain conditions, dynamics of a forced integration into the world economy can emerge, fueled for instance by accumulation through dispossession or accumulation by contamination.

$$Mr_r^{sub \rightarrow we} = \max \left(0, \min \left(0.1; \beta_1 \cdot (Cpc_{r,P30}^{we} - Cpc^{sub}) \right) \right) \quad (1)$$

$$M_{r,a}^{sub \rightarrow we} = \max \left(Mr_r^{sub \rightarrow we} \cdot P_{r,a}^{sub}; \left(\frac{\max(0; P^{sub} - MaxP^{sub})}{P^{sub}} \right) \cdot P_{r,a}^{sub} \right) \quad (2)$$

The representation of migration flows from the subsistence sector to the world economy can be used to explore accumulation by exploitation dynamics that occur when the world economy absorbs cheap labor from the subsistence regime. However, MORDRED also allows a reversal of this dynamic, i.e. reintegration into the subsistence regime. Within each region and social class (cl), the share of people that want to leave the world economy ($Mr_{r,cl}^{we \rightarrow sub}$) grows as the consumption levels in the global economy in any given class (cl) begin to approach those within the subsistence regime (3). The absolute migration flows depend on the maximum number of people that the subsistence regime can sustain in any given moment of time, and the size of the respective class (4).

$$Mr_{r,cl}^{we \rightarrow sub} = \max \left(0, \min \left(\beta_0 - \beta_1 \cdot Cpc_{r,cl}^{we} (time_step - 1) \right) \right) \quad (3)$$

$$\begin{aligned} M_{r,a}^{we \rightarrow sub} &= \max \left(0; \min \left(1; \frac{MaxP^{sub} - P^{sub}}{\sum (Mr_{r,cl}^{we \rightarrow sub} \cdot P_{r,a}^{we} \cdot class_share_{cl})} \right) \right) \\ &\cdot \sum_{cl} (Mr_{r,cl}^{we \rightarrow sub} \cdot P_{r,a}^{we} \cdot class_share_{cl}) \end{aligned} \quad (4)$$

In the land module, the land demand by the subsistence economy ($Land_{sub}^d$) depends on the number of people living in subsistence conditions, the people that want to leave the world economy and the subsistence land intensity (Int_{sub}^{Land}) (5). In the initial moment of time, the latter is given in km^2 per million people and is calculated based on the initial population that is working in the subsistence regime and the land managed per worker, estimated based on data on the farm size of African smallholders (Altieri & Koohafkan, 2008) (6). In turn, the maximum population that can be sustained in any moment of time depends on the land intensity and the land size of the subsistence regime in this moment of time (7). The demand of the global industrialized food sector for different types of land ($Land_{1,we}^d$) is calculated with sector-specific land intensities and the desired annual output of the food sector (X_1^d) (8).

Land intensity increases with global warming, reflecting a loss of land productivity due to climate change impacts such as extreme weather events (Altieri & Koohafkan, 2008; Aragón et al., 2021). For simplicity, it is assumed that land intensity increases as a linear function of changes in global average temperature compared to the pre-industrial period (9). The damage factor $a_{climate\ damage}$ can be changed in different scenario simulations, depending on the assumed resilience and adaptation capacity of the population sustaining the subsistence mode of production (Levene & Conversi, 2017; Thorlakson & Neufeldt, 2012; Touch et al., 2024). It reflects the consequences of ‘accumulation by contamination’ since the subsistence population faces a climate-change-induced loss in land productivity that is caused primarily by the greenhouse gases emissions of the global capitalist economy.

$$Land_{sub}^d = \sum_{r,a} (P_{r,a}^{sub} + M_{r,a}^{we \rightarrow sub}) \cdot Int_{sub}^{Land} \quad (5)$$

$$Int_{sub,t0}^{Land} = \frac{Int_{sub\ worker}^{Land} \cdot workers_{sub,t0}}{\sum_{r,a} (P_{r,a}^{sub})_{t0}} \quad (6)$$

$$MaxP^{sub} = Land_{sub} \cdot Int_{sub}^{Land} \quad (7)$$

$$Land_{1,we}^d = \sum_i (X_1^d \cdot Int_{1,we}^{Land}) \quad (8)$$

$$Int_{sub}^{Land} = Int_{sub,t0}^{Land} + a_{climate\ damage} \cdot (\Delta Temp_{1850} - 1) \quad (9)$$

If total land demand exceeds land supply, the model uses an allocation mechanism to prioritize different land demands, depending on the land priorities specified in the respective scenario. If land demand from the subsistence sector has a low priority, the amount of subsistence land shrinks and is integrated into the world economy. This dynamic reflects accumulation by dispossession. Other cases of dispossession, e.g. by the expansion of material extraction activities, are not directly modeled in MORDRED. However, changes in the amount of materials extracted, which are tracked by the model, can serve as indicators for extraction-related land conflicts.

The input-output data describing world economic production in 2019 (Stadler et al., 2018) that is used in MORDRED's economic module was modified for the food sector which contains the agricultural sectors. We assume that only part of the production and consumption within the subsistence regime is included in official statistics, and that this monetized subsistence consumption is concentrated in the agricultural sector, reflecting, for example, income earned through selling part of the harvest on the market. This monetized subsistence output is assumed to correspond to the monetized consumption of the subsistence population, which we estimate using an extreme poverty threshold of 2.15 2017-PPP-USD/day. By converting this value into 2019-€ and multiplying it by the initial size of the subsistence population, we derive our estimate of the subsistence output reflected in the IO table. This value is then deducted from the global food sector's output (x_1) (10). In this way, both the subsistence production and consumption have been separated from the global economy.

For simplicity, we assume that the subsistence sector does not rely on any economic inputs from the world economy. Thus, the first column of the A matrix, which contains the input coefficients of the food sector, is modified by multiplying the original values with the ratio between the sectoral output with and without the monetized subsistence output (11).

To remove labor hours of the subsistence population from the global working force, we assume that 70% of the subsistence class works in the food sector and that half of the working day of the subsistence class, i.e. 4 hours, flows into the production of output which enters the formal economy, and, thus, is monetized. The resulting estimated annual hours of subsistence work are subtracted from the original number of annual hours worked in the global food sector (12).

Last, by multiplying the initial land intensity ($Int_{sub,t0}^{Land}$) by the size of the subsistence population, the total amount of subsistence land is derived. This value is then subtracted from the sum of cropland and grassland used by the food sector, which is given in the environmental extension of Exiobase3 (13).

$$x_{1without\ sub} = x_{1with\ sub} - \sum_{r,a} (P_{r,a}^{sub})_{t0} \cdot Cpc_{sub} \quad (10)$$

$$A_{(without\ sub)} = \begin{bmatrix} a_{1,1} \cdot \frac{x_1^{with\ sub}}{x_1^{without\ sub}} & \dots & a_{1,25} \\ \vdots & \ddots & \vdots \\ a_{25,1} \cdot \frac{x_1^{with\ sub}}{x_1^{without\ sub}} & \dots & a_{25,25} \end{bmatrix} \quad (11)$$

$$L_{1^{without\ sub}} = L_{1^{with\ sub}} - (0.7 \cdot \sum_{r,a} (P_{r,a}^{sub}) \cdot \frac{4\ h}{d} \cdot \frac{5\ d}{w} \cdot 49\ w) \quad (12)$$

$$Land_{1,cropland\ \&\ pastures^{without\ sub}_{t_0}} = Land_{1,cropland\ \&\ pastures_{t_0}} - Land_{sub_{t_0}} \quad (13)$$

As a result of these simple operations, the labor and land productivity of the global food sector, as well as its input intensity increase, which is characteristic of industrialized and capitalized agriculture. Thus, MORDRED contains two somewhat artificial economic spheres that change dynamically throughout the simulation, reflecting capitalist expansion as well as incomplete integration into the world economy: The global economic sphere, devoid of any subsistence production and consumption, and the subsistence sphere, devoid of any inputs from the global economy. However, due to the high uncertainty regarding data and estimates about the subsistence sector, we stress that the model outcomes resulting from scenarios involving the subsistence regime should not be interpreted as precise quantitative projections, but rather as theoretical model dynamics that serve exploratory scenario analyses of future rural–urban interactions. The same holds for the ‘urbanization indicator’ (UI), which we added to the model as a measure of the rural poor’s integration into the world economy. The UI is calculated as the ratio between the population linked to the rural area and the total world population (14).

$\alpha_{non-workers}$ multiplies the number of workers with a factor that considers that the workers sustain the non-working population, while $\alpha_{rural\ services}$ is a correction factor that takes into account that there must be a minimum of additional non-agricultural and non-food processing economic activity to avoid rural depopulation, which requires additional workers and dependent non-working population. Both factors can vary according to the scenario.

$$UI = 1 - \left[\frac{\sum_{r,a} (P_{r,a}^{sub}) + \left(\frac{Int_1^{Labor\ hours} \cdot x_1}{annual\ hours\ worked} \right) (\alpha_{non-workers} + \alpha_{rural\ services})}{\sum_{r,a} (P_{r,a}^{sub}) + \sum_{r,a} (P_{r,a}^{we})} \right] \quad (14)$$

Figure 1 provides a graphical representation of the relationships between the world economy and the subsistence regime.

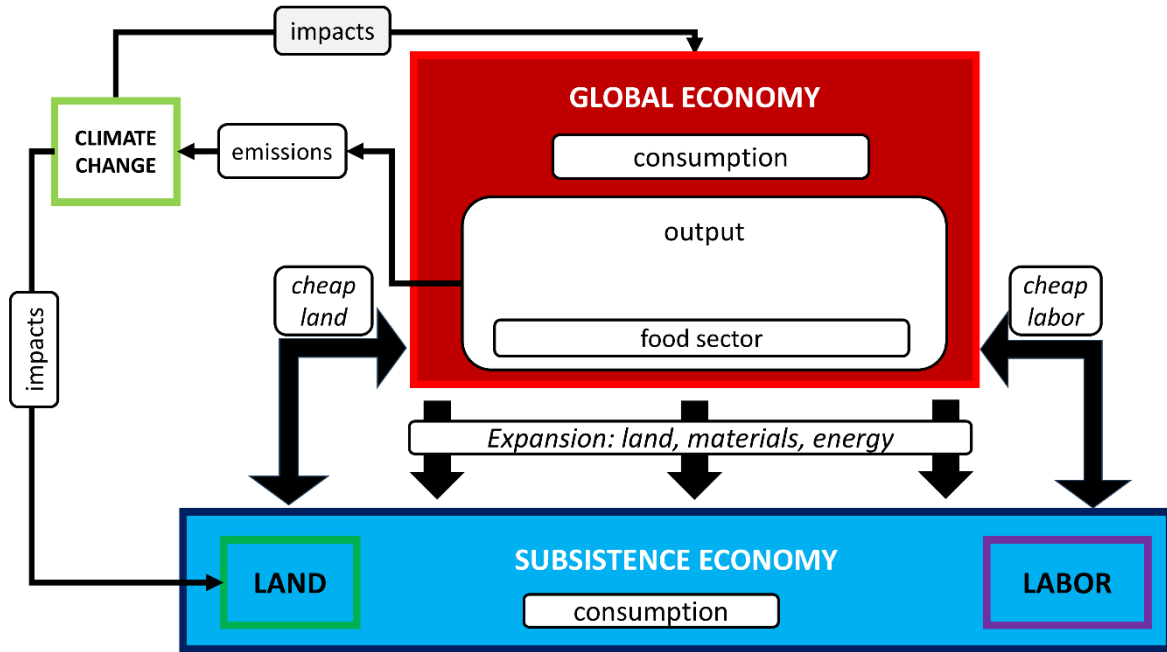


Figure 1: Representation of links between the industrialized global economy and modes of production at its margins in MORDRED. Arrows from the global economy to the outside indicate an expansion of capitalist economic activities, particularly through expanding commodity frontiers. Arrows between the world economy and the subsistence regime indicate inflows and outflows of land and labor that vary according to the simulated scenario. For simplicity, only the land and labor belonging to the subsistence economy are depicted.

2.2. Scenarios

The aim of our scenario exercise is to explore a wide range of conceivable development pathways for the capitalist world economy and the subsistence regime. Therefore, we simulate 4 scenarios (A-D) for the period 2019-2100, which differ in variables influencing subsistence-global economy interactions, while adopting the model's default values for the remaining parameters. Table 1 highlights similarities and differences between the scenarios for selected variables. The numerical values corresponding to the parametrization of these variables are provided in the Supplementary Material. The scenarios are simulated with all scarcity factors activated, except for two mechanisms that ration, and increase the input costs of, fossil extraction, resulting in very high fossil resource availability.

	Scenario A	Scenario B	Scenario C	Scenario D
Technological and economic development	Moderate energy efficiency gains, electrification and changes in electricity mix toward renewables.			
Desired annual per capita consumption growth rate	Center: 1.7% Semiperiphery: Richest 20%: 2.7%; poorest 30%: 3.5%; middle 50%: 3.2% Periphery: Richest 20%: 2.8%; poorest 30%: 3%; middle 50%: 3.1%.	Same as A but: consumption growth rate of the poorest 30% of the semiperiphery and periphery is divided by 10.		

Consumption priorities in the case of scarcity	Investment > center (public and private consumption) > rest of the world.	Investment > poorest 30% of periphery & semiperiphery > governments of all regions & center all households > remaining households.	Investment > governments & households of the center > poorest 30% periphery > poorest 30% semiperiphery > richest 20% and middle class periphery & richest 20% semiperiphery > middle class semiperiphery
Rural-urban migration	High willingness to migrate from the subsistence to the global economy.	Low willingness to migrate from the subsistence to the global economy.	
Labor productivity	High increase driven by learning and technological progress.	Increase is 10% higher than in A.	
Land intensity	Very high reductions driven by learning and technological progress.	High reductions driven by learning and technological progress.	
Land intensity subsistence	Constant.	Increasing due to climate change impacts.	Increasing due to climate change impacts; decreasing due to adaptation.
Land priorities	World economy > subsistence > natural ecosystems.		
Land availability	Higher land availability due to a lack of land protection.	Protection of 40% of primary forest.	
Fossil fuel availability	Very high .		
Climate damages	No.	Yes.	

Table 1: Similarities and differences in the scenario assumptions of scenarios A-D.

3. Results

In this section, we compare four global futures characterized by different dynamics between the subsistence system and the global economic system, and highlight the key simulation outcomes.

3.1. A: Neoliberal promises

In this scenario, resource scarcity, climate change impacts, and other negative global environmental changes are assumed to be nonexistent or to manifest only in the 22nd century. Consequently, there are no limits to the continued expansion and development of the global capitalist system.

During the first decades, economic growth is supported by an expanding global labor force, driven primarily by population growth within the world economy and by migration from the subsistence regime into the global economy. However, with increasing per capita consumption levels that are facilitated by a continuous growth in global productive capacities, the overall

birth rates in the world economy begin to decline faster than the death rates. Once the majority of the subsistence population has been absorbed into the global labor force, overall labor supply begins to fall, although by 2100 it still remains slightly above the initial level (Figure 2a). Conversely, the productivity of both labor and land grows exponentially throughout the simulation, enabling continuous expansion of global output (Figure 2b). In this scenario, the gap between the consumption levels of the world's poorest classes and those of the subsistence class widens rapidly, creating an incentive to leave subsistence regime. By 2060, the vast majority of the initial subsistence population has migrated, and by the end of the simulation the subsistence sector has disappeared entirely (Figure 2c). As the population living in subsistence declines, land demand decreases accordingly, meaning that the land used for subsistence production follows the same exponential decline (Figure 2d).

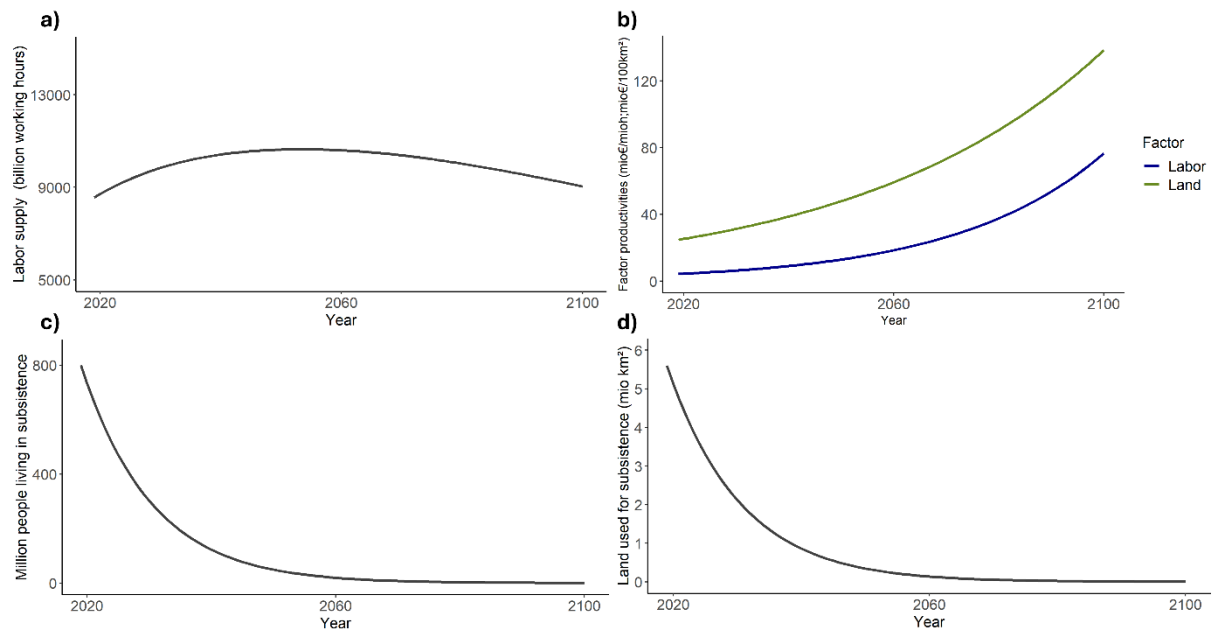


Figure 2: Evolution of a) maximum labor supply, b) labor (blue) and land (green) productivity in the food sector, c) population without full integration into the world economy and d) subsistence land in scenario A.

The disappearance of the subsistence sector, combined with large increases in labor productivity in the food sector, leads to a strong rise in the value of the urbanization indicator (Figure 3a). We interpret this as continued dominance of rural-to-urban migration patterns, particularly in peripheral and semiperipheral regions, further reinforcing dynamic urban development.

Global final demand grows steadily, reaching a level by 2100 that is approximately four times higher than at the start of the simulation (Figure 3b). The scenario is replicating the neoliberal narrative that economic growth ultimately benefits all classes: the increase in global final demand is not only driven by elites' consumption expectations but also by all other segments of the world population. As industrialization unfolds with greater strength in the periphery, extreme poverty is eradicated worldwide within four decades. Throughout the scenario, the world's poor, which are soon completely integrated into world economic production processes, experience significant increases in their living standard, especially during the second half of the simulation. In 2060, the poorest 30% of the semiperiphery consume about €5,300 per person per year and those of the periphery about €3,100. These values increase to more than €17,500 and €8,700 respectively by 2100 (Figure 3c). The middle class benefits even more: while the middle 50% of the semiperiphery consume about €11,500 per capita in 2060, by 2100 this

increases to nearly €35,000 annually. In the periphery, middle-class consumption reaches €6,000 per capita by 2060 and almost €17,500 by the end of the simulation.

Despite rapid global economic growth, final demand and household consumption begin to slow toward the end of the simulation. This dynamic results from increasing labor scarcity, as productivity gains fail to keep pace with the shrinking labor supply—driven by population decline and global aging—while consumption expectations rise continuously. Thus, notably, even in a scenario without biophysical constraints, economic growth might still diminish.

Given that scenario A exhibits high economic inequality paired with high economic growth and a considerable improvement in the poor's consumption levels, we refer to it as *Neoliberal promises*.

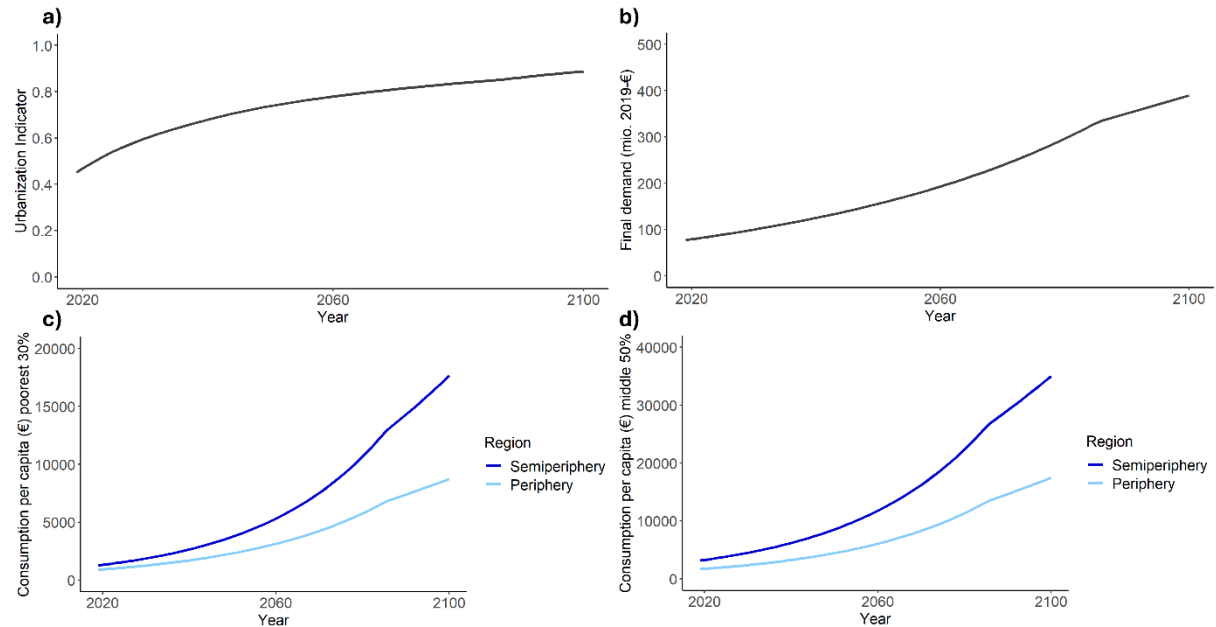


Figure 3: Projected evolution of a) the urbanization indicator, b) total annual final demand, c) annual consumption per capita of the poorest 30% of the semiperiphery and periphery; d) annual consumption per capita of the middle 30% of the semiperiphery and periphery in scenario A.

3.2. B: Shadows of neoliberal development

In scenario B, the subsistence population is less willing to migrate, and the consumption of the poorest 30% of the population in the semiperipheral and peripheral parts of the global economy grows very slowly, reflecting barriers for these groups to access employment with a decent salary. Throughout the entire simulation the consumption per capita of the poorest class only grows by 160€ in the periphery and by 280€ in the semiperiphery (Figure 4a).

Annual per capita consumption of the middle class, grows stronger: in the semiperiphery consumption reaches 6,370€ by 2060 and 10,000€/year by 2100; in the periphery, the middle classes consumes less than 5,000€ by the end of the simulation (Figure 4b).

While the low growth in consumption among the poorest classes stems from exogenous scenario assumptions, the lower consumption of the middle classes compared to Scenario A is caused by land scarcity, which emerges relatively early in the simulation, to the detriment of consumption for populations living outside the center. Whereas in Scenario A child mortality rates in the semiperiphery and periphery converge with those of the center by 2060 and 2080, in Scenario B improvements in child mortality are slower, and rates remain higher in the semiperiphery and periphery than in the center until the end of the simulation. The lower consumption levels of the poorer classes result in slower growth of global final demand (Figure 4d).

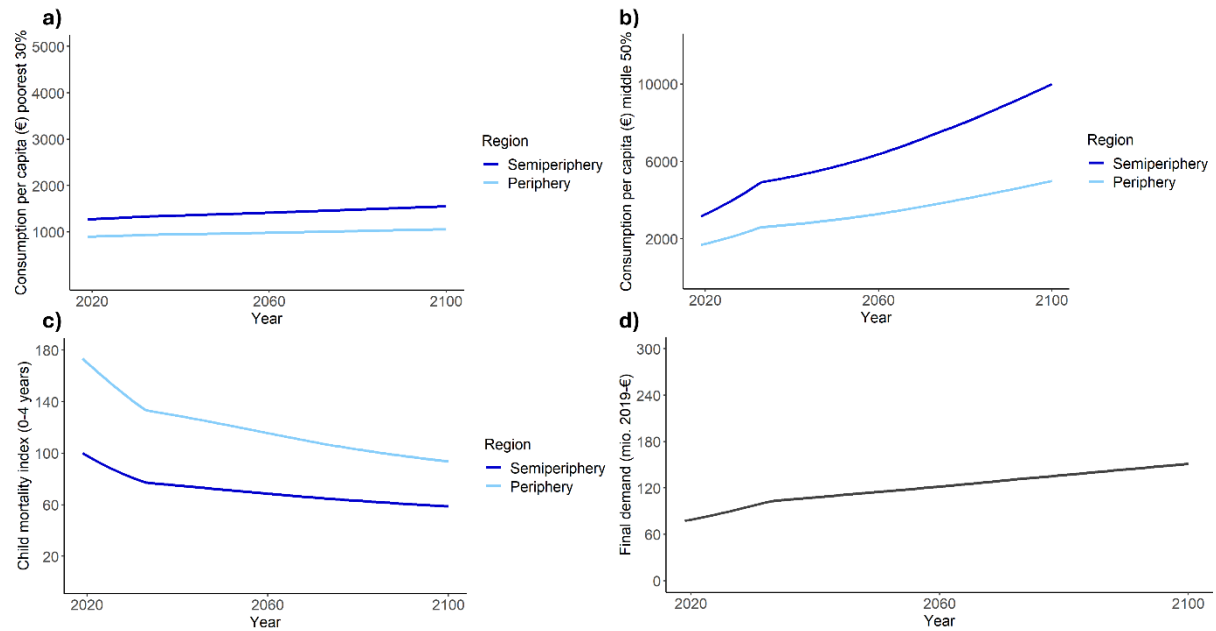


Figure 4: Per capita consumption of (a) the poorest 30%, (b) the middle 50%; (c) child mortality (calculated with respect to the child mortality rate in the periphery in 2019) and (d) global final demand in scenario B.

The less favorable macroeconomic situation, especially for the most vulnerable population groups within the world economy, reduce the incentives to leave the subsistence sector. Consequently, the population of the subsistence sector in the first 1.5 decades of the simulation declines only by about 200 million people. In 2033, however, there is a turning point after which outmigration accelerates significantly, leading to a faster decline of the subsistence population which drops to 70 million people in 2060 (Figure 5a). This dynamic is driven by the capitalist economy's expansion that leads to increasing demand for land. Due to the limited land availability and the scenario's prioritization of land demand from the world economy over land demand from the subsistence sector, part of the subsistence land is converted into land used by the global economy. Thus, scenario B represents a future featuring strong capitalist accumulation by dispossession: subsistence land is expropriated, capitalized and integrated into the world economy, thereby turning into more 'productive' land. Since land serves as a means of livelihood for the subsistence population, its loss amounts to forced outmigration from the subsistence sector and involuntary integration into capitalist labor markets, fueling accumulation by exploitation. As the subsistence population declines, demand for land decreases, leading to a further reduction in subsistence land (Figure 5b). Further indicators for

accumulation by dispossession are the continuously rising extraction levels for different materials used by the global economy (Figure 5b).

Last, the low growth of the global economy, combined with technological progress and a moderate energy transition leads CO₂ emissions to peak and decline moderately. Nevertheless, by the end of the simulation, CO₂ emissions are still comparable to initial levels, and contrary to political pledges, far from approaching ‘net zero’ (Dafnomilis et al., 2023), which shows a continued reliance of the global economy on accumulation by contamination.

Consequently, this scenario illustrates what may be termed *Shadows of neoliberal development*.

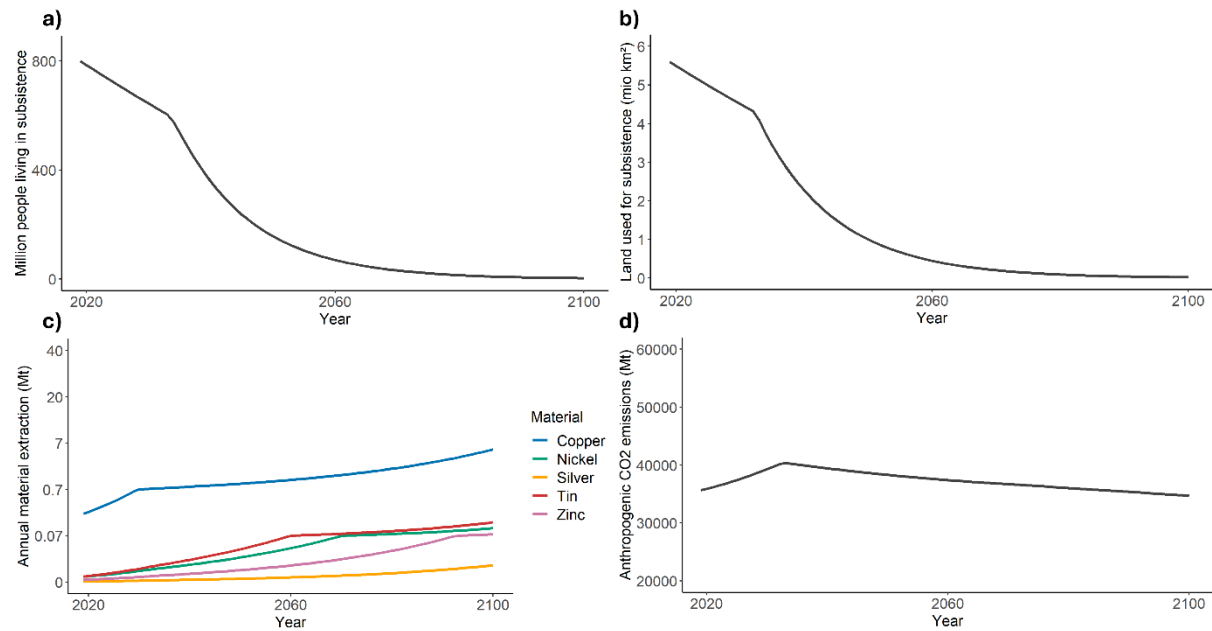


Figure 5: a) Subsistence population, b) subsistence land, c) annual material extraction for copper (blue), nickel (green), silver (orange), tin (red) and zinc (purple), d) annual anthropogenic CO₂ emissions in scenario B.

3.3. C: Breakdown of neoliberal development

Scenario C constitutes a worst-case economic and climate scenario, with outcomes that resemble a *Breakdown of neoliberal development*.

During the first 1.5 decades, the consumption of the poorest classes within the world economy peaks and then starts to decline. This reduces incentives for the subsistence population to migrate and the incorporation of cheap labor from the subsistence regime remains low.

However, rising land scarcity forces the integration of subsistence land into the world economy from 2030 onward, which—as in scenario B—generates strong accumulation by dispossession and accumulation by exploitation dynamics between 2030–2040. However, the continuous decline in the consumption level of the poorest 30% in the periphery sparks a first wave of remigration to the subsistence sector from 2040–2070. In the last decade of the simulation, a second wave

follows, as the consumption of the poorest class of the semiperiphery drops to critical levels and no policies of redistribution are implemented (Figure 6a).

Since the subsistence regime cannot absorb the entire population wishing to leave the global economy, the first and second migration waves are accompanied by a sharp increase in deaths in the two world regions, as consumption levels of those unable to migrate fall so low that mortality rates escalate (Figure 6b).

Interestingly, the land productivity in the world economy continues to grow during the entire simulation, although it does so at a much lower rate than in the absence of adverse climate impacts (Figure 6c). Changes in the area of land used by the global food industry (Figure 6d) are a result of changing productivities as well as industry and final demand for products of the food sector. Global sectoral land use peaks after two decades and declines sharply during the last decade of the simulation, reflecting a breakdown of the food sector due to the macroeconomic collapse caused and enforced by the massive outmigration of population.

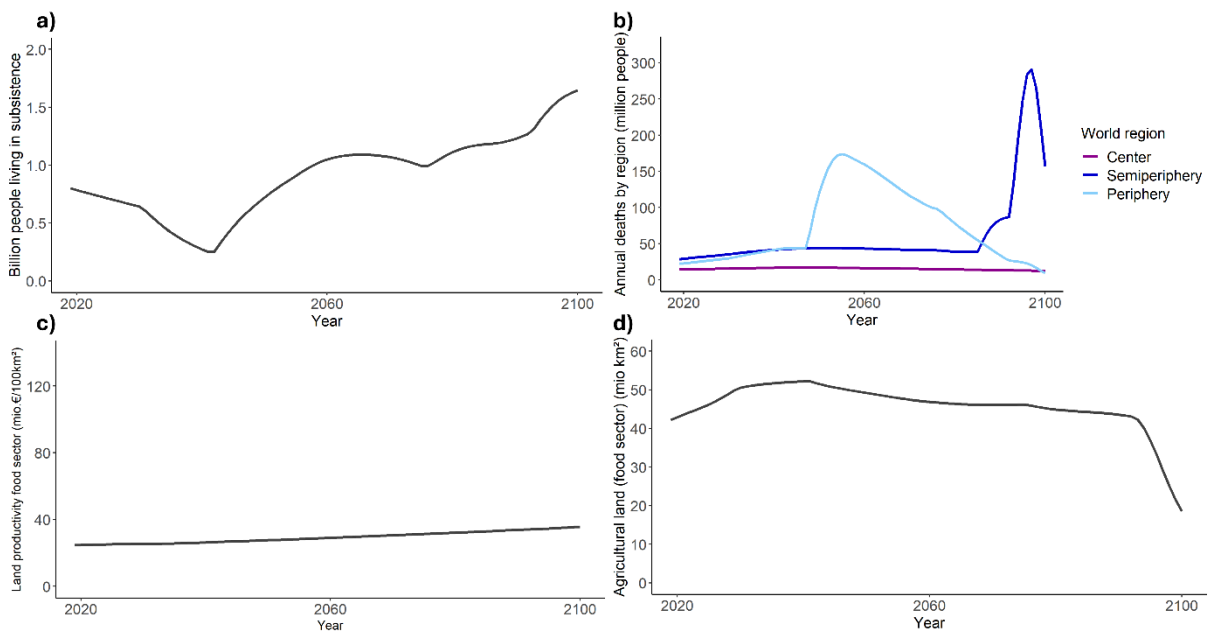


Figure 6: a) Global subsistence population, b) annual deaths in the global economy by region, c) land productivity of the food sector and d) the size of agricultural land in scenario C.

In scenario C, by 2100 global average temperature has increased by 3 °C compared to the pre-industrial period (Figure 7a). As climate damages multiply, the subsistence sector, unlike the industrialized food sector, experiences a decline in productivity (Figure 7b).

The evolution of subsistence land is highly non-linear during the simulation: it is driven by higher subsistence land demand resulting from the loss of land productivity and the migratory movements from urban to rural areas, while simultaneously constrained by land demand from the global economy. However, as the total output from the world economy begins to fall, more land is freed free and becomes available to the subsistence sector (Figure 7c). As a result of the interactions between socio-economic and environmental changes, the urbanization process slows, stabilizes and eventually reverses (Figure 7d).

Thus, Scenario C illustrates how global climate change could interact with other biophysical limits to growth, combined with diverging consumption inequality and persistent neglect of extreme poverty, to produce migration and population dynamics that may be described as a breakdown of capitalist accumulation and a partial return to the subsistence regime.

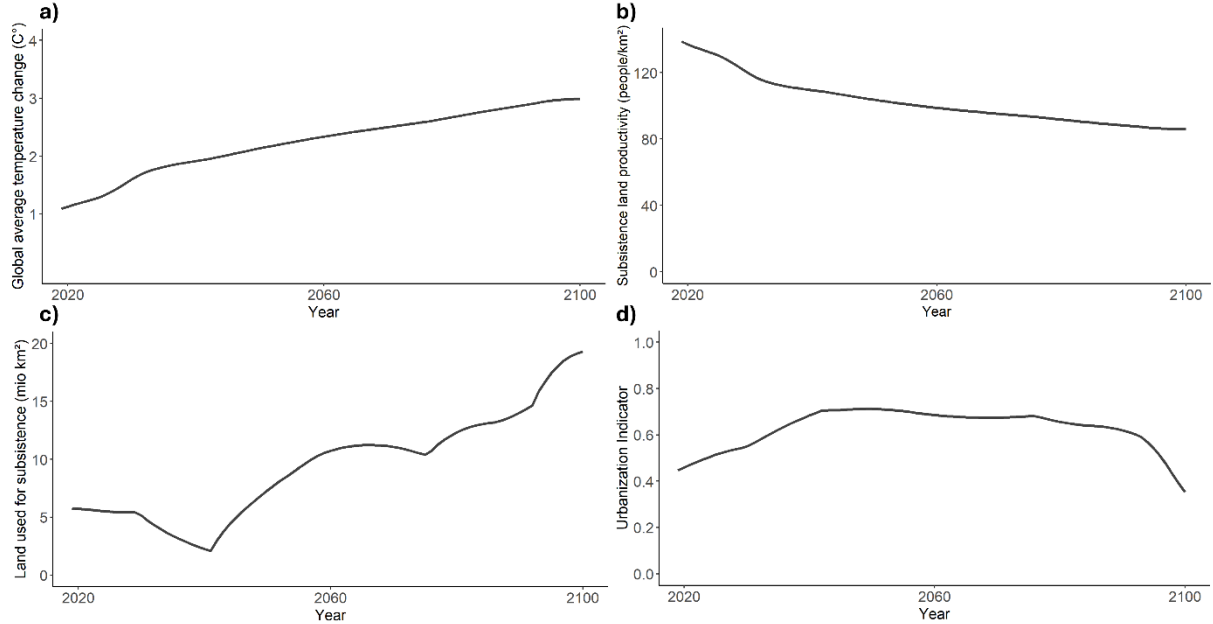


Figure 7: a) Subsistence land productivity, b) size of subsistence land, c) urbanization indicator and d) global warming in scenario C.

3.4. D: High adaptive capacity

We denominate Scenario D *High adaptive capacity of subsistence economies* because it attributes greater agency and adaptive capacity to subsistence populations than Scenarios A-C, which portray them as passive victims of global economic and environmental change. This ignores the agency of smallholders and their capacity to influence their futures (Karlin, 2025). The principal difference from Scenario C is that the subsistence population is assumed to possess a high capacity for innovation and adaptation in response to the adverse environmental impacts arising from the productive activities of the world economy.

In Scenario D, the population depending completely on the world economy peaks at over 8 billion in 2042 and afterwards declines continuously to 3.8 billion in 2090 and to 1.7 billion in 2100 (Figure 8a). This strong population loss is caused by both higher mortality rates among poorer population groups in the world economy, and by the eventual outmigration of the poorest workers. The evolution of the subsistence population is comparable to Scenario C but during the first wave of outmigration more people from the world economy can be absorbed, while the second wave occurs with a delay of various years (Figure 8b). As a result of the high adaptive capacity within the subsistence sector, the land productivity loss is smaller than in Scenario C and slows down during the simulation although the temperature increase in both scenarios is comparable (Figure 8c,d).

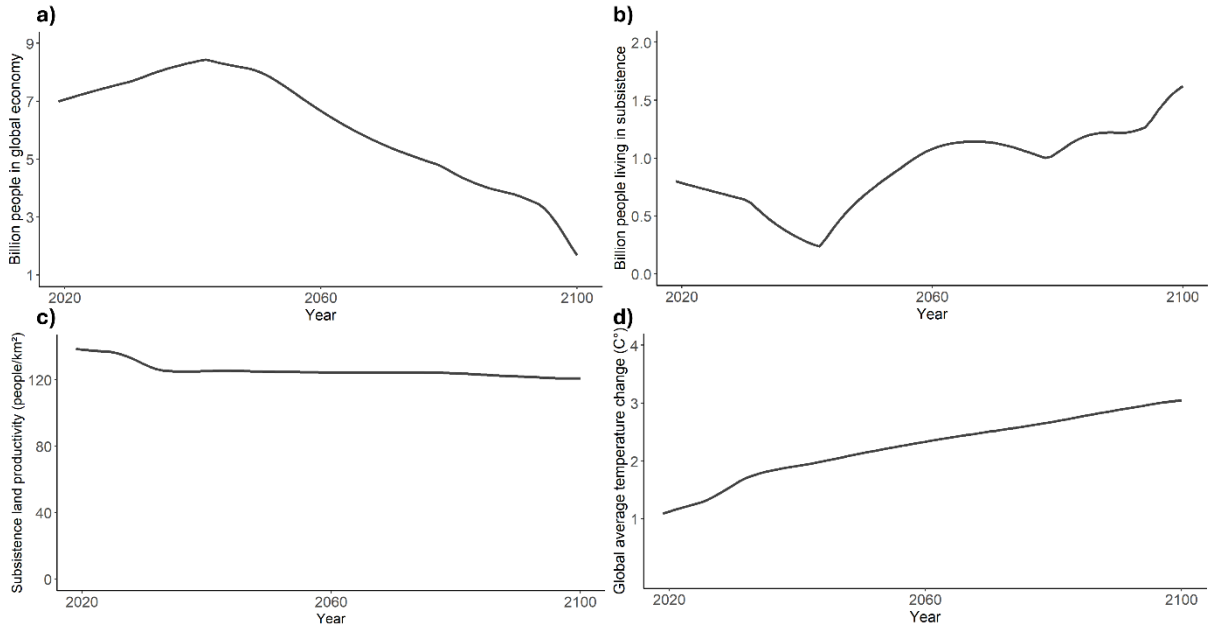


Figure 8: Evolution of a) the population depending entirely on the global economy, b) the population living outside the global economy, c) the subsistence land productivity and d) global warming in Scenario D.

The demographic changes in the global and the subsistence economy explain the changes in the urbanization indicator (Figure 9a). The dynamic is comparable to Scenario C but the final decline in the indicator's value occurs with a temporal delay. At the same time, due to the lower decline in land productivity, the area of land used by the subsistence sector is smaller than in Scenario C (Figure 9b).

Despite the massive population loss, world final demand continues to increase, implying a continued growth in consumption levels of the world's richer social classes. This dynamic is only reversed during the last decade of the simulation as the outmigration of workers from the semiperiphery leaves the world economy with an insufficient labor supply to maintain the desired level of output (Figure 9c).

Comparing the child mortality index in the global economy with those in the subsistence regime, we find that in the subsistence regime child mortality is considerably higher than in the world economy during the first three decades of the simulation. However, during the last five decades, the child mortality index for the world economy's peripheral regions surpasses that of the subsistence economy multiple times. Toward the end of the simulation, the child mortality index of the semiperipheral regions escalates as well, making the subsistence economy increasingly attractive to vulnerable population groups in the global economy (Figure 9c). Changes in the mortality of older age groups mirror the patterns observed for child mortality.

Introducing higher agency into the scenario simulation, thus, has multiple effects: high adaptive capacity leads to less biophysical constraints to the maximum population size, resulting in more people being absorbed during the first migration wave and less people dying in the world economy, although the difference is rather small. Instead, the land area of the subsistence regime is reduced considerably, which lowers the overall anthropogenic pressure on land. As a result, overall land scarcity is slightly reduced, the land demand from the world economy increases and the world economy grows at a slightly higher rate. This results in higher consumption levels within the global economy and a lower outmigration, at least as long as consumption does not reach critically low levels that cause sudden and sharp increases in

mortality in MORDRED. Thus, a higher adaptive capacity in the subsistence sector has a temporary stabilizing effect on the world economy.

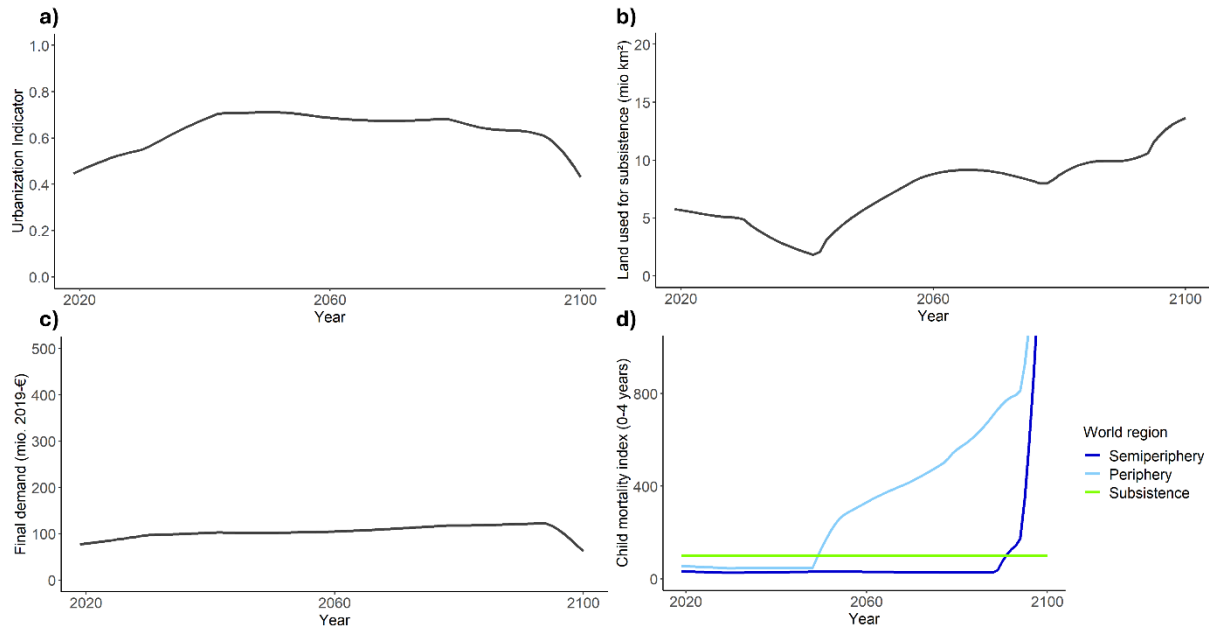


Figure 9: Evolution of a) the urbanization indicator, b) the land used by the subsistence sector, c) world final demand and d) the child mortality index for the population living in subsistence or in the global economy's semiperipheral and peripheral regions in Scenario D.

4. Discussion

The conducted explorative scenario exercise should be regarded as a first attempt to model interactions between capitalist and non-capitalist regimes, as well as urban and rural demographic dynamics within an IAM of medium complexity. Thus, unsurprisingly, our work comes with several limitations and important opportunities for future research.

First, the quality of our quantitative simulations is constrained by existing knowledge and data gaps that reflect the deep uncertainty surrounding contemporary global environmental changes and the relative neglect of non-monetized economic activities in quantitative economic and statistical research. The imbalance in data availability and reliability between high-income and low-income countries necessarily creates biases in our simulations that are difficult to control for. Although a large number of case studies in political ecology exist, and some attempts at quantifying political distribution conflicts have been made (Temper et al., 2018, 2020), a weak state presence in subsistence-dominated areas generally implies less reliable official statistics describing environmental, economic, demographic, cultural and social conditions in territories not subject to the capitalist mode of production. As a result, in addition to general uncertainties regarding the capacity of the global capitalist economy to mitigate, cope with, and adapt to climate change, little is known about the future adaptation capacity and resilience of the subsistence regime, maximum rates of rural re-migration, the rates at which land can be recovered and restored, or the speed at which local and Indigenous knowledge can be recovered and disseminated in scenarios of capitalist breakdown (cf. Aswani et al., 2018; Morton, 2007). Consequently, there is high uncertainty surrounding the more radical scenarios C and D in our scenario exercise. The discontinuous dynamics observable in these scenarios are produced by specific scenario assumptions indicated in the Methods section and the Supplementary Material.

They should not be understood as predictions of unavoidable collapse and ‘ruralization’, but they do question the stability of current trends and structures.

Second, there are limits to the model structure itself stemming from the simplified representation of the subsistence sector. For example, we do not consider gender inequalities or other power structures within subsistence regimes (Jost et al., 2016; Muzari, 2016). Likewise, the model’s dualism, i.e., the creation of two separate spheres—subsistence regime and global economy—linked only through migration flows, cannot capture hybrid agricultural regimes characterized by medium industrial input intensity. The model also cannot reflect the full complexity of rural transformation processes, which may involve additional accumulation dynamics beyond those considered here. For instance, accumulation by assimilation relies on integration under disadvantageous terms rather than dispossession, e.g. through contract farming (Marin-Burgos & Clancy, 2017; Pratama et al., 2021). Moreover, the model does not represent the economic characteristics of the urban informal sector, which plays a key role in maintaining the socio-economic metabolism of many cities in the Global South (Schindler, 2017). In MORDRED, the population engaged in informal economic activities belongs to the lowest consumption classes in the periphery and semi-periphery. Their vulnerability to economic and environmental shocks is reflected in consumption cuts rather than through explicit disruptions of informal production processes.

For these reasons, although our scenario exercise is based on quantitative data, it is best interpreted as a formal, qualitative exploration of multiple complex dynamics that may result in radically divergent rural-urban landscapes. To avoid implying a false level of quantitative precision, we only indicate three reference years (2020, 2060, 2100) in the figures showing simulation results.

In light of these limitations, future work could focus on systematizing existing case studies and surveys to create more coherent and comprehensive databases suitable for modeling rural and urban subsistence and care economies. Likewise, uncertainties could be reduced through the development of new databases focusing specifically on production-related variables in the subsistence sector, including knowledge and technology, energy and material flows, contamination, land productivity, labor productivity and division of work, as well as changes in these variables in response to environmental change.

Equally, modelers could aim to construct IAMs that incorporate differentiated economic structures, including informal and subsistence modes of (re)production, and that integrate model and scenario assumptions beyond neoclassical economic theory. We hold that scenarios introduced in current IAMs focus excessively on ‘neoliberal promises’ depicted in *scenario A*, rather than on the complex and contested urbanization dynamics and their intersections with environmental problems and uneven economic growth that have characterized development in the Global South. Our scenario exercise shows dynamics of accumulation through exploitation, dispossession, and contamination in a relatively simple way, demonstrating that it is possible to build IAMs that reflect critical perspectives on capitalist development and urbanization. It is equally conceivable to combine economic models focused on subsistence, demographic change, and unequal development with energy, emissions, and climate models to enhance their relevance for climate research.

Regarding the content of global environmental scenarios, our simulations open the possibility of futures with radically altered spatial configurations, metabolisms, migration flows, and dominant forms of economic (re)production. While the need for more disruptive and

discontinuous scenarios has already been emphasized elsewhere (Rothman et al., 2023), our scenario development exercise illustrates the importance of reflecting on the (ir)reversibility of urbanization and the (un)desirability of maintaining ways of life and modes of production outside capitalist logics (Gillen et al., 2022; Ridgeway, 2007; Wang, 2024). Actively involving actors from the subsistence sector or the urban informal sector as key stakeholders in the development of global climate, energy, land, and biodiversity scenarios would likely lead to scenarios grounded in everyday experiences and future perceptions that are too often ignored in global environmental scenario analyses, and could yield new insights into poverty reduction, vulnerability, adaptation, resilience, and socio-political mobilization.

5. Conclusion

In this article, we have integrated a simple subsistence sector and migration dynamics between the subsistence sector and the global economy into an IAM to explore different global economic and environmental futures. The scenario exercise points to several highly policy-relevant risks, such as persistent urban poverty, which could be exacerbated by future climate change impacts, and the possibility of large-scale economic breakdown and a reversal of urbanization in worst-case scenarios. Under continued environmental degradation, neoliberal development cannot deliver its promises and may instead lead to profound human suffering and social disruption. The explorative scenario work conducted here therefore highlights the importance of adopting new development paradigms that prioritize poverty eradication, basic human needs, ecological regeneration, and resilience over capital accumulation in both rural and urban contexts. Quantitative models can play an important role in informing political decision-making in this regard, but only if overly idealistic and power-blind neoclassical assumptions are problematized and adapted.

References

- Albore, A., Zenebe, A., Tesfay, G., & Abadi, N. (2024). Lowland smallholders' livelihood vulnerability to Climate change-induced hazards in Southern Ethiopia. *Environmental Challenges*, 15, 100897. <https://doi.org/10.1016/j.envc.2024.100897>
- Altieri, M. A., & Koohafkan, P. (2008). *Enduring farms: Climate change, smallholders and traditional farming communities* (Vol. 6). Third World Network (TWN) Penang.
- Aragón, F. M., Oteiza, F., & Rud, J. P. (2021). Climate change and agriculture: Subsistence farmers' response to extreme heat. *American Economic Journal: Economic Policy*, 13(1), 1–35.
- Aswani, S., Lemahieu, A., & Sauer, W. H. H. (2018). Global trends of local ecological knowledge and future implications. *PLOS ONE*, 13(4), e0195440. <https://doi.org/10.1371/journal.pone.0195440>
- Barbesgaard, M., & Whitmore, A. (2024). "Blood on the floor:" The nickel commodity frontier and inter-capitalist competition under green extractivism. *Journal of Political Ecology*, 30(1). <https://doi.org/10.2458/jpe.5458>
- Bernards, N. (2025). Exploitation, colonial capitalism, and the deep roots of climate vulnerability in West Africa. *New Political Economy*, 1–16. <https://doi.org/10.1080/13563467.2025.2531001>
- Bluwstein, J., & Cavanagh, C. (2023). Rescaling the land rush? Global political ecologies of land use and cover change in key scenario archetypes for achieving the 1.5° C Paris agreement target. *The Journal of Peasant Studies*, 50(1), 262–294.
- Bonefeld, W. (2023). Capitalist accumulation and its historical foundation and logical premise: On primitive accumulation. *Critique*, 51(1), 197–215.
- Brenner, N., & Schmid, C. (2015). Towards a new epistemology of the urban? *City*, 19(2–3), 151–182. <https://doi.org/10.1080/13604813.2015.1014712>
- Capellán-Pérez, I., de Blas, I., Nieto, J., de Castro, C., Miguel, L. J., Carpintero, Ó., Mediavilla, M., Lobejón, L. F., Ferreras-Alonso, N., & Rodrigo, P. (2020). MEDEAS: a new modeling framework integrating global biophysical and socioeconomic constraints. *Energy & Environmental Science*, 13(3), 986–1017.
- Caviedes, J., Ibarra, J. T., Calvet-Mir, L., Álvarez-Fernández, S., & Junqueira, A. B. (2024). Indigenous and local knowledge on social-ecological changes is positively associated with livelihood resilience in a Globally Important Agricultural Heritage System. *Agricultural Systems*, 216, 103885. <https://doi.org/10.1016/j.agsy.2024.103885>
- Chanza, N., & Musakwa, W. (2022). Indigenous local observations and experiences can give useful indicators of climate change in data-deficient regions. *Journal of Environmental Studies and Sciences*, 12(3), 534–546. <https://doi.org/10.1007/s13412-022-00757-x>
- Dafnomilis, I., Den Elzen, M., & Van Vuuren, D. P. (2023). Achieving net-zero emissions targets: An analysis of long-term scenarios using an integrated assessment model. *Annals of the New York Academy of Sciences*, 1522(1), 98–108. <https://doi.org/10.1111/nyas.14970>
- D'Alisa, G., & Demaria, F. (2024). Accumulation by contamination: Worldwide cost-shifting strategies of capital in waste management. *World Development*, 184, 106725.
- Demaria, F. (2015). Can the Poor Resist Capital? Conflicts over 'Accumulation by Contamination' at the Ship Breaking Yard of Alang (India) How Struggles for Environmental Justice Contribute to the Environmental Sustainability of the Economy. In *Nature, Economy and Society: Understanding the Linkages* (pp. 273–304). Springer.
- Estrada, A., Garber, P. A., Gouveia, S., Fernández-Llamazares, Á., Ascensão, F., Fuentes, A., Garnett, S. T., Shaffer, C., Bicca-Marques, J., Fa, J. E., Hockings, K., Shanee, S., Johnson, S., Shepard, G. H., Shanee, N., Golden, C. D., Cárdenas-Navarrete, A., Levey, D. R., Boonratana, R., ...

- Volampeno, S. (2022). Global importance of Indigenous Peoples, their lands, and knowledge systems for saving the world's primates from extinction. *Science Advances*, 8(32), eabn2927. <https://doi.org/10.1126/sciadv.abn2927>
- Ewing, P. M., Tu, X., Runck, B. C., Nord, A., Chikowo, R., & Snapp, S. S. (2023). Smallholder farms have and can store more carbon than previously estimated. *Global Change Biology*, 29(6), 1471–1483. <https://doi.org/10.1111/gcb.16551>
- Ford, J. D. (2012). Indigenous Health and Climate Change. *American Journal of Public Health*, 102(7), 1260–1266. <https://doi.org/10.2105/AJPH.2012.300752>
- Gatew, S., & Guyo, N. (2024). Livelihood vulnerability of Borana pastoralists to climate change and variability in Southern Ethiopia. *International Journal of Climate Change Strategies and Management*, 16(1), 157–176. <https://doi.org/10.1108/IJCCSM-06-2023-0077>
- Gillen, J., Bunnell, T., & Rigg, J. (2022). Geographies of ruralization. *Dialogues in Human Geography*, 12(2), 186–203. <https://doi.org/10.1177/20438206221075818>
- Glassman, J. (2006). Primitive accumulation, accumulation by dispossession, accumulation by 'extra-economic' means. *Progress in Human Geography*, 30(5), 608–625. <https://doi.org/10.1177/0309132506070172>
- Hall, D. (2013). Primitive Accumulation, Accumulation by Dispossession and the Global Land Grab. *Third World Quarterly*, 34(9), 1582–1604. <https://doi.org/10.1080/01436597.2013.843854>
- Harvey, D. (2003). *The New Imperialism*. Oxford University Press. <https://doi.org/10.1093/oso/9780199264315.001.0001>
- Hazarika, A., Nath, A. J., Reang, D., Pandey, R., Sileshi, G. W., & Das, A. K. (2024). Climate change vulnerability and adaptation among farmers practicing shifting agriculture in the Indian Himalayas. *Environmental and Sustainability Indicators*, 23, 100430. <https://doi.org/10.1016/j.indic.2024.100430>
- IPCC. (2023). *Climate Change 2023: Synthesis Report. Contribution of Working Groups I, II and III to the Sixth Assessment Report of the Intergovernmental Panel on Climate Change [Core Writing Team, H. Lee and J. Romero (eds.)]*. IPCC. <https://www.ipcc.ch/report/sixth-assessment-report-cycle/>
- Jenet, A., Buono, N., Di Lello, S., Gomarasca, M., Heine, C., Mason, S., Nori, M., Saavedra, R., & Van Troos, K. (2017). *Pastoralism, the backbone of the world's drylands* (P. Mundy, Ed.). VSF International.
- Jost, C., Kyazze, F., Naab, J., Neelormi, S., Kinyangi, J., Zougmore, R., Aggarwal, P., Bhatta, G., Chaudhury, M., Tapiro-Bistrom, M.-L., Nelson, S., & Kristjanson, P. (2016). Understanding gender dimensions of agriculture and climate change in smallholder farming communities. *Climate and Development*, 8(2), 133–144. <https://doi.org/10.1080/17565529.2015.1050978>
- Karlin, M. (2025). The Future of Peasants: A Multidisciplinary Review of Culture, Systems, and Movements. *Folia Geographica*, 67(2).
- Khan, D., & Karak, A. (2018). Urban development by dispossession: Planetary urbanization and primitive accumulation. *Studies in Political Economy*, 99(3), 307–330.
- Lauer, A., Carpintero, Ó., & De Castro, C. (2025). In search of a missing South: An explorative study of biases in global climate and energy scenarios. *Globalizations*, 1–22. <https://doi.org/10.1080/14747731.2025.2526295>
- Lauer, A., & Llases, L. (2025). *MORDRED: Model Of Resource Distribution and Resilient Economic Development. Model Documentation*. GitHub. <https://github.com/Pendracus/MORDRED>
- Lauer, A., Llases, L., & López-Muñoz, P. (2025). Toward global environmental scenarios for (and by) the 'bottom billion'? *Environmental Science & Policy*, 174, 104268.

- Levene, M., & Conversi, D. (2017). Subsistence societies, globalisation, climate change and genocide: Discourses of vulnerability and resilience. In *Climate Change and Genocide* (pp. 29–45). Routledge.
- Li, C. (2020). Rural Labor Mobility in the Process of Industrialization under Triple Dimensions. *Latin American Journal of Trade Policy*, 3(6), 6–31.
- Lowder, S. K., Bhalla, G., & Davis, B. (2025). Decreasing farm sizes and the viability of smallholder farmers: Implications for resilient and inclusive rural transformation. *Global Food Security*, 45, 100854. <https://doi.org/10.1016/j.gfs.2025.100854>
- Marin-Burgos, V., & Clancy, J. S. (2017). Understanding the expansion of energy crops beyond the global biofuel boom: Evidence from oil palm expansion in Colombia. *Energy, Sustainability and Society*, 7, 1–21.
- Mediavilla, M., Lifi, M., Ferreras-Alonso, N., Miguel, L. J., & De Blas, I. (2025). Analysis of the competition between land, energy and food using the TERRA module of WILIAM System Dynamics IAM. *Renewable and Sustainable Energy Reviews*, 216, 115651. <https://doi.org/10.1016/j.rser.2025.115651>
- Meyfroidt, P., Abeygunawardane, D., Baumann, M., Bey, A., Buchadas, A., Chiarella, C., Junquera, V., Kronenburg García, A., Kuemmerle, T., Le Polain De Waroux, Y., Oliveira, E., Picoli, M., Qin, S., Rodriguez García, V., & Rufin, P. (2024). Explaining the emergence of land-use frontiers. *Royal Society Open Science*, 11(7), 240295. <https://doi.org/10.1098/rsos.240295>
- Moore, J. (2000). Sugar and the expansion of the early modern world-economy: Commodity frontiers, ecological transformation, and industrialization. *Review (Fernand Braudel Center)*, 409–433.
- Moore, J. (2015). *Capitalism in the Web of Life: Ecology and the Accumulation of Capital*. Verso Books.
- Moore, J. (2017). The Capitalocene, Part I: on the nature and origins of our ecological crisis. *The Journal of Peasant Studies*, 44(3), 594–630.
- Morton, J. F. (2007). The impact of climate change on smallholder and subsistence agriculture. *Proceedings of the National Academy of Sciences*, 104(50), 19680–19685.
- Muzari, W. (2016). Gender disparities and the role of women in smallholder agriculture in Sub-Saharan Africa. *International Journal of Science and Research*, 5(1), 1869–1873.
- Negash, M., & Kanninen, M. (2015). Modeling biomass and soil carbon sequestration of indigenous agroforestry systems using CO2FIX approach. *Agriculture, Ecosystems & Environment*, 203, 147–155. <https://doi.org/10.1016/j.agee.2015.02.004>
- Nikolakis, W., Welham, C., & Greene, G. (2022). Diffusion of indigenous fire management and carbon-credit programs: Opportunities and challenges for “scaling-up” to temperate ecosystems. *Frontiers in Forests and Global Change*, 5, 967653. <https://doi.org/10.3389/ffgc.2022.967653>
- Nori, M., Taylor, M., & Sensi, A. (2008). Browsing on fences. *Pastoral Land Rights, Livelihoods and Adaptation to Climate Change. IIED Issue Paper*, 148.
- Owen, J. R., Kemp, D., Lechner, A. M., Harris, J., Zhang, R., & Lèbre, É. (2022). Energy transition minerals and their intersection with land-connected peoples. *Nature Sustainability*, 1–9.
- Parida, D., & Agrawal, S. (2023). Southern urbanism: A systematic review of concepts, debates, and future directions. *GeoJournal*, 88(3), 2587–2608.
- Peck, R., Anderson, C., & Anderson, J. (2013). Segmentation of smallholder households: Meeting the range of financial needs in agricultural families. *Focus Note*, 85.
- Picard, M., & Beigi, T. (2020). Stains of Empire: Accumulation by contamination in the Gulf. *Journal of Energy History*, 2, 1–25.

- Pratama, I. P., Winarso, H., Hudalah, D., & Syabri, I. (2021). Extended Urbanization through Capital Centralization: Contract Farming in Palm Oil-Based Agroindustrialization. *Sustainability*, 13(18), 10044. <https://doi.org/10.3390/su131810044>
- Raju Das. (2017). David Harvey's Theory of Accumulation by Dispossession: A Marxist Critique. *World Review of Political Economy*, 8(4). <https://doi.org/10.13169/worlrevipoliecon.8.4.0590>
- Ridgeway, S. (2007). Globalization from the Subsistence Perspective. *Peace Review*, 19(3), 297–304. <https://doi.org/10.1080/10402650701524659>
- Rothman, D. S., Raskin, P., Kok, K., Robinson, J., Jäger, J., Hughes, B., & Sutton, P. C. (2023). Global Discontinuity: Time for a Paradigm Shift in Global Scenario Analysis. *Sustainability*, 15(17), 12950.
- Saghai, Y. (2021). Subversive future seeks like-minded model: On the mismatch between visions of food sovereignty futures and quantified scenarios of global food futures. *Ethics & International Affairs*, 35(1), 51–67.
- Samberg, L. H., Gerber, J. S., Ramankutty, N., Herrero, M., & West, P. C. (2016). Subnational distribution of average farm size and smallholder contributions to global food production. *Environmental Research Letters*, 11(12), 124010.
- Sanyal, K. (2007). *Rethinking capitalist development: Primitive accumulation, governmentality and post-colonial capitalism*. Routledge India.
- Savo, V., Lepofsky, D., Benner, J., Kohfeld, K. E., Bailey, J., & Lertzman, K. (2016). Observations of climate change among subsistence-oriented communities around the world. *Nature Climate Change*, 6(5), 462–473.
- Scheidel, A., Sorman, A. H., Avila, S., Del Bene, D., & Ott, J. (2023). Renewables Grabbing. Land and Resource Appropriations in the Global Energy Transition. In A. Neef, C. Ngin, T. Moreda, & S. Mollett (Eds.), *Routledge handbook of global land and resource grabbing* (pp. 189–204). Routledge.
- Schindler, S. (2017). Towards a paradigm of Southern urbanism. *City*, 21(1), 47–64.
- Soto-Pinto, L., Anzueto, M., Mendoza, J., Ferrer, G. J., & De Jong, B. (2010). Carbon sequestration through agroforestry in indigenous communities of Chiapas, Mexico. *Agroforestry Systems*, 78(1), 39–51. <https://doi.org/10.1007/s10457-009-9247-5>
- Stadler, K., Wood, R., Bulavskaya, T., Södersten, C., Simas, M., Schmidt, S., Usabiaga, A., Acosta-Fernández, J., Kuenen, J., Bruckner, M., Giljum, S., Lutter, S., Merciai, S., Schmidt, J. H., Theurl, M. C., Plutzar, C., Kastner, T., Eisenmenger, N., Erb, K., ... Tukker, A. (2018). EXIOBASE 3: Developing a Time Series of Detailed Environmentally Extended Multi-Regional Input-Output Tables. *Journal of Industrial Ecology*, 22(3), 502–515. <https://doi.org/10.1111/jiec.12715>
- Temper, L., Avila, S., Del Bene, D., Gobby, J., Kosoy, N., Le Billon, P., Martinez-Alier, J., Perkins, P., Roy, B., & Scheidel, A. (2020). Movements shaping climate futures: A systematic mapping of protests against fossil fuel and low-carbon energy projects. *Environmental Research Letters*, 15(12), 123004.
- Temper, L., Demaria, F., Scheidel, A., Del Bene, D., & Martinez-Alier, J. (2018). The Global Environmental Justice Atlas (EJAtlas): Ecological distribution conflicts as forces for sustainability. *Sustainability Science*, 13(3), 573–584.
- Thorlakson, T., & Neufeldt, H. (2012). Reducing subsistence farmers' vulnerability to climate change: Evaluating the potential contributions of agroforestry in western Kenya. *Agriculture & Food Security*, 1, 1–13.
- Touch, V., Tan, D. K., Cook, B. R., Li Liu, D., Cross, R., Tran, T. A., Utomo, A., You, S., Grunbuhel, C., & Cowie, A. (2024). Smallholder farmers' challenges and opportunities: Implications for

- agricultural production, environment and food security. *Journal of Environmental Management*, 370, 122536.
- UN DESA. (2023). *The Sustainable Development Goals Report 2023: Special edition*. United Nations Publications. <https://unstats.un.org/sdgs/report/2023/The-Sustainable-Development-Goals-Report-2023.pdf>
- Wang, H. (2024). The role of informal ruralization within China's rapid urbanization. *Nature Cities*, 1(3), 205–215. <https://doi.org/10.1038/s44284-024-00038-4>
- Whiting, S. H. (2022). Land rights, industrialization, and urbanization: China in comparative context. *Journal of Chinese Political Science*, 27(2), 399–414.
- Widiono, S., Wahyuni, E. S., Kolopaking, L. M., & Satria, A. (2024). Livelihood vulnerability of indigenous people to climate change around the Kerinci Seblat National Park in Bengkulu, Indonesia. *Regional Sustainability*, 5(4), 100181. <https://doi.org/10.1016/j.regsus.2024.100181>
- World Bank. (2025a). *Indigenous Peoples*. <https://www.worldbank.org/en/topic/indigenouspeoples>
- World Bank. (2025b). *World Bank Analytical Classifications (presented in World Development Indicators)*. <https://datacatalogfiles.worldbank.org/ddh-published/0037712/DR0090754/OGHIST.xlsx>
- Zhang, Z., Li, M., Li, W., Wei, Y., & Shi, Y. (2023). A long way to go: Impacts of urbanization on migrants' livelihoods and rural ecology in less industrialized regions. *Journal of Mountain Science*, 20(12), 3450–3463. <https://doi.org/10.1007/s11629-023-8319-8>

Beyond Unidirectional Drivers: Endogenizing IPAT in an Integrated Assessment Model

Abstract

This article revisits and extends the IPAT framework ($\text{Impact} = \text{Population} \times \text{Affluence} \times \text{Technology}$) by representing the IPAT equation in a dynamic and endogenized way within the system-dynamics model MORDRED. Unlike static interpretations of IPAT that treat each component as independent and unidirectional driver of environmental impact, our approach captures the complex, reciprocal interactions between population, affluence, technological development and environmental impacts over time. Through the simulation of a business-as-usual scenario, and a range of population-, sufficiency- and efficiency-related policy scenarios, we examine the systemic implications of these interdependencies for environmental sustainability and economic stability. Our results reveal three key insights. First, the components of the IPAT equation are deeply interrelated: changes in one driver dynamically influence the others, and can both slow down and reinforce environmental degradation. Second, in the absence of ambitious and stringent policy interventions or societal changes, these interactions accelerate environmental impacts, triggering biophysical feedbacks that in turn undermine economic and demographic stability, leading to systemic collapse. Third, although combined policy measures targeting all three drivers, especially population size, can significantly reduce environmental pressures, they are far from sufficient to achieve long-term environmental sustainability. The formal integration of dynamic IPAT relationships into an IAM provides a novel lens for assessing policy effectiveness and the behavior of different social and biophysical systems. Our findings underscore the continued relevance of IPAT but also point to the importance of a detailed analysis of the underlying global cultural, economic and political institutions that fundamentally condition and shape future evolutions of every IPAT component.

Keywords

Integrated Assessment Modeling; sustainability modeling; business as usual; sufficiency; world population; system dynamics.

1. Introduction

The *IPAT* identity emerged from a debate between Ehrlich, Holdren and Commoner in the early 1970s (Commoner, 1972; Ehrlich & Holdren, 1971, 1972) and has influenced decades of research on the anthropogenic driving forces of environmental impacts due to its relative simplicity and the clear decomposition of impact into three key variables. Over the years the original equation has been modified and re-evaluated by different authors (Chertow, 2000; McGee et al., 2015; Waggoner & Ausubel, 2002; Wei, 2011; York et al., 2003b), with the STIRPAT model being one of the most prominent extensions because it enables researchers to conduct statistical analyses of the causal linkages between anthropogenic drivers and environmental impacts by quantifying their relative weights in the equation (Dietz & Rosa, 1997; Rosa & Dietz, 1998). The *IPAT* framework has been used to study a wide range of environmental impacts, ranging from pollution such as CO₂ emissions in the Soviet Union (Brizga et al., 2013) to the water use of the economy (J. Yang & Chen, 2019) and waste generation at tourist destinations (Arbulu et al., 2017). Furthermore, it has been linked to other environmental accounting frameworks such as life-cycle accounting (Font Vivanco et al., 2014) and material flow analysis (Fischer-Kowalski & Amann, 2001), and has influenced the development of the Kaya identity promoted by the IPCC, and the master equation in industrial ecology (Chertow, 2000; Magee & Devezas, 2018).

Given that *IPAT* enables modelers to project environmental impacts under different assumptions regarding future changes in population, affluence and technology the framework has also been used in different modeling and scenario studies, including the quantification of economic scenarios beyond growth in Sweden (Skånberg & Svenfelt, 2022), the exploration of different land-use scenarios under SSP1 - SSP4 (Karlsson et al., 2018) and the development of country-level emission and socio-economic pathways through the downscaling of regional scenarios (Gütschow et al., 2021).

Nevertheless, since its initial formulation research interests and trends have led to a fundamental reinterpretation of the *IPAT* framework (Chertow, 2000): while *IPAT* was originally developed to illustrate the unsustainability of harmful technology, affluence in the developed countries and population growth, it has increasingly been used to emphasize the potential of green technologies and to examine the hypothesized positive effect of affluence on environmental degradation, as suggested by the Environmental Kuznets Curve (EKC) (Xing et al., 2023; Zhao et al., 2017). Also, although Ehrlich and Holdren (1972) explicitly stated that the variables on the right-hand side of the identity are not independent from each other, many models only focus on the *affluence → technology* relationship shaping the EKC, rather than on other existing feedback dynamics between the drivers of environmental degradation. This is reflected in the technology-focus of current integrated assessment modeling: although integrated assessment models (IAMs) link demographic, economic, social and environmental systems, they often prioritize the identification of optimal technological pathways while sidestepping policies that would tackle affluence (Hickel et al., 2021; Wiedmann et al., 2020) and population growth (Alcott, 2012).

This paper introduces an IAM that reflects a reinterpretation of the *IPAT* equation stressing the interlinkages and feedback dynamics between the identity's components and the importance of considering a bidirectional causality between ecological and anthropogenic drivers and impacts. Our study makes three main contributions to the literature. First, we develop a dynamic and complex interpretation of the *IPAT* equation by disaggregating every component and formalizing different feedback relationships between the main drivers. Second, we endogenize the *IPAT*

equation in the IAM MORDRED, thereby illustrating that the structure of every coupled demographic-economic-environmental model can be interpreted and assessed through an *IPAT* lens. Last, we construct *IPAT*-informed policy scenarios and assess their isolated and combined effects on key variables of the global system.

2. Theoretical background and methods

In this section we describe different possible theoretical approaches to IPAT, the quantitative model, and the designed scenarios.

2.1. Possible theoretical approaches to IPAT

We distinguish four theoretical approaches to the *IPAT* identity that influence our modeling exercise.

Firstly, IPAT can be understood as a framework to disaggregate the drivers of environmental degradation and to analyze how changes in the different components over time affect the overall environmental impact, resulting in policy recommendations that can address P , A and T (Engström & Kolk, 2024).

$$I = P * A * T \quad (1)$$

Given that consumption is a share of economic output, X can be understood as total consumption or total economic production and influences both A and T .

$$A = \frac{X}{P} \quad (2)$$

$$T = \frac{I}{X} \quad (3)$$

Secondly, the P - A - T components can be seen as interdependent. For example, Alcott (2010) identifies nine simultaneous equations on the right-hand side of $I=PAT$ ($T=f(P)$, $A=f(T)$, $P=f(A)$ etc.).

$$I = f(P, A, T) \quad (4)$$

Thirdly, from a system dynamics perspective, the left- and the right-hand side of *IPAT* could mutually influence each other, and I can drive itself. For instance, environmental degradation can reduce the carrying capacity (Ehrlich & Ehrlich, 2013; Meadows et al., 1972) of global ecosystems, while climate tipping points (Armstrong McKay et al., 2022) serve as example of self-enforcing ‘environmental degradation’.

$$\frac{dP}{dt} = f(P, A, T, I) \quad (5)$$

$$\frac{dI}{dt} = f(P, A, T, I) \quad (6)$$

$$f(P, A, T, I) = 0 \quad (7)$$

Last, adopting a critical or constructivist approach, it is possible to argue that P , A and T are first order drivers that are themselves shaped by underlying second order drivers including economic modes of productions (e), political governance institutions (g) and hegemonic cultures (c) (Mokyr, 2016; York et al., 2003a).

$$I(P, A, T) = f(P(e, c, g), A(e, c, g), T(e, c, g)) \quad (8)$$

This approach is difficult to represent explicitly within formal models but must be considered when designing and interpreting scenarios.

2.2. Operationalizing IPAT

IAMs provide an opportunity to formalize the *IPAT* components and their mutual interactions. Thus, they facilitate the systematic exploration of different policy interventions.

This section explains how the model used for this study represents *IPAT* and to which extent it considers complex feedback relationships between *IPAT* components.

2.2.1. Model structure

MORDRED (Model of Resource Distribution and Resilient Economic Development) is an IAM well suited for investigating *IPAT*-related questions because it provides detailed representations of population dynamics, affluence levels, technological change, and environmental impacts, alongside multiple feedback mechanisms that interconnect these drivers.

MORDRED's population module represents the global population, which is disaggregated into 3 world regions, 10 classes and 20 age groups. The 'center' includes the population living in high-income countries, the 'semiperiphery' the population residing in upper-middle-income countries and the 'periphery' the population of lower-middle- and low-income countries. Within every world region except the center, the population is assumed to either be sustained by the global economy or by subsistence economies. The populations belonging to the latter constitute the 'subsistence class' whereas the population living within the world economy is divided into 3 classes per world region: the Top20 (the richest 20%), the Botttom30 (the poorest 30%) and the Middle50 (the remaining 50% of the population). Differences between the per capita consumption of the subsistence class and the Bottom30 drive migration dynamics between the two economic regimes.

Economic production is represented using an Input–Output (IO) framework comprising 25 global economic sectors, including primary, secondary, and tertiary sectors as well as multiple energy technologies. Following the IO method (Miller & Blair, 2009), the model represents inter-industry flows and the production of intermediate goods through a 25x25 A matrix. Final demand is disaggregated into household and government final demand as well as investment. The sum of all demand components and intermediate goods yields global economic output (X).

A is modeled as consumption per capita. An individual's affluence depends on overall global economic development, on the world region and on the individual's class. Overall economic development, in turn, can be restrained by the availability of a series of input factors: labor hours, different types of land, capital, and intermediate products, notably from the energy sectors.

Technology is represented in MORDRED through the A matrix and through 'impact intensities' of production. The input coefficients of the A matrix indicate the technological profile of the economy. Declining input requirements, especially from energy sectors, typically reflect

technological progress via efficiency improvements, whereas rising input requirements may point to increasing challenges in extracting, processing, and transforming raw material (Brockway et al., 2019; Igogo et al., 2021; Norgate & Haque, 2010). Material extraction for different materials is computed through material intensity factors linked mainly to the output of the mining sector while fossil fuel intensity factors for the output of the fossil fuel sectors allow the model to calculate fossil resource demand.

Impacts on the biophysical environment resulting from economic activities and represented in MORDRED include different greenhouse gas (GHG) emissions, extracted materials, increased land use changes through forest conversion, and increased air and soil pollution. For our simulation we activate feedbacks within the climate system that result in higher temperature increases for any given level of anthropogenic GHG emissions.

Adverse effects on the economic structure resulting from environmental degradation represented in MORDRED include climate change damages of capital stock, labor productivity, working force and input intensities of the food sector, as well as increasing input coefficients for the extraction of fossil fuel resources that reflect increasing depletion of the finite fossil resource stock which is estimated based on BGR data on coal reserves and oil and gas resources (2020). Given that the main motivation of this study is methodological and conceptual, we reduce the model's complexity by deactivating all climate impacts so that only the energy-depletion feedback remains active. As will be shown, this feedback mechanism is sufficient to illustrate key dynamics emerging from a system dynamics approach to *IPAT*.

A detailed explanation of MORDRED is provided in Lauer & Llases (2025).

2.2.2. Feedback relationships between I,P,A and T in MORDRED

Because of its system dynamic basis, MORDRED can represent many of the feedback relationships between the components of *IPAT*. The main causal relationships are:

- 1) $PAT \rightarrow I$: Different types of impacts result from multiplying the output of economic production (X) with conversion efficiencies T_j (j includes land, energy and CO₂). The output can be disaggregated into the population and affluence level of three regions r that each contain 3 consumption classes k , the government consumption of every region, the production of intermediate products Z , and gross fixed capital formation $GFCF$.
- 2) $I \rightarrow PAT$: Only the consequences of growing resource depletion are considered through an extraction difficulty factor (EDF) which is multiplied with the input coefficients of the fossil sectors (no. 3 and 8) of the A matrix (M); other impacts (e.g. damages from climate change, biodiversity loss etc.) are not considered although it is possible to represent them through the economic structure of the model. Direct impacts of damages on population and technologies are not represented in MORDRED.
- 3) $P \rightarrow A$: Consumption per capita is a function of total population size and economic output which in turn is a function of labor productivity T_L and labor supply. The latter depends on the size of the population aged 15-64, the participation rate (prt) and the hours worked ($whours$). Thus, both T_L and the age structure of the population determine affluence.
- 4) $A \rightarrow P$: The difference in the affluence of the poorest classes in the world economy (we) and of the people living in subsistence acts as a driver of migration dynamics between the population of the subsistence and the world economy, with higher affluence levels

acting as an attractor of population from the subsistence regime. Mortality and fertility rates follow an asymptotic pattern for most age groups a and decrease with affluence.

- 5) $P \rightarrow T$: Hypothesized effects of an increasing population size are not represented in the model.
- 6) $T \rightarrow A$: The model represents two effects of T on A . On the one hand, productivity improvements of the input factors (land, labor, energy) allow output to grow, which can rise consumption levels. At the same time, production technologies increasingly impact the environment in a negative way, which in turn negatively impacts economic production capacities, reducing affluence levels.
- 7) $T \rightarrow P$: The model represents two effects of T on P . On the one hand, land productivity increases allow for a stronger growth of the agricultural sector, leading to increased consumption, reduced mortality and a higher population. On the other hand, there is an indirect negative effect on population size through adverse impacts on the economy and reduced affluence levels that increase mortality rates.
- 8) $A \rightarrow T$: Input requirements to the production process are assumed to decrease with increasing final demand per capita, due to increased investments in research and education. In the model, T improves as a logarithmic function of A .

Table 1 illustrates how the feedback relationships are operationalized in the model while Figure 1 provides a graphical summary of the operationalization of *IPAT* components in MORDRED.

Dimension	Feedback relationship number	Model	
$PAT \rightarrow I$	1)	$I_j = \left[\left(\sum_{i=r}^3 \sum_{k=1}^3 P_{r,k} * A_{r,k} \right) + Z + \sum_{r=1}^3 C_{gov_r} + GFCF \right] * T_j$ <p>with $T_j = \frac{I_j}{X}$ and $I = \sum_{j=1}^n I_j$</p>	(9)
$I \rightarrow PAT$	2)	$M_{i,3t_{with\ impacts}} = M_{i,3t_{without\ impacts}} * EDF$ $M_{i,8t_{with\ impacts}} = M_{i,8t_{without\ impacts}} * EDF$ $EDF > 1$	(10)
$P \rightarrow A$	3)	$A = c_{per\ capita} = f(X(Labor, T_L), P)$ $Labor\ hours = Prt * whours * P_{working\ age}^{we}$	(11)
$A \rightarrow P$	4)	$Migration_{Sub \rightarrow we} = f(A_{we})$ $Mortality\ rate_a = \alpha_{MR} + (\beta_{MR} - \alpha_{MR}) * e^{-\gamma A}$ $Fertility\ rate_a = \alpha_{FR} + (\beta_{FR} - \alpha_{FR}) * e^{-\gamma A}$ <p>Except for $a_{[30;34]}$ and $a_{[35;39]}$</p>	(12)
$P \rightarrow T$	5)	-	(13)
$T \rightarrow A$	6)	$A = f(X(I), P)$ $\max(X) = \frac{J}{T_j}$ $I_j = T_j * X$	(14)

		$\frac{dX}{dI} < 0$ $T \rightarrow I \rightarrow A$	
$T \rightarrow P$	7)	$\max(X_{agriculture}) = \frac{\text{total land}}{T_{land}}$ $T_j * X = I_j$ $A = f(X(I), P)$ $Mortality rate_a = f(A)$ $T \rightarrow I \rightarrow A \rightarrow P$	(15)
$A \rightarrow T$	8)	$T_{intermediary\ products} = f(\beta_1 * \ln(A_t) + \beta_2)$	(16)

Table 1: Integration of IPAT in MORDRED.

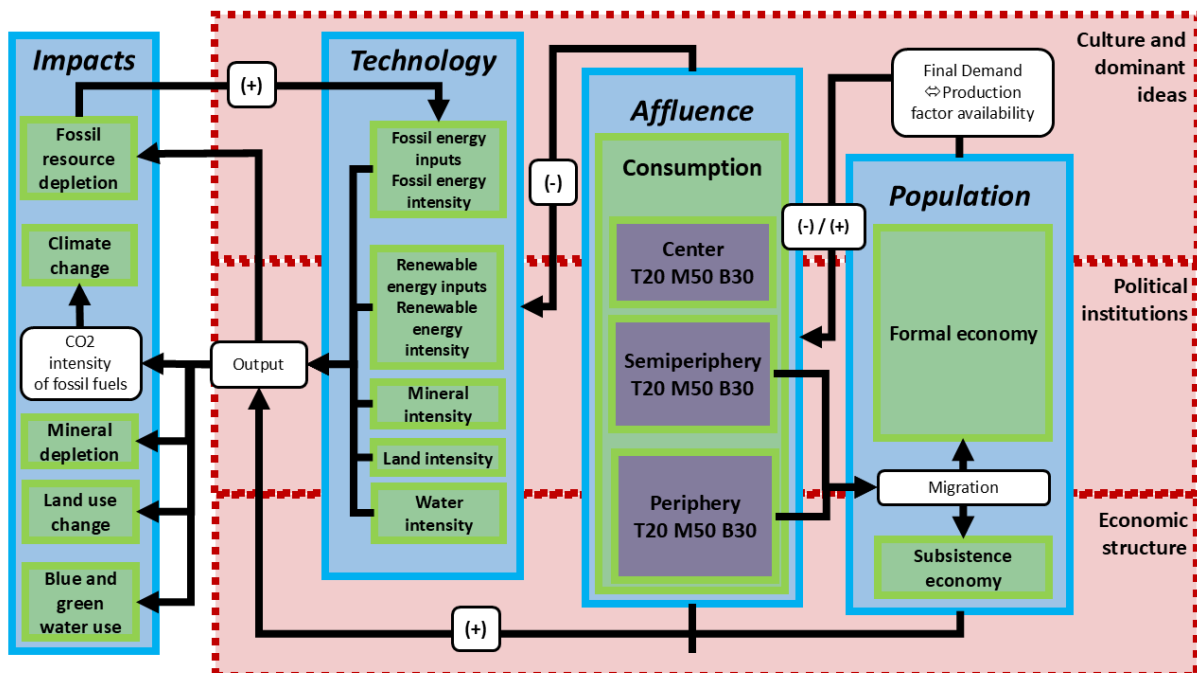


Figure 1: Relationships between the elements of IPAT in the MORDRED model.

2.3. Scenarios

We explore how IPAT plays out in the model through one baseline and four policy intervention scenarios. The baseline scenario is designed to illustrate the feedback between the left- and the right-hand side of $I=PAT$ while the policy scenarios explore the consequences of politically motivated changes in one, several or all drivers.

- *Baseline/no policy intervention*: In this scenario there are no policy interventions and, consequently, P, A, T and I develop endogenously following the basic model calibration and dynamics.
- *Population policy intervention (PPI)*: In this scenario, a global one-child policy is adopted.

- *Sufficiency policy intervention* (SPI): In this scenario, the per capita consumption of the whole world converges to the level of the Top20 of the semiperiphery until 2060.
- *Efficiency policy intervention* (EPI): In this scenario, we assume that at any given level of GDP per capita, the material and energy intensity of the economy is 5% lower than it would be in the absence of a technology-focused policy intervention. Additionally, fossil electricity is completely replaced by renewable electricity while in the baseline scenario 10% of the original fossil electricity input into the production process is maintained.
- *Population & sufficiency policy intervention* (PPI+SPI): This scenario combines the policies of PPI and SPI.
- *Population & efficiency policy intervention* (PPI + EPI): This scenario combines the policies of PPI and EPI.
- *Sufficiency & Efficiency policy intervention* (SPI+ EPI): This scenario combines the policies of SPI and EPI.
- *Integral policy intervention* (IPI = PPI + SPI + EPI): This scenario combines all policies in the IPAT framework.

To simulate the scenarios, we developed MORDRED 1.0.3 which includes four main changes compared to MORDRED 1.0:

First, we introduced a ‘technological impact factor’ (*TIF*) that changes the energy and material input requirements (*EMIR*) in the A matrix and depends on global final demand per capita.

$$Technological\ Impact\ Factor\ (TIF)_t = \beta_1 * \ln\left(\frac{FD}{P_t}\right) + \beta_2 \quad (17)$$

$$EMIR_{EMsectors,sectors_t} = TIF_t * EMIR_{EMsectors,sectors_{2019}} \quad (18)$$

EM (energy & material) sectors include the sectors 3,4,10, 12,13,14,15,16,17,18,19 and 20 (Suppl.Table1).

The parameters β_1 and β_2 ensure that *TIF* takes a value of 1 for a world final demand per capita corresponding to the initial moment of the simulation (2019) and a value of 0 when world final demand per capita approaches a high level, corresponding to approximately 80,000 € per capita based on a statistical analysis of York et al. (2003b).¹ At this point, it is assumed that the affluence elasticity of impact reaches 0, and, consequently, energy input requirements to the economy reach zero. This assumption introduces two strong optimistic biases into the analysis: First, it implies that strong absolute decoupling and complete dematerialization of the economy is possible, which contradicts thermodynamic principles. Second, while the threshold value given in York et al. applies to the affluence elasticity of CO₂, we use the same value for the affluence elasticity of energy. However, absolute decoupling for CO₂ is easier to achieve than absolute decoupling of energy use, since impacts can be shifted (e.g. from emissions to increase land use and biodiversity loss) by substituting fossil fuels with other energy sources, while overall energy intensity remains unchanged.

Second, we added an efficiency multiplier (*M_{EPI}*) that represents the effects of policy interventions aiming at accelerating the speed of technology-driven efficiency improvements:

$$TIF_{t_{EPI}} = (\beta_1 * \ln(final\ demand\ per\ capita_t) + \beta_2) * M_{EPI} \quad (19)$$

¹ The threshold value given in York et al. was converted to 2019-€.

In the EPI scenario and all other scenarios with an EPI component, the multiplier is set to 0.95, i.e. policies are assumed to accelerate the process of dematerialization by 5% at every level of economic development.

Third, we introduced the possibility to alter annual birth rates (BR) in all the regions and age groups in the model exogenously, approximating the effects of regional and/or global population policies. To simulate a global one-child policy, the sum of the birth rates over all age groups is set to 0.5, i.e. every adult has on average 0.5 children during the reproductive age (15-44 years).

$$BR_{age\ group,region_t} = \frac{1}{5} * \frac{1}{2} * \frac{BR_{age\ group_i_{2019},region}}{\sum_{i=1}^6 BR_{age\ group_i_{2019},region}} \quad (20)$$

Last, we added the option to let the consumption per capita of all classes converge toward the level of the richest 20% of the semiperiphery ($c_{T20,semip.}$) by defining exogenous growth rates ($g_{class,region}$).

$$g_{class,region_t} = e^{\ln\left(\frac{\frac{c_{T20,semip.2019}}{c_{class,region_{2019}}}}{2060-2019}\right)} - 1 \text{ if } c_{class,region_t} \neq c_{T20,semip.} \quad (21)$$

$$g_{class,region_t} = 0 \text{ if } c_{class,region_t} = c_{T20,semip.} \quad (22)$$

The Supplementary Material contains the parametrization of all scenarios that are simulated for the period 2019 - 2110.

3. Results

This section includes the key results and main insights from all scenario simulations realized in MORDRED. First, we present the simulation outcomes of the Baseline scenario which serves as a reference for the isolated policy interventions (PPI, SPI and EPI). Subsequently, we compare the development of IPAT drivers and key variables for the combined policy scenarios.

3.1. Baseline

The Baseline scenario illustrates that without IPAT-related policy interventions, the interactions between dynamically changing drivers produce strongly non-linear and historically discontinuous patterns over the course of the 21st century for key global variables (Figure 2).

Growth in world population contributes to increasing environmental impacts until 2056 when world population reaches a peak at 8.75 billion people. Afterwards, the relative importance of the driver ‘population’ decreases as global population moderately but persistently declines to 7.76 billion by 2100 (Figure 2a).

Affluence, on the other hand, grows continuously to reach a value of 42,410 (2019-)€ of annual final demand per capita by 2091, which is 4.3 times as high as the initial value (Figure 2b).

However, in the last decades of the simulation affluence levels begin to decline sharply and at an accelerated rate, reaching about 21,690 € in 2110.

The role of technological development is reflected in Figure 2c and d. Until affluence levels begin to stagnate and decline at the beginning of the 2090s, we can observe affluence-driven improvements in production technologies that result in a continuous decrease in environmental impacts per unit of production. Thus, energy intensities and the intensity at which five important minerals (copper, lead, nickel, silver, zinc) are used by the global economy decline by approximately 59%, 58%, 65%, 63%, 43% and 65%, respectively.

CO₂ exhibits a 56% decline by 2091, aside from a localized increase linked to deforestation. Nonetheless, in the simulation's final decades, this downward trend is reversed as reductions in affluence contribute to a deterioration of efficiency parameters.

Consequently, in the Baseline scenario affluence is the main driver of environmental impacts during most of the simulation time, with population growth playing a minor but still significant role. The relative contribution of 'bad' production technologies to environmental degradation decreases throughout the scenario which counterbalances increasing population and affluence levels. However, technological development does not occur fast enough to stabilize or reverse environmental impacts: material extraction rises continuously throughout the simulation (Figure 2f), as well as energy use and cumulative GHG emissions (Figure 2e). In combination with increasing natural GHG emissions due to positive feedback loops within the climate system, the anthropogenic emissions lead to a temperature increase of 4.7 °C relative to 1850 at the end of the simulation, compared to 1.09 °C in 2019.

While feedback mechanisms from material extraction or temperature increases are not at work in the Baseline scenario, the increasing depletion of fossil fuel reserves and resources leads to a worsening of the fossil energy return on energy invested, and, in general, to increasing input requirements of the fossil sectors, which from 2088 onward can no longer be counteracted by affluence-driven technological efficiency improvements (Figure 2g). Given the continued reliance of the global economy on great quantities of fossil fuel inputs, increasing extraction difficulties cause global output to decline (Figure 2h). This activates a self-reinforcing feedback loop: as output declines, affluence levels drop, which worsens the environmental impacts of production technologies, reinforcing the biophysical constraints on economic production.

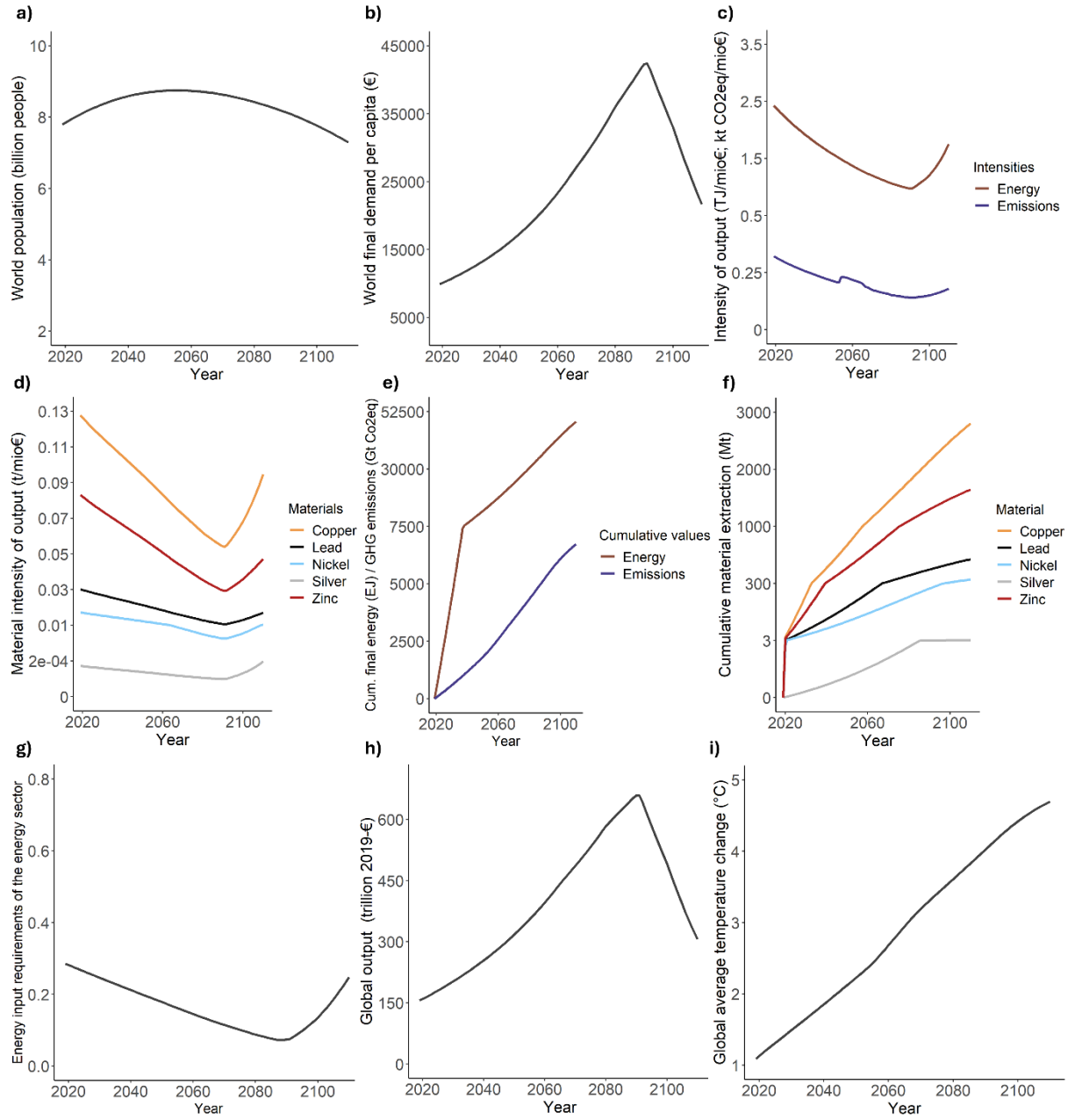


Figure 2: Key outputs of the Baseline scenario: evolution of (a) world population, (b) global average final demand per capita, (c) energy and emission intensities of output, (d) material intensity of output for copper, lead, nickel, silver and zinc, (e) cumulative final energy use and emissions (including land use change emissions), (f) cumulative material extraction for copper, lead, nickel, silver and zinc, (g) fossil energy input requirements of the fossil energy sector, (h) global output and (i) global average temperature compared to the pre-industrial period during the simulation.

3.2. Population policy scenario (PPI)

The PPI scenario shows that a reduction of the driver ‘population’ can significantly change the evolution of the other components of *IPAT* and avoid a decline in affluence due to fossil depletion during the simulation period but is insufficient to stabilize or reverse environmental degradation.

As an immediate consequence of the population policy world population declines throughout the 21st century and reaches 3.25 billion in 2100, a number comparable to world population in 1964 (Figure 3a). At the same time, affluence levels increase faster than in the Baseline scenario

and by 2100 exceed 45,000 €, which also speeds up the improvement of production technologies (Figure 3b-d). By 2110, energy intensity has declined by 64%, and GHG emission intensity by 61%, 5 percentage points more than in the Baseline scenario. GHG intensity declines less than energy intensity because emissions include greenhouse gases other than CO₂ whose emission intensities decline more slowly. Material intensities also drop faster—by 66%, 75%, 73%, 47%, and 74% by 2110 for copper, lead, nickel, silver, and zinc, respectively. Unlike in the baseline scenario, technological progress maintains its positive trajectory throughout the entire simulation. The continuous reduction in the size of the global population, driven by low birth rates, enables affluence levels to increase even though global output peaks in 2070.

Nevertheless, several indicators suggest that the population policy intervention is insufficient to lead to long-term sustainability beyond the 21st century: From 2065 onward, the rate of improvements in the fossil sector declines and growth in final demand slows down while environmental impacts, represented by cumulative material extraction and emissions, continue to increase (Figure 3e-g). In 2110, the global economy is situated in a 3.56 °C warmer and significantly older world due to the population policy intervention: the average age of the population in the formal economy is 53 in the center and the semiperiphery, and 52 in the periphery, while it was 41, 36 and 28 in 2019. The combined pressure on the working force stemming from climate-change-induced labor productivity losses and from the need to support a higher share of population beyond the working age, could lead to major economic reproduction problems beyond the simulation period.

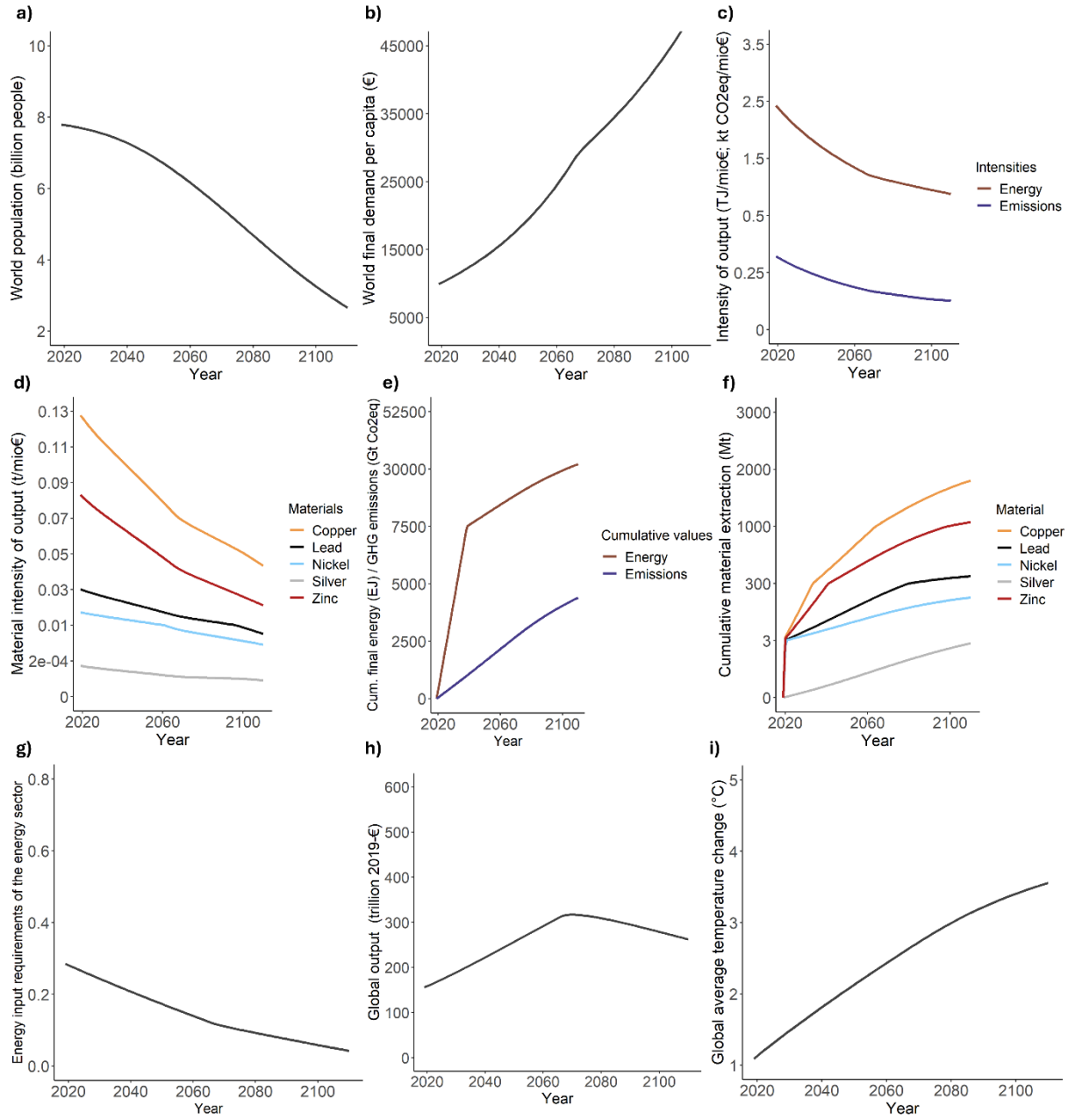


Figure 3: Key outputs of the PPI scenario: evolution of (a) world population, (b) global average final demand per capita, (c) energy and emission intensities of output, (d) material intensity of output for copper, lead, nickel, silver and zinc, (e) cumulative final energy use and emissions (including land use change emissions), (f) cumulative material extraction for copper, lead, nickel, silver and zinc, (g) fossil energy input requirements of the fossil energy sector, (h) global output and (i) global average temperature compared to the pre-industrial period during the simulation.

3.3. Sufficiency scenario (SPI)

While affluence is an important driver of environmental impacts in the Baseline scenario, and the main driver of impacts in the PPI scenario, in the SPI simulation, it plays a less significant role. Instead, during the first half of the simulation, the importance of population as driver increases, while during the second half of the simulation, environmentally harmful production technologies become the main driver of degradation, as affluence levels of the world regions and classes converge, and world population declines from a maximum of 8.55 billion in 2049 to 6.6

billion people at the end of the simulation (Figure 4a-d). The convergence of affluence to a relatively low level in the scenario has two main effects on the *P* and *T* drivers. On the one hand, affluence-induced declines in mortality rates are smaller than in fertility rates, eventually resulting in moderate population decline even at relatively low affluence levels. On the other hand, technological improvements are slower than in the Baseline and the PPI scenario, and, consequently, biophysical feedbacks on economic production via energy depletion manifest earlier (Figure 4c, d and g).

The SPI scenario performs worse than the PPI scenario but better than the baseline scenario in terms of absolute economic impacts, despite the inferior technological profile of the economy compared to the baseline: cumulative final energy use in the SPI scenario is 74% of final energy use in the baseline, while in PPI energy use is only 66% of the baseline value. This pattern is repeated for cumulative material extraction of copper, lead, nickel, silver and zinc, which is 80% (64%), 82%, (65%), 82% (65%), 76% (62%), 82% (65%) of the baseline value for the SPI (PPI) scenario. Nevertheless, the SPI scenario proves slightly more effective than the PPI scenario at limiting global warming due to a lower amount of GHG emissions other than CO₂, resulting in an increase of global average temperature of 3.54 °C compared to the pre-industrial period.

Thus, positive effects of increasing affluence levels on the *T* driver only translate into environmental impact reductions if they are combined with a population policy. Moreover, environmental impacts can be reduced via convergence policies that reduce the affluence of the richest classes and increase those of the poorest, even when assuming that the unintentional effect of convergence policies is a reduction or deterioration in technological development.

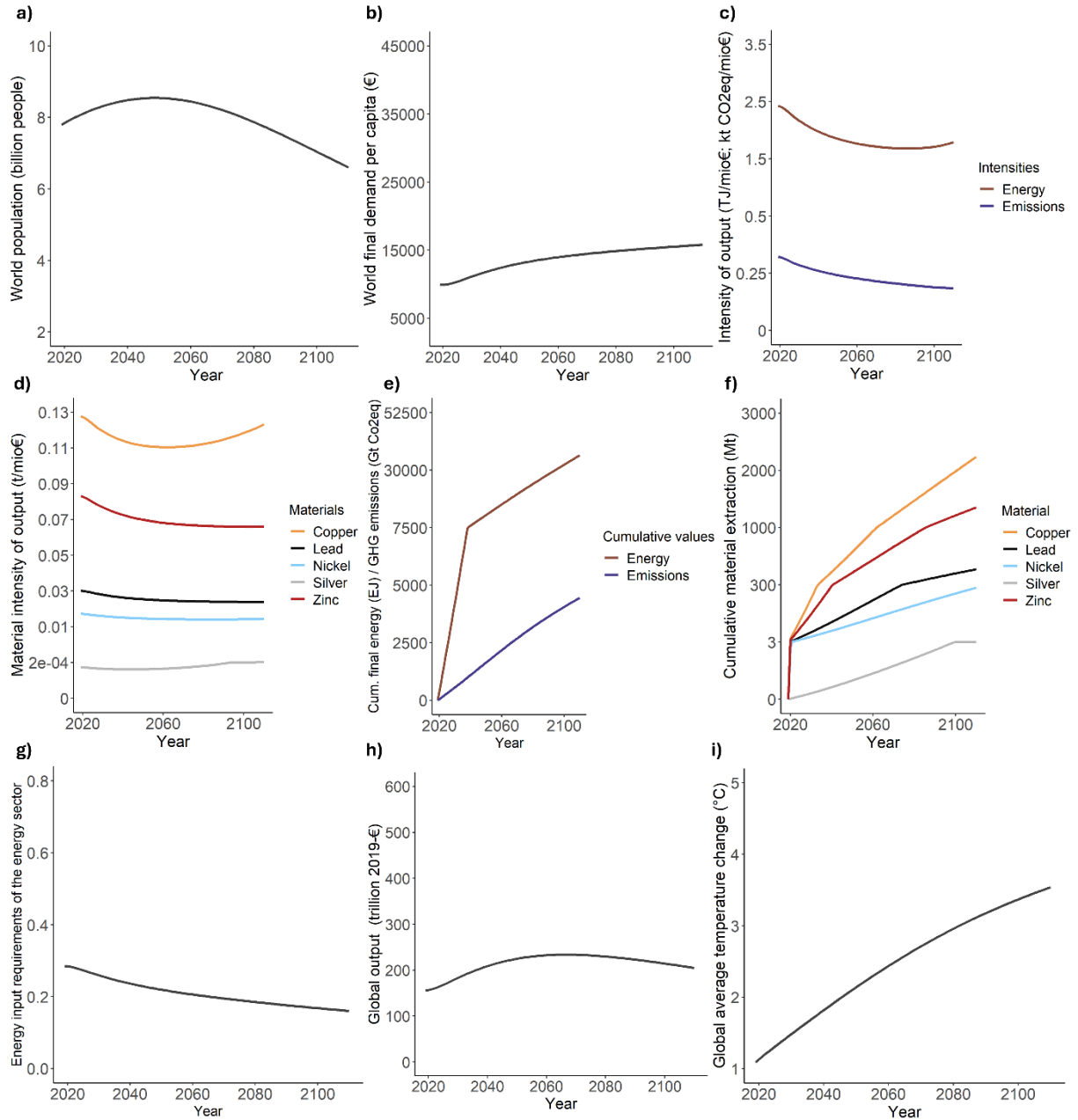


Figure 4: Key outputs of the SPI scenario: evolution of (a) world population, (b) global average final demand per capita, (c) energy and emission intensities of output, (d) material intensity of output for copper, lead, nickel, silver and zinc, (e) cumulative final energy use and emissions (including land use change emissions), (f) cumulative material extraction for copper, lead, nickel, silver and zinc, (g) fossil energy input requirements of the fossil energy sector, (h) global output and (i) global average temperature compared to the pre-industrial period during the simulation.

3.4. Efficiency scenario (EPI)

The EPI scenario essentially reproduces the patterns observed in the Baseline scenario although the higher rates of efficiency improvement allow the system to grow for a slightly longer period than in the Baseline scenario (Figure 5).

While the size of the world population peaks in the same year and at the same value as in the baseline, final demand per capita continues to grow until 2094, becoming the most significant driver of environmental impacts in the scenario. Nevertheless, the peak of 44,229 € of annual final demand per capita is still lower than the affluence achieved in the PPI scenario. Given the assumed link between rising affluence levels and rising technological sufficiency, the

technology-related variables in the EPI scenario generally improve more than in the baseline and in the SPI scenario but less than in the PPI scenario. Energy and GHG emission intensities decline one percentage point more than in the baseline, while the additional decline in material intensities compared to the baseline scenario is between -1 (silver) and +2 (nickel) percentage points.

Nevertheless, at the end of the simulation, the emergence of discontinuous non-linear developments can be observed. Affluence and output start to decline sharply and technological developments reach critical turning points (Figure 5c, d, g) indicating that even with higher political efforts to foster efficiency, the fundamentally unsustainable character of a business-as-usual development pathway as represented by the Baseline scenario cannot be altered. In the EPI scenario, global temperatures rise even more than in the baseline - to 4.74 °C by 2110 - despite a transition to 100% renewable electricity.

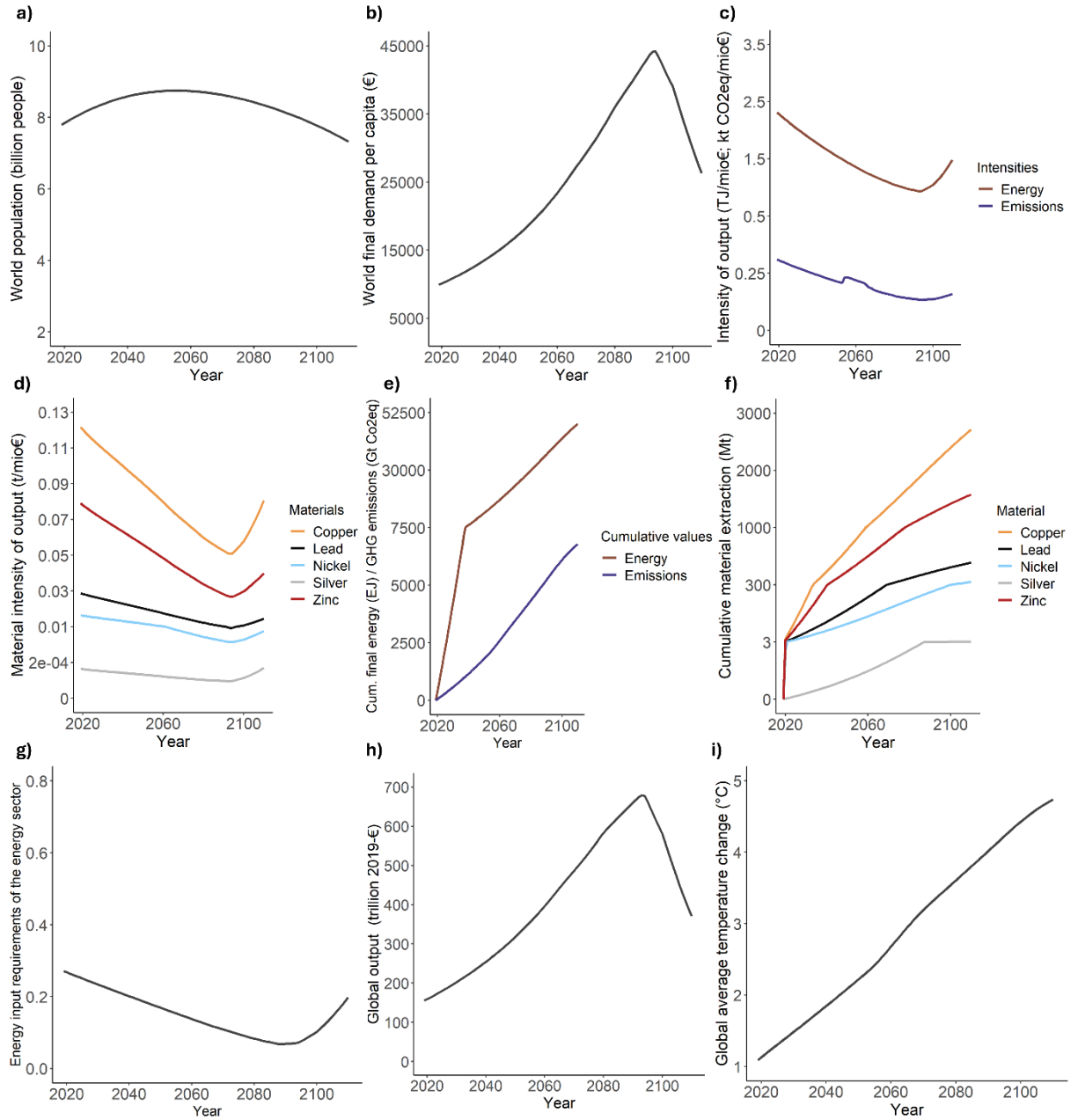


Figure 5: Key outputs of the EPI scenario: evolution of (a) world population, (b) global average final demand per capita, (c) energy and emission intensities of output, (d) material intensity of output for copper, lead, nickel, silver and zinc, (e) cumulative final energy use and emissions (including land use change emissions), (f) cumulative material extraction for copper, lead, nickel, silver and zinc, (g) fossil energy input requirements of the fossil energy sector, (h) global output and (i) global average temperature compared to the pre-industrial period during the simulation.

3.5. Combined scenarios

Unsurprisingly, all combined scenarios with a population policy element (PPI+SPI, PPI+EPI, PPI+SPI+EPI) display highly similar population trajectories, with only marginal differences in the final values (2.6 billion in 2110 for PPI+SPI and PPI+SPI+EPI; 2.66 billion in 2110 for PPI+EPI). Conversely, the combination of sufficiency and efficiency policies (SPI+EPI) results in the same population in 2110 as the isolated SPI scenario (6.6 billion in 2110) (Figure 6a).

The PPI+EPI scenario produces a continuously increasing global affluence level (about 52,000 € per capita in 2110) while in the rest of the combined scenarios, affluence in the different regions and classes converges to around 15,400 € (Figure 6b).

Regarding the *T* driver, the comparison of the combined policy interventions clearly shows that higher technological efficiency is not an indicator of lower environmental impacts (Figure 6c-g). The PPI+EPI scenario displays the most pronounced declines in energy, emission and material intensities as well as in the input requirements of the fossil sectors but nevertheless has the second highest environmental impacts, i.e. cumulative energy use, emissions and material extraction. Only the SPI+EPI scenario produces slightly higher environmental impacts, displaying also the least efficient technology profile. The PPI+SPI scenario and the scenario that addresses all three drivers follow comparable trajectories, with the latter displaying both faster technological development and lower environmental impacts, due to the assumed accelerating effects of efficiency policies on technological progress.

In the combined scenarios with SPI element, output declines due to declining affluence levels, while in combined scenarios with PPI element output declines to prevent labor scarcity from arising (Figure 6h). The finding that technological efficiency improvements do not translate into declining output levels and do not necessarily translate into a decline in impacts, illustrates the existence of rebound effects through which gains in technological efficiency are directly translated into affluence and/or population increases.

The lowest global temperature increase occurs in the PPI+SPI+EPI scenario where global warming is limited to 2.83 °C while in the PPI+SPI scenario the global average temperature increase is 2.85 °C (Figure 6i). Both values are considerably smaller than the most successful ‘isolated’ policy intervention (i.e., 3.56 °C in the PPI scenario). Thus, the combination of population intervention policies with additional policies, especially those that foster sufficiency of richer classes and world regions, constitutes a significantly more effective climate policy approach than those strategies that only address one component of *IPAT*. Likewise, we find that a global one-child policy in the simulation yields climate outcomes comparable to a global sufficiency intervention that leads final demand per capita to converge around 15,000 €, irrespective of efficiency policies.

The range of projected global warming over the baseline scenario and all policy scenarios is 2.83 °C to 4.74 °C which shows the crucial importance of climate policies that address more than only the ‘technology’ driver of the *IPAT* equation. However, even the scenario combining policy interventions that jointly address all three drivers of environmental impacts is far from reaching international climate policy goals.

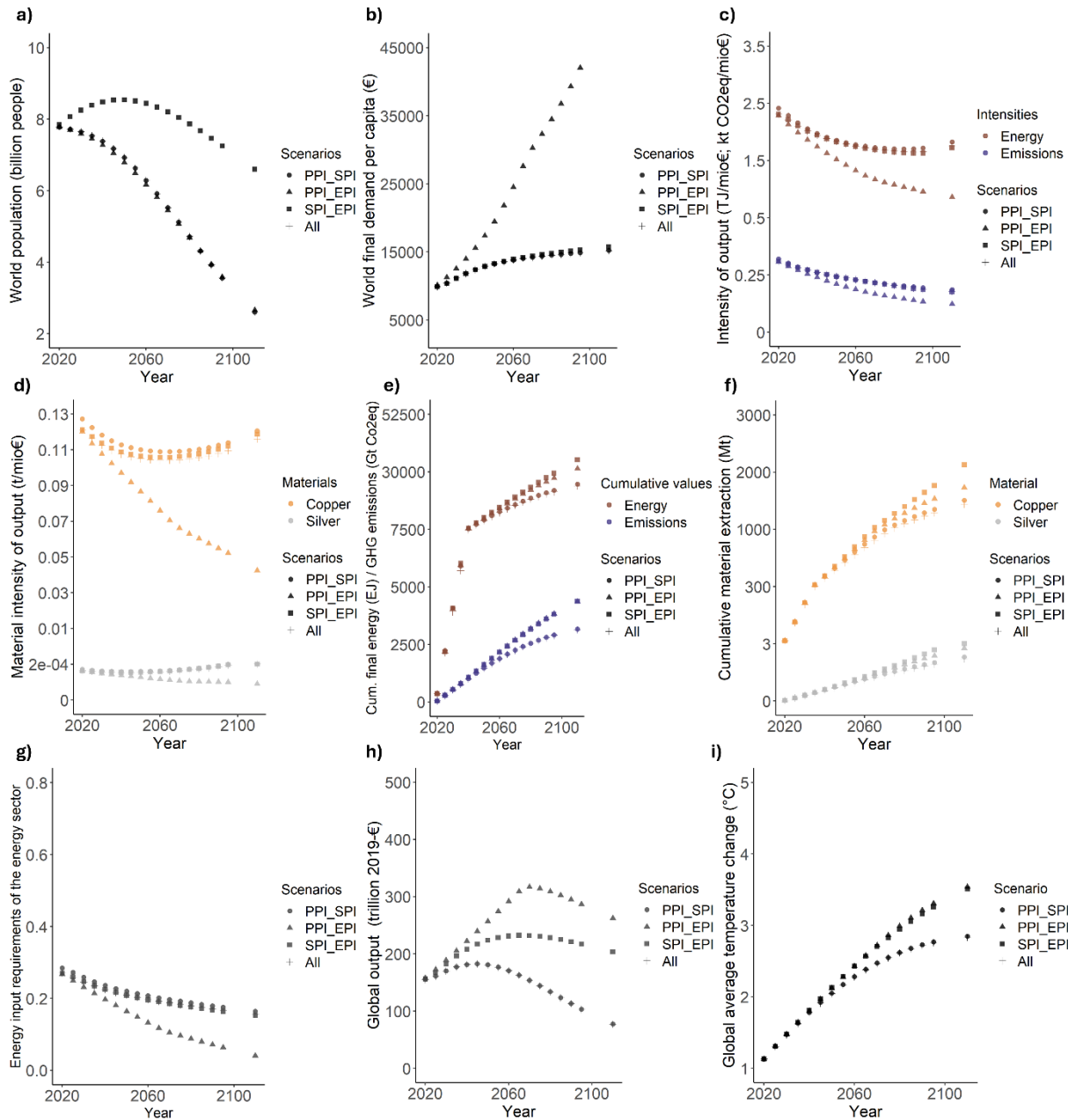


Figure 6: Key outputs of the combined policy scenarios (PPI+SPI, PPI+EPI, SPI+EPI, PPI+SPI+EPI): Evolution of (a) world population, (b) global average final demand per capita, (c) energy and emission intensities of output, (d) material intensity of output for copper and silver, (e) cumulative final energy use and emissions (including land use change emissions), (f) cumulative material extraction for copper and silver, (g) fossil energy input requirements of the fossil energy sector, (h) global output and (i) global average temperature compared to the pre-industrial period during the simulations. The development of material intensity and cumulative material extraction for lead, nickel and zinc are displayed in Suppl. Figure 1 and 2.

Considering all the simulated scenarios, we can summarize the findings in three main insights: First, all components of IPAT influence each other in dynamic ways. Consequently, isolated approaches to society-economy-environment problems are incapable of providing an accurate understanding of the problem. Second, without policy interventions or other intentional societal changes, the interactions between drivers, rather than ‘solving’ the sustainability problem, lead to escalating environmental impacts whose feedbacks on the economic system result in economic collapse. Last, policy interventions that go beyond policy-induced production

efficiency increases by addressing the drivers ‘population’, and - to a lesser extent - ‘affluence’ can significantly reduce environmental impacts but are far from reducing pressure on the environment to levels that can be expected to be sustainable in the long-term.

4. Discussion

4.1. Possible biases in scenario assumptions

As in every scenario study, scenario assumptions regarding key parameters shape simulation outcomes, jointly with the model structure and data. Thus, we want to highlight some possible biases in the assumptions made, and discuss to which extent changes in the assumptions could alter the main insights obtained (section 3.5).

We identify one ‘pessimist’ bias and three ‘optimist’ biases:

First, the mitigation potential of technology-focused policies could be underestimated as we take a rather conservative approach to the possibility of accelerating technological efficiency gains through policy interventions, due to the uncertainty about the rate at which technological progress can be accelerated by policy interventions (cf. section 4.2). Thus, we assume only a 5% improvement in the technological impact factor at a given level of affluence, and ‘only’ simulate the effects of a complete greening of the electricity sector while we do not consider policy interventions that would electrify great parts of current non-electric energy inputs. Instead, in the EPI as well as in the Baseline scenario, not more than 25% of the 2019 values for non-electric energy inputs to key economic sectors is replaced by green electricity. Likewise, we do not simulate technologies whose scalability is questionable, such as carbon capture and storage or different types of geoengineering (Braun et al., 2025; Sekera & Lichtenberger, 2020; Wewerinke-Singh et al., 2022).

This relatively conservative stance in the EPI scenario is offset by highly optimistic assumptions across all scenarios that may reflect an excessive confidence in technological progress.

First, the theoretical possibility of complete decoupling of both energy and materials from production growth at high affluence levels is highly questionable and likely overestimates the energy and material efficiency gains in all scenarios. The estimation error could be even higher if we take into account that all scenarios are driven by continuous increases in labor productivity, which are linked to increases in exergy, counteracting exergy efficiency increases that are ultimately constrained by thermodynamic limits (Furse, 2025).

Second, the inclusion of only one biophysical feedback from I to P , A and T possibly results in an overestimation of the period of time in which the system can grow before it collapses: we do neither include climate damages on economic output (Diaz & Moore, 2017; Lenton et al., 2023), nor feedbacks on the economic system triggered by land use changes and biodiversity losses (Giglio et al., 2024; Markandya, 2015). Also, we assume that there are no limits to mineral extraction. Although the latter depend on assumptions about ultimately recoverable resources (URR) and there is no imminent threat of depletion during the 21st century for none of the five

minerals included for the URR value we adopt (Henckens, 2021), the adverse economic effects of increasing input requirements resulting from falling ore grades are not depicted in the model.

Last, assumptions regarding land use productivity increases are optimistic as they assume annual productivity increases of 1.73% throughout the century irrespective of the *IPAT* drivers, and do not take into account the negative impact of soil erosion, biodiversity loss and other environmental impacts on land productivity (Bouchoms et al., 2019; FAO, 2022; Hossain et al., 2020).

Taking all biases into account, we find that the ‘techno-optimist’ tendencies in our analysis exceed those that could be characterized as ‘techno-pessimist’ or ‘techno-realist’. However, correcting for these biases by reducing techno-optimism would affirm, rather than contradict the key scenario results: (1) it would reinforce the feedback of environmental impacts (*I*) on the drivers (*P-A-T*) which would illustrate the bidirectionality of the *IPAT* framework in all the policy scenarios rather than only in the Baseline and in the EPI scenario; (2) it would lead to an even earlier collapse of economic output in the Baseline scenario, and (3) it would likely lower the mitigation effect of policy scenarios.

4.2. Feasibility of policy scenarios

An *IPAT*-based approach to policy interventions systematically considers policy options that address population and affluence as drivers of environmental degradation, apart from policies aiming at an improvement of production technologies. Although the latter is commonly given a central importance in techno-optimistic environmental policy discourses (Engström & Kolk, 2024; Leipold et al., 2019) our simulations show that the former policy options should not be neglected in environmental policy-making.

Nevertheless, there might be a trade-off between policy effectiveness and policy feasibility (Verhoef et al., 1996) for *IPAT*-related problems: population policies are barely discussed in the sustainability context since the UN Conference on Population and Development in Cairo marked the beginning of a ‘population taboo’ (O’Sullivan, 2020). Rather it is often assumed that education and access to contraceptives linked to increasing affluence will reduce population pressures. Although our analysis relies heavily on this hypothesis, we also show that affluence-driven changes in world population are insufficient to stabilize or even alleviate environmental impacts and that significant reductions in impact, in the absence of technological breakthroughs, are only achieved by relatively ‘radical’ population policies such as a globally implemented one-child policy which is maintained throughout the simulation. Apart from the current low support for such policies at the global level, an additional feasibility restriction stems from the requirement of high labor productivity improvements that have to be maintained throughout the century to counteract the loss of labor force due to an aging population.

Sufficiency policies are increasingly discussed in the academic context and beyond (Alexander & Rutherford, 2019; Kallis et al., 2024; Samadi et al., 2017) but have not yet entered the mainstream discourse (Koch, 2020). Thus, although the political feasibility of sufficiency approaches to sustainability problems might increase, it is questionable whether social classes of high-income countries would agree to degrow their consumption between 3.56% (for the richest 20% of the population) and 0,19% (for the poorest 30% of the population) per year.

Policies fostering efficiency arguably align well with currently dominant narratives of ecological modernization and green governmentality (Bäckstrand & Lövbrand, 2019) but in our scenario

play only a complementary role and, without additional policies, barely change the baseline trajectory. While our simulation shows that technology policies aiming at a 100% renewable electricity system do not achieve significant reductions in environmental impacts, the modeling of the effects of more abstract technology-centered policies is highly uncertain. Although policies can have a certain influence on the direction of technological development (Hémous & Olsen, 2021; Mazzucato et al., 2020), it is evident that faster and larger-scale politically motivated changes in production technologies encounter greater implementation challenges, thereby limiting the practical feasibility of these policies.

Thus, the scenarios – especially those with an SPI or PPI component – should be seen as stylized policy scenarios designed to determine their maximum effects. Very likely, even under favorable institutional conditions, the implementation of SPI- or PPI-related policies would be less radical than in the simulations.

4.3. Underlying institutional conditions

The development of P, A, T and I does not take place in abstract space but is shaped and constrained by underlying institutional conditions constituting the current world order.

First, population policies are designed in the context of the (nation) state and are subject to strategic national interests: assuming that states are interested in maintaining or increasing power and that a higher population generally translates into a higher working force and a higher pool of potential soldiers as well as a greater share in global environmental commons (Coleman & Rowthorn, 2011; McNicoll, 1999) we can hypothesize that states in the current world order will try to increase rather than decrease birth rates, or at least not decrease birth rates at a higher rate than other states, which considerably restricts possible policy-based development trajectories of the P driver.

Second, wealth is linked to power and technological capacity (Jovetic & Katnic, 2024), and dominant cultures and narratives promote a continued increase rather than decrease in affluence (Schmelzer, 2017, 2024), which makes sufficiency policy strategies potentially incompatible with the current world order.

Third, technology is not an isolated subsystem of the world system, nor is the direction of its development neutral. Instead, it is deeply shaped by—and entangled with—existing political, economic, and cultural power structures, reflected for example in the links between civil and military innovations (Bordin et al., 2020) and in rebound effects that undermine gains in resource efficiency (Vélez-Henao et al., 2019). Moreover, short-term and linear thinking, aligning with and fostered by dominant ways of life and values, can lead to technological fixes that exacerbate unsustainable trajectories. Last, large-scale technological transformations such as the global energy transition have deep implications on the shape of the current world order as they change geopolitical and economic power relationships (Hafner & Tagliapietra, 2020; Y. Yang et al., 2023).

From this perspective, the effect of I on $P-A-T$ can be seen as the reduction of the capacity of the material structures, ‘rules of the game’, and dominant ideas of the current civilization to reproduce themselves over time.

Thus, we stress the need for greater attention in future work to the deeper institutional conditions underlying the *IPAT* framework—factors not directly captured in our modeling study.

These conditions offer an alternative lens for assessing policy effectiveness and underscore the necessity of broader systemic change on the global level to expand the option space for environmental and economic policies.

5. Conclusion

While traditional approaches to *IPAT* have tended to focus on single drivers of environmental degradation, in this paper, we have used the MORDRED-IAM to simulate a business-as-usual scenario as well as various policy scenarios that reflect the complex and dynamic nature of the *IPAT* framework. Going beyond the commonly assumed unidirectionality of the equation, with P , A , and T driving I , we have shown that as a consequence of environmental degradation caused by the economy, P , A and T themselves can be deeply affected by emerging feedbacks from the biophysical system affecting the development possibilities of the social system. Formalizing the interdependencies between the components of *IPAT* through an IAM has enabled us to shed light on the role different drivers play in environmental degradation and to systematically compare the effectiveness of various isolated and combined policy options formulated with the *IPAT* framework. Although our work illustrates the continued relevance of *IPAT* for current environmental and sustainability-related problems, the limited success in terms of environmental outcomes of the policy scenarios points to the need of deep and fast systemic transformations on the global level and corresponding scientific analyses of sustainability-related problems that move beyond population, affluence and technology to address the underlying institutional drivers of unsustainability ingrained in the current world order.

References

- Alcott, B. (2010). Impact caps: Why population, affluence and technology strategies should be abandoned. *Journal of Cleaner Production*, 18(6), 552–560.
- Alcott, B. (2012). Population matters in ecological economics. *Ecological Economics*, 80, 109–120.
- Alexander, S., & Rutherford, J. (2019). A critique of techno-optimism: Efficiency without sufficiency is lost. In *Routledge handbook of global sustainability governance* (pp. 231–241). Routledge.
- Arbulu, I., Lozano, J., & Rey-Maquieira, J. (2017). Waste Generation Flows and Tourism Growth: A STIRPAT Model for Mallorca. *Journal of Industrial Ecology*, 21(2), 272–281.
<https://doi.org/10.1111/jiec.12420>
- Armstrong McKay, D. I., Staal, A., Abrams, J. F., Winkelmann, R., Sakschewski, B., Loriani, S., Fetzer, I., Cornell, S. E., Rockström, J., & Lenton, T. M. (2022). Exceeding 1.5 C global warming could trigger multiple climate tipping points. *Science*, 377(6611), eabn7950.
- Bäckstrand, K., & Lövbrand, E. (2019). The road to Paris: Contending climate governance discourses in the post-Copenhagen era. *Journal of Environmental Policy & Planning*, 21(5), 519–532.
- BGR. (2020). *BGR Energy Study 2019 – Data and Developments Concerning German and Global energy supplies*. Hannover.
https://www.bgr.bund.de/EN/Themen/Energie/Downloads/energiestudie_2019_en.pdf;jsessionid=ADF18B2529B3E89FC705FDF390A57BA4.internet002?__blob=publicationFile&v=6
- Bordin, G., Hristova, M., & Luque-Perez, E. (2020). *JRC horizon scanning on dual-use civil and military research*. <https://publications.jrc.ec.europa.eu/repository/handle/JRC120638>
- Bouchoms, S., Wang, Z., Vanacker, V., & Van Oost, K. (2019). Evaluating the effects of soil erosion and productivity decline on soil carbon dynamics using a model-based approach. *SOIL*, 5(2), 367–382. <https://doi.org/10.5194/soil-5-367-2019>
- Braun, J., Werner, C., Gerten, D., Stenzel, F., Schaphoff, S., & Lucht, W. (2025). Multiple planetary boundaries preclude biomass crops for carbon capture and storage outside of agricultural areas. *Communications Earth & Environment*, 6(1), 102.
- Brizga, J., Feng, K., & Hubacek, K. (2013). Drivers of CO₂ emissions in the former Soviet Union: A country level IPAT analysis from 1990 to 2010. *Energy*, 59, 743–753.
- Brockway, P. E., Owen, A., Brand-Correa, L. I., & Hardt, L. (2019). Estimation of global final-stage energy-return-on-investment for fossil fuels with comparison to renewable energy sources. *Nature Energy*, 4(7), 612–621. <https://doi.org/10.1038/s41560-019-0425-z>
- Chertow, M. R. (2000). The IPAT equation and its variants. *Journal of Industrial Ecology*, 4(4), 13–29.
- Coleman, D., & Rowthorn, R. (2011). Who's afraid of population decline? A critical examination of its consequences. *Population and Development Review*, 37, 217–248.
- Commoner, B. (1972). A Bulletin Dialogue on "The Closing Circle," Response. *Bulletin of the Atomic Scientists*.
- Diaz, D., & Moore, F. (2017). Quantifying the economic risks of climate change. *Nature Climate Change*, 7(11), 774–782. <https://doi.org/10.1038/nclimate3411>
- Dietz, T., & Rosa, E. A. (1997). Environmental impacts of population and consumption. *Environmentally Significant Consumption: Research Directions*, 92–99.
- Ehrlich, P. R., & Ehrlich, A. H. (2013). Can a collapse of global civilization be avoided? *Proceedings of the Royal Society B: Biological Sciences*, 280(1754), 20122845.

- Ehrlich, P. R., & Holdren, J. P. (1971). Impact of population growth. *Science*, 171(3977), 1212–1217.
- Ehrlich, P. R., & Holdren, J. P. (1972). A Bulletin Diaologue on “The Closing Circle,” Critique: One-dimensional ecology. *Bulletin of the Atomic Scientists*, 28(5), 16–27.
- Engström, E., & Kolk, M. (2024). Projecting environmental impacts with varying population, affluence and technology using IPAT–Climate change and land use scenarios. *Vienna Yearbook of Population Research*, 2024, 1–29.
- FAO. (2022). *Global status of black soils*. FAO. <https://doi.org/10.4060/cc3124en>
- Fischer-Kowalski, M., & Amann, C. (2001). Beyond IPAT and Kuznets curves: Globalization as a vital factor in analysing the environmental impact of socio-economic metabolism. *Population and Environment*, 23, 7–47.
- Font Vivanco, D., Kemp, R., Van Der Voet, E., & Heijungs, R. (2014). Using LCA-based Decomposition Analysis to Study the Multidimensional Contribution of Technological Innovation to Environmental Pressures. *Journal of Industrial Ecology*, 18(3), 380–392. <https://doi.org/10.1111/jiec.12118>
- Furse, S. (2025). *Are there biophysical limits to technical change? A review of societal exergy analysis and ecological macroeconomics*.
- Giglio, S., Kuchler, T., Stroebel, J., & Wang, O. (2024). *The Economics of Biodiversity Loss* (No. w32678; p. w32678). National Bureau of Economic Research. <https://doi.org/10.3386/w32678>
- Gütschow, J., Jeffery, M. L., Günther, A., & Meinshausen, M. (2021). Country-resolved combined emission and socio-economic pathways based on the Representative Concentration Pathway (RCP) and Shared Socio-Economic Pathway (SSP) scenarios. *Earth System Science Data*, 13(3), 1005–1040. <https://doi.org/10.5194/essd-13-1005-2021>
- Hafner, M., & Tagliapietra, S. (Eds.). (2020). *The Geopolitics of the Global Energy Transition* (Vol. 73). Springer International Publishing. <https://doi.org/10.1007/978-3-030-39066-2>
- Hémous, D., & Olsen, M. (2021). Directed Technical Change in Labor and Environmental Economics. *Annual Review of Economics*, 13(1), 571–597. <https://doi.org/10.1146/annurev-economics-092120-044327>
- Henckens, T. (2021). Scarce mineral resources: Extraction, consumption and limits of sustainability. *Resources, Conservation and Recycling*, 169, 105511. <https://doi.org/10.1016/j.resconrec.2021.105511>
- Hickel, J., Brockway, P., Kallis, G., Keyßer, L., Lenzen, M., Slameršak, A., Steinberger, J., & Ürge-Vorsatz, D. (2021). Urgent need for post-growth climate mitigation scenarios. *Nature Energy*, 6(8), 766–768.
- Hossain, A., Krupnik, T. J., Timsina, J., Mahboob, M. G., Chaki, A. K., Farooq, M., Bhatt, R., Fahad, S., & Hasanuzzaman, M. (2020). Agricultural Land Degradation: Processes and Problems Undermining Future Food Security. In S. Fahad, M. Hasanuzzaman, M. Alam, H. Ullah, M. Saeed, I. Ali Khan, & M. Adnan (Eds.), *Environment, Climate, Plant and Vegetation Growth* (pp. 17–61). Springer International Publishing. https://doi.org/10.1007/978-3-030-49732-3_2
- Igogo, T., Awuah-Offei, K., Newman, A., Lowder, T., & Engel-Cox, J. (2021). Integrating renewable energy into mining operations: Opportunities, challenges, and enabling approaches. *Applied Energy*, 300, 117375. <https://doi.org/10.1016/j.apenergy.2021.117375>
- Jovetic, I., & Katnic, I. (2024). Economic Power: Security, Military and Political Resource. In I. Karabegovic, A. Kovačević, & S. Mandzuka (Eds.), *New Technologies, Development and Application VII* (Vol. 1070, pp. 361–369). Springer Nature Switzerland. https://doi.org/10.1007/978-3-031-66271-3_39

- Kallis, G., Mastini, R., & Zografos, C. (2024). Perceptions of degrowth in the European Parliament. *Nature Sustainability*, 7(1), 64–72.
- Karlsson, K., Nørgård, J., Bermúdez, J. G., Balyk, O., Wackernagel, M., Glynn, J., & Kanudia, A. (2018). The Role of Population, Affluence, Technological Development and Diet in a Below 2 °C World. In G. Giannakidis, K. Karlsson, M. Labriet, & B. Ó. Gallachóir (Eds.), *Limiting Global Warming to Well Below 2 °C: Energy System Modelling and Policy Development* (Vol. 64, pp. 85–102). Springer International Publishing. https://doi.org/10.1007/978-3-319-74424-7_6
- Koch, M. (2020). Structure, action and change: A Bourdieusian perspective on the preconditions for a degrowth transition. *Sustainability: Science, Practice and Policy*, 16(1), 4–14.
- Lauer, A., & Llases, L. (2025). *MORDRED: Model Of Resource Distribution and Resilient Economic Development. Model Documentation*. GitHub. <https://github.com/Pendracus/MORDRED>
- Leipold, S., Feindt, P. H., Winkel, G., & Keller, R. (2019). Discourse analysis of environmental policy revisited: Traditions, trends, perspectives. *Journal of Environmental Policy & Planning*, 21(5), 445–463. <https://doi.org/10.1080/1523908X.2019.1660462>
- Lenton, T. M., Xu, C., Abrams, J. F., Ghadiali, A., Loriani, S., Sakschewski, B., Zimm, C., Ebi, K. L., Dunn, R. R., & Svenning, J.-C. (2023). Quantifying the human cost of global warming. *Nature Sustainability*, 6(10), 1237–1247.
- Magee, C. L., & Devezas, T. C. (2018). Specifying technology and rebound in the IPAT identity. *Procedia Manufacturing*, 21, 476–485.
- Markandya, A. (2015). *The Economic Feedbacks of Loss of Biodiversity and Ecosystem Services* (OECD Environment Working Papers No. 93; OECD Environment Working Papers, Vol. 93). <https://doi.org/10.1787/5jrqgv610fg6-en>
- Mazzucato, M., Kattel, R., & Ryan-Collins, J. (2020). Challenge-Driven Innovation Policy: Towards a New Policy Toolkit. *Journal of Industry, Competition and Trade*, 20(2), 421–437. <https://doi.org/10.1007/s10842-019-00329-w>
- McGee, J. A., Clement, M. T., & Besek, J. F. (2015). The impacts of technology: A re-evaluation of the STIRPAT model. *Environmental Sociology*, 1(2), 81–91.
- McNicoll, G. (1999). Population Weights in the International Order. *Population and Development Review*, 25(3), 411–442. <https://doi.org/10.1111/j.1728-4457.1999.00411.x>
- Meadows, D. H., Meadows, D., Randers, J., & Behrens, W. W. (1972). *The limits to growth. A report for the Club of Rome's Project on the Predicament of Mankind*. Universe Books.
- Miller, R. E., & Blair, P. D. (2009). *Input-output analysis: Foundations and extensions*. Cambridge university press.
- Mokyr, J. (2016). *A culture of growth: The origins of the modern economy*. Princeton University Press.
- Norgate, T., & Haque, N. (2010). Energy and greenhouse gas impacts of mining and mineral processing operations. *Journal of Cleaner Production*, 18(3), 266–274. <https://doi.org/10.1016/j.jclepro.2009.09.020>
- O'Sullivan, J. N. (2020). The social and environmental influences of population growth rate and demographic pressure deserve greater attention in ecological economics. *Ecological Economics*, 172, 106648. <https://doi.org/10.1016/j.ecolecon.2020.106648>
- Rosa, E. A., & Dietz, T. (1998). Climate Change and Society: Speculation, Construction and Scientific Investigation. *International Sociology*, 13(4), 421–455. <https://doi.org/10.1177/026858098013004002>
- Samadi, S., Gröne, M.-C., Schneidewind, U., Luhmann, H.-J., Venjakob, J., & Best, B. (2017). Sufficiency in energy scenario studies: Taking the potential benefits of lifestyle changes into account. *Technological Forecasting and Social Change*, 124, 126–134.

- Schmelzer, M. (2017). The growth paradigm: History, hegemony, and the contested making of economic growthmanship. In *Routledge Handbook of the History of Sustainability* (pp. 164–186). Routledge.
- Schmelzer, M. (2024). Without growth, everything is nothing': On the origins of growthism. In L. Eastwood & K. Heron (Eds.), *De Gruyter Handbook of Degrowth* (pp. 25–40). De Gruyter.
- Sekera, J., & Lichtenberger, A. (2020). Assessing carbon capture: Public policy, science, and societal need: A review of the literature on industrial carbon removal. *Biophysical Economics and Sustainability*, 5, 1–28.
- Skånberg, K., & Svenfelt, Å. (2022). Expanding the IPAT identity to quantify backcasting sustainability scenarios. *Futures & Foresight Science*, 4(2), e116.
- Vélez-Henao, J.-A., Vivanco, D. F., & Hernández-Riveros, J.-A. (2019). Technological change and the rebound effect in the STIRPAT model: A critical view. *Energy Policy*, 129, 1372–1381.
- Verhoef, E., Nijkamp, P., & Rietveld, P. (1996). The trade-off between efficiency, effectiveness, and social feasibility of regulating road transport externalities. *Transportation Planning and Technology*, 19(3–4), 247–263. <https://doi.org/10.1080/03081069608717572>
- Waggoner, P. E., & Ausubel, J. H. (2002). A framework for sustainability science: A renovated IPAT identity. *Proceedings of the National Academy of Sciences*, 99(12), 7860–7865.
- Wei, T. (2011). What STIRPAT tells about effects of population and affluence on the environment? *Ecological Economics*, 72, 70–74.
- Wewerinke-Singh, M., De Jong, I., Adelman, S., Biermann, F., Burns, W., Cramer, W., Gonzalez, C., Hey, E., Kotzé, L., & Lang, M. (2022). *Submission to the Human Rights Council Advisory Committee on the impact of new technologies for climate protection on the enjoyment of human rights: By members of the network of academics for an International Non-Use Agreement on Solar Geoengineering*. <https://hdl.handle.net/1887/3561525>
- Wiedmann, T., Lenzen, M., Keyßer, L. T., & Steinberger, J. K. (2020). Scientists' warning on affluence. *Nature Communications*, 11(1), 1–10.
- Xing, L., Khan, Y. A., Arshed, N., & Iqbal, M. (2023). Investigating the impact of economic growth on environment degradation in developing economies through STIRPAT model approach. *Renewable and Sustainable Energy Reviews*, 182, 113365.
- Yang, J., & Chen, X. (2019). Quantification of the Driving Factors of Water Use in the Productive Sector Change Using Various Decomposition Methods. *Water Resources Management*, 33(12), 4105–4121. <https://doi.org/10.1007/s11269-019-02338-0>
- Yang, Y., Xia, S., & Qian, X. (2023). Geopolitics of the energy transition. *Journal of Geographical Sciences*, 33(4), 683–704. <https://doi.org/10.1007/s11442-023-2101-2>
- York, R., Rosa, E. A., & Dietz, T. (2003a). Footprints on the Earth: The Environmental Consequences of Modernity. *American Sociological Review*, 68(2), 279. <https://doi.org/10.2307/1519769>
- York, R., Rosa, E. A., & Dietz, T. (2003b). STIRPAT, IPAT and ImPACT: analytic tools for unpacking the driving forces of environmental impacts. *Ecological Economics*, 46(3), 351–365.
- Zhao, X., Fan, X., & Liang, J. (2017). Kuznets type relationship between water use and economic growth in China. *Journal of Cleaner Production*, 168, 1091–1100.

Assessing equity and mitigation outcomes in multiple degrowth pathways

Abstract

We use a socially and environmentally extended input–output model to explore 162 global degrowth pathways. While all scenarios assume deliberate reductions in consumption by richer households they differ in the overall scale and pace of reduction, the degree of convergence between social classes and regions, and the extent of technological, structural, and behavioral change. The scenarios produce a wide range of climate outcomes, with global mean temperature increases of 2.56 – 4.49 °C above preindustrial levels. These differences in mitigation outcomes are accompanied by large variations in global output, land use, and per capita consumption. Our findings show that simply downscaling existing economic structures cannot achieve climate targets. Effective and equitable mitigation instead requires deep convergence in consumption towards low levels worldwide, coupled with transformative socio-technological changes in production systems. These results highlight the importance of integrating social equity and systemic innovation into pathways for sustainable post-growth futures.

Display items

Dimension 0 State []	Scale of degrowth (1)	Pace (2)	Convergence (3)	Electricity mix (4)	Factor intensity (5)	Agricultural production (6)	Diet (7)
[1]	Moderate (11000 €)	Fast (to 2040)	Complete	No changes	Lower [higher] labor [energy] intensity	Conventional	Meat- based
[2]	Weak (15400 €)	Moderate (to 2060)	Interregional	100% renewable	Higher [lower] labor [energy] intensity	Organic	Plant- based
[3]	Strong (6600 €)	Slow (to 2100)	Intraregional	Combination of dimensions and states generates scenario pathways, e.g. 1111111, 1211111, ..., 3332222.			

Table 1: Overview of DG scenario dimensions and possible states of the dimensions.

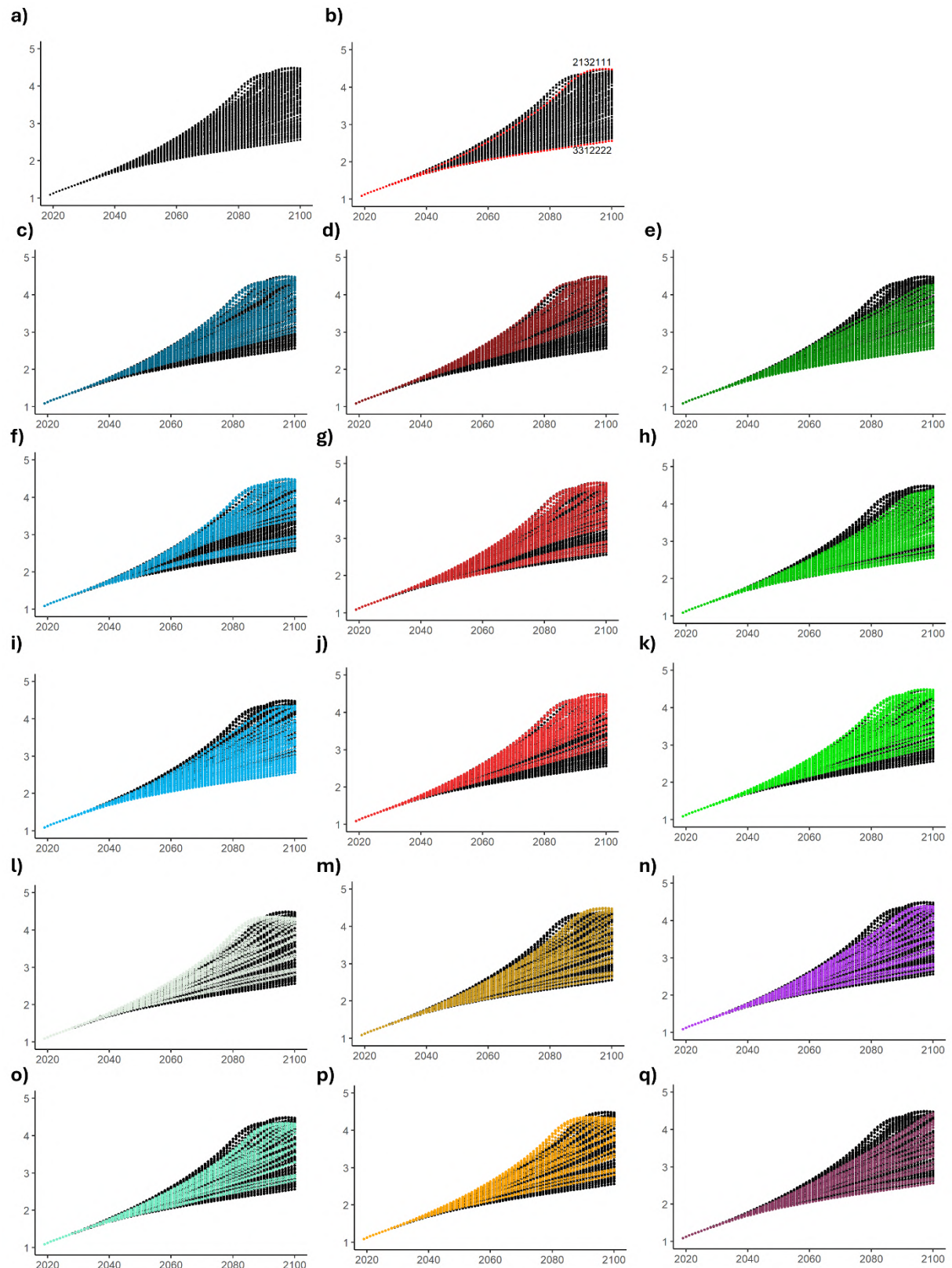


Figure 1: Temperature change (°C, reference year 1850) for all simulated scenarios. a) all pathways. b) pathways leading to the highest and the lowest temperature outcome in 2100. c) colored: pathways with moderate scale of DG. d) colored: pathways with weak scale of DG. e) colored: pathways with strong scale of DG. f) colored: pathways with fast pace of convergence. g) colored: pathways with moderate pace of convergence. h) colored: pathways with slow pace of convergence. i) colored: pathways with complete convergence. j) colored: pathways with interregional convergence. k) colored: pathways with intraregional convergence. l) colored: pathways without policies. m) colored: pathways with renewable electricity policy. n) colored: pathways with increased labor intensity policy. o) colored: pathways with

organic agriculture policy. p) colored: pathways with plant-based diet policy. q) colored: pathways with all policies applied.

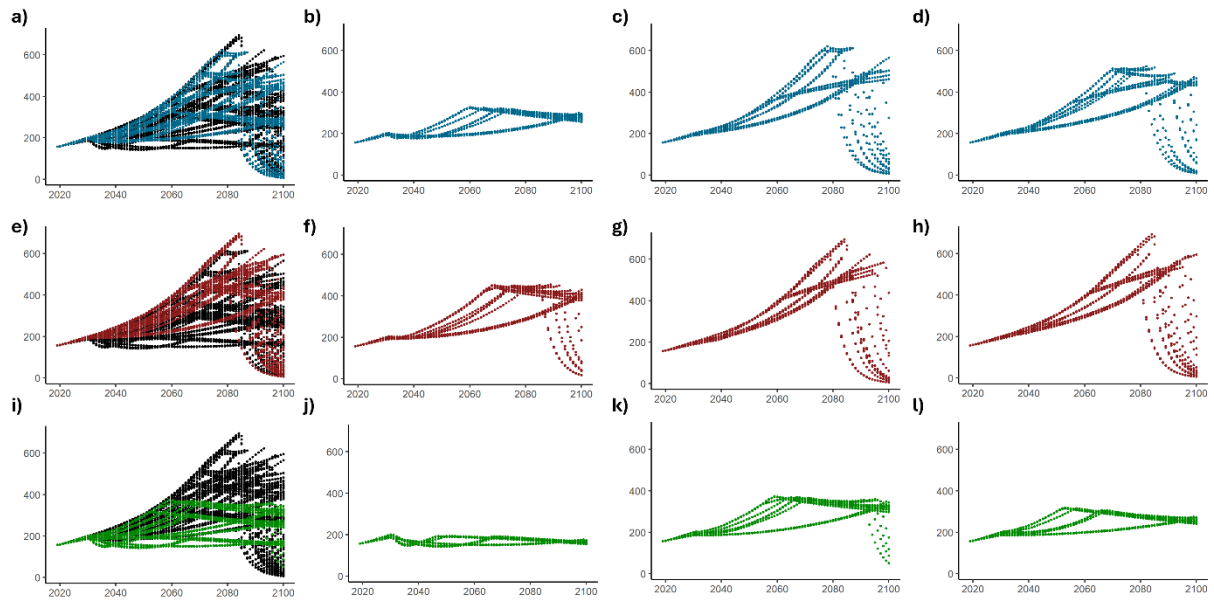


Figure 2: Annual world output (trillion €). Colored: output pathways with a) moderate scale of DG. b) moderate scale and complete convergence. c) moderate scale and interregional convergence. d) moderate scale and intraregional convergence. e) weak scale of DG. f) weak scale and complete convergence. g) weak scale and interregional convergence. h) weak scale and intraregional convergence. i) strong scale of DG. j) strong scale and complete convergence. k) strong scale and interregional convergence. l) strong scale and intraregional convergence.

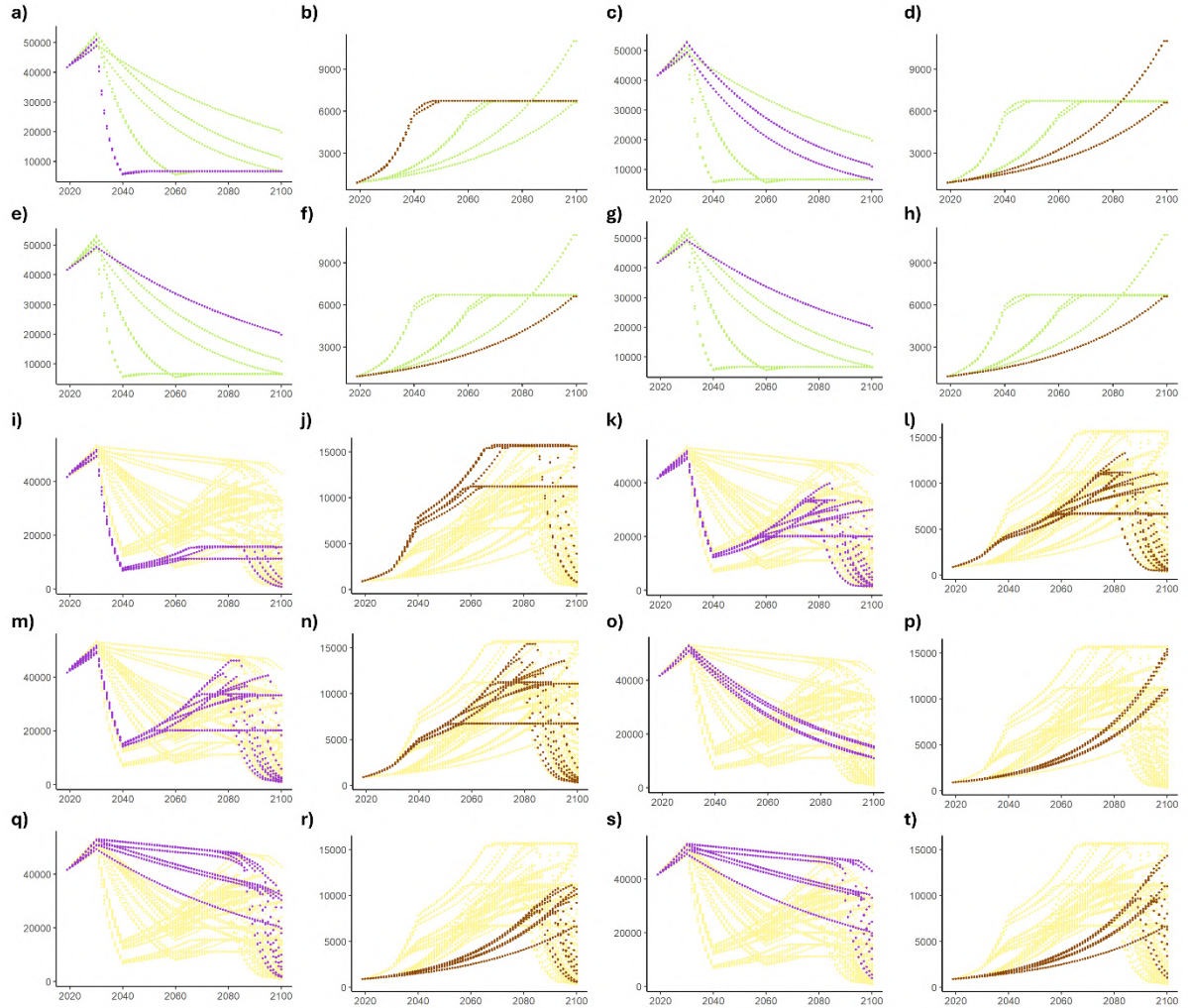


Figure 3: Consumption pathways ($\text{€ person}^{-1} \text{year}^{-1}$) under strong, moderate and weak DG for the richest 20% of the Center (T20C) (purple) and the poorest 30% of the Periphery (B30P) (brown) corresponding to lower (green) (a-h) and higher (yellow) (i-t) temperature changes at the end of the century. a) T20C consumption for fast and complete convergence (purple). b) B30P consumption for fast and complete convergence (brown). c) T20C consumption for slow and complete convergence (purple). d) B30P consumption for slow and complete convergence (brown). e) T20C consumption for slow and interregional convergence (purple). f) B30P consumption for slow and interregional convergence (brown). g) T20C consumption for slow and intraregional convergence (purple). h) B30P consumption for slow and intraregional convergence (brown). i) T20C consumption for fast and complete convergence (purple). j) B30P consumption for fast and complete convergence (brown). k) T20C consumption for fast and interregional convergence (purple). l) B30P consumption for fast and interregional convergence (brown). m) T20C consumption for fast and intraregional convergence (purple). n) B30P consumption for fast and intraregional convergence (brown). o) T20C consumption for slow and complete convergence (purple). p) B30P consumption for slow and complete convergence (brown). q) T20C consumption for slow and interregional convergence (purple). r) B30P consumption for slow and interregional convergence (brown). s) T20C consumption for slow and intraregional convergence (purple). t) B30P consumption for slow and intraregional convergence (brown).

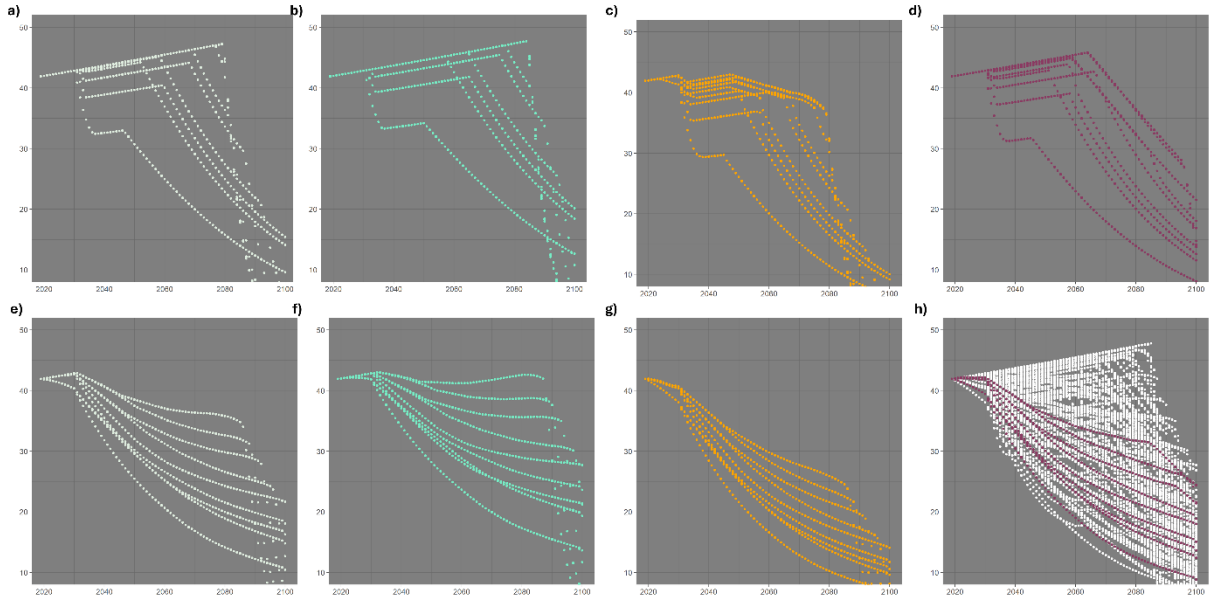


Figure 4: Use of cropland and pastures (mio. km²). Pathways with a) no policies and fast convergence (until 2040). b) organic agriculture policy and fast convergence. c) plant-based diet policy and fast convergence. d) all policies and fast convergence. e) no policies and slow convergence (until 2100). f) organic agriculture policy and fast convergence. g) plant-based diet policy and fast convergence. h) all policies and fast convergence. White-colored points: All simulated land use pathways.

Main

Existing climate mitigation scenarios compatible with the Paris Agreement often rely heavily on large-scale deployment of negative emissions technologies (NETs) that enable scenarios with both high consumption growth and high climate mitigation [1], [2]. Those scenarios have attracted criticism for violating principles of precaution and responsibility, given the unresolved technical, environmental, and social challenges of deploying NETs at the required scale [3], [4]. In light of these concerns, strategies that go beyond technological solutions and rather focus on behavioral changes, ways of life and consumption patterns have increasingly gained attention [5], [6], [7].

Degrowth (DG), understood as the intentional downscaling of production and consumption in high-income countries to reduce environmental pressures and improve equity and well-being, has emerged as one such strategy [8], [9]. In recent years, the concept has gained visibility in academic research, civil society, and policymaking, with some members of the European Parliament expressing radical positions with regard to sustainability, including support for post-growth and eco-socialism [10], [11]. This development parallels a growing body of modeling work on basic human needs and resource distribution [12], [13], post-growth and DG transitions [14], [15], [16], [17], as well as analyses of demand-side solutions [18], [19].

However, despite this progress, degrowth futures are characterized by considerable uncertainties, including the scale of reduction required, the pace of the transition, and the degree of convergence between high- and low-income countries. Quantitative modeling work on DG is still relatively scarce [20], reflected in the underrepresentation of low energy and material demand scenarios in the IPCC scenario database [21] and the absence of post-growth in the

original shared socio-economic pathways (SSP) and the resulting modeling studies [22], [23]. Traditional modeling work based on integrated assessment models (IAMs) suffers from a pro-growth bias stemming from both the models' structure and variables, and from modeling practices striving to create shared baselines among different IAMs [24]. Although some IAMs have been adapted to represent degrowing economies [17], [25] and ecological macroeconomic models have been constructed to model post-growth pathways [26], [27], DG and post-growth modeling studies often use different assumptions, system boundaries, and geographic scopes, making results difficult to compare [14]. Consequently, it remains unclear under which conditions DG could achieve climate targets while avoiding adverse impacts on living standards, or whether there is a trade-off between mitigation and poverty alleviation [13], [28].

Here, we address this gap by constructing 162 DG scenarios simulated with the IAM MORDRED. All scenarios assume deliberate consumption reductions among richer households but differ in the overall scale and pace of reduction, the degree of convergence across income groups, and the extent of technological, structural, and behavioral change. Using a single, integrated modelling framework enables systematic comparison of the scenarios in terms of climate outcomes and key socio-environmental variables, including global output, land use, and per capita consumption. This comprehensive scenario set allows us to evaluate the individual and combined effects of different DG dimensions. Our results demonstrate that simulating DG within IAMs can inform the design of equitable and precautionary climate strategies.

Results

Scenario design

We define seven dimensions linked to a DG transition: the target per capita consumption level, or scale of DG which can range between €6,600 and €15,400 (1); the pace of consumption convergence, or pace of DG i.e. convergence until 2040, 2060 or 2100 (2); the degree of convergence, which can be complete or incomplete (3); the electricity mix that can be partially or fully renewable (4); factor intensities of production i.e. a possible increase in labor intensity linked to a decrease in energy intensity (5); agricultural production techniques (organic or conventional) (6); and the composition of the human diet (meat- or plant-based) (7). The 162 pathways are constructed by varying the states of the seven dimensions across the scenarios. Table 1 summarizes the scenario design which is explained in detail in the Methods section. S1 Supplementary Information (SI) lists all scenarios with their characteristics.

Climate change mitigation under DG

Figure 1 presents projected changes in global average temperature (°C) relative to the pre-industrial period across all simulated DG scenarios. The variance is considerable: while global average temperature rises by more than 400% relative to initial values in the highest-emission scenarios, it increases by less than 230% in the lowest-emission pathways. The worst-performing scenario (pathway 2132111) reaches 4.48 °C in 2100, far beyond 'safe and just' thresholds [29] while even the best-performing pathway (3312222) is linked to an increase of 2.56 °C (Figure 1b). Accordingly, none of the 162 DG pathways achieves the 1.5 °C or 2 °C climate target, and only 25 limit warming to 3.2 °C or below. These findings are contextualized further in the Discussion section.

Although no single DG dimension determines climate outcomes, differences among pathways can be partially explained by how individual dimensions are set.

Although no single DG dimension fully determines climate outcomes, differences among pathways can be partially explained by how scale, pace, and degree of convergence are implemented. First, scenarios with a strong DG scale—defined as a per-capita consumption target of €6,600 year⁻¹ for the middle class of the semiperiphery—consistently achieve better climate outcomes than those with moderate (€11,000) or weak (€15,400) targets (Figure 1c-e). Temperature ranges are [2.56–4.27 °C] for ‘strong’ DG, [3.01–4.48 °C] for ‘moderate’ DG, and [3.33–4.49 °C] for ‘weak’ DG. This finding supports the notion of a trade-off between higher consumption levels and climate safety, demonstrating that reducing resource use in richer households is critical for limiting warming.

Second, the pace of convergence between classes and regions plays an important but nuanced role. Scenarios with slower convergence generally perform better than those with faster convergence (Figure 1f-h). Temperature ranges are [2.56–4.39 °C] for convergence by 2100, [2.66–4.49 °C] by 2060, and [2.7–4.49 °C] by 2040. Contrary to the hypothesis that faster convergence improves climate outcomes, we find that faster convergence increases the rate of consumption growth among poorer households, whose increasing demand partially offsets the reduction in consumption by richer households. Slower convergence reduces total demand and production over the century, moderating emissions. This finding illustrates a tension between equity in consumption and climate outcomes: faster convergence enhances social equality more quickly, but may exacerbate cumulative emissions if it triggers rapid demand growth.

Third, the degree of convergence matters substantially. Complete convergence yields a temperature range of [2.56–4.35 °C], outperforming both interregional ([3.11–4.49 °C]) and intraregional ([3.0–4.49 °C]) convergence scenarios (Figure 1i-k). In inter- and intraregional scenarios, inequality between the richest and poorest households or regions is reduced to a 3:1 ratio, i.e. inequality drops consistently in spite of the absence of full convergence. Thus, maintaining current inequality levels in these partial-convergence pathways would result in even less climate mitigation. These results indicate that convergence does not involve a trade-off between equity and climate mitigation, but rather fosters both objectives.

Comparing the three dimensions, scale and degree of convergence emerge as slightly more influential in shaping climate outcomes than the pace of convergence. Especially strong DG and complete convergence seem to have the potential to significantly limit global warming during the 21st century, suggesting that both cutting the per-capita consumption of richer households and reducing inequality are essential for mitigation. The pace of convergence, while secondary, modulates the timing and cumulative effect of demand shifts across the global population.

Policy interventions exhibit diverse unexpected effects and strong context dependency (Figure 1l-q). The shift to 100% renewable electricity appears in both the best- and worst-performing pathways, highlighting strong context dependency as they can both support cleaner energy production under low consumption and improve the efficiency of the total energy system as fossil resources become more costly to access, thus, prolonging the reproductive capacity of a fossil-fuel based energy infrastructure. Temperature *ceteris paribus* increases slowest when all policies are implemented. Interestingly, the plant-based diet policy slightly accelerates warming early in the century: Improvements in land-use efficiency initially do not occur fast enough to satisfy total desired consumption demand but since dietary shifts ease land constraints, a higher share of demanded consumption can be fulfilled. Thus, global output rises faster and emissions increase temporarily. Changes in factor intensities modestly improve outcomes (−0.1 °C between best-performing factor-intensity and no-policy scenarios), while the organic agriculture

policy shows a negligible effect ($-0.000004^{\circ}\text{C}$), likely due to the relatively simplistic implementation of the policy in the model (see Methods).

Of the 25 lower-temperature pathways, 22 feature strong DG, 21 complete convergence, 13 slow convergence (to 2100), and 11 a switch to renewables (alone or with other policies). The best scenario without explicit DG policies combines slow, complete convergence to a low consumption level and reaches 2.8°C in 2100.

Overall, the findings demonstrate that climate mitigation under DG depends on the interplay of consumption reductions, convergence dynamics, and context-specific policies, highlighting the need to consider social equity, consumption patterns, and structural policies together when designing DG pathways.

Development of total output

The DG scenarios produce a wide range of global output trajectories, driven primarily by demographic trends, target consumption levels, the availability of input factors and resources, and specific scenario characteristics. In the early years of the simulation, total output rises in all scenarios, reflecting limited convergence and a continuous increase in the consumption of the poorest households (B30P). From 2030 onward, differences in output dynamics are mainly determined by the scale of DG and the degree of convergence.

Under strong DG, low consumption targets that affect a large share of the global population cause world output to peak earlier and at lower levels (Figure 2.i). In contrast, scenarios in which household consumption converges toward higher levels display prolonged and stronger growth, reaching higher output peaks (Figure 2.a, e). Differences between moderate and weak DG are comparatively minor, while the contrast between strong DG and the other two variants is pronounced. Complete convergence leads to earlier and lower peaks than partial convergence, with inter- and intraregional convergence showing similar overall behavior, though interregional convergence typically produces slightly higher peaks.

A 'moderate' scale of DG with complete convergence (Figure 2.b) leads to a first peak and subsequent moderate decline in the 2030s, followed by renewed growth as global convergence progresses. The rate of increase depends primarily on the pace of convergence: faster convergence yields faster growth, with output peaking between 2060 and 2070 at more than twice its initial level. Under moderate DG with inter- or intraregional convergence (Figure 2.c-d), output peaks between two and four times the initial value, depending on the convergence pace.

A 'weak' scale of DG exhibits similar qualitative patterns, although complete convergence (Figure 2.f) produces longer and higher output growth, followed by pronounced late-century declines not observed under moderate DG (Figure 2.b). In contrast, strong DG produces sharp declines only in the final decade, particularly under interregional convergence (Figure 2.k). Strong DG combined with complete convergence leads to final output levels comparable to initial output (in 2100: $[0.99 - 1.1] \times$ initial output) (Figure 2.j) while strong DG combined with intraregional convergence yields output levels $1.5-1.7 \times$ initial output.

In scenarios lacking strong DG or complete convergence, output contracts sharply toward the end of the century due to fossil resource depletion. In 63 of 162 scenarios, global output in 2100 is more than 20 % below its initial level. These dynamics are driven by the depletion of fossil reserves and critically depend on the assumption of low fossil resource accessibility. Policies

delay but do not prevent resource scarcity; the full policy set is most effective, followed by factor-intensity change, expansion of renewable electricity, and organic agriculture.

Hence, surprisingly, even persistent DG among richer households does not necessarily reduce world output. Instead, output dynamics are shaped by the interaction between the scale of DG, convergence dynamics, and resource availability. Conversely, weak DG and incomplete convergence can produce unintended and steep output reductions under insufficient fossil fuel substitution once reserves are depleted. These findings highlight that maintaining global output under DG conditions requires not only equitable consumption convergence but also technological and structural transitions beyond the greening of the electricity mix.

Development of household consumption

Simulation results cover consumption pathways for all nine household types pertaining to the global economy, i.e. the top 20%, the bottom 30% and the remaining middle 50% of all high-income countries ('Center'), all upper-middle income countries ('Semiperiphery') and all lower-and low income countries ('Periphery'): T20C, B30C, M50C, T20S, B30S, M50S, T20P, B30P and M50P. Here, we focus on the 'extreme' cases of the T20C and B30P households, while results for the other household types are visualized in S3 of the SI.

Figure 3.a-h displays consumption pathways for low-emission scenarios ($\leq 3.2 \text{ }^{\circ}\text{C}$), while Figure 3.i-t shows consumption pathways of high-emission scenarios. Per-capita consumption of T20C ranges between €19,800 and €6,600 year $^{-1}$ under strong DG, corresponding to a reduction of 53–84 % compared to the initial level. The B30P group, by contrast, experiences a substantial increase, reaching €6,600–11,000 year $^{-1}$ —7 to 12 times its initial consumption.

Higher-emission scenarios are more numerous and often deviate from the exogenously specified convergence targets. Under moderate or weak DG with fast and complete convergence, T20C and B30P consumption levels meet around 2040 but remain below the target due to insufficient land-intensity improvements. Only in later decades, as efficiency increases, do consumption targets become attainable (Figure 3.i-j). Fast and interregional convergence leads to a sharp early rise in B30P consumption that later stabilizes or collapses under resource scarcity. The T20C pattern mirrors this behavior, with more pronounced late-century declines under intraregional convergence.

Slow but complete convergence yields steady decline in T20C consumption and a continuous rise for B30P, reaching €11,000–15,400 year $^{-1}$ by 2100 (Figure 3.o and p. In contrast, under slow inter- or intraregional convergence (Figure 3.q-t), T20C consumption remains high for most of the century before collapsing, while B30P consumption drops to much lower levels. Scenario 2332222, which retains high consumption the longest, reaches €43,000 year $^{-1}$ for T20C and €14,348 year $^{-1}$ for B30P in 2100.

Despite clear trade-offs between consumption and climate outcomes, similar temperature responses can occur across scenarios with markedly different consumption levels among the poorest households. For instance, scenario 1312222 (slow, complete convergence with all policies implemented) yields €11,000 year $^{-1}$ for B30P and a global warming of 3.01 °C, while scenario 3322222 (slow interregional convergence with all policies) produces €6,600 year $^{-1}$ for B30P and a warming of 3.11 °C.

These results highlight the central role of convergence for both equity and mitigation. Complete convergence enables sustained improvements in well-being among low-income groups while maintaining lower overall energy and material demand. In contrast, partial or delayed

convergence —whether inter- or intraregional— preserves high consumption levels among the richest households for much of the century, eventually leading to abrupt declines as resource constraints intensify.

Overall, the findings suggest that effective climate mitigation and equitable consumption outcomes depend less on absolute consumption targets and more on the speed and completeness of convergence. Even low inequality ratios can lower mitigation, indicating that sufficiency-oriented pathways with complete global convergence are essential for aligning degrowth strategies with both social and climatic goals.

Land use

Land-use dynamics for food production (cropland + grassland) vary substantially across the simulated scenario pathways (Figure 4). A slower convergence pace (to 2100) leads to stronger and more persistent reductions in land use compared to a faster convergence (to 2040), while scenarios with moderate convergence (to 2060) lie in between. Sharp declines toward the end of the century, observable in several pathways, result from collapsing output driven by fossil resource scarcity and its feedback effects on agricultural productivity and demand.

Relative to no-policy pathways (Figure 4a, e), organic agriculture increases land use, whereas plant-based diets reduce it. Under fast convergence, the lowest land-use case without policies (3111111) reaches 25 million km² in 2060, about 40% below the initial value. The best organic agriculture case (3111121) requires 28.7 million km², while the best plant-based diet case (3111112) uses 20.1 million km². When all policies are combined (3112222), total land use is about 8% lower than in the best no-policy case. Under slow convergence, these effects are more pronounced: organic agriculture occasionally increases land use, whereas plant-based diets consistently lower it.

Across all simulations, strong DG and complete convergence generally produce lower land-use outcomes, though exceptions exist. For instance, under slow convergence, scenarios combining strong DG with intraregional convergence and a plant-based diet (e.g., 3331112, 3321112) result in lower land demand than those combining strong DG with complete convergence and organic agriculture (3311121).

Overall, the differences in land-use trajectories are driven less by DG-specific land policies than by underlying land-productivity assumptions, macroeconomic developments, and a relative decline in the demand for agricultural products as consumption levels of poorer households rise. Interactions between technological efficiency, resource scarcity, and convergence speed largely determine the extent to which DG pathways reduce pressure on agricultural land. While plant-based diets reliably decrease land use, organic agriculture tends to offset some of these gains due to lower yields. Balancing sufficiency-oriented consumption changes with continued productivity improvements therefore emerges as a critical condition for achieving sustainable land-use outcomes under degrowth pathways.

Discussion

Degrowth and climate targets

Our finding that none of the DG scenarios achieves sufficient mitigation to limit global warming to 1.5 °C or 2 °C should not be understood as an indirect argument for Green Growth (GG)

approaches. To assess the performance of a DG scenario compared to a GG scenario would require a separate scenario analysis with careful scenario design and implementation in the same model to ensure comparability of results.

The relatively low mitigation effect throughout all scenario simulations can be explained by several factors. First, for methodological reasons, we make very conservative assumptions regarding energy efficiency compared to other scenarios. Our aim was to explore the effects of reducing the consumption of richer households, in combination with concrete technological changes, rather than to assess possible economy-wide future improvements in energy intensity. Second, the model reflects the growing depletion of fossil resources through an increase in the input factors of the extractive sector, which worsens energy and carbon intensity and further accelerates global warming. Last, we do not include negative emission technologies (NETs) due to concerns regarding their performance, scalability, and sustainability implications [30], [31].

It follows that DG pathways could be made compatible with climate targets if they are combined with assumptions of stronger economy-wide efficiency gains, greater availability of fossil fuels, and/or NETs. Under these conditions, DG pathways would very likely outperform GG pathways in terms of climate mitigation. Alternatively, DG pathways could be made compatible with climate targets through a complete structural reorganization of the economy resulting in changed production processes and technologies, such as 'low-tech' [32], which are very difficult to represent with models built on data from the currently existing economic structure.

Nevertheless, we would caution against unjustified overoptimism regarding DG and climate mitigation. High levels of uncertainty exist not only for possible technological and socio-economic developments but also for biophysical variables and their interactions [33], [34], [35]. Importantly, if reductions in consumption are not accompanied by deep changes in the production structure away from fossil resources, even strong DG scenarios with high energy-efficiency improvements will, in the long term, face considerable climate change and resource depletion problems.

Policy implications and feasibility

The benefits of DG policies are often linked to less pressure on land and more leisure time [36], [37]. Although this might be true in comparison to GG policies, our scenarios still depend on continued growth in labor and land productivity throughout the 21st century. In more than half of the scenarios with changes in factor intensity that increase labor and decrease energy intensity, the effect is a slowdown of the consumption growth of the poorest households, contradicting convergence goals. The higher the target consumption the greater the risk for emerging labor scarcity issues becomes. The same logic applies to land productivity improvements, and since the two policies linked to DG—a plant-based diet and a switch to organic agriculture—work in opposite directions regarding land intensity they cannot solve the problem of land scarcity.

Our simulations demonstrate that complete convergence is important to prevent ongoing poverty in the poorest households at the global scale and to achieve significant climate mitigation effects. Incomplete convergence that only addresses class or territorial inequality either depresses the consumption of poorer households or leads to continued growth in total output and emissions. However, the political feasibility of completely equalizing consumption can be doubted, given that reducing consumption inequality to a factor of 1:3 at the global level, as assumed in the scenarios of inter- and intraregional convergence, would already require unprecedented redistribution policies.

From our scenario exercise it follows that it is necessary to combine strong sufficiency and convergence in consumption with deep structural and technological changes for strong climate mitigation. Consequently, strategies of sufficiency and resource equality should be seen as complementary, not contradictory, to strategies promoting socio-technological change.

This raises critical questions about the institutional conditions that could simultaneously sustain dynamic technological progress and reduce consumption and inequality.

Methods

Model

For our scenario analysis, we use MORDRED (*Model of Resource Distribution and Resilient Economic Development*), an Integrated Assessment Model for which extensive documentation is provided in Lauer & Llases [38]. Therefore, in the following, we only provide a short summary of the model, focusing on the variables most relevant to the analysis conducted.

MORDRED was built with the intention of simulating scenarios of non-linear economic development that depart from the assumption of continued growth in world output. This is achieved by endogenizing certain variables whose development is often determined exogenously, notably demographic developments and economic output. The model consists of several modules that are coupled through various feedback relationships: Population, Economy, Labor, Energy, Land, Climate, and Environmental Stressors. The main data sources for the calibration of the model are the environmentally and socially extended IO tables from Exiobase3 for the year 2019 [39], UN population data for 2020 [40], consumption inequality data for 2014 from the GCIP database [41], climate and emission-related variables from the IPCC WGI [42] and fossil resource estimates from BGR [43].

The world population is divided into a minority that is assumed to live partially or completely outside the global economy and a majority assumed to be fully integrated into the world economy. The population pertaining to the global economy is divided into three world regions and three household types in each region. The world region ‘Center’ (C) covers all high-income countries; the world region ‘Semiperiphery’ (S) includes all upper-middle-income countries; and the world region ‘Periphery’ (P) includes all lower-middle- and low-income countries. In every region, the richest 20% constitute the T20 (Top 20) household type, the poorest 30% the B30 (Bottom 30) household type, and the remaining middle 50% the M50 (Middle 50) household type. Thus, the nine household types in MORDRED are: T20C, M50C, B30C, T20S, M50S, B30S, T20P, M50P, and B30P.

The economic core of MORDRED is a global input–output model with 25 sectors constructed by aggregating product-based Exiobase3 data. This level of aggregation allows model users to simulate environmental and economic policies that target food-related, industry-related, and service-related activities, as well as different energy sectors.

The desired total output of the world economy, which depends on the respective scenario, is the sum of sectoral output calculated with the Leontief matrix L and the desired final demand for every sector (1). The desired final demand by sector is the sum of the desired gross fixed capital formation ($GFCF_s$), the desired government consumption (G_s) and the desired household consumption (hh_s) by sector. Both desired GFCF and desired government consumption depend on the desired sectoral consumption of households. The latter depends on population size, consumption vectors whose composition varies with the level of per capita consumption, and the desired rate of consumption growth.

$$X = \sum_{s=1}^{25} L_{s,s} * (G_s + hh_s + GFCF_s) \quad (2)$$

For our simulation exercise, we used MORDRED 1.1.4. The most significant difference from the base version is the use of inequality factors ($IQ_{r,c:peri,B30_t}$) to influence the evolution of consumption pathways of the different household types. These factors exogenously determine the consumption inequality ratio between a certain household type and the poorest household type (B30P) (2).

Based on scale, pace, and convergence, the necessary growth rate of the B30P household type to reach the target value in the respective year is calculated and set as an exogenous model input (3).

$$IQ_{r,c:peri,B30P_t} = \frac{c_{r,c_t}}{c_{B30P_t}} \quad (2)$$

$$g_{B30P} = e^{\frac{\ln\left(\frac{c_{B30P_{2019}}}{c_{B30P_{20xx,target}}}\right)}{20xx-2019}} - 1 \quad (3)$$

The desired consumption pathways of the other household types are calculated by multiplying the desired per capita consumption of the B30P household type by the respective inequality factors.

In MORDRED, the desired output is only produced if all necessary input factors for the sectoral economic processes are available in the required quantity. These input factors include intermediate products, labor, different types of land, and different types of resources. Labor supply is calculated based on the population module, while land and (energy) resource availability are calculated in the respective modules. Shortages in one input factor are sufficient to slow down and reverse economic growth due to the standard input-output assumption of zero substitutability between different types of inputs. However, this assumption is softened by the very broad input categories that exist in the model. For example, the input category 'fossil fuels' implies complete substitutability between different types of fossil fuels, and the input category 'labor' implies complete substitutability between different types of workers, i.e., there is no differentiation according to skills. Likewise, the model makes optimistic assumptions regarding the convertibility of different land types; for example, forest land can always be converted into agriculturally used land.

If desired final demand is higher than what can be produced with the available production factors, the consumption of all household types is reduced to maintain the exogenously specified inequality ratios between household types.

The climate module, which is an adapted and actualized version of the climate module contained in the IAM WILIAM [44], calculates the global average temperature change (ΔT) (6), driven by emissions of different greenhouse gases generated in the Environmental Stressors module. CO₂ emissions are calculated as the sum of emissions from fossil fuel combustion, land-use change, and other CO₂ sources (4). Emissions for greenhouse gases other than CO₂ are calculated based on emission intensities (5).

$$Em_{CO2_t} = \sum_{i=1}^3 PE_i \cdot Int_{CO2_i} + forest\ land\ reduction * Int_{CO2_l} + \sum_{s=1}^{25} Int_{CO2_{st}} * x_{st} \quad (4)$$

$$Em_{j_t} = \sum_{s=1}^{25} Int_{j_{st}} * x_{st}) \quad (5)$$

$$\Delta T = f(Em_j, Em_{CO2}) \quad (6)$$

The total land demand for every land type is calculated using land-use intensities (7). The module compares the land demanded with the quantity of available land, which can result in land-use changes or limits to economic production.

$$Land\ demand_{lt} = \sum_{s=1}^{25} Int_{l_{st}} * x_{s_{desiredt}} \quad (7)$$

MORDRED contains several feedback mechanisms that link different modules, two of which were deactivated for our scenario exercise. First, our scenario analysis does not include feedback mechanisms in the climate system resulting, for example, from permafrost thawing. Second, for our simulations, we did not include possible climate impacts on economic structure and labor. Activating the first feedback mechanism would further accelerate the pace of temperature increase, while taking into account the second feedback mechanism would likely slow down economic growth as the global average temperature increases..

Scenario dimensions

In our scenario analysis, each DG scenario is characterized by seven dimensions, of which the first three are conceptual and the last four represent policies commonly associated with DG transitions [14], [45]: 1. the per capita consumption level, indicating the scale of DG; 2. the pace of convergence in per capita consumption, indicating the velocity of DG; 3. the degree of convergence in per capita consumption; 4. the electricity mix; 5. the factor intensity of production; 6. agricultural production techniques; and 7. the composition of the human diet. Each dimension can take two or three possible states, defined according to the representational capacity of MORDRED.

1. Per capita consumption level

The reference consumption level is the annual per capita consumption of the M50S household type. Three states are possible:

- (1) *Moderate DG*: the reference per capita consumption level is set to €11,000 year⁻¹. This results in an increase in per capita consumption for all household types except the richest 70% of the population in the Center. The consumption level refers solely to household consumption and excludes government consumption and investment. However, in the model, government consumption per world region is calculated as a share of regional household consumption, and investment ultimately depends on desired consumption levels. Thus, a reduction in household consumption leads to a corresponding decline in government spending and investment.

- (2) *Weak DG*: the reference consumption level increases by 40%.
- (3) *Strong DG*: the reference consumption level decreases by 40%.

This variation allows us to explore the significance of the scale of DG in the simulations. The reference level was set relatively high to avoid scenarios with excessive poverty among a minority of households in cases of strong DG and incomplete convergence between household types.

2. Pace of convergence

The pace of convergence is determined by a target year, with three possible states:

- (1) *Fast*: convergence of consumption levels by 2040.
- (2) *Moderate*: convergence of consumption levels by 2060.
- (3) *Slow*: convergence of consumption levels by 2100.

3. Degree of convergence

DG emphasizes the reduction of both intra-country and international inequality [45] which is implemented in all simulated scenarios. However, while one-third of the scenarios feature complete convergence between household types, in the remaining cases consumption inequality is not entirely eliminated. We construct three ideal types:

- (1) *Complete convergence*: in the target year, the consumption of all household types has converged to the same level.
- (2) *Interregional convergence*: in the target year, the average per capita consumption levels of all three world regions have converged. Inequality ratios between household types within a single region decline to a maximum of 3:1 between the richest (T20) and poorest (B30) household types.
- (3) *Intraregional convergence*: in the target year, the consumption of all household types within each world region has converged to the same level. Inequality ratios between the richest (Center) and poorest (Periphery) world regions drop to a maximum of 3:1.

4. Electricity mix

This dimension represents a conceivable policy in the context of a DG transition [46], [47]. Two states are possible:

- (1) *No policy*: the share of non-renewable electricity—i.e. nuclear power and electricity generated from fossil fuels (mainly carbon)—remains at its 2019 level throughout the simulation.
- (2) *Renewable electricity policy*: the share of non-renewable electricity declines to zero by 2100 and is replaced by hydro-, wind-, and solar-based electricity.

5. Factor intensity of production

This dimension represents a potential policy and reflects the idea of structural economic change towards higher labor intensity and lower energy intensity [48]. Its model implementation is

qualitative rather than quantitative, serving to illustrate basic dynamics such as potential labor scarcity or positive climate mitigation effects.

- (1) *No policy*: capital intensity remains constant; labor intensity depends solely on the scale of DG, the degree of convergence, and the model's default assumptions regarding labor productivity developments (section 2 SI).
- (2) *Factor intensity change policy*: labor intensity increases while the energy intensity of all energy inputs decreases in selected sectors (nos. 1, 5, 7, 11, 23). Consequently, the capital-to-labor ratio declines slightly in these industries.

6. Agricultural production

Two states are defined for this dimension:

- (1) *No policy*: in the absence of an agricultural production policy, industrial agricultural production remains predominantly conventional.
- (2) *Organic agriculture policy*: this policy allows us to explore some consequences of a global shift to predominantly organic agriculture. The model implementation focuses solely on direct land-use implications and their interactions with world output and emissions growth. Furthermore, the policy applies only to land used for food production, not to forestry or energy-sector land use.

7. Diet

Like agricultural production, this dimension has a policy character, can take two states, and focuses only on direct land-use implications rather than indirect emissions or climate-related effects:

- (1) *No diet policy*: land intensities follow default model assumptions.
- (2) *Planet-based diet policy*: meat-based protein and fat intake are substituted with plant-based alternatives.

Combining all dimensions and their possible states yields a theoretical scenario space of 432 potential combinations, of which 162 pathways were simulated. Each scenario pathway is denoted by a number encoding the state of each dimension. For example, a scenario of moderate DG ((1) = [1]) with fast ((2) = [1]) and complete ((3) = [1]) convergence, no changes in the electricity mix ((4) = [1]), no additional factor-intensity changes ((5) = [1]), conventional agriculture ((6) = [1]), and a meat-based diet ((7) = [1]) is labeled 1111111.

The simulated scenarios, their characteristics, and corresponding numbers are presented in Table S1. The SI also details key boundary conditions affecting simulation outcomes. Notably, boundary conditions assume no major changes in economic structure apart from moderate electrification and energy-efficiency improvements in existing industrial processes. It is assumed that for most core products of the global economy, the majority of cost-minimizing energy-efficiency measures have already been implemented. Consequently, compared to models assuming high efficiency gains, MORDRED tends to produce higher emissions from economic growth. For this study, we retained the model's default assumption to avoid conflating climate mitigation effects arising from abstract structural changes with those from explicit reductions in consumption.

Table 2 provides an overview of the scenario implementation for the selected dimensions in the model. Given the large volume of data generated by the simulations, the results section focuses on four key outputs: climate change, total output, per capita consumption, and land use for food production. The full dataset can be made available upon request.

Dimension	State	Qualitative	Quantitative
Consumption level	Moderate DG	Target consumption (c_{target}) of €11,000 year ⁻¹ person ⁻¹ for the middle class ($M50$) of the Semiperiphery. This value reflects the purchasing power corresponding to a monthly budget of €917 in the Eurozone in 2019.	$c_{target_{M50S}}$
	Weak DG	The target consumption increases by 40%.	$c_{target_{M50S}} * (1 + 0.4)$
	Strong DG	The target consumption decreases by 40%.	$c_{target_{M50S}} * (1 - 0.4)$
Pace	Fast	Inequality is reflected in inequality factors ($IQ_{r,c:peri,B30_t}$). $IQ_{r,c:peri,B30_t}$ are assumed to fall until 2030 after which the reduction accelerates further to reach the target level of convergence in 2040.	$IQ_{r,c:peri,B30_t} = \max \left\{ IQ_{r,c:peri,B30_{2019}} * e^{-k_{20401r,c}t}, 1 \right\}$ for $t \leq 2030$ $IQ_{r,c:peri,B30_t} = \max \left\{ IQ_{r,c:peri,B30_{2030}} * e^{-k_{20402r,c}t}, 1 \right\}$ for $t > 2030$ $k_{2040i_{r,c}}$ takes a value that ensures that the desired convergence level is reached in 2040.
	Moderate	$IQ_{r,c:peri,B30_t}$ are assumed to fall slightly until 2030 after which the decrease accelerates to reach the target level of convergence in 2060.	$IQ_{r,c:peri,B30_t} = \max \left\{ IQ_{r,c:peri,B30_{2019}} * e^{-k_{20601r,c}t}, 1 \right\}$ for $t \leq 2030$ $IQ_{r,c:peri,B30_t} = \max \left\{ IQ_{r,c:peri,B30_{2030}} * e^{-k_{20602r,c}t}, 1 \right\}$ for $t > 2030$

			$k_{2060}{}_{i_{r,c}}$ takes a value that ensures that the desired convergence level is reached in 2060.
	Slow	$IQ_{r,c:peri.,B30_t}$ are assumed to fall slightly until 2030 after which the decrease accelerates to reach the target level of convergence in 2100.	$Q_{r,c:peri.,B30_t} = \max \left\{ IQ_{r,c:peri.,B30_{2019}} * e^{-k_{2100}{}_{1r,c} t}, 1 \right\}$ for $t \leq 2030$ $IQ_{r,c:peri.,B30_t} = \max \left\{ IQ_{r,c:peri.,B30_{2030}} * e^{-k_{2100}{}_{2r,c} t}, 1 \right\}$ for $t > 2030$ $k_{2100}{}_{i_{r,c}}$ takes a value that ensures that the desired convergence level is reached in 2100.
Convergence	Complete	A complete convergence between all classes and regions is assumed.	$IQ_{r,c:peri.,B30_{target\ year}} = 1$
	Interregional	A complete convergence between regions and a partial convergence between classes is assumed (the richest classes consume three times as much as the poorest class).	$IQ_{center,T20:peri.,B30_{target\ year}} = 3$ $IQ_{semi,T20:peri.,B30_{target\ year}} = 2$ $IQ_{peri,T20:peri.,B30_{target\ year}} = 1$ $IQ_{center,M50:peri.,B30_{target\ year}} = 3$ $IQ_{semi,M50:peri.,B30_{target\ year}} = 2$ $IQ_{peri,M50:peri.,B30_{target\ year}} = 1$ $IQ_{center,B30:peri.,B30_{target\ year}} = 3$ $IQ_{semi,B30:peri.,B30_{target\ year}} = 2$
	Intraregional	A complete convergence between classes and a partial convergence between regions is assumed (the classes in the richest region consume three times as much as the classes in the poorest region).	$IQ_{center,T20:peri.,B30_{target\ year}} = 3$ $IQ_{semi,T20:peri.,B30_{target\ year}} = 3$ $IQ_{peri,T20:peri.,B30_{target\ year}} = 3$ $IQ_{center,M50:peri.,B30_{target\ year}} = 2$ $IQ_{semi,M50:peri.,B30_{target\ year}} = 2$

			$IQ_{peri,M50:peri,B30target\ year} = 2$ $IQ_{center,B30:peri,B30target\ year} = 1$ $IQ_{semi,B30:peri,B30target\ year} = 1$
Electricity mix	No changes	In the A matrix, input coefficients $IC_{sel,s}$ representing inputs from electricity sectors s_{el} are proportionally reduced through a process efficiency coefficient (PEC) while the relation between renewable and fossil electricity remains constant.	$IC_{Sel:S_{2100}} = PEC * IC_{Sel:S_{2019}}$ $s_{el} = \{sector\ i \mid 12 \leq i \leq 20\}$
	100% renewable	$IC_{sel,s}$ are reduced due to the PEC . Inputs from the nuclear and fossil electricity sector are shifted to renewable electricity sectors (solar PV, wind and hydro power) in industrial processes and for the consumption vector of final demand components (CV_{FD}).	$IC_{12:S_{2100}} = 0; IC_{13:S_{2100}} = 0$ $CV_{FD_{12\ 2100}} = 0; CV_{FD_{13\ 2100}} = 0$ $IC_{Sren:S_{2100}} = PEC * IC_{Sren:S_{2019}}$ $+ \frac{1}{3} (PEC(IG_{12:S_{2019}} + IC_{13:S_{2019}}))$ $S_{ren} = \{14, 15, 17\}$ $CV_{FD_{Sren\ 2100}} = CV_{FD_{Sren\ 2019}} + \frac{1}{3} (CV_{FD_{12\ 2019}} + CV_{FD_{13\ 2019}})$
Factor intensity	No additional changes	Energy intensity and labor intensity developments follow pathways specified by boundary conditions (see S2 SI).	$Labor\ intensity_s = \frac{L_s}{x_{s\ exog}}$
	Higher labor intensity	Labor intensities specified by boundary conditions are multiplied by a labor intensification factor (LIF) that increases labor intensity between 20% and 100% for selected sectors (no. 1, 5, 7, 11, 23). Those sectors that experience an increase in labor intensity also experience a decrease in energy intensity based on the assumption of	$\frac{L_s}{x_s} = \frac{L_s}{x_{s\ exog}} * LIF_s$ $LIF_{1,5,7,11,23} > 1$

		imperfect substitution between labor and energy through the reorganization of productive processes. Thus, the <i>PEC</i> of the respective sectors is multiplied by an Economic Structural Change (<i>ESC</i>) multiplier, defined as the ratio of the Imperfect Substitution Coefficient (<i>ISC</i>) to the <i>LIF</i> .	$ISC = \frac{ESC_{1,5,7,11,23}}{LIF_{1,5,7,11,11,23}}$ $PEC_{1,5,7,11,23} = PEC_{\text{default}} * ESC_{1,5,7,11,23}$
Agricultural production	Conventional	No changes in land intensity apart from those specified by boundary conditions.	$Land\ intensity_s = \frac{Land_s}{x_s \text{ exog}}$
	Organic	We take the average between the yield difference per unit of output in the case of best organic practices y_{bp} and in the case of highest comparability between conventional and organic systems y_{hc} compared to conventional practices y_{con} [49] to calculate the Intensity factor for Organic agriculture (<i>IO</i>), assuming that yield differences are proportional to land productivity differences. The policy only applies to land used to produce food products which is only demanded by sector 1.	$IO = \frac{1}{\left(1 - \frac{\frac{y_{bp}}{y_{con}} + \frac{y_{hc}}{y_{con}}}{2} \right)}$ $\frac{Foodland}{x_1} = IO * \frac{Foodland_1}{x_1 \text{ exog}}$
Diet	Meat-based	No changes in land intensity apart from those specified by boundary conditions.	$Land\ intensity_s = \frac{Land_s}{x_s \text{ exog}}$
	Plant-based	<p>Based on data for the land intensity of 15 food products ($\frac{land_j}{kcal_j}$) serving as protein source [50], we constructed two diet vectors v_i that specify the share of calories covered by every food product. The meat-based diet vector contains high shares for meat-based food products while the share of meat-based products is 0 in the plant-based diet vector.</p> <p>With the vectors and the land intensities for all food products, the weighted land intensity $\mu_{l_{i_w}}$ is calculated.</p> <p>The land intensity factor for protein calorie intake (ID_{pro}) is defined as the ratio of the weighted land intensity of a plant-based diet to that of a meat-based diet. For simplicity, we assume the same difference in land intensity also for fat-based calories in the human diet. However, since</p>	$i_1 = meat, i_2 = plant$ $\mu_{l_{i_w}} = \sum_{j=1}^{15} \frac{land}{kcal_j} * v_{j,i}$ $ID_{pro} = \frac{\mu_{l_{i_w}}}{\mu_{l_{i_m}}} < 1$

	<p>carbohydrates are mainly covered through plant-based sources in both forms of diet, the efficiency gain of a plant-based diet only applies to a share of total calories consumed. Taking this into account generates the final intensity factor for a plant-based diet (ID).</p> <p>Since we assume that the biophysical (kcal) and monetary (€) output of the agricultural sector are proportional, the ID can be applied to calculate the reduced land intensity of a plant-based diet compared to a default (meat-based) case.</p> <p>The policy only applies to land used to produce food products which is only demanded by sector 1.</p>	$ID = ID_{pro} * \left(\frac{kcal_{fat+protein}}{kcal_{total}} \right) + 1 - \left(\frac{kcal_{fat+protein}}{kcal_{total}} \right)$ $\frac{land}{kcal} = \frac{land}{\alpha * x}$ $\frac{Foodland}{x_1} = ID * \frac{Foodland_1}{x_1 \ exog}$
--	---	---

Table 2: Scenario implementation in MORDRED.

References

- [1] J. Hickel and A. Slamersak, "Existing climate mitigation scenarios perpetuate colonial inequalities," *The Lancet Planetary Health*, vol. 6, no. 7, pp. e628–e631, July 2022, doi: 10.1016/S2542-5196(22)00092-4.
- [2] J. D. Andersson, "Gambling with our climate futures: On the temporal structure of negative emissions," *Environment and Planning E: Nature and Space*, vol. 6, no. 3, pp. 1987–2007, 2023.
- [3] S. Fuss *et al.*, "Betting on negative emissions," *Nature climate change*, vol. 4, no. 10, pp. 850–853, 2014.
- [4] D. McLaren and W. Burns, "It Would Be Irresponsible, Unethical, and Unlawful to Rely on NETs at Large Scale Instead of Mitigation," in *Debating Climate Law*, 1st ed., B. Mayer and A. Zahar, Eds., Cambridge University Press, 2021, pp. 241–256. doi: 10.1017/9781108879064.019.
- [5] A. Brad *et al.*, "Existing demand-side climate change mitigation policies neglect avoid options," *Commun Earth Environ*, vol. 6, no. 1, p. 773, Oct. 2025, doi: 10.1038/s43247-025-02800-5.
- [6] U. Brand and M. Wissen, "Crisis and continuity of capitalist society-nature relationships: The imperial mode of living and the limits to environmental governance," *Review of International Political Economy*, vol. 20, no. 4, pp. 687–711, 2013.
- [7] D. Álvarez-Antelo, A. Lauer, and Í. Capellán-Pérez, "Exploring the potential of a novel passenger transport model to study the decarbonization of the transport sector," *Energy*, vol. 305, p. 132313, 2024.
- [8] G. Kallis, V. Kostakis, S. Lange, B. Muraca, S. Paulson, and M. Schmelzer, "Research on degrowth," *Annual Review of Environment and Resources*, vol. 43, no. 1, pp. 291–316, 2018.
- [9] J. Hickel, "Degrowth: a theory of radical abundance," *Real-World Economics Review*, vol. 87, no. 19, pp. 54–68, 2019.
- [10] J.-O. Engler, M.-F. Kretschmer, J. Rathgens, J. A. Ament, T. Huth, and H. von Wehrden, "15 years of degrowth research: A systematic review," *Ecological Economics*, vol. 218, p. 108101, 2024.
- [11] G. Kallis, R. Mastini, and C. Zografos, "Perceptions of degrowth in the European Parliament," *Nature Sustainability*, vol. 7, no. 1, pp. 64–72, 2024.
- [12] J. Millward-Hopkins, J. K. Steinberger, N. D. Rao, and Y. Oswald, "Providing decent living with minimum energy: A global scenario," *Global Environmental Change*, vol. 65, p. 102168, 2020.
- [13] Y. Oswald, J. Steinberger, D. Ivanova, and J. Millward-Hopkins, "Global redistribution of income and household energy footprints: a computational thought experiment," *Global Sustainability*, vol. 4, 2021.
- [14] A. Lauer, I. Capellán-Pérez, and N. Wergles, "A comparative review of de-and post-growth modeling studies," *Ecological Economics*, vol. 227, p. 108383, 2025.
- [15] A. Edwards, P. Brockway, K. Bickerstaff, and F. J. Nijssse, "Towards modelling post-growth climate futures: a review of current modelling practices and next steps," *Environmental Research Letters*, 2025.
- [16] L. Hardt and D. W. O'Neill, "Ecological macroeconomic models: assessing current developments," *Ecological economics*, vol. 134, pp. 198–211, 2017.
- [17] J. S. Kikstra *et al.*, "Downscaling down under: towards degrowth in integrated assessment models," *Economic Systems Research*, vol. 36, no. 4, pp. 576–606, Oct. 2024, doi: 10.1080/09535314.2023.2301443.

- [18] A. Grubler *et al.*, "A low energy demand scenario for meeting the 1.5 C target and sustainable development goals without negative emission technologies," *Nature energy*, vol. 3, no. 6, pp. 515–527, 2018.
- [19] F. Creutzig, J. Roy, and J. Minx, "Demand-side climate change mitigation: where do we stand and where do we go?," *Environmental Research Letters*, vol. 19, no. 4, p. 040201, 2024.
- [20] I. Savin and J. van den Bergh, "Reviewing studies of degrowth: Are claims matched by data, methods and policy analysis?," *Ecological Economics*, vol. 226, p. 108324, 2024.
- [21] M. Sugiyama *et al.*, "High with low: harnessing the power of demand-side solutions for high wellbeing with low energy and material demand," *Joule*, vol. 8, no. 1, pp. 1–6, 2024.
- [22] T. W. Wood, K. Richter, and E. Atkins, "Modelling beyond growth perspectives for sustainable climate futures: the case for rethinking Shared Socioeconomic Pathways," *Energy Research & Social Science*, vol. 117, p. 103705, 2024.
- [23] J. Hickel *et al.*, "Urgent need for post-growth climate mitigation scenarios," *Nature Energy*, vol. 6, no. 8, pp. 766–768, 2021.
- [24] B. Cointe and A. Pottier, "Understanding why degrowth is absent from mitigation scenarios: Modelling choices and practices in the IAM community," *regulation*, vol. 35, 2023, doi: 10.4000/regulation.23034.
- [25] M. Li *et al.*, "Integrated assessment modelling of degrowth scenarios for Australia," *Economic Systems Research*, pp. 1–31, 2023.
- [26] J. Nieto, Ó. Carpintero, L. J. Miguel, and I. de Blas, "Macroeconomic modelling under energy constraints: Global low carbon transition scenarios," *Energy Policy*, vol. 137, p. 111090, 2020.
- [27] S. D'Alessandro, A. Cieplinski, T. Distefano, and K. Dittmer, "Feasible alternatives to green growth," *Nature Sustainability*, vol. 3, no. 4, pp. 329–335, 2020.
- [28] J. D. Moyer, "Modeling transformational policy pathways on low growth and negative growth scenarios to assess impacts on socioeconomic development and carbon emissions," *Scientific Reports*, vol. 13, no. 1, p. 15996, 2023.
- [29] J. Rockström *et al.*, "Safe and just Earth system boundaries," *Nature*, vol. 619, no. 7968, pp. 102–111, July 2023, doi: 10.1038/s41586-023-06083-8.
- [30] J. Sekera and A. Lichtenberger, "Assessing carbon capture: Public policy, science, and societal need: A review of the literature on industrial carbon removal," *Biophysical Economics and Sustainability*, vol. 5, pp. 1–28, 2020.
- [31] J. Braun, C. Werner, D. Gerten, F. Stenzel, S. Schaphoff, and W. Lucht, "Multiple planetary boundaries preclude biomass crops for carbon capture and storage outside of agricultural areas," *Communications Earth & Environment*, vol. 6, no. 1, p. 102, 2025.
- [32] S. Alexander and P. Yacoumis, "Degrowth, energy descent, and 'low-tech'living: Potential pathways for increased resilience in times of crisis," *Journal of Cleaner Production*, vol. 197, pp. 1840–1848, 2018.
- [33] N. Wunderling *et al.*, "Climate tipping point interactions and cascades: a review," *Earth System Dynamics*, vol. 15, no. 1, pp. 41–74, 2024.
- [34] G. H. Roe and M. B. Baker, "Why Is Climate Sensitivity So Unpredictable?," *Science*, vol. 318, no. 5850, pp. 629–632, Oct. 2007, doi: 10.1126/science.1144735.
- [35] G. Wagner and M. L. Weitzman, "Potentially large equilibrium climate sensitivity tail uncertainty," *Economics Letters*, vol. 168, pp. 144–146, July 2018, doi: 10.1016/j.econlet.2018.04.036.
- [36] E. Bilancini and S. D'Alessandro, "Long-run welfare under externalities in consumption, leisure, and production: A case for happy degrowth vs. unhappy growth," *Ecological Economics*, vol. 84, pp. 194–205, 2012.

- [37] I. Otero *et al.*, "Biodiversity policy beyond economic growth," *CONSERVATION LETTERS*, vol. 13, no. 4, p. e12713, July 2020, doi: 10.1111/conl.12713.
- [38] A. Lauer and L. Llases, "MORDRED: Model Of Resource Distribution and Resilient Economic Development. Model Documentation." GitHub, 2025. [Online]. Available: <https://github.com/Pendracus/MORDRED>
- [39] K. Stadler *et al.*, "EXIOBASE 3: Developing a Time Series of Detailed Environmentally Extended Multi-Regional Input-Output Tables," *J of Industrial Ecology*, vol. 22, no. 3, pp. 502–515, June 2018, doi: 10.1111/jiec.12715.
- [40] UN DESA, "World Population Prospects 2019, Online Edition. Rev. 1. File POP/7-1: Total population (both sexes combined) by five-year age group, region, subregion and country, 1950–2100 (thousands)." 2019.
- [41] R. Lahoti, A. Jayadev, and S. Reddy, "The global consumption and income project (GCIP): An overview," *Journal of Globalization and Development*, vol. 7, no. 1, pp. 61–108, 2016.
- [42] IPCC, "Climate Change 2021: The Physical Science Basis. Contribution of Working Group I to the Sixth Assessment Report of the Intergovernmental Panel on Climate Change." Cambridge University Press. Cambridge University Press, Cambridge, UK and New York, NY, USA, 2021.
- [43] BGR, "BGR Energy Study 2019 – Data and Developments Concerning German and Global energy supplies." Hannover, 2020. [Online]. Available: https://www.bgr.bund.de/EN/Themen/Energie/Downloads/energiestudie_2019_en.pdf;jsessionid=ADF18B2529B3E89FC705FDF390A57BA4.internet002?__blob=publicationFile&v=6
- [44] M. Lifi *et al.*, "D9.3: 'Synthesis of the model, selected results, and scenario assessment.'" 2023. [Online]. Available: <https://www.locomotion-h2020.eu/resources/main-project-reports/>
- [45] N. Fitzpatrick, T. Parrique, and I. Cosme, "Exploring degrowth policy proposals: A systematic mapping with thematic synthesis," *Journal of Cleaner Production*, p. 132764, 2022.
- [46] M. R. Sers, "Ecological macroeconomic assessment of meeting a carbon budget without negative emissions," *Global Sustainability*, vol. 5, p. e6, 2022.
- [47] J. Nieto, Ó. Carpintero, L. F. Lobejón, and L. J. Miguel, "An ecological macroeconomics model: The energy transition in the EU," *Energy Policy*, vol. 145, p. 111726, 2020.
- [48] T. Jackson and P. Victor, "Productivity and work in the 'green economy': Some theoretical reflections and empirical tests," *Environmental Innovation and Societal Transitions*, vol. 1, no. 1, pp. 101–108, 2011.
- [49] V. Seufert, N. Ramankutty, and J. A. Foley, "Comparing the yields of organic and conventional agriculture," *Nature*, vol. 485, no. 7397, pp. 229–232, 2012.
- [50] J. Poore and T. Nemecek, "Reducing food's environmental impacts through producers and consumers," *Science*, vol. 360, no. 6392, pp. 987–992, June 2018, doi: 10.1126/science.aaq0216.

Supplementary Information

S.1. Overview simulated scenarios

Consumption level	Year	Convergence	Green electricity	Structural change	Organic agriculture	Plant-based diet	Scenario name
11000€ <i>person * year</i>	2040	complete	no	no	no	no	1111111
11000€ <i>person * year</i>	2040	interregional	no	no	no	no	1121111
11000€ <i>person * year</i>	2040	intraregional	no	no	no	no	1131111
11000€ <i>person * year</i>	2040	complete	yes	no	no	no	1112111
11000€ <i>person * year</i>	2040	interregional	yes	no	no	no	1122111
11000€ <i>person * year</i>	2040	intraregional	yes	no	no	no	1132111
11000€ <i>person * year</i>	2040	complete	no	yes	no	no	1111211
11000€ <i>person * year</i>	2040	interregional	no	yes	no	no	1121211
11000€ <i>person * year</i>	2040	intraregional	no	yes	no	no	1131211
11000€ <i>person * year</i>	2040	complete	no	no	yes	no	1111121
11000€ <i>person * year</i>	2040	interregional	no	no	yes	no	1121121
11000€ <i>person * year</i>	2040	intraregional	no	no	yes	no	1131121
11000€ <i>person * year</i>	2040	complete	no	no	no	yes	1111112
11000€ <i>person * year</i>	2040	interregional	no	no	no	yes	1121112
11000€ <i>person * year</i>	2040	intraregional	no	no	no	yes	1131112
11000€ <i>person * year</i>	2040	complete	yes	yes	yes	yes	1112222
11000€ <i>person * year</i>	2040	interregional	yes	yes	yes	yes	1122222
11000€ <i>person * year</i>	2040	intraregional	yes	yes	yes	yes	1132222
11000€ <i>person * year</i>	2060	complete	no	no	no	no	1211111
11000€ <i>person * year</i>	2060	interregional	no	no	no	no	1221111
11000€ <i>person * year</i>	2060	intraregional	no	no	no	no	1231111
11000€ <i>person * year</i>	2060	complete	yes	no	no	no	1212111
11000€ <i>person * year</i>	2060	interregional	yes	no	no	no	1222111
11000€ <i>person * year</i>	2060	intraregional	yes	no	no	no	1232111
11000€ <i>person * year</i>	2060	complete	no	yes	no	no	1211211

11000€ <i>person * year</i>	2060	interregional	no	yes	no	no	1221211
11000€ <i>person * year</i>	2060	intraregional	no	yes	no	no	1231211
11000€ <i>person * year</i>	2060	complete	no	no	yes	no	1211121
11000€ <i>person * year</i>	2060	interregional	no	no	yes	no	1221121
11000€ <i>person * year</i>	2060	intraregional	no	no	yes	no	1231121
11000€ <i>person * year</i>	2060	complete	no	no	no	yes	1211112
11000€ <i>person * year</i>	2060	interregional	no	no	no	yes	1221112
11000€ <i>person * year</i>	2060	intraregional	no	no	no	yes	1231112
11000€ <i>person * year</i>	2060	complete	yes	yes	yes	yes	1212222
11000€ <i>person * year</i>	2060	interregional	yes	yes	yes	yes	1222222
11000€ <i>person * year</i>	2060	intraregional	yes	yes	yes	yes	1232222
11000€ <i>person * year</i>	2100	complete	no	no	no	no	1311111
11000€ <i>person * year</i>	2100	interregional	no	no	no	no	1321111
11000€ <i>person * year</i>	2100	intraregional	no	no	no	no	1331111
11000€ <i>person * year</i>	2100	complete	yes	no	no	no	1312111
11000€ <i>person * year</i>	2100	interregional	yes	no	no	no	1322111
11000€ <i>person * year</i>	2100	intraregional	yes	no	no	no	1332111
11000€ <i>person * year</i>	2100	complete	no	yes	no	no	1311211
11000€ <i>person * year</i>	2100	interregional	no	yes	no	no	1321211
11000€ <i>person * year</i>	2100	intraregional	no	yes	no	no	1331211
11000€ <i>person * year</i>	2100	complete	no	no	yes	no	1311121
11000€ <i>person * year</i>	2100	interregional	no	no	yes	no	1321121
11000€ <i>person * year</i>	2100	intraregional	no	no	yes	no	1331121
11000€ <i>person * year</i>	2100	complete	no	no	no	yes	1311112
11000€ <i>person * year</i>	2100	interregional	no	no	no	yes	1321112
11000€ <i>person * year</i>	2100	intraregional	no	no	no	yes	1332112
11000€ <i>person * year</i>	2100	complete	yes	yes	yes	yes	1312222
11000€ <i>person * year</i>	2100	interregional	yes	yes	yes	yes	1322222
11000€ <i>person * year</i>	2100	intraregional	yes	yes	yes	yes	1332222
15400€ <i>person * year</i>	2040	complete	no	no	no	no	2111111
15400€ <i>person * year</i>	2040	interregional	no	no	no	no	2121111

15400€ <i>person * year</i>	2040	intraregional	no	no	no	no	2131111
15400€ <i>person * year</i>	2040	complete	yes	no	no	no	2112111
15400€ <i>person * year</i>	2040	interregional	yes	no	no	no	2122111
15400€ <i>person * year</i>	2040	intraregional	yes	no	no	no	2132111
15400€ <i>person * year</i>	2040	complete	no	yes	no	no	2111211
15400€ <i>person * year</i>	2040	interregional	no	yes	no	no	2121211
15400€ <i>person * year</i>	2040	intraregional	no	yes	no	no	2131211
15400€ <i>person * year</i>	2040	complete	no	no	yes	no	2111121
15400€ <i>person * year</i>	2040	interregional	no	no	yes	no	2121121
15400€ <i>person * year</i>	2040	intraregional	no	no	yes	no	2131121
15400€ <i>person * year</i>	2040	complete	no	no	no	yes	2111112
15400€ <i>person * year</i>	2040	interregional	no	no	no	yes	2121112
15400€ <i>person * year</i>	2040	intraregional	no	no	no	yes	2131112
15400€ <i>person * year</i>	2040	complete	no	no	no	yes	2131112
15400€ <i>person * year</i>	2040	interregional	yes	yes	yes	yes	2112222
15400€ <i>person * year</i>	2040	intraregional	yes	yes	yes	yes	2122222
15400€ <i>person * year</i>	2040	complete	yes	yes	yes	yes	2132222
15400€ <i>person * year</i>	2060	complete	no	no	no	no	2211111
15400€ <i>person * year</i>	2060	interregional	no	no	no	no	2221111
15400€ <i>person * year</i>	2060	intraregional	no	no	no	no	2231111
15400€ <i>person * year</i>	2060	complete	yes	no	no	no	2212111
15400€ <i>person * year</i>	2060	interregional	yes	no	no	no	2222111
15400€ <i>person * year</i>	2060	intraregional	yes	no	no	no	2232111
15400€ <i>person * year</i>	2060	complete	no	yes	no	no	2211211
15400€ <i>person * year</i>	2060	interregional	no	yes	no	no	2221211
15400€ <i>person * year</i>	2060	intraregional	no	yes	no	no	2231211
15400€ <i>person * year</i>	2060	complete	no	no	yes	no	2211121
15400€ <i>person * year</i>	2060	interregional	no	no	yes	no	2221121
15400€ <i>person * year</i>	2060	intraregional	no	no	yes	no	2231121
15400€ <i>person * year</i>	2060	complete	no	no	no	yes	2211112
15400€ <i>person * year</i>	2060	interregional	no	no	no	yes	2221112
15400€ <i>person * year</i>	2060	intraregional	no	no	no	yes	2231112

15400€ <i>person * year</i>	2060	complete	yes	yes	yes	yes	2212222
15400€ <i>person * year</i>	2060	interregional	yes	yes	yes	yes	2222222
15400€ <i>person * year</i>	2060	intraregional	yes	yes	yes	yes	2232222
15400€ <i>person * year</i>	2100	complete	no	no	no	no	2311111
15400€ <i>person * year</i>	2100	interregional	no	no	no	no	2321111
15400€ <i>person * year</i>	2100	intraregional	no	no	no	no	2331111
15400€ <i>person * year</i>	2100	complete	yes	no	no	no	2312111
15400€ <i>person * year</i>	2100	interregional	yes	no	no	no	2322111
15400€ <i>person * year</i>	2100	intraregional	yes	no	no	no	2332111
15400€ <i>person * year</i>	2100	complete	no	yes	no	no	2311211
15400€ <i>person * year</i>	2100	interregional	no	yes	no	no	2321211
15400€ <i>person * year</i>	2100	intraregional	no	yes	no	no	2331211
15400€ <i>person * year</i>	2100	complete	no	no	yes	no	2311121
15400€ <i>person * year</i>	2100	interregional	no	no	yes	no	2321121
15400€ <i>person * year</i>	2100	intraregional	no	no	yes	no	2331121
15400€ <i>person * year</i>	2100	complete	no	no	no	yes	2311112
15400€ <i>person * year</i>	2100	interregional	no	no	no	yes	2321112
15400€ <i>person * year</i>	2100	intraregional	no	no	no	yes	2331112
15400€ <i>person * year</i>	2100	complete	yes	yes	yes	yes	2312222
15400€ <i>person * year</i>	2100	interregional	yes	yes	yes	yes	2322222
15400€ <i>person * year</i>	2100	intraregional	yes	yes	yes	yes	2332222
6600€ <i>person * year</i>	2040	complete	no	no	no	no	3111111
6600€ <i>person * year</i>	2040	interregional	no	no	no	no	3121111
6600€ <i>person * year</i>	2040	intraregional	no	no	no	no	3131111
6600€ <i>person * year</i>	2040	complete	yes	no	no	no	3112111
6600€ <i>person * year</i>	2040	interregional	yes	no	no	no	3122111
6600€ <i>person * year</i>	2040	intraregional	yes	no	no	no	3132111
6600€ <i>person * year</i>	2040	complete	no	yes	no	no	3111211
6600€ <i>person * year</i>	2040	interregional	no	yes	no	no	3121211
6600€ <i>person * year</i>	2040	intraregional	no	yes	no	no	3131211
6600€ <i>person * year</i>	2040	complete	no	no	yes	no	3111121

6600€ <u>person * year</u>	2040	interregional	no	no	yes	no	3121121
6600€ <u>person * year</u>	2040	intraregional	no	no	yes	no	3131121
6600€ <u>person * year</u>	2040	complete	no	no	no	yes	3111112
6600€ <u>person * year</u>	2040	interregional	no	no	no	yes	3121112
6600€ <u>person * year</u>	2040	intraregional	no	no	no	yes	3131112
6600€ <u>person * year</u>	2040	complete	yes	yes	yes	yes	3112222
6600€ <u>person * year</u>	2040	interregional	yes	yes	yes	yes	3122222
6600€ <u>person * year</u>	2040	intraregional	yes	yes	yes	yes	3132222
6600€ <u>person * year</u>	2060	complete	no	no	no	no	3211111
6600€ <u>person * year</u>	2060	interregional	no	no	no	no	3221111
6600€ <u>person * year</u>	2060	intraregional	no	no	no	no	3231111
6600€ <u>person * year</u>	2060	complete	yes	no	no	no	3212111
6600€ <u>person * year</u>	2060	interregional	yes	no	no	no	3222111
6600€ <u>person * year</u>	2060	intraregional	yes	no	no	no	3232111
6600€ <u>person * year</u>	2060	complete	no	yes	no	no	3211211
6600€ <u>person * year</u>	2060	interregional	no	yes	no	no	3221211
6600€ <u>person * year</u>	2060	intraregional	no	yes	no	no	3231211
6600€ <u>person * year</u>	2060	complete	no	no	yes	no	3211121
6600€ <u>person * year</u>	2060	interregional	no	no	yes	no	3221121
6600€ <u>person * year</u>	2060	intraregional	no	no	yes	no	3231121
6600€ <u>person * year</u>	2060	complete	no	no	no	yes	3211112
6600€ <u>person * year</u>	2060	interregional	no	no	no	yes	3221112
6600€ <u>person * year</u>	2060	intraregional	no	no	no	yes	3231112
6600€ <u>person * year</u>	2060	complete	yes	yes	yes	yes	3212222
6600€ <u>person * year</u>	2060	interregional	yes	yes	yes	yes	3222222
6600€ <u>person * year</u>	2100	complete	no	no	no	no	3311111
6600€ <u>person * year</u>	2100	interregional	no	no	no	no	3321111
6600€ <u>person * year</u>	2100	intraregional	no	no	no	no	3331111
6600€ <u>person * year</u>	2100	Complete	yes	no	no	no	3312111
6600€ <u>person * year</u>	2100	interregional	yes	no	no	no	3322111

$\frac{6600\text{€}}{\text{person} * \text{year}}$	2100	intraregional	yes	no	no	no	3332111
$\frac{6600\text{€}}{\text{person} * \text{year}}$	2100	Complete	no	yes	no	no	3311211
$\frac{6600\text{€}}{\text{person} * \text{year}}$	2100	interregional	no	yes	no	no	3321211
$\frac{6600\text{€}}{\text{person} * \text{year}}$	2100	intraregional	no	yes	no	no	3331211
$\frac{6600\text{€}}{\text{person} * \text{year}}$	2100	Complete	no	no	yes	no	3311121
$\frac{6600\text{€}}{\text{person} * \text{year}}$	2100	interregional	no	no	yes	no	3321121
$\frac{6600\text{€}}{\text{person} * \text{year}}$	2100	intraregional	no	no	yes	no	3331121
$\frac{6600\text{€}}{\text{person} * \text{year}}$	2100	Complete	no	no	no	yes	3311112
$\frac{6600\text{€}}{\text{person} * \text{year}}$	2100	interregional	no	no	no	yes	3321112
$\frac{6600\text{€}}{\text{person} * \text{year}}$	2100	intraregional	no	no	no	yes	3331112
$\frac{6600\text{€}}{\text{person} * \text{year}}$	2100	Complete	yes	yes	yes	yes	3312222
$\frac{6600\text{€}}{\text{person} * \text{year}}$	2100	interregional	yes	yes	yes	yes	3322222
$\frac{6600\text{€}}{\text{person} * \text{year}}$	2100	intraregional	yes	yes	yes	yes	3332222

SI Table 1: Scenario characteristics of all simulated scenarios along the scenario dimensions.

S.2. Boundary conditions

Default economic structural change

In the A-Matrix, all industrial processes improve energy efficiency by 5% regarding all energy inputs (fossil fuels, electricity, biomass energy). This is done by multiplying all energy inputs by a process efficiency coefficient (PEC).

Additionally, 10% of the non-electric energy demand of households and of certain industrial sectors (no. 3, 5, 7, 8, 9, 10, 11, 12, 14, 15, 17, 21, 25) are substituted with electricity, linked to an energy efficiency gain of 50%.

Labor productivity

The key assumption behind the labor productivity developments in the scenario is a link between per capita consumption and regional economic development, with the latter being linked to higher labor productivities. Both assumptions are empirically grounded and are reflected in the country-based Exiobase3 data.

We make very optimistic assumptions regarding the future development of labor productivity in the context of degrowing consumption levels for the Global North as we assume that labor productivity in 2100 on the global scale is higher than in 2019 in the richest world region although average consumption on a global scale in 2100 is lower than in the center in 2019.

In scenarios with only intraregional convergence, we assume that labor productivity is somewhat lower as the majority of workers live in the semiperiphery and periphery. Likewise, lower labor productivity increases are assumed for ‘moderate’ and ‘strong’ DG compared to ‘weak’ DG.

SI Table 2 displays the different labor productivity assumptions for different scenario configurations.

Scale	Convergence	Sectoral labor productivity assumptions	
Soft DG	Full convergence, interregional convergence	Higher labor productivity scenarios $L_{prod.\text{higher}}$	Global labor productivity in 2100 is 1.3 times higher than labor productivity in the center in 2019
	Intraregional convergence	Upper medium labor productivity scenarios $L_{prod.\text{upper medium}} = 0.85 * L_{prod.\text{higher}}$	Global labor productivity in 2100 is 15% lower than in the higher labor productivity scenarios
Classic DG	Full convergence, interregional convergence	Lower medium labor productivity scenarios $L_{prod.\text{lower medium}} = 0.8 * L_{prod.\text{higher}}$	Global labor productivity in 2100 is 20% lower than in the higher labor productivity scenarios
	Intraregional convergence	Lower labor productivity scenarios $L_{prod.\text{lower}} = 0.75 * L_{prod.\text{higher}}$	Global labor productivity in 2100 is 25% lower than in the higher labor productivity scenarios
Hard DG	Full convergence, interregional convergence		
	Intraregional convergence		

SI Table 2: Comparison of convergence and future labor productivity assumptions.

Land intensities

Land intensity developments are not differentiated according to consumption per capita levels to increase the comparability between the scenarios and avoid excessive complexity through varying boundary conditions.

A factor of 0.2 was applied for the default intensity improvements without additional policies. This means that land intensity for all land-demanding sectors and for all land types (forests, agricultural land, land used for energy generation) is reduced by 80% compared to the global average values in 2019. As a result, the global agricultural sector is 2.85 times more productive in terms of agricultural land use than the agricultural sector of the center in 2019, and the global forestry sector is 3.63 times more productive in terms of forest land use than the forestry sector of the center in 2019. Land intensity of infrastructure in the model is driven by household demand and remains constant which could lead to an overestimation of infrastructure land demand relative to other land demands. However, water-based renewable energy technologies, notably hydropower, are assumed to have a land-intensity of zero although infrastructure needs

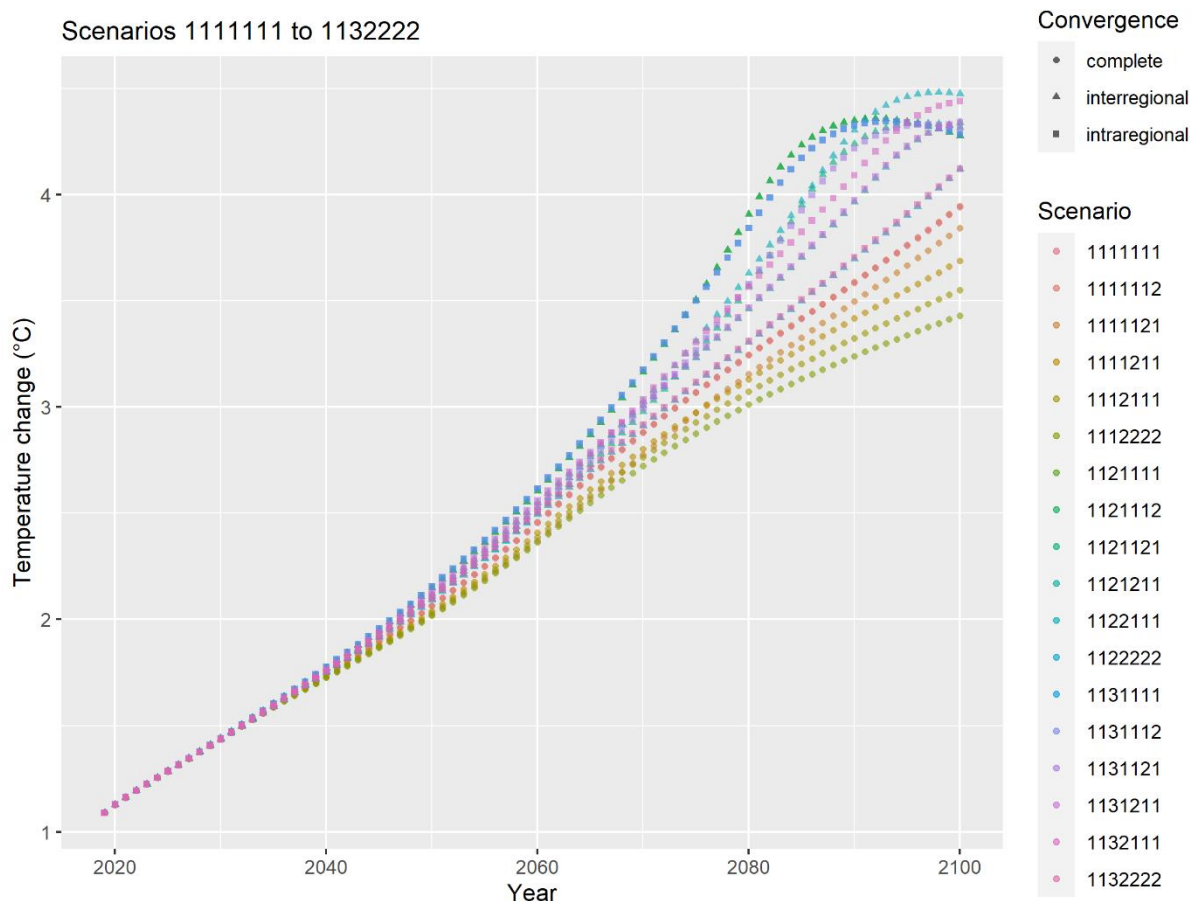
to build the plants might result in additional land-use change not represented, which reduces the possible overestimation.

Resources

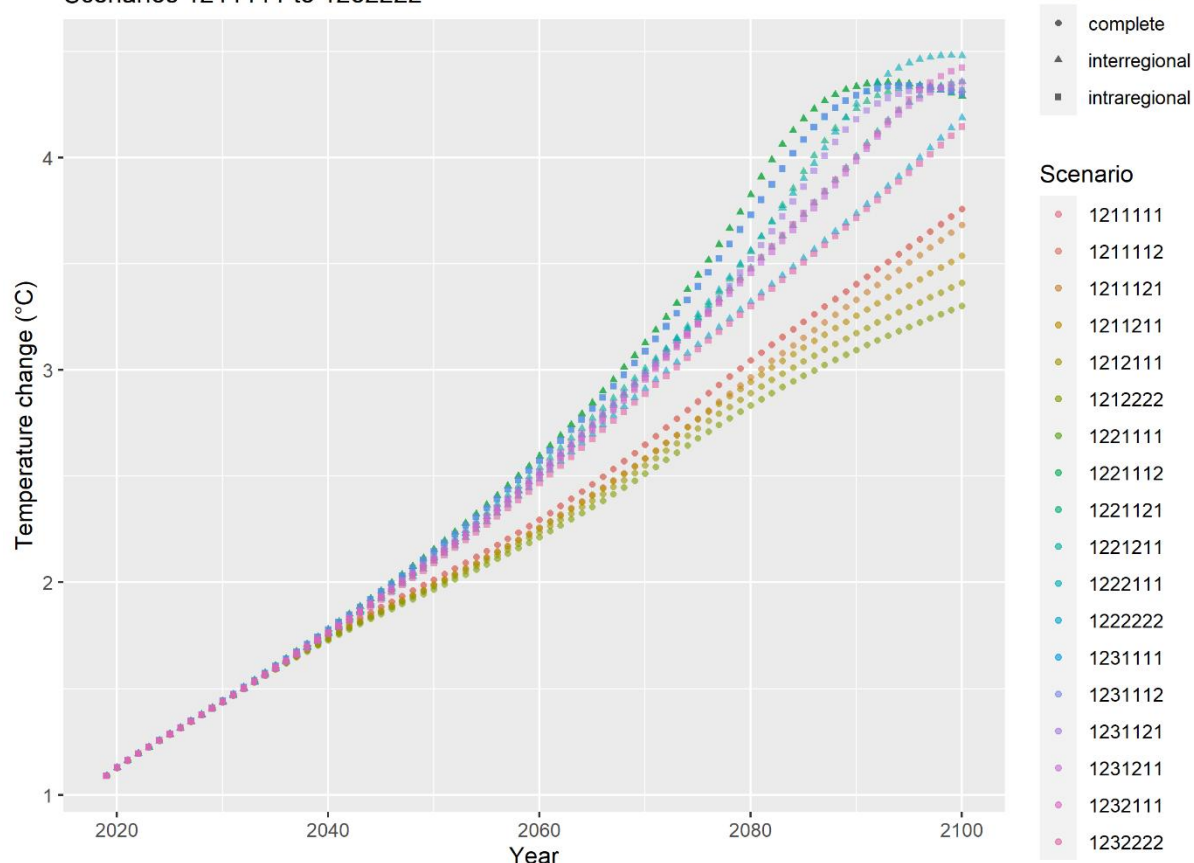
Default model assumptions that are not changed in the simulations include (1) the absence of limits regarding the quantity of extracted mineral resources; (2) linearly increasing input factors in the resource extraction sector as resource depletion increases; and (3) fossil resources that are the sum of reserve estimates for coal as well as resource estimates for natural gas and oil according to the BGR (2020). Optimistically, the model assumes complete substitutability between different types of fossil fuels.

S.3. Supplementary Figures

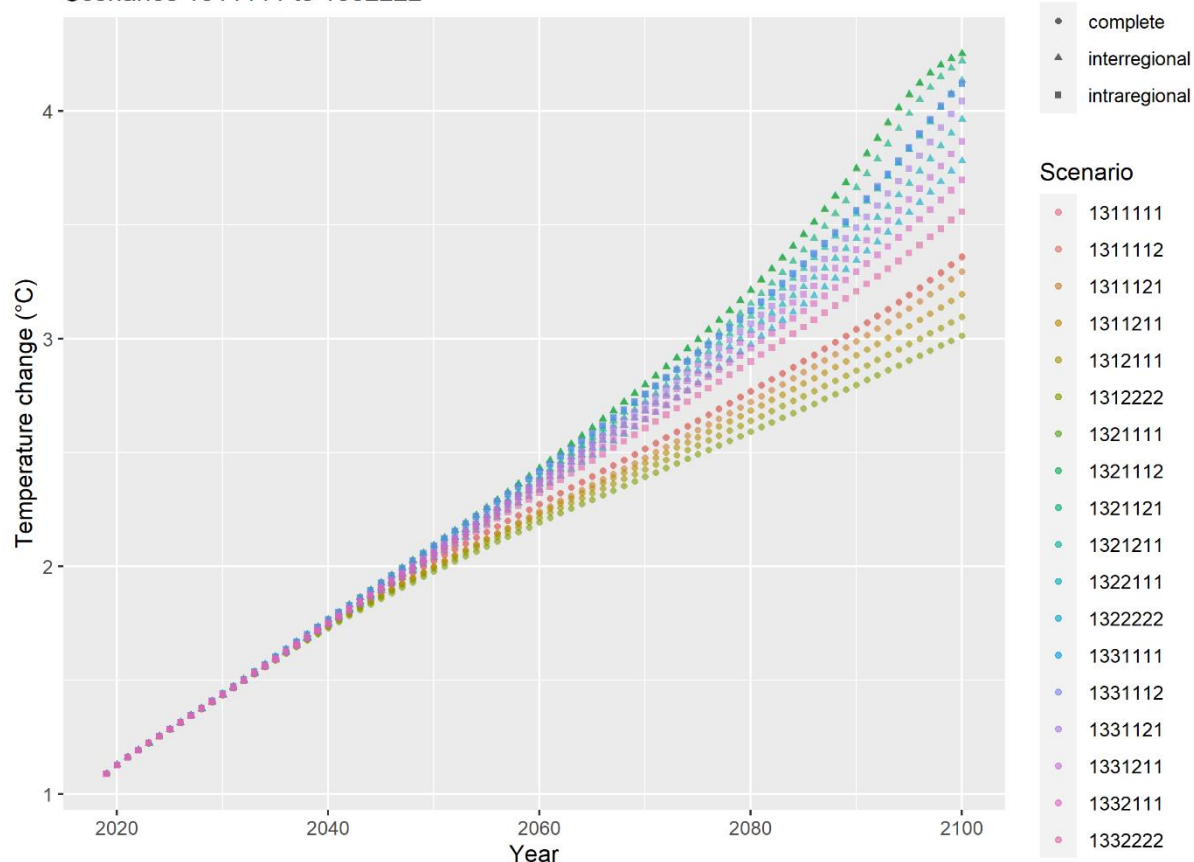
S.3.1. Temperature change



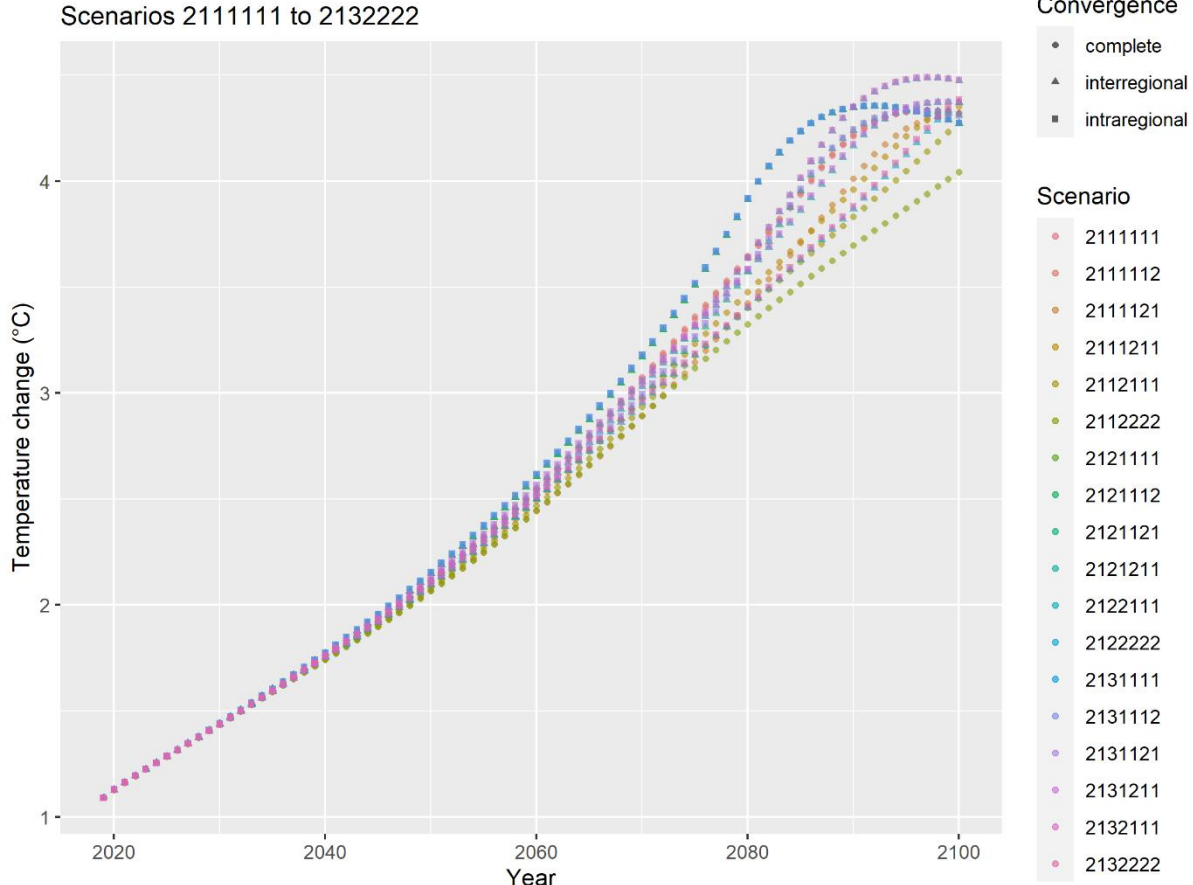
Scenarios 1211111 to 1232222



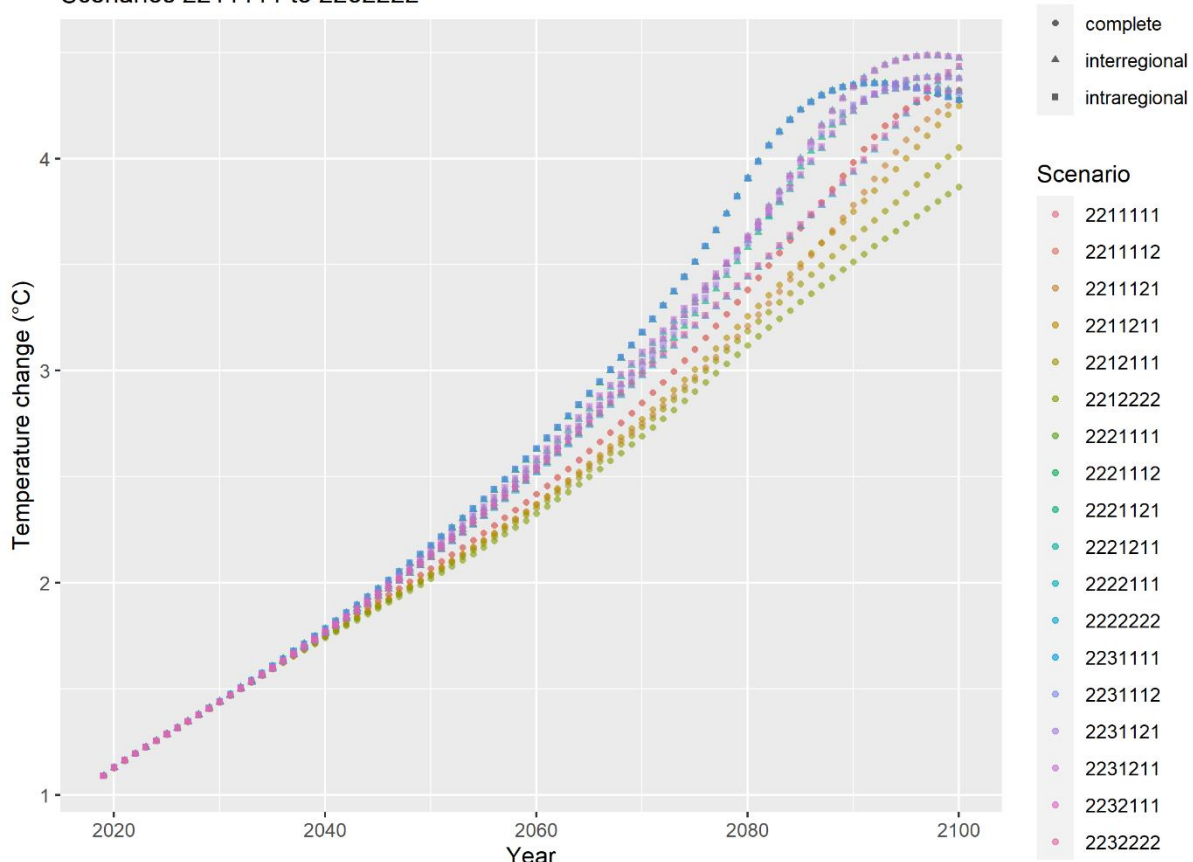
Scenarios 1311111 to 1332222



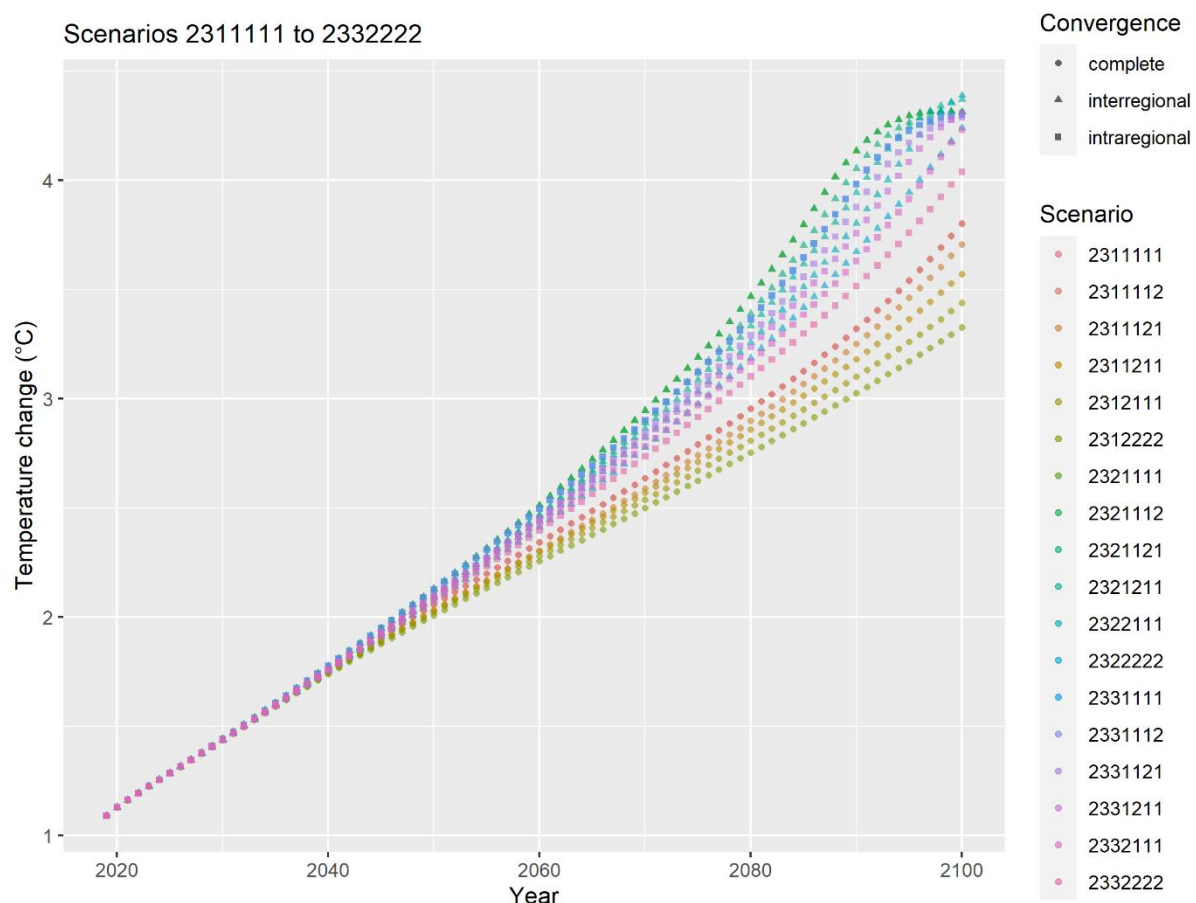
Scenarios 2111111 to 2132222



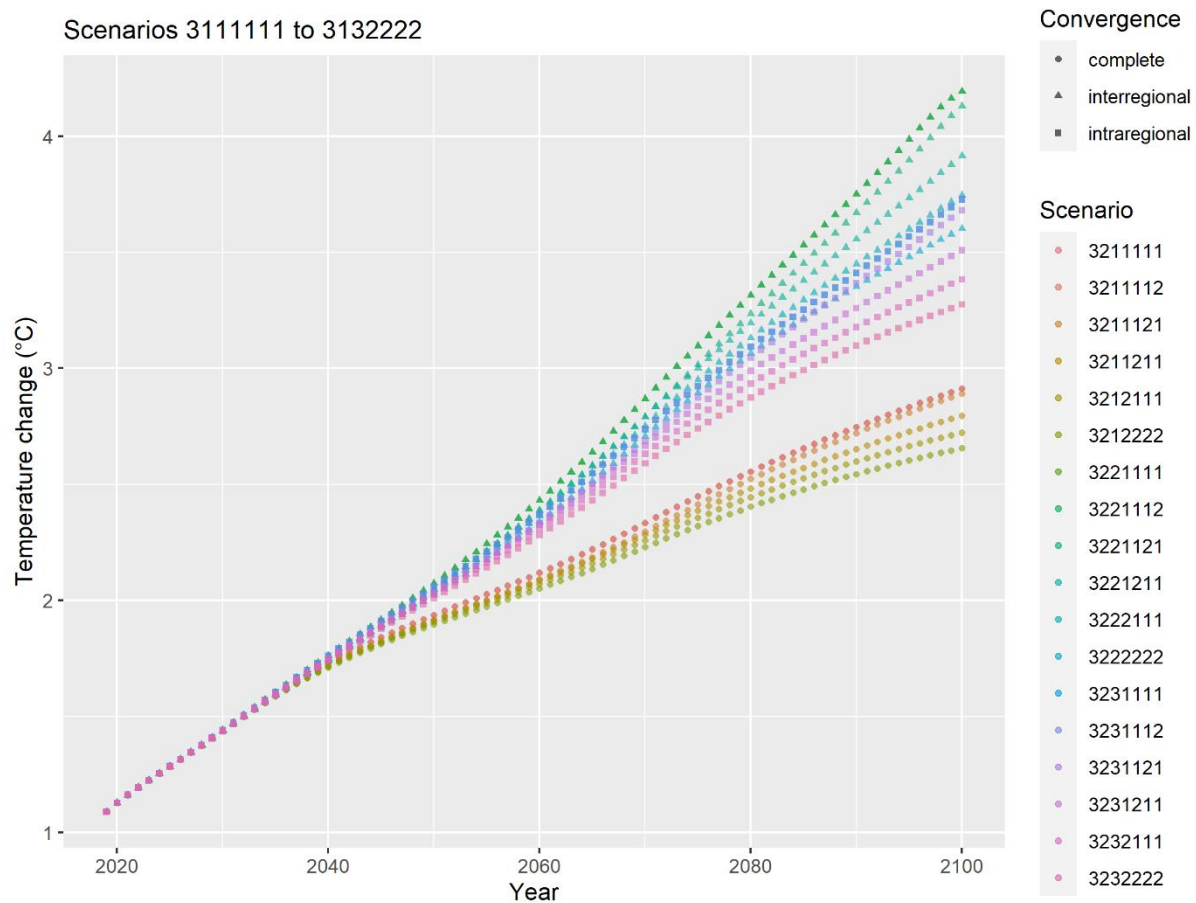
Scenarios 2211111 to 2232222

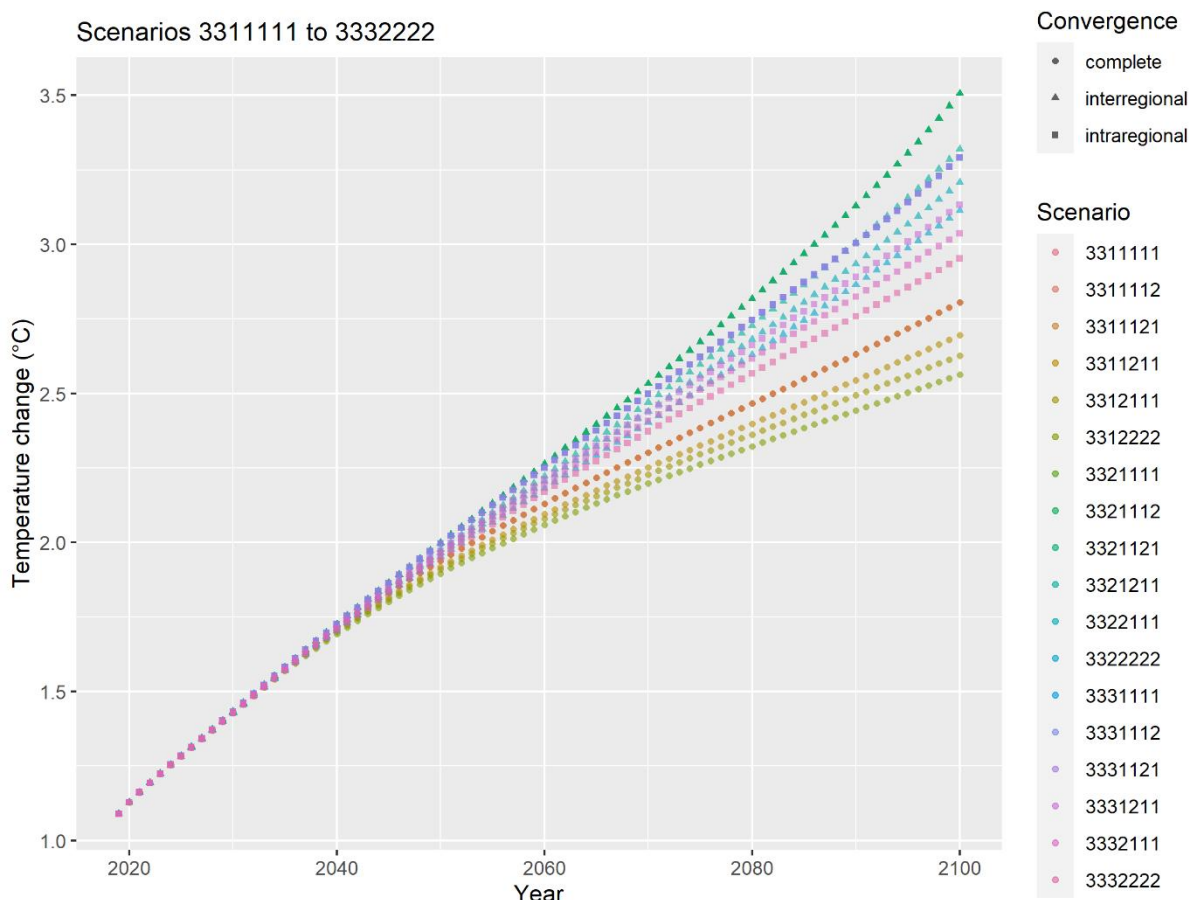
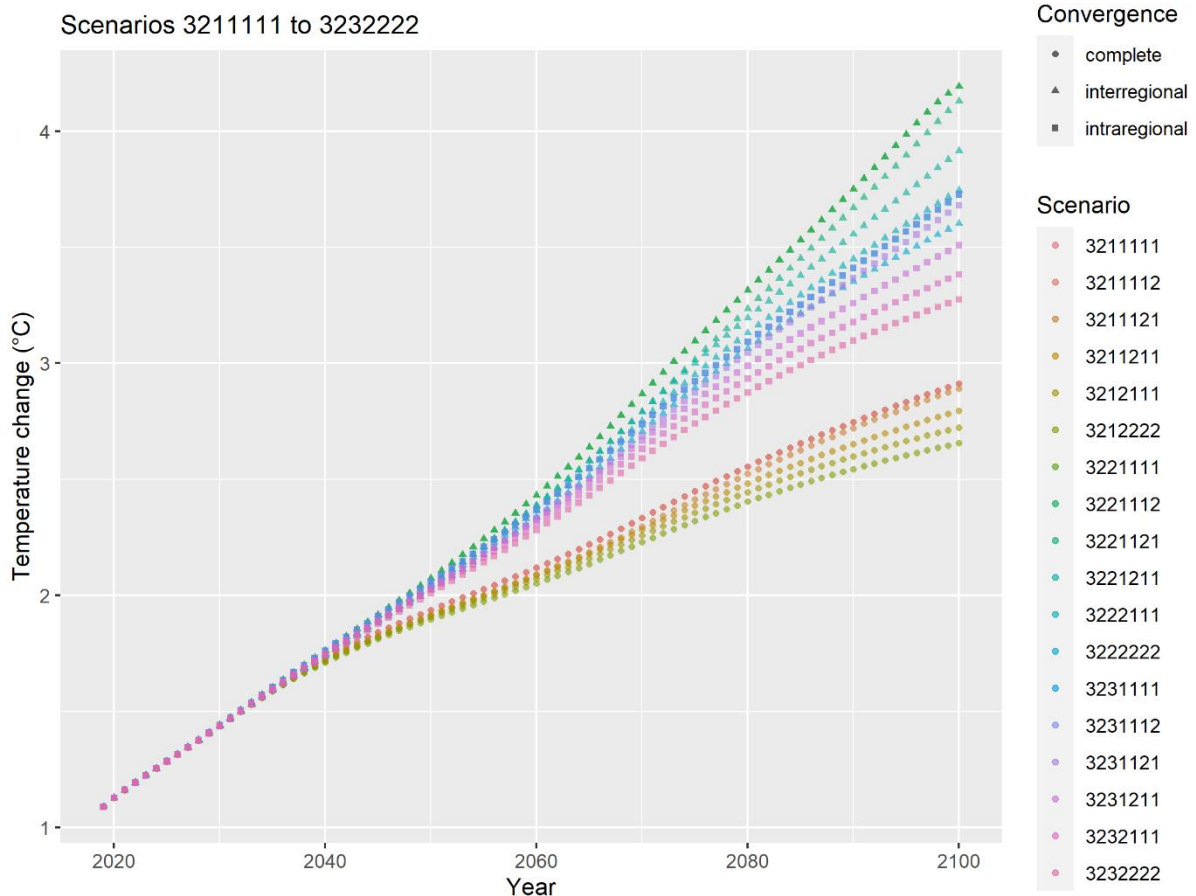


Scenarios 2311111 to 2332222

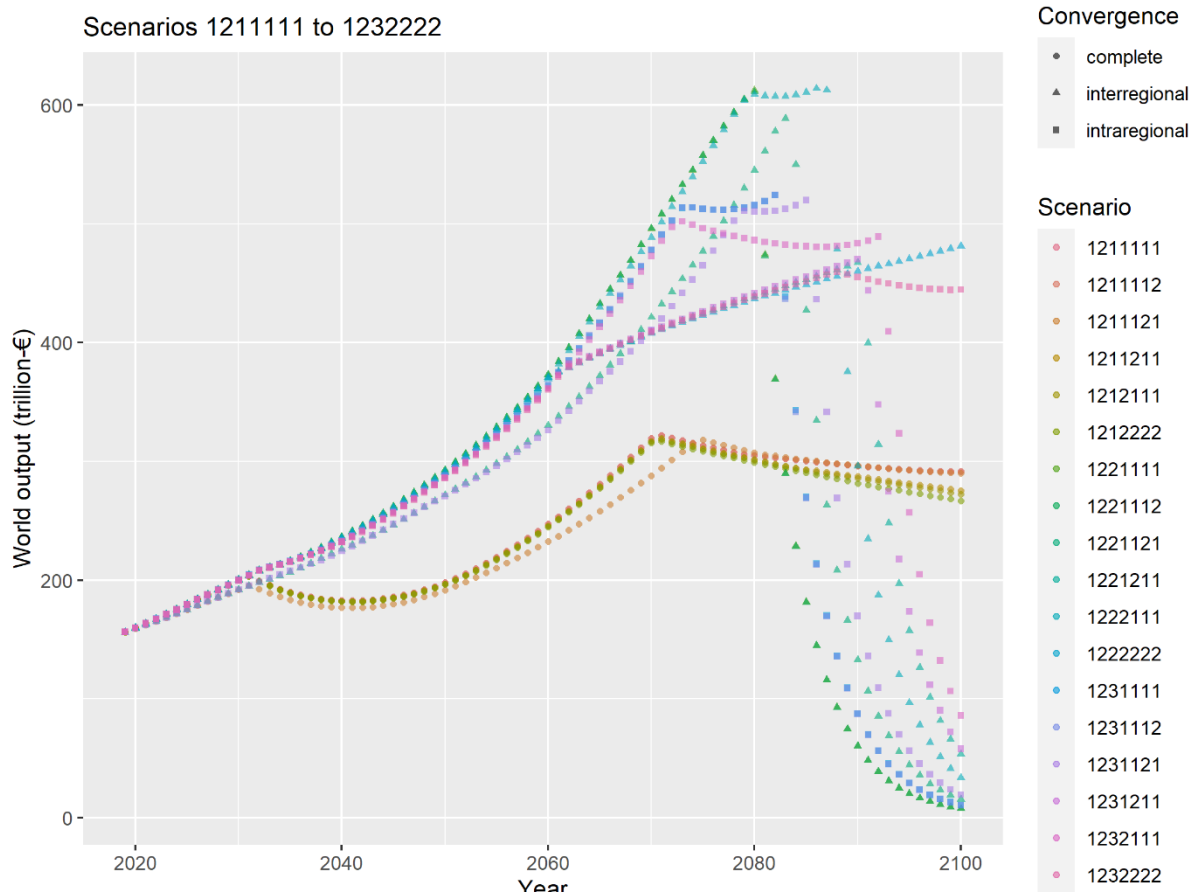
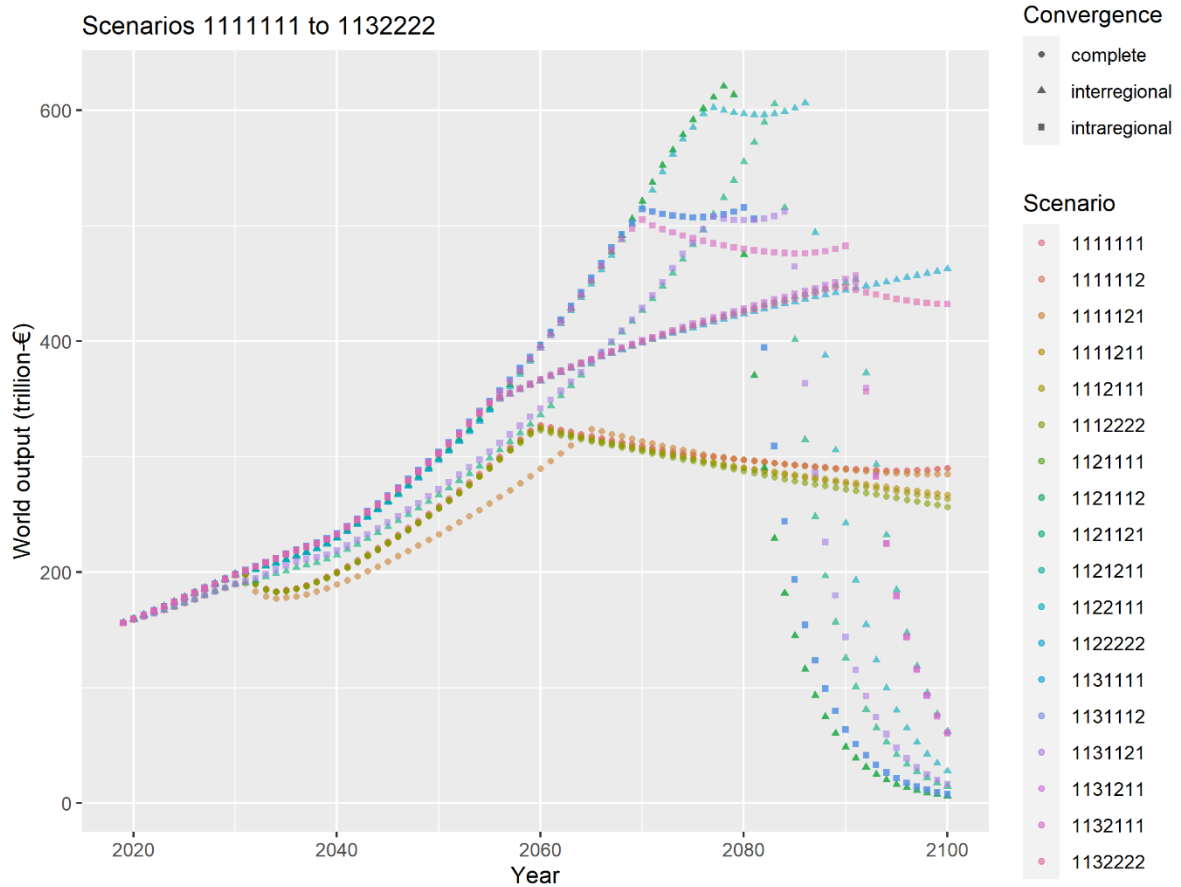


Scenarios 3111111 to 3132222

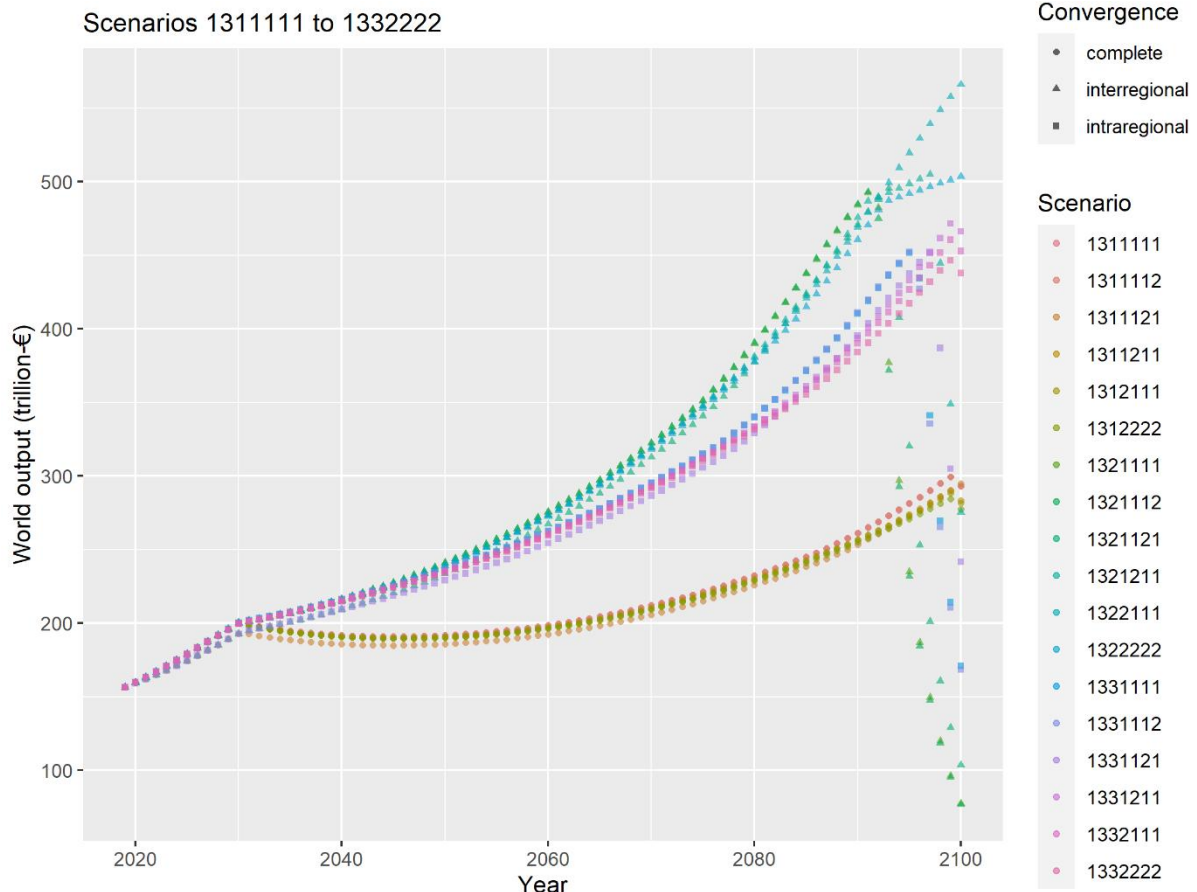




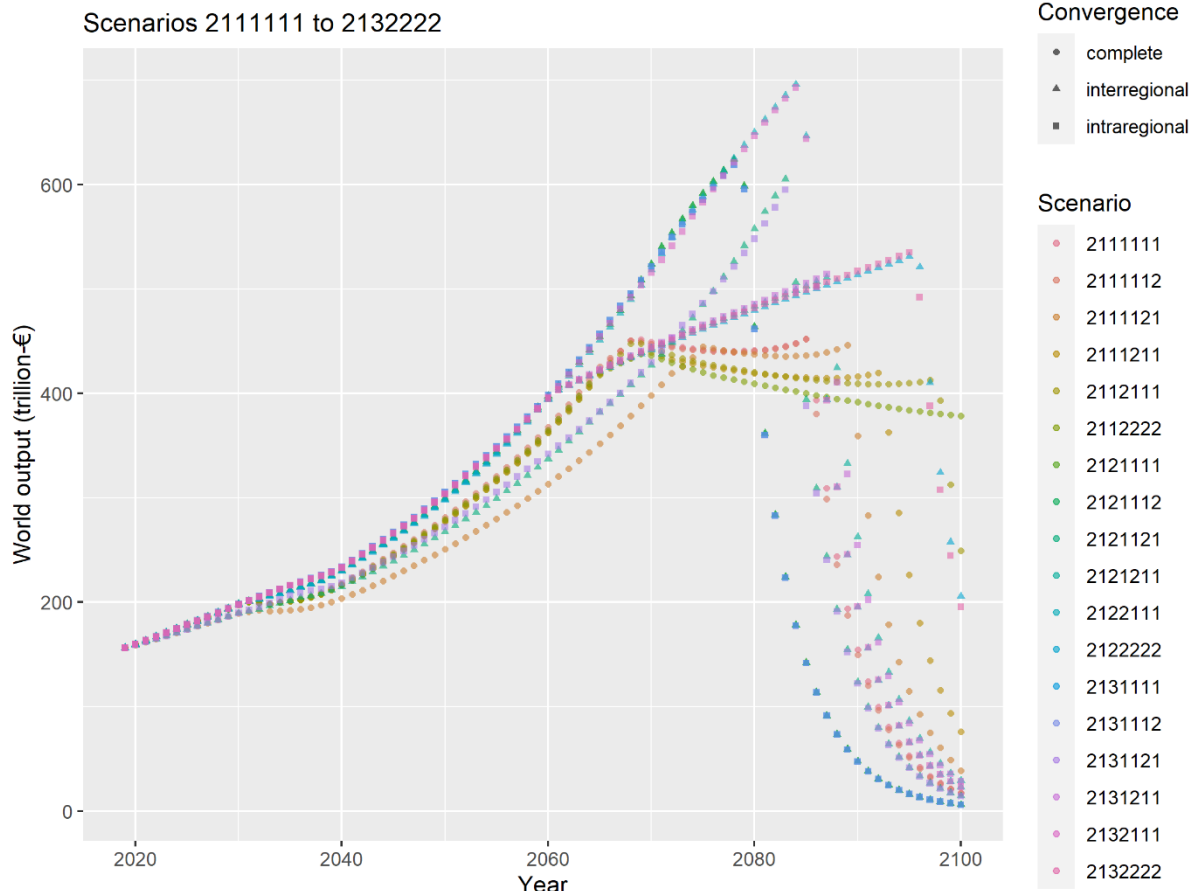
S.3.2. Output



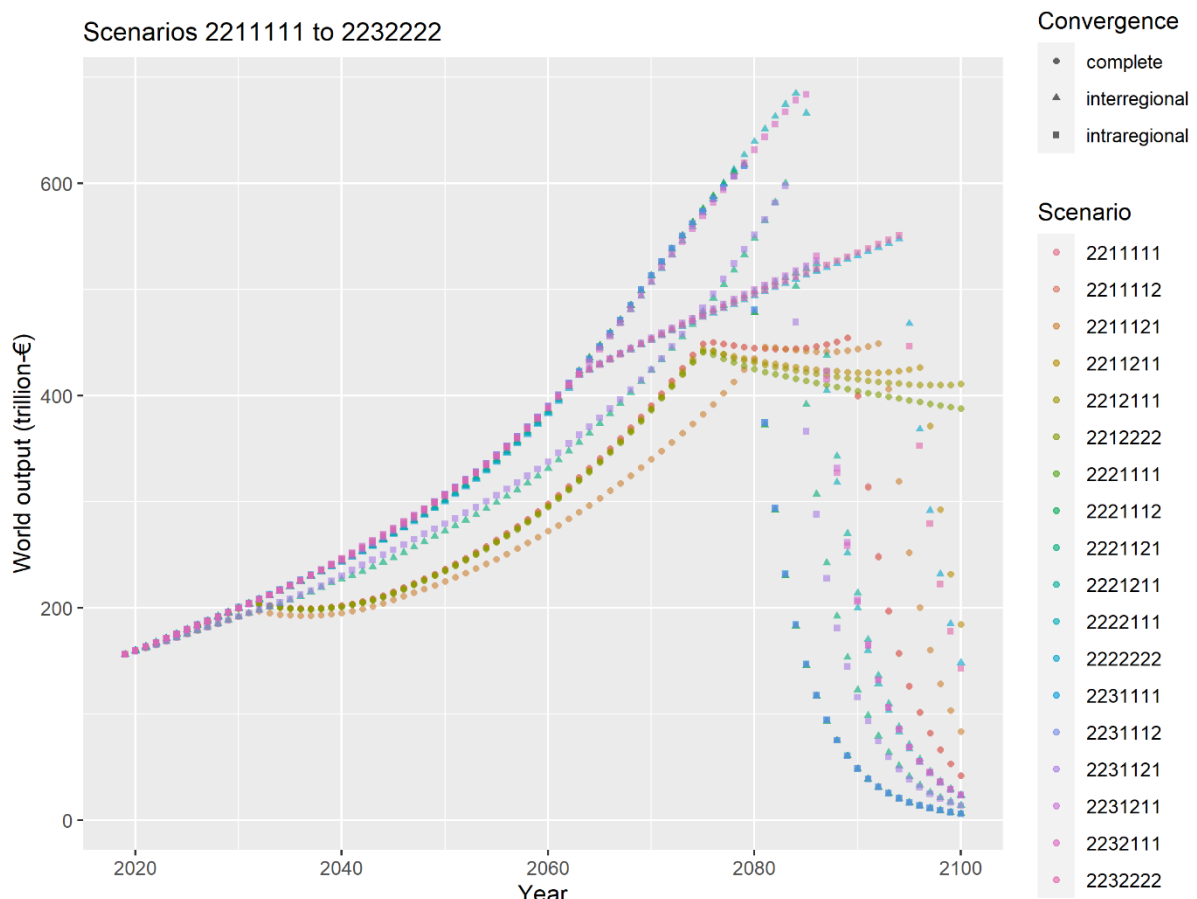
Scenarios 1311111 to 1332222



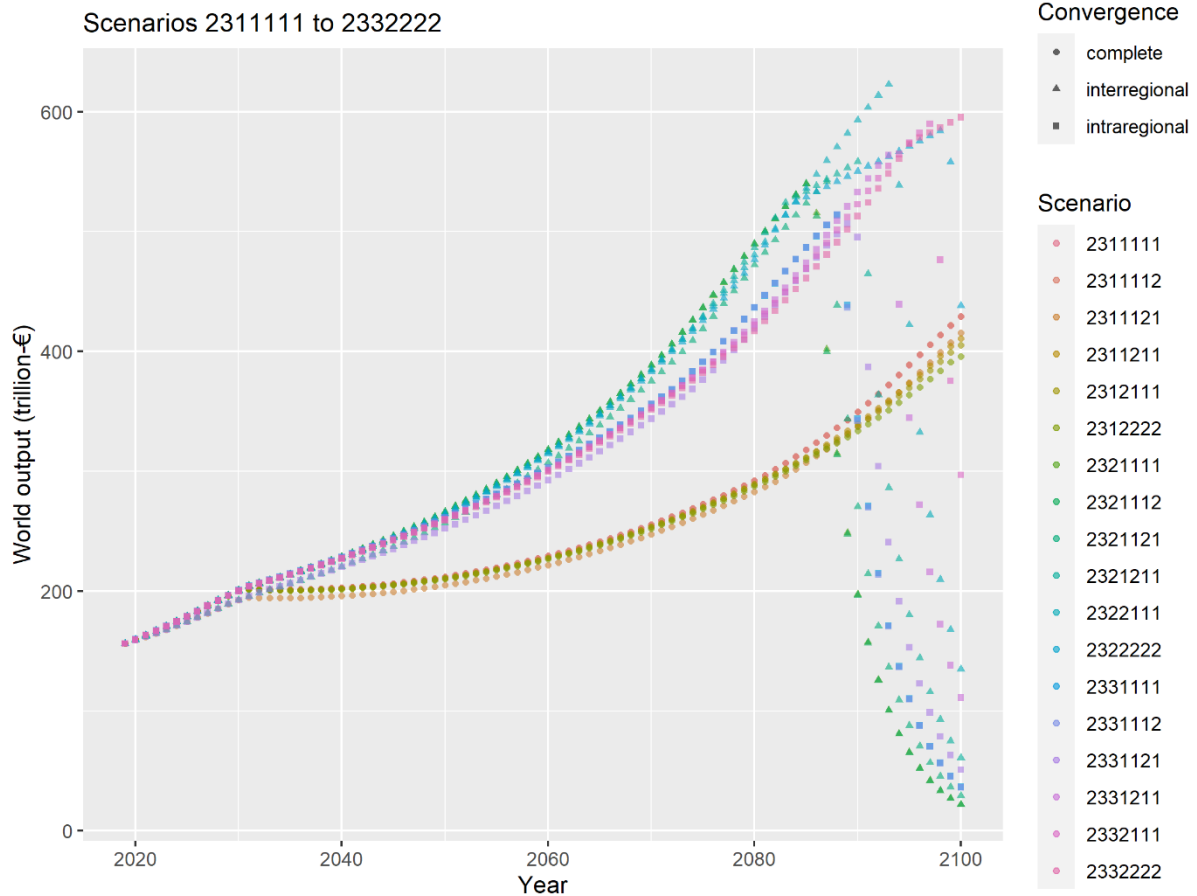
Scenarios 2111111 to 2132222



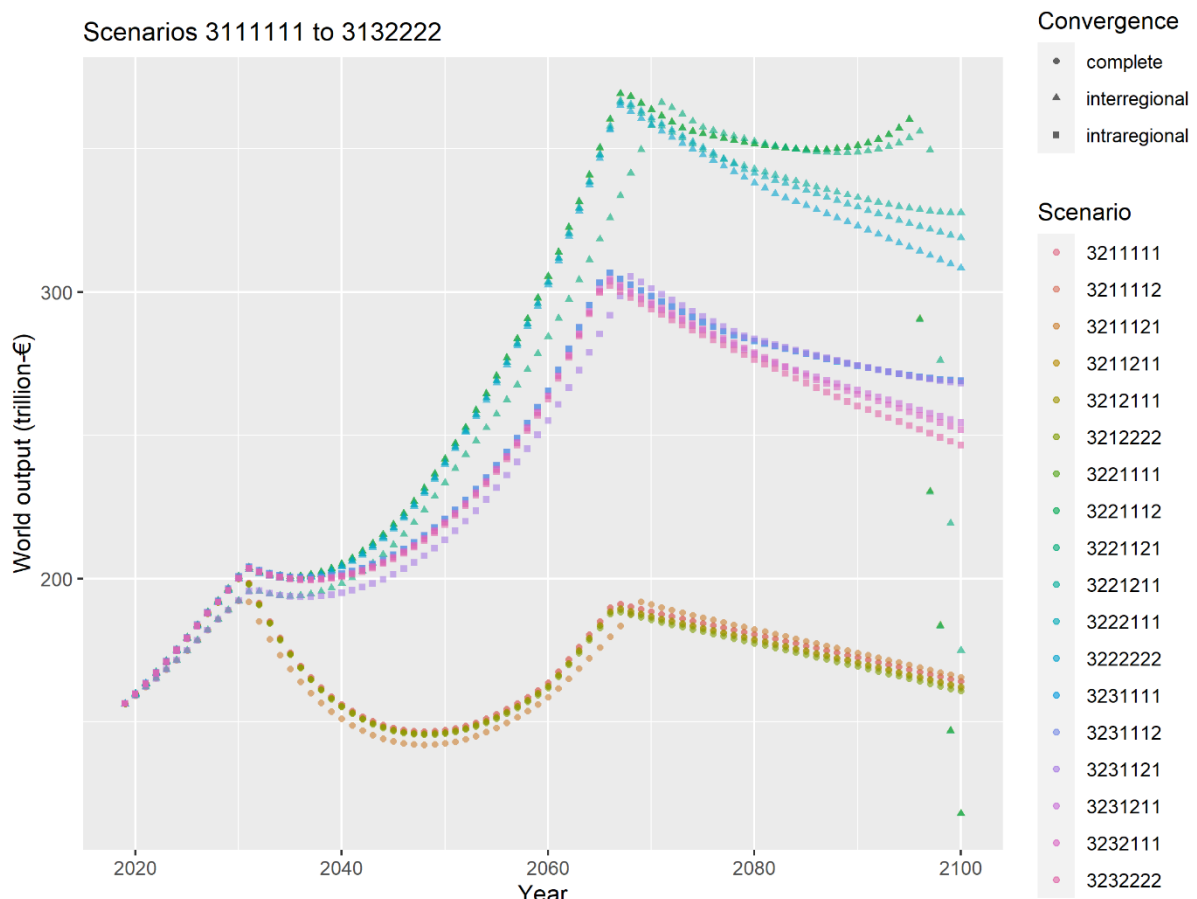
Scenarios 2211111 to 2232222



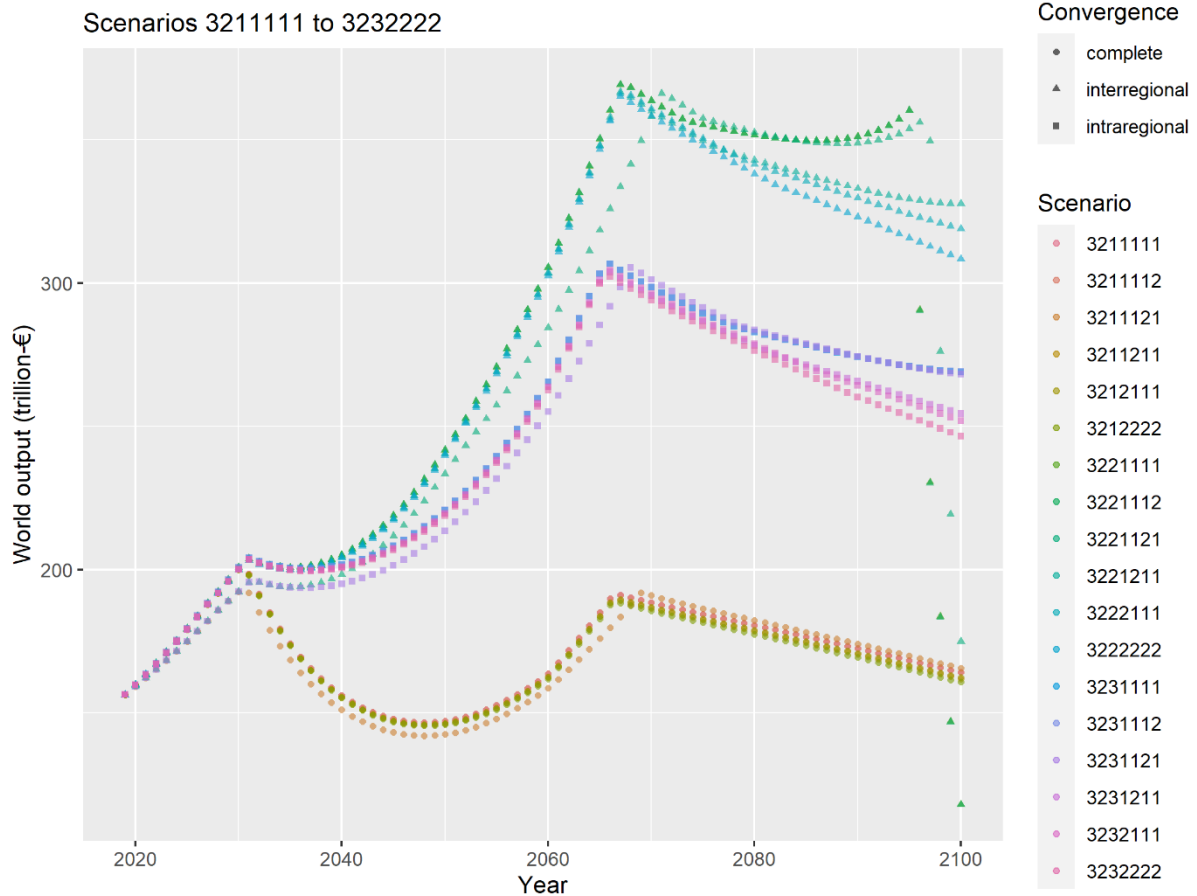
Scenarios 2311111 to 2332222



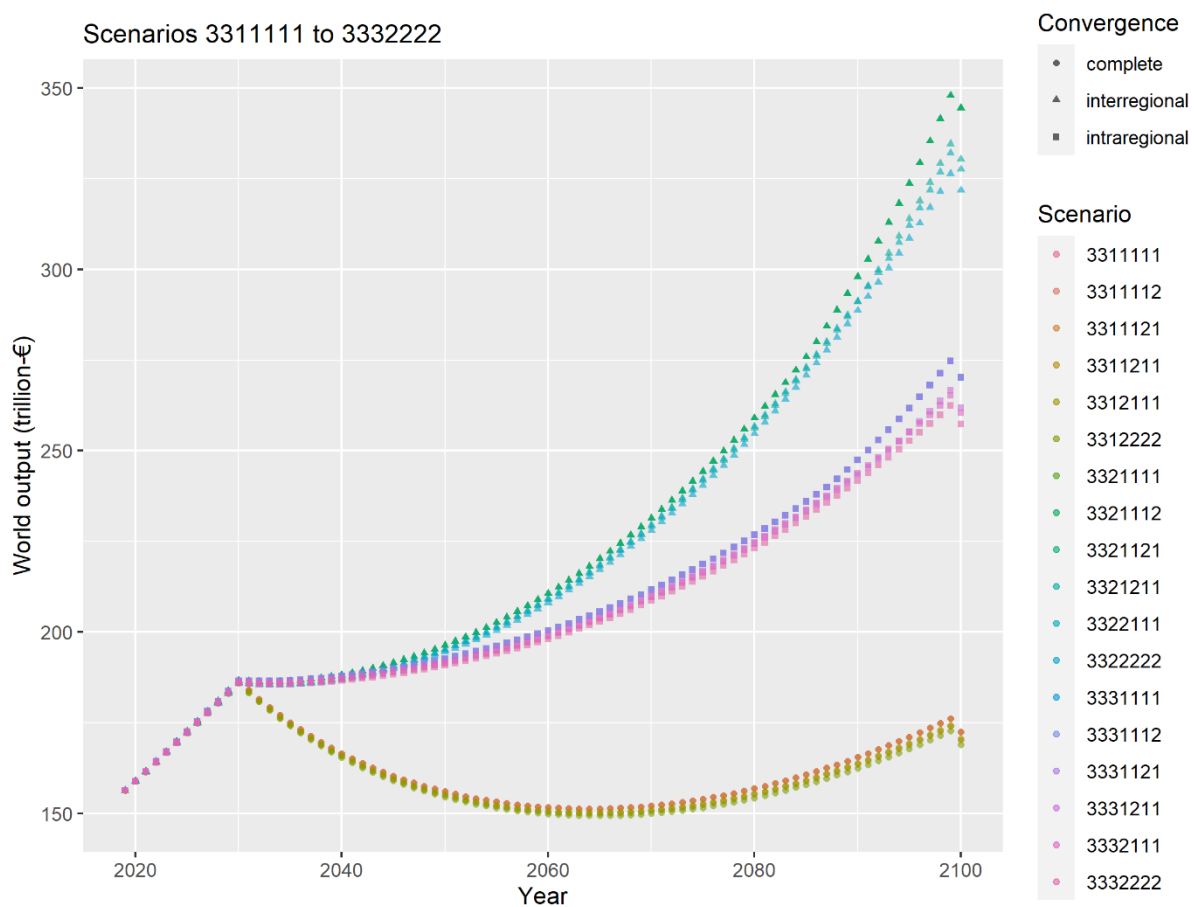
Scenarios 3111111 to 3132222



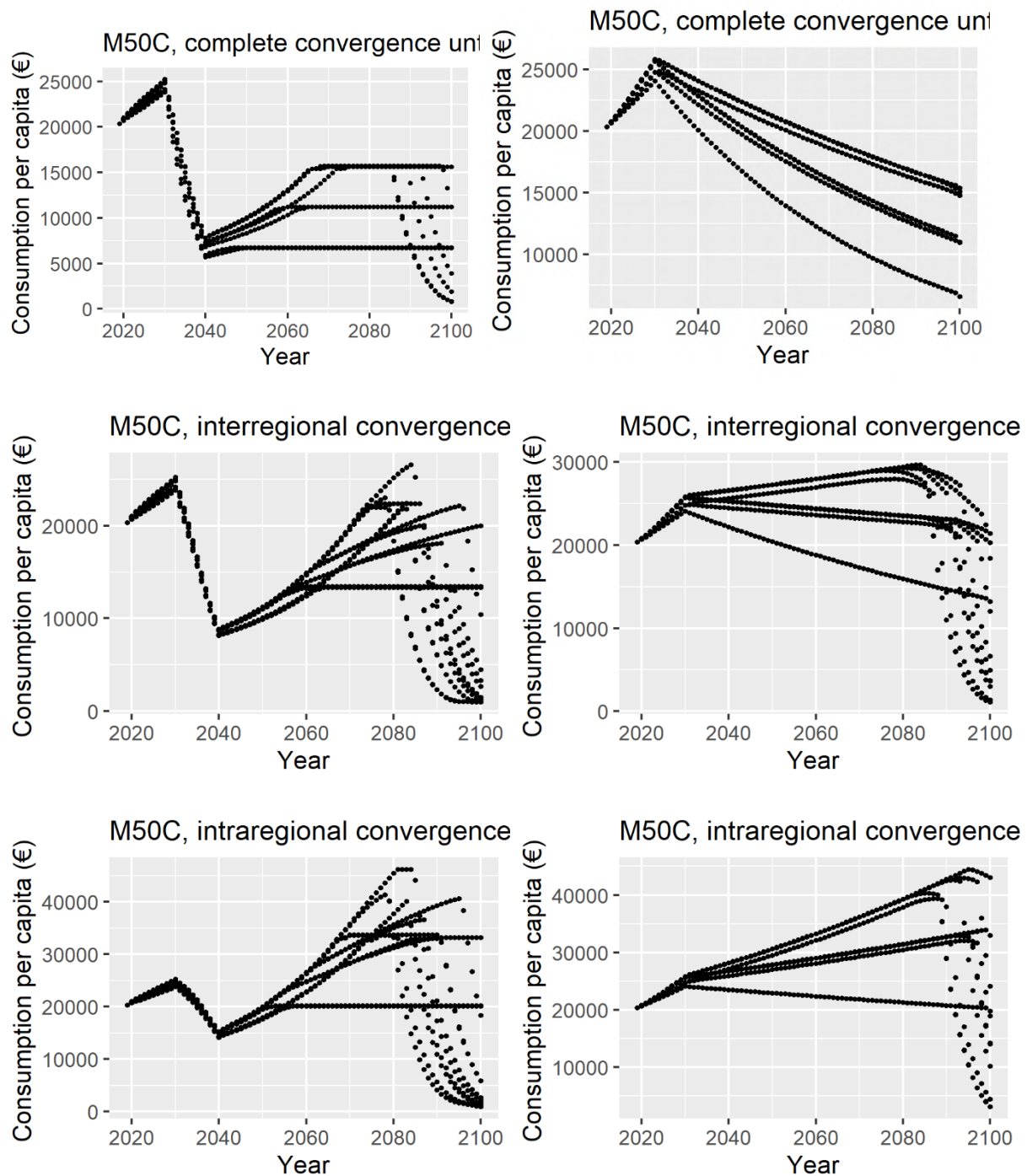
Scenarios 3211111 to 3232222



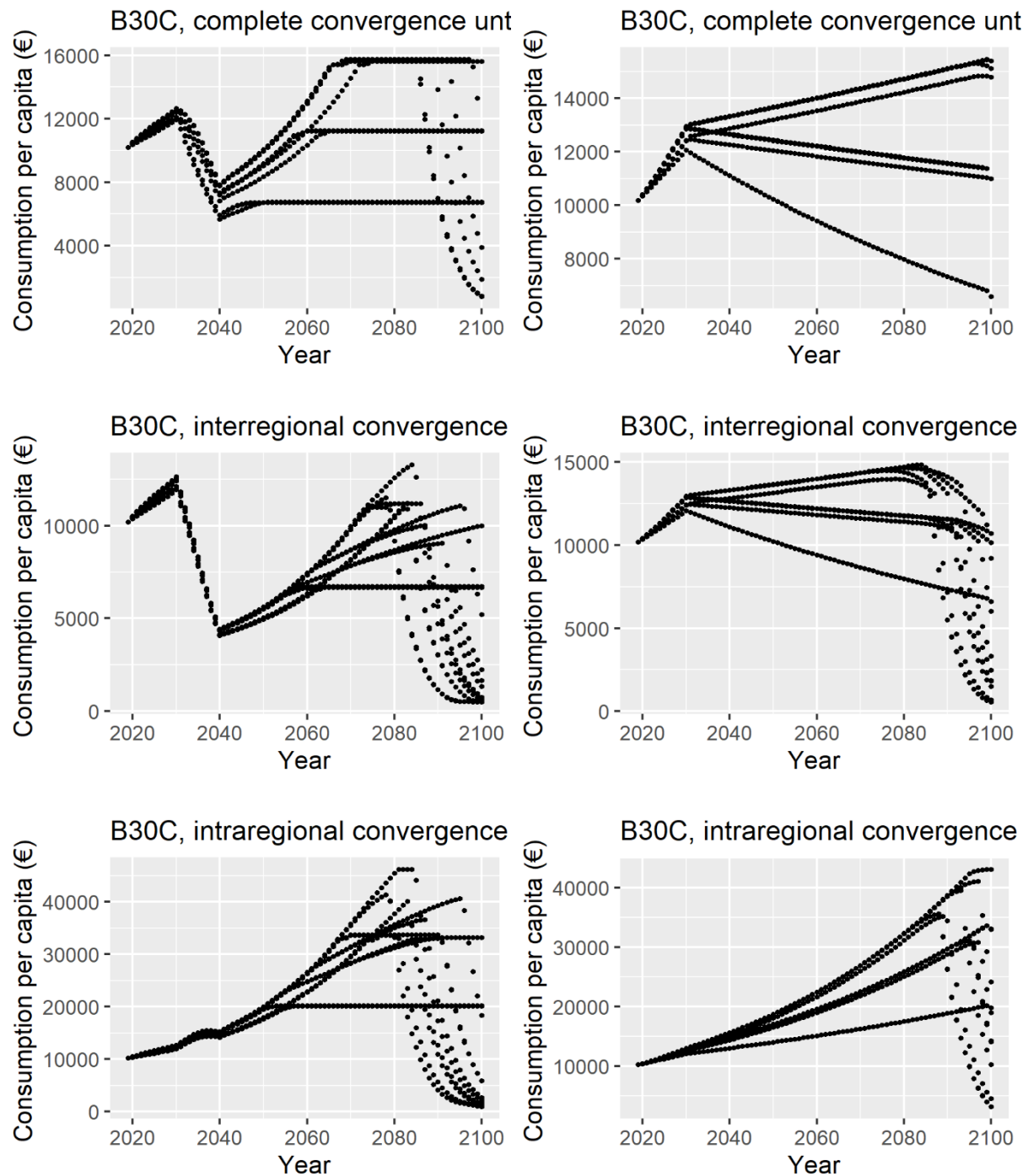
Scenarios 3311111 to 3332222



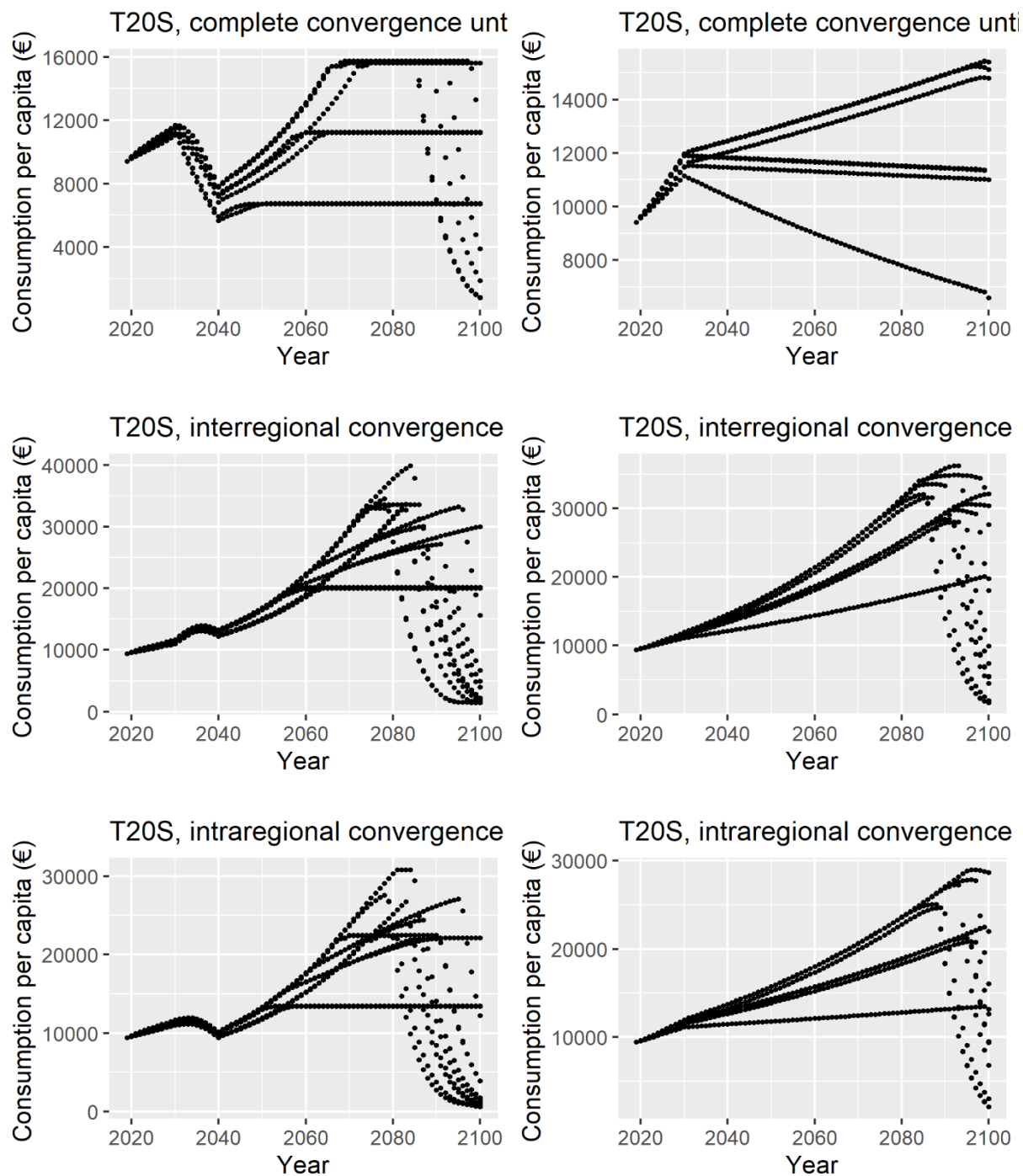
S.3.3. Consumption M50C



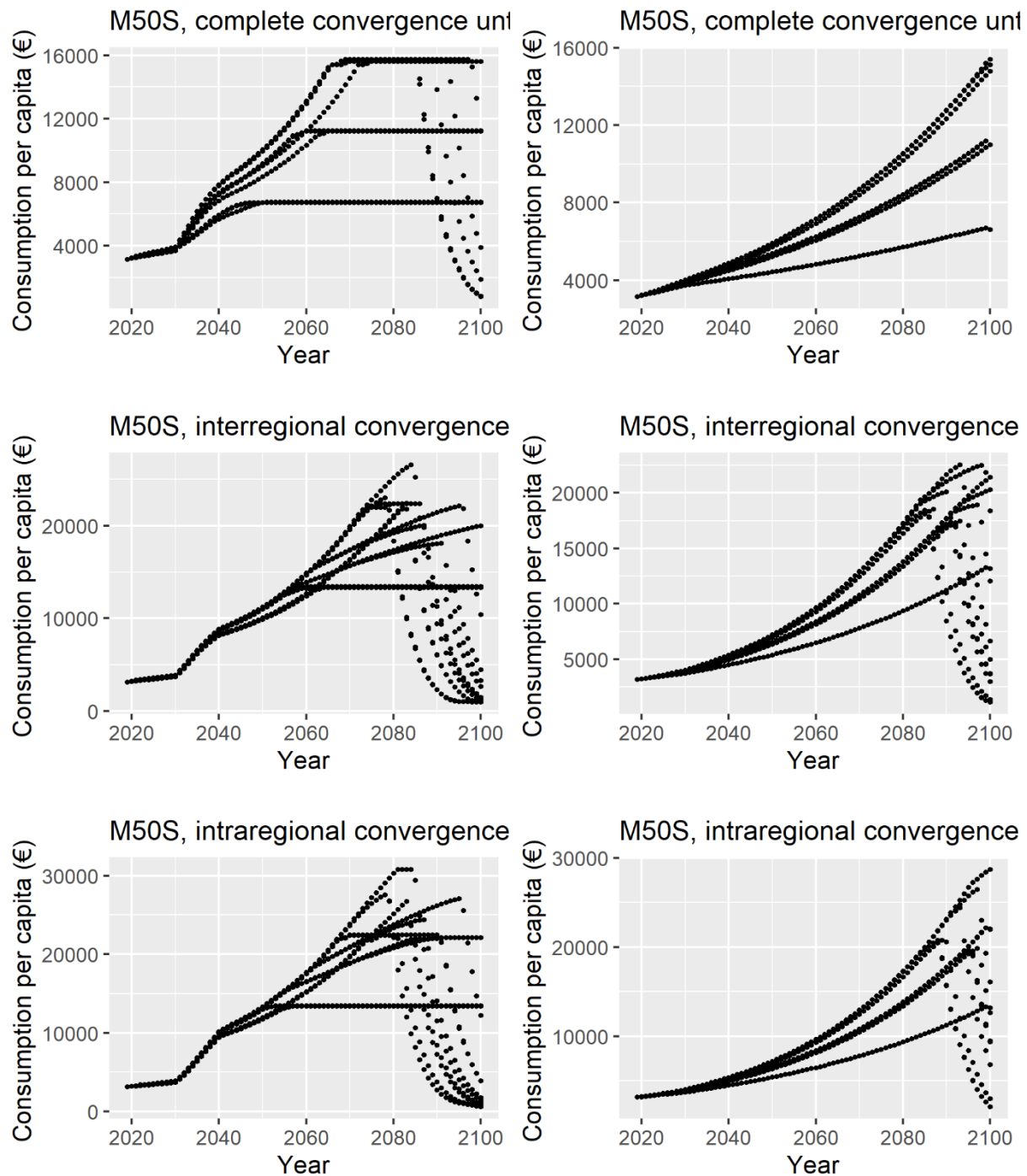
S.3.4. Consumption B30C



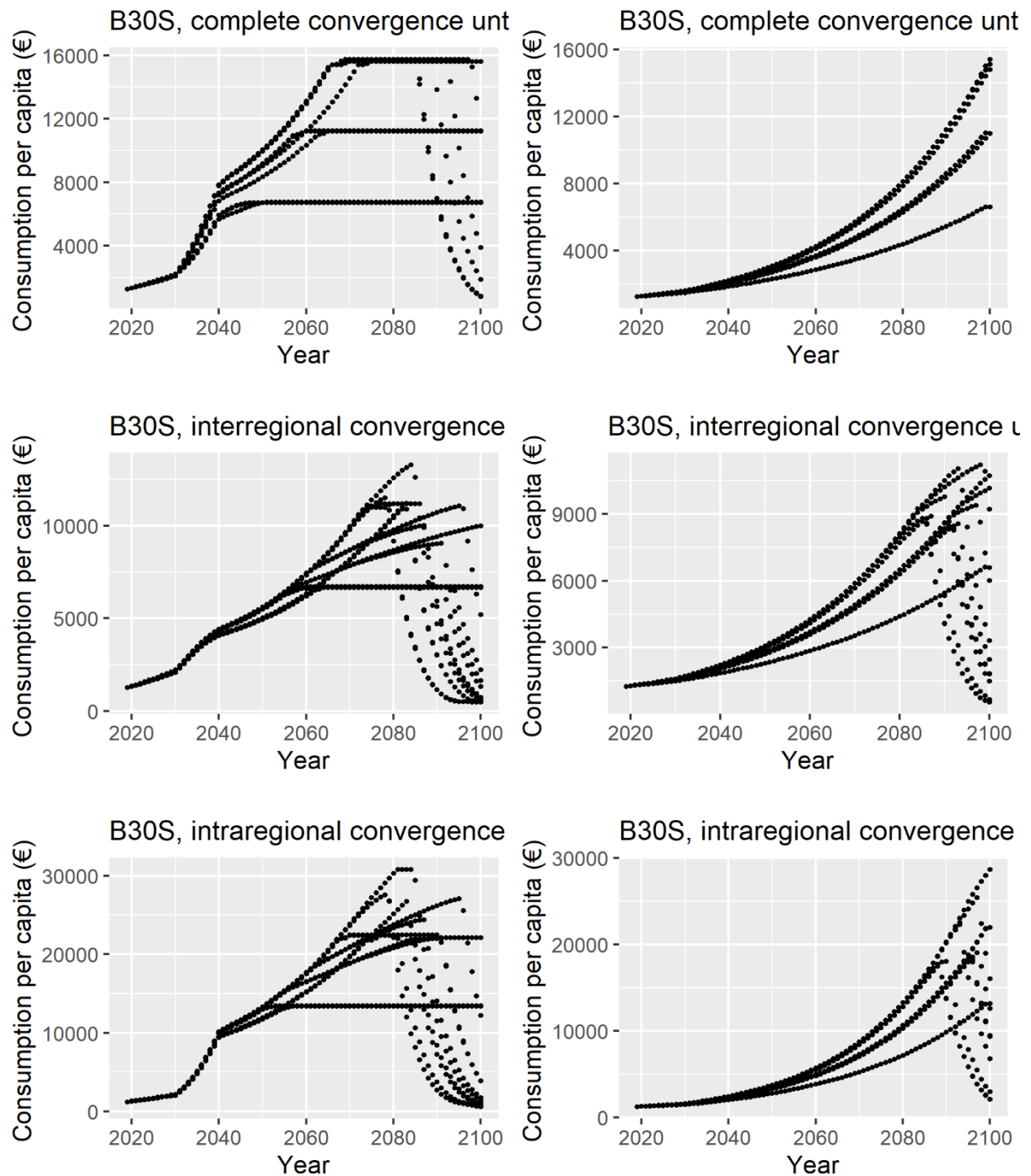
S.3.5. Consumption T20S



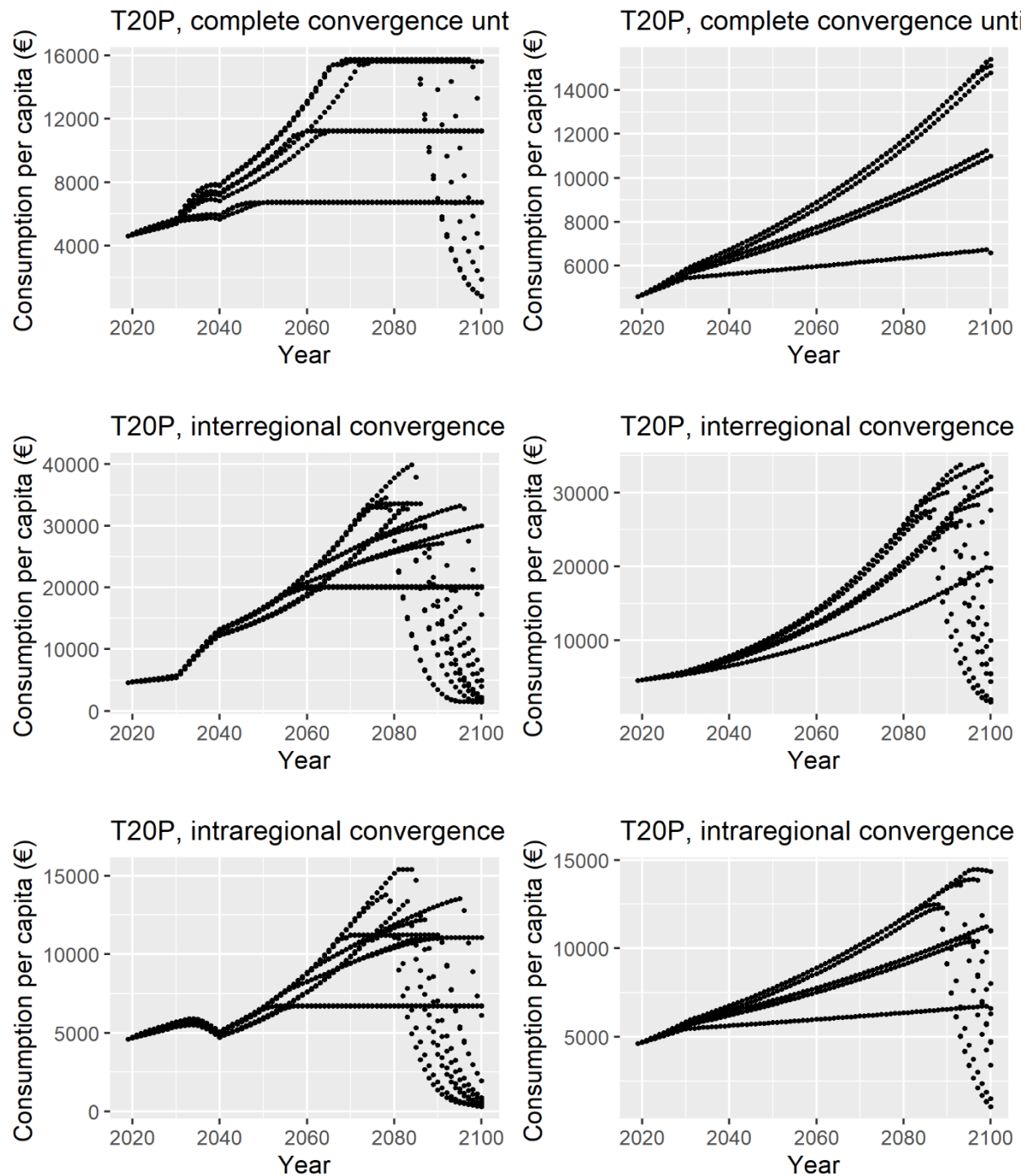
S.3.6. Consumption M50S



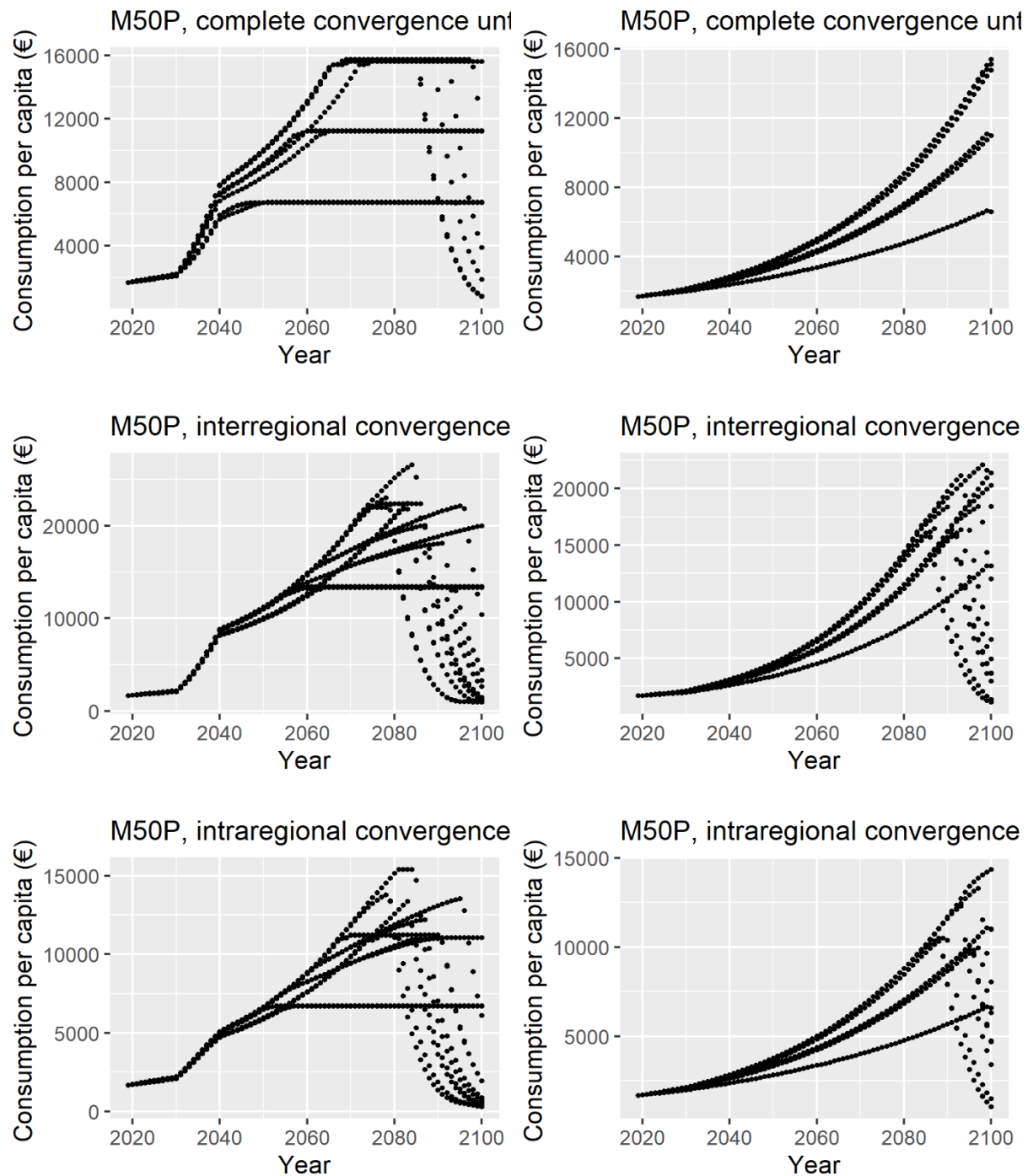
S.3.7. Consumption B30S



S.3.8. Consumption T20P



S.3.9. Consumption M50P



Degrowth vs. Green Growth: Multidimensional Impacts on Economy, Society, and Planetary Boundaries

Abstract

We employ a quantitative system dynamics model to examine the evolution of key economic, social, and biophysical variables under two contrasting development pathways: green growth (GG) and degrowth (DG). To enable a multidimensional assessment of environmental outcomes, we develop a set of planetary boundary indices that capture the degree of transgression of critical Earth system thresholds. Scenario simulations reveal broadly similar trajectories for GG and DG until the middle of the century, after which key variables diverge markedly. Results indicate that absolute decoupling of fossil energy consumption from economic growth in the GG scenario is insufficient to halt or reverse the deterioration of most planetary boundary variables. Instead, rising consumption levels across all social classes and world regions drive the Earth system irreversibly into a high-risk zone. In contrast, the DG scenario yields lower overall economic output but substantially improves the living standards of poorer populations and those in less developed regions, while the transgression of planetary boundaries is slowed or even reversed. Overall, the DG scenario outperforms GG in 10 out of 11 planetary boundary indices. Nevertheless, even under ambitious technological and social DG policies, the Earth system does not return to a safe operating space within the simulation period.

Keywords

Degrowth; Post-growth; Green growth; Earth system boundaries; convergence; integrated assessment models

1. Introduction

Despite a modest decoupling between global GDP and the adverse impacts of economic growth on planetary boundaries between 1995 and 2019 (Vázquez et al., 2023), recent assessments indicate that six of the nine planetary boundaries have already been transgressed (Richardson et al., 2023). The ‘safe and just’ operating space—defined by Earth System Boundaries that minimize exposure to significant harm to humans—is considerably narrower, implying an even higher degree of transgression and associated risks (Rockström et al., 2023). Accordingly, sustainability science is tasked with identifying development pathways capable of meeting basic human needs for the entire world population without driving the Earth system beyond the planetary conditions delineating the safe operating space (O’Neill et al., 2018). Although climate change occupies a central position in the planetary boundaries framework, the latter cannot be reduced to the former but rather opens up the possibility to study interactions between different planetary boundaries, such as feedback dynamics between land system change and climate change (Drücke et al., 2024). Moreover, global environmental change is increasingly understood as a co-evolutionary process between human societies and the biogeophysical Earth system, rather than a unidirectional causal relationship driven solely by anthropogenic pressures. This perspective can be represented through ‘World–Earth’ models that integrate socio-economic dynamics alongside a biophysical systems (Donges et al., 2019).

Within debates on sustainable future development pathways, proponents of ‘degrowth’ and ‘post-growth’ contend that reducing consumption in the Global North, coupled with reconfiguring development trajectories in the Global South away from accumulation by dispossession, is essential to achieving human well-being within a safe operating space for humanity (Kallis et al., 2025; Kronenberg et al., 2024; Sultana, 2023). However, model-based evidence demonstrating the potential of global degrowth or post-growth scenarios to reduce planetary boundary transgressions remains limited. Several factors contribute to this gap. First, quantitative modeling studies that simulate future impacts of global development pathways on Earth system boundaries often incorporate only a subset of planetary boundaries (e.g. Allen et al., 2021; Mathias et al., 2017) or operationalize them in abstract, non-biophysical terms (Gries & Naudé, 2025). Second, those studies integrating a high number of planetary boundaries either do not focus on the question of economic growth (Algunaibet et al., 2019; Engström et al., 2020) or explore different forms of green growth scenarios characterized by continuous GDP expansion (Van Vuuren et al., 2025). Finally, modeling studies associated with the degrowth or post-growth discourse tend to be conceptual or limited to the climate–economy nexus, thereby neglecting other planetary boundaries (Lauer et al., 2025). The absence of degrowth scenarios in classical Integrated Assessment Models (IAMs) can be attributed to a pro-growth bias within the IAM community, embedded in both modeling tools and modeling practice (Cointe & Pottier, 2023). Although there is no *ex ante* impossibility of simulating degrowth trajectories within IAMs (Kikstra et al., 2024), prevailing modeling conventions often constrain their capacity to represent post-growth futures (Edwards et al., 2025).

In this study, we address these gaps through a multidimensional quantitative assessment of global ‘green growth’ and ‘degrowth’ futures, evaluating their social, economic, and environmental implications. To this end, we integrate planetary boundaries into a system-dynamics-based IAM of medium complexity capable of representing non-linear economic trajectories and convergence dynamics among different social classes and world regions. By simulating both scenarios within a single modeling framework, this study constitutes the first

systematic comparison of the potential implications of degrowth and green-growth pathways for the transgression of multiple planetary boundaries.

2. Methods

2.1. Model overview

We use MORDRED 1.1 (Model Of Resource Distribution and Resilient Economic Development) to parametrize and run the scenarios. MORDRED is a data-based system dynamic model documented in Lauer & Llases (2025). For brevity, this section summarizes only the model's key characteristics and principal variables.

MORDRED comprises seven interrelated modules: population, economy, labor, energy, land, climate, and environmental stressors. The main data sources forming its quantitative basis are the environmentally and socially extended input-output (IO) tables from Exiobase3 (Stadler et al., 2018), consumption inequality estimates from the GCIP database (Lahoti et al., 2016), UN population data (UN DESA, 2019), climate and emissions data from the IPCC WGI (2021) and fossil resource estimates from BGR (2020). The model's main purpose is to enable data-informed scenario analyses that explore conceptual and theoretical questions rather than to provide probabilistic forecasts of key variables.

The economic module follows an input-output (IO) structure and includes all typical variables of IO models: of IO models: an A matrix, output at the sector level, final demand components (private consumption, public consumption, and gross fixed capital formation), and sectoral capital stocks. The model distinguishes 25 sectors, enabling users to analyze multiple energy-related industries (see Section 1 of the Supplementary Material). Total output is driven by exogenously defined growth rates for the poorest household type, as well as by consumption shares of households, governments, and investors that reflect either empirical data or scenario assumptions.

Economic production depends on labor, land, and energy inputs, which are derived from their respective modules. Production requires four land types—food (cropland and grassland), forest, land for energy generation and infrastructure, and ‘other land’ as defined by FAO. The remaining land types in the model include (non-economically used) primary forest, secondary forest and shrub. Non-economic land categories include primary forest, secondary forest, and shrubland. Economic activity is also linked to environmental stressors, including greenhouse gas emissions, which are computed in the environmental stressors module and fed into the climate module. Production may be limited by input scarcity or by adverse climate impacts on economic structure; however, this latter feedback is deactivated in the simulations to reduce model complexity.

The global population, which supplies labor and consumes most economic output, is divided into three world regions and three household types (“classes”) per region. The *center* includes high-income countries, the *semiperiphery* upper-middle-income countries, and the *periphery* lower-middle- and low-income countries. In each region, the richest 20% constitute the T20 (Top20) class, the middle 50% the M50 class, and the poorest 30% the B30 (Bottom30) class. Fertility and mortality rates depend on class-specific consumption trajectories and evolve dynamically throughout the simulation period.

2.2. Planetary Boundary Indices

To conduct the scenario analysis, we extended MORDRED 1.1 with a Planetary Boundary Indices (PBI) module. This module calculates several PBIs based on Steffen et al. (2015), Richardson et al. (2023) and model output variables. Each PBI operationalizes a planetary boundary within the limits of what the model can represent. All indices are normalized to a reference value of 100 at the simulation's starting year. Deterioration in a boundary variable is reflected as an increase in its index.

Except for aerosol loading and green freshwater, all PBIs include lower and upper threshold values. The lower threshold corresponds to the planetary boundary, while the upper threshold represents the upper end of the 'zone of increasing risk' defined by Richardson et al. (2023). For 'novel entities', we set the lower threshold to 1 and the upper to 95, given that this boundary is already considered transgressed. The boundaries for green freshwater change and atmospheric aerosol loading cannot be represented in MORDRED, as their biophysical variables are sub-global, whereas MORDRED operates at a global scale. For blue freshwater, the thresholds are derived from the uncertainty range for global blue water use reported in Steffen et al. (2015).

Values above the lower threshold indicate entry into a zone of increasing risk or zone of uncertainty while values above the upper threshold correspond to a zone of high risk, where interglacial Earth system conditions are confidently exceeded. The greater the transgression, the higher the probability of abrupt and potentially catastrophic changes in the Earth system or regional subsystems (Richardson et al., 2023; Rockström et al., 2009). Values below the lower threshold indicate a safe operating zone. Notably, the simulations begin with several PBIs already in the high-risk zone.

The first two PBIs are related to the climate change boundary and are calculated with two model variables: atmospheric CO₂ concentration (ppm) and effective radiative forcing (W/m²):

$$CO_2 \text{ concentration index} = \frac{\text{atmospheric CO}_2 \text{ concentration}_t}{\text{atmospheric CO}_2 \text{ concentration}_{t_0}} * 100 \quad (1)$$

$$\text{Radiative forcing index} = \frac{ERF_t}{ERF_{t_0}} * 100 \quad (2)$$

The PBI for ocean acidification is calculated with the aragonite saturation variable in the model.

$$\text{Ocean acidification index} = 200 - \left(\frac{\text{aragonite saturation}_t}{\text{aragonite saturation}_{t_0}} * 100 \right) \quad (3)$$

The PBI for biosphere integrity is calculated based on the different land use types in MORDRED and assumptions about the intensity with which the different land uses appropriate the Net Primary Production (NPP) of the biosphere. Infrastructure is assumed to have the highest appropriation (destruction) of NPP whereas HANPP (Human Appropriation of NPP) is assumed to be zero in the case of land types that are not subject to economic use. The estimated HANPP for the initial year of the simulation is 0.3, in line with Richardson et al. (2023).

$$HANPP_{Mordred} = \frac{\sum_{land \ type=1}^9 \alpha_{land \ type} * size_{land \ type}}{\sum_{land \ type=1}^9 = size_{land \ type}} \quad (4)$$

land type ∈ {infrastructure, energy, food (high intensity), food (low intensity), productive forest, other land, primary forest, secondary forest, shrub}

$$1 > \alpha_1 > \alpha_2 > \alpha_3 > \alpha_4 > \alpha_5 > \alpha_6 > \alpha_{7,8,9} \geq 0$$

$$\text{Biosphere integrity index} = \frac{\text{HANPP}_{\text{Mordred}_t}}{\text{HANPP}_{\text{Mordred}_{t_0}}} * 100 \quad (5)$$

The PBI for land-system change is calculated with changes in forest land types in the model. The forest cover in the initial year of the simulation is derived by aggregating primary forest, secondary forest and productive, i.e. economically used forest, and is assumed to constitute 60% of the original forest cover, following Richardson et al. (2023).

$$\begin{aligned} & \text{Land system change index} \\ &= 200 - \frac{(\text{land type}_4 + \text{land type}_6 + \text{land type}_7)_t}{(\text{land type}_4 + \text{land type}_6 + \text{land type}_7)_{t_0}} * 100 \end{aligned} \quad (6)$$

The PBIs for biogeochemical flows are approximated with two model variables. Industrial N fixation is approximated as a share of the model variable *material extraction of chemical and fertilizer minerals* and in the initial moment of the simulation reflects the current value given in Richardson et al. (2023). P flows from fertilizers to erodible soils are approximated by the model variable *phosphorus soil pollution of agriculture*. The initial value for the variable is based on estimates of P flows to soils by Lu & Tian (2017).

$$\text{Industrial N fixation}_{2019} = \alpha * \text{Chemical and fertilizer minerals}_{2019} \quad (7)$$

$$P \text{ soil pollution}_{t_0} = P_{2013} + 6 * \frac{P_{2013} - P_{1961}}{1961 - 2013} \quad (8)$$

$$\text{Biogeochemical flows index}_N = \frac{\text{Chemical and fertilizer minerals}_t}{\text{Chemical and fertilizer minerals}_{t_0}} * 100 \quad (9)$$

$$\text{Biogeochemical flows index}_P = \frac{P \text{ soil pollution}_t}{P \text{ soil pollution}_{t_0}} * 100 \quad (10)$$

The lower (l) and upper (u) threshold values for the seven indices were calculated on the basis of the lower and upper thresholds given by Richardson et al. (2023).

$$i \in \{l, u\} \quad (11)$$

$$\text{Threshold}_{i_{CO2 \text{ concentration}}} = \frac{\text{threshold value}_i}{\text{atmospheric CO2 concentration}_{t_0}} * 100$$

$$\text{Threshold}_{i_{forcing}} = \frac{\text{threshold value}_i}{ERF_{t_0}} * 100 \quad (12)$$

$$\text{Thresholds}_{i_{ocean acidification}} = 200 - \left(\frac{\text{threshold value}_i}{\text{aragonite saturation}_{t_0}} \right) * 100 \quad (13)$$

$$\text{Thresholds}_{i_{functional integrity}} = \left(\frac{\text{threshold value}_i}{\text{HANPP}_{\text{MORDRED}_{t_0}} * 100} \right) * 100 \quad (14)$$

$$\text{Thresholds}_{i_{land system change}} = 200 - \left(\frac{\text{threshold value}_i}{60} \right) * 100 \quad (15)$$

$$\text{Thresholds}_{i_N} = \frac{\text{threshold value}_i}{\text{Industrial N fixation}_{t_0}} * 100 \quad (16)$$

$$Thresholds_{i_P} = \frac{\text{threshold value}_i}{P \text{ flows to soils}_{t_0}} * 100 \quad (17)$$

MORDRED does not contain information on the percentage of synthetic chemicals that are released into the environment without safety testing. However, we assume that the quantity of novel entities is proportional to the production of the chemical sector. Thus, the PBI for novel entities is calculated with the output of the chemical industry. Similarly, the aerosol loading index is approximated using PM2.5, PM10, and NH3 pollution, as the model lacks data on interhemispheric aerosol optical depth differences.

$$\text{Novel entities index} = \frac{x_{9t}}{x_{9t_0}} * 100 \quad (18)$$

$$\text{Aerosol loading index} = \frac{PM_{2.5t} + PM_{10t} + NH3_t}{PM_{2.5t_0} + PM_{10t_0} + NH3_{t_0}} * 100 \quad (19)$$

Because MORDRED does not explicitly model human-induced disturbances of blue or green water flows, freshwater use PBIs are approximated through household and industrial blue water consumption and green water use in the food sector. For blue water, threshold values are based on the uncertainty range in Steffen et al. (2015). The Exiobase3 data yield an initial blue water estimate roughly 30% lower than Steffen et al.'s value, which may slightly overestimate the corresponding thresholds.

$$\text{Blue water index} \quad (20)$$

$$= \frac{(consumption_{blue_{hh}} + consumption_{blue_{industries}})_t}{(consumption_{blue_{hh}} + consumption_{blue_{industries}})_{t_0}} * 100$$

$$\text{Green water index} = \frac{\text{water consumption}_{green_t}}{\text{water consumption}_{green_{t_0}}} * 100 \quad (21)$$

$$Thresholds_{i_{blue\ water}} = \frac{\text{threshold value}_i}{\text{total blue water consumption}_{t_0}} * 100 \quad (22)$$

The stratospheric ozone depletion index remains constant, as ozone changes are not modeled in MORDRED. Threshold values follow Richardson et al. (2023).

$$\text{Ozone depletion index} = 100 \quad (23)$$

$$Thresholds_{ozone_i} = 200 - \left(\frac{\text{threshold}_i}{284.6 \text{ DU}} \right) * 100 \quad (24)$$

Table 1 summarizes the operationalization of the planetary boundaries in MORDRED and the corresponding lower and upper threshold values.

Planetary boundary	approximation	lower threshold	upper threshold
--------------------	---------------	-----------------	-----------------

Climate change	atmospheric CO ₂ concentration	85	110
	effective radiative forcing	37	56
Ocean acidification	aragonite saturation	93	100
Biosphere integrity	land use intensity and shares of different land types	33	66
Land-system change	% forest cover in original forest cover	75	110
Biogeochemical flows	fertilizer extraction	33	43
	P flows to soils	33	59
Novel entities	output chemical industry	1	95
Aerosol loading	industrial NH ₃ , PM _{2.5} and PM ₁₀ emissions	na	na
Blue freshwater change	household and industry blue water consumption	223	335
Green freshwater change	green water consumption	na	na
Stratospheric ozone depletion	constant value	103	108

Table 1: Overview of planetary boundary representation in MORDRED.

2.3. Scenario design

We construct two stylized scenarios reflecting distinct economic paradigms: Green Growth (GG) and Degrowth (DG). Both represent idealized transitions characterized by ambitious environmental policy assumptions. Simulations run from 2019 to 2100. Unlike other green-growth or post-growth scenario exercises (Nieto et al., 2020; Van Vuuren et al., 2017), we do not impose scenario-specific exogenous demographic assumptions, as mortality and fertility rates are endogenized in MORDRED. Moreover, unlike the International Futures model used by Moyer (2023) to simulate degrowth trajectories, demographic parameters in MORDRED depend primarily on consumption per capita rather than education or GDP per capita.

The GG scenario represents a continuation of historical development trends combined with strong green-technology deployment for global decarbonization. Economic output, labor productivity, and land productivity increase continuously throughout the century. Consumption inequality declines moderately, while all social classes and world regions experience rising consumption levels. The electricity mix becomes increasingly green, with rapid electrification and a major expansion of renewable generation. Fossil energy is progressively replaced by modern bioenergy. Agricultural intensification increases blue water use and decreases green water use.

The DG scenario entails a radical shift in global development patterns. Per capita household consumption levels converge by 2035 toward a common level of approximately €9,000 per person per year. By 2100, electricity generation relies entirely on renewable sources, and economic electrification expands—though less than in the GG scenario. As in the GG scenario, half of fossil inputs are replaced by biomass energy. Agriculture transitions from conventional to organic production, and a fully plant-based global diet is adopted. Despite this shift, land productivity continues to increase, partly due to a higher share of irrigated agriculture and reduced rain-fed production. Labor productivity also rises, though at a slower rate than under the GG scenario.

Table 2 summarizes key changes in the GG and the DG scenario while additional details on the parametrization process is provided in Section 2 of the Supplementary Material.

	GG	DG
Δ per capita consumption center	++	--
Δ per capita consumption semiperiphery	+++	+
Δ per capita consumption periphery	+++	++
Δ electrification	++	+
Δ share of renewables in electricity mix	+++	+++
Δ ratio bioenergy to fossil energy	+++	+++
Δ blue water intensity (industries)	+	+
Δ blue water intensity (households)	0	-
Δ green water intensity (industries)	-	-
Δ N2O and CH4 emission intensities	0	-- (organic agriculture + plant-based diet)
Δ N&P pollution intensity of agriculture	0	-- (organic agriculture)
Δ Labor productivity	++	+
Δ Land intensity	---	--- - (plant-based diet) + (organic agriculture)

Table 2: Key changes in the GG and DG scenario.

3. Results

In the following, we present the main results of the scenario simulations, covering the evolution of macroeconomic, social and biophysical variables.

3.1. Macroeconomic developments

Global world output follows a comparable trajectory in both scenarios until the mid-2050s, although output grows slightly slower in the DG scenario. From 2060 onwards, growth in output accelerates in the GG scenario and at the end of the century is 3.9 times its initial value.

Conversely, in the DG scenario output peaks at a level 1.6 times the initial value in 2055 and afterwards declines continuously. Towards the end of the century, world output reaches a level comparable to 2040s, which is 27% above current output values. By 2100, output in the GG scenario is three times higher than in DG. Notably, downscaling consumption and production in richer regions does not reduce total output during the first 30 years; significant divergence between DG and GG only appears due to the continued application of DG policies throughout the century.

Total capital stock begins to differ between scenarios from the mid-2020s, accumulating faster in GG than in DG. By 2060, capital stock in GG is 1.35 times higher than in DG. In the DG scenario, total capital peaks later than output and remains nearly constant between 2060 and 2100. Compared to 2019, world capital stock doubles under DG and grows 6.5-fold under GG.

Total government spending (world public consumption) follows the same patterns as total output in both scenarios, with a continuous increase until the end of the century in the case of GG and a mid-century peak and subsequent slow decline in the case of DG. Until 2050, the difference in public consumption trajectories between DG and GG is even less pronounced than for the world output trajectories. In the DG scenario, between 2050 and 2070, world public consumption plateaus at 59% above its initial value while world output during the same time period first increases and then declines. By 2100, global public consumption in GG is 2.5 times higher than in DG.

Although global public consumption grows in both scenarios, regional trajectories diverge. In GG, consumption in the center grows slowly, plateauing between 2070 and 2090 before slightly declining. In the semiperiphery, it rises steadily, almost quadrupling by 2100. In the periphery, growth accelerates from 2040, increasing sevenfold by the end of the 21st century.

In DG, strong convergence until 2035 leads to an initial sharp drop in government consumption in the center—falling by 75% from initial levels within 15 years—followed by a brief recovery and then gradual decline. In the semiperiphery, consumption rises faster than in GG during the first three decades, equalizes around 2060, and then declines whereas it continues to grow in the GG scenario. The difference between DG and GG is even more pronounced for the public consumption of the periphery: by 2040, public consumption reaches €6.5 trillion in DG—2.5 times the GG level—and remains higher for five decades. This trend is only reversed from 2074 onwards, as a result of continued growth in the GG scenario and slow decline in the DG scenario. Nevertheless, at the end of the century, in the DG scenario, public consumption in the periphery is four times as high as in the center and slightly higher than in the semiperiphery.

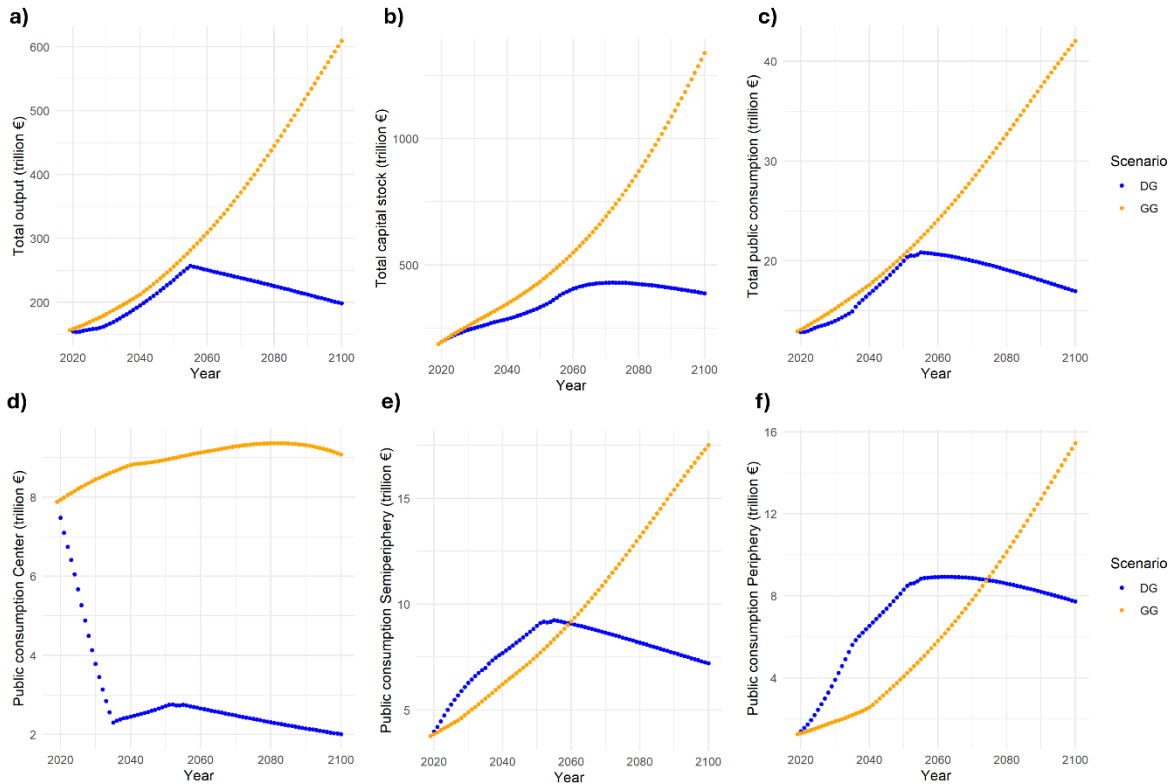


Figure 1: Development of a) total output; b) total capital stock; c) total public consumption; d) public consumption in high-income countries; e) public consumption in upper-middle income countries; f) public consumption in lower-middle and low-income countries in a Degrowth (blue) and a Green growth (orange) scenario.

3.2. Social developments

Demographic developments in the two scenarios start to diverge from 2030 onwards, with higher population growth in the GG than in the DG scenario, driven by underlying changes in household consumption. However, in both scenarios, world population peaks at a relatively low level and declines moderately until the end of the century. In the GG scenario, population peaks at 8.83 billion in 2060, returning to 2020 levels by 2100. In the DG scenario, population peaks

earlier, at 8.56 billion in 2050, reaching the initial size in the 2070s and ending at 7 billion, 10% below the initial value..

As a result of a continuous increase in labor productivity assumed in both scenarios labor demand across all sectors declines much faster than world population. Due to greater labor productivity increases assumed for the GG scenarios, the decline in labor input is stronger in the first half of the simulation. This dynamic is reversed in the second half of the simulation due to the combined effects of increasing labor productivity and decreasing or stabilizing consumption levels. In the final year of the simulation, labor demand is reduced by 70.7 % in the DG scenario, and by 42.5 % in the GG scenario compared to the initial value. However, while in a DG scenario this result can be assessed as positive as it allows for the sharing of work and an increase in leisure time (Bilancini & D'Alessandro, 2012; Houtbeckers, 2025; Vincent & Brandellero, 2023), in a GG scenario the decline in labor demand constitutes a threat to job security (D'Alessandro et al., 2020). Increasing employment in the GG scenario would mean a further increase in growth rates, followed, *ceteris paribus*, by even higher environmental impacts. For the service sector, which is the greatest sector in MORDRED, in the GG scenario the demand for workers declines fast during the first decade of the simulation, stays constant during the following three decades and then starts to decline again at an accelerated rate. Conversely, in the DG scenario, after an initial fast decline, demand increases between 2030 and 2050, reaching almost 1.3 billion people in 2050 required to work in the service sector. However, after this peak demand starts to fall persistently until the end of the century. In 2100, in the GG scenario, 1.08 billion workers are projected to work in the service industry, compared to 1.25 billion in 2019, whereas in the DG scenario this number has dropped to 557 million workers. This finding suggests that in the DG scenario high labor productivity growth might be only required during the first three decades after which the scenario would also be feasible with constant or declining labor productivities that are below the current labor productivity rates in high-income countries.

The average consumption per capita in the global world economy follows a comparable trajectory in both scenarios until 2055. Thereafter, GG consumption continues to rise, while DG stabilizes at €9,165 per person. However, significant differences appear at the class level from the start. In the GG scenario, the richest 20% in the center steadily increase consumption while in the DG scenario the consumption of the T20 class falls sharply due to global convergence, dropping from €41,722 to €6,711 by 2035, below the target level of €9,000 which is only reached in 2052. This dynamic is also present in the consumption trajectories of the other classes of the center although it is less extreme. The middle class of the center that constitutes 50% of the population sees its consumption reduced by more than 50% during the first 15 years of the simulation while the consumption of the poorest 30% declines less sharply. Whereas the richest 20% of the center consume 8 times as much in a GG scenario compared to a DG scenario at the end of the century, the middle class of the center consumes 4 times as much, and the poorest 30% of the center two times as much.

In the semiperiphery, the per capita consumption of the T20 class increases faster in the GG scenario than in the DG scenario, reaching a consumption level more than 4 times as high as in the DG scenario at the end of the simulation. However, for the remaining 70% of the population in the semiperiphery, consumption levels increase faster in the DG scenario. In the case of the middle class, consumption levels in the GG scenario only exceed those in the DG scenario from 2065 onwards while for the poorest class consumption between the two scenarios only converges towards the end of the simulation.

Last, in the periphery the consumption of the middle class in the DG scenario increases exponentially during the first 15 years of the simulation after which consumption growth slows down slightly and levels off in the middle of the century. In the GG scenario, this class reaches comparable consumption levels only in 2080. Nevertheless, due to the accelerating growth in consumption in the GG scenario, in 2100 consumption levels are 58% higher. For the poorest class of the periphery, the DG scenario leads to a higher consumption trajectory throughout the whole simulation as annual per capita consumption under a GG development pathway only reaches 7,230 € in 2100 while in the DG scenario this value is already reached in 2039. Conversely, for the 20% richest in the periphery, consumption levels between DG and GG already converge in 2040, and in the final year of the simulation, consumption per capita in the GG scenario is more than three times as high as in the DG scenario.

Overall, DG benefits poorer classes in the periphery and semiperiphery in terms of both equity and absolute consumption, while GG favors high-income households, particularly the top 20%.

The consumption of all classes in the DG scenario in the first three decades of the simulation is limited by the rates at which land intensities in the model fall. As the DG scenario implies a fast and strong growth in the consumption of poorer classes that spend a larger share of their budgets on the food sector than richer classes, the land demand resulting from the desired growth in consumption is higher than the land available for use until 2055. However, continuous land intensity improvements combined with a continuous increase in wealth of the poorer classes, and a reversal of population growth eventually dissolves the land scarcity problem and the target consumption level is reached by all classes. Thus, the simulation illustrates a potential feasibility barrier of scenarios with fast rates and high degrees of convergence in consumption due to the requirement of high land productivity increases necessary to cover the increased consumption of food products resulting from a combination of population growth and increased affluence of the world's poorer classes.

As birth rates in MORDRED are determined by region- and class-specific consumption trajectories, the earlier peak in world population in the DG scenario can be explained by the faster growth in the consumption of the world's poorest classes that reduces birth rates.

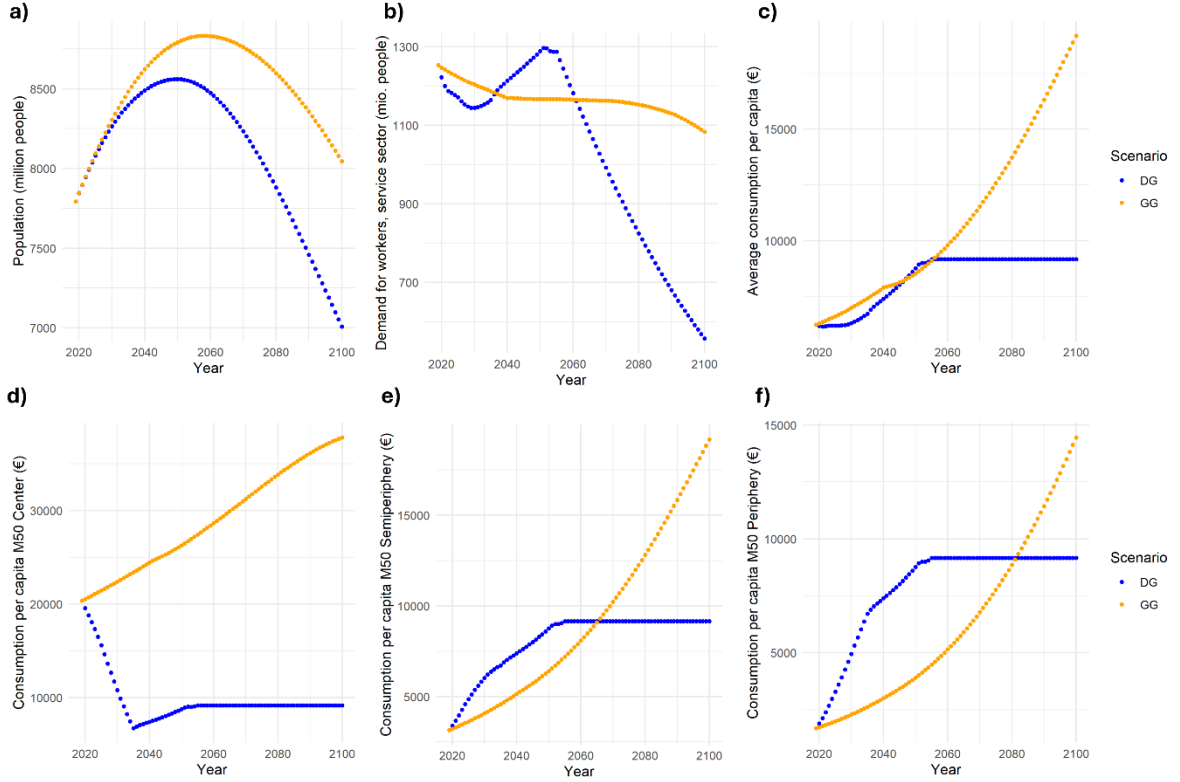


Figure 2: Evolution of a) world population; b) workers demanded in the service sector; c) average consumption per capita; d) consumption per capita of the middle class in high-income countries; e) consumption per capita of the middle class in upper-middle income countries; f) consumption per capita of the middle class in lower-middle and low-income countries in a Degrowth (blue) and a Green growth (orange) scenario.

3.3. Biophysical developments

In the GG scenario, absolute decoupling between economic growth and fossil resource use occurs between 2020 and 2040 and between 2070 and 2100 with a phase of low growth in fossil resource use in between (Figure 3a). Despite absolute decoupling, the climate-related PBIs (Figure 3e-g) continue to deteriorate and remain in or cross the high-risk zone during the last four decades of the simulation. Ultimately, the pace of decoupling is not fast enough for effective climate mitigation: in the final year of the simulation, the level of global fossil resource use has only declined by 12% compared to the 2019 level. Conversely, in the DG scenario, total fossil resource consumption declines by 68.5%. Interestingly, the DG scenario also experiences a period of absolute decoupling in the first decade of the simulation, followed by relative decoupling until the 2050s. As fossil fuel intensity continues to decline throughout the century, the consequence of the eventual degrowth in world output in the DG scenario is a significant reduction of fossil resource extraction and consumption. Although the carbon intensity of the economy by 2100 is 9% lower under GG than under DG, total fossil resource consumption is 2.8 times higher due to the continued growth in output in the GG scenario during the second half of the century.

The absolute decoupling between economic growth and total fossil resource use that can be observed in the GG scenario stems from strong reductions in the consumption of those fossil resources that are used as energy sources. As shown in Figure 3b, the amount of fossil resources used for non-energy purposes, i.e. as industry feedstocks, continues to increase. In the DG scenario, the evolution of the material use of fossil resources is comparable to the GG scenario during the first three decades of the simulation but then diverges in line with differences in

world output between the two scenarios. As oil currently constitutes 73% of the fossil fuels that are used for non-energy purposes, in both scenarios the reduction of fossil fuel combustion ‘saves’ oil resources that are required as feedstock in industrial processes.

Comparing the simulation results of both scenarios across all PBIs, we find that the DG scenario outperforms the GG scenario in 10 of 11 indices (Figure 3c-l). This result is robust to changes of the scenario assumptions in favor of GG and against DG (see the sensitivity tests in S3 Supplementary Material). The exception is the PBI for land-system change, where DG performs better 2040–2080 and GG in the last two decades (Figure 3g). Under GG, no index value is compatible with a safe operating space while under DG only indices representing biogeochemical flows reach values corresponding to a safe operating space.

The radiative forcing index and the CO₂ concentration index, which belong to the climate change planetary boundary, worsen in both scenarios during the simulation (Figure 3c and d). In the GG scenario, the radiative forcing index increases from 100 in 2019 to 225 in 2100. In the DG scenario, the index peaks in 2081 at a value of 151 and in the last two decades of the simulation declines to 148. In the case of the CO₂ concentration index, both scenarios enter the high-risk zone between 2050 and 2060. In the GG simulation, the index worsens faster than in the DG simulation, reaching a final value 13% higher than in the DG scenario, and 31% higher than the initial value. The ocean acidification index mirrors the development of the two other climate-related indices (Figure 3e), with a stabilizing dynamic in the DG simulation, and continued deterioration for the GG simulation. The index value stays in the high-risk zone between 2027 and 2100 (GG), and between 2029 and 2100 (DG).

The biosphere integrity index starts already in a high-risk zone in 2019 and stays constant during the first 15 years for both scenarios. From 2035 onwards, the index worsens in the DG scenario but starts to improve by 2050. During the following 50 years of the simulation the value improves steadily and in 2080 crosses the upper threshold, reaching a zone of uncertainty. Although the index values continue to decline, the safe operating space is not reached during the simulation period. Conversely, in the GG simulation, the index value starts to increase from 2050 onwards, indicating that the Earth system progressively advances farther into the high-risk zone for this planetary boundary (Figure 3f). The differences in the performance between the two scenarios can be explained by the differences in land use in the scenarios: Under GG, the share of economically used land is higher than under DG. Thus, in the latter, natural ecosystems associated with higher biosphere integrity have space to recover while in the former the great majority of accessible land is ‘managed’ and economically exploited.

The land system change index starts in the zone of increasing risk, located between the safe operating zone and the high-risk zone, and stays there for both scenarios during the simulation period although it evolves towards the safe-operating zone during the simulation period (Figure 3g). The index starts to improve more than 10 years earlier in the DG scenario but then stays constant during the last 50 years of the simulation at a value of 88. In the GG scenario, the index starts to continuously improve from the year 2054 and in 2100 stands at 86. The index value is driven by changes in the forest cover throughout the simulations which increases earlier in the DG than in the GG scenario. Equally, between 2050 and 2100, the share of forest not subject to economic exploitation steadily increases in the DG scenario, compared to a steady increase in economically used forest in the GG scenario.

The differences between DG and GG are highest in the case of the planetary boundaries linked to biogeochemical flows (Figure 3h and i). Both indices start at the same point located above the

upper risk threshold but take very different trajectories. In the GG simulation the index values of both N and P flows increase continuously, reaching 474 and 275 in 2100 compared to the reference values of 100 in 2019. In the case of DG, the nitrogen flow index declines from 100 in 2019 to 73.9 in 2051, increases slightly to 78 in 2055 and afterwards declines continuously until the final year of the simulation. The N-flow index enters the zone of increasing risk in 2065, and the safe operating zone in 2087 where it remains until the end of the simulation. The P-flow index reaches the zone of uncertainty in 2084 and the safe operating zone in 2094. Interestingly, in our simulations, absolute decoupling between economic growth and the N- and P-boundary cannot be observed for GG but for DG during the time period in which world output grows. One the one hand, this shows that a period of green (macroeconomic) growth in a scenario of (consumption) degrowth is not a contradiction but a plausible result due to global consumption convergence combined with technological changes (conventional to organic agriculture) and behavioral changes (from meat-based to plant-based diet). On the other hand, it demonstrates that absolute decoupling in a GG scenario limited to fossil resource use is insufficient for the Earth system to leave the high-risk zone.

The novel entities index and the aerosol loading index display comparable dynamics, with a steady deterioration of the indices under GG, reaching values of 385 (for novel entities) and 264 (for aerosol loading) at the end of the simulation. Under DG, the index values increase until global output peaks, and then start to decrease, reaching initial levels for the aerosol loading index and a value 28% above the reference value for the novel entities index (Figure 3j and k).

Industrial green water consumption increases steadily in the GG scenario, despite an assumed reduction of green water intensity due to further industrialization of the global food sector, reflected in an increase of the green water index from 100 to over 200 at the end of the simulation. The blue water index that integrates industrial and household blue water consumption increases even faster than the green water index, crossing the lower threshold for blue water consumption around the middle of the century, and the upper threshold in 2076. In the DG scenario, green water consumption peaks in 2055 and returns to the reference value towards the end of the simulation while blue water consumption increases strongly until the middle of the century and levels off afterwards, entering the zone of uncertainty (Figure 3l).

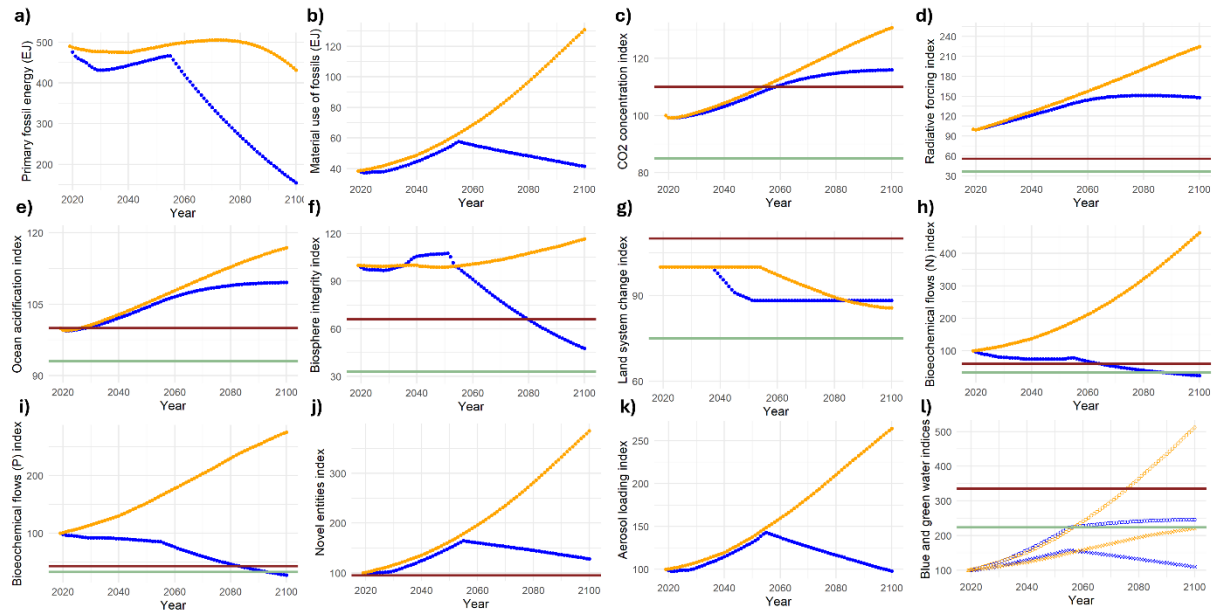


Figure 3: Development of a) fossil resource use, including oil, gas and coal, given in primary energy and in EJ; b) non-energy fossil fuel consumption in EJ; c) the biosphere integrity index; d) the land system change index; e) the radiative forcing index; f) CO₂ concentration index; g) ocean acidification index; h) biogeochemical flows (N) index; i) biogeochemical flows (P) index; j) novel entities index; k) aerosol loading index; l) blue (circle) and green (cross) water indices. All indices are dimensionless and take a reference value of 100 in the initial year of the simulation. Red lines represent upper risk thresholds while green lines represent lower risk thresholds for various planetary boundary indices. Blue lines describe developments under degrowth, orange lines developments under green growth.

Figure 4 shows the initial values for every PBI compared to the operationalized upper and lower threshold values that are known (a), alongside the projected values in 2100 for both simulation scenarios (b), highlighting the substantial changes projected by the model. The results indicate that, overall, the GG scenario falls short of producing ‘genuine green growth’, defined as growth in output that delivers absolute reductions in environmental impacts (Stoknes & Rockström, 2018).

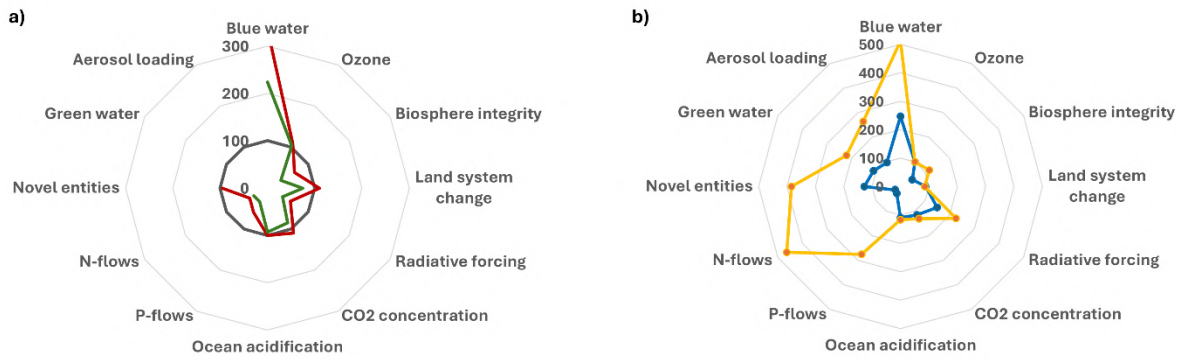


Figure 4: a) PBI values at the beginning of the simulation (grey); lower (green) and upper (red) thresholds for certain PBIs; b) PBI values at the end of the simulation for a Green growth (orange) and Degrowth (blue) scenario.

4. Discussion

4.1. Policy implications

Our results show that a DG scenario combining strong technological and behavioral changes with consumption reductions among richer households—to about €9,000 per person per year—outperforms a GG scenario not only in terms of resource equity but also environmental sustainability. Considering multiple Earth system variables represented through PBIs, we have demonstrated that GG strategies with a narrow focus on reducing the carbon intensity of the economy not only fail to achieve strong climate mitigation at the pace required to reach international climate targets but also neglect other important dimensions of global environmental change (Crona et al., 2023; Goodwin et al., 2024; Vitousek, 1994). Although our results should be interpreted as qualitative illustrations of global socio-ecological dynamics rather than exact quantitative forecasts, several implications for sustainability policy emerge.

First, significant mitigation of anthropogenic pressures on the Earth system requires a policy mix that combines green structural change with shifts in consumption patterns and social redistribution or changes in the property structure within and between societies. Given the limits to how fast and deeply the global economy can decarbonize and dematerialize, behavioral changes—such as a shift to plant-based diets and reduced private consumption by affluent households, especially in high-income countries—can slow the Earth system's drift toward unsustainable states. For some planetary boundaries, these changes eventually might allow the Earth system to enter again into a lower or low-risk zone.

Second, economic development in low-income regions and rising living standards for poorer classes are shared objectives of both GG and DG paradigms. Growth and infrastructure policies should therefore avoid locking poorer regions into carbon-dependent infrastructure (Chen et al., 2021; Unruh & Carrillo-Hermosilla, 2006). Rapid and equitable growth in these regions requires redistribution within societies and capital transfers from richer to poorer territories at both regional and global scales. However, given the persistent scarcity of capital flows to least-developed countries (UN, 2024; UNCTAD, 2023), the DG scenario may face greater feasibility challenges. Another obstacle is the strong decline in government spending observed for high-income countries in the simulation, which, under the current international ‘rules of the game’ could undermine support for DG from the Global North’s governments. Thus, achieving better social and environmental outcomes through a global DG development paradigm may require a new global political-economic logic, grounded in a radically reformed institutional architecture.

Third, sustainability policies must address all Earth system boundaries rather than focusing solely on climate mitigation, which risks adverse trade-offs (Braun et al., 2025; Suckling et al., 2021). The deterioration of N and P related PBIs in the GG simulation indicates a continued reliance on industrial fertilizer which is not only problematic due to altered biogeochemical flows but also because phosphate resources are finite and industrial nitrogen synthesis depends heavily on natural gas (Mingolla & Rosa, 2025; Sverdrup & Ragnarsdottir, 2011; Vaccari & Strigul, 2011; Van Vuuren et al., 2010). Organic agricultural practices could reduce perturbations of the N, P, and C cycles (Scialabba & Müller-Lindenlauf, 2010; Smith et al., 2015) yet their widespread adoption remains constrained by current policy regimes, infrastructure gaps, vested interests, limited knowledge, and cultural barriers (Reganold & Wachter, 2016).

Finally, in neither scenario does the Earth system return to a safe operating zone, even under optimistic assumptions about productivity and bioenergy scalability. Most PBIs remain far beyond their upper thresholds—deep in the “high-risk” zone. This finding differs substantially

from GG simulations based on SSP2 and SSP1 conducted with the IAM IMAGE which show improvements for several boundaries, including climate change, freshwater use, and biogeochemical flows (Van Vuuren et al., 2025). Thus, we argue that it is important to assess the feasibility of global development within planetary boundaries by multiple IAMs that reflect a greater diversity regarding scenario assumptions and model structure.

In MORDRED, although the DG scenario performs better than the GG scenario, several indices - including blue water, novel entities, ocean acidification, CO₂ concentration, and radiative forcing - still deteriorate. Only two PBIs return to safe levels by 2100. This suggests that even ambitious sustainability strategies may be insufficient for full recovery. Consequently, policies must not only strengthen mitigation but also enhance societal resilience and adaptation to reduce the risks associated with prolonged planetary boundary transgression.

4.2. Limitations and further research

The introduction of PBIs represents a first step toward broadening integrated environmental assessment models to systematically include multiple critical Earth system boundaries. However, their development and integration into MORDRED were constrained by model structure and remaining knowledge gaps. For example, biogeochemical PBIs rely on global rather than regional flows, the ozone depletion index is assumed constant, and the ‘novel entities’ index is proxied by chemical sector output.

A key limitation is the absence of feedbacks from the planetary boundary module to the rest of the model. As a result, our simulations capture the effects of economic development on Earth system variables, but not the reverse—how prolonged boundary transgressions might impact economic and social systems. Future research should refine the representation of individual boundaries in IAMs and explore the socio-economic consequences of the Earth system remaining in a high-risk state for extended periods. Currently, the model distinguishes only between three risk zones—safe, increased risk, and high risk—making it difficult to assess how risk scales within the high-risk zone. Developing a more nuanced, quantitative understanding of these relationships is an important next step.

Further limitations stem from the assumption of a smooth, immediate global transition, high fossil resource availability, and rapid technological progress. Future studies could relax these assumptions by incorporating feedbacks that slow land productivity improvements and by modeling biophysical limits to organic agriculture and bioenergy scalability

5. Conclusion

This study compared the economic, social, and biophysical outcomes of two global development paradigms—degrowth (DG) and green growth (GG)—using an extended version of the MORDRED model that incorporates a Planetary Boundary Indices module. The DG scenario yields lower total output but higher equity, improving living standards in poorer regions and slowing (or reversing) planetary boundary transgression. However, these improvements remain insufficient to restore a safe operating space. In contrast, the GG scenario’s continued consumption growth across all classes and regions leads to further deterioration of most PBIs, keeping the Earth system in a high-risk state. Future research should expand the biophysical scope of IAMs like MORDRED by integrating additional boundary variables and feedback mechanisms to better capture the nonlinear dynamics of long-term planetary change.

References

- Algunaibet, I. M., Pozo, C., Galán-Martín, Á., Huijbregts, M. A. J., Mac Dowell, N., & Guillén-Gosálbez, G. (2019). Powering sustainable development within planetary boundaries. *Energy & Environmental Science*, 12(6), 1890–1900.
<https://doi.org/10.1039/C8EE03423K>
- Allen, C., Metternicht, G., Wiedmann, T., & Pedercini, M. (2021). Modelling national transformations to achieve the SDGs within planetary boundaries in small island developing states. *Global Sustainability*, 4, e15. <https://doi.org/10.1017/sus.2021.13>
- BGR. (2020). *BGR Energy Study 2019 – Data and Developments Concerning German and Global energy supplies*. Hannover.
https://www.bgr.bund.de/EN/Themen/Energie/Downloads/energiestudie_2019_en.pdf?__blob=publicationFile&v=6
- Bilancini, E., & D'Alessandro, S. (2012). Long-run welfare under externalities in consumption, leisure, and production: A case for happy degrowth vs. Unhappy growth. *Ecological Economics*, 84, 194–205.
- Braun, J., Werner, C., Gerten, D., Stenzel, F., Schaphoff, S., & Lucht, W. (2025). Multiple planetary boundaries preclude biomass crops for carbon capture and storage outside of agricultural areas. *Communications Earth & Environment*, 6(1), 102.
- Chen, X., Li, Z., Gallagher, K. P., & Mauzerall, D. L. (2021). Financing carbon lock-in in developing countries: Bilateral financing for power generation technologies from China, Japan, and the United States. *Applied Energy*, 300, 117318.
<https://doi.org/10.1016/j.apenergy.2021.117318>
- Cointe, B., & Pottier, A. (2023). Understanding why degrowth is absent from mitigation scenarios: Modelling choices and practices in the IAM community. *Revue de La Régulation*, 35. <https://doi.org/10.4000/regulation.23034>
- Crona, B., Parlato, G., Lade, S., Fetzer, I., & Maus, V. (2023). Going beyond carbon: An “Earth system impact” score to better capture corporate and investment impacts on the earth system. *Journal of Cleaner Production*, 429, 139523.
<https://doi.org/10.1016/j.jclepro.2023.139523>
- D'Alessandro, S., Cieplinski, A., Distefano, T., & Dittmer, K. (2020). Feasible alternatives to green growth. *Nature Sustainability*, 3(4), 329–335.
- Donges, J. F., Heitzig, J., Barfuss, W., Wiedermann, M., Kassel, J. A., Kittel, T., Kolb, J. J., Kolster, T., Müller-Hansen, F., Otto, I. M., Zimmerer, K. B., & Lucht, W. (2019). *Earth system modeling with endogenous and dynamic human societies: The copan:CORE open World-Earth modeling framework*. <https://doi.org/10.48550/ARXIV.1909.13697>
- Drüke, M., Lucht, W., Von Bloh, W., Petri, S., Sakschewski, B., Tobian, A., Loriani, S., Schaphoff, S., Feulner, G., & Thonicke, K. (2024). The long-term impact of transgressing planetary boundaries on biophysical atmosphere–land interactions. *Earth System Dynamics*, 15(2), 467–483. <https://doi.org/10.5194/esd-15-467-2024>
- Edwards, A., Brockway, P., Bickerstaff, K., & Nijssse, F. J. (2025). Towards modelling post-growth climate futures: A review of current modelling practices and next steps. *Environmental Research Letters*.
- Engström, G., Gars, J., Krishnamurthy, C., Spiro, D., Calel, R., Lindahl, T., & Narayanan, B. (2020). Carbon pricing and planetary boundaries. *Nature Communications*, 11(1), 4688.
<https://doi.org/10.1038/s41467-020-18342-7>

- Goodwin, K., Li, M., & Wiedmann, T. (2024). Beyond greenhouse gases – Comprehensive planetary boundary footprints to measure environmental impact. *Sustainable Production and Consumption*, 52, 29–44. <https://doi.org/10.1016/j.spc.2024.10.009>
- Gries, T., & Naudé, W. (2025). Economics for a Safe Operating Space: A Green-Growth-Degrowth Model. *Institute of Labor Economics (IZA)*, 1–55.
- Houtbeckers, E. (2025). Mapping the spectrum of degrowth work. In A. Nelson (Ed.), *Routledge Handbook of Degrowth* (pp. 292–306). Routledge.
- IPCC. (2021). *Climate Change 2021: The Physical Science Basis. Contribution of Working Group I to the Sixth Assessment Report of the Intergovernmental Panel on Climate Change*. Cambridge University Press. Cambridge University Press, Cambridge, UK and New York, NY, USA.
- Kallis, G., Hickel, J., O'Neill, D. W., Jackson, T., Victor, P. A., Raworth, K., Schor, J. B., Steinberger, J. K., & Ürge-Vorsatz, D. (2025). Post-growth: The science of wellbeing within planetary boundaries. *The Lancet Planetary Health*, 9(1), e62–e78.
- Kikstra, J. S., Li, M., Brockway, P. E., Hickel, J., Keysser, L., Malik, A., Rogelj, J., Van Ruijen, B., & Lenzen, M. (2024). Downscaling down under: Towards degrowth in integrated assessment models. *Economic Systems Research*, 36(4), 576–606. <https://doi.org/10.1080/09535314.2023.2301443>
- Kronenberg, J., Andersson, E., Elmquist, T., Łaszkiewicz, E., Xue, J., & Khmara, Y. (2024). Cities, planetary boundaries, and degrowth. *The Lancet Planetary Health*, 8(4), e234–e241. [https://doi.org/10.1016/S2542-5196\(24\)00025-1](https://doi.org/10.1016/S2542-5196(24)00025-1)
- Lahoti, R., Jayadev, A., & Reddy, S. (2016). The global consumption and income project (GCIP): An overview. *Journal of Globalization and Development*, 7(1), 61–108.
- Lauer, A., Capellán-Pérez, I., & Wergles, N. (2025). A comparative review of de-and post-growth modeling studies. *Ecological Economics*, 227, 108383.
- Lauer, A., & Llases, L. (2025). *MORDRED: Model Of Resource Distribution and Resilient Economic Development. Model Documentation*. GitHub. <https://github.com/Pendracus/MORDRED>
- Lu, C., & Tian, H. (2017). Global nitrogen and phosphorus fertilizer use for agriculture production in the past half century: Shifted hot spots and nutrient imbalance. *Earth System Science Data*, 9(1), 181–192. <https://doi.org/10.5194/essd-9-181-2017>
- Mathias, J.-D., Andries, J. M., & Janssen, M. A. (2017). On our rapidly shrinking capacity to comply with the planetary boundaries on climate change. *Scientific Reports*, 7(1), 42061. <https://doi.org/10.1038/srep42061>
- Mingolla, S., & Rosa, L. (2025). Low-carbon ammonia production is essential for resilient and sustainable agriculture. *Nature Food*, 6(6), 610–621. <https://doi.org/10.1038/s43016-025-01125-y>
- Moyer, J. D. (2023). Modeling transformational policy pathways on low growth and negative growth scenarios to assess impacts on socioeconomic development and carbon emissions. *Scientific Reports*, 13(1), 15996.
- Nieto, J., Carpintero, Ó., Lobejón, L. F., & Miguel, L. J. (2020). An ecological macroeconomics model: The energy transition in the EU. *Energy Policy*, 145, 111726.
- O'Neill, D. W., Fanning, A. L., Lamb, W. F., & Steinberger, J. K. (2018). A good life for all within planetary boundaries. *Nature Sustainability*, 1(2), 88–95.
- Reganold, J. P., & Wachter, J. M. (2016). Organic agriculture in the twenty-first century. *Nature Plants*, 2(2), 15221. <https://doi.org/10.1038/nplants.2015.221>
- Richardson, K., Steffen, W., Lucht, W., Bendtsen, J., Cornell, S. E., Donges, J. F., Drücke, M., Fetzer, I., Bala, G., & von Bloh, W. (2023). Earth beyond six of nine planetary boundaries. *Science Advances*, 9(37), eadh2458.

- Rockström, J., Gupta, J., Qin, D., Lade, S. J., Abrams, J. F., Andersen, L. S., Armstrong McKay, D. I., Bai, X., Bala, G., Bunn, S. E., Ciobanu, D., DeClerck, F., Ebi, K., Gifford, L., Gordon, C., Hasan, S., Kanie, N., Lenton, T. M., Loriani, S., ... Zhang, X. (2023). Safe and just Earth system boundaries. *Nature*, 619(7968), 102–111. <https://doi.org/10.1038/s41586-023-06083-8>
- Rockström, J., Steffen, W., Noone, K., Persson, Å., Chapin, F. S. I., Lambin, E., Lenton, T., Scheffer, M., Folke, C., Schellnhuber, H. J., Nykvist, B., de Wit, C., Hughes, T., van der Leeuw, S., Rodhe, H., Sörlin, S., Snyder, P., Costanza, R., Svedin, U., ... Foley, J. (2009). Planetary Boundaries: Exploring the Safe Operating Space for Humanity. *Ecology and Society*, 14(2). <https://doi.org/10.5751/ES-03180-140232>
- Scialabba, N. E.-H., & Müller-Lindenlauf, M. (2010). Organic agriculture and climate change. *Renewable Agriculture and Food Systems*, 25(2), 158–169. <https://doi.org/10.1017/S1742170510000116>
- Smith, L. G., Williams, A. G., & Pearce, Bruce. D. (2015). The energy efficiency of organic agriculture: A review. *Renewable Agriculture and Food Systems*, 30(3), 280–301. <https://doi.org/10.1017/S1742170513000471>
- Stadler, K., Wood, R., Bulavskaya, T., Södersten, C., Simas, M., Schmidt, S., Usabiaga, A., Acosta-Fernández, J., Kuenen, J., Bruckner, M., Giljum, S., Lutter, S., Merciai, S., Schmidt, J. H., Theurl, M. C., Plutzar, C., Kastner, T., Eisenmenger, N., Erb, K., ... Tukker, A. (2018). EXIOBASE 3: Developing a Time Series of Detailed Environmentally Extended Multi-Regional Input-Output Tables. *Journal of Industrial Ecology*, 22(3), 502–515. <https://doi.org/10.1111/jiec.12715>
- Steffen, W., Richardson, K., Rockström, J., Cornell, S. E., Fetzer, I., Bennett, E. M., Biggs, R., Carpenter, S. R., de Vries, W., & de Wit, C. A. (2015). Planetary boundaries: Guiding human development on a changing planet. *Science*, 347(6223).
- Stoknes, P. E., & Rockström, J. (2018). Redefining green growth within planetary boundaries. *Energy Research & Social Science*, 44, 41–49. <https://doi.org/10.1016/j.erss.2018.04.030>
- Suckling, J., Hoolahan, C., Soutar, I., & Druckman, A. (2021). Unintended consequences: Unknowable and unavoidable, or knowable and unforgivable? *Frontiers in Climate*, 3, 737929.
- Sultana, F. (2023). Whose growth in whose planetary boundaries? Decolonising planetary justice in the Anthropocene. *Geo: Geography and Environment*, 10(2), e00128. <https://doi.org/10.1002/geo2.128>
- Sverdrup, H. U., & Ragnarsdottir, K. V. (2011). Challenging the planetary boundaries II: Assessing the sustainable global population and phosphate supply, using a systems dynamics assessment model. *Applied Geochemistry*, 26, S307–S310.
- UN. (2024). November 2024 Briefing: Economic prospects and development challenges in landlocked developing countries. *World Economic Situation and Prospects: Monthly Briefing*, 186. <https://policy.desa.un.org/sites/default/files/publications/2024-11/mb186.pdf>
- UN DESA. (2019). *World Population Prospects 2019, Online Edition. Rev. 1. File POP/7-1: Total population (both sexes combined) by five-year age group, region, subregion and country, 1950-2100 (thousands)*.
- UNCTAD. (2023). Investment flows to least developed countries affected disproportionately by global crises. *Global Investment Trends Monitor*, 45, 1–12.
- Unruh, G. C., & Carrillo-Hermosilla, J. (2006). Globalizing carbon lock-in. *Energy Policy*, 34(10), 1185–1197. <https://doi.org/10.1016/j.enpol.2004.10.013>

- Vaccari, D. A., & Strigul, N. (2011). Extrapolating phosphorus production to estimate resource reserves. *Chemosphere*, 84(6), 792–797.
- Van Vuuren, D. P., Bouwman, A. F., & Beusen, A. H. (2010). Phosphorus demand for the 1970–2100 period: A scenario analysis of resource depletion. *Global Environmental Change*, 20(3), 428–439.
- Van Vuuren, D. P., Doelman, J. C., Schmidt Tagomori, I., Beusen, A. H. W., Cornell, S. E., Röckstrom, J., Schipper, A. M., Stehfest, E., Ambrosio, G., Van Den Berg, M., Bouwman, L., Daioglou, V., Harmsen, M., Lucas, P., Van Der Wijst, K.-I., & Van Zeist, W.-J. (2025). Exploring pathways for world development within planetary boundaries. *Nature*, 641(8064), 910–916.
<https://doi.org/10.1038/s41586-025-08928-w>
- Van Vuuren, D. P., Stehfest, E., Gernaat, D. E., Doelman, J. C., Van den Berg, M., Harmsen, M., de Boer, H. S., Bouwman, L. F., Daioglou, V., & Edelenbosch, O. Y. (2017). Energy, land-use and greenhouse gas emissions trajectories under a green growth paradigm. *Global Environmental Change*, 42, 237–250.
- Vázquez, D., Galán-Martín, Á., Tulus, V., & Guillén-Gosálbez, G. (2023). Level of decoupling between economic growth and environmental pressure on Earth-system processes. *Sustainable Production and Consumption*, 43, 217–229.
<https://doi.org/10.1016/j.spc.2023.11.001>
- Vincent, O., & Brandellero, A. (2023). Transforming work: A critical literature review on degrowth, post-growth, postcapitalism and craft labor. *Journal of Cleaner Production*, 430, 139640. <https://doi.org/10.1016/j.jclepro.2023.139640>
- Vitousek, P. M. (1994). Beyond Global Warming: Ecology and Global Change. *Ecology*, 75(7), 1861–1876. <https://doi.org/10.2307/1941591>

Supplementary Material

S1 MORDRED sectors

Sector number	Sector description
1	Agriculture, food, beverages
2	Non-energy use of biomass
3	Fossil fuels used for energy
4	Mining
5	Industry not elsewhere classified
6	Recycling industry
7	Services not elsewhere classified
8	Non-energy use of fossil fuels
9	Chemical industry
10	Biomass used for energy
11	Manufacturing
12	Fossil fuel-based electricity
13	Nuclear electricity
14	Hydroelectricity
15	Wind based electricity
16	Biomass and waste based electricity
17	Solar PV electricity
18	Solar thermal electricity
19	Tide, wave and ocean based electricity
20	Geothermal electricity
21	Transport
22	Education
23	Health
24	Waste industry
25	Waste ,recycling' (biogasification & composting) industry

Table 1: Overview of the sectors represented in MORDRED. Source:
<https://github.com/Pendracus/MORDRED/blob/main/Sectors.md>

S2 Scenario parametrization

Model variable	GG	DG
<i>Labor productivity</i>	Global average productivity increases to 1.5 times the productivity levels of high-income countries in 2019.	Global average productivity increases to the productivity levels of high-income countries in 2019.
<i>Process efficiency coefficient in the A matrix</i>	Constant energy efficiency improvements through technological progress are assumed to be offset by falling labor intensity. In sector 1 a factor of 1.1 is applied due to an assumed link between higher productivity and higher energy intensity. Energy intensity declines by 30% due to the electrification of industrial processes which reach higher levels than in the DG scenario.	Process efficiency is assumed to improve compared to a GG scenario due to higher labor intensities across sectors (10% reduction in sector 1, 20% reduction in the remaining sectors). The additional labor is assumed to be employed to develop energy saving processes and/or perform physical work that allows to replace part of the required non-human energy inputs. Efficiency intensity declines by 50% due to the electrification of industrial processes.
<i>A matrix sector 11</i>	Constant.	Inputs from sector 11 decrease by 20% for sector 1, reflecting decreased fertilizer use.
<i>Energy technologies</i>	Greening (complete replacement of nuclear and fossil energy), Electrification (reduction of non-electricity inputs by 40%); non-electric greening: replacement of 50% of inputs from sector 3 with sector 10.	Greening (complete replacement of nuclear & fossil energy to 2100), Electrification (reduction of non-electricity inputs by 25%); non-electric greening: replacement of 50% of inputs from sector 3 with sector 10.
<i>Target consumption vector of governments, GFCF and households</i>	Greening, replacement, electrification, shift from fossil to biomass to the same degree as the industrial processes. The demand for food products was adjusted in the consumption vector of the poorest household type.	Greening, replacement, electrification, shift from fossil to biomass to the same degree as the industrial processes. The demand for food products was adjusted in the consumption vector of the poorest household type.
<i>Land intensity of agriculture & forestry</i>	Intensity decreases to 0.2, 0.4 and 0.7 of 2019 values for agricultural, forest and other land, respectively .	Intensity decreases to 0.2, 0.4 and 0.7 of 2019 values for agricultural, forest and other land, respectively. Additionally: land intensity declines for agricultural and other land due to diet change and land intensity increase due to organic farming factor. The plant-based diet factor is 0.65, the organic agriculture factor is 1.31.
<i>Land intensity of energy generation</i>	30% improvement for non-biomass energy, biomass increases by the average increase of agricultural and forest land, i.e. 0.3.	30% improvement for non-biomass energy, biomass increases by the average increase of agricultural and forest land. The organic agriculture factor is also applied here and increases land intensity.
<i>Greenhouse gas emission intensity of N2O and CH4</i>	Constant as there are weak incentives to reduce intensity in the absence of a global stringent emission trading system for N2O and CH4 emissions.	Decrease due to organic agricultural practices and diet changes. The introduction of organic agriculture is reflected through a decrease in N2O intensity of 80% in the food sector. The effects of a plant-based diet are

		reflected by a reduction of current CH4 intensity in the food sector by 71%.
<i>N und P pollution intensity of agriculture</i>	Constant as the tendency to increase intensity due to productivity growth is assumed to offset the tendency to decrease intensity due to technology improvements.	Changes in agricultural practices, notably the shift to organic agriculture, are assumed to lead to strong decreases in N & P pollution intensity, represented through a decrease of 80%.
<i>Industrial water intensity</i>	Green water intensity decreases while blue water consumption intensity increases due to intensification of agriculture. It is assumed that 20% of green water is substituted by blue water.	
<i>Household water intensity</i>	Behavioral changes are assumed to lead to a moderate 20% decline in household blue water consumption intensity.	
<i>Consumption growth rate</i>	Consumption rates calculated according to consumption targets: the per capita consumption of classes in the center doubles until 2100; classes in the semiperiphery consume what the respective classes in the center consumed in 2019; classes in the periphery consume 0.75 times what the respective classes in the center consumed in 2019.	Global convergence to a target level of 9000 € in 2035. Consumption is given in 2019-€.
<i>Convergence</i>	Moderate convergence to a maximum consumption ratio of 10:1 between the richest and the poorest class in 2100.	Strong and fast convergence to zero consumption inequality in 2035.
<i>Capital intensity</i>	Increases by 1.5%.	Constant.
<i>Annual working hours</i>	2080 hours.	
<i>Maximum participation rate</i>	0.9	
<i>Resources</i>	High resource availability (sum of coal, oil and gas resources: 495390 EJ).	
<i>Extraction costs</i>	Exponential curve, very favorable cost curve.	
<i>Land allocation</i>	Land demand for subsistence agriculture has lower priority than land demand for monetized economic processes within the global economy.	Land demand for subsistence agriculture has the same priority as land demand for monetized economic processes within the global economy.
<i>Land protection</i>	Protection of 20% of primary forest	Protection of 30% of primary forest.
<i>Target subsistence land intensity</i>	Model default.	
<i>Maximum land conversion rate</i>	Low: 0.004.	
<i>Climate related assumptions</i>	No climate damages, no climate feedbacks.	

Table 2: Scenario parametrization for Green growth (GG) and Degrowth (DG).

S3 Sensitivity tests

Test design

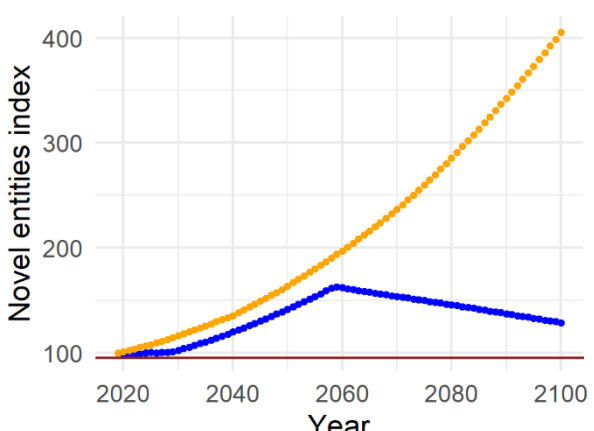
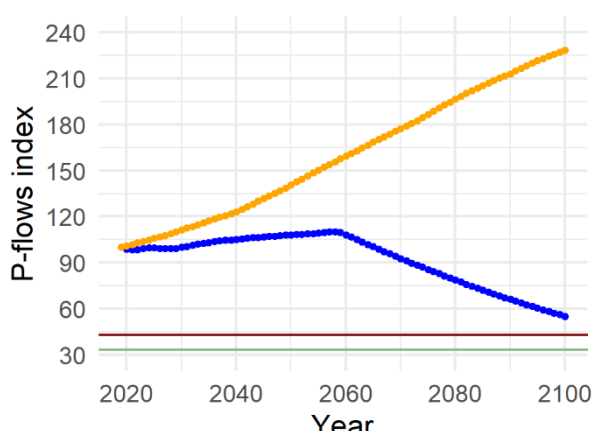
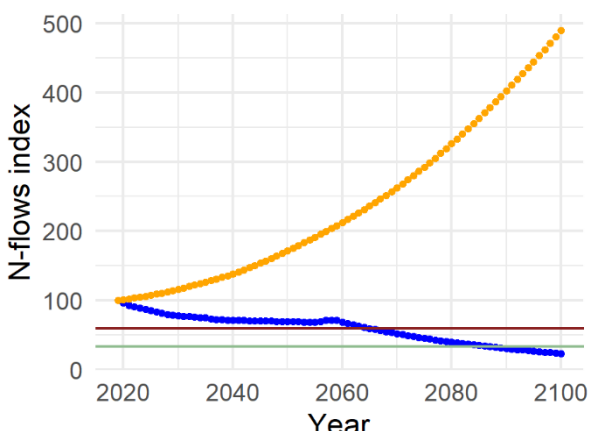
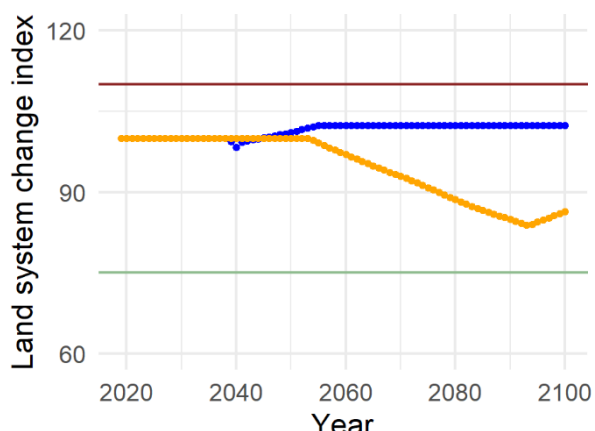
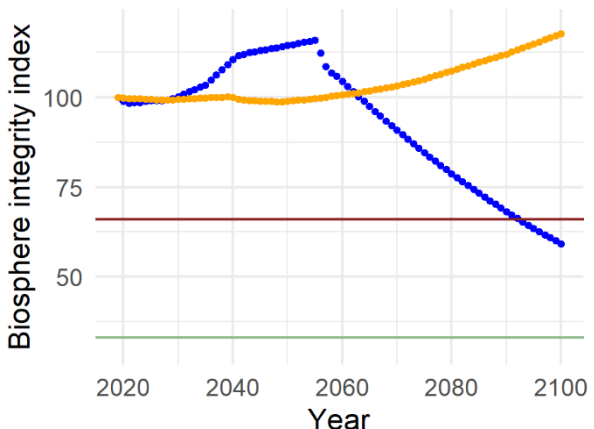
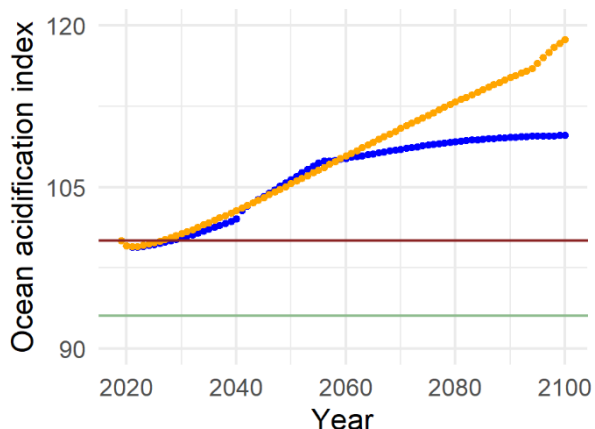
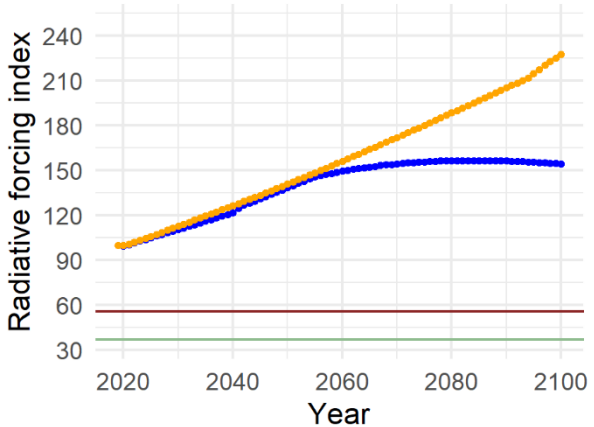
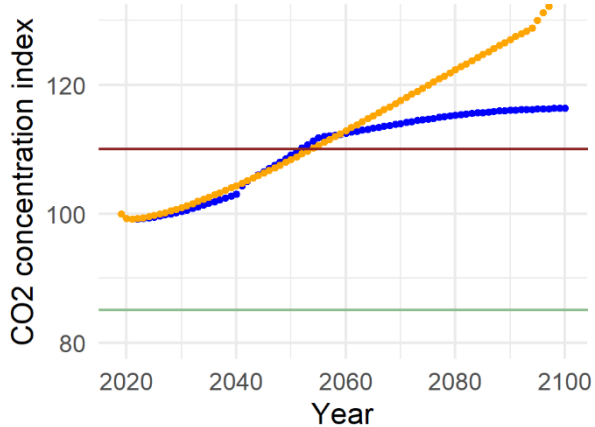
Since we find that the DG scenario performs better than the GG scenario in terms of planetary boundary indicators, the sensitivity tests aim to test the consequences of a possible overestimation of DG related intensity improvement factors and a possible underestimation of GG related improvement factors. Table 3 lists the changes made in the sensitivity tests (ST) for GG and DG.

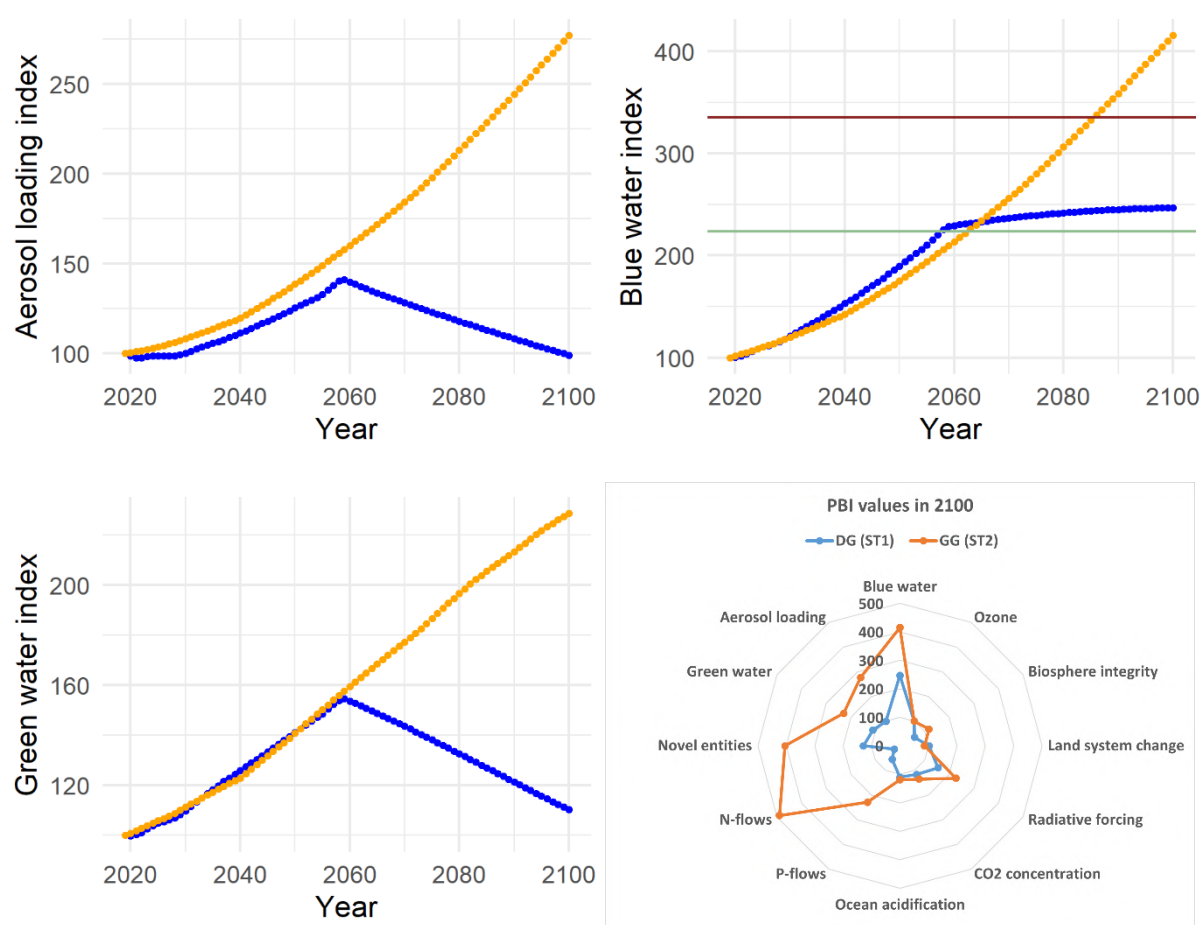
Variable	ST1: Optimistic GG	ST2: Pessimistic DG
<i>Energy intensity</i>	Original value for energy intensity reductions due to electrification multiplied by 1.5.	Original value for energy intensity reductions due to higher labor intensity multiplied by 0.5.
<i>Land intensity of energy generation</i>	Original value multiplied by 1.5.	Original value multiplied by 0.5.
<i>Greenhouse gas emission intensity of N2O and CH4</i>	Instead of a constant value, intensity is reduced by 20%.	Original values for emission intensity reduction multiplied by 0.75.
<i>N und P pollution intensity of agriculture</i>	Instead of a constant value, intensity is reduced by 20%.	Original value multiplied by 0.75.
<i>Blue water intensity</i>	Only 50% of green water reductions are substituted by blue water.	No changes to original value.
<i>Organic agriculture factor</i>	-	Factor increases by 25%, i.e. greater increase in land intensity due to organic agriculture.
<i>Plant-based diet factor</i>	-	Factor increases by 25%, i.e. less land intensity improvements due to plant-based diet.

Table 3: Parameter changes in sensitivity tests.

Test results

- Biosphere integrity: No changes in general dynamics but the index value rises higher and declines slower in the DG scenario.
- Land system change: The index in the DG scenario does not decline but increases slightly and then remains constant. The GG scenario outperforms the DG scenario earlier in the simulation (from 2050 onwards). However, there are no significant differences in the final result; in both scenarios, the index stays between the upper and lower thresholds.
- Radiative forcing: No changes in general dynamics.
- CO2 concentration: No changes in general dynamics.
- Ocean acidification: No changes in general dynamics
- Biogeochemical (N) flows: No changes in general dynamics.
- Biogeochemical (N) flows: No changes in general dynamics but the index value declines slower in the DG scenario and does not fall below the upper or lower threshold value until the end of the simulation.
- Novel entities: No changes in general dynamics although the index value increases slower in this version of the DG scenario than in the original version.
- Aerosol loading: No changes in general dynamics although the index value increases slower in this version of the DG scenario than in the original version.
- Blue & green water: No changes in general dynamics.





Graphical visualization of the evolution of the Planetary Boundary Indicators (PBIs) in ST1 and ST2.

Ideal vs. delayed just sustainability transitions: a comparative scenario analysis

Abstract

While most modeling studies focus on sustainability policies being implemented in the near future, delayed societal transition processes driven by emerging limits to growth remain underexplored. Using a quantitative system-dynamic model, we compare the socio-economic and environmental performance of two global societal just transition scenarios featuring ambitious social, economic, technological and demographic policies. The *early-transition scenario* is implemented from 2030 onwards, whereas radical sustainability policies in the *late-transition scenario* are only introduced from 2075 onwards. We find that an early transition avoids an unintentional reduction in economic production due to rising adverse environmental impacts, and achieves social consumption and redistribution targets with slower rates of change compared to a delayed transition. Conversely, the decline in the consumption levels of richer classes in the late-transition scenario is linked to environmental restraints to economic production and further accelerated by redistribution policies. A clear trade-off between maintaining high consumption levels and crossing critical ecological thresholds emerges in the simulations. While both scenarios fail to limit global warming to 2 °C above the pre-industrial period, global average temperatures in 2100 are 1.4 °C higher in the late-transition scenario than in the early-transition scenario. Radical sustainability policies during a delayed transition might temporarily stabilize the world system and prevent undesirable dynamics of accelerated economic breakdown in the context of an increasingly destabilized Earth system, whereas an earlier transition could achieve higher stability in the long-term.

Keywords

Just sustainability, post-growth, sustainability transitions, societal change, Integrated Assessment Modeling, delayed climate action.

1. Introduction

The world is experiencing multiple simultaneous shifts in the planetary environmental system, the global human energy infrastructure, the international security system, the global economic system and the information system, which could give rise to a profound polycrisis (Lawrence et al., 2024). In this context, the need to address intertwined economic, social and environmental problems has given rise to the notion of just sustainability transitions, understood as processes of transformative change aimed at enabling present and future human and non-human living beings to survive and flourish (Avelino et al., 2024).

Already in 1992 the Union of Concerned Scientists issued a ‘warning to humanity’, which was reiterated in 2017 and signed by 13,524 researchers across the world (Ripple et al., 2017). Further warnings concerning the ‘climate emergency’ (Ripple et al., 2022, 2023, 2024), (Cavicchioli et al., 2019; Ripple et al., 2022, 2023, 2024), the threats to mountain ecosystems (Schmeller et al., 2022) and insects (Harvey et al., 2023), the bidirectional impacts between climate change and microorganisms (Cavicchioli et al., 2019), the threats to ecosystems posed by invasive alien species (Pyšek et al., 2020) and on affluence as a barrier to sustainability (Wiedmann et al., 2020) have emphasized the urgency of a just transition.

Thus, time emerges as a key variable in the quest for sustainability. With every year of delayed climate action, the emission pathways consistent with international climate goals become steeper or depend more on large-scale negative emissions to achieve ‘net zero’ (cf. IPCC, 2018). The existence of non-linear dynamics and different critical thresholds suggest that if the transition occurs too slow or too late anthropogenic pressure on the Earth system could result in irreversible changes with long-term negative impacts on human development (Lenton et al., 2019). Therefore, transition scenarios in the literature are generally modeled as early transitions, with decisive changes occurring decades before, rather than after, 2050 (e.g. IEA, 2022; IPCC, 2018).

However, despite the proliferation of multilateral environmental agreements (Mitchell et al., 2020) and numerous transition efforts at the local level (Ehnert et al., 2022; Frantzeskaki et al., 2016) a global societal transition has yet to materialize. Instead, greenhouse gas emissions are at an all-time high (Ripple et al., 2024) and significant transgressions for six out of nine planetary boundaries have pushed the Earth system far beyond the ‘safe operating zone’ known to be conducive to human welfare and societal development (Richardson et al., 2023).

Because economic production remains tightly linked to material flows, preventing high rates of absolute decoupling (Haberl et al., 2020; Martinico-Perez et al., 2018; Streeck et al., 2020; Vogel & Hickel, 2023), the past decade has seen a surge in theoretical and modeling work exploring new economic development paradigms centered on the universal satisfaction of basic human needs within planetary boundaries (Brand-Correa & Steinberger, 2017; Fanning & Raworth, 2025; Hickel, 2019; Kallis et al., 2025; Millward-Hopkins et al., 2020). These approaches imply strong intra- and international convergence processes of per capita consumption to relatively low levels, and a fundamental reorientation of economic processes and policies away from the ‘growth paradigm’ (Schmelzer, 2017).

Although such alternative proposals are gaining traction both in academia and policy-making (Engler et al., 2024; Kallis et al., 2024) an ambitious and coherent implementation implies deep structural changes on the global level, including a new Earth governance structure enforcing resource extraction caps, accompanied by capital redistribution and other social policies, and in the absence of a series of positive ‘black swans’ or social tipping points it seems improbable that such a new world order will emerge within the next one or two decades (cf. Biermann et al., 2012; Fitzpatrick et al., 2022; Lauer & Llases, 2025a). At the same time, the increase in climate change induced disasters and catastrophes under certain conditions might open up new windows of opportunity for societal change (Brundiers & Eakin, 2018; Matsuura, 2022; Rizzo et al., 2022), which, in the best case, could result in a global transition, albeit with a delay of various decades compared to timely transitions occurring under ideal conditions.

Therefore, in this paper we aim to explore how the timing of a global sustainability transition influences socio-economic and environmental outcomes. While the cost of delayed climate action has been already examined in various scenario exercises (e.g. Aryanpur et al., 2024; Schaeffer et al., 2015; Winning et al., 2019), little is known about delayed ‘radical’ sustainability pathways characterized by a degrowing global economy and large-scale redistribution measures. Consequently, we are particularly interested in the following research questions:

1. How might socio-economic, demographic, and environmental developments differ under an early global just sustainability transition compared to a delayed transition?
2. Which trade-offs might appear in an early versus a late transition?
3. To what extent does the timing of the transition influence the long-term stability and resilience of the emerging socio-economic system?

To examine these questions, we conduct a quantitative modeling study grounded in two previously developed qualitative scenarios, which we parameterize and simulate using a newly developed Integrated Assessment Model (IAM). We present and discuss the main scenario results and conclude by outlining potential avenues for future research.

2. Methods

2.1. Scenario and model selection

We select two previously developed qualitative storylines called *Fast Sustainability Transition 5: sufficiency economies (FST5)* and *Business as usual - Global Emergency Governance (BAU-GEG)* that serve as examples for an ‘early’ and a ‘late’ societal transition.

In FST5, a black swan in form of a successful global movement triggers various social tipping points that result in the establishment of a Planetary Confederation in 2032. Legitimated by a global consensus for egalitarian wealth and resource distribution, as well as ecological technology development, the Planetary Confederation implements ambitious social, economic, demographic, environmental and technological policies which fundamentally change the world system during the 21st century.

In BAU-GEG, the world follows its historical development pathway characterized by weak environmental and social policies. However, as environmental conditions deteriorate and economic crises increase, legitimization for the world economic system and the institutions that support it dwindles. Under the pressure of an organized global worker movement, a world emergency regime is installed that pushes stringent environmental, social and demographic policies, focusing on minimizing resource use and pollution, disaster management and the fulfillment of human needs. The complete storylines are displayed in Lauer et al. (2025) and in Lauer & Llases (Lauer & Llases, 2025a).

Three main reasons motivated our choice of scenarios.

First, both are of global scale and provide relatively detailed information on social, (geo)political, economic and environmental variables and their interlinkages. One scenario represents an ‘ideal’, intentional, swift and early transition while the other illustrates a delayed transition that only occurs as biophysical limits to growth emerge, political tensions increase and social forces have built up enough pressure to impose radical changes at the global level. Their similarity in scale and variables, combined with the difference in the timing of the transition, renders them particularly suitable for a comparative scenario analysis.

Second, they feature non-linear changes in key variables that are assumed to be influenced by strong social, ecological, environmental and demographic policies. Therefore, the transition in the selected scenarios is not limited to the technological realm. Notably, both can be classified as ‘post-growth’ scenarios as they foresee a reduction in the consumption level of richer classes, a more equitable access to resources and economic goods and change in production patterns to reduce human impacts on Earth systems (Edwards et al., 2025; Van Eynde et al., 2025). Hence, they are built on the basic premise that ultimately neither continued environmental degradation nor environmental restoration are compatible with permanently increasing consumption levels. Last, both scenarios are linked to a relatively extensive scenario translation protocol, which facilitates the quantification process and renders the parametrization of the scenarios more transparent.

For the scenario quantification we use the system-dynamic-based simulation model *MORDRED* (Model Of Resource Distribution and Resilient Economic Development). *MORDRED* was built following various calls in the literature for more heterogeneous and diverse futures that break with the ‘continuity bias’ and integrate systemic shocks as well as alternative economic paradigms and systems (Hickel et al., 2021; Lauer et al., 2024; Raskin & Swart, 2020; Rothman et al., 2023). The model differs from other IAMs due to the high number of endogenously evolving, interlinked variables and due to its attention to different economic input factors that might limit economic growth. Its modular structure, the option to activate different feedback mechanisms, as well as the user-friendly programming software allow the model to be tailored to different scenarios by adapting the simulation time and adding new necessary variables. These characteristics facilitate the simulation of non-linear futures with strong deviations from historical trends and render the model suitable for the quantification of the selected transition scenarios.

MORDRED consists of several interlinked modules, the principal ones being the demographic, economic, labor, land, energy and climate modules. The demographic module calculates changes in the world population, which consists of 20 age cohorts and three world regions: the ‘center’,

covering all high-income countries, the ‘semiperiphery’, which includes all upper-middle-income countries, and the ‘periphery’, containing the lower-middle- and low-income-countries. Changes in the demographic module influence the labor module by changing the labor supply which consists of the segment of the world population aged 15 to 64, as well as the economy module via changes in the final demand for different products. At the same time, changes occurring in the economic module, such as changes in production and consumption per capita impact age-specific mortality and fertility rates in the demographic module. The economic, labor, land and energy modules are linked via sectoral labor, land and energy intensities. As human labor, different land types (forest, land for renewable energy generation, land for food cultivation, land classified as ‘other land’ by FAO) and different energy types (fossil fuels, bioenergy, fossil-based- and non-fossil-based electricity) are necessary input factors into the economic process, they can act as limiting factors to growth if the required inputs to meet global demand for economic goods exceed the available stock of input factors. Last, the economic module influences the climate module via different greenhouse gas emissions, primarily caused by the combustion of fossil fuels, while changes in the climate module impact the economic module through climate damages that increase nonlinearly with global average temperatures.

The economic module is based on an input-output framework. Thus, it differentiates between different final demand components (private consumption, public consumption and gross fixed capital formation) and sectoral demands for intermediate goods that are disaggregated into 25 sectors. Given that one of the core concerns behind the development of MORDRED was to explore inequality in consumption and living standards, the model disaggregates private (household) consumption within the global economy into 9 classes: The richest 20%, poorest 30% and the remaining middle class of the center (R20C, P30C, M50C), the richest 20%, poorest 30% and the remaining 50% of the semiperiphery (R20S, P30S, M50S), as well as the richest 20%, poorest 30% and the remaining middle class of the periphery (R20P, P30P, M50P).

For the simulations, we created two new model versions - MORDRED 1.1.5 and 1.1.6. A detailed description of the base model and data sources, the model versions and the 25 economic sectors is given in Lauer & Llases (2025b). Additionally, the Supplementary Material (SM) contains the main causal loop diagrams for the most important modules.

The two model versions allow us to differentiate between technological, economic, demographic and social developments before and after the transition starts. Additionally, we partly endogenized changes in the intensity of food land, forest land and land classified as ‘other land’ by the FAO in both model versions and added an endogenous component to the evolution of sectoral labor intensities in the model version used to simulate the BAU-GEG scenario. The default simulation time in the model covers the period 2019 – 2100, which we adapt, since we consider the period long enough to show the most significant changes caused by transition policies as well as differences between an early and a late transition.

2.2. Scenario parametrization

By comparing the scenario storylines and the scenario parametrization protocols provided for FST5 and BAU-GEG with the capacity of MORDRED to represent the envisioned changes (cf. SM section 2), we developed a list of variables that are at the same time represented by the model and relevant for both scenario storylines. Subsequently, the selected variables were parametrized considering the information provided in the translation protocols (Table 1). To increase the comparability between the scenarios and highlight differences caused by the *timing* of the transition, we selected rather similar technological and socio-economic parameter values. Notable differences include a higher birth reduction policy and a lower primary forest protection policy in BAU-GEG, compared to FST5. Also, while social redistribution policies occur within 10 years after the beginning of the transition in both scenarios, technological changes such as changes in the energy mix, take 70 years in the FST5 scenarios and only 50 years in the BAU-GEG, reflecting higher urgency.

The start of the transition was set to 2030 for FST5, following the information in the scenario storyline. Conversely, as no specific timeframe is given for the BAU-GEG scenario, we chose 2075 as starting point, which on the one hand constitutes a significant delay relative to the ‘early’ transition, but on the other hand still allows us to explore possible changes caused by the ‘late’ transition during the last 25 years of the simulation period.

Table 1: Parametrization of the two selected qualitative scenarios.

Variable	Early transition (based on FST5)	Late transition (based on BAU-GEG)
Key parameters before the transition		
<i>Desired consumption growth rate before the transition</i>	Highest desired consumption growth rate (P30P): 3.04%; lowest desired consumption growth rate (R20C): 0.86%; moderate convergence in consumption inequality.	
<i>Technological changes in the A matrix and in final demand components</i>	Until 2030: energy efficiency in all economic processes improves by 2.25%; electrification of 2.5% of non-electric fossil energy inputs, substitution of 5% of fossil-based electricity through renewable electricity (solar PV, hydro, wind) in production processes and in final demand.	Until 2075: energy efficiency in all economic processes improves by 5%; electrification of 10% of non-electric fossil energy inputs, substitution of 5% of fossil energy inputs through bioenergy, substitution of 30% of fossil-based electricity and 20% of nuclear electricity through renewable electricity (solar PV, hydro, wind) in production processes and in final demand.
<i>Start of the transition</i>	2030.	2075.
Key parameters during the transition		

<i>Inequality between and within societies</i>	Complete convergence between classes and regions to 7,500 €.	Relatively high convergence between classes and regions around 7,500 €.
<i>Consumption inequality</i>	<p>Consumption inequality (CI) between classes is represented through a vector containing the consumption ratios between all 9 classes of the global economy and the P30P class. The target consumption ratios in 2040 can be described by a matrix with the columns describing the world regions (center, semiperiphery, periphery) and the rows describing the classes (R20, M50, P30).</p> $CI_{2040} = \begin{matrix} & 1 & 1 & 1 \\ 1 & & 1 & 1 \\ & 1 & 1 & 1 \end{matrix}$	<p>The target consumption ratios in 2085 are described as:</p> $CI_{2084} = \begin{matrix} 1.68 & 1.54 & 1.3 \\ 1.44 & 1.32 & 1.2 \\ 1.2 & 1.1 & 1 \end{matrix}$ <p>(first column: center; second column: semiperiphery; third column: periphery; first row: R20, second row: M50; third row: P30).</p>
<i>Population policy</i>	Fertility rates reduced by 30% across all regions and age groups in the reproductive age.	Fertility rates reduced by 50% across all regions and age groups in the reproductive age.
<i>Green electrification</i>	100% renewable energy (fossil & nuclear = 0) to 2100.	100% renewable energy (fossil = 0, nuclear reduced by 50%) to 2125.
<i>Forest protection</i>	20% of the primary forest in 2019.	10% of the primary forest in 2019.
<i>Government spending</i>	Shift in government consumption vector from services to health and education.	Reduced shift in government consumption from services to health.
<i>Carbon intensity</i>	By 2100: 100% greening of electricity, substitution of 40% of fossil energy with green electricity, shift of 60% of fossil to bioenergy.	By 2125: 100% greening of electricity, substitution of 40% of fossil energy with green electricity, shift of 60% of fossil to bioenergy.
<i>Energy intensity</i>	By 2100: 10% gain in process efficiency due to higher labor intensity (additional labor hours assumed to be dedicated to the optimization of production processes) and efficiency gains from electrification.	By 2125: 5% gain in process efficiency due to lower labor intensity, efficiency gains from electrification.
<i>Mineral intensity</i>	20% reduction of inputs from the mining sector in A matrix.	
<i>Water intensity</i>	20% reduction in water intensity.	

<i>Product use duration</i>	Multiply input coefficients in the target A matrix by 0.25 to represent a 4-fold increase in product duration and use for the industry, manufacturing, transport and service sector. A matrix starts to develop toward the A matrix when the transition begins and reaches the target A matrix 70 years after the transition in FST5 and 50 years after the transition in GE.	
<i>Reuse of products</i>	Reduction of water intensity of industries and households by 50%, reduction of inputs from the mining and the non-energy biomass sector in the A matrix by 50%.	
<i>Material recycling</i>	25% reduction in inputs from the mining sector in A matrix.	
Key boundary conditions		
<i>Land intensity</i>	<p>Evolution of land intensities of the economic production are divided into a time-dependent, an output-dependent and an affluence-dependent component.</p> <p>Time-dependent component: land intensities of the energy sectors decline by 10% until 2100; forest, agricultural and 'other' land intensities decline by 20% until 2100, compared to the 2019 level.</p> <p>Output-dependent component (only for non-energy related land uses): represented through a land intensity multiplier that declines exponentially with rising output per capita levels in the food- and forestry-related sectors. The multiplier is set to reduce land intensities by 50% by the time output per capita levels have doubled. Affluence-dependent component: share of consumption budget spent on food-related products decreases as per capita consumption levels increase, which reduces the land intensity of the global economy.</p>	
<i>Labor intensity</i>	<p>Exogenous sectoral labor intensities, as changes in labor intensities are assumed to be a consequence of exogenous policies, rather than of endogenous changes in economic development. Labor intensity is assumed to fall by 10% until 2100, compared to the global 2019 levels.</p>	<p>Evolution of sectoral labor intensities has a time-dependent and an affluence-dependent component. Time-dependent component: by 2100, sectoral labor productivities reach 80% of the labor productivities of the center in 2019. Affluence-dependent component: labor intensities decline with increasing global average per capita consumption levels. The labor intensity multiplier is set to reduce labor intensities by 40% by the time global average per capita consumption reaches the average</p>

		consumption level in the center at the beginning of the simulation.
<i>Capital intensity</i>	Constant.	
<i>Feedback mechanisms</i>	Land, labor, fuel scarcity and climate damages activated; feedbacks in the climate system activated.	

3. Results

To compare the two scenarios, we organize the simulation results into three categories: (i) socio-economic and demographic variables, (ii) biophysical variables, and (iii) system-level indicators from which we can draw hypotheses regarding the stability of the world system toward the end of the simulation and beyond the simulation period. To describe the scenarios, we will use 'FST5/early-transition scenario', and 'BAU-GEG/late-transition scenario' interchangeably.

3.1. Socio-economic performance

The evolution of socio-economic variables is comparable in both scenarios until the moment when transition policies are implemented in the early-transition scenario (Fig. 1). In FST5, a population policy that reduces birth rates across all world regions and age groups in the reproductive age (15 – 44), combined with rising per capita consumption levels of the poorer social classes, results in a world population peak in 2033 and a steady decline afterwards to 4.86 billion in 2100. Conversely, in the BAU-GEG scenario world population starts to level off in the 2060s and declines significantly during the late transition period between 2075 and 2100. Although the birth reduction policy is stronger in the late-transition scenario, the population declines less and stands at 6.63 billion in 2100 (Fig. 1a). Fig. 1b-d shows the population by social class in the center, semiperiphery and periphery, illustrating both the significant difference in population size and the changes occurring during the scenarios. While the population trend is negative in both scenarios in the center, with an early transition accelerating the decline, in the semiperiphery and periphery the early transition leads to an earlier peak in population, which, in the case of the middle class of the periphery, is about half a billion lower than in the late-transition scenario. Already in 2019, the center is by far the smallest world region, and the difference grows over time in both scenarios. For example, in the late transition scenario, at the start of the simulation the size of the wealthiest 20% of the semiperiphery is still slightly smaller than half of the center's population (559 million compared to 620 million people). However, by the end of the simulation the smallest class in the semiperiphery exceeds the biggest class in the center by almost 100 million people (410 million vs. 318 million). Similarly, while the middle class of the periphery in the early-transition scenarios approaches the initial size at the end of the simulation, the size of the semiperiphery's middle class is reduced by 50% compared to 2019. Both the general decrease in world population and the relative increase in the size of classes with lower consumption levels drive reductions in total final demand, causing a

slowdown of environmental degradation. As output and investment ultimately depend on final consumption demands, the evolution of the variables Fig. 1e-h can be better understood in the context of demographic changes. Both total production and investment drop strongly during the global redistribution phase between 2030 and 2040 in the early-transition scenario as global consumption demands are reorganized. Once the target consumption rate is reached across all social classes, total output and investment decline steadily until the end of the population, driven by the decline in world population. Importantly, the output of the food sector increases during the transition period and only reaches its peak in 2049 (Fig. 1g). This is explained by the fact that the poorest classes spend a larger share of their consumption budget on food. Only as consumption levels continue to increase this share starts to shrink, eventually causing production in this sector to peak. Conversely, output in the mining and non-fossil extraction sector decreases faster than in other sectors due to the assumed technological changes that reduce the dependency of the economy on the extractive sector (Fig. 1h).

In the BAU-GEG scenario, world output, investment, food production and mineral extraction reach a plateau already before the transition occurs, reflecting the emerging restraints to further economic accumulation described in the storyline. The transition leads to a pronounced and steep decline of these variables in the period 2075-2085, which resembles dynamics of economic collapse. During the last 15 years of the simulation economic activity continues to fall but at a slower rate. Thus, in a late-transition scenario, the rate of both growth and decline is much higher than in an early transition, but due to the difference in world population, economic production is still higher in the BAU-GEG than in the FST5 scenario by 2100. Thus, an early transition avoids a potential unintentional decline in economic production imposed by emerging limits to economic growth and achieves the intended social consumption and redistribution targets with slower rates of change.

Last, Fig. 1i-l shows differences in energy-related final demand that reflects the economic impacts of technological transition policies. As with sectoral output variables, final demand for fossil (non-electric) energy (coal, gas, oil) and fossil-based electricity peak and decline at an earlier and lower level in the early-transition scenario. The decrease in final fossil energy and electricity demand in the BAU-GEG scenario (Fig. 1i & j) can be divided into three phases. The first phase between 2060 and 2075 is driven mainly by a combination of a stagnating economic production, and slow but persistent efficiency increases and substitution processes of fossil energy through renewable energy, especially renewable electricity. The second phase between 2075 and 2085 is driven primarily by a general significant reduction in overall final demand, as well as more ambitious green energy policies. The last phase (2085-2100) demonstrates the effects of the unfolding technological change policies that lead to a replacement of fossil energy types. However, final demand for fossil energy in the late-transition scenario in 2100 is still three times higher than in the case of an early transition. Also, while demand for fossil electricity reaches zero in the FST1 scenario, it is still significant in BAU-GEG.

Interestingly, demand for bioenergy and renewable electricity in the two scenarios is comparable during the majority of the simulation. As both bioenergy and renewable electricity gain importance during the transition, they increase in the early-transition scenario despite a general decrease in economic activity. Conversely, during the BAU phase of the late-transition scenario, the demand for bioenergy and renewable electricity grows primarily due to a general increase in economic scale

that has to be powered by energy. Somewhat counterintuitively, the late transition in BAU-GEG causes the demand for renewable electricity to fall below the levels of the early transition scenario. This results from the strong declines in output and demand, as well as from the fact that the energy mix in the late-transition scenario during the last 15 years of the simulation, despite the implementation of ambitious technological change policies, is still ‘dirtier’ than the energy mix in the early-transition scenario.

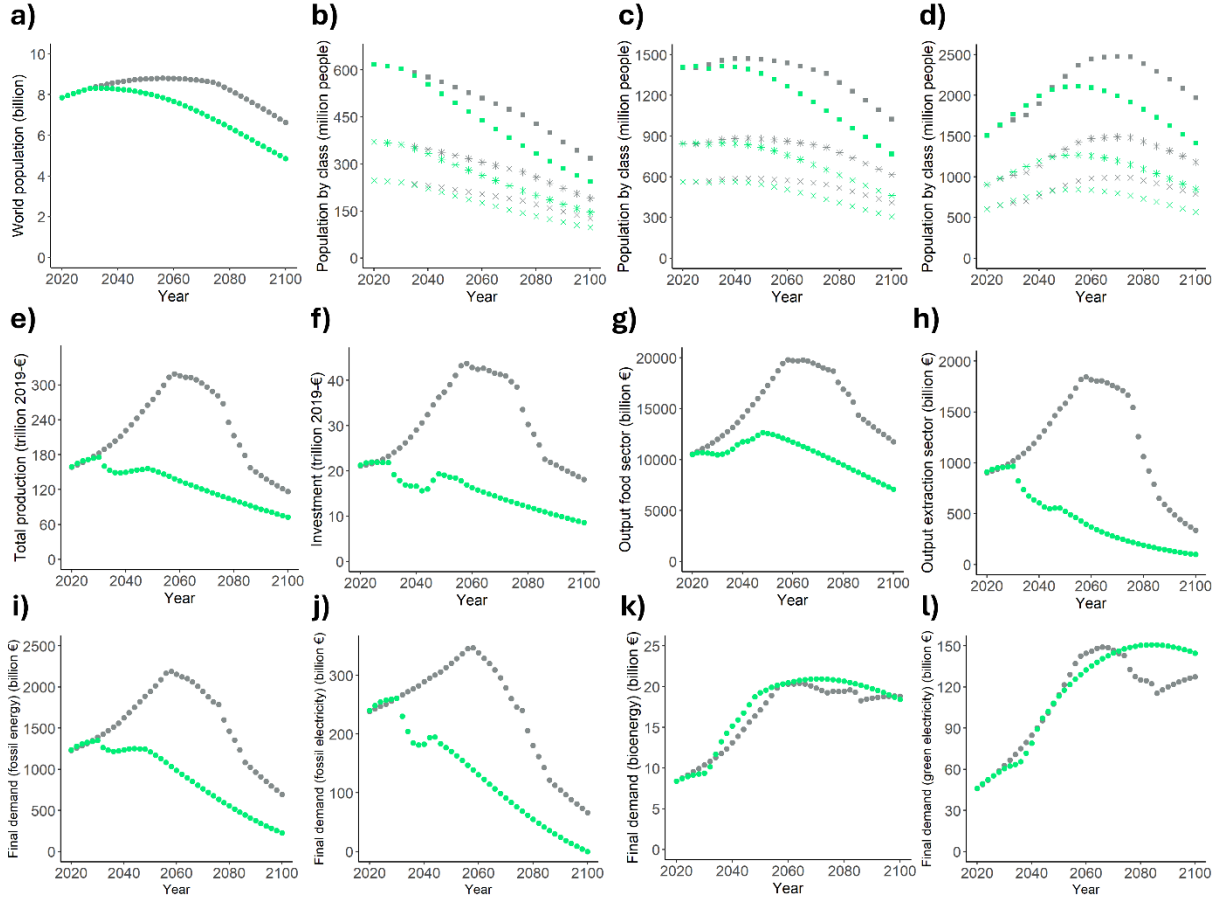


Fig. 1: Evolution of a) the world population, b) the population of the center, divided into the richest 20% (crosses), the poorest 30% (stars) and the middle 50% (squares); c) the population of the semiperiphery, divided into the richest 20% (crosses), the poorest 30% (stars) and the middle 50% (squares); d) the population of the periphery, divided into the richest 20% (crosses), the poorest 30% (stars) and the middle 50% (squares); e) world output; f) gross fixed capital formation; g) output of the food sector; h) output of the non-fossil fuel extraction sector; i) final demand for non-electric fossil energy; j) final demand for fossil-based electricity; k) final demand for biomass-based non-electric energy; l) final demand for renewable-based electricity in the early (green) and late (grey) transition scenario.

Disaggregating consumption per capita pathways by region and class, we find significant differences between an early- and a late-transition scenario for the majority of classes and during the majority of the simulation time. Consumption pathways are comparable in both scenarios for all classes until redistribution policies are implemented in the early-transition scenario after which the consumption levels of all classes in the center and the richest class in the semiperiphery decrease strongly, while they continue to grow until approximately 2060 in the late-transition scenario. However, during the last 15 years of the simulation the consumption levels in these classes

converge again due to the implementation of the late-transition social policies (Fig. 2a-d). Notably, in the late-transition scenario, the decline of consumption levels for richer classes is driven primarily by emerging limits to growth, with redistribution policies further accelerating the process.

In the case of the richest 20% of the periphery, the early transition causes consumption levels to stabilize around 2040, whereas in the late-transition scenario they continue to grow for more than two decades, reaching a level 1.8 times higher than in the early-transition scenario by 2066 (Fig. 2g). At the same time, an early transition accelerates the growth in consumption levels of the poorest 30% of the semiperiphery and the periphery as well as the middle class of the periphery. Conversely, in a late transition consumption levels of these classes begin to stagnate from the 2060s onwards, only increase with the onset of the late transition in 2075, and do not reach the levels obtained in the early-transition scenario despite the redistribution policies (Fig. 2f, h, i).

Finally, the consumption levels of the middle class of the semiperiphery follow approximately the same pathways independent from the timing of the transition (Fig. 2e).

Thus, an early transition benefits the consumption and living standards of the poorest classes of the semiperiphery and periphery, which, in 2100, constitute more than half of humanity (56% of the world population in FST5, 57% in BAU-GEG). Conversely, a late transition allows the classes of the center and the richest class of the semiperiphery and periphery to grow their consumption during a

longer time, thereby maintaining their privileged access to resources. However, by 2100 these classes make up less than a third of the world population in both scenarios.

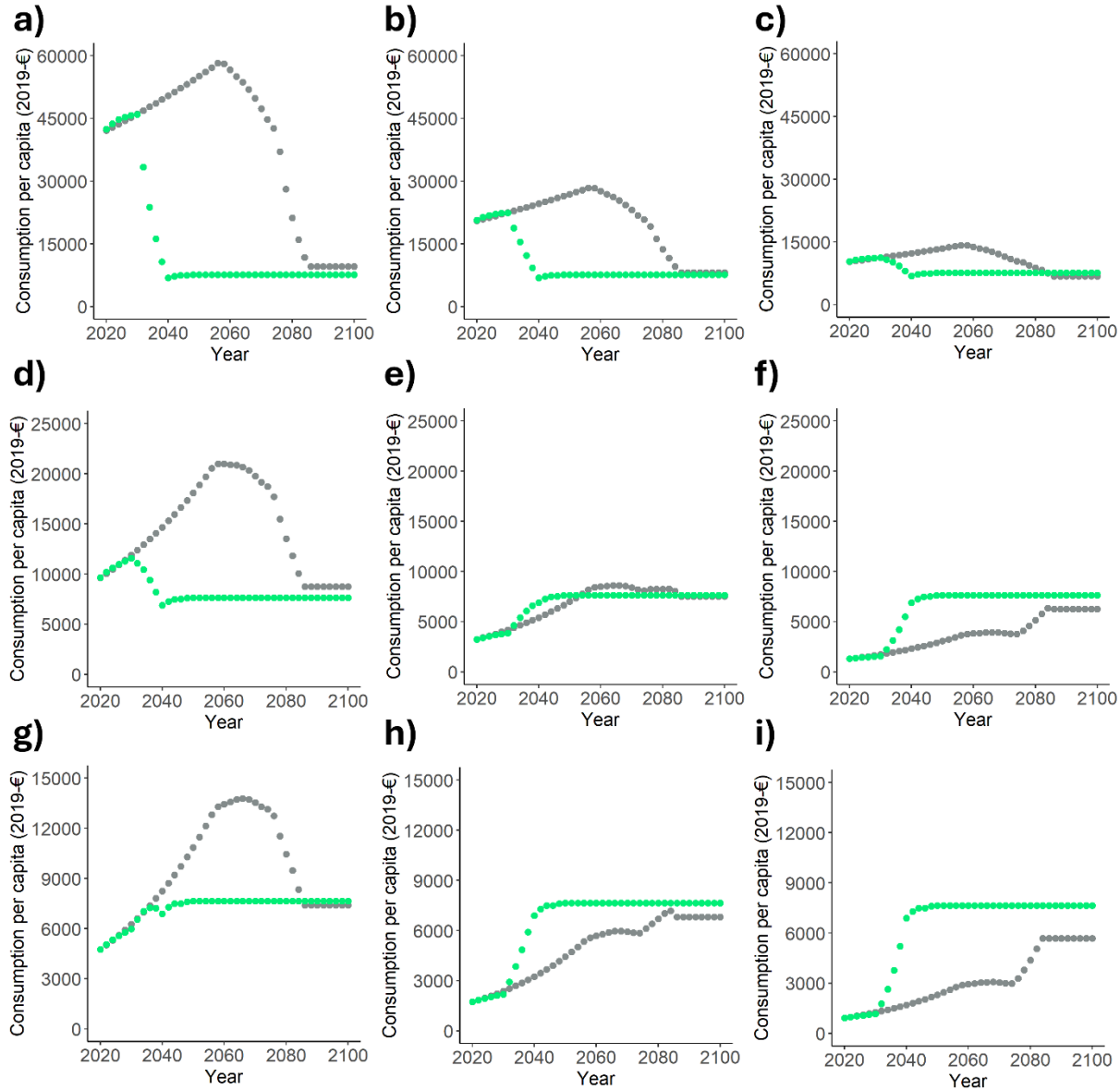


Fig. 2: Evolution of the annual consumption per capita of a) the richest 20%, b) the middle 50% and c) the poorest 30% of the center; d) the richest 20%, e) the middle 50% and f) the poorest 30% of the semiperiphery; g) the richest 20%, h) the middle 50% and i) the poorest 30% of the periphery in the early (green) and late (grey) transition scenario.

3.2. Environmental performance

Fig. 3 shows a selection of environmental indicators that point to stark differences in the environmental ‘performance’ of a delayed compared to a swift global transition. While cumulative greenhouse gas emissions follow a comparable pathway during the first two decades of the simulation, from 2040 onwards, the transition policies in the early-transition scenario strongly curb the increase in emissions. In the late-transition scenario, a slowdown in emissions can be observed from 2080 onwards, resulting in cumulative emission levels in 2100 that are more than twice as high as in the early-transition scenario (Fig. 3a). This difference is reflected in the projected changes in global average temperatures (Fig. 3a). Activated feedbacks in the climate system as well as conservative assumptions about the future evolution of greenhouse gas intensities other than CO₂ result in a temperature increase of 2.56 °C in 2100 compared to pre-industrial levels, i.e. a failure to reach the 2 °C target in the early-transition scenario, despite the strong reductions in overall CO₂ emissions. A late-transition scenario, however, not only fails to reach the 2 °C climate goal but is linked to a temperature increase of 3.95 °C which is far beyond levels of climate change considered safe (Rockström et al., 2023). Thus, both cumulative emissions and temperature changes indicate that practicing ‘business-as-usual’ beyond the second half of the 21st century will likely push the climate system into high-risk zones and that the timing of the transition might turn out to be crucial for desirable climate outcomes. However, the simulations also indicate that under the boundary conditions chosen for our simulations even an ambitious transition envisioned to start already in 2030 might turn out to be too late to avoid an ‘overshoot’, i.e. average temperatures more than 2°C higher than the pre-industrial level, during more than half a century. At the same time, although the early-transition scenario might not prevent the activation of several climate tipping points, the late-transition scenario carries a substantially higher risk of pushing the climate system into an irreversible state shift (Armstrong McKay et al., 2022; Wunderling et al., 2024).

However, not only climate variables but also other environmental variables evolve differently across the two scenarios. For example, the share of primary forest in total land area (Fig. 3c) falls earlier and further in the late-transition scenario—from nearly 11% in 2019 to 1% in 2046—with only the assumed forest protection policy preventing additional losses. In the early-transition scenario the loss of primary forest is less pronounced: by 2050, the share of primary forest in total land only has fallen from 11% to 8%, and no further losses occur during the second half of the 21st century. This result is remarkable since land intensity declines faster in the late-transition scenario than in the early-transition scenario. However, the lower levels of output of the food and (non-energy) biomass sector in the early-transition scenario more than offset the higher land intensity.

At the same time, the share of land used for the generation of renewable biomass energy or electricity in total habitable land increases faster in the late-transition scenario and, between 2050 and 2077, is higher than 10%. Only the implementation of transition policies lowers the demand for energy, and thus, the associated land demand. In the early-transition scenario, the maximum share of land used for energy generation is reached in 2049 at 7% and falls slowly afterwards to 5% in 2100. Despite the significant decline in land demand, by the end of the simulation, the land share in the late-transition scenario is still 1% higher than in the early-transition scenario (Fig. 3d). The land shares of economically used forests (Fig. 3e) and of cropland and pastures (Fig. 3f) evolve similarly in both scenarios until 2045 despite the implementation of the early-transition policies between

2030 and 2040. During the second half of the 21st century, the variables start to diverge: In the early-transition case, from 2045 onwards the share of economically used forest in total land consistently falls while in the late-transition scenario the variable stabilizes and only begins to fall with the onset of the late-transition policies. In 2100 the share of economically used forest in total land is 55% and 32% below the initial level for the early- and the late-transition scenario, respectively. In both scenarios, the land used by the industrial food sector is projected to occupy almost half of the habitable land by 2045. However, while the early transition in the long term considerably lowers the size of land used for food production, in the late-transition scenario land used for industrialized agriculture grows to occupy more than 53% in 2075 as both economic growth and land intensity improvements start to reverse in the 2060s.

Although late-transition policies manage to lower the share of land dedicated to food production to the initial level, the long periods of time in which energy and food production claim large shares of the total inhabitable land, coupled with the higher loss of primary forest, implies that the pressure on biodiversity and ecosystem integrity is much higher during the GEG scenario than during the FST5 scenario.

Fig. 3g-h shows the projected global production trends of copper, tin, and silver, which serve as essential raw materials for both general industrial applications and renewable energy technologies. In both scenarios, the share of copper, tin and silver production that is required for renewable energy technologies increases considerably, especially toward the end of the simulation period. Since total metal extraction falls faster in the early-transition scenario while the demand for renewable electricity is comparable in both scenarios the share of metals dedicated to the renewable energy sector is significantly higher in the early-transition scenario. By the end of the simulation, in the late-transition scenario half of the tin and silver production is used for the production of renewable energy technologies, the other half being processed by the remaining sectors, while in the early-transition scenario the amount of tin and silver required for renewable energies is significantly higher than the quantity of metals demanded by the rest of the economy. In the case of copper, in the late-transition scenario the rest of the economy still requires 3.45 times more material than the renewable energy sectors while in the early-transition scenario copper demand of the remaining sectors has decreased to such an extent that half of the total copper production is used for renewable energy technologies.

Comparing the simulation results across multiple environmental indicators, we can detect a trade-off between a reduction of anthropogenic pressure on the environment and a prolonged period of high consumption for richer classes. This trade-off is especially strong in the case of non-renewable stocks and non-linear tipping points in ecosystems and the climate system. For example, climate tipping points or irreversible state shifts in the Earth's biosphere (Barnosky et al., 2012) could greatly reduce the positive impacts of a late transition on the environment. Likewise, a loss of primary forest and of relatively easily accessible fossil and mineral resources during a time of prolonged 'business-as-usual' can no longer be reversed during a delayed transition.

For the poorer classes, a growth-versus-climate trade-off does not seem to apply since in both scenarios, poorer classes see their consumption levels increase during the transition while annual emissions decrease strongly. However, we find a limited trade-off with respect to agricultural land,

as rising consumption levels, especially in the case of the poorest classes, in our simulations result in higher demand for agricultural land, and thus, a higher pressure for land conversion.

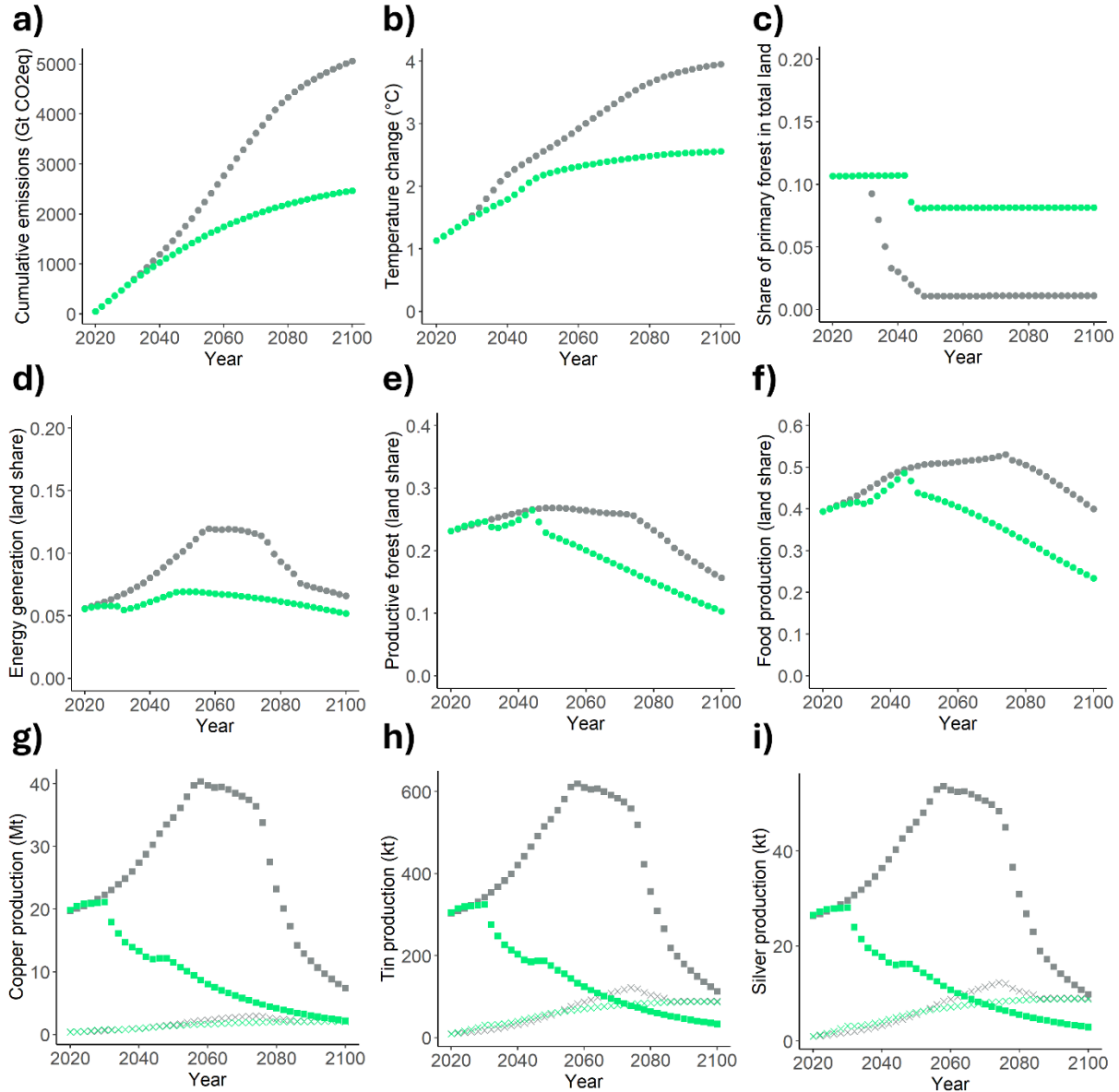


Fig. 3: Changes in a) cumulative greenhouse gas emissions between 2019 and 2100; b) global average temperature compared to pre-industrial (1850) levels; c) the share of primary forest in total land; d) the share of land used by the renewable energy sectors in total land; e) the share of economically used forest in total land; f) the share of land used by the food sector in total land; g) annual copper production for renewable energy technologies (crosses) and for the rest of the economy (squares); h) annual tin production for renewable energy technologies (crosses) and for the rest of the economy (squares); i) annual silver production for renewable energy technologies (crosses) and for the rest of the economy (squares) in the early (green) and late (grey) transition scenario.

3.2. Stability assessment

We identify five dimensions that indicate the stability and plausibility of the scenarios toward the end and beyond the 21st century: resource availability, climate change, use of input factors, public and private consumption levels, and mortality rates.

The first three dimensions point to problems in the economic reproduction process: declining resource availability can prevent the economy from fulfilling the desired consumption levels, climate change disturbs economic activities and if the intensity of input factors increases, the probability of scarcity issues increases. The last two dimensions indicate risks to social reproduction processes: declines in public spending and private consumption levels, as well as increasing mortality rates might spark social unrest and fuel distribution conflicts.

While the early-transition scenario causes fossil fuel extraction to peak in the 2030, in the late-transition scenario, fossil resource use peaks in 2057 and afterwards remains on high levels until the start of the transition. The additional extraction during the BAU phase of the late-transition scenario amounts to more than 19,000 EJ by 2075, almost half of the coal, gas and oil reserves in the model. Consequently, by 2080, despite the start of the transition, the fossil reserves have been depleted, while in the early-transition case, there are still fossil reserves left by the end of the century. With increasing depletion, resource extraction becomes costlier in terms of input factors required to produce one unit of output in the fossil resource sectors. This is reflected in an increase in the ‘extraction difficulty factor’ (Fig. 4a) that grows during the late transition but stays constant in the early transition. Since the higher degree of resource depletion cannot be reversed through transition policies, the late-transition scenario appears less stable in the long-term than the early-transition scenario, especially because both scenarios continue to rely on a small but consistent flow of fossil resources, that are used, *inter alia*, as material feedstocks.

Another source for long-term instability comes from the accelerated changes in the global climate system produced during the BAU phase of the BAU-GEG scenario (Fig. 3b). By the end of the century, the late-transition scenario is projected to face significantly higher levels of climate damages than the early-transition scenario, which exert permanent pressure on the economic production process. The high-emission pathway before the transition risks triggering critical thresholds in the climate system such as an irreversible decline of the northern AMOC (Drijfhout et al., 2025) which can lead to additional, permanent damages to the economy that are not represented by the model.

Last, comparing different intensity parameters of the two scenarios (Fig. 4b-f) we find some interesting dynamics. First, during the BAU phase of the late transition scenario, the improvement in different land and labor intensity parameters slows down and reverses. This change in the long-term trend can be interpreted as a sign of rising instability of the scenario. The implementation of transition policies, however, manages to slow down the increase of land intensities. Due to the exogenous labor intensity component in the model labor intensities eventually even begins to fall again, despite ongoing climate damages negatively affecting labor productivities. Thus, the late transition yields at least some temporal stability to the BAU-GEG scenario.

Due to different boundary conditions, land and labor intensities in the early-transition scenario are consistently higher than in the late-transition scenario. However, unlike in the late-transition scenario, the long-term trend in land productivities is positive. The impact of climate damages can be clearly seen through rising labor intensities in different sectors. The ratio between labor demand and labor supply is high but stable throughout the scenario. Thus, interestingly, despite the losses in productivity due to climate damages and the loss of labor supply due to a strong decrease and aging of the world population, there is no sign of an emergent labor scarcity issue in the early-transition scenario.

An additional variable linked to the use of input factors is the ratio between final demand and total output (Fig. 4g). The decline in this ratio can be considered a sign of increasing instability as a greater part of economic activity is dedicated to satisfy industry demand through the production of intermediate goods, rather than final demand. The transition exerts a positive effect by increasing the value of this variable under both scenarios; however, the final value attained is comparatively higher in the case of an early transition.

Turning to the potential risks for social reproduction processes, we find that by the end of the simulation projected per capita levels are at a comparable low level in both scenarios, with a slightly higher consumption of the poorest classes in the early-transition scenario. Although global public consumption is higher in the late-transition scenario (Fig. 4i), public per capita expenditures for health and education after the transition are lower than in the early-transition scenario (Fig. 4h), given that the storyline of this scenario foresees higher public expenses for security. Consequently, the key stability risk in the late-transition scenario arises less from low overall consumption than from the sharper declines affecting central regions and the richest classes elsewhere. Since these groups experience prolonged growth before the downturn, their perceived losses are greater than in the early-transition scenario, increasing the likelihood of social tensions.

Finally, the changes in mortality rates caused by transition policies are comparable in both scenarios, and benefit the semiperiphery and periphery. Thus, there is a certain trade-off between the evolution of the mortality rates in the three world regions: In an early-transition scenario, the center sees its mortality rate increase early in time, due to a strong decrease in consumption, while the periphery's mortality rates fall significantly. In the late-transition scenario, the mortality rates of the center stay low during most of the simulation period, while the mortality rates of the other world regions decline at a lower rate than in the early-transition scenario. The mortality index depicted in Fig. 4j-k is calculated to take a value of 1 for the initial mortality rate in the semiperiphery for people aged 45 to 49, and approaches 0.7 in both scenarios and in all world regions by the end of the simulation. Thus, despite the loss of life expectancy in the center, the early- as well as the late-transition policies can prevent the risks of an excessive increase in mortality rates in poorer regions due to emerging limits to growth.

In conclusion, while a late transition might be capable of temporarily increasing the world system's stability and prevent undesirable dynamics of accelerated economic breakdown, an early transition is linked to higher stability in the longer term.

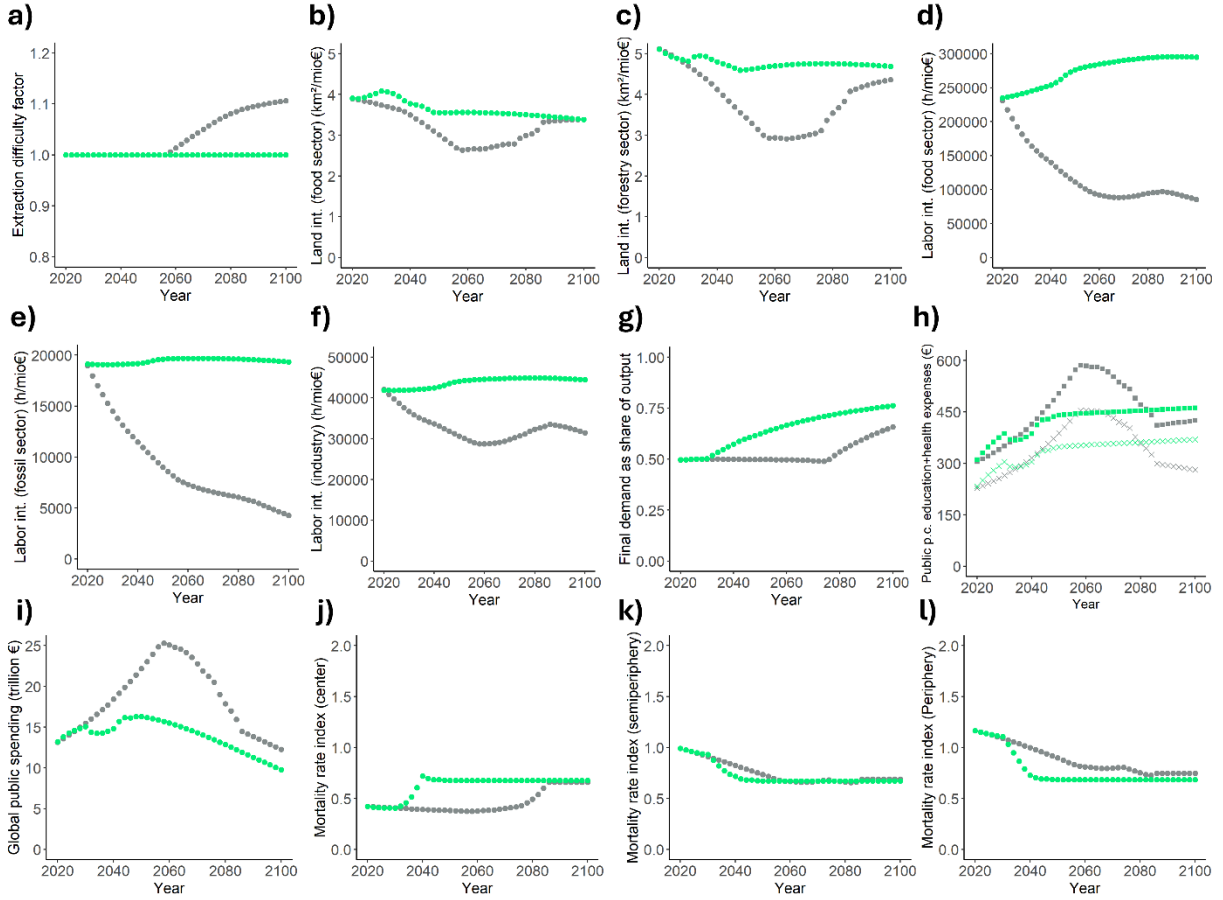


Fig. 4: Evolution of a) the fossil fuel extraction difficulty factor; b) agricultural land intensity; c) forest land intensity; d) labor intensity of the food sector; e) labor intensity of the fossil energy sector; f) labor intensity of the industrial sector; g) final demand as share of output; h) public per capita education (crosses) and health (squares) expenses; i) global public spending; j) the mortality rate index in the center; k) the mortality rate index in the semiperiphery; l) the mortality rate index in the periphery in the early (green) and late (grey) transition scenario.

Discussion

As with every other modeling study, it is important to interpret our results in the context of the model used and the assumptions made. Thus, in the following, we highlight several key scenario assumptions that influence the quantitative simulation results presented in the previous section.

First, in both the early and the delayed transition scenarios, we assume relatively fast rates of social and political change that can even surpass the rates of technological change. For example, in the GEG scenario, major social changes occur within 10 years, while technological changes take 50 years to reach the scenario targets. This sets our scenario analysis apart from modeling studies that project fast improvement rates in energy and CO₂ intensity while excluding fast structural change in the social realm (Grandjean et al., 2019). Although various theories of socio-technological change

have attempted to formalize the non-linear dynamics occurring under sustainability transitions (Petrović, 2023), maximum future rates of change in critical variables remain highly uncertain.

Second, our scenario assumptions reflect a certain optimism bias (Korteling & Toet, 2022), i.e. a possible overestimation of technological progress combined with a possible underestimation of environmental damages: On the one hand, we simulate a range of positive technological changes, such as an economy-wide shift from fossil to bioenergy, and considerable efficiency improvements due to product reuse and material recycling. On the other hand, the climate damage factors used for the simulations do not consider high-impact events with low or unknown probability, which would arguably lead to more severe disruptions of economic and governance processes. Regarding ecosystem properties, our scenarios are consistent with the assumption of highly resilient ecosystems, while they would likely cease to be feasible under brittle ecosystems (Cumming et al., 2005).

Last, the assumed decrease in land, labor and energy intensities due to learning and technological progress that take place over time, could, in theory, render an early transition less efficient than a late transition. However, in our simulations this trade-off does not manifest, since the reduction in overall economic activity is large enough to make a successful transition feasible even with higher intensities.

Despite these caveats, our work contributes to the literature on sustainability transitions by illustrating the feedback dynamics unfolding under scenarios of early and delayed global transitions. Our simulations validate the qualitative storylines by demonstrating that narrative descriptions of key patterns can be replicated through quantitative modeling. Focusing on the factor of *time* in radical just sustainability transitions, we show that an early transition is clearly desirable in terms of system stability, consumption of poorer classes, and environmental outcomes. However, while our findings support the urgency of just transitions, they also illustrate that it is never *too late* for ambitious social, ecological, and economic policies. Thus, even when emerging limiting factors begin to affect the global accumulation regime, there remain policy options to avoid worst-case socio-ecological outcomes. Nevertheless, our simulations also point to the framework conditions necessary to achieve strong climate mitigation and avoid a massive surge in mortality rates among poorer classes – namely, a declining world population size, ambitious technological policies and extremely fast and strong convergence and reductions in consumption. Based on our simulations, we hypothesize that the later the transition occurs, the higher the probability that it will take on a ‘radical’ post-growth character, since the adverse impacts of a destabilized Earth system on productive capacities increase the need for redistribution and equitable resource access to prevent the exclusion of an ever greater part of the world population from access to basic economic goods.

Consequently, we propose that future research further explore sustainability transitions occurring under *non-ideal* circumstances, including delays, maladaptation, adoption of non-optimal technological options, insufficient social redistribution, and planning failures. Quantifying such scenarios could provide society and policymakers with more realistic assessments of the socio-environmental outcomes that can be expected of future societal transitions and inform the design of policies aimed at enhancing system resilience and minimizing catastrophic harm to vulnerable human populations.

Conclusion

In this paper, we examined how the timing of a global ‘just sustainability transition’ shapes socio-economic and ecological outcomes using a comparative scenario analysis with the MORDRED-IAM. Our findings show that an early transition can prevent unintentional economic degrowth caused by environmental degradation, while achieving social consumption and redistribution targets through slower rates of change. In contrast, a delayed transition implies that the consumption declines among wealthier groups are driven first by emerging biophysical limits and later intensified by redistribution policies. Both pathways involve trade-offs—most notably between sustaining higher consumption levels and breaching critical ecological thresholds. Although a delayed transition may temporarily stabilize the global system and avoid a catastrophic economic breakdown, an earlier start of radical post-growth policies yields greater long-term resilience. Our results underscore the importance of modeling sustainability transitions under non-ideal conditions and indicate the important role radical post-growth policies could play in societal transitions that occur relatively late and in the context of mounting environmental pressures.

References

- Armstrong McKay, D. I., Staal, A., Abrams, J. F., Winkelmann, R., Sakschewski, B., Loriani, S., Fetzer, I., Cornell, S. E., Rockström, J., & Lenton, T. M. (2022). Exceeding 1.5 C global warming could trigger multiple climate tipping points. *Science*, 377(6611), eabn7950.
- Aryanpur, V., Balyk, O., Glynn, J., Gaur, A., McGuire, J., & Daly, H. (2024). Implications of accelerated and delayed climate action for Ireland's energy transition under carbon budgets. *Npj Climate Action*, 3(1), 97. <https://doi.org/10.1038/s44168-024-00181-7>
- Avelino, F., Wijsman, K., Van Steenbergen, F., Jhagroo, S., Wittmayer, J., Akerboom, S., Bogner, K., Jansen, E. F., Frantzeskaki, N., & Kalfagianni, A. (2024). Just Sustainability Transitions: Politics, Power, and Prefiguration in Transformative Change Toward Justice and Sustainability. *Annual Review of Environment and Resources*, 49(1), 519–547. <https://doi.org/10.1146/annurev-environ-112321-081722>
- Barnosky, A. D., Hadly, E. A., Bascompte, J., Berlow, E. L., Brown, J. H., Fortelius, M., Getz, W. M., Harte, J., Hastings, A., Marquet, P. A., Martinez, N. D., Mooers, A., Roopnarine, P., Vermeij, G., Williams, J. W., Gillespie, R., Kitzes, J., Marshall, C., Matzke, N., ... Smith, A. B. (2012). Approaching a state shift in Earth's biosphere. *Nature*, 486(7401), 52–58. <https://doi.org/10.1038/nature11018>
- Biermann, F., Abbott, K., Andresen, S., Bäckstrand, K., Bernstein, S., Betsill, M. M., Bulkeley, H., Cashore, B., Clapp, J., Folke, C., Gupta, A., Gupta, J., Haas, P. M., Jordan, A., Kanis, N., Kluvánková-Oravská, T., Lebel, L., Liverman, D., Meadowcroft, J., ... Zondervan, R. (2012). Transforming governance and institutions for global sustainability: Key insights from the Earth System Governance Project. *Current Opinion in Environmental Sustainability*, 4(1), 51–60. <https://doi.org/10.1016/j.cosust.2012.01.014>
- Brand-Correa, L. I., & Steinberger, J. K. (2017). A framework for decoupling human need satisfaction from energy use. *Ecological Economics*, 141, 43–52.
- Brundiers, K., & Eakin, H. C. (2018). Leveraging Post-Disaster Windows of Opportunities for Change towards Sustainability: A Framework. *Sustainability*, 10(5), 1390. <https://doi.org/10.3390/su10051390>
- Cavicchioli, R., Ripple, W. J., Timmis, K. N., Azam, F., Bakken, L. R., Baylis, M., Behrenfeld, M. J., Boetius, A., Boyd, P. W., & Classen, A. T. (2019). Scientists' warning to humanity: Microorganisms and climate change. *Nature Reviews Microbiology*, 17(9), 569–586.
- Cumming, G. S., Alcamo, J., Sala, O., Swart, R., Bennett, E. M., & Zurek, M. (2005). Are Existing Global Scenarios Consistent with Ecological Feedbacks? *Ecosystems*, 8(2), 143–152. <https://doi.org/10.1007/s10021-004-0075-1>
- Drijfhout, S., Angevaare, J. R., Mecking, J., van Westen, R. M., & Rahmstorf, S. (2025). Shutdown of northern Atlantic overturning after 2100 following deep mixing collapse in CMIP6 projections. *Environmental Research Letters*, 20(9), 094062.

- Edwards, A., Brockway, P., Bickerstaff, K., & Nijssse, F. J. (2025). Towards modelling post-growth climate futures: A review of current modelling practices and next steps. *Environmental Research Letters*.
- Ehnert, F., Egermann, M., & Betsch, A. (2022). The role of niche and regime intermediaries in building partnerships for urban transitions towards sustainability. *Journal of Environmental Policy & Planning*, 24(2), 137–159.
<https://doi.org/10.1080/1523908X.2021.1981266>
- Engler, J.-O., Kretschmer, M.-F., Rathgens, J., Ament, J. A., Huth, T., & von Wehrden, H. (2024). 15 years of degrowth research: A systematic review. *Ecological Economics*, 218, 108101.
- Fanning, A. L., & Raworth, K. (2025). Doughnut of social and planetary boundaries monitors a world out of balance. *Nature*, 646(8083), 47–56. <https://doi.org/10.1038/s41586-025-09385-1>
- Fitzpatrick, N., Parrique, T., & Cosme, I. (2022). Exploring degrowth policy proposals: A systematic mapping with thematic synthesis. *Journal of Cleaner Production*, 132764.
- Frantzeskaki, N., Dumitru, A., Anguelovski, I., Avelino, F., Bach, M., Best, B., Binder, C., Barnes, J., Carrus, G., Egermann, M., Haxeltine, A., Moore, M.-L., Mira, R. G., Loorbach, D., Uzzell, D., Omann, I., Olsson, P., Silvestri, G., Stedman, R., ... Rauschmayer, F. (2016). Elucidating the changing roles of civil society in urban sustainability transitions. *Current Opinion in Environmental Sustainability*, 22, 41–50.
<https://doi.org/10.1016/j.cosust.2017.04.008>
- Grandjean, R., Lepetit, M., & Morel, L. (2019). *Energy and climate scenarios. Evaluation and guidance*. AFEP. https://theshiftproject.org/app/uploads/2025/02/Etude-Scenarios-Afep_TSP-Rapport-final-EN.pdf
- Haberl, H., Wiedenhofer, D., Virág, D., Kalt, G., Plank, B., Brockway, P., Fishman, T., Hausknost, D., Krausmann, F., & Leon-Gruchalski, B. (2020). A systematic review of the evidence on decoupling of GDP, resource use and GHG emissions, part II: synthesizing the insights. *Environmental research letters*, 15(6), 065003.
- Harvey, J. A., Tougeron, K., Gols, R., Heinen, R., Abarca, M., Abram, P. K., Basset, Y., Berg, M., Boggs, C., & Brodeur, J. (2023). Scientists' warning on climate change and insects. *Ecological monographs*, 93(1), e1553.
- Hickel, J. (2019). Is it possible to achieve a good life for all within planetary boundaries? *Third World Quarterly*, 40(1), 18–35.
<https://doi.org/10.1080/01436597.2018.1535895>
- Hickel, J., Brockway, P., Kallis, G., Keyßer, L., Lenzen, M., Slameršák, A., Steinberger, J., & Ürge-Vorsatz, D. (2021). Urgent need for post-growth climate mitigation scenarios. *Nature Energy*, 6(8), 766–768.
- IEA. (2022). *World Energy Outlook 2022*. <https://www.iea.org/reports/world-energy-outlook-2022>

- IPCC. (2018). *Global Warming of 1.5°C: IPCC Special Report on Impacts of Global Warming of 1.5°C above Pre-industrial Levels in Context of Strengthening Response to Climate Change, Sustainable Development, and Efforts to Eradicate Poverty* (1. Aufl.). Cambridge University Press. <https://doi.org/10.1017/9781009157940>
- Kallis, G., Hickel, J., O'Neill, D. W., Jackson, T., Victor, P. A., Raworth, K., Schor, J. B., Steinberger, J. K., & Ürge-Vorsatz, D. (2025). Post-growth: The science of wellbeing within planetary boundaries. *The Lancet Planetary Health*, 9(1), e62–e78.
- Kallis, G., Mastini, R., & Zografos, C. (2024). Perceptions of degrowth in the European Parliament. *Nature Sustainability*, 7(1), 64–72.
- Korteling, J. E., & Toet, A. (2022). Cognitive Biases. In *Encyclopedia of Behavioral Neuroscience*, 2nd edition (S. 610–619). Elsevier. <https://doi.org/10.1016/B978-0-12-809324-5.24105-9>
- Lauer, A., de Castro, C., & Carpintero, Ó. (2024). Between continuous presents and disruptive futures: Identifying the ideological backbones of Global Environmental Scenarios. *Futures*, 103460.
- Lauer, A., De Castro, C., & Carpintero, Ó. (2025). Beyond Green capitalism: Global scenarios for fast societal transitions toward sustainability. *Environmental Innovation and Societal Transitions*, 56, 100981. <https://doi.org/10.1016/j.eist.2025.100981>
- Lauer, A., & Llases, L. (2025a). Business as usual on the highway to hell? Limits to growth and future world orders. *Under Review*.
- Lauer, A., & Llases, L. (2025b). *MORDRED: Model Of Resource Distribution and Resilient Economic Development. Model Documentation*. GitHub. <https://github.com/Pendracus/MORDRED>
- Lawrence, M., Homer-Dixon, T., Janzwood, S., Rockström, J., Renn, O., & Donges, J. F. (2024). Global polycrisis: The causal mechanisms of crisis entanglement. *Global Sustainability*, 7, e6.
- Lenton, T. M., Rockström, J., Gaffney, O., Rahmstorf, S., Richardson, K., Steffen, W., & Schellnhuber, H. J. (2019). Climate tipping points—Too risky to bet against. *Nature*, 575(7784), 592–595.
- Martinico-Perez, M. F. G., Schandl, H., Fishman, T., & Tanikawa, H. (2018). The Socio-Economic Metabolism of an Emerging Economy: Monitoring Progress of Decoupling of Economic Growth and Environmental Pressures in the Philippines. *Ecological Economics*, 147, 155–166. <https://doi.org/10.1016/j.ecolecon.2018.01.012>
- Matsuura, M. (2022). Disasters as Enablers of Negotiation for Sustainability Transition: A Case from Odaka, Fukushima. *Sustainability*, 14(5), 3101. <https://doi.org/10.3390/su14053101>
- Millward-Hopkins, J., Steinberger, J. K., Rao, N. D., & Oswald, Y. (2020). Providing decent living with minimum energy: A global scenario. *Global Environmental Change*, 65, 102168.

- Mitchell, R. B., Andonova, L. B., Axelrod, M., Balsiger, J., Bernauer, T., Green, J. F., Hollway, J., Kim, R. E., & Morin, J.-F. (2020). What We Know (and Could Know) About International Environmental Agreements. *Global Environmental Politics*, 20(1), 103–121. https://doi.org/10.1162/glep_a_00544
- Petrović, E. K. (2023). Sustainability Transition Framework: An Integrated Conceptualisation of Sustainability Change. *Sustainability*, 16(1), 217. <https://doi.org/10.3390/su16010217>
- Pyšek, P., Hulme, P. E., Simberloff, D., Bacher, S., Blackburn, T. M., Carlton, J. T., Dawson, W., Essl, F., Foxcroft, L. C., & Genovesi, P. (2020). Scientists' warning on invasive alien species. *Biological Reviews*, 95(6), 1511–1534.
- Raskin, P., & Swart, R. (2020). Excluded futures: The continuity bias in scenario assessments. *Sustainable Earth*, 3(1), 1–5.
- Richardson, K., Steffen, W., Lucht, W., Bendtsen, J., Cornell, S. E., Donges, J. F., Drücke, M., Fetzer, I., Bala, G., & von Bloh, W. (2023). Earth beyond six of nine planetary boundaries. *Science advances*, 9(37), eadh2458.
- Ripple, W. J., Wolf, C., Gregg, J. W., Levin, K., Rockström, J., Newsome, T. M., Betts, M. G., Huq, S., Law, B. E., & Kemp, L. (2022). *World scientists' warning of a climate emergency* 2022.
- Ripple, W. J., Wolf, C., Gregg, J. W., Rockström, J., Mann, M. E., Oreskes, N., Lenton, T. M., Rahmstorf, S., Newsome, T. M., Xu, C., Svenning, J.-C., Pereira, C. C., Law, B. E., & Crowther, T. W. (2024). The 2024 state of the climate report: Perilous times on planet Earth. *BioScience*, 74(12), 812–824. <https://doi.org/10.1093/biosci/biae087>
- Ripple, W. J., Wolf, C., Gregg, J. W., Rockström, J., Newsome, T. M., Law, B. E., Marques, L., Lenton, T. M., Xu, C., & Huq, S. (2023). The 2023 state of the climate report: Entering uncharted territory. *BioScience*, 73(12), 841–850.
- Ripple, W. J., Wolf, C., Newsome, T. M., Galetti, M., Alamgir, M., Crist, E., Mahmoud, M. I., Laurance, W. F., & 15, 364 Scientist Signatories from 184 Countries. (2017). World scientists' warning to humanity: A second notice. *BioScience*, 67(12), 1026–1028.
- Rizzo, A., Cappellano, F., Pierantoni, I., & Sargolini, M. (2022). Do natural disasters accelerate sustainability transitions? Insights from the Central Italy earthquake. *European Planning Studies*, 30(11), 2224–2244. <https://doi.org/10.1080/09654313.2021.2022104>
- Rockström, J., Gupta, J., Qin, D., Lade, S. J., Abrams, J. F., Andersen, L. S., Armstrong McKay, D. I., Bai, X., Bala, G., Bunn, S. E., Ciobanu, D., DeClerck, F., Ebi, K., Gifford, L., Gordon, C., Hasan, S., Kanie, N., Lenton, T. M., Loriani, S., ... Zhang, X. (2023). Safe and just Earth system boundaries. *Nature*, 619(7968), 102–111. <https://doi.org/10.1038/s41586-023-06083-8>
- Rothman, D. S., Raskin, P., Kok, K., Robinson, J., Jäger, J., Hughes, B., & Sutton, P. C. (2023). Global Discontinuity: Time for a Paradigm Shift in Global Scenario Analysis. *Sustainability*, 15(17), 12950.

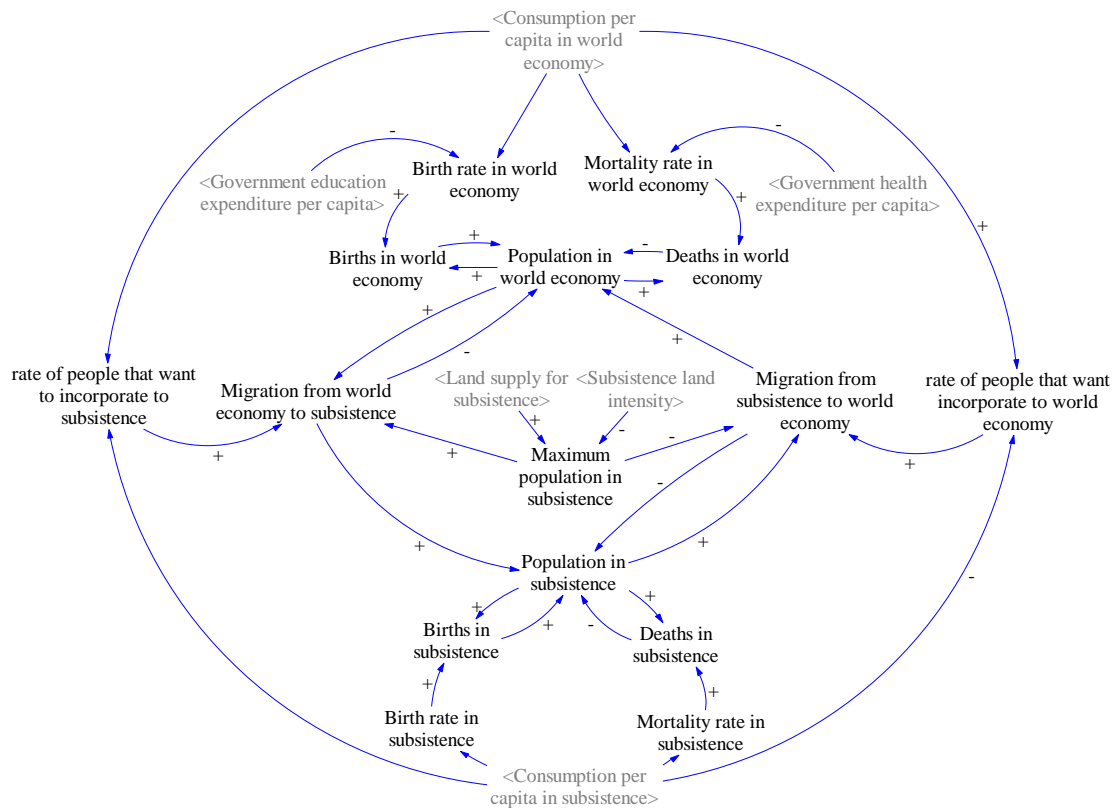
- Schaeffer, M., Gohar, L., Kriegler, E., Lowe, J., Riahi, K., & Van Vuuren, D. (2015). Mid- and long-term climate projections for fragmented and delayed-action scenarios. *Technological Forecasting and Social Change*, 90, 257–268.
<https://doi.org/10.1016/j.techfore.2013.09.013>
- Schmeller, D. S., Urbach, D., Bates, K., Catalan, J., Cogălniceanu, D., Fisher, M. C., Friesen, J., Füreder, L., Gaube, V., & Haver, M. (2022). Scientists' warning of threats to mountains. *Science of the Total Environment*, 853, 158611.
- Schmelzer, M. (2017). The growth paradigm: History, hegemony, and the contested making of economic growthmanship. In *Routledge Handbook of the History of Sustainability* (S. 164–186). Routledge.
- Streeck, J., Wiedenhofer, D., Krausmann, F., & Haberl, H. (2020). Stock-flow relations in the socio-economic metabolism of the United Kingdom 1800–2017. *Resources, Conservation and Recycling*, 161, 104960.
<https://doi.org/10.1016/j.resconrec.2020.104960>
- Van Eynde, R., Dillman, K. J., Vogel, J., & O'Neill, D. W. (2025). What is required for a post-growth model? *arXiv preprint arXiv:2508.07974*.
- Vogel, J., & Hickel, J. (2023). Is green growth happening? An empirical analysis of achieved versus Paris-compliant CO₂-GDP decoupling in high-income countries. *The Lancet Planetary Health*, 7(9), e759–e769.
- Wiedmann, T., Lenzen, M., Keyßer, L. T., & Steinberger, J. K. (2020). Scientists' warning on affluence. *Nature communications*, 11(1), 1–10.
- Winning, M., Price, J., Ekins, P., Pye, S., Glynn, J., Watson, J., & McGlade, C. (2019). Nationally Determined Contributions under the Paris Agreement and the costs of delayed action. *Climate Policy*, 19(8), 947–958.
<https://doi.org/10.1080/14693062.2019.1615858>
- Wunderling, N., von der Heydt, A. S., Aksenenov, Y., Barker, S., Bastiaansen, R., Brovkin, V., Brunetti, M., Couplet, V., Kleinen, T., & Lear, C. H. (2024). Climate tipping point interactions and cascades: A review. *Earth System Dynamics*, 15(1), 41–74.

Supplementary Material

1. Feedback links between core model variables

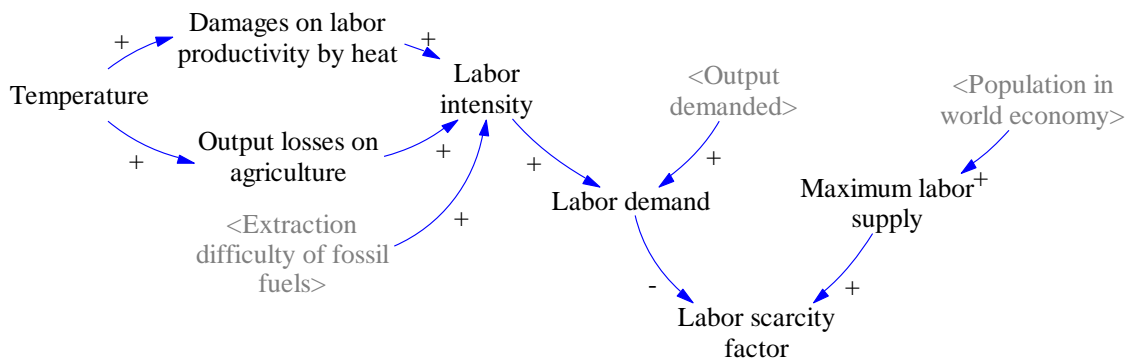
Source for all figures: https://github.com/Pendracus/MORDRED/blob/main/Diagrams_MORDRED.pdf.

Demography module



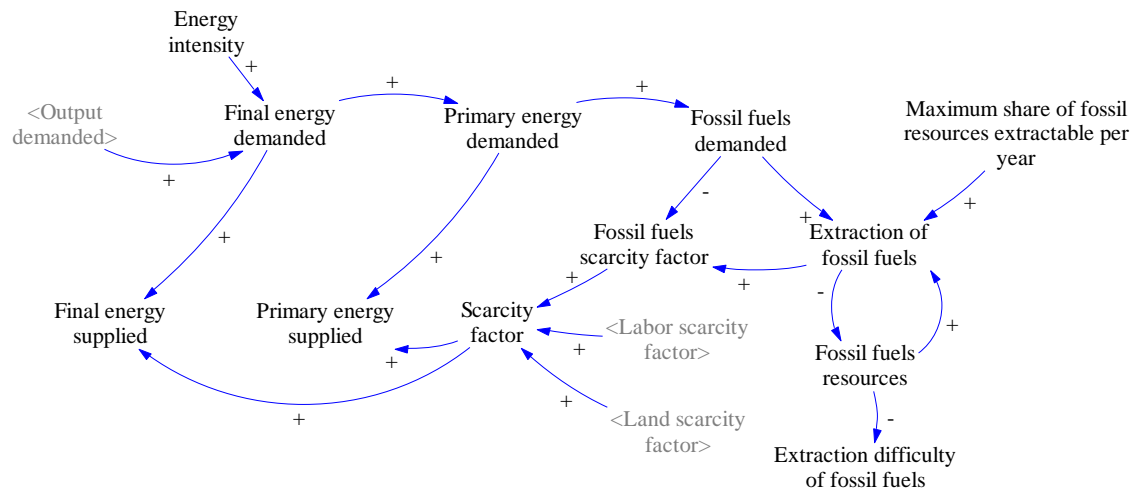
Suppl. Figure 1: Key variables and dynamics in the demographic module.

Labor module



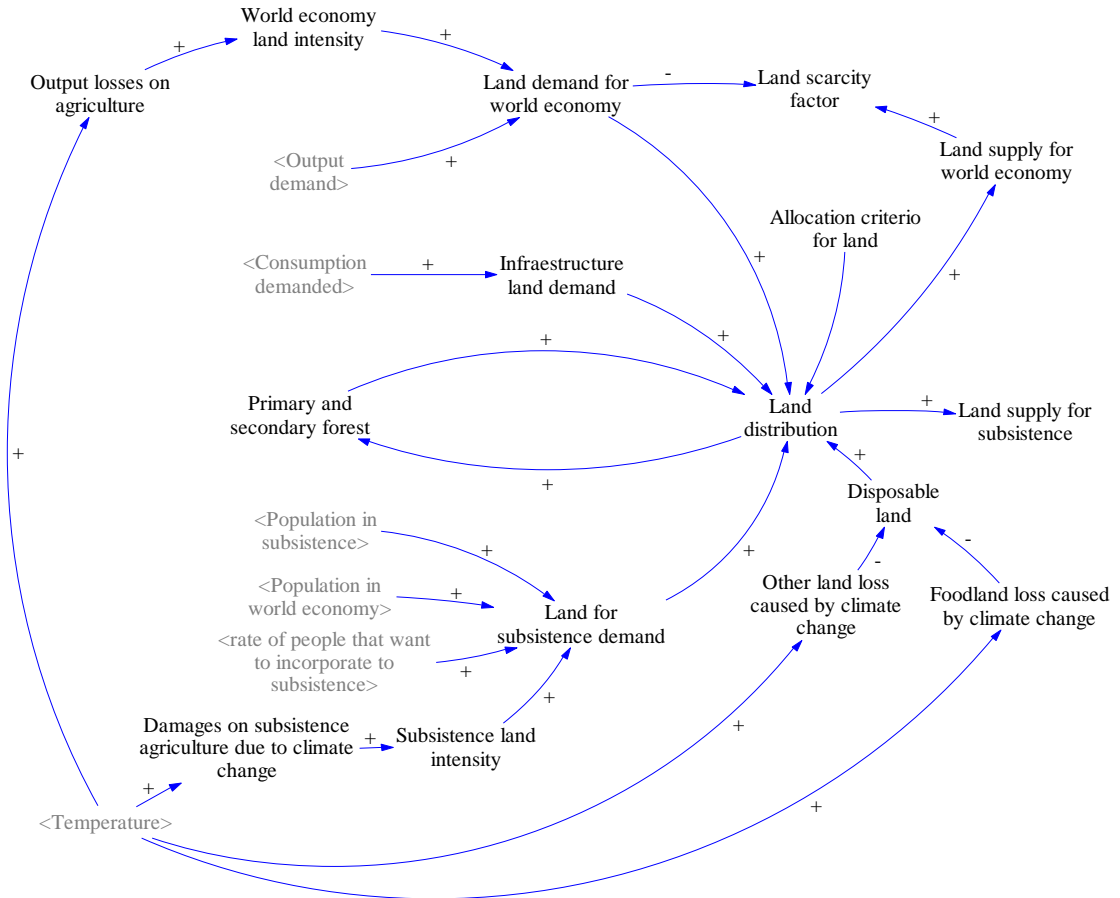
Suppl. Figure 2: Key variables and dynamics in the labor module.

Energy module



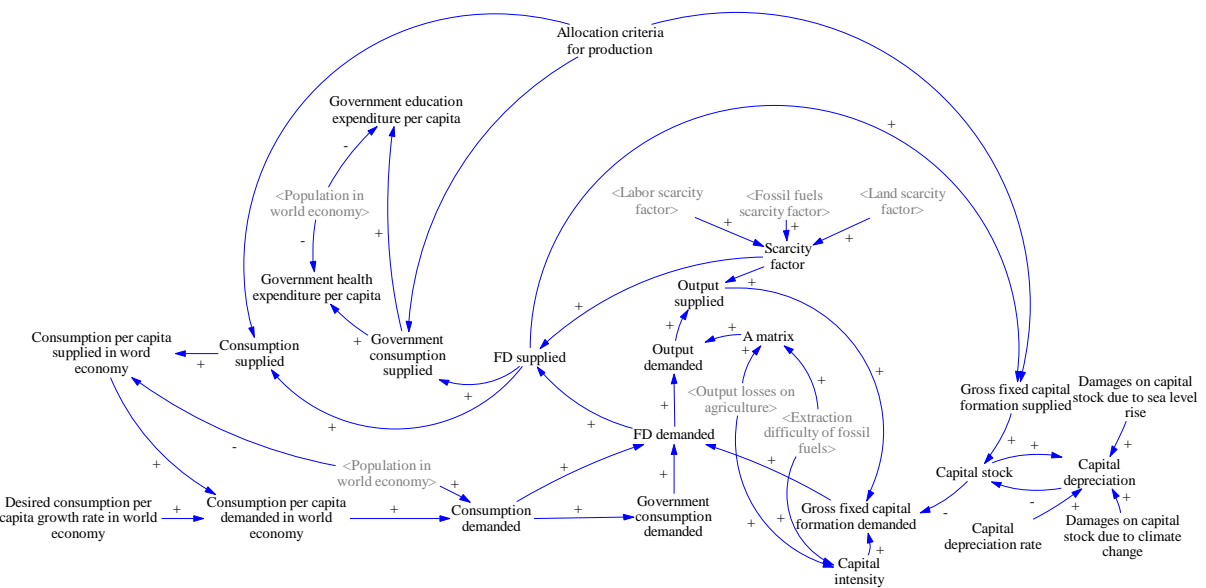
Suppl. Figure 3: Key variables and dynamics in the energy module.

Land module



Suppl. Figure 4: Key variables and dynamics in the land module.

Economy module



Suppl. Figure 5: Key variables and dynamics in the economy module.

2. Comparison of qualitative scenario variables with model variables

Suppl.Table 1 contains a comparison between important variables from the selected scenarios and representation of those variables in MORDRED. The scenario variables are drawn from the translation protocols for the two scenarios which are mentioned in the main text. Although not all variables are reflected in the model's structure, we consider the representation sufficient to take the two storylines as basis for an 'early' and a 'late' transition scenario. Nevertheless, we wish to point out that it is important to keep in mind the missing variables when interpreting our simulation results.

Scenario variable (FST5 / BAU-GEG)	Model representation
<i>Changes in the scale of economic activities</i>	Overall economic scale depends on sectoral output which changes endogenously in the model
<i>Changes in the size of human population</i>	Overall size of the human population depends on region- and age-specific death and birth rates which change endogenously in the model
<i>Economic scale in relation to well-being requirements</i>	No explicit well-being indicators; implicit through life expectancy and consumption of different basic goods (health, education etc.)
<i>Economic scale in relation to energy & material flows within the bioregion</i>	No representation
<i>Military & security</i>	Security expenses included in the public consumption of services
<i>Earth intensities</i>	Fossil fuel, energy, land, mineral, biomass and water intensity represented
<i>Duration of materials in economic sphere</i>	Representation through A-Matrix
<i>Changes in labor & capital intensity</i>	Increases or reductions possible
<i>Consumption inequality</i>	Increases or reductions possible

<i>Need-based allocation</i>	No representation
<i>Control over productive capacity</i>	No representation
Influence of unequal consumption on life expectancy	Mortality rates increase with decreases in per capita consumption
Influence of climate damages on life expectancy	Mortality rates are negatively affected by climate damages through reduced per capita consumption
Influence of violent conflicts on life expectancy	No representation
Evolution of per capita consumption	Consumption per capita disaggregated into 4 different classes and 3 world regions
Hegemonic discourse and values	No representation
Power distribution, monopoly of violence, political actors, conflict resolution	No representation
Trade regime	Global production system
Interregional inequality	Increases or reductions possible
Class inequality	Increases or reductions possible
Social policy	Increases or reductions in total government spending and spending in certain sectors
Military policy	Indirect representation through sectorial government spending for services and industry
Migration policy	Migration between formal and subsistence economy; no representation of other types of migration
Environmental policy	Reduction or increase of available fuels, protection of different land types (subsistence land, primary, secondary forests and agricultural land), changes in material inputs into the economic process, caused by recycling or product reuse
Economic policy	Representation of distribution, investment and technology.
Mode of production, goal and control of production	No representation of economic mode of production and socio-economic configurations
Allocation principles	Representation of territorial, class based, age based and egalitarian allocation
Productivity/intensity of economic production	Representation of labor productivity, capital productivity, land intensity, energy intensity, material intensity of production;
Energy types	Representation of carbon, petroleum and gas, fossil electricity, hydro-electricity, solar PV, wind electricity, nuclear electricity, biomass based energy
Mitigation	Mitigation through changes in economic structure
Adaptation	No explicit representation of adaptation. Adaptation capacity assumed to be a function of consumption per capita
Earth system	Representation of climate system, different land types, land conversion, energy, material, biomass and water extraction. Climate damages affecting output, land, labor and capital stocks, as well as land, labor and capital intensities. Pollution flows: air pollution, P&N pollution.

Suppl.Table 1: Comparison of scenario and model variables.

From Greener growth to sufficiency: modeling alternative global sustainability pathways

Abstract

This study quantifies two contrasting global sustainability transition scenarios—FST1: Greener Growth and FST5: Sufficiency Economies—using the MORDRED system dynamics model. While both scenarios pursue high levels of decarbonization without relying on speculative technologies, they embody distinct paradigms: FST1 prioritizes economic growth through green technology and efficiency improvements, whereas FST5 centers on sufficiency, redistribution, and social well-being within ecological limits. The quantitative simulations generate demographic, economic, and biophysical trajectories that complement their qualitative storylines, allowing a plausibility assessment of each transition pathway. Results show that FST1 achieves rapid technological decarbonization but remains constrained by resource and land scarcity, resulting in persistent inequalities and a failure to achieve international climate goals. In contrast, FST5 achieves strong convergence in consumption and mortality rates across regions and classes, stabilizing global warming at 1.9 °C by 2100 while reducing material and water extraction as well as pressures on land systems. At the same time, strong decarbonization increases the renewable sector's share of global resource extraction. Both scenarios appear stable beyond the end of the qualitative storyline in 2075, although the greater level of environmental pressure and inequality in FST1 pose mid- and long-term risks for its stability. Sensitivity analyses demonstrate that scenario plausibility depends on assumptions about climate sensitivity as well as land and labor productivity growth. Overall, this study underscores the importance of integrating qualitative narratives with quantitative modeling to explore plausible global transformation pathways and highlights that sufficiency-oriented transitions may offer more robust sustainability outcomes than growth-oriented ones.

Keywords

Integrated assessment modeling, global environmental scenarios, sustainability transitions, convergence, green growth, decarbonization

1. Introduction

Meeting global climate and sustainability objectives requires profound societal transformations and ambitious policy interventions that break with ‘business-as-usual’ practices, although concrete transition pathways remain contested (Köhler et al., 2019; Scoones et al., 2020; Wiedmann et al., 2020). Sustainability transitions have been linked to Green economies in both the Global North and South (Brown et al., 2014; Hochstetler, 2025; Lederer et al., 2018) as well as to the development of a circular economy (Abunyewah et al., 2023; Fetanat et al., 2021; Flynn et al., 2019), but also to more radical post-growth or degrowth transitions emphasizing the need to reduce consumption inequality and to overcome the ‘growth paradigm’ (Hickel, 2019; Kallis et al., 2025; Schmelzer, 2017).

Debates about sustainability transitions can be informed and enriched by the development of global environmental scenarios that provide visions for desirable futures but also identify socio-economic and biophysical risks within the scenario space (Juri et al., 2025; Msangi, 2013; Pereira et al., 2021; Wilkinson & Mangalagiu, 2012). Ideally, qualitative and quantitative approaches should complement and inform each other through iterative feedbacks, resulting in scenarios rich in narrative detail and supported by quantitative modeling (Alcamo, 2008). In practice, however, modeling and time constraints often lead to scenario exercises that focus predominantly on either storyline creation or model development.

For instance, many quantitative modeling studies of low-demand or sufficiency transitions lack the narrative context provided by detailed storylines that situate modeled measures within coherent and plausible socio-political trajectories (Millward-Hopkins et al., 2020; Wiese, Taillard, et al., 2024; Wiese, Zell-Ziegler, et al., 2024). Moreover, scenario studies with a quantitative component often embody a ‘continuity bias’ (Raskin & Swart, 2020) characterized by the absence of transformative structural changes in the economic, political, and cultural realms that deviate from the status quo (Lauer et al., 2024). For example, strong climate mitigation pathways based on the Low Energy Demand (LED) scenario (Grubler et al., 2018) or SSP2 (Van Vuuren et al., 2018) do not engage with the systemic politico-economic and cultural preconditions that would render the modeled policies feasible. Global sustainability scenarios featuring strong and rapid convergence between the Global North and South toward energy levels compatible with meeting basic human needs remain underexplored (Hickel & Slamersak, 2022). Likewise, systematic model-based comparisons of radically different global-scale transformation pathways and policies have yet to be conducted.

Conversely, many qualitative scenarios reflecting more radical approaches to sustainability are characterized by absent or insufficient quantification (Durán et al., 2023; Otero et al., 2020; Sessa & Ricci, 2014), partly due to the limited capacity of existing integrated assessment models (IAMs) to represent radical systemic change. As a result, their concrete implications for material flows, inequality, and environmental outcomes remain invisible.

Further examples for qualitatively rich scenarios lacking a model-based quantitative exploration are the six recently developed ‘fast sustainability transition scenarios’ (FSTs) (Lauer et al., 2025), which narrate alternative sustainability transformation pathways based on competing socio-economic paradigms and approaches to addressing global socio-economic and environmental challenges, including strong convergence and relocalization as well as eco-socialist and green capitalist growth strategies.

This article aims to complement the FST development by quantifying two of the six FSTs (‘FST1 – Greener Growth’ and ‘FST5 – Sufficiency Economies’) using a recently developed IAM. The

quantification exercise serves four purposes. First, to enrich the qualitative scenario content with a quantitative dimension that illustrates the rate and scale of the envisioned changes. Second, to assess the extent to which the simulated quantitative dynamics align with the scenario storylines and, where relevant, to uncover unexpected dynamics or contradictions between the qualitative and quantitative versions. Third, to compare projected developments in social, economic, and environmental systems across two scenarios featuring transformative changes grounded in distinct sustainability approaches. Finally, to explore how variations in boundary conditions affect simulation results, thereby narrowing the parameter range within which quantitative dynamics align with qualitative scenario content, enabling a plausibility assessment of both scenarios.

2. Methods

2.1. Scenario and model description

FST1 and FST5 are two of six global sustainability scenarios describing potential changes in world order, cultural hegemony, (geo)political alliances and global modes of production that align to form global societal transition pathways spanning several decades. We selected the scenarios because they represent fundamentally different approaches to solving the ‘sustainability conundrum’. Although both aim to achieve greater social, environmental, and economic sustainability throughout the 21st century, in cases of conflict between these goals, FST1 prioritizes economic growth over environmental and social objectives, whereas in FST5, well-being—linked to the notion of ‘sufficiency’—is given the highest political priority.

In FST1, by the end of the 2020s, a new historical bloc emerges that successfully advances a global ‘green growth’ agenda, which becomes mainstreamed into economic and social policies with the support of international institutions, civil society, and intellectuals. While the development of green technological innovation is promoted, less attention is paid to social welfare and inequality. Conversely, in FST5, by the late 2020s, a global movement grounded in strong ecological and social values persuades a group of states to advocate for the establishment of a Planetary Confederation to fundamentally transform the global economic system and decisively address socio-environmental challenges, focusing particularly on basic human needs and sufficiency in consumption.

The complete storylines, which narrate power struggles among social actors, shifts in public discourse, and the implementation of diverse sustainability policies, are detailed in Lauer et al (2025).

The model used to quantify FST1 and FST5 is called MORDRED (Model Of Resource Distribution and Resilient Economic Development). MORDRED is an environmentally and socially extended input-output (IO) model coupled with a demographic model and a climate model, reflecting the growing interest in linking IAM and IO modeling approaches (Lefèvre, 2024; Malik & Schaeffer, 2024). The model was developed to portray non-linear global environmental futures characterized by historical discontinuities in economic growth and demographic developments, as well as scenarios of strong redistribution between and within societies. MORDRED’s subcomponents, structure, and data sources are described in detail in the model documentation (Lauer & Llases, 2025).

The model’s components represent and project future developments across different systems at the global level. The evolution of the world population results from changes in mortality and

fertility rates across three world regions and 20 age cohorts, which are driven by individuals' per capita consumption levels and by public per capita expenditures on health and education. These variables depend on both the region of residence and the individual's social class. At the beginning of each model simulation, the world region 'center'—comprising high-income countries—has the highest per capita health and education expenditures, followed by the 'semiperiphery', consisting of upper-middle-income countries, and the 'periphery', which aggregates all low- and lower-middle-income countries. Within each region, the population fully participating in the global economy is divided into three segments: the richest 20%, the poorest 30%, and the remaining 50%, constituting the middle class. Exogenous scenario assumptions determine how the global distribution of economic consumption goods evolves over the simulation period, enabling the modeling of economic convergence and divergence. Thus, MORDRED can represent different socio-economic groups and inequalities, as well as various forms of distributional justice—an important step toward incorporating justice considerations into IAMs (Low et al., 2025).

Global economic production is represented through Leontief production functions and disaggregated into 25 sectors listed in the Supplementary Material (SM). This sectoral disaggregation allows for the projection of scenario-based developments across different energy sectors, including fossil fuels, biomass, hydropower, solar PV, wind, nuclear, and fossil electricity.

MORDRED's environmental modules project changes in the global climate and land systems and also track the evolution of various forms of air, soil, and water pollution. Additionally, the model converts the economic output of the mining sector into biophysical quantities of extracted materials, including several key minerals for the energy (Owen et al., 2022; Valero et al., 2018).

Importantly, the model incorporates a set of linkages between variables that may constrain economic growth. These constraints operate through several channels. First, labor scarcity arises when the demand for labor hours exceeds the maximum labor supply, which depends on the size of the global working-age population. Second, land scarcity occurs when the demand for specific land types surpasses their available supply. Third, fossil energy scarcity results from the progressive depletion of fossil fuel reserves, ultimately limiting the amount of extractable energy resources per unit of time and increasing extraction costs. Fourth, climate-related damages affect economic performance by reducing the availability and productivity of labor and land, as well as diminishing the capital stock. In addition, production in any sector may decline if the demand for intermediate goods required in the production process cannot be met.

The structure of MORDRED allows scenario developers to selectively activate or deactivate policies, feedback mechanisms, or entire submodules. Depending on the scenario, exogenous parameters can be modified, and new parameters can be added to simulate the effects of different policies—for example, population policies or changes in government expenditure.

Using a single model to quantify both scenarios not only simplifies parameterization and simulation but also enhances the comparability of results. Consequently, differences in the development of key variables arise exclusively from differences in scenario parameter assumptions based on their respective storylines, rather than from differences in model structure.

2.2. Scenario parametrization

To quantify the FST1 and FST5 storylines, we use the translation protocol outlined in Lauer et al. (2025), which consists of a series of scenario objectives pursued to different degrees in each FST. In every scenario, each objective is assigned a level ranging from 0, indicating that the objective is not pursued, to 4, indicating that it is strongly pursued. Consequently, the main part of the parametrization process consisted of identifying which scenario objectives could be represented in MORDRED and assigning the relevant variables numerical values that reflect the indicated level. In this way, the qualitative differences between FST1 and FST5 were ‘translated’ into quantitative differences.

When determining the concrete numerical values, we sought to balance two goals: selecting values that reproduce the developments described in the storylines, and avoiding rates of change that would appear implausible or unfeasible. As a certain degree of subjectivity and uncertainty is unavoidable in this process, all parametrized scenario variables for FST1 and FST5 are enumerated in Table 1, allowing researchers to replicate the simulations using other models and/or alternative rates of change for the variables.

The SM includes the numerical values for the main model variables, many of which depend on the quantified scenario objectives (Table 1). For the remaining model variables, MORDRED’s default values were adopted. The only exception is the model parameter regulating the evolution of different greenhouse gas (GHG) intensities, including CO₂ from non-combustion processes, CH₄, N₂O, SF₆, HFC and PFC. Since this type of intensity is not listed among the scenario objectives, we include it in Table 1 as an additional variable.

Following the storylines, we set the beginning of the global societal transition in 2029. The preceding decade (2019–2029) is assumed to represent a ‘business-as-usual’ (BAU) period, marked by limited political effort in the social, environmental, economic, and technological spheres, alongside high consumption demands across all social classes. Therefore, technological and consumption parameters during ‘BAU’ are defined separately and are overwritten by the parameters corresponding to FST1 and FST5 from 2029 onwards. Although the narratives only cover the period until 2075, we simulate them until 2100 to assess their stability beyond the temporal end of the storyline.

Rather than focusing on the projection of future changes within an isolated subsystem of the world, we are interested in the development of the world system as a whole, including interactions and feedback effects between human and natural systems and their impacts on variables featured in FST1 and FST5. Accordingly, all interlinkages and feedback mechanisms between model variables are activated during the simulations.

Scenario objectives	FST1	Quantification	FST5	Quantification
Scale of economic/transformation activities				
Increase scale of economic activities	4	<i>Consumption growth rates of 1% (center) to 2.5% (periphery).</i>	0	<i>Consumption growth rates of 1% (center) to 2.5% (periphery) until 2029.</i>
Decrease scale of economic activities	0	<i>Growth rates only become negative as a consequence of biophysical limits to growth.</i>	3	<i>Consumption decreases and converges to 7,500 (2019-€) between 2029 and 2039.</i>
Reduce size of human population	0	<i>Human population only drops as a result of increased mortality rates.</i>	1	<i>Birth rate multiplier of 0.7 for all regions.</i>

Adapt scale of economic activity to well-being requirements	1	<i>Target growth of poorest social classes and regions assumed to represent well-being requirements.</i>	4	<i>Target consumption level assumed to represent well-being requirements.</i>
Render scale of economy compatible with E&M flows of bioregion	<i>No representation of regional E&M flows</i>			
Increase military & security forces	2	<i>Shift 10% of government expenditures on services (sector 7, including public administration and defense) to education (sector 22) and health (sector 23).</i>	0	-
Decrease military & security forces	0	-	3	<i>Shift 15% of government expenditures from sector 7 to 22 and 23.</i>
Average 'Earth intensity' of economic activities (depends on sectoral composition and technologies)				
Reduce fossil fuel intensity	4	<i>100% greening of electricity, substitution of 60% of fossil energy with green electricity, shift of 50% of remaining fossil energy demands to bioenergy.</i>	4	<i>100% greening of electricity, substitution of 40% of fossil energy with green electricity, shift 60% of remaining fossil energy demands to bioenergy.</i>
Reduce GHG emission intensity	2	<i>Emission intensity of CH4, N2O, SF6, HFC, PFC and non-combustion related CO2 reduced by 35%.</i>	2	<i>Emission intensity of CH4, N2O, SF6, HFC, PFC and non-combustion related CO2 reduced by 35%.</i>
Reduce energy intensity	3	<i>Process efficiency and efficiency gains from electrification.</i>	4	<i>Higher process efficiency due to higher labor intensity (labor dedicated to the optimization of processes) and higher efficiency gains from electrification (due to lower share of electrification).</i>
Reduce land intensity	2	<i>World adopts the productivity levels that the center held in 2019 for the agriculture and forest sectors, contained in sector 1 & 2; land intensity of renewable electricity technologies improves by 30%; land intensity of biomass energy improves by the same rate as the average of agriculture and forest land.</i>	2	<i>World adopts productivity levels of the center for sector 1 & 2; land intensity of renewable electricity technologies improves by 30%; land intensity of biomass energy improves by the same rate as the average of agriculture and forest land.</i>
Reduce mineral intensity	1	<i>10% reduction in the inputs from sector 4 (mining) in A matrix.</i>	2	<i>20% reduction in the inputs from sector 4 in A matrix.</i>
Reduce biomass intensity	1	<i>10% reduction in the inputs from sector 2 (biomass) in A matrix.</i>	0	-
Reduce water intensity	0	-	2	<i>20% reduction in water intensity.</i>
'Circularity' of economy (duration of materials in economic sphere)				
Increase product use duration	0	-	4	<i>Multiply input coefficients in A matrix by 0.25 for sectors 5, 11, 7, 21 (industry, manufacturing, services and transport) to</i>

				<i>represent a 4-fold increase in product duration and use.</i>
Increase reuse of water, biomass and mineral based products	0	-	4	<i>Water intensity of industries and households reduced by 50%, inputs from sector 2 and 4 in A matrix reduced by 50%.</i>
Increase recycling of materials (minerals)	1	<i>10% reduction in the inputs from sector 4 in A matrix.</i>	3	<i>25% reduction in the inputs from sector 4 in A matrix.</i>
Labor/Capital-intensity				
Increase labor intensity in production process	0	<i>Strong labor intensity decline to 0.8 times the sectoral labor intensities held by the Center in 2019.</i>	4	<i>Increase of initial global average values by 10%.</i>
Increase capital intensity in production process	4	<i>Capital intensity increases by 30%.</i>	0	<i>Constant capital intensity.</i>
Distribution of consumption goods				
Reduce inequalities in consumption /unequal access to consumption goods	0	-	4	<i>Complete elimination of inter- and intraregional inequality, i.e. complete convergence in access to consumption goods.</i>
Aim at need-based allocation of consumption goods	<i>No representation of needs in model.</i>			
Control of productive capacity / the development of productive forces				
Strengthen individual decisions about production	<i>Model does not distinguish between different types of ownership, decision-making and/or ways of production.</i>			
Strengthen collective decisions about production				
Decrease inequality in (private or collective) ownership of means of production				

Table 1: Quantification of FST1 and FST5 storylines, following the translation protocol outlined in Lauer et al. (2025). All changes refer to 2100 as target year. The numbers and names of the economic sector in MORDRED are contained in the SM.

Finally, to test to which extent key model dynamics differ when important boundary conditions are altered, we conducted three additional simulations for both FST scenarios. In each additional simulation, certain scenario parameters were modified.

In the first scenario variation (SV1), which is simulated for both FST1 and FST5, we reduced non-combustion-related GHG intensities by only 10% and increased the sensitivity of the climate system to anthropogenic pressure—specifically by increasing the equilibrium climate sensitivity (ECS) by 10% and assuming a higher sensitivity of natural CH₄ emissions and of carbon uptake by biomass from the atmosphere to temperature changes (cf. Kaufhold et al., 2025).

In SV2, also simulated for both FST1 and FST5, the reduction in the land intensity of renewable energy sectors is set to 10% by 2100, i.e. it is assumed that only limited land-use savings can be achieved in renewable energy generation without reducing technological performance (Capellán-Pérez et al., 2017).

SV3 differs between FST1 and FST5. For FST1, we assess the consequences of lower demand for land, resulting from both reduced land intensities and a lower reliance on biomass-based renewable energy. Compared to the ‘default’ FST1 run, the target land intensity in 2100 is reduced by 50% for all non-energy-related land uses. Additionally, it is assumed that only 5% of

non-electric fossil energy is substituted by biomass. For FST5, SV3 explores the effects of a greater reduction in labor productivity on scenario outcomes. Accordingly, the global average sectoral labor intensities are set to increase by 50% by 2100.

Scenario variation	FST1	FST5
SV1	Higher climate sensitivity and less GHG intensity reductions	
SV2	Lower reductions in the land intensity of renewable energy sectors	
SV3	Less pressure on land	More pressure on labor

Table 2: Overview of additional scenario simulations.

3. Results

3.1. FST1: Greener growth

The main economic and socio-demographic changes during the simulation are shown in Fig. 1 while key developments in the biophysical domain are presented in Fig. 2. During the *Greener Growth* scenario, global economic activity continues to expand throughout the 21st century. World output increases by 50% between 2030 and 2100, while the global capital stock nearly doubles over the same period. However, land scarcity constrains economic expansion: compared to a scenario assuming infinite land availability (grey dashed line in Fig. 1a), economic growth in FST1 is considerably lower. By 2075, output in the unlimited-land scenario is almost 1.6 times higher than in FST1.

The increase in output is linked to growing final demand components. The largest component by far is household (private) consumption, followed by gross fixed capital formation and government (public) consumption. Under *Greener Growth*, both private and public consumption rise significantly during the 21st century, although their growth slows in the second half of the simulation. Thus, between 2060 and 2100, total household consumption increases by only 7 trillion 2019-€, compared to an increase of more than 23 trillion € between 2020 and 2060, rising from €44.3 trillion to €67.5 trillion. Global public consumption grows by 6 trillion € in the first half of the simulation, but only 1 trillion € in the second, from 19 to 20 trillion €.

Conversely, due to the increasing capital intensity of production and higher depreciation rates from climate-related damages, investment rises almost linearly throughout the entire simulation, reaching 37.6 trillion €/year at the end of the storyline and 45.5 trillion €/year by 2100. The expansion of capital stock and investment is mirrored in industrial output, which grows by 11.2 trillion € between 2029 and 2075, compared to 4.7, 3.3, and 2.2 trillion € in the food, health, and education sectors, respectively. Even in relative terms, industry exhibits the highest growth rates, reflecting FST1's focus on capital accumulation rather than on the development of food, health, and education provisioning systems.

During the transition period (2029–2075), global average per capita consumption rises moderately from 6,859 €/year to 8,097 €/year, reaching 9,152 €/year by 2100. All classes in the center, as well as the richest 20 % of the semiperiphery, remain above the global average throughout the simulation, while the poorer 80 % of the semiperiphery and periphery never reach it. The top 20 % in the periphery, however, grow rapidly and reach the global average

around 2040 (Fig. 1f). In 2075, the average regional consumption in the center is still three times as high as the global average, converges towards the global level in the semiperiphery, and remains below the global average in the periphery although the gap narrows substantially toward the end of the simulation.

The large population size of the poorest 80% of the semiperiphery and periphery explains the difference between the global average and high consumption levels in the center. Rising consumption across all classes reflects the universal aspiration for continuous consumption growth depicted in the FST1 storyline. However, a peak and subsequent decline in consumption can be observed among the center's classes (Fig. 1f), signaling an involuntary break with historical trends and political ambitions. The richest class of the center does not exceed 50,000 per capita consumption per year. After the final year of the storyline, per capita consumption continues to rise in the semiperiphery and periphery but declines gradually in the center (Fig. 1d-f), implying a geopolitical shift not mentioned in the qualitative storyline.

The FST1 storyline also lacks explicit demographic information, which the quantification provides. Model results show that global population peaks around mid-century at 8.8 billion, then begins to decline, reaching 8.7 billion by 2075—slightly above the 8.3 billion observed at the start of the global transition in 2029. Driven by the development trajectory, global birth rates fall sharply, especially outside the center, leading to a moderate decline in the semiperiphery's population and stabilization in the periphery by 2075 (Fig. 1g). The mortality rate index—calculated for each age group relative to the semiperiphery's base-year value (set to 1)—is projected to decrease for all age cohorts in the semiperiphery and periphery, and to remain constant in the center. Child mortality declines significantly, while progress among older populations is more limited (Fig. 1h & i). Nevertheless, regional disparities persist, reflecting the scenario's reliance on economic development rather than global redistribution, which proves insufficient to eliminate inequalities in life expectancy.

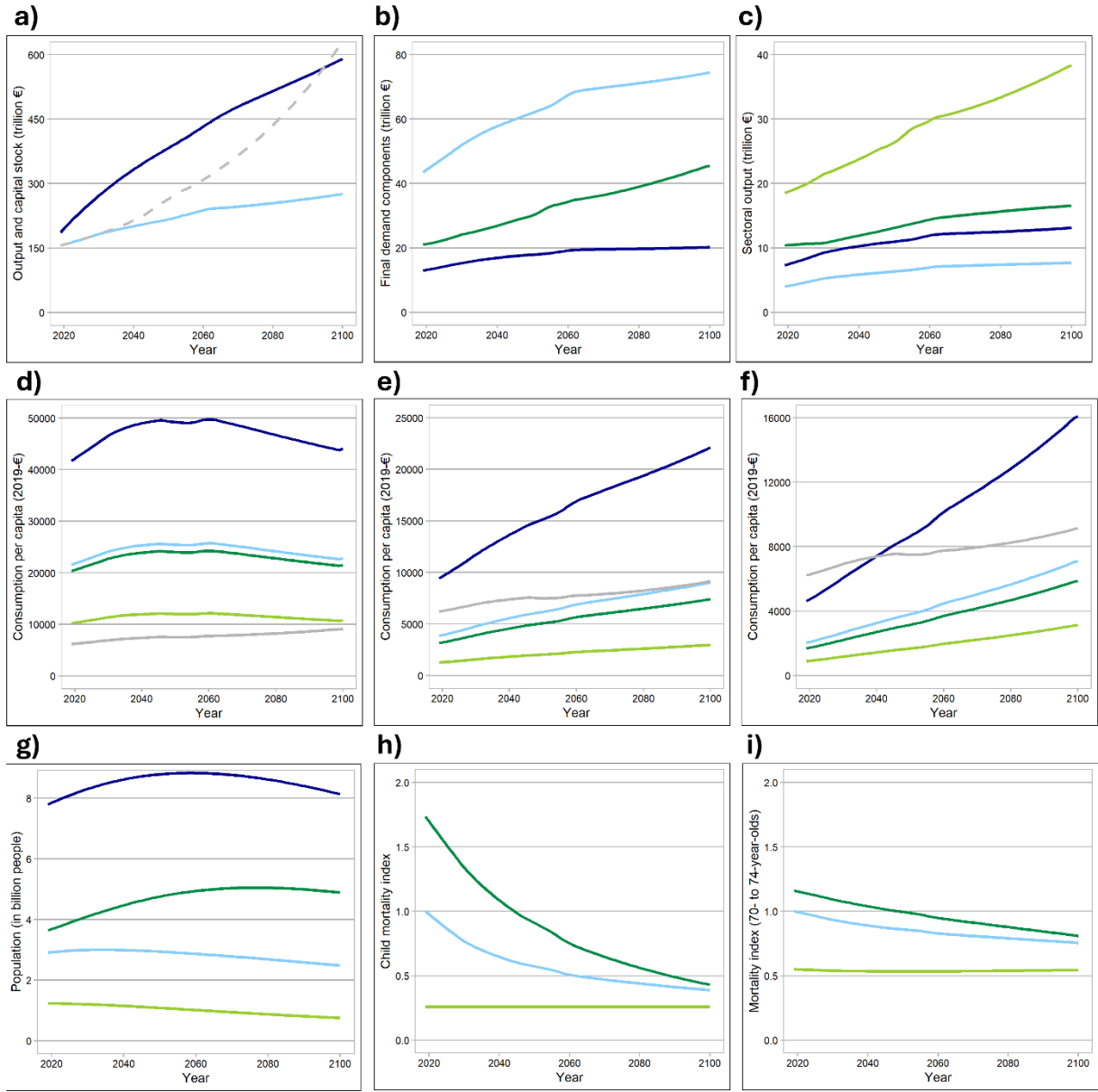


Fig. 1: Evolution of a) world output (light blue), world output without land restrictions on growth (dashed grey line) and total capital stock (dark blue); b) annual investment (dark green), private consumption (light blue) and public consumption (dark blue); c) output of the industry (light green), food (dark green), education (light blue) and health (dark blue) sector; d) average per capita consumption of the world (grey), the center (light blue), the richest 20% (dark blue), the poorest 30% (light green) and the middle class of the center (dark green); e) average per capita consumption of the world (grey), the semiperiphery (light blue), the richest 20% (dark blue), the poorest 30% (light green) and the middle class of the semiperiphery (dark green); f) average per capita consumption of the world (grey), the periphery (light blue), the richest 20% (dark blue), the poorest 30% (light green) and the middle class of the periphery (dark green); g) world population (dark blue), population in the center (light green), semiperiphery (light blue) and periphery (dark green); h) child mortality index for the center (light green), semiperiphery (light blue) and periphery (dark green); i) mortality index (people aged 70 to 74-year-olds) for the center (light green), semiperiphery (light blue) and periphery (dark green) in the FST1 scenario.

The political efforts to promote the decarbonization of the global economy in FST1 are mirrored in a continuous and fast reduction of total GHG emissions caused by the global sustainability transition (Fig. 2d). Global GHG emissions peak at 54.7 Gt in 2030 and then decline steadily. From 2060 onward, declining population further accelerates the reduction. By 2075, GHG emissions have been reduced by 37% compared to 2030, and by 2100 are more than 50 % below 2019 levels.

The reduction is primarily driven by falling CO₂ emissions (Fig. 2a). Anthropogenic CH₄ emissions peak with the onset of the transition and decline moderately during the simulation (Fig. 2b), while N₂O emissions only peak around 2060 (Fig. 2c). However, despite these reductions, the change of global average temperature compared to the pre-industrial period crosses the 2 °C threshold in 2045, reaching 2.4 °C by 2075 and 2.6 °C by 2100 (Fig. 2e).

Notably, emissions decline despite continuous growth in total energy use, reflecting substantial progress in decarbonization. This is enabled by a sharp reduction in fossil energy use, including the complete phaseout of fossil-based electricity by 2100, and a strong expansion of electric and non-electric renewables (Fig. 2j-l), consistent with the FST1 narrative of large-scale investment in green technologies.

However, the transition involves significant increases in mineral demand. Due to the strong increase in renewable electricity, copper extraction rises significantly during the simulation. By 2100, one-third of global copper output serves the renewable energy sector (Fig. 2g). Similar patterns occur for other minerals critical to the energy transition. Bulk materials such as iron and sand also increase steadily, while fossil resources used as industrial feedstocks continue to rise modestly (Fig. 2i). Industrial blue water use more than doubles between 2029 and 2075 (Fig. 2h), and green water use also increases, suggesting that freshwater consumption may exceed ecological thresholds (Rockström et al., 2009). These trends indicate a neglect of non-fossil-fuel-related environmental pressures in the FST1 development paradigm.

Last, technological changes in FST1 reshape global land systems. Due to land-use pressures, primary forest area declines by 80 % over the simulation while land devoted to built infrastructure and energy generation expands sharply, occupying 3.4 % and 9 %, respectively, of global habitable land by 2075 (Fig. 2f). Importantly, the slow-down of economic growth is caused by an excessive demand for land to generate renewable energies which stems from the effort to substitute fossil fuels with biomass-based energy, and which cannot be satisfied fast enough.

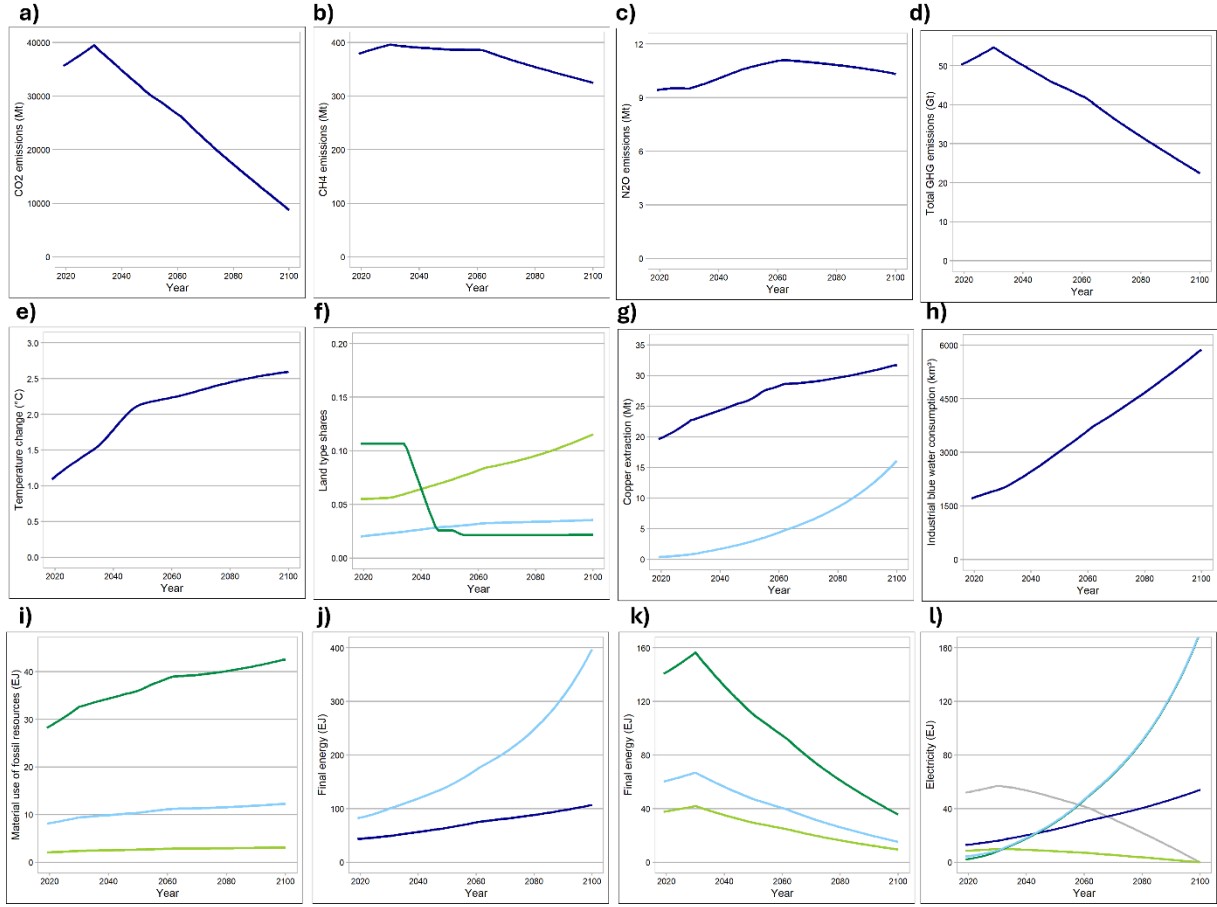


Fig. 2: Evolution of a) anthropogenic CO₂ emissions without land use change emissions; b) CH₄ emissions; c) N₂O emissions; d) total GHG emissions without land use change per year; e) global average temperature change compared to 1850; f) share of primary forest (dark green), land used for energy generation (light green), and infrastructure (blue) in total habitable land area; g) annual copper extraction for renewable energy technologies (light blue) and for the rest of economic production (dark blue); h) annual industrial blue water consumption; i) final non-energy use of oil (dark green), gas (blue) and coal (light green); j) final (non-electric) energy from biomass (dark blue) and electric energy (light blue); k) final (non-electric) energy from oil (dark green), gas (blue), coal (light green); l) fossil fuel- (grey), hydro- (dark blue), nuclear- (light green), solar PV- (dark green) and wind-based (light blue) electricity in the FST1 scenario.

Hence, compared to the storyline, the quantitative scenario simulation yields some additional insights on ‘FST1 – greener growth’, notably demographic developments, such as changes in population size and mortality, and projections of biophysical variables enabling a more precise assessment of environmental impacts. Some aspects, however, remain beyond the model’s scope, including green trade, speculative technologies (e.g., carbon capture, nuclear fusion), and interregional financial flows.

Overall, the simulation results confirm key shortcomings of the FST1 approach to the sustainability conundrum, as identified in the storyline: higher material extraction rates and increased risks of ecological distribution conflicts (Martinez-Alier, 2003, 2004) due to expanding commodity frontiers, alongside failure to meet the Paris Agreement and rising climate-related damages impacting the food sector. Thus, the title of FST1 is pertinent: Grows becomes greener, especially in terms of decarbonization, yet not green enough to prevent intensifying anthropogenic pressure on planetary systems.

While the storyline does not specify the rate of economic growth, the simulations indicate continued, though slower, expansion of the world economy during the transition, constrained by

land scarcity linked to bioenergy expansion. This underscores the growing conflict between accumulation and the ecological imperative in FST1.

On the social side, the simulations confirm FST1's narrative of limited economic convergence. However, the 'burden' of slower economic growth in the simulation is shared between the classes of the semiperiphery and periphery that face a slower decline of poverty, and the classes of the center, that see their consumption levels decline in absolute terms. Thus, in our simulation the weakening of pro-labor policies and unemployment support mentioned in the FST1 storyline mainly affects poorer classes of the center. Since the storyline does not specify how relative losses in growth are distributed across regions, alternative quantifications remain conceivable in which consumption stagnates or declines for poorer classes outside the center, while the center continues to expand.

3.2. FST5: Sufficiency economies

In the quantified version of FST5, world output grows to 170 trillion € at the start of the global transition, then declines by 30% and during the next decades increases slowly to reach a second peak at 139 trillion € in 2058. During the second half of the simulation output declines slowly, reaching 109 trillion € by 2075 and 72 trillion € by 2100 (Fig. 3a). Although capital intensity is assumed to remain constant, due to endogenous economic developments that are affected by increasing climate damages and by the growth in relatively capital-intensive sectors, the economic-wide capital-stock-to-output ratio increases moderately during the scenario while the development of total capital stock fluctuates with changing output. As a result of the general decrease in economic activity in FST5, investment approximates public consumption during the transition and by the end of the storyline has even dropped below the public consumption level (Fig. 3b). Meanwhile, global private consumption reaches a peak in 2058 at 59 trillion € and subsequently declines to 52 trillion by 2075 and 38 trillion € by 2100.

The lower demand for capital goods during the transition drives reductions in the output of the industrial sector. Output in all four sectors, depicted in Fig. 3c, peaks between 2055 and 2060 at low levels that do not surpass 12.6 trillion €/year. By 2100, with 6.9 trillion, the output in the food sector is the highest among the four sectors, followed by health sector. After its peak, the industrial sector's output declines faster compared to the other sectors, and by 2100, is only marginally higher than the education sector's output. These changes indicate the relative importance of food, health and education in FST5 compared to industrial development.

Due to global redistribution policies rapid convergence between classes to the global average consumption can be observed in all world regions (Fig. 3d-f). The class that experiences the greatest consumption cuts in absolute terms is the richest class of the center whose consumption drops from almost 45,000 €/year in 2029 to 5,243 €/year in 2033. Between 2029 and 2039 the richest class of the semiperiphery as well as the remaining classes of the center loose a significant share of their consumption budget while the poorer classes of the semiperiphery and especially the periphery see their consumption grow at very high rates. As a result of global transition policies, between 2029 and 2055 the per capita consumption of the poorest 30% of the semiperiphery and periphery increases almost 5 and more than 6.5 times, respectively. The target per capita consumption of 7,500 €/year is reached in 2056; by 2059, global per capita consumption has reached 7,676 €/year. This value is maintained until the end of the simulation period.

The consumption reduction of richer classes to levels below the target level, as well as the multiple peaks and small instabilities observed in Fig. 3a-c at the end of the 2020s, during the

early years of the 2030s and at the end of the 2050s are caused by labor and land scarcity that constrains the desired economic development in FST5. Excessive land and labor demand lead to a lower growth of the poorest class of the periphery, which, in combination with complete and fast consumption convergence, results in global consumption levels lower than the 7,500 € target. Since household consumption influences all other relevant economic variables, e.g. public consumption, investment and output, the impacts of scarcity are also observable in the latter. Thus, a more plausible dynamic would show partial convergence during the first three decades of the transition, preventing the consumption of richer classes from falling below the €7,500 target, while allowing poorer classes to gradually approach the target consumption level. However, an undesired side effect of this quantification would be an increase of overall anthropogenic pressure on planetary systems and a reduction in climate mitigation (Fig. 4).

Due to the population policy implemented in FST5, world population already peaks in 2033 and afterwards declines to 6.78 billion people by the end of the storyline. The periphery is the only world region where population continues to grow despite the population policy. However, this trend is reversed in 2049. As a result of these demographic developments, in 2075 the population of the periphery is 5 times as large as the population of the center, and more than 1.5 times as large as the population in the semiperiphery (Fig. 3g). Combined with the convergence in per capita consumption this implies a much higher weight of the periphery in the 'Planetary Confederation' of FST5. Thus, countries of these world region would likely no longer be 'peripheral' to the global economy but become its central driving force.

Mortality rates in all age groups and regions converge to a global value by 2039, which is significantly lower than initial mortality in the semiperiphery and periphery but slightly higher than initial mortality levels in the center for child mortality (Fig. 3h), and considerably higher than the initial center-values for the mortality of the older population (aged 70 to 74 years in Fig. 3i). This points to the importance of an analysis disaggregated not only by class but also by age when studying the effects of economic development on mortality and fertility.

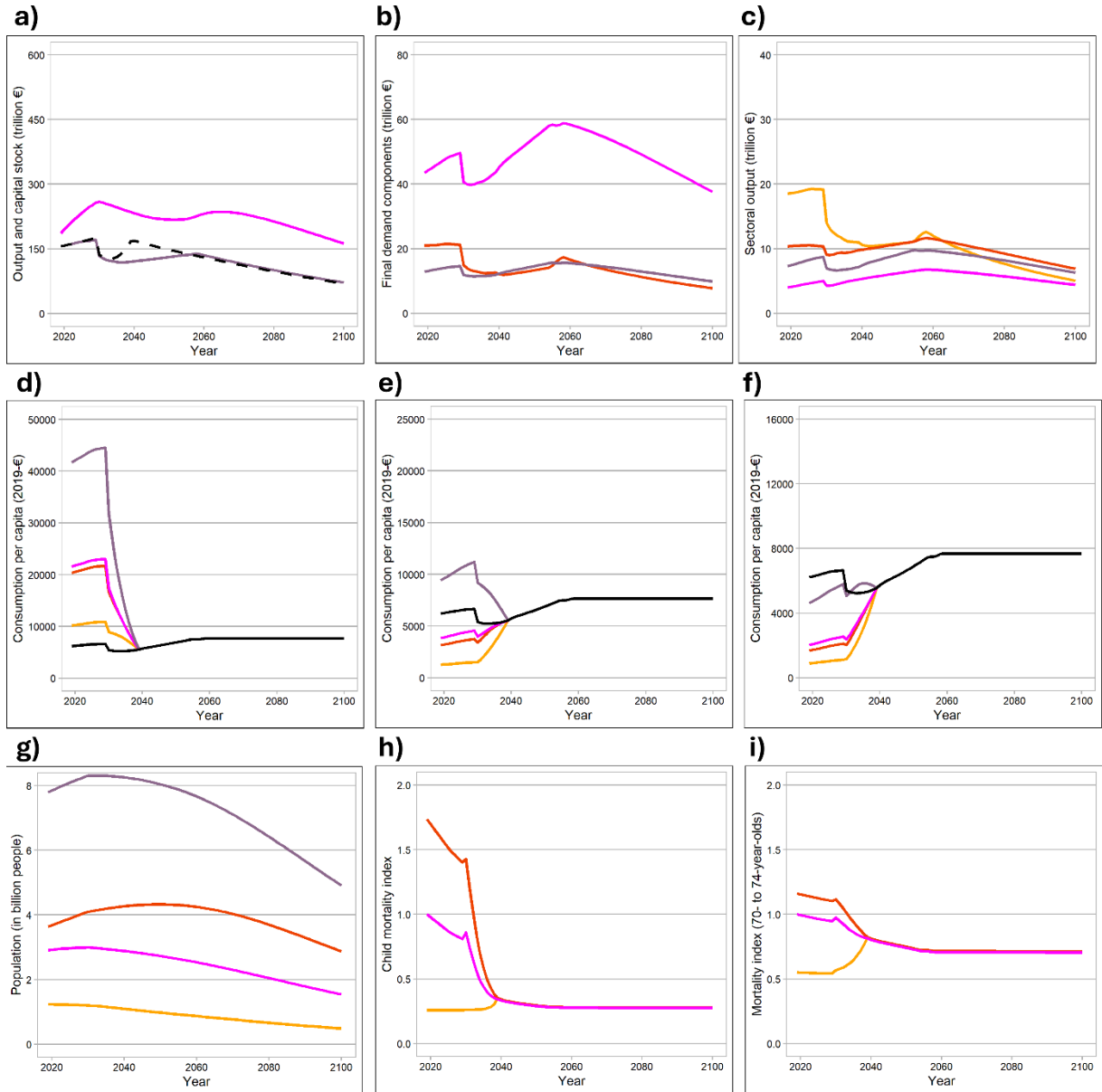


Fig. 3: Evolution of a) world output (purple) and total capital stock (pink) (dashed line: world output without land restrictions); b) annual investment (red), private consumption (pink) and public consumption (purple); c) output of the industry (orange), food (red), education (pink) and health (purple) sector; d) average per capita consumption of the world (black), the center (pink), the richest 20% of the center (purple), the poorest 30% of the center (orange) and the middle class of the center (red); e) average per capita consumption of the world (black), the semiperiphery (pink), the richest 20% (purple), the poorest 30% (orange) and the middle class of the semiperiphery (red); f) average per capita consumption of the world (black), the periphery (pink), the richest 20% (purple), the poorest 30% (orange) and the middle class of the periphery (red); g) world population (purple), population in the center (orange), semiperiphery (pink) and periphery (red); h) child mortality index for the center (orange), semiperiphery (pink) and periphery (red); i) mortality index (people aged 70 to 74) for the center (orange), semiperiphery (pink) and periphery (red) in the FST5 scenario.

During the first 10 years of the global sustainability transition in FST5 total GHG emissions fall drastically. The reduction slows down between 2040 and 2060 and accelerates again during the second half of the simulation period (Fig. 4d). This dynamic is driven mostly by global CO₂ emissions (Fig. 4a) and is reinforced by CH₄ and N₂O emissions which start to fall from 2060 onwards, driven especially by a decline in the food sector's output, as well as falling GHG emission intensities (Fig. 4b-c).

The statement in the FST5 storyline that the transition to a Planetary Confederation occurs too late to reach the 1.5 °C climate goal is confirmed in the simulation (Fig. 4e). Nevertheless, it is a remarkable achievement of FST5 to keep global warming below 2 °C during the entire simulation period: The global sustainability transition manages to slow down the increase in global average temperatures, and consequently, between 2029 and 2075 global average temperature only increases by 0.5 °C. By 2100 the world is 1.88°C warmer than in the pre-industrial (1850) reference period. Although this degree of warming already risks triggering multiple climate tipping points (Armstrong McKay et al., 2022) and is linked to significant climate-induced damages, adaptation possibilities are much higher than in scenarios with higher levels of climate change (cf. IPCC, 2022)

The transition manages to leave the extent of the world's primary forests unchanged, which is partly explained by the low peaks in the land shares human-built infrastructure and land used for energy generation (Fig. 4f). Additionally, the growth in industrial blue water consumption slows down during the transition and eventually global blue water extraction declines. By 2100, industrial blue water consumption is projected to be 48% lower than in 2019 (Fig. 4h). The final energy use of fossil resources declines steeply during the entire transition period while renewable electricity grows to reach 20.9 EJ, 21 EJ and 13.1 EJ in 2075 for wind, solar PV and hydropower, respectively (Fig. 4k & l). By 2100, fossil-based electricity has disappeared, while the non-electric energetic use of coal, gas and oil has been reduced by 93% compared to the start of the transition. The growth in electric- and non-electric energy does not offset the degrowth of energetic fossil resource use, resulting in a strong net reduction of energy use in FST5.

The growth in renewables compared with the general degrowth in the economy and the assumed improvements in material intensity and material recycling leads to a strong increase in material extraction for the renewable sector and a simultaneous strong decline in material extraction for the rest of the economy. For example, by 2100, half of the total copper production is dedicated to the maintenance of the renewable electricity infrastructure (Fig. 4g).

At the same time, the use of fossil resources as material feedstock decreases, although at a lower rate compared to reductions in fossil fuel combustion (Fig. 4i). By 2075, the world still relies on fossil resource extraction to use the equivalent of 12.7 EJ of oil, 3.7 EJ of gas and 0.9 EJ of coal in industrial processes. The small amount of coal used as industrial feedstock, coupled with the reduction of coal in the electricity sector points to a strong loss of significance of the coal sector in FST5.

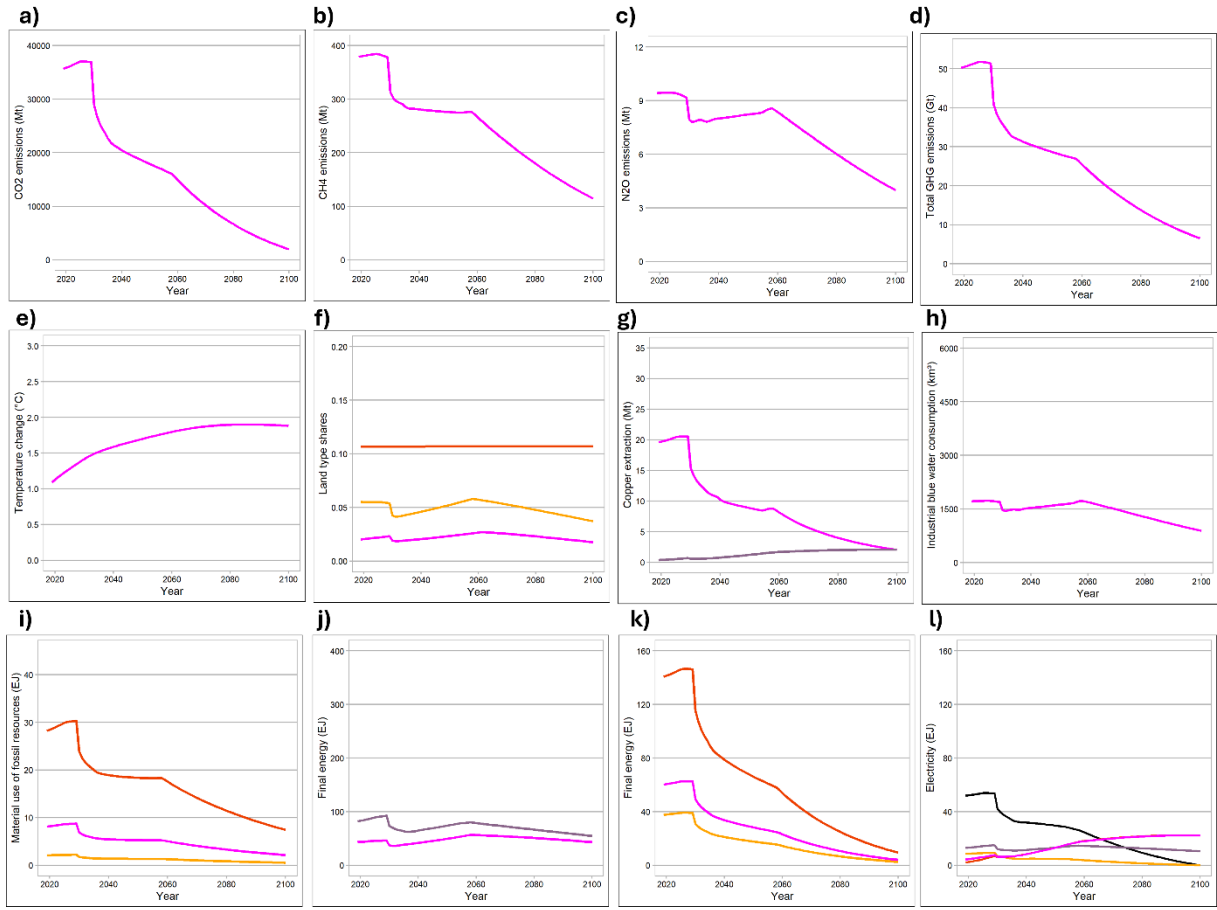


Fig. 4: Evolution of a) anthropogenic CO₂ emissions without land use change emissions; b) CH₄ emissions; c) N₂O emissions; d) total GHG emissions without land use change per year; e) global average temperature change compared to 1850; f) share of primary forest (red), land used for energy generation (orange), and infrastructure (pink) in total habitable land area; g) annual copper extraction for renewable energy technologies (purple) and for the rest of economic production (pink); h) annual industrial blue water consumption; i) final non-energy use of oil (red), gas (pink) and coal (orange); j) final (non-electric) energy from biomass (pink) and electric energy (purple); k) final (non-electric) energy from oil (red), gas (pink), coal (orange); l) fossil fuel- (black), hydro- (purple), nuclear- (orange), solar PV- (red) and wind-based (pink) electricity in the FST5 scenario.

Overall, the simulation outcomes fit the FST5 storyline: The egalitarian distribution of wealth is reflected through strong convergence in household consumption while investment in the model exclusively serves to realize private and public consumption and does not lead to increasing inequalities over time through private capital accumulation. The convergence in living standards and mortality rates is strong and fast, while the extraction of both rare and bulk materials is reduced throughout and beyond the scenario, despite the expansion of the renewable sector. The simulation shows a low but permanent reliance on fossil resources for material uses, as well as GHG emissions and annual material extraction rates greater than zero, which points to the absence of an ‘ideal’ circular economy with closed material circles.

Nevertheless, some additional insights can be gained from the quantification: First, the climate damages represented in the model, which increase with global average temperature, are not significant enough to pose a threat to economic reproduction during and beyond the FST5 scenario storyline, despite the higher labor productivity in this scenario and the negative impact of global warming on labor productivity (Dasgupta et al., 2021).

Second, temporal land and labor scarcity issues can endanger the feasibility of FST5. In other words, higher land and labor productivities, or at least faster growth rates in the first half of the

simulation, would likely create a smoother development pathway under FST5. The simulation also indicates that fast growth rates in the poorer classes – such as over 20% in the poorest classes at the global level – might pose feasibility problems.

Additionally, the scenario quantification demonstrates that FST5 only works with significant improvements in land productivity because at low consumption levels, food expenses make up a relatively large share of total expenditure. Thus, an increase in consumption will generate a higher demand for land than a similar increase at a higher consumption level. If land productivity improvements do not match the consumption growth of poorer classes, land conversions and the associated loss of biodiversity and increase in GHG emissions become more probable.

Finally, a dynamic that reduces anthropogenic pressure on ecosystems and sustains high levels of climate mitigation beyond 2075 is the continuous population decline, which is not explicitly considered in the FST5 storyline. This demographic trend emerges as an important stabilizing factor in the scenario. With the exception of temporary labor shortages in the first half of the simulation, no significant labor scarcity is observed in the second half, despite the aging population. However, workforce utilization remains high throughout the simulation and increases slowly but steadily over the last four decades, suggesting that long-term stability of FST5 will ultimately require either population stabilization or renewed growth in labor productivity.

3.3. Comparison of FST1 and FST5

Comparing the two scenario simulations we find that FST5 is linked to considerably lower levels of anthropogenic pressure on planetary systems. While FST5 manages to keep global warming below 2°C by 2100, in FST1 none of the climate objectives of the Paris Agreement are reached. Additionally, FST1 has a narrow focus on climate mitigation and ignores other environmental stressors such as water consumption, the material use of fossil resources, material extraction or land use conversion, while in FST5 these variables improve during the scenario. Last, the effect of the presence or absence of limits to growth imposed by the availability of land is much higher in FST1 than in FST5 (compare dashed lines in Fig. 1a and Fig. 3a).

While life expectancy and per capita consumption of the poorest increase in both scenarios, class and territorial inequalities are reduced considerably faster in FST5. Thus, in FST1, the poorest 30% of the periphery live with very low consumption levels throughout and beyond the global transition. At the same time, although the richest classes in the center eventually see their consumption levels decline in both scenarios, the loss in consumption is much more pronounced in FST5.

Once the global-level policies are implemented, both scenarios are stable beyond the final year of the storyline (2075), although the greater level of environmental pressure and inequality in FST1 pose mid- and long-term risks for its stability.

4. Discussion

4.1. Boundary conditions and scenario plausibility

By changing key boundary conditions in the simulations, we can identify which scenario assumptions must hold for the outcomes to resemble the FST storylines. These assumptions can then be evaluated in terms of their plausibility.

For each dimension (economic, social, environmental) we select one key variable for assessment: *output*, because it represents the scale of overall economic activity; *consumption per capita*, because in the model this variable influences life expectancy and serves as an indicator of well-being (at least until a certain consumption level) (Carver & Grimes, 2019; Vollebregt et al., 2024); and *changes in global average temperature*, because they serve as an indicator of anthropogenic pressure on planetary systems.

Simulating the first scenario variation (SV1) we find that more pessimistic assumptions about the climate system's sensitivity lead to higher levels of global warming, lower output due to climate damages, and reduced per capita consumption (Fig. 5a-d). The output loss is significantly greater for FST1 than for FST5, and it causes the consumption of the richest class to fall below their initial level by 2100, while the reduction in consumption of the poorest class further hampers poverty elimination. Because even small changes in the magnitude of global warming visibly alter the scenario outcomes, we conclude that the quantifications—especially for FST1—are sensitive to assumptions about the climate system, and that greater climate sensitivity diminishes the scenarios' long-term stability and renders them less plausible.

In SV2 we observe relatively small deviations from the original scenario outcomes (Fig. 5e-h); these deviations are reduced in FST1 and nearly eliminated in FST5 during the second half of the simulation. Interestingly, this suggests that technological progress in (land) efficiency of renewables has a comparatively minor influence on the feasibility of the scenarios.

For FST1, SV3 diverges notably from the original scenario simulation, with higher outcomes, elevated consumption levels and weak climate mitigation. Despite the substantial improvement in land intensity—which buffers the increasing climate-change-related land damages—growing difficulties in sustaining economic growth become apparent toward the end of the simulation. Since a low level of fossil-bioenergy substitution does not align with the FST1 storyline, and the very high land-intensity improvements required to achieve the same growth rate through biomass-based energy seem difficult to attain (especially given factors that tend to reduce land productivity, such as soil-fertility loss (Cherlet et al., 2018) or forest productivity decline (Mohr et al., 2025)), FST1 appears plausible only under lower-than-desirable growth levels.

For FST5, SV3 demonstrates that the assumed increase in labor intensity in the original quantification represents an upper bound: with lower labor productivity levels, the consumption target of FST5 can no longer be met (Fig. 5o,p). Thus, assuming a stronger increase in labor intensity—as in SV3—reduces the feasibility of FST5.

There are other important boundary conditions that we did not vary in the scenario analyses. These include resource availability, the severity of damages, and impacts of biodiversity loss. Estimates of remaining and accessible fossil resources vary widely (Delannoy et al., 2021; Fricko et al., 2017; Laherrère et al., 2022; Turner, 2008). However, using a medium estimate in our simulations, we find that by 2100 only 74 % of estimated fossil reserves have been extracted in FST1 and only 45 % in FST5. Thus, in sustainability transition scenarios, uncertainty about fossil resources plays a lesser role than in high-emission pathways. Regarding the accessibility of

minerals, comparing the quantities of tin and copper extracted between 2019 and 2100 in FST1 and FST5 with the Ultimately Available Resources (UAR) estimates of Henckens (2021), we find extracted shares of 18 % and 5 % for tin, and 27 % and 8 % for copper, respectively. We conclude that mineral resource availability has a relatively minor impact on scenario plausibility—especially for FST5.

The severity of climate damages was not varied in the scenarios, although they certainly influence development pathways (IPCC, 2022). Nevertheless, since damages evolve nonlinearly, we argue that the question of severity is more central for worst-case climate scenarios, while the transition scenarios modeled here exhibit comparatively moderate temperature rises.

Finally, given that MORDRED does not represent potential effects of declining ecosystem services on economic reproduction the scenario outcomes are likely over-optimistic, especially for FST1 which exhibits higher resource and land pressures.

In general, the rates of change assumed during transitions in FST1 and FST5 are far higher than historical rates of change. However, we maintain that this does not make them implausible, since both scenarios are built on the premise of a substantial change in world order and a reconfiguration of political priorities.

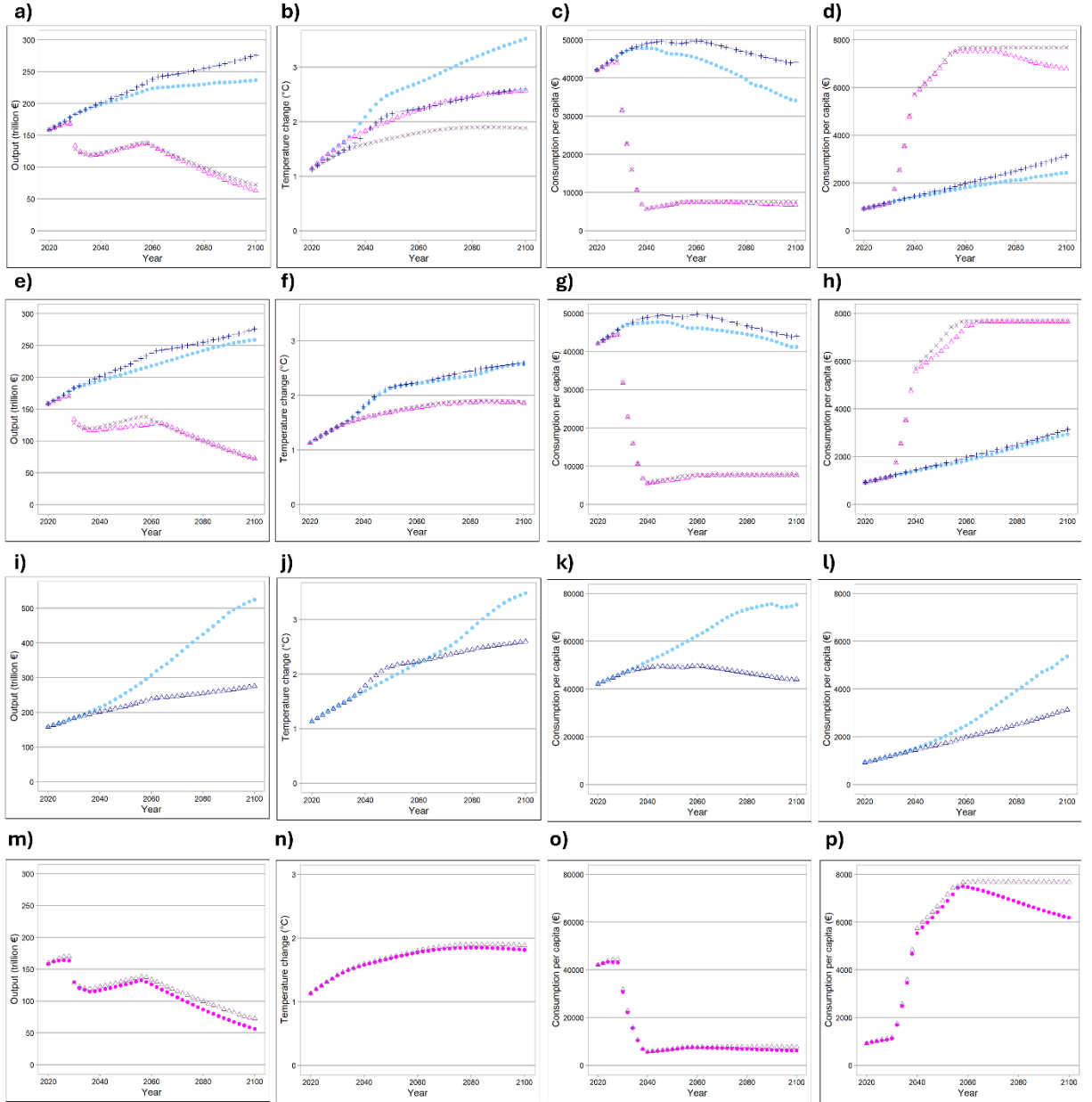


Fig. 5: Evolution of key output variables in scenarios with changed boundary conditions (FST1 = light blue, FST5 = pink), compared to the baseline scenario results (FST1 = dark blue, FST5 = purple). a, e, i, m: total world output; b, f, j, n: global average temperature change compared to 1850; c, g, k, o: consumption per capita of the richest 20% of the center; d, h, l, p: consumption per capita of the poorest 30% of the periphery. a-d) Baseline scenarios compared to scenarios with higher climate sensitivity and less GHG intensity reductions; e-h) Baseline scenarios compared to scenarios with lower reductions in the land intensity of renewable energy sectors; i-l) Baseline compared to a scenario with higher land intensity reductions and lower substitution of fossil energy through bioenergy. m-p) Baseline compared to a scenario with a higher labor intensity increase.

4.2. Policy relevance and future work

Our simulations are not predictions of the future but data-based imagined futures supporting societal and political decision-making and planning (Juri et al., 2025). As we focus on very broad development at the global level, the policy relevance of our work equally is of global character since regional or local policies can be better informed by concrete case-specific modeling studies. Three key policy-relevant insights can be formulated based on the simulation outcomes of FST1 and FST5.

First, the modeling results clearly indicate that FST5 has better chances to meet both environmental and social sustainability goals, namely a slowdown of environmental degradation, the eradication of poverty and the reduction of social inequality. FST1 does not only fail to achieve climate goals but is also characterized by a constant decrease in the workforce utilization rate, pointing at a risk of emerging unemployment issues, which has already been discussed by O'Neill (2020). Thus, our work provides model-based support for those strands in the ongoing debate on sustainability transitions that promote development paradigms and policies similar to those in FST5, such as degrowth, post-growth or steady-state economics (Daly, 2013; Fitzpatrick et al., 2022).

Second, the simulations show that strong reductions of anthropogenic pressure on planetary systems are possible even in the absence of speculative technologies or technological breakthroughs such as negative emission technologies (NETs) or nuclear fusion. However, successful mitigation depends critically on radical convergence, consumption reduction and a series of changes in production processes such as recycling, product reuse etc. Importantly, in the simulation, policy measures are implemented fast and throughout the world. Thus, our scenario study confirms the urgent need to look for radical solutions beyond national boundaries, which in turn, can only be implemented under a changed world order with new institutional 'rules of the game' shaping global economic, political and cultural systems.

Last, the scenario quantification exercise reaffirms the importance of holistic sustainability policies targeting demographic, economic, social, cultural and technological developments, since it is the combination of simultaneous changes in different sub-modules that drive simulation outcomes in both FSTs. For example, the population policy in FST5 significantly contributes to its mitigation success. Likewise, the rapid decarbonization of the economy in both scenarios increases the relative importance of GHG emissions from other sources than fossil fuel combustion, such as N₂O or SF₆ that should be addressed with specific globally harmonized policies.

Our simulations could be refined in future work by integrating more biophysical feedbacks to address the optimistic bias of the simulations, by improving the representation of land-related processes, and by updating the IO data used (Stadler et al., 2018). Equally, multiple FST scenarios, including FST1 and FST5, could be introduced into different IAMs. This would enable comparing the performance of different sustainability paradigms in models other than MORDRED but also would serve to explore differences in outcomes stemming from differences in model structures. Since many IAMs use NETs it can be expected that climate-related results would improve for both FSTs. Additionally, the emission pathways generated by MORDRED could be fed into more sophisticated climate modules to explore possible variations in the level of global warming. Finally, researchers could develop new models that focus on aspects of the FSTs that neither MORDRED nor other existing IAMs can represent, such as ownership structures, decision-making processes in economic production, basic human needs and a need-based allocation of goods (Table 1).

5. Conclusion

In this article, we quantified two global sustainability transition scenarios—FST1: Greener Growth and FST5: Sufficiency Economy—using the MORDRED-IAM. Overall, the scenario outcomes align well with their respective storylines, supporting their plausibility. The

simulations complement the qualitative narratives by generating demographic, consumption, production, and emission pathways. Both scenarios achieve substantial decarbonization without relying on speculative technologies; however, only FST5 limits global warming to below 2 °C. Future research could extend this work by quantifying the remaining FSTs, implementing FST1 and FST5 in other IAMs, and developing new models to explore aspects not covered in this analysis, such as shifts in ownership structures or need-based goods allocation.

References

- Abunyewah, M., Erdiaw-Kwasie, M. O., Okyere, S. A., & Boateng, F. G. (2023). Advancing a slum-circular economy model for sustainability transition in cities of the Global South. *Nature Sustainability*, 6(11), 1304–1311. <https://doi.org/10.1038/s41893-023-01176-8>
- Alcamo, J. (2008). Chapter six the SAS approach: Combining qualitative and quantitative knowledge in environmental scenarios. *Developments in Integrated Environmental Assessment*, 2, 123–150.
- Armstrong McKay, D. I., Staal, A., Abrams, J. F., Winkelmann, R., Sakschewski, B., Loriani, S., Fetzer, I., Cornell, S. E., Rockström, J., & Lenton, T. M. (2022). Exceeding 1.5 C global warming could trigger multiple climate tipping points. *Science*, 377(6611), eabn7950.
- Brown, E., Cloke, J., Gent, D., Johnson, P. H., & Hill, C. (2014). Green growth or ecological commodification: Debating the green economy in the global south. *Geografiska Annaler: Series B, Human Geography*, 96(3), 245–259. <https://doi.org/10.1111/geob.12049>
- Capellán-Pérez, I., De Castro, C., & Arto, I. (2017). Assessing vulnerabilities and limits in the transition to renewable energies: Land requirements under 100% solar energy scenarios. *Renewable and Sustainable Energy Reviews*, 77, 760–782.
- Carver, T., & Grimes, A. (2019). Income or Consumption: Which Better Predicts Subjective Well-Being? *Review of Income and Wealth*, 65(S1). <https://doi.org/10.1111/roiw.12414>
- Cherlet, M., Hutchinson, C., Reynolds, J., Hill, J., Sommer, S., & von Maltitz, G. (2018). *World Atlas of Desertification*. Publication Office of the European Union. https://wad.jrc.ec.europa.eu/sites/default/files/atlas_pdf/JRC_WAD_fullVersion.pdf
- Daly, H. (2013). Top 10 policies for a steady-state economy. *Daily News*, 28.
- Dasgupta, S., van Maanen, N., Gosling, S. N., Piontek, F., Otto, C., & Schleussner, C.-F. (2021). Effects of climate change on combined labour productivity and supply: An empirical, multi-model study. *The Lancet Planetary Health*, 5(7), e455–e465.
- Delannoy, L., Longaretti, P.-Y., Murphy, D. J., & Prados, E. (2021). Peak oil and the low-carbon energy transition: A net-energy perspective. *Applied Energy*, 304, 117843.
- Durán, A. P., Kuiper, J. J., Aguiar, A. P. D., Cheung, W. W., Diaw, M. C., Halouani, G., Hashimoto, S., Gasalla, M. A., Peterson, G. D., & Schoolenberg, M. A. (2023). Bringing the Nature Futures Framework to life: Creating a set of illustrative narratives of nature futures. *Sustainability Science*, 1–20.
- Fetanat, A., Tayebi, M., & Shafipour, G. (2021). Management of waste electrical and electronic equipment based on circular economy strategies: Navigating a sustainability transition toward waste management sector. *Clean Technologies and Environmental Policy*, 23(2), 343–369. <https://doi.org/10.1007/s10098-020-02006-7>
- Fitzpatrick, N., Parrique, T., & Cosme, I. (2022). Exploring degrowth policy proposals: A systematic mapping with thematic synthesis. *Journal of Cleaner Production*, 132764.
- Flynn, A., Hacking, N., & Xie, L. (2019). Governance of the circular economy: A comparative examination of the use of standards by China and the United Kingdom. *Environmental Innovation and Societal Transitions*, 33, 282–300.

- Fricko, O., Havlik, P., Rogelj, J., Klimont, Z., Gusti, M., Johnson, N., Kolp, P., Strubegger, M., Valin, H., & Amann, M. (2017). The marker quantification of the Shared Socioeconomic Pathway 2: A middle-of-the-road scenario for the 21st century. *Global Environmental Change*, 42, 251–267.
- Grubler, A., Wilson, C., Bento, N., Boza-Kiss, B., Krey, V., McCollum, D. L., Rao, N. D., Riahi, K., Rogelj, J., & De Stercke, S. (2018). A low energy demand scenario for meeting the 1.5 C target and sustainable development goals without negative emission technologies. *Nature Energy*, 3(6), 515–527.
- Henckens, T. (2021). Scarce mineral resources: Extraction, consumption and limits of sustainability. *Resources, Conservation and Recycling*, 169, 105511. <https://doi.org/10.1016/j.resconrec.2021.105511>
- Hickel, J. (2019). Is it possible to achieve a good life for all within planetary boundaries? *Third World Quarterly*, 40(1), 18–35.
- Hickel, J., & Slamersak, A. (2022). Existing climate mitigation scenarios perpetuate colonial inequalities. *The Lancet Planetary Health*, 6(7), e628–e631. [https://doi.org/10.1016/S2542-5196\(22\)00092-4](https://doi.org/10.1016/S2542-5196(22)00092-4)
- Hochstetler, K. (2025). The Green Economy and the Global South. *Regulation & Governance*, 19(2), 515–519. <https://doi.org/10.1111/rego.70008>
- IPCC. (2022). *Climate Change 2022: Impacts, Adaptation and Vulnerability. Contribution of Working Group II to the Sixth Assessment Report of the Intergovernmental Panel on Climate Change*. Cambridge University Press. Cambridge University Press, Cambridge, UK and New York, NY, USA.,
- Juri, S., Marais-Potgieter, A., Achieng, T., Gianelli, I., Kabisa, M., Nkgothoe, B., Ojino, J., Tcheton, S., Carpenter-Urquhart, L., & Pereira, L. M. (2025). Transforming towards what? A review of futures-thinking applied in the quest for navigating sustainability transformations. *Environmental Research Letters*, 20(5), 053006. <https://doi.org/10.1088/1748-9326/adcbc4>
- Kallis, G., Hickel, J., O'Neill, D. W., Jackson, T., Victor, P. A., Raworth, K., Schor, J. B., Steinberger, J. K., & Ürge-Vorsatz, D. (2025). Post-growth: The science of wellbeing within planetary boundaries. *The Lancet Planetary Health*, 9(1), e62–e78.
- Kaufhold, C., Willeit, M., Talento, S., Ganopolski, A., & Rockström, J. (2025). Interplay between climate and carbon cycle feedbacks could substantially enhance future warming. *Environmental Research Letters*, 20(4), 044027. <https://doi.org/10.1088/1748-9326/adb6be>
- Köhler, J., Geels, F. W., Kern, F., Markard, J., Onsongo, E., Wieczorek, A., Alkemade, F., Avelino, F., Bergek, A., Boons, F., Fünschilling, L., Hess, D., Holtz, G., Hyysalo, S., Jenkins, K., Kivimaa, P., Martiskainen, M., McMeekin, A., Mühlmeier, M. S., ... Wells, P. (2019). An agenda for sustainability transitions research: State of the art and future directions. *Environmental Innovation and Societal Transitions*, 31, 1–32. <https://doi.org/10.1016/j.eist.2019.01.004>
- Laherrère, J., Hall, C. A., & Bentley, R. (2022). How much oil remains for the world to produce? Comparing assessment methods, and separating fact from fiction. *Current Research in Environmental Sustainability*, 4, 100174.
- Lauer, A., de Castro, C., & Carpintero, Ó. (2024). Between continuous presents and disruptive futures: Identifying the ideological backbones of Global Environmental Scenarios. *Futures*, 103460.
- Lauer, A., De Castro, C., & Carpintero, Ó. (2025). Beyond Green capitalism: Global scenarios for fast societal transitions toward sustainability. *Environmental Innovation and Societal Transitions*, 56, 100981. <https://doi.org/10.1016/j.eist.2025.100981>

- Lauer, A., & Llases, L. (2025). *MORDRED: Model Of Resource Distribution and Resilient Economic Development. Model Documentation*. GitHub. <https://github.com/Pendracus/MORDRED>
- Lederer, M., Wallbott, L., & Bauer, S. (2018). Tracing Sustainability Transformations and Drivers of Green Economy Approaches in the Global South. *The Journal of Environment & Development*, 27(1), 3–25. <https://doi.org/10.1177/1070496517747661>
- Lefèvre, J. (2024). Integrated assessment models and input–output analysis: Bridging fields for advancing sustainability scenarios research. *Economic Systems Research*, 36(4), 675–698. <https://doi.org/10.1080/09535314.2023.2266559>
- Low, S., Brutschin, E., Baum, C. M., & Sovacool, B. K. (2025). Expert perspectives on incorporating justice considerations into integrated assessment modelling. *Npj Climate Action*, 4(1), 10. <https://doi.org/10.1038/s44168-025-00218-5>
- Malik, A., & Schaeffer, R. (2024). Integrated assessment modelling and input-output analysis. *Economic Systems Research*, 36(4), 501–507. <https://doi.org/10.1080/09535314.2024.2408660>
- Martinez-Alier, J. (2003). *The Environmentalism of the poor: A study of ecological conflicts and valuation*. Edward Elgar Publishing.
- Martinez-Alier, J. (2004). Ecological distribution conflicts and indicators of sustainability. *International Journal of Political Economy*, 34(1), 13–30.
- Millward-Hopkins, J., Steinberger, J. K., Rao, N. D., & Oswald, Y. (2020). Providing decent living with minimum energy: A global scenario. *Global Environmental Change*, 65, 102168.
- Mohr, J. S., Bastit, F., Grünig, M., Knoke, T., Rammer, W., Senf, C., Thom, D., & Seidl, R. (2025). Rising cost of disturbances for forestry in Europe under climate change. *Nature Climate Change*, 15(10), 1078–1083. <https://doi.org/10.1038/s41558-025-02408-9>
- Msangi, S. (2013). Visioning Change and Alternative Futures: Foresight as a research and planning tool. *Development*, 56(4), 491–499. <https://doi.org/10.1057/dev.2014.51>
- O'Neill, D. W. (2020). Beyond green growth. *Nature Sustainability*, 3(4), 260–261.
- Otero, I., Farrell, K. N., Pueyo, S., Kallis, G., Kehoe, L., Haberl, H., Plutzar, C., Hobson, P., García-Márquez, J., & Rodríguez-Labajos, B. (2020). Biodiversity policy beyond economic growth. *Conservation Letters*, 13(4), e12713.
- Owen, J. R., Kemp, D., Lechner, A. M., Harris, J., Zhang, R., & Lèbre, É. (2022). Energy transition minerals and their intersection with land-connected peoples. *Nature Sustainability*, 1–9.
- Pereira, L., Kuiper, J. J., Selomane, O., Aguiar, A. P. D., Asrar, G. R., Bennett, E. M., Biggs, R., Calvin, K., Hedden, S., & Hsu, A. (2021). Advancing a toolkit of diverse futures approaches for global environmental assessments. *Ecosystems and People*, 17(1), 191–204.
- Raskin, P., & Swart, R. (2020). Excluded futures: The continuity bias in scenario assessments. *Sustainable Earth*, 3(1), 1–5.
- Rockström, J., Steffen, W., Noone, K., Persson, Å., Chapin III, F. S., Lambin, E., Lenton, T. M., Scheffer, M., Folke, C., & Schellnhuber, H. J. (2009). Planetary boundaries: Exploring the safe operating space for humanity. *Ecology and Society*, 14(2).
- Schmelzer, M. (2017). The growth paradigm: History, hegemony, and the contested making of economic growthmanship. In *Routledge Handbook of the History of Sustainability* (pp. 164–186). Routledge.
- Scoones, I., Stirling, A., Abrol, D., Atela, J., Charli-Joseph, L., Eakin, H., Ely, A., Olsson, P., Pereira, L., & Priya, R. (2020). Transformations to sustainability: Combining structural, systemic and enabling approaches. *Current Opinion in Environmental Sustainability*, 42, 65–75.
- Sessa, C., & Ricci, A. (2014). The world in 2050 and the New Welfare scenario. *Futures*, 58, 77–90.
- Stadler, K., Wood, R., Bulavskaya, T., Södersten, C., Simas, M., Schmidt, S., Usobiaga, A., Acosta-Fernández, J., Kuenen, J., Bruckner, M., Giljum, S., Lutter, S., Merciai, S., Schmidt, J. H.,

- Theurl, M. C., Plutzar, C., Kastner, T., Eisenmenger, N., Erb, K., ... Tukker, A. (2018). EXIOBASE 3: Developing a Time Series of Detailed Environmentally Extended Multi-Regional Input-Output Tables. *Journal of Industrial Ecology*, 22(3), 502–515. <https://doi.org/10.1111/jiec.12715>
- Turner, G. (2008). A comparison of The Limits to Growth with 30 years of reality. *Global Environmental Change*, 18(3), 397–411. <https://doi.org/10.1016/j.gloenvcha.2008.05.001>
- Valero, A., Valero, A., Calvo, G., & Ortego, A. (2018). Material bottlenecks in the future development of green technologies. *Renewable and Sustainable Energy Reviews*, 93, 178–200.
- Van Vuuren, D. P., Stehfest, E., Gernaat, D. E. H. J., Van Den Berg, M., Bijl, D. L., De Boer, H. S., Daioglou, V., Doelman, J. C., Edelenbosch, O. Y., Harmsen, M., Hof, A. F., & Van Sluisveld, M. A. E. (2018). Alternative pathways to the 1.5 °C target reduce the need for negative emission technologies. *Nature Climate Change*, 8(5), 391–397. <https://doi.org/10.1038/s41558-018-0119-8>
- Vollebregt, M., Mugge, R., Thürridl, C., & Van Dolen, W. (2024). Reducing without losing: Reduced consumption and its implications for well-being. *Sustainable Production and Consumption*, 45, 91–103. <https://doi.org/10.1016/j.spc.2023.12.023>
- Wiedmann, T., Lenzen, M., Keyßer, L. T., & Steinberger, J. K. (2020). Scientists' warning on affluence. *Nature Communications*, 11(1), 1–10.
- Wiese, F., Taillard, N., Balembois, E., Best, B., Bourgeois, S., Campos, J., Cordroch, L., Djelali, M., Gabert, A., Jacob, A., Johnson, E., Meyer, S., Munkácsy, B., Pagliano, L., Quoilin, S., Roscetti, A., Thema, J., Thiran, P., Toledano, A., ... Marignac, Y. (2024). The key role of sufficiency for low demand-based carbon neutrality and energy security across Europe. *Nature Communications*, 15(1), 9043. <https://doi.org/10.1038/s41467-024-53393-0>
- Wiese, F., Zell-Ziegler, C., Burghardt, C., Kloos, Y., & Schäfer, M. (2024). Reducing demand: A quantitative analysis of energy service demand indicators in sufficiency-oriented scenarios. *Environmental Research Communications*, 6(12), 121003. <https://doi.org/10.1088/2515-7620/ad966e>
- Wilkinson, A., & Mangalagiu, D. (2012). Learning with futures to realise progress towards sustainability: The WBCSD Vision 2050 Initiative. *Futures*, 44(4), 372–384.

MORDRED: Model Of Resource Distribution and Resilient Economic Development.

Model Documentation 1.0

11 / 2025

Arthur Lauer & Luis Llases

1. Previous remarks

We have extended this documentation various times to make it as comprehensive as possible. It corresponds to the model version MORDRED 1.0 and allows to understand all other model versions and extensions. The development of different parts of the model and the corresponding scenario analyses is described in several working papers and articles. One module that is not strictly needed for MORDRED to run is the so-called ‘Planetary Boundaries’ module because the variables of this module do not feedback into other modules. We removed this module from MORDRED 1.0 and refrain from describing it here given that its structure, equation and data are described in detail in the corresponding article.

Since this is a system dynamics model it is not meant to be run backwards and historical analyses can only be done by adapting the parameters to the empirical context prior to 2019. MORDRED is built to explore a wide range of global socio-environmental scenarios that can deviate strongly from historical tendencies. Thus, while the model is a structural representation of the recent past (it is based on data ranging from 1995 – 2020) simulation outcomes critically depend on scenario assumptions that are independent from model assumptions.

Limitations:

1. The mathematical form chosen to model the majority of the changes in fertility rates, combined with the exclusion of cultural and political factors results in a tendency of the model to underestimate population growth in simulations without population policies which also implies an underestimation of environmental pressure.
2. The focus on the materiality of economic processes leads to scenarios with conservative abstract energy efficiency improvements (overestimation of environmental pressure) and low growth in consumption and GDP (underestimation of environmental pressure), i.e. the model does not focus on abstract economic production without a material basis.
3. Capital stock and land requirements corresponding to renewable energy technologies are subject to uncertainty. Projections could be improved if better data were available.
4. Damage estimates are not comprehensive and do not take into account structural disruptions (underestimation of economic impacts) but the severity of damage could be mitigated by adaptation which is not explicitly modeled (overestimation of economic impacts).

2. Model structure

Mordred is a system dynamics model programmed in Vensim and designed to represent the broad socio-economic dynamics at a global scale and their relationship with the environment. The model can be divided into several modules, each corresponding to a specific aspect of the system it aims to represent: demographics, economy, labor, energy, land use, climate and stressors.

The demographic module computes the evolution of the global population, divided into three world regions based on income levels: the core, semi-periphery, and periphery. This evolution depends on birth and death rates, which are themselves influenced by per capita consumption levels across different regions and social classes within the model (each region is divided into three social classes: the wealthiest 20%, the poorest 30%, and the remaining 50% in between). Additionally, birth and death rates are affected by per capita public spending on healthcare and education.

The demographic module also accounts for populations living in subsistence conditions, at the margins of the global economic system. For each region, migration between subsistence and the global economy is modeled as a function of the difference in living standards between the lowest-income class and subsistence conditions.

The economic module calculates the volume of goods and services produced in the global economy and their distribution across regions and social classes based on exogenously defined per capita consumption levels for each class and region. Government consumption is computed as a fixed percentage of individual consumption, while investment is determined endogenously by the quantity of capital goods required for production. However, the actual output of goods and services may not match demand, as it is constrained by the availability of energy, labor, and land. Additionally, production is affected by adverse climate change impacts and broader environmental degradation.

In the labor module the available workforce is computed and an upper limit on production capacity is imposed. Labor productivity trends are set exogenously through scenario assumptions. The maximum feasible labor input is also reduced by environmental deterioration. Similarly, labor productivity itself may suffer negative impacts from climate change.

The energy module calculates the total energy demanded by the system. First, it determines final energy consumption and then uses this variable to compute primary energy requirements. For fossil fuels, the module also accounts for the depletion of available resources and the increasing extraction difficulty as reserves are used up.

The land use module tracks land availability and its allocation among different uses. This allocation depends on predefined priorities for each land use according to scenario assumptions, and the land intensity of production processes and other land uses. As with labor, land productivity trends are set exogenously based on scenarios, although they can also be endogenously affected by environmental degradation damages.

The climate module is adapted from the climate submodule contained in WILIAM v1.3 (Lifi et al., 2023) and calculates changes in global average temperatures that are driven by different greenhouse gas emissions which are calculated in the stressors module. The latter quantifies the impact of human activity on the environment across multiple dimensions. Apart from greenhouse gas emissions, it also tracks human water usage, extraction of various materials, and water/air pollution from different contaminants.

The following sections describes each module with its key equations.

2.1. Demography

The demographic module simulates global population dynamics by dividing the world into three regions—center, semi-periphery, and periphery—and into 20 five-year age cohorts ranging from 0–4 to 95 and older. The population is further categorized into two groups: those integrated into the global economy and those engaged in subsistence activities.

To calculate the evolution of the population integrated into the global economy, the following factors are considered: the initial population stock (divided, as previously mentioned, by age and region), the flow of births, the flow of deaths, the flow of population transitioning from the global economy to subsistence, the flow of population moving from subsistence to the global economy, and the population shifting from one age group to another.

For the 0–4 age group the population stock is described as:

$$P_{r,c04}^{we} = \int_{t_0}^t \left(B_r^{we} - D_{r,c04}^{we} + M_{r,c04}^{sub2we} - M_{r,c04}^{we2sub} - \frac{P_{r,c04}^{we}}{5} \right) dt + P_{r,c04}^{we}(t_0);$$

for intermediate population stocks as:

$$P_{r,am}^{we} = \int_{t_0}^t \left(\frac{P_{r,ay}^{we}}{5} - D_{r,am}^{we} + M_{r,am}^{sub2we} - M_{r,am}^{we2sub} - \frac{P_{r,am}^{we}}{5} \right) dt + P_{r,am}^{we}(t_0) \text{ and}$$

for the population stock aged 95 or older:

$$P_{r,c95+}^{we} = \int_{t_0}^t \left(\frac{P_{r,c9094}^{we}}{5} - D_{r,c95+}^{we} + M_{r,c95+}^{sub2we} - M_{r,c95+}^{we2sub} \right) dt + P_{r,c95+}^{we}(t_0)$$

In addition, the population is divided into three social classes. However, the division into social classes is made apart from the previously established divisions and follows a different logic. The population stock only has the division into ages and regions and evolves from these with the equations that we are exposing. The division into three classes is established a posteriori: given a certain evolution of the population as a whole, in each time step each age cohort is divided into the richest 20%, the poorest 30% and the intermediate 50%.

The different components that determine population dynamics are calculated as follows. The birth flow is calculated using the population stock of age groups within the fertile range and the birth rate of each group. Birth rates are endogenously computed based on

per capita consumption, divided into three social classes, and per capita public education spending, which is calculated in the economic module. Different functional forms have been used to estimate birth rates across age groups to achieve a better statistical fit.

Additionally, when per capita consumption falls below the monetized subsistence level (a fixed amount of 729 € at constant prices of 2019), a different function is applied to calculate the birth rate. This function is the same for all age cohorts, and its parameters are adjusted so that when per capita consumption is half the subsistence level, the birth rate drops to zero. The rates represent births every five years, so they must be divided by five to obtain annual figures.

If per capita consumption > subsistence consumption:

$$Br5y_{r,c1519}^{we} = \sum_{cl} \left(\left(yf_{c1519}^{Br5y} + (y0_{c1519}^{Br5y} - yf_{c1519}^{Br5y}) \cdot e^{-\alpha_{c1519}^{Br5y} \cdot (Cpc_{r,cl}^{we,s} + Edpc_r)} \right) \cdot clsh_{cl} \right)$$

$$Br5y_{r,c2024}^{we} = \sum_{cl} \left(\left(yf_{c2024}^{Br5y} + (y0_{c2024}^{Br5y} - yf_{c2024}^{Br5y}) \cdot e^{-\alpha_{c2024}^{Br5y} \cdot (Cpc_{r,cl}^{we,s} + Edpc_r)} \right) \cdot clsh_{cl} \right)$$

$$Br5y_{r,c2529}^{we} = \sum_{cl} \left(\left(yf_{c2529}^{Br5y} + (y0_{c2529}^{Br5y} - yf_{c2529}^{Br5y}) \cdot e^{-\alpha_{c2529}^{Br5y} \cdot (Cpc_{r,cl}^{we,s} + Edpc_r)} \right) \cdot clsh_{cl} \right)$$

$$Br5y_{r,c3034}^{we} = \sum_{cl} \left(\left(\beta_1_{c3034}^{Br5y} + \beta_2_{c3034}^{Br5y} \cdot \ln(Cpc_{r,cl}^{we,s} + Edpc_r) \right) \cdot clsh_{cl} \right)$$

$$Br5y_{r,c3539}^{we} = \sum_{cl} \left(\left(\beta_1_{c3539}^{Br5y} + \beta_2_{c3539}^{Br5y} \cdot (Cpc_{r,cl}^{we,s} + Edpc_r) \right) \cdot clsh_{cl} \right)$$

$$Br5y_{r,c4044}^{we} = \sum_{cl} \left(\left(yf_{c4044}^{Br5y} + (y0_{c4044}^{Br5y} - yf_{c4044}^{Br5y}) \cdot e^{-\alpha_{c4044}^{Br5y} \cdot (Cpc_{r,cl}^{we,s} + Edpc_r)} \right) \cdot clsh_{cl} \right)$$

If per capita consumption < subsistence consumption:

$$Br5y_{r,a}^{we} = \max \left(0, \sum_{cl} \left((\beta_0_a^{Br5y} + \beta_1_a^{Br5y} \cdot Cpc_{r,cl}^{we,s}) \cdot clsh_{cl} \right) \right)$$

For age cohorts below 15 or above 44, the birth rate is always zero, regardless of whether consumption is above or below the subsistence threshold.

To obtain annual birth rates and births, we divide by five and multiply with the population size.

$$Br_{r,a}^{we} = \frac{Br5y_{r,a}^{we}}{5}$$

$$B_r^{we} = \sum_a (P_{r,a}^{we} \cdot Br_{r,a}^{we})$$

Deaths are calculated using the population stock of different age groups and their respective mortality rates. These mortality rates depend on per capita consumption—divided into social classes—and per capita public healthcare spending. As with birth rates, death rates represent deaths every five years, so they must be divided by five to obtain annual figures. When per capita consumption is below subsistence consumption, a different equation is used which sets the mortality rate over five years to 5 when per capita consumption is reduced to half of subsistence consumption as physical survival becomes impossible at those low levels of consumption.

If per capita consumption > subsistence consumption:

$$Dr5y_{r,a}^{we} = \sum_{cl} \left(\left(yf_a^{Dr5y} + (y0_a^{Dr5y} - yf_a^{Dr5y}) \cdot e^{-\alpha_a^{Dr5y} \cdot (Cpc_{r,cl}^{we,s} + Hpc_r)} \right) \cdot clsh_{cl} \right)$$

If per capita consumption < subsistence consumption:

$$Dr5y_{r,a}^{we} = \min \left(5, \sum_{cl} \left((\beta_0_a^{Dr5y} + \beta_1_a^{Dr5y} \cdot Cpc_{r,cl}^{we,s}) \cdot clsh_{cl} \right) \right)$$

To obtain annual mortality rates and deaths we divide by five and multiply with the population size.

$$Dr_{r,a}^{we} = \frac{Dr5y_{r,a}^{we}}{5}$$

$$D_{r,a}^{we} = P_{r,a}^{we} \cdot Dr_{r,a}^{we}$$

To calculate the population flow from the global economy to the subsistence economy, first, the ratio of the population that wishes to move to the subsistence sector is calculated for each region and social class. This ratio is then used to determine the flow. The ratio is calculated based on per capita consumption¹ and always ranges between 0 and 0.1. The flow is constrained by the availability of land for subsistence agriculture, which is calculated in the land use module:

$$Mr_{r,cl}^{we2sub} = \max \left(0, \min \left(0.1, \beta_0 - \beta_1 \cdot Cpc_{r,cl}^{we,s} (ts - 1) \right) \right)$$

$$MaxP^{sub} = Lnd_s \cdot Int_{sub_lnd}^{Lnd}$$

$$M_{r,a}^{we2sub} = \max \left(0; \min \left(1; \frac{MaxP^{sub} - P^{sub}}{\sum (Mr_{r,cl}^{we2sub} \cdot P_{r,a}^{we} \cdot clsh_{cl})} \right) \right) \cdot \sum_{cl} (Mr_{r,cl}^{we2sub} \cdot P_{r,a}^{we} \cdot clsh_{cl})$$

On the other hand, the flow from the subsistence economy to the global economy is calculated using a ratio and the stock of population living in subsistence conditions. The ratio is determined based on the per capita consumption in the lowest classes of the

¹ In this case, as in some others, the value of the variable in the previous time step is used to avoid simultaneous equations.

different regions within the global economy and the fixed per capita consumption in subsistence.

Additionally, if there is insufficient land to sustain the subsistence population, forced integration into the global economy occurs. This process is independent of the previously mentioned ratio and serves as an adjustment mechanism when subsistence conditions cannot support the existing population.

$$Mr_r^{sub2we} = \max(0, \min(0.1; \beta_1 \cdot (Cpc_{r,low}^{we,s} - Cpc^{sub})))$$

$$M_{r,a}^{sub2we} = \max\left(Mr_r^{sub2we} \cdot P_{r,a}^{sub}; \left(\frac{\max(0; P^{sub} - MaxP^{sub})}{P^{sub}}\right) \cdot P_{r,a}^{sub}\right)$$

The same equations used for the population integrated into the global economy are applied to the population belonging to the subsistence sector, with only two differences. The first difference is that, instead of using the per capita consumption of the corresponding region and social class plus per capita public spending on health or education to calculate birth and death rates, the per capita subsistence consumption is used—which, as previously mentioned, is a constant. The second difference lies in the equations used to calculate population changes, where migration terms have reversed signs. This is because migrations from the global economy to subsistence represent an inflow for the subsistence population but an outflow for the global economy's population stock. Conversely, migrations from subsistence back to the global economy constitute an outflow for the subsistence population and an inflow for the global economy.

2.2. Economy

The economic module follows an input-output structure where production is determined by final demand and a series of other factors (technological changes, environmental degradation damages, resource scarcity, etc.) that we will examine below.

We begin by explaining the calculation of demand components before moving on to the calculation of production and the physical constraints that can limit production.

Final demand, like production, is calculated at a global scale and divided into sectors. Furthermore, final demand consists of three components: private consumption, public consumption, and investment.

Private consumption is calculated using exogenous per capita consumption trajectories. This approach allows for the direct simulation of different inequality scenarios in a straightforward manner. However, the mechanisms leading to inequality are not explicitly represented—only the final outcome is reflected, namely that per capita consumption differs across the three classes in the three represented regions.

To implement these trajectories in the model, initial per capita consumption is specified for each class and region, along with a growth rate for each consumption level. Additionally, as will be shown later, not all consumption demand may necessarily be met, since various production constraints can arise.

$$Cpc_{r,cl}^{we,d} = \int_{t_0}^t (Cpc_{r,cl}^{we,d} \cdot Cpc_gr_{r,cl}^{we} - Cpc_nc_{r,cl}^{we}) dt + Cpc_{r,cl}^{we,d}(t_0)$$

The sectoral distribution of per capita consumption is calculated using final consumption data from EXIOBASE3 (Stadler et al., 2018) that is aggregated to approximate the three MORDRED world regions. Thus, we obtain three sectoral distributions that belong to three per capita consumption levels (cf. section 3.2.3.5). The minimum consumption level corresponds to average household consumption in those Exiobase3 countries and regions that were matched with the MORDRED region ‘periphery’. The maximum consumption level corresponds to average household consumption in those Exiobase3 countries that were matched with the MORDRED region ‘center’. The medium value corresponds to the average household consumption in those Exiobase3 countries and regions that were matched with the MORDRED region ‘semiperiphery’.

For per capita consumption levels below the approximated average ‘periphery’ consumption level the sectoral distribution corresponding to this minimum level is maintained. For levels above the average ‘center’ consumption, the sectoral distribution corresponding to this maximum level is maintained. For intermediate levels, an interpolation is established using the three available data points.

$$Cpc_{r,cl,i}^{we,d} = Cpc_{r,cl}^{we,d} \cdot Cpc_ssh_{r,cl,i}$$

Once per capita consumption by sector is determined, it is multiplied by the population of each class and region to obtain total consumption per class and region. By aggregating across all classes and regions, we derive global private consumption by sector.

$$C_{r,cl,i}^d = Cpc_{r,cl,i}^{we,d} \cdot P_r^{we} \cdot clsh_{cl}$$

$$C_{r,i}^d = \sum_{cl} C_{r,cl,i}^d$$

$$C_i^d = \sum_r C_{r,i}^d$$

Public consumption is calculated based on private consumption, maintaining a constant ratio between the two (though future scenarios could potentially be designed where this ratio evolves over time). Next, a sectoral distribution is applied for each region, remaining constant throughout the simulation period. To obtain global public consumption by sector, we aggregate the public consumption across all three regions.

$$G_r^d = C_r^d \cdot G2Cr_r$$

$$G_{r,i}^d = G_r^d \cdot G_ssh_{r,i}$$

$$G_i^d = \sum_r G_{r,i}^d$$

Last, investment is calculated by sector and directly at the global level, aiming to maintain a specific 'capital stock to production' ratio for each sector, depending on the capital intensity of the sector. Therefore, to calculate investment, both the capital intensity and the sector's production are taken into account, as well as the depreciation rate of the sector's capital stock.

Both capital intensity and the depreciation rate have an endogenous and an exogenous component. The exogenous component either evolves according to the technological changes assumed in the scenario or remains constant. The endogenous component depends on various changes occurring in the natural environment.

In the case of capital intensity, the exogenous part evolves according to technological changes, while the endogenous part is affected by two distinct factors. In the fossil fuel production sectors (sector 3 and 8), it is affected by the increasing difficulty of extraction as recoverable fossil resources become increasingly depleted. In agriculture (contained in sector 1), it is influenced by the damages caused by climate change on this sector. While damages in agriculture have been represented as an output loss ratio, extraction difficulty has been modeled as a factor that multiplies the factors of production required to extract fossil resources.

$$Int_1^k = \frac{Int_1^{k,bd}}{(1 - X_loss_1)}$$

$$Int_{3,8}^k = Int_{3,8}^k \cdot Edf$$

For the rest of the sectors:

$$Int_i^k = Int_i^{k,bd}$$

The global mean temperature appears in most damage functions and enters the model as the difference between the global mean temperature at time t and in 1850.

$$\Delta Temp = Temp(t) - Temp(1850)$$

The function determining extraction difficulty is described in the energy section, while the corresponding output loss in the agricultural sector is modeled as:

$$X_loss_1 = \beta^{X_loss} \cdot \left(\frac{\Delta Temp - 1}{3} \right)$$

For the depreciation rate, the exogenous component remains constant, while the endogenous component depends on both temperature rise and sea level rise. Ultimately, sea level rise also depends on temperature, but the damage function is modeled differently in each case. When the damage is related to temperature increases, the function is continuous and affects the depreciation rate unevenly across different sectors. In contrast, when the damage depends on sea level rise, it is applied after certain temperature thresholds are exceeded (2°C, 3°C, and 4°C), following a Gaussian function and affecting all sectors' depreciation rates equally. In other words, the damage is assumed to affect the capital stock as a whole without sectoral differentiation.

Damage caused directly by temperature:

$$\delta_i^{temp} = \beta_i^{\delta_temp} \cdot \left(\frac{(\Delta Temp - 1)^2}{9} \right)$$

Damage caused by sea level rise:

$$\delta_i^{slr} = \beta 0^{2^\circ C_slr} \cdot e^{-\left(\frac{(t-10-t^{2^\circ C})^2}{\beta 1^{2^\circ C_slr}}\right)} + \beta 0^{3^\circ C_slr} \cdot e^{-\left(\frac{(t-10-t^{3^\circ C})^2}{\beta 1^{3^\circ C_slr}}\right)} + \beta 0^{4^\circ C_slr} \cdot e^{-\left(\frac{(t-10-t^{4^\circ C})^2}{\beta 1^{4^\circ C_slr}}\right)}$$

Calculation of depreciation by sector:

$$\delta_i = \delta_i^{bd} + \delta_i^{temp} + \delta_i^{slr}$$

Once capital intensity and depreciation are known, sectoral investment can be calculated using the sector's output in the previous time step, its capital stock, and an adjustment parameter that regulates the investment speed. This ensures the investment isn't concentrated in a single period.

$$Inv_i^d = \max(0; \beta^{Inv} \cdot (X_i^s(ts - 1) \cdot Int_i^k - K_i) + \delta_i \cdot K_i)$$

The capital stock simply increases with investment and decreases with depreciation.

$$K_i = \int_{t_0}^t (Inv_i^s - \delta_i \cdot K_i) dt + K_i(t_0)$$

The sum of investment across all sectors yields total investment. Subsequently, to calculate gross fixed capital formation as a demand component, total investment is multiplied by a vector indicating which portion of the total investment goods each sector is responsible for producing. Additionally, there is supplementary gross fixed capital formation that becomes necessary when the temperature increase exceeds 2°C above pre-industrial levels due to assumed increased hard coastal protection. This additional investment is applied for 40 years once this temperature threshold is reached.

$$GFCF_i^d = GFCF_ssh_i \cdot \sum_i (Inv_i^d) + Extra_GFCF^{slr}$$

The sum of the three demand components yields final demand.

$$FD_i^d = C_i^d + G_i^d + GFCF_i^d$$

To calculate the output required to meet this final demand, using the input-output table is essential. Like capital intensity, the input-output table has both an exogenous component—which evolves according to hypothesized technological changes—and an endogenous component that depends on increasing fossil resource extraction difficulty and food sector damages.

Damage to the food sector is modeled as a factor that increases intermediate consumption of this sector. If temperature < 1.4 °C:

$$Adf^{io} = 1$$

If temperature >1.4 °C:

$$Adf^{io} = \beta 0^{Adf_io} + \beta 1^{Adf_io} \cdot \Delta Temp + \beta 2^{Adf_io} \cdot \Delta Temp^2$$

Column 1 (food sector) of the input-output matrix:

$$a_{i,1} = a_{i,1}^{bd} \cdot Adf^{io}$$

Column 3 and 8 (fossil fuels) of the input-output matrix:

$$a_{i,3,8} = a_{i,3,8}^{bd} \cdot Edf$$

For the remaining sectors contained in the input-output matrix:

$$a_{i,j} = a_{i,j}^{bd}$$

Using final demand and the input-output table, the output vector required to satisfy final demand can be calculated through the Leontief inverse.

$$\bar{X}^d = (Id - A)^{-1} \cdot \bar{FD}^d$$

In this way, it is possible to determine the land, fossil resources, and labor required for the desired overall production. This calculation is performed in the respective modules (land use, energy, and labor). Since the production function used in the model is a Leontief production function, if there is scarcity in any of these resources, production is reduced proportionally to adjust to the resource's availability. In other words, there is no substitutability between the different production factors.

To represent this, a scarcity factor ranging from 0 to 1 is calculated in each of the corresponding modules. The smallest of these scarcity factors is then multiplied by the demanded output to determine the actual output produced. By convention, we will refer to this output as the supplied output (X^s).

$$Sf = \min (Sf^{Lb}; Sf^{ff}; Sf^{Lnd})$$

$$X_i^s = X_i^d \cdot Sf$$

This same scarcity factor is also applied to final demand to calculate the actual satisfied final demand, as well as to the productive factors to determine the resources that have actually been used.

$$FD_i^s = FD_i^d \cdot Sf$$

Regarding the application of scarcity within final demand—that is, to its different components—there are two possible methods. Either the scarcity factor is applied uniformly to all components, or an allocation function is used to prioritize certain components over others.

Vensim offers several allocation-type functions, and the one used in this model is the ALLOCATE AVAILABLE function. This function distributes a limited quantity (in this case, the total final demand that can be satisfied with the available production factors) among

multiple claimants (the different demand components) based on a set of parameters. These parameters determine each claimant's priority, establishing who receives resources first and at what threshold of satisfied demand the allocation shifts to the next claimant. While the mechanics of this function are complex, they are thoroughly documented in Vensim's help section.²

Once the demand components are calculated, the per capita consumption for each class and region can be derived by dividing the consumption allocated to the corresponding group by the population that constitutes it.

$$Cpc_{r,cl}^{we,s} = \frac{\sum_i (C_{r,cl,i}^s)}{\sum_a (P_{r,a}^{we}) \cdot clsh_{cl}}$$

The per capita consumption not covered, which appears in the per capita consumption demand calculation equation, is computed as the difference between the demanded per capita consumption and the supplied per capita consumption.

$$Cpc_nc_{r,cl}^{we} = Cpc_{r,cl}^{we,d} - Cpc_{r,cl}^{we,s}$$

2.3. Labor

The function of the labor module is to account for labor demand, the available workforce, the number of hours that can contribute to production, and the production limit imposed by this factor.

Labor demand is determined by the desired sectoral production and the labor intensity of different sectors. As with capital intensity, labor intensity also has an exogenous component, which varies depending on technological advancements in the proposed scenarios, and an endogenous component, which represents the damage caused by environmental degradation on labor productivity. Additional endogenous components have been introduced in extended MORDRED versions that are not described here.

The endogenous component is divided into three types of damage: damage to the food sector, the increased difficulty of fossil fuel extraction—both of which have been mentioned previously—and the damage caused by extreme heat on labor productivity. The first is modeled in the same way as for capital intensity, i.e. as a loss of output. In fact, the same variable is used (X_loss_1). The second is calculated in the energy module, as previously mentioned.

The third damage type is unique to this module and applies to all sectors, though with different strengths for each sector. It is modeled as a reduction in sectoral labor productivity.

$$HD_i^{Lb_prod} = \beta_i^{HB_Lb_prod} \cdot \left(\frac{(\Delta Temp - 1)^2}{4} \right)$$

² https://www.vensim.com/documentation/fn_allocations.html

Taking into account the endogenous and exogenous components, the labor intensity can be calculated.

For sector 1:

$$Int_1^{Lb} = \frac{Int_1^{Lb,bd}}{(1 - X_loss_1 - HD_1^{Lb_prod})}$$

For sector 3 and 8:

$$Int_{3,8}^{Lb} = \frac{Int_{3,8}^{Lb,bd}}{(1 - HD_{3,8}^{Lb_prod})} \cdot Edf$$

For the remaining sectors:

$$Int_i^{Lb} = \frac{Int_i^{Lb,bd}}{(1 - HD_i^{Lb_prod})}$$

Based on the output demanded by sector and the respective intensities, the sectoral labor demand and the total labor demand are computed:

$$Lb_i^d = X_i^d \cdot Int_i^{Lb}$$

$$Lb^d = \sum_i Lb_i^d$$

On the other hand, the maximum labor supply is calculated based on the population integrated into the global economy aged 15 – 64, a maximum participation rate, and a maximum number of working hours per worker. Additionally, when determining the maximum labor supply, a factor representing losses in labor supply due to rising temperatures is also applied.

$$HD^{Max_Lb} = \beta^{HB_Max_Lb} \cdot \left(\frac{(\Delta Temp - 1)^2}{9} \right)$$

$$Max_Lb = \sum_{r,[1519,...,6064]} (P_{r,[1519,...,6064]}^{we}) \cdot Prt_r \cdot Max_h \cdot (1 - HD^{Max_Lb})$$

From the total labor demand and the maximum labor supply, the labor scarcity factor is calculated. This factor indicates whether there is a labor shortage and, if so, its extent in meeting the demanded production.

$$Sf^{Lb} = \min \left(1; \frac{Max_Lb}{Lb^d} \right)$$

2.4. Energy

The energy module calculates energy consumption, including both final energy and primary energy. It also accounts for the amount of remaining extractable non-renewable energy resources and estimates extraction difficulty, allowing the corresponding modules

to adjust extraction costs i.e. required intermediate inputs, labor hours, and capital needed per extracted unit.

To calculate final energy demand, the module multiplies the unadjusted desired sectoral output by conversion factors that convert monetary units into energy units.³ On the one hand, the energy use of goods constituting final energy is computed, and on the other, non-energy use is determined. By adding up the two variables, the final energy demand is obtained.

$$FE_{i,en}^{d,eu} = X_i^d \cdot Cf_{i,en}^{eu}$$

$$FE_{i,en}^{d,neu} = X_i^d \cdot Cf_{i,en}^{neu}$$

$$FE_{i,en}^d = FE_{i,en}^{d,eu} + FE_{i,en}^{d,neu}$$

Subsequently, using the final energy demand, the module calculates the primary energy demand for fossil resources (oil, natural gas, and coal).⁴ Fossil fuel consumption is later used to update the remaining amount of extractable resources.

$$PE_{ff}^d = \sum_i (FE_{i,ff}^d) \cdot FE2PE_{ff}$$

The model allows for rationing the extraction of non-renewable resources by imposing an annual maximum extraction ratio relative to the total extractable resource. Using both the demand for non-renewable resources and the maximum extractable amount, the energy scarcity factor is calculated. This factor ranges from 0 to 1 and indicates the fraction of the demanded output that can actually be produced. The extractable fossil fuel resource is derived by aggregating all types of fossil fuels.

$$Max_ff = Max_Er \cdot Rsc_ff$$

$$Sf_{ff} = \frac{Max_ff}{\sum_{ff}(PE_{ff}^d)}$$

The model calculates the actual energy production quantities by using both the general scarcity factor (which accounts for various production limits) and the demanded energy amounts. This approach ensures that output adjustments properly reflect all constrained resources across the economic system.

$$FE_{i,en}^s = FE_{i,en}^d \cdot Sf$$

$$PE_{ff}^s = PE_{ff}^d \cdot Sf$$

³ Only the output of the energy sectors is used, thus, the conversion factor takes the value 0 when the sectors are not energy sectors.

⁴ The final energy types cover oil, natural gas, coal, electricity, biofuels and waste, and other final energy. However, only oil, natural gas and coal are computed as primary energies. In the programming structure, final energies constitute the energy vector (en). Additionally, a subset of this vector - the fossil fuels subvector (ff) - is used for calculating primary energies.

Fossil energy production is the only outflow from the stock of extractable non-renewable energy resources, so the evolution of the latter can be calculated using the former:

$$Rsc_{ff} = Rsc_{ff(t_0)} - \int_{t_0}^t \sum_{ff} (PE_{ff}^s) dt$$

Finally, the stock of extractable resources is used to calculate the extraction difficulty factor, which increases the intensity of the productive factors needed to extract fossil energy.

$$Edf = \max\left(1; \beta 0^{Edf} \cdot e^{\beta 1^{Edf} \cdot \left(1 - \frac{Rsc_{ff}}{Rsc_{ff(t_0)}}\right)}\right)$$

2.5. Land

The land module tracks available land for productive uses and its allocation. The available land can be divided into nine categories: built infrastructure, land used for renewable energy generation (energy land), land used for food generation by the global economy (food land), land used for food generation by the subsistence sector (subsistence land), forest that is used by productive sectors (forest land), primary forest with no productive use, secondary forest with no productive use, other productively used land (other land), and shrubland (this category describes land that is not a forest and not productively used).

Land demand depends on different variables and varying usage intensities. Firstly, for infrastructure land, consumption serves as a proxy variable along with land use intensity for infrastructure. Secondly, for land uses related to production, an intensity matrix is employed that links sectoral production with the land required to meet the demanded output. A comprehensive matrix including all sectors is used for programming convenience, though most cases show zero intensity. For instance, only the food sector requires food land, and only energy sectors demand energy land.

$$Lnd_{inf}^d = \sum_{r,cl,i} (C_{r,cl,i}^d) \cdot Int_{inf}^{Lnd}$$

$$Lnd_{prod_Lnd}^d = \sum_i (X_i^d \cdot Int_{i,prod_Lnd}^{Lnd})$$

In the third place, the demand for subsistence land depends on the number of people living in subsistence, plus the inflow of those seeking to join the subsistence sector.

$$Lnd_{sub}^d = \sum_{r,a} (P_{r,a}^{sub} + M_{r,a}^{we2sub}) \cdot Int_{sub_Lnd}^{Lnd}$$

The usage intensities for productive land and subsistence land change exogenously according to different scenarios. Furthermore, for food land—both for the global economy and subsistence—there is also an exogenous component dependent on climate change. For the global economy, the damage has been modeled in the same way as for capital and

labor, as an output loss. For subsistence, it has been modeled as an additional intensity that sums to the pre-damage intensity.

$$Ext_Int_{sub_lnd}^{Lnd} = \beta^{Ext_Int_Lnd_sub} \cdot (\Delta Temp - 1)$$

$$Int_{sub_lnd}^{Lnd} = Int_{sub_lnd}^{Lnd,bd} + Ext_Int_{sub_lnd}^{Lnd}$$

$$Int_{foodland_we}^{Lnd} = \frac{Int_{foodland_we}^{Lnd,bd}}{(1 - X_loss_1)}$$

The "demand" for primary forest always equals the amount of primary forest from the previous period, meaning it only disappears if subsequent land allocation assigns its space to other uses. A similar approach applies to secondary forest—its "demand" equals the previous period's secondary forest plus the productive-use forest, ensuring that abandoned productive forest is converted into secondary forest. Finally, the "demand" for shrubland equals all available land. This programming treats shrubland as residual land; during allocation, its "demand" is only fulfilled after other land demands are satisfied. However, if no other land types were demanded, all available land would turn into shrubland.

$$Lnd_{pfrst}^d = Lnd_{pfrst}^s(ts - 1)$$

$$Lnd_{sfrst}^d = Lnd_{sfrst}^s(ts - 1) + Lnd_{prod_frst}^s(ts - 1)$$

$$Lnd_{shrub}^d = Dsp_Lnd$$

The quantity of available land may decrease during the simulation due to environmental impacts that result in land losses.

Additionally, depending on the scenarios, there is an option to protect either a portion of primary forest or land used in the subsistence sector. If this option is activated, it comes at the expense of reducing the total land available for allocation.

$$Lnd_loss = \beta^{Lnd_loss} \cdot \left(\frac{(\Delta Temp - 1)^2}{9} \right)$$

$$Foodland_loss = \beta^{Foodland_loss} \cdot \left(\frac{(\Delta Temp - 1)^2}{9} \right)$$

$$Dsp_Lnd = Dsp_Lnd^{bd} - Lnd_loss - Foodland_loss - Prt_Lnd_{sub_lnd} - Prt_Lnd_{pfrst}$$

The land allocation process begins after all land demands have been calculated. The system employs the ALLOCATE AVAILABLE function to determine land distribution, using the same methodology applied for allocating scarce production capacities among different demand components.

Following land allocation, the model calculates the land scarcity factor based on productive sectors' land demand versus available land supply. This factor reflects the tension between resource requirements and availability.

$$Sf^{Lnd} = \min \left(\frac{Lnd_{en_lnd}^s}{Lnd_{en_lnd}^d}, \frac{Lnd_{foodland_we}^s}{Lnd_{foodland_we}^d}, \frac{Lnd_{prod_frst}^s}{Lnd_{prod_frst}^d}, \frac{Lnd_{oth_lnd}^s}{Lnd_{oth_lnd}^d} \right)$$

2.6. Stressors

The stressors module calculates human-generated emissions of various pollutants. Some impact other model components, while others serve solely as indicators.

The module tracks multiple stressor variables. The first group of variables is composed of different greenhouse gases: CO2, CH4, N2O, SF6, HFCs, and PFCs.

Emissions are derived from economic output and emission intensity factors. These intensity factors evolve exogenously based on technological change assumptions in each scenario. For the food sector, emission intensities are impacted by climate change damage effects.

Intensity in sector 1:

$$Int_{1,ghg}^{em} = \frac{Int_{1,ghg}^{em,bd}}{(1 - X_loss_1)}$$

Intensity in the rest of sectors:

$$Int_{i,ghg}^{em} = Int_{i,ghg}^{em,bd}$$

Emissions:

$$Em_{ghg} = \sum_i (X_i^s \cdot Int_{i,ghg}^{em})$$

The exception is CO2, where a distinction is made between emissions from fossil fuel combustion (calculated based on the primary fossil energy consumption), emissions from land-use changes, and emissions from non-combustion production processes. This differentiation allows for a more precise tracking of CO2 emission sources and their respective drivers within the model.

$$Em_{CO2}^{comb} = \sum_i (PE_{i,ff}^s) \cdot Int_{ff,co2}^{em}$$

$$Em_{CO2}^{land} = Frst_lnd_rdct \cdot Int^{em,land}$$

$$Em_{CO2}^{other} = \sum_i (X_i^s \cdot Int_{i,CO2}^{em,other})$$

$$Em_{CO2} = Em_{CO2}^{comb} + Em_{CO2}^{land} + Em_{CO2}^{other}$$

The second group consists of variables related to water consumption. A distinction is made between green water consumption and blue water consumption. Green water consumption is linked to food production and is therefore calculated using the sector's output along with a green water intensity factor. This intensity factor contains both an

exogenous component and an endogenous component that reflects climate change impacts on the agricultural sector.

$$Int^{WC,green_w} = \frac{Int^{WC,green_w,bd}}{(1 - X_loss_1)}$$

$$WC^{green} = X_1^s \cdot Int^{WC,green_w}$$

Blue water consumption is divided into industrial water consumption, industrial water withdrawal, household water consumption, and household water withdrawal. The first two variables are calculated based on sectoral output and their respective blue water intensity factors. These intensity factors vary exogenously according to technological change assumptions. For the food sector, in addition to exogenous variations, they are also affected by climate change impacts.

Intensity for sector 1:

$$Int_1^{WC,blue_w,prod} = \frac{Int_1^{WC,blue_w,prod,bd}}{(1 - X_loss_1)}$$

$$Int_1^{WW,blue_w,prod} = \frac{Int_1^{WW,blue_w,prod,bd}}{(1 - X_loss_1)}$$

Intensity for the rest of the sectors:

$$Int_i^{WC,blue_w,prod} = Int_i^{WC,blue_w,prod,bd}$$

$$Int_i^{WW,blue_w,prod} = Int_i^{WW,blue_w,prod,bd}$$

Blue water consumption and withdrawal in production:

$$WC^{blue_w,prod} = \sum_i (X_i^s \cdot Int_i^{WC,blue_w,prod})$$

$$WW^{blue_w,prod} = \sum_i (X_i^s \cdot Int_i^{WW,blue_w,prod})$$

The second two are calculated from household consumption. The intensity of this water consumption varies exogenously.

$$WC^{blue_w,hh} = \sum_i (C_{r,cl,i}^s) \cdot Int^{WC,blue_w,hh}$$

$$WW^{blue_w,hh} = \sum_i (C_{r,cl,i}^s) \cdot Int^{WW,blue_w,hh}$$

The third group of stressors consists of extraction flows for 19 material types. The extraction is divided into used material extraction and unused material extraction. In both cases, the calculation is based on sectoral output and a specific extraction intensity for each material. These extraction intensities remain constant throughout the simulation.

$$Mat_{mat}^{used} = \sum_i (X_i^s \cdot Int_{i,mat}^{mat_used})$$

$$Mat_{mat}^{unused} = \sum_i (X_i^s \cdot Int_{i,mat}^{mat_unused})$$

$$Mat_{mat} = Mat_{mat}^{used} + Mat_{mat}^{unused}$$

Fourth, the model addresses phosphorus and nitrogen pollution. The pollution flow is calculated based on sectoral output⁵ and intensity factors that evolve exogenously, with an additional endogenous component applied specifically to the food sector. Within the model, phosphorus and nitrogen pollution is categorized into three types: water pollution by nitrogen, water pollution by phosphorus, and soil pollution by phosphorus.

Intensity for sector 1:

$$Int_{1,P\&N} = \frac{Int_{1,P\&N}^{bd}}{(1 - X_loss_1)}$$

Intensity for the rest of the sectors:

$$Int_{i,P\&N} = Int_{1,P\&N}^{bd}$$

Nitrogen and phosphorus contamination:

$$P\&N_Poll_{P\&N} = \sum_i (X_i^s \cdot Int_{i,P\&N})$$

Fifth, the model calculates air pollution. This is computed using sectoral output and exogenously evolving intensity factors, with an additional endogenous component for the food sector. The model classifies air pollution into three categories: NH3, PM2.5, and PM10.

Intensity for sector 1:

$$Int_{1,air_poll} = \frac{Int_{1,air_poll}^{bd}}{(1 - X_loss_1)}$$

Intensity for all other sectors:

$$Int_{i,air_poll} = Int_{1,air_poll}^{bd}$$

Air pollution:

$$Air_Poll_{air_poll} = \sum_i (X_i^s \cdot Int_{i,air_poll})$$

⁵ In practice, only sectors 1, 24, and 25 are used to calculate the generation of these pollutants. However, as in previous cases, the programming implementation calculates it across all sectors for convenience, with generation intensities set to 0 for the remaining sectors.

Finally, the consumption of industrial roundwood is calculated from the output of sector 2 and a conversion factor.

$$IRW = X_2^S \cdot Cf^{IRW}$$

3. Model data

3.1. Demography

3.1.1. Initial population

The raw data comes from the United Nations, Department of Economic and Social Affairs, Population Division (UN DESA, 2019c). The data for 2020 were taken because there are no data for 2019.

The data was matched to all the countries aggregated in Exiobase3.

There are 21 age categories in the raw data (from 0-4 years, 5-9 years, 10-14 years, ..., 95-99 years, 100+years) whereas MORDRED has 20 age groups (from 0-4 years, 5-9, 10-14, etc., with the last category being people aged 95+). Thus, the last two age groups were aggregated. For every age group, the population of the respective countries was aggregated into the three MORDRED world regions (cf section 3.1.4).

Initial population in the formal and informal economy

The total initial population in the three world regions and in the 20 age groups were further sub-divided into population sustained by and working for the global economy, and population sustained by and working in a subsistence economy.

We estimate that in 2019 at least 800 million people lived not fully integrated or even apart from the global economy in different forms of subsistence regimes, focusing on the poorest population groups among the 380 to 510 million smallholder farms and the high intersection between subsistence farming and extreme poverty (Lowder et al., 2025; Samberg et al., 2016). For simplicity, we assume that (1) the share of people living in subsistence regimes does not vary by age group or gender, and (2) the vast majority of individuals living at the margins of the global economy reside in the periphery, with the remainder living in the semi-periphery. Due to the lack of precise data, we operationalized these qualitative assumptions by allocating 85% of the population in subsistence regimes to the periphery and 15% to the semi-periphery at the start of the simulations in 2019.

As mentioned in section 2.2, this ‘subsistence class’ is characterized by high but stable death and birth rates and very low but stable per capita consumption, which is only partially monetized. Fertility and mortality rates for the different age groups for the subsistence class are computed using the monetized per capita consumption of the subsistence class which we approximate by using the World Bank’s extreme poverty line (World Bank, 2025) (2.15\$ in 2017-PPP, converted to 1.997 (2019-)€ per day) which gives a per capita consumption of 729 € per year for 2019.

The remaining population in the center, semiperiphery and periphery lives within the formal economy and is matched to one of three classes within each MORDRED region.

3.1.2. Mortality and fertility parameters

The raw data for the calculation of birth and death parameters comes from UN DESA (2019b, 2019c, 2019a) and from Exiobase3 final demand data for 1995, 2000, 2005, 2010, 2015 and 2020 (Stadler et al., 2021).

The Exiobase3 data was converted to 2019-€ using the ECB deflator. All Exiobase sectors were aggregated into one single sector, apart from the 'Education (80)' and the 'Health and social work (85)' sector, which were matched to sector no. 22 (education) and sector no. 23 sectors, respectively (Table 3).

The original regional disaggregation of Exiobase with 44 countries and 5 (rest of the) world regions was preserved (cf. section 3.1.4).

The average government final demand for the education and health sector for all 49 Exiobase regions were calculated for the time periods 1995-2000, 2000-2005, 2005-2010, 2010-2015 and 2015-2020.

The average population size for every Exiobase region for the time periods 1995-2000, 2000-2005, 2005-2010, 2010-2015 and 2015-2020 was calculated by aggregating the 21 age groups and by aggregating country data into the 5 Exiobase world regions (WA, WL, WF, WE, WM).

By dividing government final demand by population size a series of different average per capita government expenditures for health and education were generated.

The average household consumption per capita for the time periods 1995-2000, 2000-2005, 2005-2010, 2010-2015 and 2015-2020 for the 49 Exiobase regions was calculated by 1) adding the Exiobase final demand categories of 'households' and 'non-profit organizations serving households' and summing over all sectors; 2) dividing the resulting final demand by the total population in the respective regions and time periods.

Mortality and fertility rates over 5 years were derived by:

1.) calculating total deaths and births for every country over five years for the respective periods (1995-2000, 2000-2005, 2005-2010, 2010-2015 and 2015-2020) and respective age groups. This requires taking into account that the original data give births per 1000 women and per year.

2.) aggregating the death and births of the respective countries into deaths and births for the five Exiobase world regions (the rest of the countries can be incorporated without further changes).

3.) dividing the deaths and births by the total population in the respective age groups and regions. This gives mortality and fertility rates for every age group and for every Exiobase region (i.e. 44 countries and 5 world regions) which, multiplied by the respective population, indicate the number of deaths in the different age groups and the number of births coming from the different age groups that occur during 5 years.

With these results, we constructed a database containing 245 observations which we used to conduct a regression analysis. Each observation has 29 dimensions: the

consumption of households per capita; the education expenses of governments per capita; the health expenses of governments per capita; the mortality rate for people aged 0-4; 5-9; 15-19; 20-24; 25-29; 30-34; 35-39; 40-44; 45-49; 50-54; 55-59; 60-64; 65-69; 70-74; 75-79; 80-84; 85-89; 90-94; 95+; the fertility rate for people aged 15-19; 20-24; 25-29; 30-34; 35-39; 40-44; 45-49.

We assume that mortality and fertility rates are fully determined by a range of variables, the most important of which being consumption per capita as well as health and education expenses. Thus, we do not assume the abstract variable 'time' to influence mortality and fertility rates and consequently do not factor 'time' into the regression analysis. This has a methodological-logical reason: Introducing a time-effect into the estimation of mortality and fertility rates can lead to serious distortions in a simulation-based dynamic model. For example, if time is found to decrease mortality, even in a context of extreme poverty and environmental impacts mortality would continue to decrease over time, which constitutes a contradiction. Apart from that, we use data spanning a period of only 25 years which we assume to be short enough to avoid 'correcting' for time.

The regression analysis links per capita consumption and government expenses for health and education to mortality and fertility rate of the different age groups.

In total, we construct 25 regression models covering all relevant age groups. Most of the age groups exhibit exponentially decaying, asymptotic patterns (Figure 1).

For all mortality rates, we used self-starting Nonlinear Least Squares Asymptotic Regression Models (cf. section the equation for $Dr5y_{r,a}^{we}$ in section 2.1) that were calculated in R via the NLS/SSasymp commands from the stats package because they provided better fits than logistic regressions. We made no further adjustments to the calculated automated best guess.

While the dependent variable is the mortality rate in the respective age group the independent variable is the sum of the per capita consumption and the per capita government expense for health.

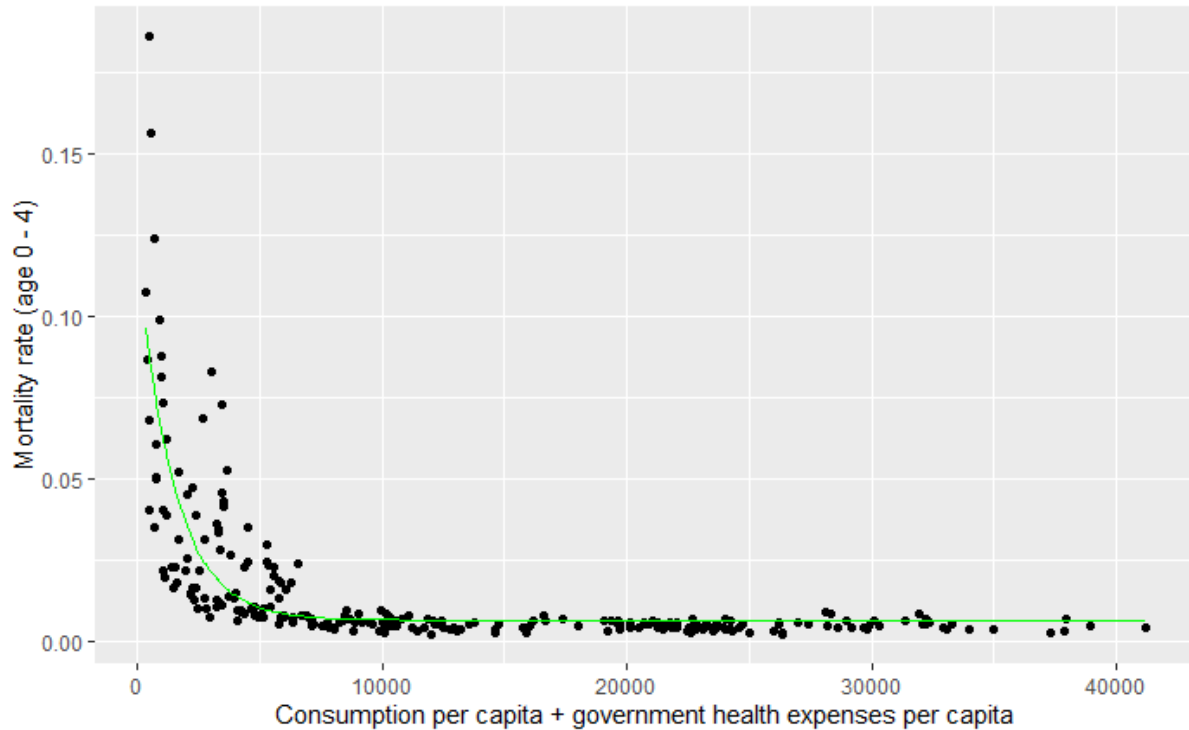


Figure 1: Mortality rates decrease with increasing consumption and health expenses. The green line is calculated from the parameters obtained from the NLS Asymptotic Regression Model.

For the birth rates the independent variable is the sum of the per capita consumption and the per capita government expense for education. For four age groups (15-19, 20-24, 25-29 and 40-44) we used the same function as for mortality rates whereas the birth rate of the age group 30-34 is best approximated through a logarithmic regression and the fertility rate of the age group 35-39 is best approximated through a linear regression.

To prevent illogical model outcomes in simulations where variables might take extreme values, in the model an upper bound of 1 for the mortality rate and a lower bound of 0 for the birth rate is applied. Since the model for the fertility of the age group 35-39 is a linear model, an upper bound of 0.25 is introduced which only begins to apply in the case of per capita consumption levels far above current levels (Figure 2).

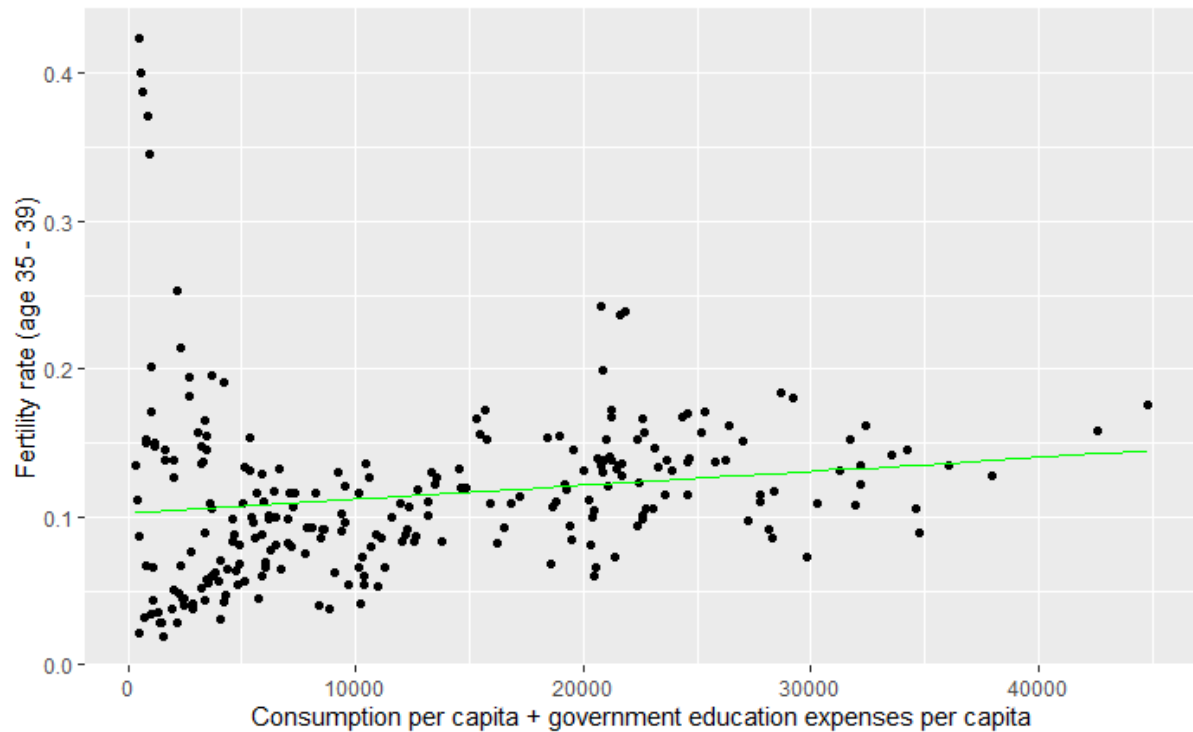


Figure 2: Fertility rates for the age group 35-39 increase with consumption and education expenses.

Fertility and mortality in the case of extremely low consumption values

The data that provide the basis for the regression analysis give mortality and fertility rates that are high but not excessively high for very low per capita consumption, which is due to the fact that these low per capita consumption values belong to the subsistence class and are based on the monetized consumption, thus, leaving out one part of the actual consumption. Thus, the regression functions are not suitable to describe death and birth rates at extremely low consumption of the classes that are sustained by the world economy because they do not have any other non-monetized consumption.

Thus, once the consumption per capita drops below the monetized subsistence level for a class that is sustained by the global economy linear functions that depend on per capita consumption ensure that mortality rates converge to 1 and birth rates to 0.

3.1.3. Migration between subsistence and world economy

The parameters regulating migration between the subsistence and the global economy reflect qualitative reasoning rather than any specific quantitative data sources and can be changes in different scenarios.

3.1.4. Aggregation of countries and EXIOBASE regions into MORDRED regions

The MORDRED regions *center*, *semiperiphery* and *periphery* are operationalized through the World Bank's income-based classification of countries for the year 2019 (World Bank, 2024d). For countries without a world bank classification, their GDP per capita was compared to countries with a world bank classification and comparable income per capita levels. In these cases, the value in the 'Worldbank classification' column of Table 1 is marked in *Italics*. Countries without UN population data are marked in *Italics* as well. Most of these countries have a very small population that is not significant at the global level, thus, their populations are set to zero.

Country number	Country Name	Worldbank classification	Exiobase3 Regions	MORDRED regions
1	Austria	H	AT	Center
2	Australia	H	AU	Center
3	Belgium	H	BE	Center
4	Bulgaria	UM	BG	Semiperiphery
5	Brazil	UM	BR	Semiperiphery
6	Canada	H	CA	Center
7	Switzerland	H	CH	Center
8	China	UM	CN	Semiperiphery
9	Cyprus	H	CY	Center
10	Czech Republic	H	CZ	Center
11	Germany	H	DE	Center
12	Denmark	H	DK	Center
13	Estonia	H	EE	Center
14	Spain	H	ES	Center
15	Finland	H	FI	Center
16	France	H	FR	Center
17	United Kingdom	H	GB	Center
18	Greece	H	GR	Center
19	Croatia	H	HR	Center
20	Hungary	H	HU	Center
21	Indonesia	UM	ID	Semiperiphery
22	Ireland	H	IE	Center
23	India	LM	IN	Periphery
24	Italy	H	IT	Center
25	Japan	H	JP	Center
26	South Korea	H	KR	Center
27	Lithuania	H	LT	Center
28	Luxembourg	H	LU	Center
29	Latvia	H	LV	Center
30	Malta	H	MT	Center
31	Mexico	UM	MX	Semiperiphery
32	Netherlands	H	NL	Center
33	Norway	H	NO	Center
34	Poland	H	PL	Center
35	Portugal	H	PT	Center
36	Romania	H	RO	Center

37	Russian Federation	UM	RU	Semiperiphery
38	Sweden	H	SE	Center
39	Slovenia	H	SI	Center
40	Slovak Republic	H	SK	Center
41	Türkiye	UM	TR	Semiperiphery
42	Taiwan, China	H	TW	Center
43	United States	H	US	Center
44	Afghanistan	L	WA	Periphery
45	Armenia	UM	WA	Semiperiphery
46	Azerbaijan	UM	WA	Semiperiphery
47	Bangladesh	LM	WA	Periphery
48	Bhutan	LM	WA	Periphery
49	Brunei Darussalam	H	WA	Center
50	Cambodia	LM	WA	Periphery
51	Hong Kong SAR, China	H	WA	Center
52	Macao SAR, China	H	WA	Center
53	Korea, Dem. Rep.	L	WA	Periphery
54	Fiji	UM	WA	Semiperiphery
55	French Polynesia	H	WA	Center
56	Georgia	UM	WA	Semiperiphery
57	Guam	H	WA	Center
58	Kazakhstan	UM	WA	Semiperiphery
59	Kiribati	LM	WA	Periphery
60	Kyrgyz Republic	LM	WA	Periphery
61	Lao PDR	LM	WA	Periphery
62	Malaysia	UM	WA	Semiperiphery
63	Maldives	UM	WA	Semiperiphery
64	Micronesia, Fed. Sts.	LM	WA	Periphery
65	Mongolia	LM	WA	Periphery
66	Myanmar	LM	WA	Periphery
67	Nepal	LM	WA	Periphery
68	New Caledonia	H	WA	Center
69	New Zealand	H	WA	Center
70	Pakistan	LM	WA	Periphery
71	Papua New Guinea	LM	WA	Periphery
72	Philippines	LM	WA	Periphery
73	Samoa	UM	WA	Semiperiphery
74	Singapore	H	WA	Center
75	Solomon Islands	LM	WA	Periphery
76	Sri Lanka	LM	WA	Periphery
77	Tajikistan	L	WA	Periphery
78	Thailand	UM	WA	Semiperiphery
79	Timor-Leste	LM	WA	Periphery
80	Tonga	UM	WA	Semiperiphery
81	Turkmenistan	UM	WA	Semiperiphery
82	Uzbekistan	LM	WA	Periphery
83	Vanuatu	LM	WA	Periphery
84	Vietnam <i>United States Minor Outlying Islands</i>	LM	WA	Periphery
85		L	WA	Periphery

86	<i>American Samoa</i>	UM	WA	Semiperiphery
87	<i>Antarctica</i>	L	WA	Periphery
88	<i>Bouvet Island</i>	L	WA	Periphery
89	<i>British Indian Ocean Territory</i>	L	WA	Periphery
90	<i>Wallis & Futuna</i>	L	WA	Periphery
91	<i>Christmas Island</i>	L	WA	Periphery
92	<i>Cocos Island</i>	L	WA	Periphery
93	<i>Cook Islands</i> <i>Heard Island and McDonald Islands</i>	L	WA	Periphery
94		L	WA	Periphery
95	<i>Marshall Islands</i>	UM	WA	Semiperiphery
96	<i>Niue</i>	L	WA	Periphery
97	<i>Norfolk Island</i>	L	WA	Periphery
98	<i>Northern Mariana Islands</i>	H	WA	Center
99	<i>Nauru</i>	H	WA	Center
100	<i>Palau</i> <i>South Georgia and the South Sandwich Islands</i>	H	WA	Center
101		L	WA	Periphery
102	<i>Pitcairn</i>	L	WA	Periphery
103	<i>Tokelau</i>	L	WA	Periphery
104	<i>Tuvalu</i>	UM	WA	Semiperiphery
105	<i>Albania</i>	UM	WE	Semiperiphery
106	<i>Belarus</i>	UM	WE	Semiperiphery
107	<i>Bosnia and Herzegovina</i> <i>Channel Islands (Gurenesey and Jersey)</i>	UM	WE	Semiperiphery
108		H	WE	Center
109	<i>Iceland</i>	H	WE	Center
110	<i>Montenegro</i>	UM	WE	Semiperiphery
111	<i>North Macedonia</i>	UM	WE	Semiperiphery
112	<i>Moldova</i>	LM	WE	Periphery
113	<i>Serbia</i>	UM	WE	Semiperiphery
114	<i>Ukraine</i>	LM	WE	Periphery
115	<i>Aland Islands</i>	H	WE	Center
116	<i>Andorra</i>	H	WE	Center
117	<i>Vatican</i>	H	WE	Center
118	<i>Faeroe Islands</i>	H	WE	Center
119	<i>Gibraltar</i>	H	WE	Center
120	<i>Monaco</i>	H	WE	Center
121	<i>Isle of Man</i>	H	WE	Center
122	<i>Kosovo</i>	UM	WE	Semiperiphery
123	<i>Liechtenstein</i>	H	WE	Center
124	<i>San Marino</i>	H	WE	Center
125	<i>Svalbard</i>	H	WE	Center
126	<i>Algeria</i>	LM	WF	Periphery
127	<i>Angola</i>	LM	WF	Periphery
128	<i>Benin</i>	LM	WF	Periphery
129	<i>Botswana</i>	UM	WF	Semiperiphery
130	<i>Burkina Faso</i>	L	WF	Periphery
131	<i>Burundi</i>	L	WF	Periphery
132	<i>Cabo Verde</i>	LM	WF	Periphery
133	<i>Cameroon</i>	LM	WF	Periphery

134	Central African Republic	L	WF	Periphery
135	Chad	L	WF	Periphery
136	Comoros	LM	WF	Periphery
137	Congo, Rep.	LM	WF	Periphery
138	Côte d'Ivoire	LM	WF	Periphery
139	Congo, Dem. Rep.	L	WF	Periphery
140	Djibouti	LM	WF	Periphery
141	Equatorial Guinea	UM	WF	Semiperiphery
142	Eritrea	L	WF	Periphery
143	Eswatini	LM	WF	Periphery
144	Ethiopia	L	WF	Periphery
145	Gabon	UM	WF	Semiperiphery
146	Gambia, The	L	WF	Periphery
147	Ghana	LM	WF	Periphery
148	Guinea	L	WF	Periphery
149	Guinea-Bissau	L	WF	Periphery
150	Kenya	LM	WF	Periphery
151	Lesotho	LM	WF	Periphery
152	Liberia	L	WF	Periphery
153	Libya	UM	WF	Semiperiphery
154	Madagascar	L	WF	Periphery
155	Malawi	L	WF	Periphery
156	Mali	L	WF	Periphery
157	Mauritania	LM	WF	Periphery
158	Mauritius	H	WF	Center
159	Mayotte	LM	WF	Periphery
160	Morocco	LM	WF	Periphery
161	Mozambique	L	WF	Periphery
162	Namibia	UM	WF	Semiperiphery
163	Niger	L	WF	Periphery
164	Nigeria	LM	WF	Periphery
165	Rwanda	L	WF	Periphery
166	Reunion	H	WF	Center
167	São Tomé and Príncipe	LM	WF	Periphery
168	Senegal	LM	WF	Periphery
169	Seychelles	H	WF	Center
170	Sierra Leone	L	WF	Periphery
171	Somalia	L	WF	Periphery
172	South Sudan	L	WF	Periphery
173	Sudan	L	WF	Periphery
174	Togo	L	WF	Periphery
175	Tunisia	LM	WF	Periphery
176	Uganda	L	WF	Periphery
177	Tanzania	LM	WF	Periphery
178	Western Sahara	LM	WF	Periphery
179	Zambia	LM	WF	Periphery
180	Zimbabwe	LM	WF	Periphery
181	<i>French Southern Territories</i>	L	WF	Periphery
182	<i>Saint Helena</i>	LM	WF	Periphery

183	Antigua and Barbuda	H	WL	Center
184	Argentina	UM	WL	Semiperiphery
185	Aruba	H	WL	Center
186	Bahamas, The	H	WL	Center
187	Barbados	H	WL	Center
188	Belize	UM	WL	Semiperiphery
189	Bolivia	LM	WL	Periphery
190	Chile	H	WL	Center
191	Colombia	UM	WL	Semiperiphery
192	Costa Rica	UM	WL	Semiperiphery
193	Cuba	UM	WL	Semiperiphery
194	Curaçao	H	WL	Center
195	Dominican Republic	UM	WL	Semiperiphery
196	Ecuador	UM	WL	Semiperiphery
197	El Salvador	LM	WL	Periphery
198	French Guiana	UM	WL	Semiperiphery
199	Grenada	UM	WL	Semiperiphery
200	Guadeloupe	H	WL	Center
201	Guatemala	UM	WL	Semiperiphery
202	Guyana	UM	WL	Semiperiphery
203	Haiti	L	WL	Periphery
204	Honduras	LM	WL	Periphery
205	Jamaica	UM	WL	Semiperiphery
206	Martinique	H	WL	Center
207	Nicaragua	LM	WL	Periphery
208	Panama	H	WL	Center
209	Paraguay	UM	WL	Semiperiphery
210	Peru	UM	WL	Semiperiphery
211	Puerto Rico	H	WL	Center
212	St. Lucia	UM	WL	Semiperiphery
213	St. Vincent and the Grenadines	UM	WL	Semiperiphery
214	Suriname	UM	WL	Semiperiphery
215	Trinidad and Tobago	H	WL	Center
216	Virgin Islands (U.S.)	H	WL	Center
217	Uruguay	H	WL	Center
218	Venezuela, RB	UM	WL	Semiperiphery
219	<i>Bermuda</i>	H	WL	Center
220	<i>Bonaire, Saint Eustatius and Saba</i>	H	WL	Center
221	<i>British Virgin Islands</i>	H	WL	Center
222	<i>Cayman Islands</i>	H	WL	Center
224	<i>Falkland Islands</i>	H	WL	Center
225	<i>Greenland</i>	H	WL	Center
226	<i>Dominica</i>	UM	WL	Semiperiphery
227	<i>St. Kitts and Nevis</i>	H	WL	Center
228	<i>Montserrat</i>	UM	WL	Semiperiphery
229	<i>Sint Maarten (Dutch part)</i>	H	WL	Center
230	<i>Saint Barthelemy</i>	H	WL	Center
231	<i>Saint Pierre and Miquelon</i>	H	WL	Center
232	<i>St. Martin (French part)</i>	H	WL	Center

233	<i>Turks and Caicos Islands</i>	H	WL	Center
234	<i>Anguilla</i>	H	WL	Center
235	Bahrain	H	WM	Center
236	Egypt, Arab Rep.	LM	WM	Periphery
237	Iran, Islamic Rep.	UM	WM	Semiperiphery
238	Iraq	UM	WM	Semiperiphery
239	Israel	H	WM	Center
240	Jordan	UM	WM	Semiperiphery
241	Kuwait	H	WM	Center
242	Lebanon	UM	WM	Semiperiphery
243	Oman	H	WM	Center
244	Qatar	H	WM	Center
245	Saudi Arabia	H	WM	Center
246	West Bank and Gaza	LM	WM	Periphery
247	Syrian Arab Republic	L	WM	Periphery
248	United Arab Emirates	H	WM	Center
249	Yemen, Rep.	L	WM	Periphery
250	South Africa	UM	ZA	Semiperiphery

Table 1: Aggregation of population data into MORDRED regions. L = low-income, LM = lower-middle income; UM = upper-middle income, H = High income.

Economy

3.1.5. Production

The original data source for the economic module in MORDRED is Exiobase3 version 3.8.2 (Stadler et al., 2018, 2021) for the year 2019 in product by product format, downloadable as *IOT_2019_pxp.zip*. Includes data for the A matrix (A), sectoral output (x), final demand (Y) and inter-sectoral flows (Z) in million 2019-€. The data was processed with the *pymrio* python package (Stadler, 2021).

3.1.5.1. Data aggregation

The 200 sectoral categories in the Exiobase3 pxp data for 2019 were aggregated into 25 sectors while the 44 countries and 5 world regions in Exiobase were aggregated into one world region.

Original sectors aggregated to MORDRED sectors

Table 2 shows which Exiobase3 sectors were matched to which MORDRED sectors.

Exiobase3 Sector Number	Exiobase 3 Sector Name	Exiobase 3 Sector Abbreviation	MORDRED Sector Number
1	Paddy rice	AUT_Paddy rice	1
2	Wheat	AUT_Wheat	1
3	Cereal grains nec	AUT_Cereal grains nec	1
4	Vegetables, fruit, nuts	AUT_Vegetables, fruit, nuts	1
5	Oil seeds	AUT_Oil seeds	1
6	Sugar cane, sugar beet	AUT_Sugar cane, sugar beet	1
7	Plant-based fibers	AUT_Plant-based fibers	1
8	Crops nec	AUT_Crops nec	1
9	Cattle	AUT_Cattle	1
10	Pigs	AUT_Pigs	1
11	Poultry	AUT_Poultry	1
12	Meat animals nec	AUT_Meat animals nec	1
13	Animal products nec	AUT_Animal products nec	1
14	Raw milk	AUT_Raw milk	1
15	Wool, silk-worm cocoons	AUT_Wool, silk-worm cocoons	2
16	Manure (conventional treatment)	AUT_Manure (conventional treatment)	1
17	Manure (biogas treatment)	AUT_Manure (biogas treatment)	1
18	Products of forestry, logging and related services (02)	AUT_Products of forestry, logging and related services (02)	2
19	Fish and other fishing products; services incidental of fishing (05)	AUT_Fish and other fishing products; services incidental of fishing (05)	1
20	Anthracite	AUT_Anthracite	3
21	Coking Coal	AUT_Coking Coal	3

22	Other Bituminous Coal	AUT_Other Bituminous Coal	3
23	Sub-Bituminous Coal	AUT_Sub-Bituminous Coal	3
24	Patent Fuel	AUT_Patent Fuel	3
25	Lignite/Brown Coal	AUT_Lignite/Brown Coal	3
26	BKB/Peat Briquettes	AUT_BKB/Peat Briquettes	3
27	Peat	AUT_Peat	3
28	Crude petroleum and services related to crude oil extraction, excluding surveying	AUT_Crude petroleum and services related to crude oil extraction, excluding surveying	3
29	Natural gas and services related to natural gas extraction, excluding surveying	AUT_Natural gas and services related to natural gas extraction, excluding surveying	3
30	Natural Gas Liquids	AUT_Natural Gas Liquids	3
31	Other Hydrocarbons	AUT_Other Hydrocarbons	3
32	Uranium and thorium ores (12)	AUT_Uranium and thorium ores (12)	4
33	Iron ores	AUT_Iron ores	4
34	Copper ores and concentrates	AUT_Copper ores and concentrates	4
35	Nickel ores and concentrates	AUT_Nickel ores and concentrates	4
36	Aluminium ores and concentrates	AUT_Aluminium ores and concentrates	4
37	Precious metal ores and concentrates	AUT_Precious metal ores and concentrates	4
38	Lead, zinc and tin ores and concentrates	AUT_Lead, zinc and tin ores and concentrates	4
39	Other non-ferrous metal ores and concentrates	AUT_Other non-ferrous metal ores and concentrates	4
40	Stone	AUT_Stone	4
41	Sand and clay	AUT_Sand and clay	4
42	Chemical and fertilizer minerals, salt and other mining and quarrying products nec	AUT_Chemical and fertilizer minerals, salt and other mining and quarrying products n.e.c.	4
43	Products of meat cattle	AUT_Products of meat cattle	1
44	Products of meat pigs	AUT_Products of meat pigs	1
45	Products of meat poultry	AUT_Products of meat poultry	1
46	Meat products nec	AUT_Meat products nec	1
47	products of Vegetable oils and fats	AUT_products of Vegetable oils and fats	1
48	Dairy products	AUT_Dairy products	1
49	Processed rice	AUT_Processed rice	1
50	Sugar	AUT_Sugar	1
51	Food products nec	AUT_Food products nec	1
52	Beverages	AUT_Beverages	1
53	Fish products	AUT_Fish products	1
54	Tobacco products (16)	AUT_Tobacco products (16)	2
55	Textiles (17)	AUT_Textiles (17)	2

56	Wearing apparel; furs (18)	AUT_Wearing apparel; furs (18)	2
57	Leather and leather products (19)	AUT_Leather and leather products (19)	2
58	Wood and products of wood and cork (except furniture); articles of straw and plaiting materials (20)	AUT_Wood and products of wood and cork (except furniture); articles of straw and plaiting materials (20)	5
59	Wood material for treatment, Re-processing of secondary wood material into new wood material	AUT_Wood material for treatment, Re-processing of secondary wood material into new wood material	6
60	Pulp	AUT_Pulp	5
61	Secondary paper for treatment, Re-processing of secondary paper into new pulp	AUT_Secondary paper for treatment, Re-processing of secondary paper into new pulp	6
62	Paper and paper products	AUT_Paper and paper products	2
63	Printed matter and recorded media (22)	AUT_Printed matter and recorded media (22)	7
64	Coke Oven Coke	AUT_Coke Oven Coke	3
65	Gas Coke	AUT_Gas Coke	3
66	Coal Tar	AUT_Coal Tar	8
67	Motor Gasoline	AUT_Motor Gasoline	3
68	Aviation Gasoline	AUT_Aviation Gasoline	3
69	Gasoline Type Jet Fuel	AUT_Gasoline Type Jet Fuel	3
70	Kerosene Type Jet Fuel	AUT_Kerosene Type Jet Fuel	3
71	Kerosene	AUT_Kerosene	3
72	Gas/Diesel Oil	AUT_Gas/Diesel Oil	3
73	Heavy Fuel Oil	AUT_Heavy Fuel Oil	3
74	Refinery Gas	AUT_Refinery Gas	3
75	Liquefied Petroleum Gases (LPG)	AUT_Liquefied Petroleum Gases (LPG)	3
76	Refinery Feedstocks	AUT_Refinery Feedstocks	8
77	Ethane	AUT_Ethane	8
78	Naphtha	AUT_Naphtha	8
79	White Spirit & SBP	AUT_White Spirit & SBP	8
80	Lubricants	AUT_Lubricants	8
81	Bitumen	AUT_Bitumen	8
82	Paraffin Waxes	AUT_Paraffin Waxes	8
83	Petroleum Coke	AUT_Petroleum Coke	3
84	Non-specified Petroleum Products	AUT_Non-specified Petroleum Products	8
85	Nuclear fuel	AUT_Nuclear fuel	4
86	Plastics, basic	AUT_Plastics, basic	5
87	Secondary plastic for treatment, Re-processing of secondary plastic into new plastic	AUT_Secondary plastic for treatment, Re-processing of secondary plastic into new plastic	6
88	N-fertiliser	AUT_N-fertiliser	9
89	P- and other fertiliser	AUT_P- and other fertiliser	9

90	Chemicals nec	AUT_Chemicals nec	9
91	Charcoal	AUT_Charcoal	3
92	Additives/Blending Components	AUT_Additives/Blending Components	9
93	Biogasoline	AUT_Biogasoline	10
94	Biodiesels	AUT_Biodiesels	10
95	Other Liquid Biofuels	AUT_Other Liquid Biofuels	10
96	Rubber and plastic products (25)	AUT_Rubber and plastic products (25)	9
97	Glass and glass products	AUT_Glass and glass products	5
98	Secondary glass for treatment, Re-processing of secondary glass into new glass	AUT_Secondary glass for treatment, Re-processing of secondary glass into new glass	6
99	Ceramic goods	AUT_Ceramic goods	11
100	Bricks, tiles and construction products, in baked clay	AUT_Bricks, tiles and construction products, in baked clay	11
101	Cement, lime and plaster	AUT_Cement, lime and plaster	5
102	Ash for treatment, Re-processing of ash into clinker	AUT_Ash for treatment, Re-processing of ash into clinker	6
103	Other non-metallic mineral products	AUT_Other non-metallic mineral products	11
104	Basic iron and steel and of ferro-alloys and first products thereof	AUT_Basic iron and steel and of ferro-alloys and first products thereof	5
105	Secondary steel for treatment, Re-processing of secondary steel into new steel	AUT_Secondary steel for treatment, Re-processing of secondary steel into new steel	6
106	Precious metals	AUT_Precious metals	5
107	Secondary precious metals for treatment, Re-processing of secondary precious metals into new precious metals	AUT_Secondary preciuos metals for treatment, Re-processing of secondary preciuos metals into new preciuos metals	6
108	Aluminium and aluminium products	AUT_Aluminium and aluminium products	5
109	Secondary aluminium for treatment, Re-processing of secondary aluminium into new aluminium	AUT_Secondary aluminium for treatment, Re-processing of secondary aluminium into new aluminium	6
110	Lead, zinc and tin and products thereof	AUT_Lead, zinc and tin and products thereof	5
111	Secondary lead for treatment, Re-processing of secondary lead into new lead	AUT_Secondary lead for treatment, Re-processing of secondary lead into new lead	6
112	Copper products	AUT_Copper products	5
113	Secondary copper for treatment, Re-processing of secondary copper into new copper	AUT_Secondary copper for treatment, Re-processing of secondary copper into new copper	6
114	Other non-ferrous metal products	AUT_Other non-ferrous metal products	5
115	Secondary other non-ferrous metals for treatment, Re-processing of secondary other non-ferrous metals into new other non-ferrous metals	AUT_Secondary other non-ferrous metals for treatment, Re-processing of secondary other non-ferrous	6

		metals into new other non-ferrous metals	
116	Foundry work services	AUT_Foundry work services	11
117	Fabricated metal products, except machinery and equipment (28)	AUT_Fabricated metal products, except machinery and equipment (28)	11
118	Machinery and equipment nec (29)	AUT_Machinery and equipment n.e.c. (29)	11
119	Office machinery and computers (30)	AUT_Office machinery and computers (30)	11
120	Electrical machinery and apparatus nec (31)	AUT_Electrical machinery and apparatus n.e.c. (31)	11
121	Radio, television and communication equipment and apparatus (32)	AUT_Radio, television and communication equipment and apparatus (32)	11
122	Medical, precision and optical instruments, watches and clocks (33)	AUT_Medical, precision and optical instruments, watches and clocks (33)	11
123	Motor vehicles, trailers and semi-trailers (34)	AUT_Motor vehicles, trailers and semi-trailers (34)	11
124	Other transport equipment (35)	AUT_Other transport equipment (35)	11
125	Furniture; other manufactured goods nec (36)	AUT_Furniture; other manufactured goods n.e.c. (36)	11
126	Secondary raw materials	AUT_Secondary raw materials	5
127	Bottles for treatment, Recycling of bottles by direct reuse	AUT_Bottles for treatment, Recycling of bottles by direct reuse	6
128	Electricity by coal	AUT_Electricity by coal	12
129	Electricity by gas	AUT_Electricity by gas	12
130	Electricity by nuclear	AUT_Electricity by nuclear	13
131	Electricity by hydro	AUT_Electricity by hydro	14
132	Electricity by wind	AUT_Electricity by wind	15
133	Electricity by petroleum and other oil derivatives	AUT_Electricity by petroleum and other oil derivatives	12
134	Electricity by biomass and waste	AUT_Electricity by biomass and waste	16
135	Electricity by solar photovoltaic	AUT_Electricity by solar photovoltaic	17
136	Electricity by solar thermal	AUT_Electricity by solar thermal	18
137	Electricity by tide, wave, ocean	AUT_Electricity by tide, wave, ocean	19
138	Electricity by Geothermal	AUT_Electricity by Geothermal	20
139	Electricity nec	AUT_Electricity nec	12
140	Transmission services of electricity	AUT_Transmission services of electricity	7
141	Distribution and trade services of electricity	AUT_Distribution and trade services of electricity	7
142	Coke oven gas	AUT_Coke oven gas	3
143	Blast Furnace Gas	AUT_Blast Furnace Gas	3
144	Oxygen Steel Furnace Gas	AUT_Oxygen Steel Furnace Gas	3

145	Gas Works Gas	AUT_Gas Works Gas	3
146	Biogas	AUT_Biogas	10
147	Distribution services of gaseous fuels through mains	AUT_Distribution services of gaseous fuels through mains	7
148	Steam and hot water supply services	AUT_Steam and hot water supply services	7
149	Collected and purified water; distribution services of water (41)	AUT_Collected and purified water, distribution services of water (41)	7
150	Construction work (45)	AUT_Construction work (45)	5
151	Secondary construction material for treatment, Re-processing of secondary construction material into aggregates	AUT_Secondary construction material for treatment, Re-processing of secondary construction material into aggregates	6
152	Sale, maintenance, repair of motor vehicles, motor vehicles parts, motorcycles, motor cycles parts and accessories	AUT_Sale, maintenance, repair of motor vehicles, motor vehicles parts, motorcycles, motor cycles parts and accessories	7
153	Retail trade services of motor fuel	AUT_Retail trade services of motor fuel	7
154	Wholesale trade and commission trade services, except of motor vehicles and motorcycles (51)	AUT_Wholesale trade and commission trade services, except of motor vehicles and motorcycles (51)	7
155	Retail trade services, except of motor vehicles and motorcycles; repair services of personal and household goods (52)	AUT_Retail trade services, except of motor vehicles and motorcycles; repair services of personal and household goods (52)	7
156	Hotel and restaurant services (55)	AUT_Hotel and restaurant services (55)	7
157	Railway transportation services	AUT_Railway transportation services	21
158	Other land transportation services	AUT_Other land transportation services	21
159	Transportation services via pipelines	AUT_Transportation services via pipelines	21
160	Sea and coastal water transportation services	AUT_Sea and coastal water transportation services	21
161	Inland water transportation services	AUT_Inland water transportation services	21
162	Air transport services (62)	AUT_Air transport services (62)	21
163	Supporting and auxiliary transport services; travel agency services (63)	AUT_Supporting and auxiliary transport services; travel agency services (63)	7
164	Post and telecommunication services (64)	AUT_Post and telecommunication services (64)	7
165	Financial intermediation services, except insurance and pension funding services (65)	AUT_Financial intermediation services, except insurance and pension funding services (65)	7
166	Insurance and pension funding services, except compulsory social security services (66)	AUT_Insurance and pension funding services, except compulsory social security services (66)	7
167	Services auxiliary to financial intermediation (67)	AUT_Services auxiliary to financial intermediation (67)	7

168	Real estate services (70)	AUT_Real estate services (70)	7
169	Renting services of machinery and equipment without operator and of personal and household goods (71)	AUT_Renting services of machinery and equipment without operator and of personal and household goods (71)	7
170	Computer and related services (72)	AUT_Computer and related services (72)	7
171	Research and development services (73)	AUT_Research and development services (73)	7
172	Other business services (74)	AUT_Other business services (74)	7
173	Public administration and defence services; compulsory social security services (75)	AUT_Public administration and defence services; compulsory social security services (75)	7
174	Education services (80)	AUT_Education services (80)	22
175	Health and social work services (85)	AUT_Health and social work services (85)	23
176	Food waste for treatment: incineration	AUT_Food waste for treatment: incineration	24
177	Paper waste for treatment: incineration	AUT_Paper waste for treatment: incineration	24
178	Plastic waste for treatment: incineration	AUT_Plastic waste for treatment: incineration	24
179	Inert/metal waste for treatment: incineration	AUT_Inert/metal waste for treatment: incineration	24
180	Textiles waste for treatment: incineration	AUT_Textiles waste for treatment: incineration	24
181	Wood waste for treatment: incineration	AUT_Wood waste for treatment: incineration	24
182	Oil/hazardous waste for treatment: incineration	AUT_Oil/hazardous waste for treatment: incineration	24
183	Food waste for treatment: biogasification and land application	AUT_Food waste for treatment: biogasification and land application	25
184	Paper waste for treatment: biogasification and land application	AUT_Paper waste for treatment: biogasification and land application	25
185	Sewage sludge for treatment: biogasification and land application	AUT_Sewage sludge for treatment: biogasification and land application	25
186	Food waste for treatment: composting and land application	AUT_Food waste for treatment: composting and land application	25
187	Paper and wood waste for treatment: composting and land application	AUT_Paper and wood waste for treatment: composting and land application	25
188	Food waste for treatment: waste water treatment	AUT_Food waste for treatment: waste water treatment	24
189	Other waste for treatment: waste water treatment	AUT_Other waste for treatment: waste water treatment	24
190	Food waste for treatment: landfill	AUT_Food waste for treatment: landfill	24
191	Paper for treatment: landfill	AUT_Paper for treatment: landfill	24
192	Plastic waste for treatment: landfill	AUT_Plastic waste for treatment: landfill	24
193	Inert/metal/hazardous waste for treatment: landfill	AUT_Inert/metal/hazardous waste for treatment: landfill	24

194	Textiles waste for treatment: landfill	AUT_Textiles waste for treatment: landfill	24
195	Wood waste for treatment: landfill	AUT_Wood waste for treatment: landfill	24
196	Membership organisation services nec (91)	AUT_Membership organisation services n.e.c. (91)	7
197	Recreational, cultural and sporting services (92)	AUT_Recreational, cultural and sporting services (92)	7
198	Other services (93)	AUT_Other services (93)	7
199	Private households with employed persons (95)	AUT_Private households with employed persons (95)	7
200	Extra-territorial organizations and bodies	AUT_Extra-territorial organizations and bodies	7

Table 2: Aggregation of Exiobase sectors into MORDRED sectors.

From the aggregated Exiobase3 data for 2019 we derive a 25X25 A matrix, the initial output and the sectoral shares of total gross fixed capital formation on a global scale.

Table 3 shows the order of the sectors in the A matrix.

Sector number	Sector description
1	Agriculture, food, beverages
2	Non-energy use of biomass
3	Fossil fuels used for energy
4	Mining
5	Industry not elsewhere classified
6	Recycling industry
7	Services not elsewhere classified
8	Non-energy use of fossil fuels
9	Chemical industry
10	Biomass used for energy
11	Manufacturing
12	Fossil fuel-based electricity
13	Nuclear electricity
14	Hydroelectricity
15	Wind based electricity
16	Biomass and waste based electricity
17	Solar PV electricity
18	Solar thermal electricity
19	Tide, wave and ocean based electricity
20	Geothermal electricity
21	Transport
22	Education
23	Health
24	Waste industry
25	Waste ,recycling' (biogasification & composting) industry

Table 3: Overview MORDRED sectors.

3.1.5.2. Data modification

In MORDRED, there is a separation between the production and consumption of the subsistence class and the production and consumption within the formal economy. Thus, the part of the subsistence economy that is included in Exiobase3 is excluded in MORDRED.

We assume that the monetized output of the subsistence sector is concentrated in sector 1, which includes agricultural products, and that no intermediary inputs from the global economy are needed to produce output. The monetized output equals the monetized subsistence per capita consumption per capita times the subsistence population size.

We assume that 70% of the subsistence class works and that half of the working day of the subsistence class, i.e. 4 hours, goes to the production of output, which enters the formal economy, and, thus, is monetized.

Therefore, we deduct the monetized output of the subsistence sector from the sectoral output of sector 1, and deduct the amount of hours worked from the hours worked in sector 1.

The A-Matrix is modified for the column containing the intermediary products sector 1 demands from the 25 sectors to reflect the change in output.

As a side effect, both the labor productivity and the input intensity of sector 1 increases, as the more labor-intensive and less input-reliant subsistence regime gets excluded from the IO structure.

This modification allows us to have two separate economic structures and different mortality and fertility patterns for the subsistence class and the rest of classes in the case of very low per capita consumption. It also allows us to better reflect the higher labor productivity in agriculture for industrialized agriculture.

3.1.6. Capital

3.1.6.1. Capital output ratios

In MORDRED, the capital stock is calculated via sector specific capital-output ratios.

To estimate the capital-output ratios for the different MORDRED sectors at the global level, we draw on different data sources: for the estimations of capital stock we use the EU KLEMS database (2023 release, which also includes data for Japan, the UK and the US) (Bontadini et al., 2023; LUISS, 2023), the IndiaKLEMS database (2024 release) (RBI, 2024) and the China CIP 4.0 database (2023 release) (RIETI, 2023).

The following steps were taken:

1. Extraction of all capital stock and output data for all available countries:

We extracted the net capital stock for all assets (K_GFCF) for the year 2019 from the Capital Accounts excel sheets as well as the gross output (GO_CP) for the year 2019 from the National Accounts for all the available countries in EUKLEMS (in current prices, millions of national currency): Japan, UK, US, Austria, Belgium, Czechia, Germany, Denmark, Estonia, Greece, Spain, Finland, France, Hungary, Ireland, Italy, Lithuania,

Luxembourg, Latvia, Malta, Netherlands, Poland, Portugal, Romania, Sweden, Slovenia, Slovakia. Subsequently, the national currencies were converted to 2019-€, using the official exchange rates for 2019 provided by the World Bank. As the capital stock estimates for Japan constitute an outlier with respect to the other countries and as the quality of those estimates were questionable, we excluded Japan from the sample.

We extracted the net capital stock (K) as well as the gross output (GO) for the year 2019-20 (in crore of 2019-rupees) from IndiaKLEMS.

In the case of China, the most actual data is for the year 2017. To obtain the real net capital stock for this year, the net capital stock in 2000 in the different sectors (CHINA_CIP_4.0_(2023)_2.2.xlsx) is multiplied by the real net capital stock growth index for 2017 in the different sectors (CIP_4.0_(2023)_4.xlsx) and a conversion factor is applied to convert the data from mio. of 2000-yuan to mio. of 2017-yuan. We extract the output for the year 2017 from the CIP_4.0 (2023)1.3.xlsx excel sheet which contains the gross value of output by industry in millions of current (2017-) yuan.

Due to a lack of data for other countries, the countries in EUKLEMS are treated as a representative sample of the center, China is treated as a representative sample of the semiperiphery, and India is treated a representative sample of the periphery.

2. Matching of sectors with MORDRED sectors

EUKLEMS contains 52 sector categories (Table 4).

Sector abbreviation	Sector description
A	Agriculture, forestry and fishing
B	Mining and quarrying
C	Manufacturing
C10-C12	Manufacture of food products; beverages and tobacco products
C13-C15	Manufacture of textiles, wearing apparel, leather and related products
C16-C18	Manufacture of wood, paper, printing and reproduction
C19	Manufacture of coke and refined petroleum products
C20	Manufacture of chemicals and chemical products
C20-C21	Chemicals; basic pharmaceutical products
C21	Manufacture of basic pharmaceutical products and pharmaceutical preparations
C22-C23	Manufacture of rubber and plastic products and other non-metallic mineral products
C24-C25	Manufacture of basic metals and fabricated metal products, except machinery and equipment
C26	Manufacture of computer, electronic and optical products
C26-C27	Computer, electronic, optical products; electrical equipment
C27	Manufacture of electrical equipment
C28	Manufacture of machinery and equipment n.e.c.

C29-C30	Manufacture of motor vehicles, trailers, semi-trailers and of other transport equipment Manufacture of furniture; jewellery, musical instruments, toys; repair and installation of machinery and equipment
C31-C33	Electricity, gas, steam and air conditioning supply Electricity, gas, steam; water supply, sewerage, waste management
D	Water supply; sewerage, waste management and remediation activities
D-E	Construction
E	Wholesale and retail trade; repair of motor vehicles and motorcycles
F	Wholesale and retail trade and repair of motor vehicles and motorcycles
G	Wholesale trade, except of motor vehicles and motorcycles
G45	Retail trade, except of motor vehicles and motorcycles
G46	Transportation and storage
G47	Land transport and transport via pipelines
H	Water transport
H49	Air transport
H50	Warehousing and support activities for transportation
H51	Postal and courier activities
H52	Accommodation and food service activities
H53	Information and communication
I	Publishing, motion picture, video, television programme production; sound recording, programming and broadcasting activities
J	Telecommunications
J58-J60	Computer programming, consultancy, and information service activities
J61	Financial and insurance activities
J62-J63	Real estate activities
K	Imputed rents of owner-occupied dwellings
L	Professional, scientific and technical activities
L68A	Professional, scientific and technical activities; administrative and support service activities
M	Administrative and support service activities
M-N	Public administration and defence; compulsory social security
N	Public administration, defence, education, human health and social work activities
O	Education
O-Q	Human health and social work activities
P	Human health activities
Q	Residential care activities and social work activities without accommodation
Q86	Arts, entertainment and recreation
Q87-Q88	
R	

R-S
S

Arts, entertainment, recreation; other services and service activities, etc.
Other service activities

Table 4: Sectors in EUKLEMS.

The sectors contained in the country (*cnt*) data of EUKLEMS (except for Japan) were matched to the MORDRED sectors in the following way:

$$\begin{aligned}\frac{K}{X_{center_1}} &= \frac{\sum_{cnt=1}^{26} (K_{A_{cnt}} + K_{C10-C12_{cnt}})}{\sum_{cnt=1}^{26} (X_{A_{cnt}} + X_{C10-C12_{cnt}})} \\ \frac{K}{X_{center_2}} &= \frac{\sum_{cnt=1}^{26} (K_{C13-C15_{cnt}} + K_{C16-C18_{cnt}})}{\sum_{cnt=1}^{26} (X_{C13-C15_{cnt}} + X_{C16-C18_{cnt}})} \\ \frac{K}{X_{center_{3,8}}} &= \frac{\sum_{cnt=1}^{26} K_{C19_{cnt}}}{\sum_{cnt=1}^{26} X_{C19_{cnt}}}\end{aligned}$$

(The same capital-output ratio is used for the sectors 3 and 8.)

$$\begin{aligned}\frac{K}{X_{center_4}} &= \frac{\sum_{cnt=1}^{26} K_{B_{cnt}}}{\sum_{cnt=1}^{26} X_{B_{cnt}}} \\ \frac{K}{X_{center_5}} &= \frac{\sum_{cnt=1}^{26} (K_{C24-C25_{cnt}} + K_{F_{cnt}})}{\sum_{cnt=1}^{26} (X_{C24-C25_{cnt}} + X_{F_{cnt}})} \\ \frac{K}{X_{center_6}} &= 0 \\ \frac{K}{X_{center_{7,10,12,13,14,15,16,17,18,19,20,24,25}}} &= \frac{\sum_{cnt=1}^{26} (K_{([D]+[D-E]+[E]+[G]+[G45]+[G46]+[G47]+[H52]+[H53]+[I]+[J]+[J58-J60]+[J61]+[J62-J63]+[K]+[L])_{cnt}})}{\sum_{cnt=1}^{26} (X_{([D]+[D-E]+[E]+[G]+[G45]+[G46]+[G47]+[H52]+[H53]+[I]+[J]+[J58-J60]+[J61]+[J62-J63]+[K]+[L])_{cnt}})}\end{aligned}$$

(Due to a lack of disaggregation, the same capital-output ratio is used for the sectors no. 7, 10, 12 to 20 [12;20], 24 and 25.)

$$\frac{K}{X_{center_9}} = \frac{\sum_{cnt=1}^{26} (K_{C20_{cnt}} + K_{C20-C21_{cnt}} + K_{C21_{cnt}} + K_{C22-C23_{cnt}})}{\sum_{cnt=1}^{26} (X_{C20_{cnt}} + X_{C20-C21_{cnt}} + X_{C21_{cnt}} + X_{C22-C23_{cnt}})}$$

$$\begin{aligned}\frac{K}{X_{center_{21}}} &= \frac{\sum_{cnt=1}^{26} (K_{([H]+[H49]+[H50]+[H51])_{cnt}})}{\sum_{cnt=1}^{26} (X_{([H]+[H49]+[H50]+[H51])_{cnt}})} \\ \frac{K}{X_{center_{22}}} &= \frac{\sum_{cnt=1}^{26} (K_{P_{cnt}})}{\sum_{cnt=1}^{26} (X_{P_{cnt}})}\end{aligned}$$

$$\frac{K}{X_{center_{23}}} = \frac{\sum_{cnt=1}^{26} (K_{Q_{cnt}})}{\sum_{cnt=1}^{26} (X_{Q_{cnt}})}$$

For this sector, the sub-categories Q86-Q88 were not included given that they are subsectors of Q and all countries had data estimates for Q but not for the subcategories.

The China CIP database contains 37 sectors that were matched with MORDRED sectors.

CIP sector number	CIP sector description	MORDRED sector
1	Agriculture, forestry, animal husbandry & fishery	1
2	Coal mining	3, 8
3	Oil & gas excavation	3, 8
4	Metal mining	4
5	Non-metallic minerals mining	4
6	Food and kindred products	1
7	Tobacco products	2
8	Textile mill products	2
9	Apparel and other textile products	2
10	Leather and leather products	2
11	Saw mill products, furniture, fixtures	11
12	Paper products, printing & publishing	2
13	Petroleum and coal products	3, 8
14	Chemicals and allied products	9
15	Rubber and plastics products	9
16	Stone, clay, and glass products	5
17	Primary & fabricated metal industries	5
18	Metal products (excluding rolling products)	5
19	Industrial machinery and equipment	11
20	Electric equipment	11
21	Electronic and telecommunication equipment	11
22	Instruments and office equipment	11
23	Motor vehicles & other transportation equipment	11
24	Miscellaneous manufacturing industries	11
25	Power, steam, gas and tap water supply	[12;20]
26	Construction	5
27	Wholesale and retail trades	7
28	Hotels and restaurants	7
29	Transport, storage & post services	21
30	Information & computer services	7
31	Financial Intermediations	7
32	Real estate services	7

33	Leasing, technical, science & business services	7
34	Government, public administration, and political and social organizations, etc.	7
35	Education	22
36	Healthcare and social security services	23
37	Cultural, sports, entertainment services; residential and other services	7

Table 5: CIP sectors matched to MORDRED sectors.

This gives the following capital-output ratios (all based on data for China):

$$\frac{K}{X_{semiperiphy_1}} = \frac{K_1 + K_6}{X_1 + X_6}$$

$$\frac{K}{X_{semiperiphy_2}} = \frac{K_7 + K_8 + K_9 + K_{10} + K_{12}}{X_7 + X_8 + X_9 + X_{10} + X_{12}}$$

$$\frac{K}{X_{semiperiphy_{3,8}}} = \frac{K_2 + K_3 + K_{13}}{X_2 + X_3 + X_{13}}$$

$$\frac{K}{X_{semiperiphy_4}} = \frac{K_4 + K_5}{X_4 + X_5}$$

$$\frac{K}{X_{semiperiphy_5}} = \frac{K_{16} + K_{17} + K_{18} + K_{26}}{X_{16} + X_{17} + X_{18} + X_{26}}$$

$$\frac{K}{X_{semiperiphy_6}} = 0$$

$$\frac{K}{X_{semiperiphy_{7,10,12,13,14,15,16,17,18,19,20,24,25}}} = \frac{K_{25} + K_{27} + K_{28} + K_{30} + K_{31} + K_{32} + K_{33} + K_{34} + K_{37}}{X_{25} + X_{27} + X_{28} + X_{30} + X_{31} + X_{32} + X_{33} + X_{34} + X_{37}}$$

$$\frac{K}{X_{semiperiphy_9}} = \frac{K_{14} + K_{15}}{X_{14} + X_{15}}$$

$$\frac{K}{X_{semiperiphy_{11}}} = \frac{K_{11} + K_{19} + K_{20} + K_{21} + K_{22} + K_{23} + K_{24}}{X_{11} + X_{19} + X_{20} + X_{21} + X_{22} + X_{23} + X_{24}}$$

$$\frac{K}{X_{semiperiphy_{21}}} = \frac{K_{29}}{X_{29}}$$

$$\frac{K}{X_{semiperiphy_{22}}} = \frac{K_{35}}{X_{35}}$$

$$\frac{K}{X_{semiperiphy_{23}}} = \frac{K_{36}}{X_{36}}$$

The INDIAKLEMS database contains 27 sectors that were matched with MORDRED sectors.

IndiaKlems sector number	IndiaKLEMS sector description	MORDRED sector
1	Agriculture,Hunting,Forestry and Fishing	1
2	Mining and Quarrying	4
3	Food Products,Beverages and Tobacco	1
4	Textiles, Textile Products, Leather and Footwear	2
5	Wood and Products of wood	2
6	Pulp, Paper,Paper products,Printing and Publishing	2
7	Coke, Refined Petroleum Products and Nuclear fuel	3, 8
8	Chemicals and Chemical Products	9
9	Rubber and Plastic Products	9
10	Other Non-Metallic Mineral Products	9
11	Basic Metals and Fabricated Metal Products	5
12	Machinery, nec.	11
13	Electrical and Optical Equipment	11
14	Transport Equipment	11
15	Manufacturing, nec; recycling	11
16	Electricity, Gas and Water Supply	[12; 20], 7, 10
17	Construction	5
18	Trade	7
19	Hotels and Restaurants	7
20	Transport and Storage	21
21	Post and Telecommunication	7
22	Financial Services	7
23	Business Service	7
24	Public Administration and Defense; Compulsory Social Security	7
25	Education	22
26	Health and Social Work	23
27	Other services	7, 24, 25

Table 6: IndiaKLEMS sectors matched to MORDRED sectors.

This gives the following capital-output ratios (all based on data for India):

$$\frac{K}{X_{periphy_1}} = \frac{K_1 + K_3}{X_1 + X_3}$$

$$\frac{K}{X_{periphy_2}} = \frac{K_4 + K_5 + K_6}{X_4 + X_5 + X_6}$$

$$\frac{K}{X_{periphy_{3,8}}} = \frac{K_7}{X_7}$$

$$\begin{aligned}\frac{K}{\bar{X}_{periphy_4}} &= \frac{K_2}{X_2} \\ \frac{K}{\bar{X}_{periphy_5}} &= \frac{K_{11} + K_{17}}{X_{11} + X_{17}} \\ \frac{K}{\bar{X}_{periphy_6}} &= 0 \\ \frac{K}{\bar{X}_{periphy_{7,10,12,13,14,15,16,17,18,19,20,24,25}}} &= \frac{K_{16} + K_{18} + K_{19} + K_{21} + K_{22} + K_{23} + K_{24} + K_{27}}{X_{16} + X_{18} + X_{19} + X_{21} + X_{22} + X_{23} + X_{24} + X_{27}}\end{aligned}$$

$$\begin{aligned}\frac{K}{\bar{X}_{semiperiphy_9}} &= \frac{K_8 + K_9 + K_{10}}{X_8 + X_9 + X_{10}} \\ \frac{K}{\bar{X}_{semiperiphy_{11}}} &= \frac{K_{12} + K_{13} + K_{14} + K_{15}}{X_{12} + X_{13} + X_{14} + X_{15}} \\ \frac{K}{\bar{X}_{semiperiphy_{21}}} &= \frac{K_{20}}{X_{20}} \\ \frac{K}{\bar{X}_{semiperiphy_{22}}} &= \frac{K_{25}}{X_{25}} \\ \frac{K}{\bar{X}_{semiperiphy_{23}}} &= \frac{K_{26}}{X_{26}}\end{aligned}$$

In this way, we construct three 12-dimensional vectors containing the capital-output ratios for different MORDRED sectors for every MORDRED region:

$$\frac{K}{\bar{X}_{center}}, \frac{K}{\bar{X}_{semiperiphery}}, \frac{K}{\bar{X}_{periphery}}.$$

3. Global estimates

To obtain the capital-output ratios for the MORDRED sectors at the global scale, we draw a weighted average of the three capital-output ratio vectors. The weights are the shares of the respective regions in the total output generated by the EUKLEMS countries, China and India.

To obtain the shares of the output in total output, we use Exiobase3 country data for 2019 which we aggregate according to the sectors contained in the capital:output vectors: sector no. 1; 2; 3 + 8; 4; 5; 6; 7 + 10 + [12;20] + 24 + 25; 9; 11; 21; 22; 23.

The respective shares are:

$$share_{center} = \left(\frac{\sum_{cnt=1}^{26} X_{cnt1}}{\sum_{cnt=1}^{26} X_{i_1} + X_{CN_1} + X_{IN_1}}, \frac{\sum_{cnt=1}^{26} X_{cnt2}}{\sum_{cnt=1}^{26} X_{i_2} + X_{CN_2} + X_{IN_2}}, \dots, \frac{\sum_{cnt=1}^{26} X_{cnt12}}{\sum_{cnt=1}^{26} X_{i_{12}} + X_{CN_{12}} + X_{IN_{12}}} \right)$$

cnt denotes the 27 countries of the center included in the EUKLEMS database (except for Japan).

$share_{semiperiphery}$

$$= \left(\frac{X_{CN_1}}{\sum_{cnt=1}^{26} X_{cnt_1} + x_{CN_1} + x_{IN_1}}, \frac{X_{CN_2}}{\sum_{cnt=1}^{26} X_{i_2} + X_{CN_2} + X_{IN_2}}, \dots, \frac{X_{CN_{12}}}{\sum_{cnt=1}^{26} X_{i_{12}} + X_{CN_{12}} + X_{IN_{12}}} \right)$$

$share_{periphery}$

$$= \left(\frac{X_{IN_1}}{\sum_{cnt=1}^{26} X_{i_1} + X_{CN_1} + X_{IN_1}}, \frac{X_{IN_2}}{\sum_{cnt=1}^{26} X_{i_2} + X_{CN_2} + X_{IN_2}}, \dots, \frac{X_{IN_{12}}}{\sum_{cnt=1}^{26} X_{i_{12}} + X_{CN_{12}} + X_{IN_{12}}} \right)$$

The global capital-output vector is:

$$\frac{K}{X_{world_i}} = \sum_{r=1}^3 \frac{K}{X_{i_r}} * share_{i_r} \text{ with } r \text{ denoting the three regions.}$$

This vector can be converted from a 12-dimensional vector into a 25-dimensional vector by disaggregating those sector categories that contain various MORDRED sectors, using the same value for all MORDRED sectors that belong to the respective category.

4. Correction factor

Last, we apply a correction factor $\alpha_{\frac{basic}{acquisition}}$ to convert the acquisition prices of the capital stock into basic prices, given that the output in Exibase is assumed to be given in basic prices.

$$\frac{K}{X_{world_{i basic prices}}} = \frac{K_{i acquisition prices}}{X_{i basic prices}} * \alpha_{\frac{basic}{acquisition}}$$

$\alpha_{\frac{basic}{acquisition}}$ is obtained in the following way:

We draw on WIOD 2016 data (Timmer et al., 2015; WIOD, 2016) for the year 2014 for all countries used to estimate capital-output ratios at the global level. For all countries with available data in WIOD (i.e. all countries except from China and the US) we extract the GFCF data for total intermediate consumption in basic prices and information on taxes less subsidies on products and international transport margins. $\alpha_{\frac{basic}{acquisition}}$ is calculated as:

$$\begin{aligned} \alpha_{\frac{basic}{acquisition}} &= \frac{\sum_{i=cnt}^{26} GFCF_{total intermediate consumption_{cnt}}}{\sum_{cnt=1}^{26} GFCF_{total intermediate consumption_{cnt}} + \sum_{cnt=1}^{26} taxes - subsidies_{cnt} + \sum_{cnt=1}^{26} Transport_{cnt}} \end{aligned}$$

3.1.6.2. Sectoral share of GFCF and capital depreciation

Both the data for annual sector-specific Gross Fixed Capital Formation (GFCF) and capital depreciation come from Exiobase3. In MORDRED, GFCF is the sum of the final demand categories GFCF, changes in inventories and changes in valuables. The sectoral share in GFCF is obtained by dividing GFCF in the respective sector by total GFCF.

$$GFCF_{share} = \frac{GFCF_i + \text{changes in inventories}_i + \text{changes in valuable}_i}{\sum_{i=1}^{25} (GFCF_i + \text{changes in inventories}_i + \text{changes in valuable}_i)}$$

The capital depreciation in million € for the different sectors is contained in the Exiobase3 Extension F: Operating surplus: Consumption of fixed capital. Since it is assumed to be given in acquisition prices, the $\alpha_{\frac{\text{basic}}{\text{acquisition}}}$ correction factor is applied to convert the data into basic prices.

3.1.7. Consumption side

In MORDRED, there are three world regions ('Center', 'Semiperiphery' and 'Periphery') and within each world region, there are four classes (Top20, Middle50, Bottom30 and Subsistence). The per capita consumption of an individual, thus, depends on the specific class and territory (cf. section 2.2).

3.1.7.1. Initial inequality in consumption between world regions: Regional share in global final demand without GFCF

Data on the global final demand of households is obtained by aggregating the Exiobase categories 'households' and 'non-profit organizations serving households', and data for final demand for GFCF by aggregating the Exiobase categories 'GFC', 'changes in inventories' and 'changes in valuables'. The government final demand can be directly taken from Exiobase.

We assume that final demand of households and governments is distributed unequally between regions. Although GFCF is also unequally distributed between regions, in MORDRED this does not affect consumption per capita and life expectancy, thus, there is no need for disaggregation.

The inequality in the regional share in the global final demand without GFCF is approximated based on World Bank data containing the 'Final consumption expenditure (%) of GDP' (World Bank, 2024a) and 'GDP (current US\$)' (World Bank, 2024b) for the year 2019.

We included 249 countries that were matched to the MORDRED regions according to their World Bank classification as high (center), upper-middle (semiperiphery), lower-middle and low (periphery) income.

Using all the available data, we calculated the average final consumption expenditure as percentage of GDP for the center, semiperiphery and periphery. Countries that lacked

data for final consumption expenditure as percentage of GDP were given the average value of their region. Countries without GDP data were left out of the analysis.

The total consumption for every region was derived by summing over the consumption of every country belonging to the region.

The regional share in global final demand without GFCF was calculated by dividing the final demand of the respective region by the sum of final demand of all regions

Given that the periphery had the most missing values for GDP (21 countries) and that the data was given in current rather than in PPP-USD, we multiplied the share of the periphery with a factor of 1.6 and deducted the increase in share of the periphery from the share of the center.

The resulting regional shares in global final demand without GFCF are: 0.6073 for the center, 0.2559 for the semiperiphery and 0.1367 for the periphery.

3.1.7.2. Household and government share in regional final demand without GFCF

To approximate differences in the shares of households and governments in final demand between MORDRED regions, we use Exiobase3 data on final demand for the year 2019 because this data has a relatively high regional disaggregation and differentiates between final demand from governments and from households (when we speak of household consumption or demand in the context of Exiobase3, we always refer to the Exiobase categories 'households' and 'non-profit organizations serving households' which are added into one MORDRED category 'households (hh)').

We use pymrio (Stadler, 2021) to aggregate Exiobase countries and regions in a way that they approximate the MORDRED regions (Table 7).

MORDRED	Exiobase countries/regions
Center	Austria, Belgium, Cyprus, Czech Republic, Germany, Denmark, Estonia, Spain, Finland, France, Greece, Croatia, Hungary, Ireland, Italy, Lithuania, Luxembourg, Latvia, Malta, Netherlands, Poland, Portugal, Romania, Sweden, Slovenia, Slovak Republic, Great Britain, USA, Japan, Canada, South Korea, Australia, Switzerland, Taiwan, Norway
Semiperiphery	Bulgaria, China, Brazil, Mexico, Russia Federation, Türkiye, Indonesia, South Africa, Rest of the World Latin America (WL), Rest of the World Middle East (WM)
Periphery	India, Rest of the World Asia (WA), Rest of the World Europe (WE), Rest of the World Africa (WF)

Table 7: Matching Exiobase countries and regions to MORDRED regions.

To allocate the Rest of the World Exiobase regions to the MORDRED regions we calculated for every region the percentage of people living in countries classified as

'center', 'semiperiphery' and 'periphery', using the UN population data for 2020 (cf. section 3.1.1). WA, WL, WF and WE were matched to the MORDRED region where the highest share of population lived: In WA, 83.7% of the population lives in countries classified as 'periphery'; In WL, 74.63% of the population lives in countries classified as 'semiperiphery'; in WF, 98.5% of the population lives in countries classified as 'periphery'; in WE, 63.4% of the population lives in countries classified as 'periphery'. In WM, 42.6% of the population lives in the periphery, 38.88% lives in the semiperiphery and 18.53% lives in the center. Thus, while less than half of the population lives in peripheral countries, more than half of the population lives in semiperipheral or central countries. Consequently, WM as a whole was matched to the semiperiphery.

For every region, the share of government consumption in total consumption is calculated by aggregating the sectoral final demand of the government and households.

$$G2Cr_r = \frac{\sum_{i=1}^{25} G_{r_i}}{\sum_{i=1}^{25} G_{r_i} + \sum_{i=1}^{25} C_{r_i}}$$

The resulting share of government consumption in the regional final demand without GFCF is 22.5% for the center, 25.5% for the semiperiphery and 16% for the periphery.

3.1.7.3. Inequality in consumption between classes within world regions

In MORDRED, within every region the population that does not live in subsistence is divided into three consumption classes: The richest 20%, the poorest 30% and the remaining half of the population constituting the middle class. In this way, the MORDRED reflects inequalities between as well as within world regions. Additionally, there is a subsistence class which consumes 729 € per capita independent from the world region.

To derive realistic per capita consumption of these classes we rely on the GCIP database which provides real monthly consumption estimates for every decile for the majority of the countries in the world and more than half a century (Lahoti et al., 2016).

We use only the data for 2014, which is the closest to the start of the simulation year in MORDRED and includes the most countries (159 observations). The data is given in 2011-PPP-USD. Since we are only interested in the consumption shares of the different percentiles, it is not necessary to convert the data into another currency.

The 159 countries for which data was available were matched to the MORDRED regions and the respective UN population estimates for 2020 was added for every country.

Missing data: The distribution of consumption among percentiles for countries with considerable population that were not included in the GCIP data was approximated by other countries in the same region (if possible, neighboring countries) with similar GDP per capita. For the comparison, data from the World Bank (2024c) on GDP per capita was taken for the year 2011. Countries not included in the World Bank dataset were left out of the analysis. If there were no countries with similar GDP per capita levels in the region, other regions were taken as reference. Table 8 shows the missing countries in the GCIP and how they were replaced.

Country	Consumption distribution approximated through
Guyana	Ecuador
Puerto Rico	Bahamas
Bahrain	USA
Iraq	Iran
Kuwait	Singapore
Lebanon	Iran
Oman	USA
Quatar	Luxembourg
United Arab Emirates	Singapore
Yemen	Egypt
Saudi Arabia	USA
Brunei Darussalam	Singapore
Equatorial Guinea	Gabon
Eritrea	Ethiopia
Eswatini	South Africa
Gambia	Chad
Libya	Gabon
Macao	Singapore
Solomon Islands	Papua-New-Guinea
South Sudan	Sudan
Vanuatu	Papua-New-Guinea
Zimbabwe	Zambia

Table 8: Approximation of countries missing in the GCIP dataset.

The remaining countries not included in the GPIC database either had no UN population data, very small population size (<200000 people) and/or no World Bank data, and, thus, were left out from the analysis.

For Myanmar the average mean consumption in 2011-PPP USD was corrected by multiplying it by 100 because the value was two orders of magnitude lower than all the other values in the countries constituting the periphery, indicating a mistaken position of the comma.

For the conversion of the country-level data into regional-level data we used the gpinter interpolation tool of the World Inequality Database that allows users to merge the income distribution of several countries into a single one. The population of the respective countries serves to assign different weights to the respective inequality distributions. To this end, we restructured the data to fit the required format (shares, average values and threshold values for every percentile as well as the population size of the respective country). Because everyone within one percentile consumes the same, the consumption of the percentile is the average consumption of the percentile, and the threshold value was set to be 1 USD below the consumption value.

The aggregation tool estimated a consumption distribution for every MORDRED region on a percentile basis. Thus, for every region, the consumption share of the poorest 30% was derived by summing over the share of the first 30 percentiles; the consumption share of the Middle50 was derived by summing over the share of the following 50

percentiles; and the consumption share of the richest 20% was derived by summing over the shares of the remaining percentiles.

3.1.7.4. Shares and Calculations

The consumption distribution for the Top20, Middle50 and Bottom30 includes the consumption of the people living in subsistence within the Bottom30 because the survey data used to calculate inequalities in consumption do not exclude people living in subsistence. However, in MORDRED, the population belonging to the Top20, Middle50 and Bottom30 in every region is calculated as 20%, 50% and 30% of the population living fully integrated in the global economy.

Thus, for the semiperiphery and periphery, we first calculate the overall consumption of the richest 20%, the middle50% and the 30% poorest percent by applying regional shares, household shares and class shares to global total consumption.

Dividing these values by 20%, 50% and 30% of the population gives three average per capita consumption values.

We subtract the population sustained by the subsistence sector from the total population in the two MORDRED regions and construct the actual Top20, Middle50 and Bottom30 classes which are smaller than the previous numbers. This leads to a re-classification of a part of the population: the poorest members of the population become the subsistence class ($n_{low \rightarrow Subsistence}$), some people belonging to the middle 50% are now part of the Bottom30 ($n_{middle \rightarrow low}$), and some people belonging to the richest 20% now become part of the Middle50 ($n_{high \rightarrow middle}$). The original number of people in every segment is written as n_{high_0} , n_{middle_0} and n_{low_0} .

We construct the overall consumption of the actual classes and their average per capita consumption. For the Top20 we multiply the population belonging to the actual Top20 with the per capita consumption of the richest 20% of the total population

$$(n_{high} - n_{high \rightarrow middle}) * av_T20_0.$$

Thus, while the top class shrinks in number, its average per capita consumption remains unchanged and high: $av_T20_1 = av_T20_0$.

The new overall consumption of the actual Middle50 is the sum of the total consumption of the people that were previously classified as part of the richest 20% and the total consumption of the people that still belong to the Middle50:

$$C_{middle} = n_{high \rightarrow middle} * av_T20_0 + (n_{middle} - n_{middle \rightarrow low}) * av_M50_0$$

Dividing the overall consumption by the new population belong to the Middle50 gives the average per capita consumption for this class

$$av_M50_1 = \frac{(n_{high \rightarrow middle} * av_T20_0 + (n_{middle} - n_{middle \rightarrow low}) * av_M50_0)}{n_{middle_0} + n_{high \rightarrow middle} - n_{middle \rightarrow low}} \text{ with } av_M50_1 > av_M50_0.$$

To obtain the new overall consumption of the actual Bottom30 class we subtract the consumption of the population that is now part of the subsistence class (this class has a

fixed monetized per capita consumption of $C_{Subsistence} = 729 \text{ € /year}$) from the total consumption of the original B30 class and add the overall consumption of the people that were previously classified as part of the middle 50% :

$$C_{low_1} = C_{low_0} + n_{middle \rightarrow low} * av_M50_0 - n_{low \rightarrow Subsistence} * C_{Subsistence}$$

Dividing the overall consumption by the new population belonging to the Bottom30 gives the average per capita consumption for this class:

$$av_B30_1 = \frac{(C_{low_1})}{n_{low_0} + n_{middle \rightarrow low} - n_{low \rightarrow Subsistence}} \text{ with } av_B30_1 > av_B30_0.$$

In this way, the inequality in consumption between classes is preserved and the consumption of the subsistence class is separated from the consumption of the rest of the classes.

3.1.7.5. Consumption vectors of households

The consumption vector of households that describes how the final demand of households (classes) is distributed among the MORDRED sectors, i.e. a 25-dimensional vector containing the sectoral shares for a given level of total consumption per capita (evidently, the sum of 25 shares equals 1).

The vector changes along two linear functions of per capita consumption. The first linear function contains the points 1,356 €/(person*year) and 3,838.5 €/(person*year). The second linear function contains the points 3,838.5 €/(person*year) and 24,672.6 €/(person*year). At consumption levels below 1,356 €/person or above 24,672.6 €/person the consumption vector stays at the distribution corresponding to these minimum and maximum values (cf. section 2.2). In this way, we are able to depict the most significant changes in consumption patterns as the population grows richer, namely, a reduction of the relative importance of the food sector (sector 1), and an increase in the relative importance of the service sector (sector 7).

The consumption vector for households is only calculated for the population belonging to the global economy given that the consumption of the subsistence class is completely separated from the IO structure.

To construct the function describing changes in the consumption vector we use Exiobase3 data for 2019 that was aggregated in two ways: the sectoral aggregation resulted in the 25 MORDRED sectors, while the regional aggregation approximated the Exiobase countries and regions to the MORDRED regions (Table 7).

For every approximated MORDRED region we calculated the average annual per capita household final demand and the corresponding shares of the 25 sectors in the final demand. Thus, the minimum value of 1,355.8 €/(person*year) and the corresponding consumption vector comes from the approximated ‘periphery’, the middle value of 3,838.5 €/(person*year) with the corresponding consumption vector comes from the approximated ‘semiperiphery’ and the maximum value and consumption vector from the Exiobase3 ‘center’.

Using the three consumption vectors corresponding to the three per capita consumption levels we calculated the sectoral consumption of every class in MORDRED, using their

initial consumption per capita level. Aggregating the sectoral consumption of every class yielded a relatively accurate approximation of the actual total sectoral household final demand on the global level: the sectors with the highest overestimation of demand were sector 8 (1.27 times above the ‘real’ global household demand) and sector 1 (1.18 times above) while the sectors with the highest underestimation of demand were sector 18 (solar thermal based electricity) and sector 15 (wind power based electricity) with 84% and 86% of ‘real’ global sectoral household demand. More than half of the sectors had an aggregated demand of around 0.94 and 1.07 of the actual global demand. Thus, to achieve a complete equivalence between the aggregated and the global final demand in the initial moment of the simulation, the three original consumption vectors were divided by a 25-dimensional vector correcting for over- and underestimation of household demand in the different sectors.

3.1.7.6. Consumption vectors of governments

The consumption vector of governments describes how the final demand of governments in each MORDRED region is distributed among the MORDRED sectors, i.e. a 25-dimensional vector containing the sectoral shares (evidently, the sum of 25 shares equals 1).

Given that a preliminary analysis of government expenditures in the three approximated MORDRED regions of the 2019 Exiobase3 data did not yield significant differences in sectoral shares we assume that the share of each sector in government consumption is equal in the periphery, semiperiphery and center of MORDRED.

Thus, the sectoral shares on the regional level are the same as on the global level and the consumption vector of governments can be obtained by dividing the global government final demand of the respective sector by total global government final demand.

3.2. Labor

We obtain the data on labor intensity from the Exiobase3 extensions (.S) which gives data in million work hours per million euros for different employment categories.

To obtain the general labor intensity, we aggregate the employment categories ‘Low-skilled male’, ‘Low-skilled female’, ‘Medium-skilled male’, ‘Medium-skilled female’, ‘High-skilled male’ and ‘High-skilled female’.

The labor intensity of sector no. 1 is derived by dividing the new hours worked in sector no. 1 (without the hours belonging to subsistence output) by the new output of sector no. 1 (without the subsistence output) (cf. section 3.2.1.2).

3.3. Energy

3.3.1. Electricity production

In MORDRED, different sectors are assumed to produce the electricity that is consumed in productive processes as is depicted in Table 9. The data on the quantity of the different types of final energy produced in the initial year (2019) of the simulation on the global level comes from the IEA and from OWD. The data for electricity production was converted into EJ and then scaled down to reflect electricity consumption (consumption < production) because the non-energy sectors demand electricity that can actually be consumed in their production processes from the energy sectors. The share of oil, gas and coal in the fossil electricity sector was calculated with data for the base year and is kept constant during the simulation.

Sector number	Biophysical output	Data source
12	electricity produced with fossil fuels (coal, gas, oil)	IEA (2021)
13	nuclear electricity	ibid.
14	hydroelectricity	ibid.
15	electricity from wind power plants	ibid.
16	electricity from bioenergy	OWD (2024)
17	electricity from solar	ibid.
18	estimated electricity from solar thermal	The IEA does not give explicit estimates of electricity from solar thermal, tidal energy and geothermal but rather gives data on 'other renewable energy' apart from hydropower. Thus, it is assumed that solar thermal, tidal and geothermal 'fill up' with equal shares the remaining gap between the sum of electricity from wind, solar and bioenergy, and amount of 'other renewable energy'. This yields a value in the same order of magnitude as the OWD data for 'other renewables' which include waste, geothermal, wave and tidal energy.
19	estimated electricity from tide	ibid.
20	estimated electricity from geothermal	ibid.

Table 9: Electricity sectors in MORDRED.

3.3.2. Biomass and fossil fuels

MORDRED also includes the production of energy from biomass and the production of fossil fuels (Table 10). One part of the fossil fuels is used as material feedstock rather than as energy source, and, thus, is matched to sector 8, while the remaining fossil fuels are matched with sector 3. Fossil-based electricity is produced in sector 12.

Sector number	Biophysical output	Data source
10	biofuels and energy from waste	IEA (2021)
3	oil, natural gas and coal products used as energy source; 'other' energy not contained in all the other sectors	ibid. This does not include fossil primary energy used for the production of fossil electricity. All values are for energy consumption rather than production.
8	oil, natural gas and coal products used as feedstock	ibid; p. 38-40 of the IEA's Key World Energy Statistics report (2021) gives the percentage of non-energy use for the three types of fossil fuels for 2019. Applying those percentages to the overall fossil fuel consumption for each type gives the amount of fossil fuels used as feedstock.

Table 10: Fossil and biomass energy in MORDRED.

3.3.3. Link between biophysical and monetary values

The biophysical output of the sectors can be linked to their monetary output by dividing the former by the latter. This yields a conversion parameter α_i for every sector and allows the model to calculate the biophysical energy production associated to a certain monetary output of a sector.

$$\alpha_{biophysical:monetary_i} = \frac{x[final\ energy]_i [EJ]}{x[money]_s [mio\ €]}.$$

For sector 8, the conversion parameter links feedstock to monetary output.

$$\alpha_{feedstock_{ff}:money_8} = \frac{x[feedstock_{ff}]_8 [EJ]}{x[money]_8 [mio\ €]} \text{ with } ff = \text{oil, gas, coal}.$$

3.3.4. Primary energy

The data for the primary energy in 2019 comes from the IEA (2021). The conversion factor to calculate the primary energy of oil, gas and coal needed for fossil electricity production are based on ECOFYS estimates on average global efficiencies of coal, natural gas and oil-fired power generation (Nierop & Humperdinck, 2018).

3.3.5. Fossil fuel reserves and resources

Reserve and resource estimates included in MORDRED

We use estimates for different fossil fuel reserves and resources from the energy study of the German Federal Institute for Geosciences and Natural Resources (BGR, 2020, p. 41) which, except for the coal resource estimates are in the same order of magnitude as other estimates of future fuel production (e.g. Maggio & Cacciola, 2012; Mohr et al., 2015).

3.4. Land

3.4.1. Initial land and land types

The size of land used for human built infrastructure comes from Exiobase3 for the year 2019.

Energy land is the land needed for the extraction (biomass) as well as the installation and maintenance of different renewable energy technologies. The land demand from the energy sectors (sector 10, sector 14-20) in the initial moment of the simulation is obtained by multiplying the land intensity of the different energy sectors with their respective output.

Food land is required by the world economy to grow food and includes cropland and pastures. By aggregating the data of all cropland categories ($n=13$) and all pasture categories ($n=3$) in Exiobase3 for 2019 and subtracting the size of subsistence food land as well as the estimated size of land used to generate bioenergy we obtain the initial size of this land type.

Subsistence land is required by the subsistence economy to grow food and includes cropland and pastures. Since Exiobase3 does not differentiate between subsistence and global economy, we approximated the size of this land type by multiplying the estimated number of subsistence workers with the estimated land managed per subsistence worker.

The number of subsistence workers is determined by our initial assumptions about the population size living in subsistence (cf. section 3.2.1.2). The size of the land managed by each subsistence worker is assumed to be 1 ha, consistent with estimates on the farm size of smallholders (Altieri & Koohafkan, 2008; Lowder et al., 2025; Samberg et al., 2016).

The size of non-primary forests, i.e. secondary forest and forest plantations, at the beginning of the simulation is obtained by deducting the size of primary forests from the total forest land extension given by OWD (Ritchie & Roser, 2024) which is compatible with FAO forest data. The size of primary forest is based on estimates of FAO (2020).

The remaining habitable land (which does not include barren land (like deserts), glaciers or water bodies (like lakes)) contains non-forest ecosystems, marginalized lands and land not classified elsewhere, i.e. the Exiobase category 'other land'. The size of this land type in the initial moment of the simulation is derived by subtracting the sum of all previously discussed land types from the total habitable land on the Earth's surface without water bodies (Ritchie & Roser, 2024).

3.4.2. Production-driven land demand

The world economy in MORDRED generates demand for energy, food, forest and other land (cf. section 2.5) The land use intensity is measured in $\frac{km^2 Lnd}{mio\epsilon X_i}$.

Sector 1 is the only sector from which all demands for food land originate:

$$Int_{foodland_we} = \left(\frac{Food\ Lnd_{t0}}{X_1}, 0_2, \dots, 0_{25} \right)$$

Sector 2 is the only sector from which all demands for forest land originate:

$$Int_{prod_frst} = (0_1, \frac{Forest\ Lnd_{t0}}{X_2}, 0_3, \dots, 0_{25})$$

According to Exiobase3 data, in the initial moment of the simulation, the economic use of forest land covers 84% of non-primary forests.

In Exiobase3, sector 1 and 2 also demand 'Other Land':

$$Int_{Other} = \left(\frac{Other\ Lnd_{1t0}}{x_1}, \frac{Other\ Lnd_{2t0}}{x_2}, 0_3, \dots, 0_{25} \right)$$

The energy sectors in MORDRED generate land use demands according to the energy demanded which in MORDRED is directly related to the outputs of the sectors.

Given the lack of data in Exiobase3 for land demanded by the energy infrastructure, we use data from the IAM MEDEAS (Capellán-Pérez et al., 2020) on the power density of different renewable energy technologies. MEDEAS does not include land use of mining and fossil fuel extraction, thus, there is a slight underestimation of demand.

The renewable energy sectors in MORDRED were matched to technologies contained in [MEDEAS]: sector 14 and sector 19 were matched to [hydropower]; sector 20 to [geothermal], sector 17 to [PV], sector 18 to [CSP], sector 15 to the average of [wind onshore] and [wind offshore], and finally, sector 16 and sector 10 were matched to [biofuels grown on cropland]. We chose the MEDEAS category [biofuels (cropland, second generation)] and neglect the category [biofuels (marginal land)] which has a lower productivity.

Subsequently, we obtained the land demand per energy production and energy production per output for every technology:

Sector 10:

$$\text{power density}_{10} \left[\frac{EJ}{km^2} \right] = \alpha_{10} * \left(\frac{\text{Land productivity}_{biofuels}}{Mha} \right) * \frac{Mha}{10^4 km^2}$$

$$\frac{Energy\ Lnd_{10}}{Energy_{10}} = \frac{1}{\text{power density}_{10}}$$

$\alpha_{10} = 1.8$ is a correction factor that takes into account that the output of sector 10 is assumed to also include energy from waste, other non-biofuel biomass-based energy and more advanced biofuel production, and that there can be a degree of co-use of land for food and energy production, both of which reduce land demand relative to energy production. This estimate should be improved in further work based on a meticulous assessment of global present and future land intensity of biomass-based energy that can substitute fossil fuels.

Sector 14:

$$\text{power density}_{14} \left[\frac{\text{EJ}}{\text{km}^2} \right] = \left[\frac{\text{Twe}_{\text{hydro}}}{\text{Mha}} \right] * \alpha_{\text{we} \rightarrow \text{wh}} \left[\frac{\text{wh}}{\text{we}} \right] * \left[\frac{3.6 \text{ Mha} * \text{EJ}}{10^7 \text{Twh} * \text{km}^2} \right]$$

$\alpha_{\text{we} \rightarrow \text{wh}}$ denotes the conversion factor to wh.

$$\frac{\text{Energy Lnd}_{14}}{\text{Energy}_{14}} = \frac{1}{\text{power density}_{14}}$$

However, given that we assume that hydropower demands water bodies, and MORDRED does not contain water bodies (rivers, lakes etc.), this variable takes the value 0.

Sector 15:

$$\text{power density}_{15} \left[\frac{\text{EJ}}{\text{km}^2} \right] = \left[\frac{\frac{\text{Twe}_{\text{wind onshore}}}{\text{Mha}} + \frac{\text{Twe}_{\text{wind onshore}}}{\text{Mha}}}{2} \right] * \alpha_{\text{we} \rightarrow \text{wh}} \left[\frac{\text{wh}}{\text{we}} \right] * \left[\frac{3.6 \text{ Mha} * \text{EJ}}{10^7 \text{Twh} * \text{km}^2} \right]$$

$$\frac{\text{Energy Lnd}_{15}}{\text{Energy}_{15}} = \frac{1}{\text{power density}_{15}}$$

Sector 16:

$$\text{power density}_{16} \left[\frac{\text{EJ}}{\text{km}^2} \right] = \alpha_{16} * \frac{\text{Land productivity}_{\text{biofuels}}}{\text{Mha}} * \frac{\text{Mha}}{10^4 \text{km}^2}$$

$\alpha_{16}=1.18$ is a correction factor as we optimistically assumed that biomass-based electricity can be compared to advanced generations biofuel production regarding land intensity.

$$\frac{\text{Energy Lnd}_{16}}{\text{Energy}_{16}} = \frac{1}{\text{power density}_{16}}$$

Sector 17:

The power density given in MEDEAS 1.4 corresponds to the average value given in de Castro (2013). The power density can be calculated following the formula given in de Castro (2013) which multiplies (a) the average solar irradiance by (b) the conversion efficiency of solar radiation into electricity, (c) the averaged performance ratio over the park's life cycle and (d) the actual land occupation of PV cells. (a) and (c) are adopted from de Castro (2013) and (d) from Capellán-Pérez et al. (2017) while we choose a value of 0.2 for (b) to reflect a higher cell conversion efficiency in the future. This yields a power density value slightly above the upper bound for future power density given in de Castro (2013).

$$\text{power density}_{17} \left[\frac{\text{EJ}}{\text{km}^2} \right] = \left[\frac{\text{Twe}_{\text{solar PV}}}{\text{Mha}} \right] * \alpha_{\text{we} \rightarrow \text{wh}} \left[\frac{\text{wh}}{\text{we}} \right] * \left[\frac{3.6 \text{ Mha} * \text{EJ}}{10^7 \text{Twh} * \text{km}^2} \right]$$

$$\frac{\text{Energy Lnd}_{17}}{\text{Energy}_{17}} = \frac{1}{\text{power density}_{17}}$$

Sector 18:

$$\text{power density}_{18} \left[\frac{\text{EJ}}{\text{km}^2} \right] = \left[\frac{\text{Twe}_{\text{CSP}}}{\text{Mha}} \right] * \alpha_{\text{we} \rightarrow \text{wh}} \left[\frac{\text{wh}}{\text{we}} \right] * \left[\frac{3.6 \text{ Mha} * \text{EJ}}{10^7 \text{Twh} * \text{km}^2} \right]$$

$$\frac{Energy\ Lnd_{18}}{Energy_{18}} = \frac{1}{power\ density_{18}}$$

Sector 19: this technology takes the same intensity as sector 14.

Sector 20:

$$power\ density_{20} \left[\frac{EJ}{km^2} \right] = \left[\frac{Twe_{geothermal}}{Mha} \right] * \alpha_{we \rightarrow wh} \left[\frac{wh}{we} \right] * \left[\frac{3.6\ Mha * EJ}{10^7 Twh * km^2} \right]$$

$$\frac{Energy\ Lnd_{20}}{Energy_{20}} = \frac{1}{power\ density_{20}}$$

$\frac{Energy_i}{X_i}$ for every sector is calculated based on the data contained in the energy and the economy module.

We calculated the intensities of land demand for the different energy sectors in $km^2/mio\epsilon$:

$$Intensity_{i\ Energy\ Lnd} = \frac{Energy\ Lnd_i [km^2]}{Energy_i [EJ]} * \frac{Energy_i [EJ]}{X_i [mio\epsilon]}$$

$$Intensity_{19\ Energy\ Lnd} = Intensity_{14\ Energy\ Lnd}$$

3.4.3. Consumption-driven land demand

In MORDRED, demand for infrastructure is assumed to correlate with overall household consumption since, arguably, there is not a single sector driving the demand for infrastructure. The more households consume, the more infrastructure has to be build to deliver the products, the more expansion of settlements becomes possible etc.

$$Int_{infr} = \left(\frac{Infrastructure_{t0}}{\sum_{s=i}^{25} C_s} \right)$$

3.4.4. Population-driven land demand

In MORDRED, the overall population living in subsistence is assumed to drive the quantity of the subsistence sector's land demand.

$$Int_{sub_lnd}^{Lnd,bd} = \left(\frac{Sub_Lnd_{t0}}{\sum_{r=1}^3 P_r^{sub} t_0} \right)$$

This gives the land demand per member of the subsistence class.

3.5. Climate

3.5.1. Climate system

The climate module is a greatly simplified and updated version of the climate module contained in the system dynamics model WILIAM 1.3 (Lifi et al., 2023; Samsó et al., 2023), which in turn is based on the climate sub-module contained in the C-Roads model.

In MORDRED 1.0 there are three climate feedbacks that can be activated. The first activated feedback affects C uptake in response to temperature changes. The second activated feedback affects changes in natural CH₄ emissions in response to temperature changes. The last feedback determines whether there are any emissions from permafrost and clathrate when certain temperature thresholds are crossed. Additionally, the ECS value can be modified, as well as the sensitivity of CH₄ and C from permafrost and clathrate to temperature changes and the temperature threshold for CH₄ emissions from permafrost and clathrate.

Apart from removing variables and submodules not considered strictly necessary for this part of MORDRED, e.g. the submodule on tipping points or waste emissions, sea-level sensitivity from ice-sheet melting, climate-related variables at the regional level, ...) the following modifications were made to the climate submodel incorporated in WILIAM:

Reserves and resources for three types of fossil fuels (coal, gas, oil) were added, based on estimations of the BGR (2020), which are used by the IPCC WG1 contribution to the AR6 (IPCC, 2021). This completes the carbon cycle part of the climate module as anthropogenic combustion of fossil fuels create a flow from fossil fuel reserves/resources to the atmosphere.

MORDRED-specific variables for CO₂ emissions from land use changes were introduced into the climate module. These are calculated in the Stressors module (cf. section 3.7).

The variables used to calculate sea-level rise were modified to reflect the starting year of MORDRED simulations.

Given that Exiobase3 does not distinguish between different HFC types, we assume that all HFC emissions in MORDRED are of the type HFC134a. Given the different warming potentials of different HFC types, this could yield a small estimation error which is assumed to be negligible due to the relatively small contribution of HFC gases to global warming.

The values of the model parameters (such as the climate sensitivity, preindustrial concentration of different greenhouse gases, global warming potentials of different greenhouse gases etc.) have been updated according to WG1 IPCC (2021) and according to the newest C-Road model version.

The calculation of different GHG emissions in MORDRED does not distinguish between several regions and uses emission intensities from Exiobase3 for CH₄, N₂O, HFC, PFC and SF₆.

The value for the variable ‘Other forcings’ was calculated based on values given in Table 7.8 IPCC WG1 (2021). This variable is needed to calculate total anthropogenic ERF which is estimated as 2.72 W/m^2 over the industrial era by the IPCC and is set to 2.70 W/m^2 in MORDRED in the initial moment of the simulation.

3.5.2. Climate damages

3.5.2.1. Capital stock

Extreme weather events

Extreme weather events of different types cause damages in capital stock and are assumed to increase in frequency and severity as global temperatures increase (IPCC, 2021).

To obtain the sectoral shares of capital damages from extreme weather events compared to the overall sectoral stock at the global level, we follow three steps.

First step: estimation of total capital stock damage at 4°C :

The estimated total global damages of capital stock (DK) from extreme weather events at 4 degrees of global warming are calculated as:

$$DK_{total\ 4^\circ\text{C}} = \sum_{e=1}^4 \left(\left(D_{2010-2019 > \text{billion\$ events}_e} + D_{2010-2019 < \text{billion\$ events}_e} \right) * \alpha_{World_e} \right. \\ \left. * \alpha_{f,i,minmax_e} * \alpha_{compound} \right) + D_{2010-2019_{hw}} * \alpha_{World_{hw}} * \alpha_{f,i,minmax_e} \\ * \alpha_{compound}$$

e denotes the type of extreme weather event with $e_1 = \text{drought}$, $e_2 = \text{flood}$, $e_3 = \text{storm}$, $e_4 = \text{wildfire}$, $e_5 = \text{heatwave (hw)}$.

For the first 4 types of extreme weather events we use the NCEI data on billion-dollar events that affected the USA over the period 2010 to 2019 (A. Smith, 2025). For the fifth type we use estimates by Forzieri et al. (2018) for Europe (EU28, Switzerland, Norway and Iceland). To obtain the estimated heatwave damages in the period 2010-2019, a weighted average is taken between the damages occurring between 1981 and 2010, and the damages they calculate for 2020. The data for the first 4 types is converted into 2015-USD, using the CPI deflator, while the data for the fifth type is converted into 2015-€, using the EZB GDP deflator.

The data of the NCEI only provides data for $D_{2010-2019 > billion\$ events_e}$. To estimate $D_{2010-2019 < billion\$ events_e}$ we assume an inverse relationship between the frequency of an event and the severity of the damages: $D_{2010-2019 < billion\$ events_{e=1,2,3,4}} = \sum_{n=1}^4 \alpha_{freq}^n * \frac{D_{< billion}}{2^{(n-1)}}$ and apply a maximum of 4 billion which could lead to a slight underestimation of this type of damage. α_{freq} and $D_{< billion}$ take the same value for all e .

$D_{2010-2019_{hw}}$ is obtained by multiplying the share of heatwave-related damages in the total capital stock of the EU with the capital stock of the US based on EUKLEMS capital stock data for 2015. EUKLEMS does not contain data for Switzerland, Norway and Iceland. However, it is assumed that, due to their geography, these countries bear an insignificant amount of heatwave related damages, thus, we assume that they are de facto excluded from both damages and stock.

$$D_{2010-2019_{hw}} = \frac{D_{hw\ 2010-2019_{EUplus}}}{total\ K_{2015_{EUplus}}} * total\ K_{2015_{US}}$$

α_{World_e} is an adjustment factor that takes into account that we are estimating global capital stock damages based on country-specific data, i.e. the US (for the first 4 types of extreme weather events) and Europe (for the last type).

Extreme weather type	Reasoning adjustment	α_{World_e}
Drought	Drought-risks outside of the US are significantly higher (Meza et al., 2020).	1.5
Flood	No significant difference in vulnerability assumed.	1
Storm	No significant difference in vulnerability assumed.	1
Wildfire	No significant difference in vulnerability assumed.	1
Heatwave	World outside of EUplus is significantly more exposed to heatwaves (Hu et al., 2023).	2

Table 11: Adjustment factors for extreme weather damages.

$\alpha_{f,i,minmax_e}$ is a multiplier to take into account changes in damages as global temperatures increase to 4°C due to an increase in the frequency and intensity of different types of extreme weather events.

Based on IPCC (2021), Ch.11 estimates on temperature-related increases in the intensity and frequency of extreme weather events, we obtain a minimum and a maximum value for every extreme weather type that describes the change in damages at 4 °C compared to 1 °C of global temperature change. In the public MORDRED 1.0 version, the minimum value is used.

Last, $\alpha_{compound}$ is a factor that takes into account the increased severity of damages caused by compound events, i.e. by similarly occurring extreme weather events.

$D_{total\ 4^\circ C}$ gives an estimate of damages in capital stock at 4 degrees of warming for a fictitious ‘world’ of the economic size of the US. Of course, the ‘real’ damages would be significantly higher. However, since we are interested in the ratio between capital

damages and capital stock, and we divide the damages by the capital stock of the US (see below), this ‘error’ is insignificant.

Second step: capital stock data

Capital stock data for the US for 2015 comes from EUKLEMS. We obtain the total capital stock (K_{total}) as well as the capital stock of specific sectors especially affected by climate damages. The latter were matched with the MORDRED sectors.

EUKLEMS sector description and abbreviation	MORDRED sector
Agriculture, forestry and fishing stock (A)	1
Manufacture of food products; beverages and tobacco (C10-C12)	
Transportation and storage (H)	21
Electricity, gas, steam; water supply, sewerage, waste management (D-E)	[12;20], 3, 8, 24, 25
Manufacture of coke and refined petroleum products (C19)	

Table 12: Matching EUKLEMS sectors with MORDRED sectors for climate damage calculations.

Thus, the capital stock of sector 1 (K_1) is approximated as the sum of the capital stock in A and C10-C12; the capital stock of sector 21 (K_{21}) is approximated as H, and the capital stock of sector 3, 8, 24, 25 and all forms of electricity (sectors 12 to 20) ($K_{3,8,12,13,14,15,16,17,18,19,20,24,25}$) is approximated as the sum of D-E and C19. Summing up these capital stocks gives the overall ‘vulnerable’ capital stock:

$$K_{vulnerable} = K_1 + K_{21} + K_{3,8,12,13,14,15,16,17,18,19,20,24,25}$$

Third step: sectoral shares of damages in stock

One part of the overall damage at 4 degree of global warming is assumed to affect the whole economy, i.e. all sectors. The rest of the overall damage is assumed to be concentrated in sectors assumed to be especially vulnerable to climate damages. These sectors experience an additional damage apart from the general damage.

$$D_{4^{\circ}C \text{ all sectors}} = \beta_{split} * D_{total \text{ } 4^{\circ}C}; \text{add. } D_{4^{\circ}C \text{ vulnerable sectors}} = (1 - \beta_{split}) * D_{total \text{ } 4^{\circ}C}$$

In MORDRED 1.0, $\beta_{split}=0.7$.

With this assumption, the sectoral shares of damages in the stock of the respective sectors can be calculated.

$$\text{share}_{\text{damage in } K_{2,4,5,7,9,11,22,23}} = \frac{D_{4^{\circ}C \text{ total}}}{K_{total}} = \beta_{2,4,5,7,9,11,22,23}^{\delta_{temp}}$$

$$\begin{aligned} \text{share}_{\text{damge in } K_{1,3,8,12,13,14,15,16,17,18,19,20,21,24,25}} &= \frac{D_{4^{\circ}C \text{ total}}}{K_{total}} + \frac{\text{add. } D_{4^{\circ}C \text{ vulnerable}}}{K_{vulnerable}} \\ &= \beta_{1,3,8,12,13,14,15,16,17,18,19,20,21,24,25}^{\delta_{temp}} \end{aligned}$$

The sectoral shares of damage from extreme weather events in capital stock are assumed to increase non-linearly to reach the values corresponding to an increase of 4°C when the temperature in the model reaches 4 °C.

$$\delta_i^{\text{temp}} = \beta_i^{\delta_{\text{temp}}} * \frac{(\text{temp} - 1)^2}{9}$$

Sea-level rise

Under a high-emission scenario and/or Antarctic instability, between 4% and 7 % of the global population could be flooded annually by the end of the century (cf. Hinkel et al., 2014; Kulp & Strauss, 2019). We assume that population is directly correlated to the size of the capital stock, and that capital assets are more concentrated in coastal areas (e.g. ports, refineries etc.). Thus, we assume that between 6% and 9% of the global capital assets could be threatened by annual flooding under a temperature increase of ~4 °C.

We assume that half of the capital stock can be protected by hard coastal protection (e.g. dykes) while the other half is lost as populations realize a managed retreat. This leads to an overall loss of 3% to 4.5% of global capital stock as temperatures approach and cross the 4°C mark.

The modeling of sea-level rise related damages is described in section 2.2.

3.5.2.2. Capital intensity and input coefficients

Agriculture

Output losses in sector 1 mean that to produce the same amount of output as before, more capital stock is needed. We consider output losses due to insect pests (Deutsch et al., 2018) and heat (Zhao et al., 2017). The losses per unit of output (or the percentage of losses in total output) due to these stressors are:

$$\beta^{X_loss} = (\alpha_{insects} + \alpha_{heat}) \text{ for } 4 \text{ °C of warming.}$$

Consequently, capital intensity in sector 1 increases as a function of temperature (see section 2.2).

The factor multiplied with the column in the A matrix corresponding to sector 1 is given as:

$$Adf^{io}(\Delta Temp = 4) = \frac{1}{(1 - \beta^{X_loss})}$$

which is parametrized as

$$Adf^{io} = \beta 0^{Adf_io} + \beta 1^{Adf_io} \cdot \Delta Temp + \beta 2^{Adf_io} \cdot \Delta Temp^2$$

3.5.2.3. Additional investment

Sea-level rise

The costs for the hard coastal protection is modeled as additional investment in sector 5, which includes the construction sector.

We take half of the costs for dyke construction from Hinkel et al. (2014) in a RCP8.5 scenario (because we assume that only half of the coastline can be protected while the other is 'lost'), convert them to 2019-€ and multiply the costs by a factor of 2 because they do not take into account that a loss of coral reef protection implied by temperature changes higher than 1.5 °C to 2 °C doubles the exposure of built capital and people to flooding (Beck et al., 2018). It is further assumed that the total coastal protection system has to be renewed once during the simulation.

$$Extra_GFCF_5^{slr} = \frac{costs_{Hinkel \text{ et al. } 2019\text{€}} * \alpha_{coral \text{ reef } loss} * \alpha_{life \text{ time}}}{2}$$

3.5.2.4. Labor force, working day, maximum labor supply

We assume no additional effects on mortality due to climate change impacts such as the spread of vector- or water-borne diseases or the increase in natural disasters given that the actual effect of those factors on mortality are strongly mediated by the socio-economic context (Béguin et al., 2011; Franklino et al., 2019).

However, we assume that the annual working hours can be negatively affected by increases in deadly heat (Mora et al., 2017).

$$\beta^{HB_Max_Lb} = \frac{days_{deadly \text{ heat}}}{days_{year}} * \frac{workers_{low \text{ resistance}}}{workers}$$

$\frac{days_{deadly \text{ heat}}}{days_{year}}$ describes the share of days with deadly heat in a year, and $\frac{workers_{low \text{ resistance}}}{workers}$ denote the share of workers that are not able to work due to deadly heat conditions. $\frac{days_{deadly \text{ heat}}}{days_{year}}$ is estimated based on Mora et al. (2017) while $\frac{workers_{high \text{ resistance}}}{workers}$ is assumed to be 0.5.

3.5.2.5. Labor intensity

Heat

The literature finds that for 3 °C global effective labor (which includes both a drop in productivity and a reduction in hours worked) decreases by 18% ($\alpha_{Lprod_{low}}$) for low-exposure and by 25% ($\alpha_{Lprod_{high}}$) for high exposure activities (Dasgupta et al., 2021). For simplicity, we assume that the hours worked remain constant, with a de facto labor productivity of zero for those hours that people do no longer work.

Low-exposure working conditions are defined as work outside in the shade or indoors while high-exposure working conditions are defined as works outside with no shade. The MORDRED sectors were classified as having predominantly low or high exposure working conditions.

Predominantly high-exposure	Sector 1, 4, 5
Predominantly low-exposure	rest of sectors

Table 13: Low- and high-exposure sectors.

$$\beta_{1,4,5}^{HB_Lb_prod} = 1 - \alpha_{Lprod_{high}}$$

$$\beta_{!=1,4,5}^{HB_Lb_prod} = 1 - \alpha_{Lprod_{low}}$$

Loss in Output

In the case of sector 1, the assumed output loss (section 3.6.2.2) also implies an additional reduction of labor productivity in this sector (see section 2.2).

3.5.2.6. Land

All estimates on land losses are cumulative values rather than annual values.

Sea level rise

To estimate the total land lost until the end of the century (β^{Lnd_loss}) in a high-emission scenario, we draw an average between the land loss estimate of Bamber et al. (Bamber et al., 2019) and the higher of the two estimates made by Hinkel et al. (2014) given that in a high-emission scenario the natural coastal protection by mangroves and reefs will be severely weakened or lost. We divide this average value by 2 since we assume that half of the inundation-threatened land will be maintained through hard coastal protection (cf. section 3.6.2.2).

River floods

The literature provides estimates on the amount of flood-prone global cropland that would be exposed to a doubling of current 100-year flood frequency by 2050 in a high-emission scenario (Arnell et al., 2016), and the risks can be expected to increase until the end of the century. Thus, we assume that half of this exposed cropland will be rendered unsuitable for agriculture and lost. Although the authors do not mention deltas, it is very probable that the land loss will concentrate in the world's deltas (Nienhuis & van de Wal, 2021).

Temperature, humidity change

Zhang & Cai (2011) calculate changes in potential arable land areas under different climate change scenarios. Given that in MORDRED it is optimistically assumed that forestland can always be converted into land to grow food, we sum only the negative

changes, i.e. losses, for the different world regions indicated in the study, and draw an average between the total land lost in the A1B-SAM and the A1b-RMSEMM scenario.

The total loss of cropland as a function of temperature is given as:

$$L\beta^{Foodland_loss} = Loss_{floods} + Loss_{temp\&humid}$$

3.5.2.7. Land intensity

Sector 1

In the case of sector 1, the assumed output loss (cf. section 3.6.2.2) also implies a reduction of land productivity in this sector.

Damages on subsistence land

It is assumed that as temperature increases and extreme weather events become more severe and frequent, less people can be sustained per unit of land.

$$\beta^{Ext_Int_Lnd_sub} = \frac{Int_{sub_lnd}^{Lnd,bd}}{3}$$

3.6. Stressors

All stressors are represented in the form of ‘intensities’. Most stressors take the form [stressor / monetary output] but some also take the form [stressor / land] or [stressor / energy]. In the first case stressors are represented as 25-dimensional vectors and contain the intensity for every sector. To construct these vectors, for every sector the quantity of the stressor emanating from the sector is divided by the sector’s output.

In the case of stressors apart from emissions, we obtain all the data from the Exiobase3 extension (.F) which gives the stressor in absolute quantities. These quantities are matched to the sectors generating the stressors and divided by the sectoral outputs to obtain the respective sectorial intensities.

3.6.1. Greenhouse gas emissions

3.6.1.1. CO₂ emissions

CO₂ emissions from fossil fuel combustion

The data for CO₂ emissions from fossil fuel combustion comes from the IEA (IEA, 2021, p. 54) and is compatible with the data contained in Exiobase3. Given that this category concerns combustion, fossil fuels that are used as feedstock are not considered. For every fossil fuel (oil, gas, coal) the emission intensity is calculated as Mt of CO₂ emitted per EJ of primary energy of this fuel.

$$Int_{CO_2:Combustion_{ff}} = \frac{CO_2_{ff} [Mt]}{PE_{ff}^{neu} [EJ]}$$

CO₂ emissions from land use changes

MORDRED includes estimates of emissions resulting from the conversion of forest land into infrastructure, land used for energy generation, land used for cultivation of food within the global economy, land used for food within the subsistence economy and into ‘other land’.

Emissions from land use changes were approximated in the following way:

First, we estimate the carbon content per unit of forest land above and below the ground.

$$Int_{Carbon} = \frac{Carbon_{above} [Mt C] + Carbon_{below} [Mt C]}{Forest land [km^2]}$$

To obtain an Int_{Carbon} which is representative of different forest types, we take the average of the carbon content in tropical rainforests and boreal coniferous forests, as these represent the two extreme ends of the spectrum — high above-ground and low below-ground carbon in tropical forests, and the opposite pattern in boreal forests, using data from Houghton & Castanho (2023).

Second, we estimate the carbon which is lost per unit of forest land that is converted into another land type in a time step.

$$Carbon\ lost = \frac{Carbon_{above_{t0}} - Carbon_{above_{t1}} + Carbon_{below_{t0}} - Carbon_{below_{t1}}}{Forest\ land\ [km^2]}$$

If forest is converted to infrastructure it is assumed that the carbon above ground is almost entirely lost given the difficulty of having forest vegetation and hard infrastructure at the same place. The literature indicates that carbon below ground is also lost at a significant rate (Tao et al., 2015). Thus,

$$Carbon_{above_{t1}} = 0.05 * Carbon_{above_{t0}}$$

and

$$Carbon_{below_{t1}} = 0.5 * Carbon_{below_{t0}}$$

For the conversion of forest to energy land it is assumed that the carbon above ground is almost entirely lost given the difficulty of having forest vegetation and energy infrastructure at the same place while it is optimistically assumed that no carbon below ground is lost. Thus,

$$Carbon_{above_{t1}} = 0.05 * Carbon_{above_{t0}}$$

$$Carbon_{below_{t1}} = Carbon_{below_{t0}}$$

For the conversion of forest to industrialized agriculture the loss of above-ground carbon for conversion to cropland and pasture was estimated based on Houghton et al. (2012) by comparing the above-ground carbon content of tropical rainforests with the carbon content of cropland and pasture after conversion. Since conversion into cropland results in higher carbon losses than conversion into pasture, and since the shares of cropland and pasture are not the same, the average of carbon loss associated to cropland and pasture is weighted with the shares these land types have in 'food land' claimed by the global economy in the initial moment of the simulation.

Consequently,

$$Carbon_{above_{t1}} = (\alpha_{croplnd}^{we} * 0.389 * Carbon_{above_{t0}} + (1 - \alpha_{croplnd}^{we}) * 0.505 * Carbon_{above_{t0}})$$

$$Carbon_{below_{t1}} = Carbon_{below_{t0}}$$

with $\alpha_{croplnd}$ denoting the share of cropland, and $1 - \alpha_{croplnd}$ denoting the share of pasture in total food land.

For the conversion of forest to subsistence agriculture, we use data from Houghton et al. (2012) calculate a weighted average based on the estimated shares of cropland and pasture within subsistence land (given the low-intensity use of grassland, we conservatively assume that on average the share of cropland in total land used by the subsistence economy is 0.4). Thus,

$$\begin{aligned}
Carbon_{above_{t_1}} &= (\alpha_{cropLnd}^{sub} * 0.389 * Carbon_{above_{t_0}} + (1 - \alpha_{cropLnd}^{sub}) * 0.505 * Carbon_{below_{t_0}}) \\
Carbon_{below_{t_1}} &= Carbon_{below_{t_0}}
\end{aligned}$$

For the conversion of forest to other land we assume the same carbon loss as conversion to industrialized agriculture, thus, we optimistically assume that those lands tend to be used for agriculture rather than for infrastructure and energy generation.

For simplicity, we assume that a conversion of primary into secondary forests or forest plantations will not result in additional emissions. Depending on the management, managed forests can accumulate more carbon than secondary forests (Brown et al., 2020).

Last, we convert the lost carbon into CO₂ by multiplying with a factor $\gamma_{C \rightarrow CO_2}$.

The resulting stressors take the form

$$Int_{CO_2:conversion_{Lnd}} = Carbon\ lost_{Lnd} * \gamma_{C \rightarrow CO_2}$$

CO₂ emissions from other processes

Exiobase3 contains information on CO₂ emissions that do not stem from the direct combustion of fossil fuels but are generated in the waste sector, in industry due to cement and lime production, and in agriculture due to peat decay. Consequently, the respective emissions were matched with the sectors 1,5, 24 and 25.⁶ Given that we assume that a conversion to agricultural land implies no loss of carbon below the ground (soil carbon) (cf. section 8.1.1.2) when calculating the emissions due to land use, including CO₂ emissions from agriculture does not constitute a double counting of emissions.

$$Str_{CO_2:other} = \left(\frac{CO_2_{agriculture}}{X_1}, 0_2, 0_3, 0_4, \frac{CO_2_{cement}}{X_5}, \dots, \frac{CO_2_{fossil\ waste}}{X_{24}} + \frac{CO_2_{biogenic\ waste}}{X_{24} + X_{25}}, \frac{CO_2_{biogenic\ waste}}{X_{24} + X_{25}} \right)$$

In section 8.1.1.1, we did not include fossil fuels used as feedstock. Eventually, the latter also emit CO₂ but with a time lag that can be significant. It is assumed that the annual emissions from sector 24 include the emissions generated by fossil feedstock at their end of life. Due to a lack of more specific data, this intensity is assumed to be constant in MORDRED which can lead to estimation errors regarding the emissions from fossil resources used as feedstock as the simulation develops.

⁶ CO₂ emissions from biogenic waste were matched equally to sector 24 and 25 while CO₂ emissions from fossil waste were only matched to sector 24.

1.7.1.2. Other greenhouse gas emissions

The information on emissions of other greenhouse gas emissions comes from the Exiobase3 extension ".F" which gives the emissions in absolute quantities. The extension .F contains a list of stressors that were matched to the MORDRED sectors.

Greenhouse gas	Stressor	Sector number
CH4	combustion - air	10, 25
	waste - air	24, 25
	non combustion - Extraction/production of (natural) gas - air	3, 8
	non combustion - Extraction/production of crude oil - air	
	non combustion - Mining of antracite - air	
	non combustion - Mining of bituminous coal - air	
	non combustion - Mining of coking coal - air	
	non combustion - Mining of lignite (brown coal) - air	
	non combustion - Mining of sub-bituminous coal - air	
	non combustion - Oil refinery - air	
N2O	agriculture - air	1
	combustion - air	3
	agriculture	1
SF6	air	12, 13, 14, 15, 16, 17, 18, 19, 20
HFC	air	11
PFC	air	4, 5, 25

Table 14: Greenhouse gas emissions and sectors causing them.

The units of the Exiobase3 data were modified to fit the climate module, which most notably involved converting the CO2 equivalents of HFC and PFC in Exiobase3 into tons of HFC and PFC, using the GWP-100 values given by the IPCC for HFC134-a and PFC-14 in the Supplementary Material for Chapter 7 of the Contribution of WGI to AR6 (C. Smith et al., 2021, pp. 17, 21).

The resulting stressors are:

$$Int_{CH4} = \left(\frac{CH4_{agriculture}}{X_1}, 0_2, \frac{\sum CH4_{combustion}}{X_3 + X_8}, 0_4, 0_5, 0_6, 0_7, \frac{\sum CH4_{combustion}}{X_3 + X_8}, 0_9, \frac{CH4_{combustion}}{X_{10} + X_{25}}, 0_{11}, \dots, \frac{CH4_{waste}}{X_{24} + X_{25}}, \frac{CH4_{combustion}}{X_{10} + X_{25}} + \frac{CH4_{waste}}{X_{24} + X_{25}} \right)$$

$$Int_{N2O} = \left(\frac{N2O_{agriculture}}{X_1}, 0_2, \frac{N2O_{combustion}}{X_3}, 0_4, 0_5, \dots, 0_{25} \right)$$

$$Int_{SF6} = \left(0_1, \dots, 0_{11}, \frac{SF6}{\sum_{i=12}^{20} X_i}, 0_{21}, \dots, 0_{25} \right)$$

$$Int_{HFC} = \left(0_1, 0_2, \dots, \frac{HFC}{X_{11}}, \dots, 0_{25} \right)$$

$$Int_{PFC} = \left(0_1, \dots, 0_3, \frac{PFC}{X_4 + X_5 + X_{24}}, \frac{PFC}{X_4 + X_5 + X_{24}}, 0_6, \dots, 0_{23}, \frac{PFC}{X_4 + X_5 + X_{24}}, 0_{25} \right)$$

3.6.2. Water

3.6.2.1. Industrial water consumption

Exiobase3 differentiates between green and blue water consumption.

Green water consumption results mainly from agricultural activity. Thus, all green water stressors in Exiobase3 were aggregated and matched to sector 1.

$$WC_{green} = \left(\frac{\sum_{v=1}^{13} Green\ water_v [mm^3]}{X_1 [mio\epsilon]}, 0_2, \dots, 0_{25} \right)$$

v denotes the different agricultural sub-sectors in which the water is used (rice, wheat, other cereals, roots and tubers, sugar crops, pulses, nuts, oil crops, vegetables, fruits, fibres, other crops, fodder crops).

Blue water consumption results from agricultural as well as from industrial activity. The sub-stressors were matched to the following sectors:

Sector no.	Sub-Stressor	w
1	Water Consumption Blue - rice	1
	[...] wheat	2
	[...] other cereals	3
	[...] roots and tubers	4
	[...] sugar crops	5
	[...] pulses	6
	[...] nuts	7
	[...] oil crops	8
	[...] vegetables	9
	[...] fruits	10
	[...] fibres	11
	[...] other crops	12
	[...] fodder crops	13
	[...] Livestock - dairy cattle	14
	[...] Livestock - nondairy cattle	15
	[...] Livestock - pigs	16
	[...] Livestock - sheep	17
	[...] Livestock - goats	18
	[...] Livestock - buffaloes	19
	[...] Livestock - camels	20
	[...] Livestock - horses	21
	[...] Livestock - chicken	22
	[...] Livestock - turkeys	23
	[...] Livestock - ducks	24
	[...] Livestock - geese	25
	[...] Products of meat cattle	26
	[...] Products of meat pigs	27
	[...] Products of meat poultry	28
	[...] Meat products nec	29
	[...] products of Vegetable oils and fats	30

	[...] Manufacturing - Dairy products	31
	[...] Processed rice	32
	[...] Sugar	33
	[...] Food products nec	34
	[...] Beverages	35
	[...] Fish products	36
2	[...] Tobacco products (16)	37
	[...] Textiles (17)	38
	[...] Wearing apparel; furs (18)	39
	[...] Leather and leather products (19)	40
	[...] Paper and paper products	41
7	[...] Printed matter and recorded media (22)	42
9	[...] N-fertiliser	43
	[...] P- and other fertiliser	44
	[...] Chemicals nec	45
	[...] Rubber and plastic products (25)	46
5	[...] Glass and glass products	47
	[...] Plastics, basic	48
	[...] Pulp	49
	[...] Cement, lime and plaster	50
	[...] Basic iron and steel and of ferro-alloys and first products thereof	51
	[...] Precious metals	52
	[...] Aluminium and aluminium products	53
	[...] Lead, zinc and tin and products thereof	54
	[...] Copper products	55
	[...] Other non-ferrous metal products	56
11	[...] Ceramic goods	57
	[...] Bricks, tiles and construction products, in baked clay	58
	[...] Other non-metallic mineral products	59
	[...] Fabricated metal products, except machinery and equipment (28)	60
	[...] Machinery and equipment n.e.c. (29)	61
	[...] Office machinery and computers (30)	62
	[...] Electrical machinery and apparatus n.e.c. (31)	63
	[...] Radio, television and communication equipment and apparatus (32)	64
	[...] Medical, precision and optical instruments, watches and clocks (33)	65
	[...] Motor vehicles, trailers and semi-trailers (34)	66
	[...] Other transport equipment (35)	67
	[...] Furniture; other manufactured goods n.e.c. (36)	68
12	[...] Electricity - tower - Electricity by coal	69
	[...] Electricity - tower - Electricity by gas	70
	[...] Electricity - tower - Electricity by petroleum and other oil derivatives	71
	[...] Electricity - once-through - Electricity by coal	72
	[...] Electricity - once-through - Electricity by gas	73

	[...] Electricity - once-through - Electricity by petroleum and other oil derivatives	74
13	[...] Electricity - tower - Electricity by nuclear	75
	[...] Electricity - once-through - Electricity by nuclear	76
16	[...] Electricity - tower - Electricity by biomass and waste	77
	[...] Electricity - once-through - Electricity by biomass and waste	78
18	[...] Electricity - tower - Electricity by solar thermal	79
	[...] Electricity - once-through - Electricity by solar thermal	80
20	[...] Electricity - tower - Electricity by Geothermal	81
	[...] Electricity - once-through - Electricity by Geothermal	82

Table 15: Matching blue water sub-stressor to MORDRED sectors.

The resulting stressor is:

$$\begin{aligned} Int_{WC_{blue}} \\ = \left(\frac{\sum_{w=1}^{36} Blue\ water_w}{X_1}, \frac{\sum_{w=37}^{41} Blue\ water_w}{X_2}, 0_3, 0_4, \frac{\sum_{w=47}^{56} Blue\ water_w}{X_5}, \dots, \frac{Blue\ water_{42}}{X_7}, 0_8, \frac{\sum_{w=43}^{46} Blue\ water_w}{X_9}, 0_{10}, \frac{\sum_{w=57}^{68} Blue\ water_w}{X_{11}}, \right. \\ \left. \frac{\sum_{w=69}^{74} Blue\ water_w}{X_{12}}, \frac{\sum_{w=75}^{76} Blue\ water_w}{X_{13}}, \frac{\sum_{w=75}^{76} Blue\ water_w}{X_{13}}, 0_{14}, 0_{15}, \frac{\sum_{w=77}^{78} Blue\ water_w}{X_{16}}, 0_{17}, \frac{\sum_{w=79}^{80} Blue\ water_w}{X_{18}}, 0_{19}, \frac{\sum_{w=81}^{82} Blue\ water_w}{X_{20}}, 0_{21}, \dots 0_{25} \right) \end{aligned}$$

3.6.2.2. Industrial water withdrawal

The stressors for industrial blue water withdrawal are the same as for industrial blue water consumption. Consequently, they are matched to the different sectors according to section 3.7.2.1, and the stressors are calculated by dividing the sum of all sub-stressors by the output of the respective sectors.

3.6.2.3. Household water consumption

The intensity of the water consumption of households is derived by dividing the total household water consumption given in Exiobase3 by the global aggregated consumption of all households. This either neglects the water consumption of the subsistence class or slightly overestimates the water consumption of the population sustained completely by the global economy (in the case that the water consumption of the subsistence class is contained in Exiobase3 through estimations).

$$Int_{WC} = \left(\frac{Q_{water}}{C} \right)$$

3.6.3. Material extraction and mineral production

Remark: In the following, we describe the data used for MORDRED 1.0 which is based on Exiobase3 data on used and unused domestic extraction. In some extended versions (e.g. 1.0.5, 1.1.1), we use global mineral production data rather than used domestic extraction for those materials for which there are global estimates provided by the US Geological Survey (USGS, 2020) or by secondary sources (Henckens, 2021), namely aluminium,

copper, gold, iron, lead, nickel, silver, tin, zinc, kaolin clay and salt. Intensities are derived in the same way. For the rest of materials, the Exiobase data on used material extraction is kept. Note that we used version Exiobase3 version 3.8.2 when we started with the development of the model. There is a new version available (3.9.6) which updates used domestic extraction and excludes unused domestic extraction. The newer data could be used to improve data quality for this part of the stressor module.

3.6.3.1. Used material extraction

The basic version of MORDRED includes the used domestic material extraction intensity in kt/mio€ for 19 materials as given by Exiobase3 for 2019: m_1 = Bauxite and aluminium, m_2 =Copper, m_3 = Gold, m_4 = Iron, m_5 = Lead, m_6 = Nickel, m_7 = Other non-ferrous metal, m_8 = PGM, m_9 = Silver, m_{10} = Tin, m_{11} = Zinc, m_{12} = Building stones, m_{13} = Chemical and fertilizer minerals, m_{14} = Clays and kaolin, m_{15} = Gravel and sand, m_{16} = Limestone, gypsum, chalk, dolomite, m_{17} = Other minerals, m_{18} = Salt, m_{19} = Slate.

MORDRED differentiates between two types of material extraction: Material extraction for general use and material extraction for the generation and maintenance of renewable energy systems. Given that sector 4 is the mining and extraction sector, we follow Exiobase3 in assuming that all material extraction for general use originates from sector 4.

Regarding the material extraction for renewable energy systems, the MEDEAS model contains material needs for different renewable energy technologies. The MORDRED sector 17 was matched to the MEDEAS technology solar PV, sector 18 was matched to CSP, and sector 15 was matched to the average material extraction requirements of wind onshore and wind offshore. Subsequently, the materials included both in Exiobase3 and in MEDEAS were identified: $m_1, m_2, m_4, m_5, m_6, m_9, m_{10}, m_{11}, m_{15}, m_{16}$. For these materials, MEDEAS gives estimates of material needs per new TW installed for every technology (kt/new TW). We considered only the material needs in the construction phase, which leads to a slight underestimation of the material requirements of renewable energy systems. The material requirements of the renewable system depend decisively on the life time and capacity factor of the installations as, after the end of life of the systems, they have to be constructed again. Due to uncertainties and lack of data regarding recycling systems for renewable energy systems, we conservatively assume that the complete energy infrastructure has to be replaced with new material after its end of life. This arguably leads to an overestimation of the material requirements of renewable energy systems towards the end of the simulation.

For sector 15 we calculated the total energy generated over the lifetime of the technology per TW installed:

$$\frac{\text{Total energy}_{15}}{\text{TW}_{\text{installed}}} = 0.5 * \left[(1 \text{ TW} * \alpha_{we \rightarrow wh} * \alpha_{TWh \rightarrow EJ} * \text{lifetime}_{wind_{offshore}} * \text{capacity factor}_{wind_{offshore}}) + (1 \text{ TW} * \alpha_{we \rightarrow wh} * \alpha_{TWh \rightarrow EJ} * \text{lifetime}_{wind_{onshore}} * \text{capacity factor}_{wind_{onshore}}) \right]$$

$$\alpha_{biophysical:monetary_{15}} = \frac{X[final\ energy]_{15}[EJ]}{X[money]_{15}[mio\epsilon]} \text{ (cf. section 3.4.3)}$$

We express the generated energy in monetary units.

$$Energy_{monetary_{15}} \left[\frac{mio\epsilon}{TW_{installed}} \right] = \frac{1}{\alpha_{biophysical:monetary_{15}}} * \frac{Total\ energy_{15}}{TW_{installed}}$$

$$Int_{m_{15}} \left[\frac{kt}{mio\epsilon} \right] = \frac{Q_{m_{15}}}{TW_{installed}} * \frac{1}{Energy_{monetary_{15}}}$$

For sector 17 we calculated the total energy generated over the lifetime of the technology per TW installed.

$$\frac{Total\ energy_{17}}{TW_{installed}} = 1\ TW * \alpha_{we \rightarrow wh} * \alpha_{TWh \rightarrow EJ} * lifetime_{solarPV} * capacity\ factor_{solarPV}$$

$$\alpha_{biophysical:monetary_{17}} = \frac{X[final\ energy]_{17}[EJ]}{X[money]_{17}[mio\epsilon]}$$

We express the generated energy in monetary units.

$$Energy_{monetary_{17}} \left[\frac{mio\epsilon}{TW_{installed}} \right] = \frac{1}{\alpha_{biophysical:monetary_{17}}} * \frac{Total\ energy_{17}}{TW_{installed}}$$

$$Int_{m_{17}} \left[\frac{kt}{mio\epsilon} \right] = \frac{Q_{m_{17}}}{TW_{installed}} * \frac{1}{Energy_{monetary_{17}}}$$

Equally, for sector 18 we calculated the total energy generated over the lifetime of the technology per TW installed.

$$\frac{Total\ energy_{18}}{TW_{installed}} = 1\ TW * \alpha_{we \rightarrow wh} * \alpha_{TWh \rightarrow EJ} * lifetime_{solarPV} * capacity\ factor_{CSP}$$

$$\alpha_{biophysical:monetary_{18}} = \frac{X[final\ energy]_{18}[EJ]}{X[money]_{18}[mio\epsilon]}$$

$$Energy_{monetary_{18}} \left[\frac{mio\epsilon}{TW_{installed}} \right] = \frac{1}{\alpha_{biophysical:monetary_{18}}} * \frac{Total\ energy_{18}}{TW_{installed}}$$

$$Int_{m_{18}} \left[\frac{kt}{mio\epsilon} \right] = \frac{Q_{m_{18}}}{TW_{installed}} * \frac{1}{Energy_{monetary_{18}}}$$

The material intensities of sector 4 were derived by subtracting the material extraction for renewable energy systems ($Q_{wind+PV+stherm}$) from the total material extraction (Q_{total}) and dividing the result by the output of sector 4. $Q_{wind,PV,stherm}$ are obtained by multiplying the respective stressors [kt/mio€] by the renewable energy sectors' initial output.

$$Int_{m_4} \left[\frac{kt}{mio\epsilon} \right] = \frac{(Q_{m_{total}} - Q_{m_{wind+PV+stherm}})}{X_4}$$

$$Q_{m_{wind+PV+stherm}} = 0$$

For $m = 3,7,8,12,13,14,17,18,19$ $Q_{m_{wind+PV+stherm}}$ is zero, for the rest of materials it is the sum of the product of output and material intensity of the wind, PV and stherm sectors.

3.6.3.2. Unused material extraction

The stressors included in the category ‘unused material extraction’ are the same materials as in the category ‘used material extraction’ and have the unit [kt/mio€]. Given that no data on unused material for the renewable energy sectors is available, following Exiobase3 we assume that all stressors originate from sector 4. Thus, all stressors take the form

$$Int_m = (0_1, \dots, Int_{4m}, 0_5, \dots, 0_{25}) \text{ with } m = (\text{Bauxite\&aluminium}_1, \dots, \text{Slate}_{19})$$

3.6.4. Nitrogen and Phosphorus pollution

The amount of N released into the water is classified as ‘N – agriculture – water’ and ‘N – waste – water’ in Exiobase. The former stressor is matched to sector no. 1, the latter equally to sector 24 and 25.

$$Int_{N_{water}} = \left(\frac{N_{agriculture} [\text{kg}]}{X_1 [\text{mio€}]}, 0_2, \dots, 0_{23}, \frac{N_{waste} [\text{kg}]}{X_{24} + X_{25} [\text{mio€}]}, \frac{N_{waste} [\text{kg}]}{X_{24} + X_{25} [\text{mio€}]} \right)$$

The amount of P released into the water is classified as ‘P – agriculture – water’ and ‘P – waste – water’ in Exiobase. The former stressor is matched to sector 1, the latter equally to sector 24 and 25.

$$Int_{P_{water}} = \left(\frac{P_{agriculture} [\text{kg}]}{X_1 [\text{mio€}]}, 0_2, \dots, 0_{23}, \frac{P_{waste} [\text{kg}]}{X_{24} + X_{25} [\text{mio€}]}, \frac{P_{waste} [\text{kg}]}{X_{24} + X_{25} [\text{mio€}]} \right)$$

The amount of P released into the soil is classified as ‘P – agriculture – soil’ in Exiobase and, thus, matched to sector 1.

$$Int_{P_{soil}} = \left(\frac{P_{soil} [\text{kg}]}{X_1 [\text{mio€}]}, 0_2, \dots, 0_{25} \right)$$

3.6.5. Air pollution

MORDRED includes data on 3 types of air pollution intensities from industrial activity in kg/mio€: NH3, PM2.5 and PM10.

NH3 consists of 4 sub-stressors: (1) NH3 from combustion was matched with sector 1, 2, 5, 9, 24, 25; (2) NH3 from agriculture with sector 1; (3) NH3 from waste with sector 24 and 25; (4) NH3 from N fertilizer production with sector 9.

$$Int_{NH3} = \left(\begin{array}{l} \frac{NH3_{combustion}}{X_1 + X_2 + X_5 + X_9 + X_{24} + X_{25}} + \frac{NH3_{agriculture}}{X_1} \cdot \frac{NH3_{combustion}}{X_1 + X_2 + X_5 + X_9 + X_{24} + X_{25}}, 0_3, 0_4, \frac{NH3_{combustion}}{X_1 + X_2 + X_5 + X_9 + X_{24} + X_{25}}, \\ 0_6, \dots, \frac{NH3_{combustion}}{X_1 + X_2 + X_5 + X_9 + X_{24} + X_{25}} + \frac{NH3_{fertilizer\ production}}{X_9}, 0_{10}, \dots, 0_{23}, \\ \frac{NH3_{combustion}}{X_1 + X_2 + X_5 + X_9 + X_{24} + X_{25}} + \frac{NH3_{waste}}{X_{24} + X_{25}}, \frac{NH3_{combustion}}{X_1 + X_2 + X_5 + X_9 + X_{24} + X_{25}} + \frac{NH3_{waste}}{X_{24} + X_{25}} \end{array} \right)$$

PM2.5 consists of a series of substressors which were matched to different sectors, following the matching in Exiobase.

Sector no.	Sub-Stressor	p
3	PM2.5 – non combustion – Production of gascoke	1
	[...] combustion	2
	[...] non combustion – Production of coke oven coke	3
	[...] non combustion – Carbon black production	4
	[...] non combustion – Oil refinery	5
	[...] non combustion – Briquettes production	6
	[...] non combustion – Mining of antracite	7
	[...] non combustion – Mining of bituminous coal	8
	[...] non combustion – Mining of coking coal	9
	[...] non combustion – Mining of lignite	10
	[...] non combustion – Mining of sub-bituminous coal	11
4	[...] non combustion – Aluminium ores and concentrates (Bauxite)	12
	[...] non combustion – Zinc ores and concentrates	13
	[...] non combustion – Silver ores and concentrates	14
	[...] non combustion – Tin ores and concentrates	15
	[...] non combustion – Platinum ores and concentrates	16
	[...] non combustion – Molybdenum ores and concentrates	17
	[...] non combustion – Chromium ores and concentrates	18
	[...] non combustion – Copper ores and concentrates	19
	[...] non combustion – Gold ores and concentrates	20
	[...] non combustion – Iron ores and concentrates	21
	[...] non combustion – Lead ores and concentrates	22
	[...] non combustion – Nickel ores and concentrates	23
	[...] non combustion - Nickel, unwrought	24
	[...] non combustion – Primary aluminium production	25
	[...] non combustion – Glass production	26
5	[...] non combustion – Steel production: basic oxygen furnace	27
	[...] non combustion – Steel production: electric arc furnace	28
	[...] non combustion – Steel production: open hearth furnace	29
	[...] non combustion – Chemical wood pulp, dissolving grades	30

	[...] non combustion - Chemical wood pulp, soda and sulphate, other than dissolving grades	31
	[...] non combustion - Chemical wood pulp, sulphite, other than dissolving grades	32
	[...] non combustion – Semi-chemical wood pulp, pulp of fibres other than wood	33
	[...] non combustion – Cement production	34
	[...]non combustion – Lime production	35
	[...] non combustion – Refined copper; unwrought, not alloyed	36
	[...] non combustion – Refined lead; unwrought	37
	[...] Unrefined copper; copper anodes for electrolytic refining	38
	[...] non combustion – Zinc; unwrought, not alloyed	39
	[...] non combustion – Pig iron production, blast furnace	40
	[...] non combustion – Cast iron production (grey iron foundries)	41
	[...] non combustion – Agglomeration plant – pellets air	42
	[...] non combustion – Agglomeration plant – sinter air	43
8	[...] non combustion – Production of gascoke	44
	[...] non combustion – Mining of antracite	45
	[...] non combustion – Mining of bituminous coal	46
	[...] non combustion – Mining of coking coal	47
	[...] non combustion – Mining of lignite	48
	[...] non combustion – Mining of sub-bituminous coal	49
9	[...] non combustion – N-fertilizer production	50
	[...]non combustion –Fertilizer-production	51
10	[...] combustion	52
11	[...] non combustion – Bricks production	53
24	[...] waste	54
25	[...] waste	55

Table 16: Matching MORDRED sectors with PM 2.5 sub-stressors.

The stressor vector is:

$$Int_{PM2.5} = \left(0_1, 0_2, \frac{\sum_{p=1}^{11} PM2.5_p}{X_3}, \frac{\sum_{p=12}^4 PM2.5_p}{X_4}, \frac{\sum_{p=25}^{43} PM2.5_p}{X_5}, 0_6, 0_7, \frac{\sum_{p=44}^{49} PM2.5_p}{X_8}, \frac{\sum_{p=50}^{51} PM2.5_p}{X_9}, \frac{PM2.5_{52}}{X_{10}}, \frac{PM2.5_{53}}{X_{11}}, 0_{12}, \dots, 0_{23}, \frac{PM2.5_{54}}{X_{24}}, \frac{PM2.5_{55}}{X_{25}} \right)$$

PM10 consists of a series of sub-stressors which are equal to PM2.5 sub-stressors and which were matched to the following respective sectors following Exiobase.

Sector	Sub-stressor	p
3	PM10 – non combustion – Production of gascoke	1
	[...] combustion	2
	[...] non combustion – Production of coke oven coke	3
	[...] non combustion – Carbon black production	4
	[...] non combustion – Oil refinery	5

	[...] non combustion – Briquettes production	6
	[...] non combustion – Mining of antracite	7
	[...] non combustion – Mining of bituminous coal	8
	[...] non combustion – Mining of coking coal	9
	[...] non combustion – Mining of lignite	10
	[...] non combustion – Mining of sub-bituminous coal	11
4	[...] non combustion – Aluminium ores and concentrates (Bauxite)	12
	[...] non combustion – Zinc ores and concentrates	13
	[...] non combustion – Silver ores and concentrates	14
	[...] non combustion – Tin ores and concentrates	15
	[...] non combustion – Platinum ores and concentrates	16
	[...] non combustion – Molybdenum ores and concentrates	17
	[...] non combustion – Chromium ores and concentrates	18
	[...] non combustion – Copper ores and concentrates	19
	[...] non combustion – Gold ores and concentrates	20
	[...] non combustion – Iron ores and concentrates	21
	[...] non combustion – Lead ores and concentrates	22
	[...] non combustion – Nickel ores and concentrates	23
	[...] non combustion - Nickel, unwrought	24
5	[...] non combustion – Primary aluminium production	25
	[...] non combustion – Glass production	26
	[...] non combustion – Steel production: basic oxygen furnace	27
	[...] non combustion – Steel production: electric arc furnace	28
	[...] non combustion – Steel production: open hearth furnace	29
	[...] non combustion – Chemical wood pulp, dissolving grades	30
	[...] non combustion - Chemical wood pulp, soda and sulphate, other than dissolving grades	31
	[...] non combustion - Chemical wood pulp, sulphite, other than dissolving grades	32
	[...] non combustion – Semi-chemical wood pulp, pulp of fibres other than wood	33
	[...] non combustion – Cement production	34
	[...]non combustion – Lime production	35
	[...] non combustion – Refined copper; unwrought, not alloyed	36
	[...] non combustion – Refined lead; unwrought	37
	[...] Unrefined copper; copper anodes for electrolytic refining	38
	[...] non combustion – Zinc; unwrought, not alloyed	39
	[...] non combustion – Pig iron production, blast furnace	40
	[...] non combustion – Cast iron production (grey iron foundries)	41
	[...] non combustion – Agglomeration plant – pellets air	42
	[...] non combustion – Agglomeration plant – sinter air	43
8	[...] non combustion – Production of gascoke	44
	[...] non combustion – Mining of antracite	45
	[...] non combustion – Mining of bituminous coal	46
	[...] non combustion – Mining of coking coal	47
	[...] non combustion – Mining of lignite	48

	[...] non combustion – Mining of sub-bituminous coal	49
9	[...] non combustion – N-fertilizer production	50
	[...]non combustion –Fertilizer-production	51
10	[...] combustion	52
11	[...] non combustion – Bricks production	53

Table 17: Matching MORDRED sectors with PM 10 sub-stressors.

$$\begin{aligned} Int_{PM10} \\ = \left(0_1, 0_2, \frac{\sum_{p=1}^{11} PM10_p}{X_3}, \frac{\sum_{p=12}^{24} PM10_p}{X_4}, \frac{\sum_{p=25}^{43} PM10_p}{X_5}, 0_6, 0_7, \frac{\sum_{p=44}^{49} PM10_p}{X_8}, \frac{\sum_{p=50}^{51} PM10_p}{X_9}, \frac{PM10_{52}}{X_{10}}, \frac{PM10_{53}}{X_{11}}, 0_{12}, \dots, 0_{25} \right) \end{aligned}$$

3.6.6. Industrial roundwood

For version 1.0, the Exiobase3 data for ‘Domestic Extraction Used - Forestry - Coniferous wood - Industrial roundwood’ and ‘Domestic Extraction Used - Forestry - Non-coniferous wood - Industrial roundwood’ was added and matched with sector no. 2, following the matching in Exiobase3. To obtain the intensity, the quantity of industrial roundwood extracted (kt) was divided by the output of the sector (in mio€).

$$Int_{IRW_{extraction}} = \left(0_1, \frac{Q_{wood}[kt]}{X_2[mio\text{€}]}, 0_3, \dots, 0_{25} \right)$$

For some extended versions, we replace the Exiobase data with data from FAO for 2016 (FAO, 2017) on global industrial roundwood production which is given in m³. To derive the intensity of production, we matched the value to sector no. 2 and divided it by the output of the sector (in mio€).

$$Int_{IRW_{production}} = \left(0_1, \frac{Q_{wood}[m^3]}{X_2[mio\text{€}]}, 0_3, \dots, 0_{25} \right)$$

4. Abbreviations, subscripts and superscripts

4.1. Abbreviations

Abbreviation	Definition
ΔTemp	Change in global average temperature with respect to 1850
a	Element of the A matrix
A	A matrix
Adf	Agriculture damage factor
Air_Poll	Air pollution
B	Births
Br	Birth rate
Br5y	Birth rate per five years
C	Private consumption
Cf	Conversion factor
clsh	Class share
Cpc	Consumption per capita
Cpc_gr	Consumption per capita growth rate
Cpc_nc	Consumption per capita not covered
Cpc_ssh	Consumption per capita sectorial share
D	Deaths
Dam	Damage
Dr	Death rate
Dsp_Lnd	Disposable land
Edf	Extraction difficulty factor
Edpc	Public expenditure on education per capita
Em	Emissions
Ext_Int	Extra intensity
Extra_GFCF	Extra gross fixed capital formation
FD	Final demand
FE	Final energy
FE2PE	Final energy to primary energy
Foodland_loss	Foodland loss
Frst_lnd_rdct	Forest land reduction
G	Government consumption
G_ssh	Government consumption sectorial share
G2Cr	Government consumption to Private consumption ratio
GFCF	Gross fixed capital formation
GFCF_ssh	Gross fixed capital formation sectorial share
Hpc	Public expenditure on health per capita
Id	Identity matrix
Int	Intensity
Inv	Investment
IRW	Industrial roundwood
K	Capital stock

Lb	Labour
Lnd	Land
M	Migrations
Mat	Materials
Max_Er	Maximum extraction rate of fossil fuels
Max_ff	Maximum fossil fuels annual extraction
Max_h	Maximum annual working hours
Max_Lb	Maximum labour
MaxP	Maximum population
Mr	Migration rate
P	Population
P&N_Poll	Phosphorus and nitrogen pollution
PE	Primary energy
Prt_Lnd	Protected land
Prt_r	Participation rate
Rsc_ff	Extractable fossil fuel resources
Sf	Scarcity factor
t	time
t0	Initial time of simulation
ts	Time step
WC	Water consumption
WW	Water withdrawal
X	Output
X_loss	Output loss (applicable to agriculture)
δ	Depreciation rate

4.2. Model Subscripts

The subscripts denote vectors, subvectors or elements thereof, programmed in the model.

Abbreviation	Type	Definition
1 to 25 (numbers)	Elements of vector sector	Numbers corresponding to the productive sectors
a	Vector	Age chort
air_poll	Vector	Air pollution
am	Generic element created for the transition of population from one cohort to another	Age middle (generic cohort)
ay	Generic element created for the transition of population from one cohort to another. It is the cohort prior to the middle age cohort	Age young (generic cohort)
c04	Element (inside vector age cohort)	Cohort 0 to 4 years
c1519	Element (inside vector age cohort)	Cohort 15 to 19 years

c2024	Element (inside vector age cohort)	Cohort 20 to 24 years
c2529	Element (inside vector age cohort)	Cohort 25 to 29 years
c3034	Element (inside vector age cohort)	Cohort 30 to 34 years
c3539	Element (inside vector age cohort)	Cohort 35 to 39 years
c4044	Element (inside vector age cohort)	Cohort 40 to 44 years
c95+	Element (inside vector age cohort)	Cohort 95 years or more
Chem&FertMin	Element (inside vector materials)	Chemical and fertilizer minerals
cl	Vector	Class
cnt	Vector	country
CO2	Element (inside vector greenhouse gas emissions)	Carbon dioxide
e	Vector	Extreme weather events
elec	Element (inside vector energy)	Electricity
en	Vector	Energy
ff	Subvector (inside vector energy)	Fossil fuels (oil, gas, coal)
foodland_we	Element (inside vector land)	Foodland for the use of the world economy
ghg	Vector	Greenhouse gas emissions
hw	Element (inside vector extreme weather events)	Heat waves
high	Element (inside vector class)	High class
i	Vector	Sector
inf	Element (inside vector land)	Infraestructure
j	Vector identical to i to construct the input-output. In the input-output, i denotes the rows and j the columns	Sector
Lnd	Vector	Land
low	Element (inside vector class)	Low class
mat	Vector	Materials
middle	Element (inside vector class)	Middle class
P&N	Vector	Phosphorus and nitrogen pollution
P_soil	Element (inside vector Phosphorus and nitrogen pollution)	Soil phosphorus pollution
pfrst	Element (inside vector land)	Primary forest
prod_frst	Element (inside vector land)	Productive forest
prod_Land	Subvector (inside vector land)	Productive land
r	Vector	Region
sfrst	Element (inside vector land)	Secondary forest
shrub	Element (inside vector land)	Shrub

sub_lnd	Element (inside vector land)	Land in use by the population in a subsistence state
---------	------------------------------	--

4.3. Model Superscripts

The superscripts serve only to complete the names of the variables or to link parameters to the variables to be calculated. The vectorization of the model is represented only in the subscripts.

Abbreviation	Definition
2°C	Superscript associated with the variable t to refer to the time at which 2°C is reached.
2°C_slr	2°C sea level rise
3°C	Superscript associated with the variable t to refer to the time at which 3°C is reached.
3°C_slr	3°C sea level rise
4°C	Superscript associated with the variable t to refer to the time at which 4°C is reached.
4°C_slr	4°C sea level rise
Adf_io	Agriculture damage factor for the input output
bd	Before damage
blue_w	Blue water
Br5y	Birth rate per five years
comb	Combustion
d	Demand
Dr5y	Death rate per five years
Edf	Extraction difficulty factor
em	Emissions
eu	Energy use
Ext_Int_Lnd_sub	Extra land intensity
ff	Fossil fuels
Foodland_loss	Foodland loss
green_w	Green water
HB_Max_Lb	Heat damage to maximum labour
HD_Lb_prod	Heat damage to labour productivity
hh	Households
Inv	Investment
io	input output
IRW	Industrial roundwood
k	Capital stock
Lb_prod	Labour productivity
Lnd	Land
Lnd	Land
Lnd_loss	Land loss
mat_unused	Material unused
mat_used	Material used
neu	Non energy use

other	Other CO2 emission sources
prod	Production
s	Supply
slr	Sea level rise
sub	Subsistence
sub2we	Subsistence to world economy
temp	Temperature
we	World economy
CW	Water consumption
WW	Water withdrawal
X_loss	Output loss (in the food sector)
δ_{temp}	Depreciation rate temperature. Abbreviation associated with parameter used to calculate changes in depreciation due to change in global average temperature.

5. References

- Altieri, M. A., & Koohafkan, P. (2008). *Enduring farms: Climate change, smallholders and traditional farming communities* (Vol. 6). Third World Network (TWN) Penang.
- Arnell, N. W., Brown, S., Gosling, S. N., Gottschalk, P., Hinkel, J., Huntingford, C., Lloyd-Hughes, B., Lowe, J. A., Nicholls, R., & Osborn, T. (2016). The impacts of climate change across the globe: A multi-sectoral assessment. *Climatic Change*, 134(3), 457–474.
- Bamber, J. L., Oppenheimer, M., Kopp, R. E., Aspinall, W. P., & Cooke, R. M. (2019). Ice sheet contributions to future sea-level rise from structured expert judgment. *Proceedings of the National Academy of Sciences*, 116(23), 11195–11200.
- Beck, M. W., Losada, I. J., Menéndez, P., Reguero, B. G., Díaz-Simal, P., & Fernández, F. (2018). The global flood protection savings provided by coral reefs. *Nature Communications*, 9(1), 2186.
- Béguin, A., Hales, S., Rocklöv, J., Åström, C., Louis, V. R., & Sauerborn, R. (2011). The opposing effects of climate change and socio-economic development on the global distribution of malaria. *Global Environmental Change*, 21(4), 1209–1214.
- BGR. (2020). *BGR Energy Study 2019 – Data and Developments Concerning German and Global energy supplies*. Hannover.
https://www.bgr.bund.de/EN/Themen/Energie/Downloads/energiestudie_2019_en.pdf;jsessionid=ADF18B2529B3E89FC705FDF390A57BA4.internet002?__blob=publicationFile&v=6
- Bontadini, F., Corrado, C., Haskel, J., Iommi, M., & Jona-Lasinio, C. (2023). EUKLEMS & INTANProd: Industry productivity accounts with intangibles—Sources of growth and productivity trends: Methods and main measurement challenges. *The Luiss*

Lab of European Economics. [Https://Euklems-Intanprod-Llee. Luiss. It/\(Data](Https://Euklems-Intanprod-Llee. Luiss. It/(Data)
Extracted on 21 February 2023).

Brown, H. C. A., Berninger, F. A., Larjavaara, M., & Appiah, M. (2020). Above-ground carbon stocks and timber value of old timber plantations, secondary and primary forests in southern Ghana. *Forest Ecology and Management*, 472, 118236.

<https://doi.org/10.1016/j.foreco.2020.118236>

Capellán-Pérez, I., de Blas, I., Nieto, J., de Castro, C., Miguel, L. J., Carpintero, Ó., Mediavilla, M., Lobejón, L. F., Ferreras-Alonso, N., & Rodrigo, P. (2020). MEDEAS: a new modeling framework integrating global biophysical and socioeconomic constraints. *Energy & Environmental Science*, 13(3), 986–1017.

Capellán-Pérez, I., De Castro, C., & Arto, I. (2017). Assessing vulnerabilities and limits in the transition to renewable energies: Land requirements under 100% solar energy scenarios. *Renewable and Sustainable Energy Reviews*, 77, 760–782.

Dasgupta, S., van Maanen, N., Gosling, S. N., Piontek, F., Otto, C., & Schleussner, C.-F. (2021). Effects of climate change on combined labour productivity and supply: An empirical, multi-model study. *The Lancet Planetary Health*, 5(7), e455–e465.

De Castro, C., Mediavilla, M., Miguel, L. J., & Frechoso, F. (2013). Global solar electric potential: A review of their technical and sustainable limits. *Renewable and Sustainable Energy Reviews*, 28, 824–835.

Deutsch, C. A., Tewksbury, J. J., Tigchelaar, M., Battisti, D. S., Merrill, S. C., Huey, R. B., & Naylor, R. L. (2018). Increase in crop losses to insect pests in a warming climate. *Science*, 361(6405), 916–919.

FAO. (2017). *Global forest products. Facts and figures 2016*.

<https://openknowledge.fao.org/server/api/core/bitstreams/16e00ac5-32f4-4ccd-89f6-4e902d299e02/content>

FAO. (2020). *Global Forest Resources Assessment 2020*.

<https://www.fao.org/interactive/forest-resources-assessment/2020/en/>

Forzieri, G., Bianchi, A., e Silva, F. B., Herrera, M. A. M., Leblois, A., Lavalle, C., Aerts, J. C., & Feyen, L. (2018). Escalating impacts of climate extremes on critical infrastructures in Europe. *Global Environmental Change*, 48, 97–107.

Franklinos, L. H., Jones, K. E., Redding, D. W., & Abubakar, I. (2019). The effect of global change on mosquito-borne disease. *The Lancet Infectious Diseases*, 19(9), e302–e312.

Henckens, T. (2021). Scarce mineral resources: Extraction, consumption and limits of sustainability. *Resources, Conservation and Recycling*, 169, 105511.

<https://doi.org/10.1016/j.resconrec.2021.105511>

Hinkel, J., Lincke, D., Vafeidis, A. T., Perrette, M., Nicholls, R. J., Tol, R. S., Marzeion, B., Fettweis, X., Ionescu, C., & Levermann, A. (2014). Coastal flood damage and adaptation costs under 21st century sea-level rise. *Proceedings of the National Academy of Sciences*, 111(9), 3292–3297.

Houghton, R. A., & Castanho, A. (2023). Annual emissions of carbon from land use, land-use change, and forestry from 1850 to 2020. *Earth System Science Data*, 15(5), 2025–2054. <https://doi.org/10.5194/essd-15-2025-2023>

Houghton, R. A., House, J. I., Pongratz, J., Van Der Werf, G. R., DeFries, R. S., Hansen, M. C., Le Quéré, C., & Ramankutty, N. (2012). Carbon emissions from land use and land-cover change. *Biogeosciences*, 9(12), 5125–5142. <https://doi.org/10.5194/bg-9-5125-2012>

Hu, Y., Jia, G., Gao, H., Li, Y., Hou, M., Li, J., & Miao, C. (2023). Spatial characterization of global heat waves using satellite-based land surface temperature. *International Journal of Applied Earth Observation and Geoinformation*, 125, 103604.

IEA. (2021). *Key World Energy Statistics 2021*. IEA. <https://www.iea.org/reports/key-world-energy-statistics-2021>

IPCC. (2021). *Climate Change 2021: The Physical Science Basis. Contribution of Working Group I to the Sixth Assessment Report of the Intergovernmental Panel on Climate Change*. Cambridge University Press. Cambridge University Press, Cambridge, UK and New York, NY, USA.,

Kulp, S. A., & Strauss, B. H. (2019). New elevation data triple estimates of global vulnerability to sea-level rise and coastal flooding. *Nature Communications*, 10(1), 1–12.

Lahoti, R., Jayadev, A., & Reddy, S. (2016). The global consumption and income project (GCIP): An overview. *Journal of Globalization and Development*, 7(1), 61–108.

Lifi, M., de Blas, I., Capellan-Perez, I., Mediavilla, M., Miguel, L. J., Parrado-Hernando, G., Llases, L., Álvarez-Antelo, D., Calleja, M., Wergles, N., Ferreras, N., Ramos, I., Arto, I., Calheiros, T., Capela Lourenco, T., Morlin, G., D'Alessandro, S., van Allen, O., Eggler, L., ... Oakes, R. (2023). *Synthesis of the model, selected results, and scenario assessment. WP9, Task 9.2, D.9.3. LOCOMOTION*.

<https://zenodo.org/records/10813034>

Lowder, S. K., Bhalla, G., & Davis, B. (2025). Decreasing farm sizes and the viability of smallholder farmers: Implications for resilient and inclusive rural transformation. *Global Food Security*, 45, 100854. <https://doi.org/10.1016/j.gfs.2025.100854>

LUISS. (2023). EUKLEMS & INTANProd. <https://euklems-intanprod-llee.luiss.it/download/>

Maggio, G., & Cacciola, G. (2012). When will oil, natural gas, and coal peak? *Fuel*, 98, 111–123.

- Meza, I., Siebert, S., Döll, P., Kusche, J., Herbert, C., Eyshi Rezaei, E., Nouri, H., Gerdener, H., Popat, E., & Frischen, J. (2020). Global-scale drought risk assessment for agricultural systems. *Natural Hazards and Earth System Sciences*, 20(2), 695–712.
- Mohr, S. H., Wang, J., Ellem, G., Ward, J., & Giurco, D. (2015). Projection of world fossil fuels by country. *Fuel*, 141, 120–135.
- Mora, C., Doussot, B., Caldwell, I. R., Powell, F. E., Geronimo, R. C., Bielecki, C. R., Counsell, C. W., Dietrich, B. S., Johnston, E. T., & Louis, L. V. (2017). Global risk of deadly heat. *Nature Climate Change*, 7(7), 501–506.
- Nienhuis, J. H., & van de Wal, R. S. (2021). Projections of global delta land loss from sea-level rise in the 21st century. *Geophysical Research Letters*, 48(14), e2021GL093368.
- Nierop, S., & Humperdinck, S. (2018). *International comparison of fossil power efficiency and CO₂ intensity – Update 2018*. ECOFYS. <https://guidehouse.com/-/media/www/site/downloads/energy/2018/intl-comparison-of-fossil-power-efficiency--co2-in.pdf>
- Our World in Data. (2024). *Electricity production by source, World*. <https://ourworldindata.org/electricity-mix>
- RBI. (2024). *KLEMS Database*. <https://rbi.org.in/Scripts/KLEMS.aspx>
- RIETI. (2023). *CIP Database 2023*. <https://www.rieti.go.jp/en/database/CIP2023/index.html>
- Ritchie, H., & Roser, M. (2024). *Half of the world's habitable land is used for agriculture*. <https://ourworldindata.org/global-land-for-agriculture>
- Samberg, L. H., Gerber, J. S., Ramankutty, N., Herrero, M., & West, P. C. (2016). Subnational distribution of average farm size and smallholder contributions to global food production. *Environmental Research Letters*, 11(12), 124010.

Samsó, R., Ramos, I., Ferreras, N., Lifi, M., Mediavilla, M., Llases, L., de Blas, I., Capellán-Pérez, I., Parrado-Hernando, G., Calleja, M., Álvarez-Antelo, D., Markovska, N., Arto, I., Calheiros, T., Papagianni, S., van Aken, O., & Eggler, L. (2023). *D11.2: "Python translation and e-Handbook for model sharing and transparency."*

https://www.locomotion-h2020.eu/wp-content/uploads/2023/11/D11.2_Python_translation_and_e-Handbook-1.pdf

Smith, A. (2025). *U.S. Billion-dollar Weather and Climate Disasters, 1980—Present (NCEI Accession 0209268)* [Dataset]. NOAA National Centers for Environmental Information. <https://doi.org/10.25921/STKW-7W73>

Smith, C., Nicholls, Z. R. J., Armour, K., Collins, W., Forster, P., Meinshausen, M., Palmer, M. D., & Watanabe, M. (2021). The Earth's Energy Budget, Climate Feedbacks, and Climate Sensitivity Supplementary Material. In V. Masson-Delmotte, P. Zhai, A. Pirani, S. L. Connors, C. Péan, S. Berger, N. Caud, Y. Chen, L. Goldfarb, M. I. Gomis, M. Huang, K. Leitzell, E. Lonnoy, J. B. R. Matthews, T. K. Maycock, T. Waterfield, O. Yelekçi, R. Yu, & B. Zhou (Eds.), *Climate Change 2021: The Physical Science Basis. Contribution of Working Group I to the Sixth Assessment Report of the Intergovernmental Panel on Climate Change.*

https://www.ipcc.ch/report/ar6/wg1/downloads/report/IPCC_AR6_WGI_Chapter07_SM.pdf

Stadler, K. (2021). *Pymrio—A Python based multi-regional input-output analysis toolbox.*

Stadler, K., Wood, R., Bulavskaya, T., Södersten, C., Simas, M., Schmidt, S., Usobiaga, A., Acosta-Fernández, J., Kuenen, J., Bruckner, M., Giljum, S., Lutter, S., Merciai, S., Schmidt, J. H., Theurl, M. C., Plutzar, C., Kastner, T., Eisenmenger, N., Erb, K., ...

Tukker, A. (2018). EXIOBASE 3: Developing a Time Series of Detailed

Environmentally Extended Multi-Regional Input-Output Tables. *Journal of Industrial Ecology*, 22(3), 502–515. <https://doi.org/10.1111/jiec.12715>

Stadler, K., Wood, R., Bulavskaya, T., Södersten, C.-J., Simas, M., Schmidt, S., Usobiaga, A., Acosta-Fernández, J., Kuenen, J., Bruckner, M., Giljum, S., Lutter, S., Merciai, S., Schmidt, J. H., Theurl, M. C., Plutzar, C., Kastner, T., Eisenmenger, N., Erb, K.-H., ... Tukker, A. (2021). EXIOBASE 3 (Version 3.8.2) [Dataset]. Zenodo.

<https://doi.org/10.5281/ZENODO.5589597>

Tao, Y., Li, F., Wang, R., & Zhao, D. (2015). Effects of land use and cover change on terrestrial carbon stocks in urbanized areas: A study from Changzhou, China. *Journal of Cleaner Production*, 103, 651–657.

<https://doi.org/10.1016/j.jclepro.2014.07.055>

Timmer, M. P., Dietzenbacher, E., Los, B., Stehrer, R., & De Vries, G. J. (2015). An Illustrated User Guide to the World Input–Output Database: The Case of Global Automotive Production. *Review of International Economics*, 23(3), 575–605.

<https://doi.org/10.1111/roie.12178>

UN DESA. (2019a). *World Population Prospects 2019, Online Edition. Rev. 1. File FERT/7: Age-specific fertility rates by region, subregion and country, 1950-2100 (births per 1,000 women)*, WPP2019_FERT_F07_AGE_SPECIFIC_FERTILITY.xlsx. This data gives age-specific fertility rates for 7 age categories (15-19, 20-24, ..., 45-49).

UN DESA. (2019b). *World Population Prospects 2019, Online Edition. Rev. 1. File MORT/4-1: Deaths (both sexes combined) by five-year age group, region, subregion and country, 1950-2100 (thousands)*, WPP2019_MORT_F04_1_DEATHS_BY_AGE_BOTH_SEXES.xlsx.

UN DESA. (2019c). *World Population Prospects 2019, Online Edition. Rev. 1. File POP/7-1: Total population (both sexes combined) by five-year age group, region, subregion and country, 1950-2100 (thousands).*

USGS. (2020). *Minerals Yearbook—Metals and Minerals. (Volume I.—Metals and Minerals).*

U.S. Geological Survey. <https://www.usgs.gov/centers/national-minerals-information-center/minerals-yearbook-metals-and-minerals>

WIOD. (2016). *World Input-Output Database 2016 Release, 2000-2014* (Version 2.1, pp. 527389, 971011, 548889, 5536437, 62241593, 19308, 14196475, 68437603, 564746464, 641578409, 858823444, 638963496, 919328606, 49465)

[Application/pdf,application/pdf,application/pdf,application/vnd.openxmlformats-

officedocument.spreadsheetml.sheet,application/zip,application/vnd.openxmlformats-

officedocument.spreadsheetml.sheet,application/zip,application/zip,application/zip,application/zip,application/zip,application/zip,application/zip,application/pdf]. DataverseNL. <https://doi.org/10.34894/PJ2M1C>

World Bank. (2024a). *Final consumption expenditure (% of GDP).*

<https://data.worldbank.org/indicator/NE.CON.TOTL.ZS>

World Bank. (2024b). *GDP (current US\$).*

<https://data.worldbank.org/indicator/NY.GDP.MKTP.CD>

World Bank. (2024c). *GDP per capita, PPP (current international \$).*

<https://data.worldbank.org/indicator/NY.GDP.PCAP.PP.CD>

World Bank. (2024d). *World Bank Analytical Classifications.*

<https://datacatalogfiles.worldbank.org/ddh-published/0037712/DR0090754/OGHIST.xlsx>

World Bank. (2025). *Poverty headcount ratio (2017 PPP, \$2.15) (% of population)*.

https://data360.worldbank.org/en/indicator/WB_PIP_HEADCOUNT_IPL

Zhang, X., & Cai, X. (2011). Climate change impacts on global agricultural land

availability. *Environmental Research Letters*, 6(1), 014014.

Zhao, C., Liu, B., Piao, S., Wang, X., Lobell, D. B., Huang, Y., Huang, M., Yao, Y., Bassu, S., &

Ciais, P. (2017). Temperature increase reduces global yields of major crops in four

independent estimates. *Proceedings of the National Academy of Sciences*, 114(35),

9326–9331.